(ISSN 0161-8202)

Journal of ARACHNOLOGY

PUBLISHED BY THE AMERICAN ARACHNOLOGICAL SOCIETY

VOLUME 44 2016 NUMBER 3

The *Journal of Arachnology* (ISSN 0161-8202), a publication devoted to the study of Arachnida, is published three times each year by *The American Arachnological Society*. **Memberships (yearly):** Membership is open to all those interested in Arachnida. A subscription to the *Journal of Arachnology* and annual meeting notices are included with membership in the Society. Regular, $55; Students, $30; Institutional, $125. Inquiries should be directed to the Membership Secretary (see below). **Back Issues:** James Carrel, 209 Tucker Hall, Missouri University, Columbia, Missouri 65211-7400 USA. Telephone: (573) 882-3037. **Undelivered Issues:** Allen Press, Inc., 810 E. 10th Street, P.O. Box 368, Lawrence, Kansas 66044 USA.

Cover photo: Two views of an unidentified female orb-weaving spider in the genus *Poltys* (Araneidae) from a rainforest near Mengla in southwestern China. In the field the unusual morphology and coloration of the spider makes it very diffieult to detect visually when it adopts the posture shown on the left (see page 397). Photos by Matjaž Kuntner.

Publication date: 23 November 2016

♾ **This paper meets the requirements of ANSI/NISO Z39.48-1992 (Permanence of Paper).**

2016. Journal of Arachnology 44:257–271

Pseudoscorpion diversity and distribution in the West Indies: sequence data confirm single island endemism for some clades, but not others

Julia G. Cosgrove[1,4], **Ingi Agnarsson**[2], **Mark S. Harvey**[3] and **Greta J. Binford**[1]: [1]Lewis & Clark College, Department of Biology, 0615 SW Palatine Hill Rd., Portland, Oregon, 97219, USA. E-mail: juliacosgrove@g.harvard.edu; [2]University of Vermont, Department of Biology, 109 Carrigan Drive, Burlington, Vermont, 05405, USA; [3]Department of Terrestrial Zoology, Western Australian Museum, Locked Bag 49, Welshpool DC, Western Australia 6986, Australia; [4]Current address: Museum of Comparative Zoology, Department of Organismic and Evolutionary Biology, Harvard University, 26 Oxford St, Cambridge, Massachusetts, 02138, USA

Abstract. The Caribbean Islands are a biodiversity hotspot harboring high levels of endemic biodiversity. In an effort to contribute to the characterization of invertebrate diversity in the region, we present an assessment of pseudoscorpion (Arachnida: Pseudoseorpiones) diversity and distribution with a focus on the superfamily Chthonioidea and the family Olpiidae. We used three markers (cytochrome *c* oxidase subunit I, histone H3 and 28S rRNA) to infer the first molecular phylogenies for each lineage and identified 32 putative new speeies in need of taxonomic assessment. These new records include the documentation of the genera *Pseudochthonius* Balzan, 1892 *Lagynochthonius* Beier, 1951, *Tyrannochthonius* Chamberlin, 1929 (Chthoniidae), *Antillolpium* Muchmore, 1991, *Novohorus* Hoff, 1945, and *Pachyolpium* Beier, 1931 (Olpiidae) on various islands. Chthonioid genera are strongly structured geographically, suggesting that many Caribbean species may be short-range endemics and excellent candidate systems for testing biogeographic hypotheses. The olpiid genus *Pachyolpium* is less geographically structured, which is consistent with the hypothesis that olpiids are better dispersers than chthonioids. This study aims to provide a foundation for taxonomic and biogeographic work on Caribbean pseudoscorpions, revealing a diversity that is far richer than is documented in the literature.

Keywords: Caribbean, Pseudoscorpiones, phylogeography, dispersal, new records

When E.O. Wilson coined the term nesiophilia – an inordinate fondness and hungering for islands (Wilson 2010) – he had his fellow biogeographers in mind, who recognize the unique opportunities for diversification that isolated biological systems provide. Of critical importance in understanding island processes are the evolution and maintenance of endemic species, which are typically also 'short-range endemic' (SRE) species (Harvey 2002). Paired together with MacArthur and Wilson's classic theory of island biogeography (1967) and modern phylogenetic methods, SRE lineages become powerful not only for predicting species richness given island area and isolation, but also for informing our hypotheses about when, where, and how a lineage first colonized an island, and shedding light on the geological and evolutionary processes that drive diversification.

Caribbean biogeography.—The Caribbean islands (also commonly referred to as the West Indies, Fig. 1) are a natural laboratory for studying evolutionary processes (Ricklefs & Bermingham 2008) due to their varying degrees of isolation from the mainland and the heterogeneity of their geological histories. Additionally, the West Indies region was identified as one of 25 biodiversity hotspots for conservation priorities as characterized by high levels of endemicity in plants and vertebrates and high rates of habitat loss (Myers et al. 2000), although Aide et al. (2013) found that reforestation also played an important role in shaping the Caribbean landscape between 2001–2010. The Greater Antilles (Cuba, Jamaica, Hispaniola [Haiti and Dominican Republic], and Puerto Rico) are the largest of the Caribbean islands, and include a combination of fragment and non-volcanic Darwinian islands, many of which have been historically connected to continental landmasses and/or each other (Iturralde-Vinent 2006; Ricklefs & Bermingham 2008). As is predicted by the species-area relationship posited by MacArthur & Wilson (1967), these islands harbor the majority of Caribbean biodiversity, and similarly, within this system species richness is often highest on Cuba, followed by Hispaniola, then Jamaica and Puerto Rico (e.g., Losos 1996; Crews & Gillespie 2010; Alonso et al. 2012).

The Lesser Antilles, which span from the northernmost US/British Virgin Islands south to Trinidad & Tobago, and also include the former Netherlands Antilles (Aruba, Bonaire, and Curaçao), are smaller and mostly younger, volcanic, Darwinian islands that have never been connected to other landmasses (with a few exceptions, such as Trinidad; Ricklefs & Bermingham 2008). Lastly, the Bahamas and the Turks and Caicos Islands, made up of around 700 'platform islands', have always been adjacent to North America and have been intermittently submerged throughout their history (Ricklefs & Bermingham 2008, and geological references therein).

While isolation and area have been identified as two of the main abiotic factors that shape biogeographic patterns (theory of island biogeography), an organism's life history, potential and realized niche, evolutionary age, and dispersal capability (Claramunt et al. 2012; Agnarsson et al. 2014) are also key factors in determining its potential for colonization and subsequent diversification on an island (as well as its status as an SRE) (Harvey 2002; Lomolino 2010). For example, at the two extremes, poorly dispersing lineages typically have smaller ranges and are more geographically structured than lineages that disperse easily, as they are more likely to have established themselves on an island via a single chance colonization event or through vicariance. Groups that are better dispersers are more likely to lack biogeographic fidelity, making it difficult to infer their true geographic history. Here we assess the

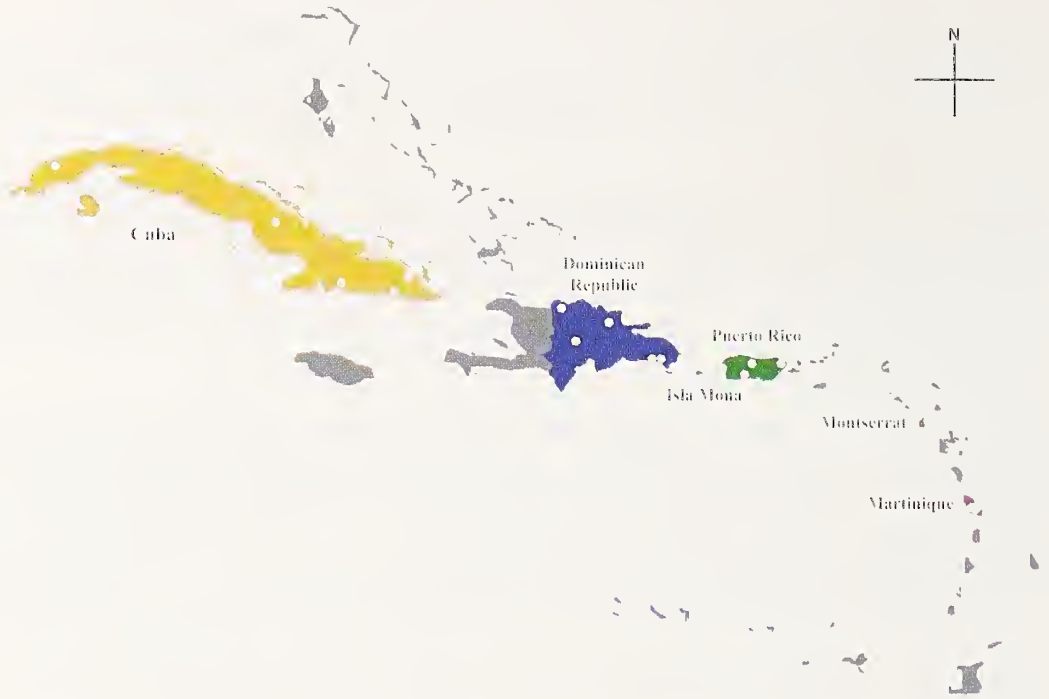

Figure 1.—The Caribbean Islands, or West Indies, with sampled localities marked by white dots.

Caribbean diversity of one of the lesser-known arachnid orders, Pseudoscorpiones, in order to contribute to the characterization of the group's overall distribution and to identify particular groups that may be useful for testing biogeographic hypotheses.

Pseudoscorpiones.—Pseudoscorpions are small, inconspicuous arachnids found in terrestrial habitats all over the world; most commonly in leaf litter, but also on tidal flats, in caves, and in the cracks of bark and rocks (Weygoldt 1969; Murienne et al. 2008; Harvey 2013). All pseudoscorpions are predatory, and species within the suborder Iocheirata use venom secreted from one or more of their chelal fingers (distal 'hand' of the pedipalp) for prey capture (Chamberlin 1931; Harvey 1992). These animals are generally considered to be poor dispersers, although some exhibit phoretic behavior (i.e., individuals hitch rides on larger animals), allowing them to disperse as far as their hosts (e.g., Poinar et al. 1998; Zeh et al. 2003). While few phylogenetic analyses have been performed to establish relationships between and within the 25 families (~3,500 species) (Harvey 2013), molecular and morphological data support the order Pseudoscorpiones as monophyletic (Shultz 2007; Murienne et al. 2008).

The oldest documented pseudoscorpion fossil is from the mid Devonian (~380 million years old), and many younger fossils placed in extant families, including specimens from Dominican amber have also been described (e.g., Schawaller et al. 1991; Judson 2012; Harvey 2013). The Caribbean fossils suggest that several pseudoscorpion families have been present in this region for at least the last ~20 million years (Judson 1998), during which time some of the Greater Antilles split apart from each other (Pindell & Barrett 1990). Currently there are 147 extant species of pseudoscorpions (47 genera, 17 families) described from the Caribbean region, 120 of which are endemic to the Caribbean islands and 93 of which are single island endemics (Table 1; Harvey 2013). Further sampling may find that not all are truly restricted to single islands, or may show an even finer scale of species boundaries than currently appreciated. The diversity of Caribbean pseudoscorpions, both extant and extinct, as well as a wide range of dispersal abilities makes these animals excellent candidates for biogeographic analysis in this region.

Although considerable work has been done on vertebrate diversification in the Caribbean, few studies have analyzed the patterns and timing of colonization by invertebrates, and researchers have not yet identified any overarching principles

Table 1.—Total number of previously described Caribbean pseudoscorpion genera and species (Harvey 2013). Focal lineages are in boldface text.

Family	Genera	Species
Chthoniidae	**8**	**26**
Lechytiidae	**1**	**4**
Tridenchthoniidae	1	5
Bochicidae	4	9
Ideoroncidae	2	3
Syarinidae	3	11
Garypidae	1	1
Garypinidae	2	2
Geogarypidae	1	1
Olpiidae	**10**	**24**
Cheiridiidae	4	5
Pseudochiridiidae	1	1
Sternophoridae	2	3
Atemnidae	4	6
Cheliferidae	4	7
Chernetidae	22	34
Withiidae	4	5
Total	74	147

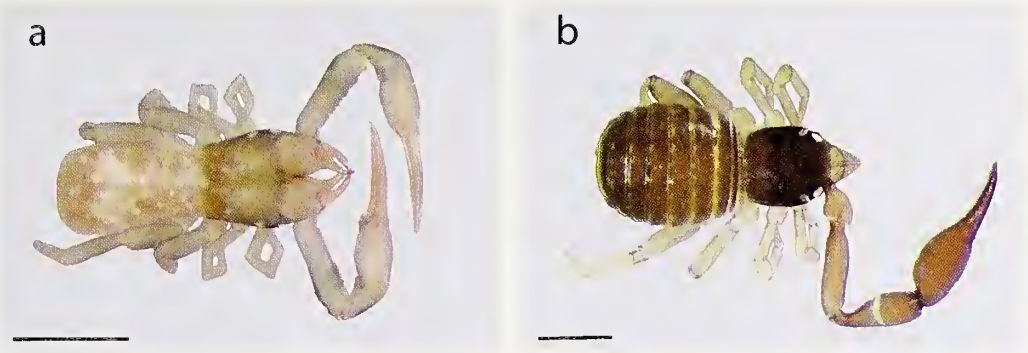

Figure 2.—Representative taxa: a, *Tyrannochthonius* sp.; b, *Pachyolpium cp033*. Scale bars represent 0.5 mm.

to explain the processes driving diversification in this biodiversity hotspot (*sensu* Myers 2000; Gillespie 2013). Nevertheless, an emerging pattern from the current project (CarBio, see islandbiogeography.org) indicates an important role of vicariant events and subsequent within-island radiation for various arachnid groups consisting of relatively poor dispersers (*Spintharus* Hentz, 1850: Dziki et al. 2015; *Phrynus* Lamarck, 1801: Esposito et al. 2015; *Micrathena* Sundevall, 1833: McHugh et al. 2014; *Loxosceles* Heineken & Lowe, 1832: Petersen et al. unpubl. data; *Deinopis* MacLeay, 1839: Chamberland et al. unpubl. data, and others). This study was undertaken to assess pseudoscorpion diversity in the Caribbean with a primary focus on two of the most diverse groups in the region: the superfamily Chthonioidea and the family Olpiidae (Fig. 2). We inferred the first molecular phylogenies for each clade in the Caribbean using three genes (cytochrome *c* oxidase subunit I (COI), 28S rRNA, and histone H3) and evaluated the phylogeographic structure of each lineage in order to identify patterns for future investigation.

METHODS

Taxon sampling and identification.—Specimens were collected into 95% ethanol by the CarBio field teams as part of an arachnid wide Caribbean inventory between 2010–2012. Pseudoscorpions were collected manually from trees, rocks, and sifted leaf litter, and extracted from litter using Berlese funnels. A variety of collecting methods decreases bias toward any particular taxonomic group or life stage; hand sorting tends to be biased towards larger and mature individuals, and Berlese funnels yield a more representative sample of juveniles and smaller individuals (Gabbutt 1970).

Using a stereomicroscope, specimens were first sorted to family using characters as described by Muchmore (1990) and Harvey (1992). Tissue samples (legs or a single pedipalp dissected from the body, depending on the size of the specimen) were taken for molecular work from 228 individuals belonging to Chthonioidea and Olpiidae, as these two groups were the most abundant in our collections (see Fig. 2 for images of the most highly represented genera in our samples). Specimens were then prepared for closer morphological examination using temporary slide mounts (as in Edward & Harvey 2008), and images of whole specimens, coxal spines (Chthonioidea), and chelal hands were taken through a compound (Chthonioidea) or light (Olpiidae) microscope using Automontage software. Each specimen was examined and diagnostic characters were compared to published descriptions of congeneric taxa in the Caribbean and adjacent regions. Individuals that matched these descriptions were identified to species, and individuals that did not match any published descriptions were identified to the genus level and further analyzed using the generated molecular data (see below). All specimens were returned to 95% ethanol after examination and stored at –20°C at Lewis & Clark College.

DNA extraction, amplification and sequencing.—DNA was extracted and purified from 96 specimens (of 228) using the Qiagen DNeasy Blood & Tissue Kit (Qiagen, Valencia, CA, USA) at Lewis & Clark College. DNA was extracted and purified from the remaining 132 specimens in the Smithsonian Laboratories of Analytical Biology (LAB) in Washington, DC using an Autogenprep965 for an automated phenol chloroform extraction (Smithsonian Institution 2013). All extractions were made from the four left legs and left pedipalp of chthonioids and the left pedipalp of olpiids.

Purified genomic DNA was used as a template to amplify cytochrome *c* oxidase subunit I (COI, ~1000 bp), histone H3 (H3, ~300 bp) and the large nuclear ribosomal subunit 28S rRNA (~1000 bp) (see Table 2 for primers and PCR conditions). COI and 28S rRNA have been useful for conducting phylogenetic analyses of pseudoscorpions at the genus level (Murienne et al. 2008), while histone H3 has been used to infer phylogenies and analyze evolutionary rates in other invertebrates (e.g. Colgan et al. 2000).

Table 2.—PCR conditions and target fragment length for each molecular marker.

Gene	Primers	MasterAmp™ buffer	Annealing temperature	Fragment length (bp)
COI	LCO11490/HCO12198	B	46.2°	~1000
28S	28spsF/28spsR	D	45°	~1000
H3	H3aR/H3nF	B	46.2°	~300

Table 3.—Taxa included in concatenated analyses.

	Species	Country/Island	Voucher	COI	28S	H3
Outgroups	*Feaella anderseni*	Australia	DNA 102369	EU559500.1	-	-
	Pseudogarypus bicornis	USA	DNA 102449	EU559501.1	EU559472.1	-
	Neopseudogarypus scutellatus	Australia	DNA 102431	EU559502.1	EU559456.1	-
	Afrosternophorus sp.	Australia	DNA 102437	EU559568.1	EU559461.1	-
	Lustrochernes sp.	Colombia	DNA 102430	EU559553.1	EU559455.1	-
	Ideoblothrus sp.	Colombia	DNA 102457	EU559562.1	EU559480.1	-
Chthonioidea	*Lagynochthonius* cp005	Puerto Rico	921A	KX263366	KX263326	KX263406
	Lagynochthonius cp006	Puerto Rico	782954	KX263365	KX263327	KX263407
	Lagynochthonius cp007	Puerto Rico	783084	KX263364	KX263328	KX263408
	Lagynochthonius proximus	Martinique	654A	KX263363	KX263325	KX263405
	Lechytia sini	Dominican Republic	782992	KX263367	KX263329	KX263409
	Pseudochthonius cp001	Dominican Republic	728A	KX263372	KX263333	KX263413
	Pseudochthonius cp001	Dominican Republic	782983	KX263375	KX263336	KX263416
	Pseudochthonius cp001	Dominican Republic	782996	KX263374	KX263338	KX263418
	Pseudochthonius cp001	Cuba	692A	KX263371	KX263332	KX263412
	Pseudochthonius cp001	Dominican Republic	917A	KX263373	KX263335	KX263415
	Pseudochthonius cp002	Mona	782995	KX263376	KX263337	KX263417
	Pseudochthonius cp003	Martinique	280A	KX263369	KX263330	KX263410
	Pseudochthonius cp003	Martinique	873A	KX263368	KX263334	KX263414
	Pseudochthonius cp004	Cuba	662A	KX263370	KX263331	KX263411
	Tyrannochthonius cp008	Cuba	986A	KX263394	KX263351	KX263431
	Tyrannochthonius cp009	Cuba	781A	KX263389	KX263343	KX263423
	Tyrannochthonius cp010	Cuba	931A	KX263380	KX263348	KX263428
	Tyrannochthonius cp011	Cuba	995A	KX263379	KX263352	KX263432
	Tyrannochthonius cp012	Cuba	675A	KX263390	KX263341	KX263421
	Tyrannochthonius cp013	Cuba	835A	KX263388	KX263346	KX263426
	Tyrannochthonius cp014	Dominican Republic	924A	KX263386	KX263347	KX263427
	Tyrannochthonius cp015	Dominican Republic	782997	KX263387	KX263355	KX263436
	Tyrannochthonius cp016	Cuba	805A	KX263385	KX263344	KX263424
	Tyrannochthonius cp017	Cuba	747A	KX263381	KX263342	KX263422
	Tyrannochthonius cp018	Cuba	942A	KX263382	KX263350	KX263430
	Tyrannochthonius cp019	Cuba	826A	KX263383	KX263345	KX263425
	Tyrannochthonius cp020	Cuba	655A	KX263384	KX263340	KX263420
	Tyrannochthonius cp021	Cuba	937A	KX263378	KX263349	KX263429
	Tyrannochthonius cp022	Mona	782976	KX263391	—	KX263435
	Tyrannochthonius cp023	Puerto Rico	782960	KX263393	KX263354	KX263434
	Tyrannochthonius cp024	Puerto Rico	782958	KX263392	KX263353	KX263433
	Tyrannochthonius insulae	Puerto Rico	782966	KX263377	KX263339	KX263419
Olpiidae	*Antillolpium* cp026	Dominican Republic	783047	KX263396	KX263357	KX263438
	Antillolpium cp027	Cuba	772A	KX263395	KX263356	KX263437
	Aphelolpium cp028	Puerto Rico	783054	KX263397	—	KX263439
	Apolpium parvum	Trinidad	DNA103134	EU559541.1	EU559489.1	—
	Pachyolpium cp029	Puerto Rico	783044	KX263402	—	KX263444
	Pachyolpium cp030	Puerto Rico	783059	KX263404	—	KX263446
	Pachyolpium cp031	Puerto Rico	783012	KX263400	KX263360	KX263442
	Pachyolpium cp032	Dominican Republic	783040	KX263401	KX263361	KX263443
	Pachyolpium cp033	Cuba	965A	KX263399	KX263359	KX263441
	Pachyolpium cp033	Cuba	866A	KX263398	KX263358	KX263440
	Pachyolpium cp033	Dominican Republic	783048	KX263403	KX263362	KX263445
	Pachyolpium sp.	Trinidad	DNA103132	EU559542.1	EU559488.1	—

For gDNA that was purified at LAB, COI was amplified and sequenced at the Smithsonian using LAB protocols (S.I. 2013). All other PCR amplifications were run at Lewis & Clark College. PCR products were validated using agarose gel electrophoresis (1% agarose), and successfully amplified reactions were cleaned up for sequencing with EXOSAP (0.5 μL/5 μL PCR product, 45 min incubation at 37°C and 15 min deactivation at 80°C). Final PCR products were Sanger-sequenced in both directions either at the University of Arizona Genomic Analysis and Technology Core, or at the LAB. Sequences for two chthonioid specimens and two olpiid specimens from Trinidad were obtained from GenBank (for vouchers see Table 3) and included in the analyses.

Sequence editing.—Sequences were assembled using SEQUENCHER 4.7 (Gene Codes Corp.), and contigs were aligned using MAFFT version 7 (Katoh 2013). MAFFT

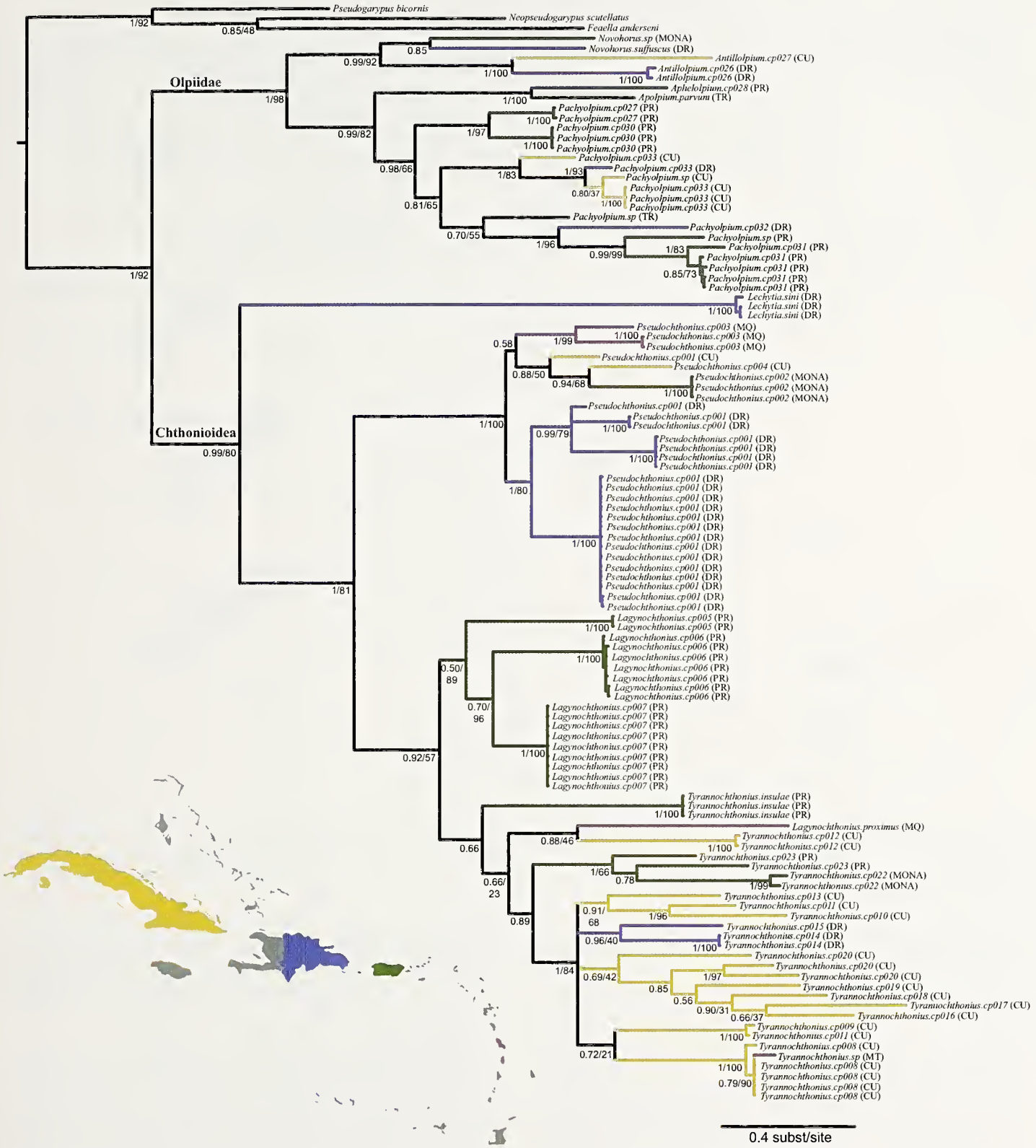

Figure 3.—Bayesian analysis of COI data from all sampled specimens supports Chthonioidea, Olpiidae, and most genera within these groups as monophyletic (all except *Lagynochthonius* + *Tyrannochthonius* which are recovered together in one clade). Posterior probabilities and bootstrap values are printed at each node for those nodes recovered by both MrBayes and RAxML (posterior probability/bootstrap value), and nodes recovered only in the Bayesian analysis are labeled with a single posterior probability value. Branches are colored by island and correspond to the colors on the map insert. CU = Cuba; DR = Dominican Republic; MQ = Martinique; MT = Montserrat; PR = Puerto Rico; TR = Trinidad.

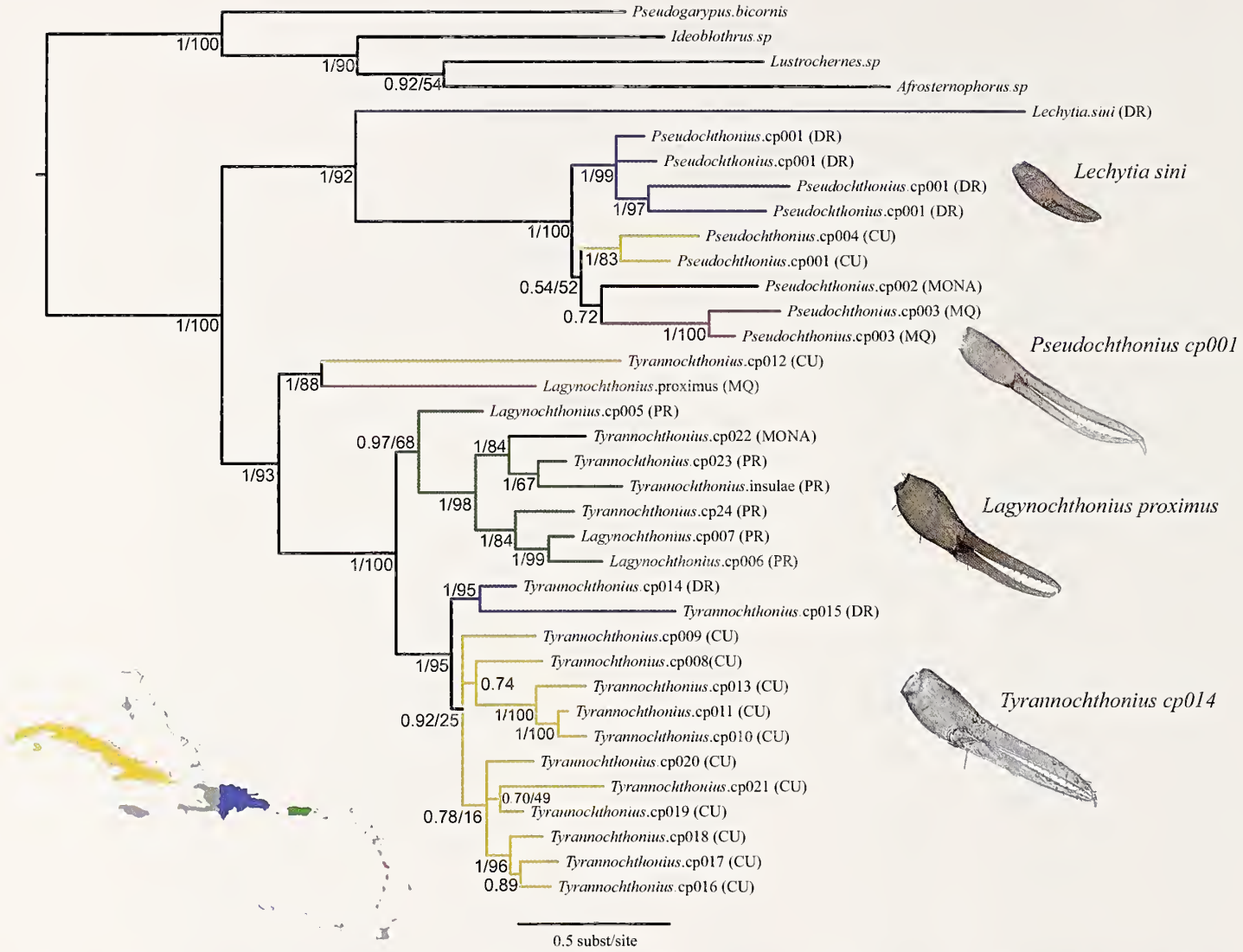

Figure 4.—Bayesian majority rule consensus tree of the concatenated matrix including COI, 28S, and H3 sequence data for Chthonioidea species and putative species. Posterior probabilities and bootstrap values are printed at each node for those nodes recovered by both MrBayes and RAxML (posterior probability/bootstrap value), and nodes recovered only in the Bayesian analysis are labeled with a single posterior probability value. Branches are colored by island and correspond to the colors on the map insert. CU = Cuba; DR = Dominican Republic; MQ = Martinique; PR = Puerto Rico.

settings changed from the default included: direction of nucleotide sequences [adjust direction according to the first sequence]; parameters, scoring matrix for nucleotide sequences [1PAM/k = 20]; align unrelated segments, too? [leave gappy regions]; unalignlevel [0.0]. Conserved blocks were selected using the less-stringent selection options in Gblocks version 0.91b (Castresana 2000), and the resulting alignments were used for all further analyses. Raw *p*-distances were calculated in Geneious v.8.1.7 (Kearse et al. 2012). All individuals for which COI successfully amplified were included in the complete COI analysis (n = 105), and individuals with sequence data from at least two genes were included in the final concatenated matrices (n = 42). Clades containing multiple individuals with identical COI haplotypes were pruned to include only one terminal in the concatenated datasets. MESQUITE (Maddison & Maddison 2011) was used to create concatenated matrices with all three genes for Chthonioidea and Olpiidae, and PartitionFinder v1.1.1 (Lanfear et al. 2012) was used to identify the best partitioning schemes for the concatenated analyses, defining seven possible partitions: 28S and positions one, two, and three for COI and H3, respectively.

Phylogenetic analyses.—RAxML version 8.2.3 (Stamatakis 2014) was used to run maximum likelihood (ML) analyses on an all-inclusive COI dataset through the CIPRES Science Gateway (Miller et al. 2010), as well as run ML analyses on the other individual genes and concatenated datasets for both Chthonioidea and Olpiidae (i.e., seven ML analyses in total; see Results, below). All ML analyses used the GTRGAMMA model with rapid bootstrapping (1000), specifying the random seed 555, and specifying the best partitioning scheme as identified by PartitionFinder (*raxmlHPC-HYBRID -T 4 -f a -n [alignment.file] -s [infile.txt] -N 1000 -p 555 –q [partition.file.txt] -m GTRGAMMA -x 555*).

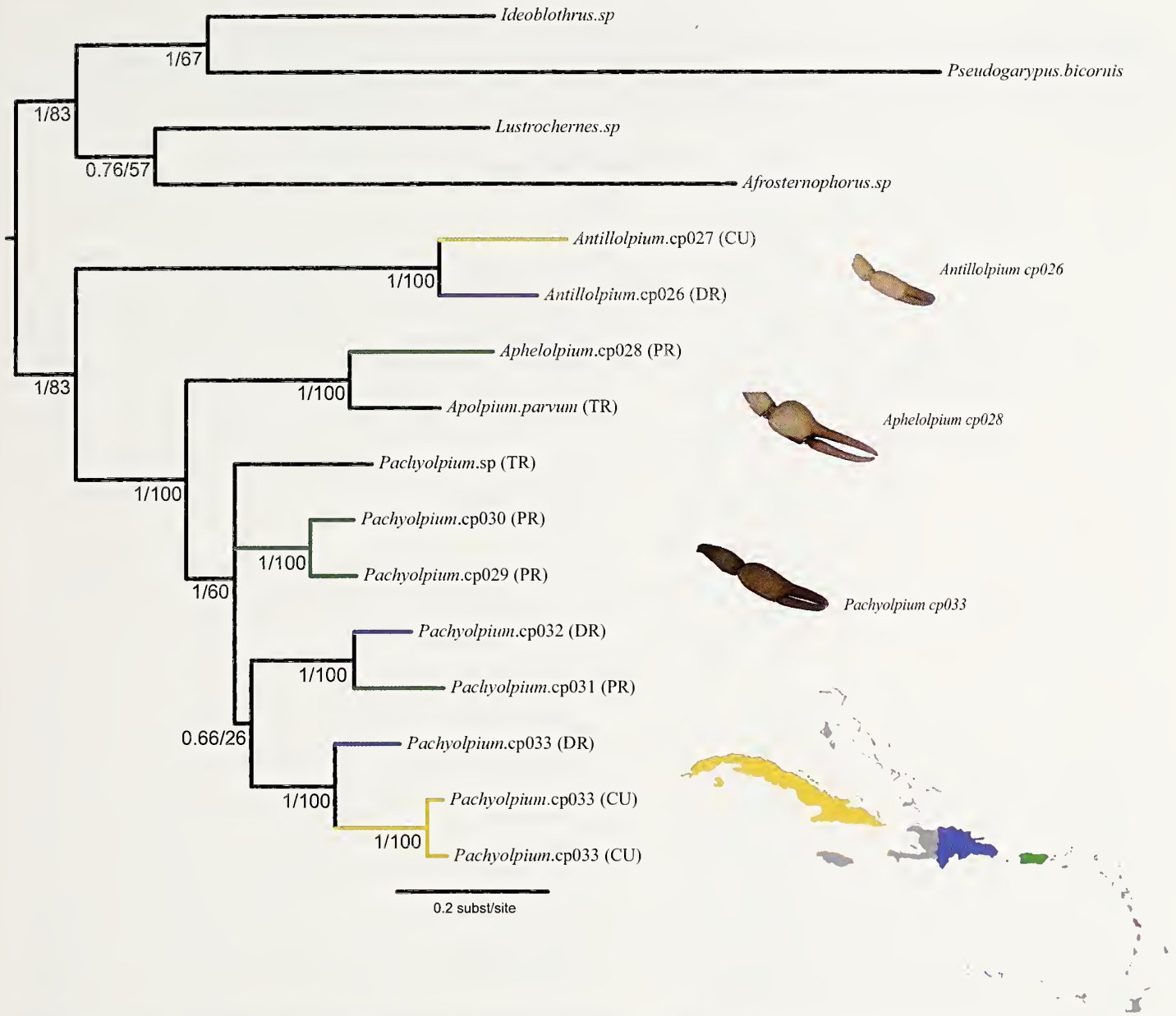

Figure 5.—Bayesian majority rule consensus tree of the concatenated matrix including COI, 28S, and H3 sequence data for Olpiidae species and putative species. Posterior probabilities and bootstrap values are printed at each node for those nodes recovered by both MrBayes and RAxML (posterior probability/bootstrap value), and nodes recovered only in the Bayesian analysis are labeled with a single posterior probability value. Branches are colored by island and correspond to the colors on the map insert. CU = Cuba; DR = Dominican Republic; MQ = Martinique; PR = Puerto Rico; TR = Trinidad.

Bayesian analyses were also run for the same seven datasets through the CIPRES Science Gateway (i.e., an all-inclusive COI dataset, as well as each individual gene matrix and the concatenated data sets for both Chthonioidea and Olpiidae) using MrBayes 3.2.1 (Huelsenbeck & Ronquist 2001). Evolutionary models selected using the Akaike Information Criterion (AIC) and Bayesian Information Criterion (BIC) in jModelTest 2.1.7 v 20141120 (Darriba et al. 2012) were applied to the individual gene Bayesian analyses, and models selected using PartitionFinder were applied to each partition in the concatenated datasets. MrBayes was used to run two Markov chain Monte Carlo (MCMC) analyses of four chains each for 10 million generations (mcmc ngen = 10000000 nchains = 4 nruns = 2 temp = 0.1 samplefreq = 1000). The two independent MCMC runs were considered converged if the average standard deviation of split frequencies was ≤ 0.01, chain stationarity and mixing was confirmed in Tracer v1.6 (Rambaut & Drummond 2007), and a strong correlation between split frequencies in each run was confirmed using the AWTY online "compare" tool (Nylander et al. 2008). After discarding burn-in replicates, the remaining sampled trees were used to build a 50% majority-rule consensus tree, where the frequency of the nodes was represented by clade posterior probabilities.

The all-inclusive COI dataset with both chthonioids and olpiids was rooted with three pseudoscorpions belonging to

Table 4.—Distribution of Chthonioidea and Olpiidae in the Caribbean (Harvey 2013). First time records presented in this study are in boldface text.

	Genus	*Species*	Caribbean Distribution
Chthonioidea	*Aphrastochthonius*	*cubanus*	Cuba
	Caribchthonius	*butleri*	U.S. Virgin Islands
	Chthonius	*tetrachelatus*	Cuba
	Lagynochthonius	*callidus*	Jamaica
		cavicola	Jamaica
		inuoxius	Jamaica
		proximus	Dominican Republic, Jamaica
		typhlus	Jamaica
		dominicanus	Dominican Republic
			Martinique, Puerto Rico
	Paraliochthonius	*carpenteri*	The Bahamas
		insulae	Jamaica
		puertoricensis	Puerto Rico
	Pseudochthonius	*arubensis*	Aruba
		clarus	Jamaica
		doctus	Jamaica
		heterodentatus	Trinidad and Tobago
		insularis	St Vincent and the Grenadines
		inundanus	Jamaica
		thibaudi	Guadeloupe
			Isla Mona, Martinique, Cuba, Dominican Republic
	Tyrannochthonius	*bahamensis*	The Bahamas
		curazavius	Curaçao
		guadeloupensis	Guadeloupe
		hoffi	Jamaica
		inititatus	Dominican Republic, Jamaica
		insulae	Trinidad and Tobago
		ovatus	Martinique
			Cuba, Puerto Rico, Isla Mona
	Lechytia	*chthoniiformis*	Jamaica
		delamarei	Guadeloupe
		martiniquensis	Martinique
		trinitatis	Dominican Republic, Trinidad and Tobago
	Tridenchthonius	*cubanus*	Cuba, Jamaica
		donaldi	Trinidad and Tobago
		gratus	Jamaica
		mexicanus	Trinidad and Tobago
		trinidadensis	Trinidad and Tobago
Olpiidae	*Aphelolpium*	*brachytarsus*	Aruba
		longidigitatum	Cayman Islands, Puerto Rico, U.S. Virgin Islands, Venezuela
		scitulum	Jamaica, Aruba, Bonaire, Curaçao
		thibaudi	Guadeloupe, Martinique
	Apolpium	*parvum*	Trinidad and Tobago
	Planctolpium	*arboreum*	Dominican Republic, Jamaica, Mexico
	Antillolpium	*cubanum*	Cuba
		hummelincki	Cayman Islands
			Dominican Republic
	Hoffhorus	*cinereus*	Trinidad and Tobago
	Leptolpium	*prospaeum*	Aruba, Bonaire, Curaçao
	Neopachyolpium	*longum*	Trinidad and Tobago
	Novohorus	*incertus*	Anguilla, St Martin, Puerto Rico, U.K. Virgin Islands, U.S. Virgin Islands,
		suffuscus	Jamaica, Mona, Puerto Rico
			Dominican Republic
	Olpiolum	*amphum*	Jamaica
		aureum	Mona, Puerto Rico
		confundens	Puerto Rico
		puertoricense	Puerto Rico
	Pachyolpium	*arubense*	Aruba, Bonaire, Curaçao, Klein Curaçao
		brevifemoratum	U.K. Virgin Islands
		brevipes	Martinique, St Vincent and the Grenadines
		confusum	St Eustatius

Table 4.—Continued.

Genus	*Species*	Caribbean Distribution
	furculiferum	Cayman Islands, St Vincent and the Grenadines, U.S. Virgin Islands, Venezuela
	isolatum	Jamaica, Panama
	medium	Dominican Republic, Jamaica, Puerto Rico, Florida
		Cuba

the superfamily Feaelloidea: *Feaella anderseni* Harvey, 1989, *Pseudogarypus bicornis* (Banks, 1895) and *Neopseudogarypus scutellatus* (Morris, 1948) (see Table 3 for GenBank accession numbers). The Feaelloidea are a basal group within Pseudoscorpiones consistently recovered as monophyletic (Harvey 1992; Murienne et al. 2008). The Chthonioidea and Olpiidae datasets (each with a concatenated matrix and two individual gene matrices for 28S and H3) were rooted with four pseudoscorpions belonging to four different superfamilies: *P. bicornis* (Feaelloidea), *Afrosternophorus* sp. (Sternophoroidea), *Lustrochernes* sp. (Cheliferoidea), and *Ideoblothrus* sp. (Neobisioidea).

Identifying putative species.—We used the Bayesian implementation of the Poisson tree processes model (bPTP) (http://www.exelixis-lab.org/, default parameters) to estimate the number of distinct species in our dataset including identical sequences that were removed for concatenation (Zhang et al. 2013). As this method tends to overestimate species richness when the numbers of individuals per haplotype are uneven (Zhang et al. 2013), and this was true for our dataset, we chose to use raw COI distances to identify putative species. Terminal taxa in the concatenated analyses that exhibited more than 10% divergence (uncorrected *p*-distances, COI) were defined as putative species and given a unique five-digit name beginning with *cp* (Caribbean pseudoscorpion), followed by three integers (001–033) assigned in order of morphological examination. We recognize that >10% COI divergence is neither a strict nor all-encompassing species-delimiting threshold, as Young & Hebert (2015) found that the average COI BIN (species proxy) distance within pseudoscorpion families is 0.190 (Demetras 2010), and up to 13.8% divergence has been observed between populations of the Neotropical pseudoscorpion species *Cordylochernes scorpioides* Linnaeus, 1758 (Wilcox et al. 1997), and up to 20% divergence between conspecifics of other arachnid lineages (Boyer et al. 2007; Fernández & Giribet 2014; Esposito et al. 2015). However, our main goal was not to define species within this subsample of Caribbean pseudoscorpions, but to assess the distribution of our focal lineages.

RESULTS

After alignment and selection of conserved blocks our final matrices were structured as follows: COI Chthonioidea + Olpiidae (taxa = 110, sites = 647 [95% of original alignment]); 28S Chthonioidea (taxa = 35, sites = 926 [81% of original alignment]); 28S Olpiidae (taxa = 13, sites = 1051 [90% of original alignment]); H3 Chthonioidea (taxa = 32, sites = 287 [100% of original alignment]); H3 Olpiidae (taxa = 10, sites = 375 [98% of original alignment]); concatenation Chthonioidea (taxa = 36, sites = 1915); concatenation Olpiidae (taxa = 16, sites = 2079).

The best fitting evolutionary models identified for our individual gene data sets were as follow: Chthonioidea + Olpiidae COI (GTR + G + I); Chthonioidea & Olpiidae 28S (GTR + G + I); Chthonioidea H3 (SYM + G); Olpiidae H3 (K80 + G). The best partitioning scheme identified for the concatenated Chthonioidea dataset included three subsets: [(COI_codon1, COI_codon3), (COI_codon2, H3_codon1, H3_codon2), (28S, H3_codon3)], for which the best-fit evolutionary models were identified as GTR+I+G, SYM+I+G and GTR+I+G, respectively. The best partitioning scheme identified for the concatenated Olpiidae dataset included seven subsets, one for each codon position in COI and H3 and one for 28S. The best-fit evolutionary models identified for these subsets were: COI_codon1 (GTR+I+G); COI_codon2 (F81+G); COI_codon3 (HKY+I+G); 28S (GTR+I+G); H3_codon1 (SYM); H3_codon2 (JC); and H3_codon3 (K80+I).

Phylogenetic analyses.—Convergence between runs was supported for each of our Bayesian analyses as defined by an average standard deviation of split frequencies ≤ 0.01, stationarity and mixing visualized in Tracer v1.6, and a strong correlation observed between run split frequencies using AWTY. Stationarity was achieved by one million generations (1000 sampled trees) in each of our analyses, so we used burn-in values of 1000 (10%) to summarize statistics in MrBayes.

Gene tree topologies differed slightly between the two phylogenetic methods. Both ML and Bayesian inference using our COI dataset recovered Chthonioidea and Olpiidae as monophyletic (posterior probability = 1, bootstrap value = 92), however our ML analysis only recovered six of nine genera as monophyletic while Bayesian inference recovered seven of nine. Both methods yielded identical topologies for our 28S matrices and the Chthonioidea H3 matrix, but ML analysis of our olpiid H3 matrix recovered *Apheloipinm* Hoff, 1964 nested within the *Pachyolpium* Beier, 1931 clade while Bayesian inference recovered *Apheloipinm* as sister to the *Pachyolpium* clade. Between methods, the topologies inferred from our concatenated datasets were identical for Olpiidae and nearly identical for Chthonioidea. Trees shown here are Bayesian majority rule consensus trees (Figs. 3–5). The three differences observed within Chthonioidea occurred at the putative species level within poorly resolved clades (see Figs. 4, 5).

Chthonioidea.—Our concatenated molecular phylogenetic analysis included 32 genetically distinct terminal taxa in the superfamily Chthonioidea, representing four genera: *Lechytia* Balzan, 1892, *Pseudochthonius* Balzan, 1892, *Tyrannochthonius* Chamberlin, 1929 and *Lagynochthonius* Beier, 1951 (Fig. 4).

Table 5.—Raw COI p-distances between putative *Pseudochthonius* species (*P.*), putative *Tyrannochthonius* and *Lagynochthonius* (*T.* and *L.*), and putative Olpiidae species.

	P. cp003 (MQ)	*P. cp003* (MQ)	*P. cp004* (CU)	*P. cp001* (CU)	*P. cp001* (DR)	*P. cp001* (DR)	*P. cp001* (DR)	*P. cp001* (DR)
P. cp003 (MQ)	-							
P. cp003 (MQ)	0.094	-						
P. cp004 (CU)	0.136	0.116	-					
P. cp001 (CU)	0.114	0.118	0.101	-				
P. cp001 (DR)	0.132	0.123	0.114	0.092	-			
P. cp001 (DR)	0.116	0.127	0.116	0.107	0.118	-		
P. cp001 (DR)	0.112	0.114	0.119	0.09	0.092	0.078	-	
P. cp001 (DR)	0.112	0.121	0.128	0.09	0.103	0.099	0.058	-
P. cp002 (MONA)	0.134	0.152	0.121	0.11	0.137	0.128	0.132	0.141

	T. cp021 (CU)	*T. cp011* (CU)	*T. cp010* (CU)	*T. cp017* (CU)	*T. cp018* (CU)	*T. cp019* (CU)	*T. cp020* (CU)	*T. cp016* (CU)
T. cp021 (CU)	-							
T. cp011 (CU)	0.172	-						
T. cp010 (CU)	0.195	0.110	-					
T. cp017 (CU)	0.172	0.174	0.175	-				
T. cp018 (CU)	0.157	0.161	0.179	0.137	-			
T. cp019 (CU)	0.154	0.146	0.179	0.168	0.139	-		
T. cp020 (CU)	0.159	0.146	0.174	0.139	0.157	0.134	-	
T. cp016 (CU)	0.161	0.166	0.179	0.145	0.136	0.152	0.152	-
T. cp015 (DR)	0.163	0.161	0.192	0.166	0.175	0.179	0.156	0.163
T. cp014 (DR)	0.165	0.157	0.165	0.175	0.159	0.177	0.157	0.163
T. cp013 (CU)	0.17	0.165	0.179	0.186	0.163	0.172	0.154	0.154
T. cp009 (CU)	0.177	0.166	0.204	0.163	0.170	0.165	0.163	0.179
T. cp022 (MONA)	0.163	0.165	0.179	0.175	0.172	0.161	0.152	0.179
T. cp024 (PR)	0.17	0.163	0.192	0.175	0.165	0.177	0.165	0.179
T. cp023 (PR)	0.165	0.179	0.186	0.184	0.177	0.177	0.181	0.177
T. cp012 (CU)	0.19	0.192	0.195	0.163	0.168	0.184	0.166	0.188
T. cp008 (CU)	0.174	0.172	0.165	0.172	0.172	0.165	0.159	0.184
L. cp005 (PR)	0.186	0.190	0.193	0.195	0.199	0.193	0.166	0.199
L. cp007 (PR)	0.166	0.174	0.197	0.179	0.175	0.177	0.156	0.172
L. cp006 (PR)	0.179	0.197	0.206	0.201	0.204	0.188	0.188	0.157
L. proximus (MQ)	0.201	0.186	0.208	0.208	0.186	0.213	0.195	0.204
T. insulae (PR)	0.197	0.206	0.217	0.222	0.206	0.212	0.172	0.212

	Antillolpium cp026 (DR)	*Antillolpium cp027* (CU)	*Aphelolpium cp028* (PR)	*Apolpium parvum* (TR)	*Pachyolpium cp029* (PR)	*Pachyolpium cp030* (PR)	*Pachyolpium cp033* (CU)	*Pachyolpium cp033* (CU)
Antillolpium cp026 (DR)	-							
Antillolpium cp027 (CU)	0.203	-						
Aphelolpium cp028 (PR)	0.256	0.271	-					
Apolpium parvum (TR)	0.251	0.298	0.178	-				
Pachyolpium cp029 (PR)	0.241	0.256	0.216	0.218	-			
Pachyolpium cp030 (PR)	0.246	0.238	0.218	0.213	0.113	-		
Pachyolpium cp033 (CU)	0.223	0.258	0.203	0.208	0.160	0.170	-	
Pachyolpium cp033 (CU)	0.253	0.271	0.231	0.218	0.178	0.175	0.108	-
Pachyolpium cp033(DR)	0.241	0.263	0.223	0.221	0.163	0.165	0.090	0.065
Pachyolpium sp (TR)	0.258	0.271	0.231	0.211	0.173	0.170	0.175	0.168
Pachyolpium cp031 (PR)	0.283	0.296	0.253	0.258	0.228	0.221	0.198	0.203
Pachyolpium cp032 (DR)	0.248	0.296	0.251	0.231	0.201	0.203	0.198	0.213
Novohorus cp025 (MONA)	0.193	0.216	0.236	0.226	0.211	0.216	0.206	0.216
Novohorus suffuscus (DR)	0.208	0.233	0.208	0.251	0.213	0.213	0.193	0.195

Table 5.—Extended.

P. cp002 (MONA)	*T. cp015* (DR)	*T. cp014* (DR)	*T. cp013* (CU)	*T. cp009* (CU)	*T. cp022* (MONA)	*T. cp024* (PR)	*T. cp023* (PR)	*T. cp012* (CU)	*T. cp008* (CU)	*L. cp005* (PR)	*L. cp007* (PR)	*L. cp006* (PR)	*L. proximus* (MQ)	*T. insulae* (PR)	*Pachyolpium cp033* (DR)	*Pachyolpium* sp (TR)	*Pachyolpium cp031* (PR)	*Pachyolpium cp032* (DR)	*Novohorus cp025* (MONA)	*Novohorus suffuscus* (DR)
-																				
0.146	-																			
0.154	0.159	-																		
0.165	0.174	0.170	-																	
0.168	0.190	0.168	0.184	-																
0.168	0.166	0.192	0.183	0.134	-															
0.159	0.193	0.199	0.208	0.136	0.141	-														
0.192	0.192	0.184	0.188	0.159	0.181	0.150	-													
0.163	0.175	0.174	0.163	0.165	0.159	0.161	0.148	-												
0.184	0.203	0.193	0.201	0.166	0.177	0.201	0.212	0.193	-											
0.168	0.181	0.188	0.179	0.165	0.163	0.157	0.170	0.168	0.141	-										
0.183	0.186	0.190	0.197	0.190	0.188	0.197	0.197	0.206	0.172	0.125	-									
0.206	0.193	0.208	0.230	0.192	0.188	0.199	0.166	0.192	0.206	0.195	0.213	-								
0.188	0.208	0.213	0.201	0.172	0.201	0.186	0.186	0.174	0.184	0.170	0.192	0.199	-							
															-					
															0.175	-				
															0.188	0.195	-			
															0.193	0.190	0.208	-		
															0.211	0.233	0.273	0.246	-	
															0.198	0.216	0.256	0.253	0.148	-

Three of these taxa were described species that had previously been documented in the Caribbean region: *Lechytia sini* Muchmore, 1975, *Lagynochthonius proximus* (Hoff, 1959) and *Tyrannochthonius insulae* (Hoff, 1946), while the remaining taxa represent 24 putative new species. The bPTP model estimated 38 distinct species from the same dataset. These include the first *Pseudochthonius* species recorded from Isla Mona, Martinique, Cuba, and the Dominican Republic (except for extinct *Pseudochthonius squamosus* Schawaller, 1980 found in Dominican Amber), the first *Tyrannochthonius* species from Isla Mona and Cuba, and the first *Lagynochthonius* species from Puerto Rico and Martinique (Table 4).

The smallest raw COI *p*-distance between putative *Pseudochthonius* species was 0.101 and between *Tyrannochthonius* and *Lagynochthonius* species 0.110 (Table 5). Within the superfamily, *Tyrannochthonius* + *Lagynochthonius* formed a monophyletic group as did *Pseudochthonius* and *Lechytia* (Fig. 4). Within the *Pseudochthonius* clade, each individual island was monophyletic (Fig. 4), although relationships among islands were not resolved. Within the *Tyrannochthonius* + *Lagynochthonius* clade, individuals from Dominican Republic and Puerto Rico/Mona Island were monophyletic and individuals from Cuba were polyphyletic, due to a single rogue taxon (Fig. 4).

Olpiidae.—Our concatenated molecular phylogenetic analysis included 12 genetically distinct terminal taxa representing four genera: *Antillolpium* Muchmore, 1991, *Aphelolpium*, *Apolpium* Chamberlin, 1930, and *Pachyolpium*. One of these taxa was a previously described species: *Apolpium parvum* Hoff, 1945 from Trinidad (sequence data from Murienne et al. 2008), another was an undescribed species also from Trinidad: *Pachyolpium* sp. (sequence data from Murienne et al. 2008), and the remaining 10 taxa represent eight putative new species. The bPTP model estimated 15 distinct species from the same dataset. The Olpiidae specimens include the first records of *Antillolpium* from the Dominican Republic and the first *Pachyolpium* species from Cuba (Table 4). Additionally, our samples also contained the first records of the olpiid genus *Novohorus* Hoff, 1945 from the Dominican Republic, however these specimens did not yield sufficient molecular data to be included in the concatenated dataset. The smallest raw COI *p*-distance between putative *Pachyolpium* species was 0.113 (Table 5). The genus *Pachyolpium* formed a monophyletic group, and within this clade individual specimens from Cuba and Trinidad were monophyletic; individuals from Puerto Rico and Dominican Republic were polyphyletic (Fig. 5). The other olpiid genera are not discussed due to small sample sizes.

DISCUSSION

Our initial assessment of pseudoscorpion diversity in the Caribbean has focused on only a fraction of the order: nine of 47 known genera, and only seven of the 41 known species within those genera (Harvey 2013). We found 32 genetically distinct taxa that are also morphologically distinct from currently described Caribbean species and warrant closer taxonomic assessment (Figs. 3–5). We also documented first time island records of six genera: *Pseudochthonius, Lagynochthonius, Tyrannochthonius, Antillolpium, Novohorus* and *Pachyolpium* (Table 4). While geographic coverage is not dense within any genus, this sampling allows for a preliminary assessment of island-level monophyly for a few genera.

Chthonioidea.—Relationships among Caribbean chthonioid genera in our analyses are consistent with previous systematic hypotheses (Murienne et al. 2008). In an order-wide molecular phylogeny, *Pseudochthonius* and *Lechytia* formed part of a larger clade that also included *Anaulacodithella* Beier, 1944 and *Sathrochthonius* Chamberlin, 1962, both of which are temperate Gondwanan groups (Murienne et al. 2008). The genera *Tyrannochthonius* and *Lagynochthonius* were also found to be closely related (Murienne et al. 2008). The *Lechytia* + *Pseudochthonius* clade inferred in the current study contains *Lechytia sini* from the Dominican Republic, which is sister to four putative *Pseudochthonius* species (Fig. 4). While we only have at most four terminal taxa on any particular island, the *Pseudochthonius* putative species groups form island clades (Fig. 4). This geographic structure is consistent with low expected dispersal within the group, and suggests that the biogeographic history of *Pseudochthonius* species in the Caribbean may reflect geological events.

The *Tyrannochthonius* + *Lagynochthonius* clade is the most diverse in our analysis, with 22 species including 20 putative new species and raw *p*-distances ranging from 0.110 to 0.230 (Table 5). It is most likely that this group represents one or a few undescribed species complexes, as 10% divergence in COI exceeds typical, though arbitrary, species delimitation thresholds. This clade also contains two notable within-island radiations: six putative *Tyrannochthonius* + *Lagynochthonius* species on Puerto Rico, and 12 putative *Tyrannochthonius* species on Cuba (Fig. 4), where this genus has not been previously documented. Further morphological and molecular analyses will be necessary to determine the taxonomic status of these putative species, however after examination of diagnostic characters, we are confident that they do not fit any published species description.

Tyrannochthonius and *Lagynochthonius* species are nested in one clade with no clear genetic distinction, which is consistent with the historic paraphyly of these groups [*Lagynochthonius* was considered a subgenus of *Tyrannochthonius* until 1962 (Chamberlin 1962), and the taxonomic status of this group is still debated], and with the results of a study on Australian members of these genera (Harrison et al. 2014). Despite this paraphyly, the geographic structure of this group is still notable. This structure, as well as previous work showing that hypogean *Tyrannochthonius* and *Lagynochthonius* species in Western Australia are SREs (Edward & Harvey 2008; Harrison et al. 2014), calls for thorough biogeographical analysis of these groups in the Caribbean region.

Within our chthonioid dataset the total number of putative species is highest on Cuba (14), which is consistent with the species-area relationship discussed by MacArthur & Wilson (1967), however only four putative species were found on Hispaniola while six were found on Puerto Rico. This could be an artifact of Hispaniola only being represented by the Dominican Republic in our study. When our putative species are added to the currently described species lists for these three islands, diversity is consistent with species-area relationships (Cuba: 17; Hispaniola: 8; Puerto Rico: 9).

Olpiidae.—Our molecular phylogenetic analysis of Caribbean olpiids is consistent with current taxonomic rankings, as

each currently described genus forms a monophyletic group. The subfamily Hesperolpiinae is represented by two genera, *Aphelolpium* and *Apolpium*, which form a clade nested within the rest of the olpiids belonging to the subfamily Olpiinae: *Antillolpium* and *Pachyolpium* (Fig. 5). The relationship between these two subfamilies remains unclear, and a thorough molecular and morphological analysis will be necessary to resolve the Olpiidae phylogeny.

Polyphyletic island groups within the genus *Pachyolpium* indicate multiple dispersal events (Fig. 5), although this genus is not strongly supported in our ML concatenated dataset (posterior probability = 1, bootstrap value = 60). In our COI analysis, *Pachyolpium* has higher bootstrap support (posterior probability = 0.98, bootstrap value = 66, Fig. 3), but more thorough sampling will be necessary to infer the true biogeographic history of olpiids in the Caribbean. Should further biogeographic analyses find patterns consistent with olpiids dispersing between islands more frequently than expected for a non-phoretic lineage and thus more frequently than chthonioids, we propose two hypotheses: (1) that olpiids are typically found in more xeric environments than chthonioids, and (2) may therefore be better suited to colonizing drier, coastal environments after an initial dispersal event (Wilson 1959; Judson 2003). Although the 'predation hypothesis' which states that phoresy in pseudoscorpions is a byproduct of predation (Vachon 1940, 1954; Muchmore 1971) was rejected by Zeh & Zeh (1992), it is possible that the pedipalp morphology of venomous pseudoscorpions (including Olpiidae) is more conducive to latching onto a larger, flying arthropod than that of the non-venomous pseudoscorpions (including Chthonioidea), which tend to have longer, more slender palpal fingers (see Figs. 2, 4, 5).

Within the olpiids, the number of putative species is highest on Puerto Rico (4), followed by Hispaniola (3), and Cuba (2). This trend is upheld when previously described olpiid species are also added to the list: Puerto Rico: 11; Hispaniola: 5; Cuba: 3. As the classic species-area relationship has been suggested to be driven primarily by *in situ* diversification (Losos & Parent 2010), the opposite pattern observed in olpiids is consistent with dispersal playing a dominant role in shaping their diversity in the Caribbean.

In conclusion, this study suggests that there is a great wealth of undocumented pseudoscorpion diversity in the Caribbean. A more thorough sampling and morphological assessment will elucidate how many new species and/or species complexes these genetically distinct taxa represent. Species of *Tyrannochthonius*, *Lagynochthonius* and *Pseudochthonius* form island specific clades, suggesting that they may be short-range endemics and thus highly informative to biogeographers and conservation biologists. Species of *Pachyolpium* form polyphyletic island groups, suggesting that they have likely dispersed between islands multiple times. More sampling within genera across the Caribbean and from adjacent continents will allow us to infer the directionality of dispersal and time-calibrate these phylogenies, empirically testing the biogeographical hypotheses inspired by the present data. There is a great need for integrated taxonomic research on these lineages in order to understand more deeply their diversity, distributions, evolutionary histories and taxonomy.

ACKNOWLEDGMENTS

We are grateful to the entire CarBio team (see islandbiogeography.org) for collecting the specimens analyzed in this study, in particular to those who participated in expeditions to Puerto Rico (2011), the Dominican Republic (2012), Cuba (2012), and the Lesser Antilles (2013). Many collaborators helped to obtain permits including Alexander Sánchez (Cuba), Lauren Esposito, Gabriel de los Santos, Solanlly Carrero, and Kelvin Guerrero (Dominican Republic) and Lauren Esposito (Lesser Antilles). Many collaborators participated in field work including Nadine Dupérré, Carlos Víquez, Abel Pérez González, Giraldo Alayón, Franklyn Cala-Riquelme, Aylin Alegre, Hanna Madden, Rodrigo Monjaraz, Bernhard Huber, Matjaž Kuntner, and many more. Members of the Agnarsson and the Binford labs were also instrumental in organizing and executing fieldwork, including Anne McHugh, Zamira Yusseff-Vanegas, Gigi Veve, Lisa Chamberland, Federico Lopez-Osorio, Carol Yablonsky, Sarah Kechejian, Laura Caicedo-Quiroga, Jose Sanchez, Angela Alicea, Trevor Bloom, Ian Petersen, Alex Nishida, Katy Loubet-Senear, Ian Voorhees, Angela Chuang, Micah Machina and many more. The Terrestrial Zoology department at the Western Australian Museum provided space and resources for morphological analysis. Dr. Pamela Zobel-Thropp made the presented molecular analyses possible by providing JC with all necessary lab training. This project was funded by NSF DEB-1050187, 1050253, 1314749 to Ingi Agnarsson and Greta J. Binford and the Lewis & Clark College Miller Internship Award to Julia G. Cosgrove. We would also like to thank Gonzalo Giribet, referees Sarah Crews and Prashant Sharma, and editor Michael Rix for reviewing this manuscript.

LITERATURE CITED

Agnarsson, I., R. Cheng & M. Kuntner. 2014. A multi-clade test supports the intermediate dispersal model of biogeography. PloS ONE 9:e86780.

Aide, T.M., M.L. Clark, H.R. Grau, D. López-Carr, M.A. Levy, D. Redo et al. 2013. Deforestation and reforestation of Latin America and the Caribbean (2001–2010). Biotropica 45:262–271.

Alonso, R., A.J. Crawford & E. Bermingham. 2012. Molecular phylogeny of an endemic radiation of Cuban toads (Bufonidae: *Peltophryne*) based on mitochondrial and nuclear genes. Journal of Biogeography 39:434–451.

Boyer, S.L., J.M. Baker & G. Giribet. 2007. Deep genetic divergences in *Aoraki denticulata* (Arachnida, Opiliones, Cyphophthalmi): a widespread 'mite harvestman' defies DNA taxonomy. Molecular Ecology 16:4999–5016.

Castresana, J. 2000. Selection of conserved blocks from multiple alignments for their use in phylogenetic analysis. Molecular Biology and Evolution 17:540–552.

Chamberlin, J.C. 1931. The arachnid order Chelonethida. Stanford University Publications, Biological Sciences 7:11–284.

Chamberlin, J.C. 1962. New and little-known false scorpions, principally from caves, belonging to the families Chthoniidae and Neobisiidae Arachnida, Chelonethida. Bulletin of the American Museum of Natural History 123:303–352.

Claramunt, S., E. Derryberry, J. Remsen & R. Brumfield. 2012. High dispersal ability inhibits speciation in a continental radiation of

passerine birds. Proceedings of the Royal Society of London Series B, Biological Sciences 279:1567–1574.

Colgan, D.J., W.F. Ponder & P.E. Eggler. 2000. Gastropod evolutionary rates and phylogenetic relationships assessed using partial 28S rDNA and histone H3 sequences. Zoologica Scripta 29:29–63.

Crews, S.C. & R.G. Gillespie. 2010. Molecular systematics of *Selenops* spiders (Araneae: Selenopidae) from North and Central America: implications for Caribbean biogeography. Biological Journal of the Linnean Society 101:288–322.

Darriba D., G.L. Taboada, R. Doallo & D. Posada. 2012. jModelTest 2: more models, new heuristics and parallel computing. Nature Methods 9:772.

Demetras, N.J., I.D. Hogg, J.C. Banks & B.J. Adams. 2010. Latitudinal distribution and mitochondrial DNA COI variability of *Stereotydeus* spp. (Acari: Prostigmata) in Victoria Land and the central Transantarctic Mountains. Antarctic Science 22:749–756.

Dziki, A., G.J. Binford, J.A. Coddington & I. Agnarsson. 2015. *Spintharus flavidus* in the Caribbean—a 30 million year biogeographical history and radiation of a 'widespread species'. PeerJ 3:e1422; DOI 10.7717/peerj.1422.

Edward, K.L. & M.S. Harvey. 2008. Short-range endemism in hypogean environments: the pseudoscorpion genera *Tyrannochthonius* and *Lagynochthonius* (Pseudoscorpiones: Chthoniidae) in the semiarid zone of Western Australia. Invertebrate Systematics 22:259–293.

Esposito, L.A., T. Bloom, L. Caicedo-Quiroga, A.M. Alicea-Serrano, J.A. Sánchez-Ruíz, L.J. May-Collado et al. 2015. Islands within islands: diversification of tailless whip spiders (Amblypygi, *Phrynus*) in Caribbean caves. Molecular Phylogenetics and Evolution 93:107–117.

Fernández, R. & G. Giribet. 2014. Phylogeography and species delimitation in the New Zealand endemic, genetically hypervariable harvestman species, *Aoraki denticulata* (Araehnida, Opiliones, Cyphophthalmi). Invertebrate Systematics 28:401–414.

Gabbutt, P.D. 1970. Sampling problems and the validity of life history analyses of pseudoscorpions. Journal of Natural History 4:1–15.

Gillespie, R.G. 2013. Biogeography: from testing patterns to understanding processes in spiders and related arachnids. Pp. 154–185. *In* Spider Research in the 21st Century: Trends & Perspectives. (D. Penney, ed.). Siri Scientific Press, Manchester.

Harrison, S.E., M.T. Guzik, M.S. Harvey & A.D. Austin. 2014. Molecular phylogenetic analysis of Western Australian troglobitic chthoniid pseudoscorpions (Pseudoscorpiones: Chthoniidae) points to multiple independent subterranean clades. Invertebrate Systematics 28:386–400.

Harvey, M.S. 1992. The phylogeny and classification of the Pseudoscorpionida (Chelicerata: Arachnida). Invertebrate Systematics 6:1373–1435.

Harvey, M.S. 2002. Short-range endemism in the Australian fauna: some examples from non-marine environments. Invertebrate Systematics 16:555–570.

Harvey, M.S. 2013. Pseudoscorpions of the World, version 3.0. Accessed July 2013. Western Australian Museum, Perth. Online at http://www.museum.wa.gov.au/catalogues/pseudoscorpions

Huelsenbeek, J.P. & F.R. Ronquist. 2001. MrBayes: Bayesian inference of phylogeny. Biometrics 17:754–755.

Iturralde-Vinent, M.A. 2006. Meso-Cenozoic Caribbean paleogeography: implications for the historical biogeography of the region. International Geology Review 48:791–827.

Judson, M.L.I. 1998. A sternophorid pseudoscorpion (Chelonethi) in Dominican Amber, with remarks on the family. Journal of Arachnology 26:419–428.

Judson, M.L.I. 2003. Baltic amber fossil of *Garypinus electri* Beier provides first evidence of phoresy in the pseudoscorpion family Garypinidae (Arachnida: Chelonethi). Proceedings of the 21st European Colloquium of Arachnology, St.-Petersburg:127–131.

Judson, M.L.I. 2012. Reinterpretation of *Dracochela deprehendor* (Arachnida: Pseudoscorpiones) as a stem-group pseudoscorpion. Palaeontology 55:261–283.

Katoh, S. 2013. MAFFT multiple sequence alignment software version 7: improvements in performance and usability. Molecular Biology and Evolution 30:772–780.

Kearse, M., R. Moir, A. Wilson, S. Stones-Havas, M. Cheung, S. Sturrock et al. 2012. Geneious Basic: an integrated and extendable desktop software platform for the organization and analysis of sequence data. Bioinformatics 28:1647–1649.

Lanfear, R., B. Calcott, S.Y.W. Ho, S. Guindon. 2012. PartitionFinder: combined selection of partitioning schemes and substitution models for phylogenetic analyses. Molecular Biology and Evolution 29:1695–1701.Online at http://dx.doi.org/10.1093/molbev/mss020

Lomolino, M. 2010. Biogeography 4th Edition. Sinauer Associates, Sunderland, Massachusetts.

Losos, J.B. 1996. Ecological and evolutionary determinants of the species-area relation in Caribbean anoline lizards. Philosophical Transactions of the Royal Society B 351:847–854.

Losos, J.B. & C.E Parent. 2010. The speciation-area relationship. Pp. 415–438. *In* The Theory of Island Biogeography Revisited. (J.B. Losos & R.E. Ricklefs, eds.). Princeton University Press, Princeton.

MacArthur, R.H & E.O. Wilson. 1967. The Theory of Island Biogeography. Princeton University Press, Princeton.

Maddison, W.P. & D.R. Maddison. 2011. Mesquite: a modular system for evolutionary analysis. Version 2.75. Online at http://mesquiteproject.org

McHugh, A., C. Yablonsky, G. Binford & I. Agnarsson. 2014. Molecular phylogenetics of Caribbean *Micrathena* (Araneae: Araneidae) suggests multiple colonisation events and single island endemism. Invertebrate Systematics 28:337–349.

Miller, M.A., W. Pfeiffer & T. Schwartz. 2010. Creating the CIPRES Science Gateway for inference of large phylogenetic trees. Proceedings of the Gateway Computing Environments Workshop (GCE), 14 Nov. 2010, New Orleans 1–8.

Muchmore, W.B. 1971. Phoresy by North and Central American pseudoscorpions. Proceedings of the Rochester Academy of Science 12:79–97.

Muchmore, W.B. 1990. Pseudoscorpionida. Pp 503–527. *In* Soil Biology Guide. (D.L. Dindal, ed.). John Wiley & Sons, New York.

Murienne, J., M.S. Harvey & G. Giribet. 2008. First molecular phylogeny of the major clades of Pseudoscorpiones (Arthropoda: Chelicerata). Molecular Phylogenetics and Evolution 49:170–184.

Myers, N., R.A. Mittermeier, C.G. Mittermeier, G.A. Da Fonseca & J. Kent. 2000. Biodiversity hotspots for conservation priorities. Nature 403:853–858.

Nylander, J.A.A., J.C. Wilgenbusch, D.L. Warren & D.L. Swofford. 2008. AWTY (are we there yet?): a system for graphical exploration of MCMC convergence in Bayesian phylogenetics. Bioinformatics 24:581–583.

Pindell, J.L. & S.F. Barrett. 1990. Geological evolution of the Caribbean region: a plate-tectonic perspective. Pp 405–432. *In* The Caribbean Region. (G. Dengo, J.E. Case, eds.). Geological Society of America, Boulder, Colorado.

Poinar, G.O., Jr., B.P.M. Curcic & J.C. Cokendolpher. 1998. Arthropod phoresy involving pseudoscorpions in the past and present. Acta Arachnologica 47:79–96.

Rambaut, A. & A.J. Drummond. 2007. Tracer v1.6. Online at http://beast.bio.ed.ac.uk/Tracer

Ricklefs, R. & E. Bermingham. 2008. The West Indies as a laboratory of biogeography and evolution. Philosophical Transactions: Biological Sciences 363:2393–2413.

Schawaller, W., W.A. Shear & P.M. Bonamo. 1991. The first Paleozoic pseudoscorpions (Arachnida, Pseudoscorpionida). American Museum Novitates 3009:1–24.

Shultz, J.W. 2007. A phylogenetic analysis of the arachnid orders based on morphological characters. Zoological Journal of the Linnean Society 150:221–265.

Smithsonian Institution. 2013. DNA Barcoding Resources. Online at http://www.mnh.si.edu/rc/lab/resources.html

Stamatakis, A. 2014. RAxML version 8: a tool for phylogenetic analysis and post-analysis of large phylogenies. Bioinformatics 30:1312–1313.

Vachon, M. 1940. Remarques sur la phorésie des Pseudoscorpions. Annales de la Sociéte entomologique de France 109:1–18.

Vachon, M. 1954. Nouvelles captures de Pseudoscorpions (Arachnides) tranportés par des insectes. Bulletin du Muséum National d'Histoire Naturelle, Paris 26:590–592.

Weygoldt, P. 1969. The Biology of Pseudoscorpions. Harvard University Press, Cambridge, Massachusetts.

Wilcox, T.P., L. Hugg, J.A. Zeh & D.W. Zeh. 1997. Mitochondrial DNA sequencing reveals extreme genetic differentiation in a cryptic species complex of neotropical pseudoscorpions. Molecular Phylogenetics and Evolution 7:208–216.

Wilson, E.O. 1959. Adaptive shift and dispersal in a tropical ant fauna. Evolution 13:122–144.

Wilson, E.O. 2010. Island biogeography in the 1960s. Pp. 1–12. *In* The Theory of Island Biogeography Revisited. (J.B. Losos & R.E. Ricklefs, eds.). Princeton University Press, Princeton.

Young, M. & P. Hebert. 2015. Patterns of protein evolution in cytochrome c oxidase 1 (COI) from the Class Arachnida. PloS ONE 10:e0135053.

Zeh, D.W. & J.A. Zeh. 1992. Failed predation or transportation? Causes and eonsequences of phoretic behavior in the pseudoscorpion *Dinocheirus arizonensis* (Pseudoscorpionida: Chernetidae). Journal of Insect Behavior 5:37–49.

Zeh, J.A., D.W. Zeh & M.M. Bonilla. 2003. Phylogeography of the harlequin beetle-riding pseudoscorpion and the rise of the Isthmus of Panamá. Molecular Ecology 12: 2759–2769.

Zhang, J., P. Kapli, P. Pavlidis & A. Stamatakis. 2013. A general species delimitation method with applications to phylogenetic placements. Bioinformatics 29:2869–2876.

Manuscript received 14 November 2015, revised 2 August 2016.

2016. Journal of Arachnology 44:272–329

The systematics of the pseudoscorpion family Ideoroncidae (Pseudoscorpiones: Neobisioidea) in the Asian region

Mark S. Harvey: Department of Terrestrial Zoology, Western Australian Museum, Locked Bag 49, Welshpool DC, Western Australia 6986, Australia; Research Associate, Division of Invertebrate Zoology, American Museum of Natural History, New York, USA; Research Associate, Department of Entomology, California Academy of Sciences, San Francisco, California, USA; Adjunct, School of Animal Biology, University of Western Australia, Crawley, Western Australia 6009, Australia; Adjunct, School of Natural Sciences, Edith Cowan University, Joondalup, Western Australia 6027, Australia. E-mail: mark.harvey@museum.wa.gov.au

Abstract. A review of the pseudoscorpion family Ideoroncidae in the Asian region reveals three genera: *Dhanus* Chamberlin, 1930, *Shravana* Chamberlin, 1930 and a new genus. *Dhanus* includes four species, *D. sumatranus* (Redikorzev, 1922), *D. hashimi* sp. nov. and *D. tioman* sp. nov. from Malaysia, and *D. hunaris* sp. nov. from Cambodia. *Dhanus doveri* Bristowe, 1952 is newly synonymized with *D. sumatranus*, and the type locality of *D. sumatranus* is confirmed as the Dark Cave, in the Batu Cave system, near Kuala Lumpur. *Shravana* is confirmed as a senior synonym of *Nhatrangia* Redikorzev, 1938 and includes 13 species: *S. laminata* (With, 1906) and S. *schwendingeri* sp. nov., from Thailand, *S. charas* sp. nov. and *S. withi* sp. nov. from Malaysia, *S. dawydoffi* (Redikorzev, 1938), comb. nov. (transferred from *Nhatrangia*) from Cambodia, Laos, Vietnam and the Spratly Islands, *S. indica* (Murthy & Ananthakrishnan, 1977), comb. nov. (transferred from *Dhanus*) from India, *S. ceylonensis* (Mahnert, 1984), comb. nov. (transferred from *Nhatrangia*) from Sri Lanka, *S. afghanica* (Beier, 1959), comb. nov. (transferred from *Dhanus*) and *S. magnifica* sp. nov. from Afghanistan, *S. latens* sp. nov. from Iran, and *S. pohli* (Mahnert, 2007), comb. nov. (transferred from *Dhanus*), *S. socotraensis* (Mahnert, 2007), comb. nov. (transferred from *Dhanus*), and *S. taitii* (Mahnert, 2007), comb. nov. (transferred from *Dhanus*) from Socotra. A new genus, *Sironcus*, is described for the type species *Ideobisium (Ideoroncus) siamensis* With, 1906 from Thailand and five new species, *S. rhiodontus* sp. nov. and *S. stonei* sp. nov. from Thailand, *S. sierwaldae* sp. nov. from Thailand and Myanmar, *S. jerai* sp. nov. from northern peninsular Malaysia and *S. belaga* sp. nov. from Sarawak.

Keywords: *Nhatrangia*, morphology, new species, post-embryonic development

ZooBank publication: http://zoobank.org/references/urn:lsid:zoobank.org:pub:72DA641E-F9B8-4F66-915F-4CEBDB358054

The pseudoscorpion family Ideoroncidae is discontinuously distributed around the world with 71 described species in the Americas, Africa and Asia (Harvey 2013; Harvey & Muchmore 2013; Harvey & Du Preez 2014). The American fauna consists of 43 species in seven genera, *Albiorix* Chamberlin, 1930, *Ideoroncus* Balzan, 1887, *Mahnertius* Harvey & Muchmore, 2013, *Muchmoreus* Harvey, 2013, *Pseudalbiorix* Harvey, Barba, Muchmore & Perez, 2007, *Typhloroncus* Muchmore, 1979, and *Xorilbio* Harvey & Mahnert, 2006, ranging from the western U.S.A. to central Chile (Harvey & Muchmore 2013). The African fauna consists of 16 species in four genera, *Botswanoncus* Harvey & du Preez, 2014, *Negroroncus* Beier, 1931, *Nannoroncus* Beier, 1955 and *Afroroncus* Mahnert, 1981 (Harvey 2013; Harvey & Du Preez 2014). The remaining 11 species are found in the Asian region occurring as far west as Socotra and Iran, and as far east as Malaysia, and are currently placed in a further three genera, *Dhanus* Chamberlin, 1930, *Nhatrangia* Redikorzev, 1938 and *Shravana* Chamberlin, 1930 (Harvey 2013). The first ideoroncids described from Asia were *Ideobisium (Ideoroncus) siamensis* With, 1906 and *Ideobisium (Ideoroncus) laminatus* With, 1906 from Thailand (With 1906), followed by *Ideoroncus sumatranus* Redikorzev, 1922 from 'Datu Caves, Sumatra' (Redikorzev 1922). These species were later transferred to other genera, with *I. siamensis* and *I. sumatranus* comprising the genus *Dhanus*, and *I. laminatus* the sole species of *Shravana* (Chamberlin 1930). *Nhatrangia* was erected by Redikorzev (1938) for *N. dawydoffi* Redikorzev, 1938 from Vietnam, and the genus now includes a second species, *N. ceylonensis* Mahnert, 1984 from Sri Lanka (Mahnert 1984). Several additional species have since been added to *Dhanus*, including *D. doveri* Bristowe, 1952 from Batu Caves, Malaysia (Bristowe 1952), *D. afghanicus* Beier, 1959 from Afghanistan and Iran (Beier 1959, 1971), *D. indicus* Murthy and Ananthakrishnan, 1977 from southern India (Murthy & Ananthakrishnan 1977), and *D. pohli* Mahnert, 2007, *D. socotraensis* Mahnert, 2007 and *D. taitii* Mahnert, 2007 from Socotra (Mahnert 2007). The Asian ideoroncids occur in several disparate areas in Asia, where they occupy a number of habitats such as rainforests, caves and semi-arid regions.

A review of the generic classification of the Ideoroncidae by Mahnert (1984) placed particular emphasis on trichobothriotaxy and highlighted many deficiencies in our knowledge of the systematics of this well-defined family (Harvey 1992). Unfortunately, specimens of *Dhanus sumatranus*, the type species of the genus, were unavailable to Mahnert (1984) and all previous descriptions of the species (Redikorzev 1922; Chamberlin 1930; Beier 1932b) have proved to be inadequate by modern standards. The lack of a suitable description for this species has hampered our understanding of the relationships of the other Asian ideoroncids, and the description presented below based on a syntype of *D. sumatranus*, the three specimens examined by Chamberlin (1930) and numerous newly collected specimens from the type locality that allows some firm decisions to be made regarding the status of *Dhanus*, *Shravana* and

Figure 1.—*Dhanus sumatranus* (Redikorzev), from Gua Pandan, Batu Caves, Malaysia: A. Adult; B. Two adults, one feeding on a juvenile cave cockroach, *Pycnoscelus striata* (Kirby).

Nhatrangia. In addition, the generic placement of *D. siamensis* is reassessed, which is found to be sufficiently distinct from both *Dhanus* and *Shravana* to warrant a new genus, *Sironcus*.

METHODS

The specimens examined for this study are lodged in the following institutions: Australian National Insect Collection, CSIRO, Canberra (ANIC); Museum of Natural History, London (BMNH); Bishop Museum, Honolulu (BPBM); California Academy of Sciences, California (CAS); Muséum d'histoire naturelle, Genèva (MHNG); Muséum national d'histoire naturelle, Paris (MNHN); Naturhistorisches Museum, Wien (NHMW); Staatliches Museum für Naturkunde, Stuttgart (SMNS); Western Australian Museum, Perth (WAM); Zoological Institute of the Russian Academy of Sciences, St Petersburg (ZISP); Zoological Museum of the University of Malaya, Kuala Lumpur (ZMUM; currently lodged in WAM); and Zoologisk Museum, Copenhaven (ZMC).

The specimens were examined by preparing temporary slide mounts by immersing the specimen in 75% lactic acid at room temperature for one to several days, and mounting them on microscope slides with 10 or 12 mm coverslips supported by small sections of 0.25 mm or 0.50 mm diameter nylon fishing line. Specimens were examined with a Leica MZ16 dissecting microscope, Leica DM2500 or Olympus BH–2 compound microscopes, and illustrated with the aid of a drawing tube. Measurements were taken at the highest possible magnification using an ocular graticule. After study, the specimens were rinsed in water and returned to 75% ethanol with the dissected portions and placed in 12 × 3 mm glass genitalia microvials (BioQuip Products, Inc.).

The setae of the carapace are shown as a solid line if present, but depicted with a dashed line if the seta was missing from the specimen. Other small dots depicted in the illustrations are small pores, and not setal areolae.

The genera and species treated in this monograph are arranged alphabetically. Terminology and mensuration largely follow Chamberlin (1931), with the exception of the nomenclature of the pedipalps, legs and with some minor modifications to the terminology of the trichobothria (Harvey 1992), chelicera (Harvey & Edward 2007; Judson 2007) and faces of the appendages (Harvey et al. 2012). The notation of the supernumerary trichobothria follows (Mahnert 1984).

Coordinates for the collection localities were calculated using Google Earth or obtained from various other on-line resources. Maps throughout this publication were created using ArcGIS® software by Esri (www.esri.com).

SYSTEMATICS

Family Ideoroncidae Chamberlin, 1930
http://zoobank.org/NomenclaturalActs/urn:lsid:zoobank.org:act:3D32F8DC-8B61-404C-B9D7-921922DACE5F

Ideoroncidae Chamberlin, 1930: 42.

Diagnosis.—Members of the family Ideoroncidae differ from all other pseudoscorpion families by the increased number of chelal trichobothria (17–31 on the fixed chelal finger and 9–14 on the movable chelal finger) (e.g., Figs. 3, 10, 24C), and the sub-basal position of the median maxillary lyrifissure (Figs. 4A, 11A, 23A).

Description.—See Harvey & Muchmore (2013).

Post-embryonic development.—Of the three genera treated in this paper, nymphal stages are known for 15 species, including the tritonymph and deutonymph of *Dhanus hashimi* sp. nov., *D. tioman* sp. nov., *Shravana afghanica*, *S. ceylonensis*, *S. magnifica* sp. nov., *S. schwendingeri* sp. nov. and *Sironcus rhiodontus* sp. nov., the tritonymph of *D. sumatranus*, *S. latens* sp. nov., *S. taitii* sp. nov., *S. withi* sp. nov. and *S. stonei* sp. nov., the deutonymph of *S. charas* sp. nov. and *S. socotraensis*, and all three nymphal stages of *Sironcus jerai* sp. nov. (Table 1). As in all other pseudoscorpions (e.g., Vachon 1964), trichobothrial numbers increase at each stage. Protonymphs of *S. jerai* have three trichobothria on the fixed finger and one trichobothrium on the movable finger, forming a pattern of 3/1. Several trichobothria are added at the deutonymph stage, forming a pattern of 9/6, at the tritonymph stage forming 14/8, and finally at the adult forming 20/10. This 20/10 pattern, and the highly similar 21/10 and 22/10, are the most common patterns among the Ideoroncidae, and are also found in *Afroroncus* (Mahnert 1981), *Albiorix* (Harvey & Muchmore 2013), *Ideoroncus* (Mahnert 1984), *Mahnertius* (Harvey & Muchmore 2013), *Muchmoreus* (Harvey & Muchmore 2013), *Nannoroncus* (Mahnert 1981), *Negroroncus* (except *N. jeanneli* Vachon, 1958) (Mahnert 1981), *Pseudalbiorix* (Harvey et al. 2007), *Typhlo-*

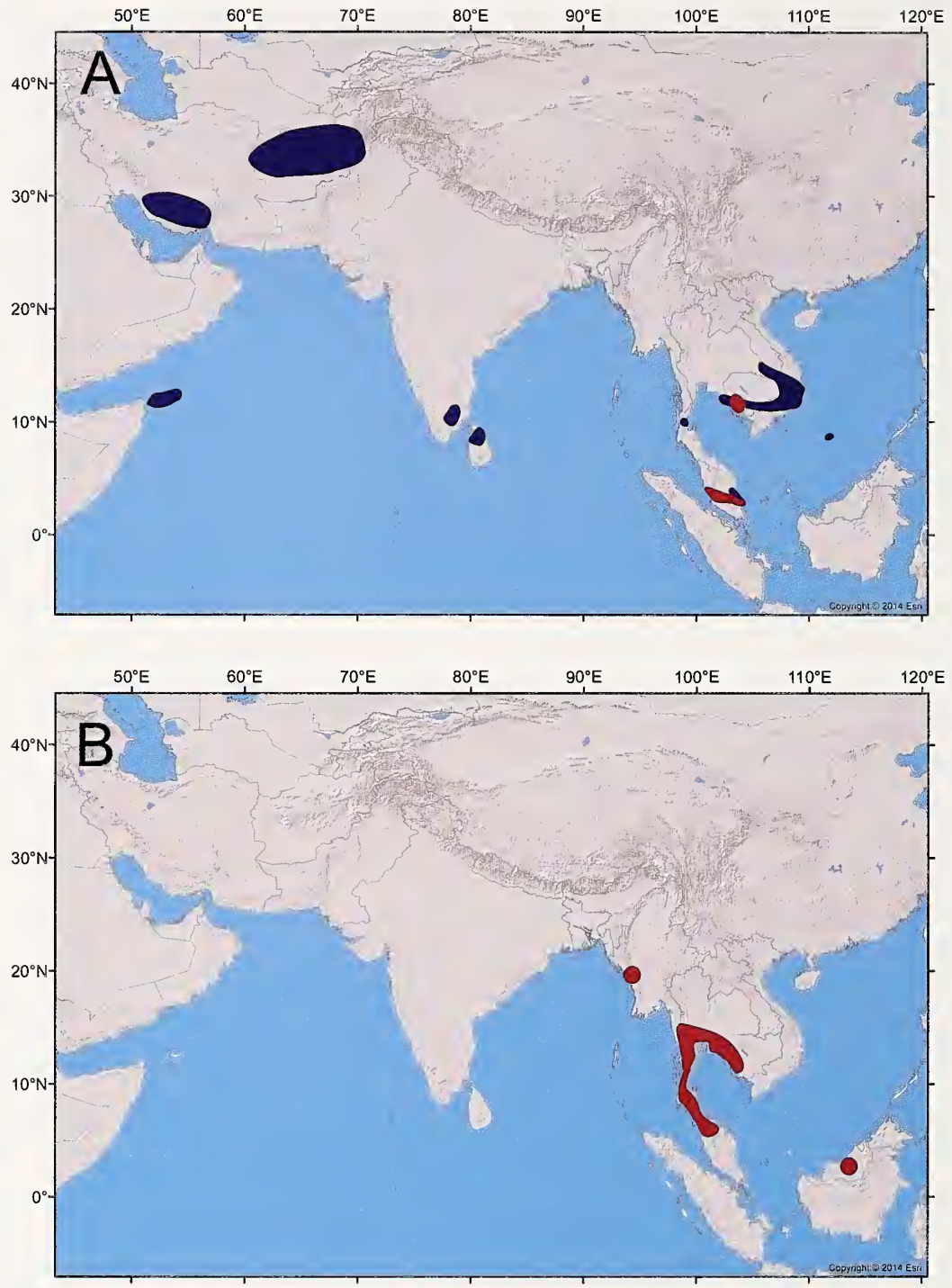

Figure 2.—Distribution of Asian Ideoroncidae: A. *Shravana* species (blue), *Dhanus* species (red); B. *Sironcus* species.

roncus (Harvey & Muchmore 2013) and *Xorilbia* (Mahnert 1984, 1985), as summarized in Harvey and Du Preez (2014). Lower numbers are found in *Botswanoncus* which has 17/9 (Harvey & Du Preez 2014), and higher numbers occur in *Negroroncus jeanneli*, all species of *Dhanus* and all species of *Shravana* except *S. socotraensis* (Vachon 1958; Mahnert 1984; 2007; this study). The generally high adult trichobothrial numbers of species of *Dhanus* and *Shravana* are reflected in the deutonymph and tritonymph patterns which are generally higher than those found in other ideoroncids, with deutonymphs having 10–20/7–10 trichobothria and tritonymphs with 16–25/8–12. Deutonymphs of other genera have 9/6 (10 species in eight genera, including *S. socotraensis*), and tritonymphs have 14/8 or 15/8 (20 species in 8 genera). Protonymphs of only seven ideoroncid species are known, *Albiorix chilensis* (Ellingsen, 1905), *Ideoroncus setosus* Mahnert, 1984, *Negroroncus* sp., *Pseudalbiorix reddelli* (Muchmore, 1982), *Sironcus jerai*, *Xorilbia arboricola* (Mahnert, 1979) and *X. gracilis* (Mahnert, 1985) (Mahnert 1981, 1984; Harvey et al. 2007; Harvey & Muchmore 2013), and all have a 3/1 pattern. It seems quite likely that

Table 1.—The number of trichobothria occurring in species of *Dhanus*, *Shravana* and *Sironcus*, including known nymphal stages.

	eb	*esb*	*est*	*et*	*ib*	*isb*	*ist*	*it*	*b*	*sb*	*st*	*t*	Fixed finger, total	Movable finger, total	Reference
Dhanus hashimi															
Adult	1	1	6–7	1	5	1	7	1	3	1	1	6	23–24	11	This study
Tritonymph	1	1	4	1	4	-	4	1	3	-	1	5	16	9	This study
Deutonymph	1	-	3	1	2	-	2	1	3	-	-	4	10	7	This study
Dhanus lunaris															
Adult	2	1	8	1	6	1	9	1	4	1	1	6	29	12	This study
Dhanus sumatranus															
Adult	1	1	6–8	1	5	1	7–9	1	3	1	1	6	24–26	11	This study
Tritonymph	1	1	5	1	4	-	4	1	3	-	1	5	17	9	This study
Dhanus tionan															
Adult	2	1	9	1	7	1	9	1	4	1	1	7	31	13	This study
Tritonymph	2	1	7	1	5	-	6	1	4	-	1	7	23	12	This study
Deutonymph	2	-	5	1	4	-	3	1	4	-	-	6	16	10	This study
Shravana afghanica															
Adult	3	1	12	1	4–5	1	8–9	1	4	1	1	8	32	14	This study
Tritonymph	3	1	7	1	4	-	7	1	4	-	1	6	24	11	This study
Deutonymph	3	-	6	1	3	-	5	1	4	-	-	6	19	10	This study
Shravana ceylonensis															
Adult	2	1	9	1	6	1	9	1	4	1	1	8	30	14	Mahnert (1984)
Tritonymph	2	1	7	1	4	-	6	1	4	-	1	7	22	12	Mahnert (1984)
Deutonymph	2	-	4	1	4	-	4	1	4	-	-	6	16	10	Mahnert (1984)
Shravana charas															
Adult	2	1	9	1	6	1	11	1	4	1	1	8	32	14	This study
Deutonymph	2	-	5	1	3	-	4	1	4	-	-	6	16	10	This study
Shravana dawydoffi															
Adult	2	1	9	1	5–6	1	9–10	1	4	1	1	8	29–31	14	Mahnert (1984)
Shravana indica															
Adult	1	1	6	1	5	1	7	1	3	1	1	7	23	12	This study
Shravana laminata															
Adult	1	1	6	1	5	1	7	1	3	1	1	7	23	12	Mahnert (1984)
Shravana latens															
Adult	2	1	8	1	5	1	9	1	3	1	1	7	28	12	This study
Tritonymph	2	1	6	1	4	-	7	1	3	-	1	6	22	10	This study
Shravana magnifica															
Adult	3	1	13	1	5	1	8–9	1	4	1	1	8	31–32	14	This study
Tritonymph	3	1	8	1	4	-	7	1	4	-	1	7	25	11	This study
Deutonymph	2	-	6	1	3	-	6	1	4	-	-	6	20	10	This study
Shravana pohli															
Adult	2	1	6	1	5–6	1	6	1	2	1	1–2	7	23–24	11–12	Mahnert (2007); Mahnert (in litt., April 2016)
Shravana schwendingeri															
Adult	1	1	6	1	5	1	7	1	3	1	1	6	23	11	This study
Tritonymph	1	1	5	1	4	-	3	1	3	-	1	5	16	8	This study
Deutonymph	1	-	3	1	2	-	2	1	3	-	-	4	10	7	This study
Shravana socotraensis															
Adult	1	1	6	1	4	1	5	1	2	1	1	6	20	10	Mahnert (2007)
Deutonymph	?	-	?	1	?	-	?	1	?	-	-	?	9	6	Mahnert (2007)
Shravana taitii															
Adult	2	1	8	1	4	1	7	1	3	1	1	7	25	12	Mahnert (2007)
Tritonymph	2	1	6	1	4	-	4	1	3	-	1	5	19	9	Mahnert (2007)
Shravana withi															
Adult	1	1	6	1	5	1	8	1	3	1	1	7	24	12	This study
Tritonymph	1	1	5	1	4	-	3	1	3	-	1	6	16	10	This study
Sironcus belaga															
Adult	1	1	6	1	4	1	5	1	2	1	1	6	20	10	This study
Sironcus jerai															
Adult	1	1	6	1	4	1	5	1	2	1	1	6	20	10	Harvey (1992); this study
Tritonymph	1	1	3	1	3	-	4	1	2	-	1	5	14	8	Harvey (1992); this study
Deutonymph	1	-	2	1	2	-	2	1	2	-	-	4	9	6	Harvey (1992); this study
Protonymph	1	-	-	1	-	-	1	-	-	-	-	1	3	1	Harvey (1992); this study

Table 1.—Continued.

	eb	*esb*	*est*	*et*	*ib*	*isb*	*ist*	*it*	*b*	*sb*	*st*	*t*	Fixed finger, total	Movable finger, total	Reference
Sironcus rhiodontus															
Adult	1	1	6	1	4	1	5	1	2	1	1	6	20	10	This study
Tritonymph	1	1	3	1	3	-	4	1	2	-	1	5	14	8	This study
Deutonymph	1	-	2	1	2	-	2	1	2	-	-	4	9	6	This study
Sironcus siamensis															
Adult	1	1	6	1	4	1	5	1	2	1	1	6	20	10	This study
Sironcus sierwaldae															
Adult	1	1	6	1	4	1	5	1	2	1	1	6	20	10	This study
Sironcus stonei															
Adult	1	1	6	1	4	1	5	1	2	1	1	6	20	10	This study
Tritonymph	1	1	3	1	3	-	4	1	2	-	1	5	14	8	This study

KEY TO GENERA OF *IDEORONCIDAE*

1. Chelal fingers with stout, mesal setae; rallum with two distal-most blades serrate, other blades smooth 2
   Chelal fingers without stout, mesal setae; rallum with all blades serrate (e.g., Figs. 14E, 27C) 3
2. Trichobothria *b* virtually adjacent and quite close to *sb* ..... *Nannoroncus* (East Africa)
   Trichobothria *b* somewhat separated and far from *sb* ..... *Afroroncus* (East Africa)
3. Arolium with small hooked process on ventral surface (e.g., Fig. 27H) 4
   Arolium without small hooked process on ventral surface (e.g., Figs. 8J, 17E) 8
4. Distal teeth of fixed chelal finger raised into a short ridge ..... *Mahnertius* (South America)
   Distal teeth of fixed chelal finger not raised into a short ridge 5
5. Anal operculum abutting sternite X ..... *Typhloroncus* (Central America)
   Anal operculum not abutting sternite X 6
6. Chelal teeth juxtadentate (contiguous) 7
   Chelal teeth diastemodentate (widely spaced) ..... *Xorilbia* (South America)
7. Lamina exterior present ..... *Negroroncus* (central and eastern Africa)
   Lamina exterior absent (Fig. 27B) ..... *Sironcus* (south-east Asia)
8. Condyle on external margin of chelal hand small and rounded 9
   Condyle on external margin of chelal hand large and bifurcate ..... *Pseudalbiorix* (Central America)
9. Lamina exterior present (e.g., 8F, 14D) 10
   Lamina exterior absent 11
10. Arolium shorter than claws or as long as claws (e.g., Fig. 8J) ..... *Dhanus* (south-east Asia)
    Arolium extending beyond claws (e.g., Fig. 17E) ..... *Shravana* (Socotra to south-east Asia)
11. Chelal fingers with 26 trichobothria, 17 on fixed finger and 9 on movable finger ..... *Botswanoncus* (southern Africa)
    Chelal fingers with 30–32 trichobothria, 20–22 on fixed finger and 10 on movable finger 12
12. Arolium divided, much longer than claws ..... *Albiorix* (Americas)
    Arolium undivided, slightly longer than claws or about same length as claws 13
13. Sternites with median suture line; each spiracular plate with 1 seta ..... *Ideoroncus* (South America)
    Sternites without median suture line; each spiracular plate with 2 or 3 setae ..... *Muchmoreus* (Central America)

protonymphs of *Dhanus* and *Shravana* will also have a 3/1 pattern.

Dhanus Chamberlin, 1930
http://zoobank.org/NomenclaturalActs/urn:lsid:zoobank.org:act:914CD39F-6BB5-4C07-B18B-82E00FDFC748

Dhanus Chamberlin, 1930:47; Beier, 1932a:173; Murthy and Ananthakrishnan, 1977:26; Harvey, 1991:318; Harvey, 2013: unpaginated.

Type species.—*Ideoroncus sumatranus* Redikorzev, 1922, by original designation.

Diagnosis.—Species of *Dhanus* differ from all other genera except *Shravana* and *Negroroncus* by the presence of a thin lamina exterior on the chelicera (e.g., Figs. 8F, 14D). They differ from *Shravana* by the short arolium (e.g., Figs. 6, 8), and from *Negroroncus* by the lack of a ventral hooked process on the arolium (e.g. Figs. 6, 8).

Description (adult).—*Setae:* generally long, straight or slightly curved, and acicular.

Chelicera (Figs. 6B, 7C, 8F): hand with 7–9 long, acuminate setae; movable finger with 1 long subdistal seta; rallum of 4 thickened blades, all blades serrate; lamina exterior present; galea long and slender.

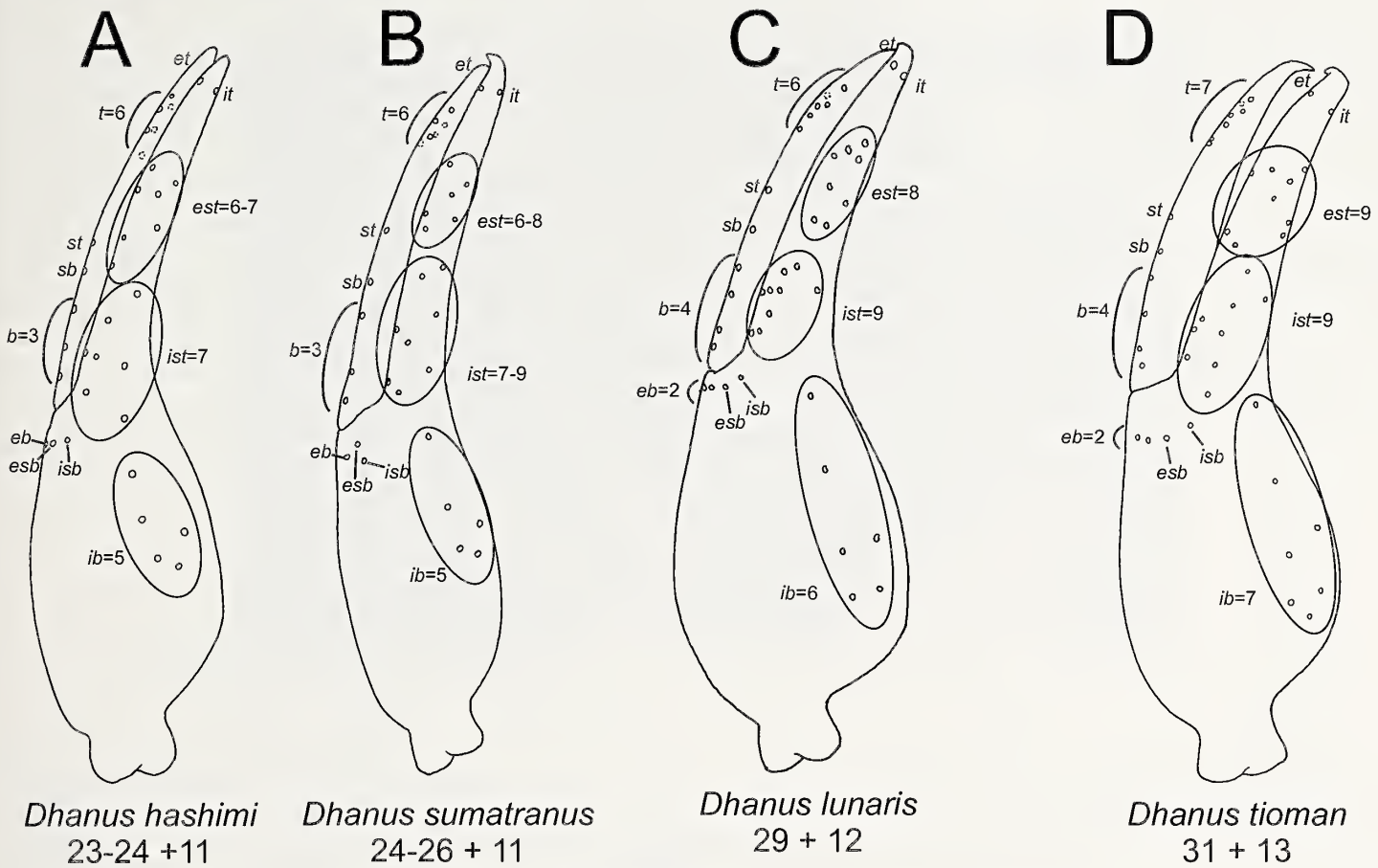

Figure 3.—Trichobothrial patterns of *Dhanus* species, taken from left chela (or a mirror image of the right chela), arranged in order of increasing trichobothrial number.

Pedipalp: long and slender; patella with disto-prolateral excavation. Fixed chelal finger with 23–28 trichobothria, movable chelal finger with 11–14 trichobothria (e.g., Fig. 3): *eb* region with 1–2 trichobothria; *est* region with 6–9 trichobothria; *ib* region with 5–6 trichobothria; *ist* region with 7 trichobothria; *b* region with 3–4 trichobothria; and *t* region with 6 trichobothria. Venom apparatus present in both chelal fingers, venom duct terminating in nodus ramosus near *est* region in fixed finger and near *t* region in movable finger (Figs. 6D, 7D, 8C, 9C). Chelal teeth juxtadentate; base of fixed chelal finger without small denticles; chelal hand with retrolateral condyle small and rounded.

Carapace (Figs. 6A, 7A, 8A, 9A): with 2 small, bulging eyes; epistome present; with shallow posterior furrow.

Coxal region (Fig. 4A): manducatory process with 2 long distal setae; median maxillary lyrifissure present and subbasally situated.

Legs (Figs. 7F, G, 8H, I): femur I and II without basal swelling; femur I much longer than patella I; suture line between femur IV and patella IV transverse; metatarsus shorter than tarsus; subterminal tarsal setae bifurcate; arolium undivided and shorter than claws or about same length as claws, without ventral hooked process (Figs. 6H, 7H, 8J); claws slender and simple.

Abdomen: tergites and sternites usually with indication of medial division, consisting of an anterior and posterior desclerotisation of the sclerite. Pleural membrane longitudinally striate (Fig. 4C). Each stigmatic sclerite with 1 seta; spiracles simple, with spiracular helix. Anal operculum not abutting sternite X (Fig. 4B).

Genitalia: male median genital sac deeply bipartite (Fig. 4E); female with large gonosac covered with pores (Fig. 4G).

Description (tritonymph).—*Pedipalp*: fixed finger and hand with 16–23 trichobothria, movable finger with 9–12 trichobothria (Figs. 6F, 8E, 9D); *esb*, *it* and *et* regions each with 1 trichobothrium; *eb* region with 1–2 trichobothria; *ib* region with 3–5 trichobothria; *ist* region with 4–6 trichobothria; *est* region with 4–7 trichobothria; *et* slightly distal to *it*; *b* region with 3–4 trichobothria; *st* region with 1 trichobothrium; *t* region with 5–7 trichobothria; *isb* and *sb* absent.

Description (deutonymph).—*Pedipalp*: fixed finger and hand with 10 trichobothria, movable finger with 7 trichobothria (Figs. 6G, 9E); *eb*, *ist*, *it* and *et* regions each with 1 trichobothrium; *ib* region with 2 trichobothria; *est* region with 3 trichobothria; *et* slightly distal to *it*; *b* region with 3 trichobothria; *t* region with 4 trichobothria; *esb*, *isb*, *sb* and *st* absent.

Description (protonymph).—Unknown.

Remarks.—Chamberlin (1930) included two Asian species when proposing the genus *Dhanus*: the type species *D. sumatranus* and *D. siamensis*. The third Asian ideoroncid described at the time, *Ideobisium laminatus*, was placed in a separate genus, *Shravana*. Chamberlin (1930) relied on the length of the arolium to separate *Dhanus* and *Shravana*, with *Dhanus* having a short arolium and *Shravana* having a long

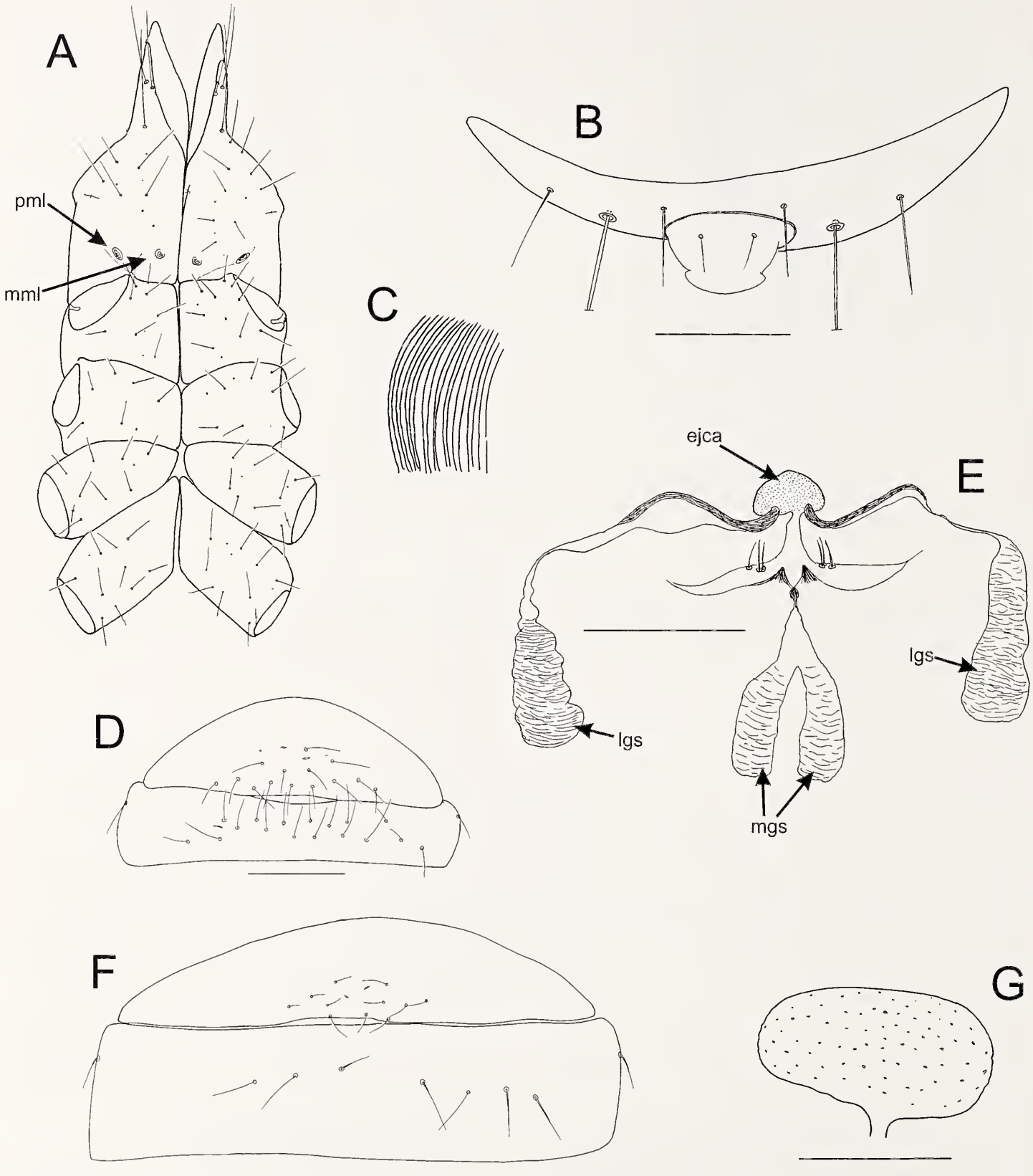

Figure 4.—*Dhanus sumatranus* (Redikorzev) from Gua Pandan, Batu Caves, Malaysia (WAM T135077): A. Cephalothorax, ventral, male; B. Sternite XI and anal operculum; C. Pleural membrane; D. Sternites III and IV, male, ventral; E. Male genitalia, ventral; F. Sternites III and IV, female, ventral; G. Female genitalia, ventral. Abbreviations: ejca, ejaculatory canal atrium; lgs, lateral genital sac; mgs, median genital sac; mml, median maxillary lyrifissure; pml, posterior maxillary lyrifissure. Scale lines = 0.2 mm (B, D–G).

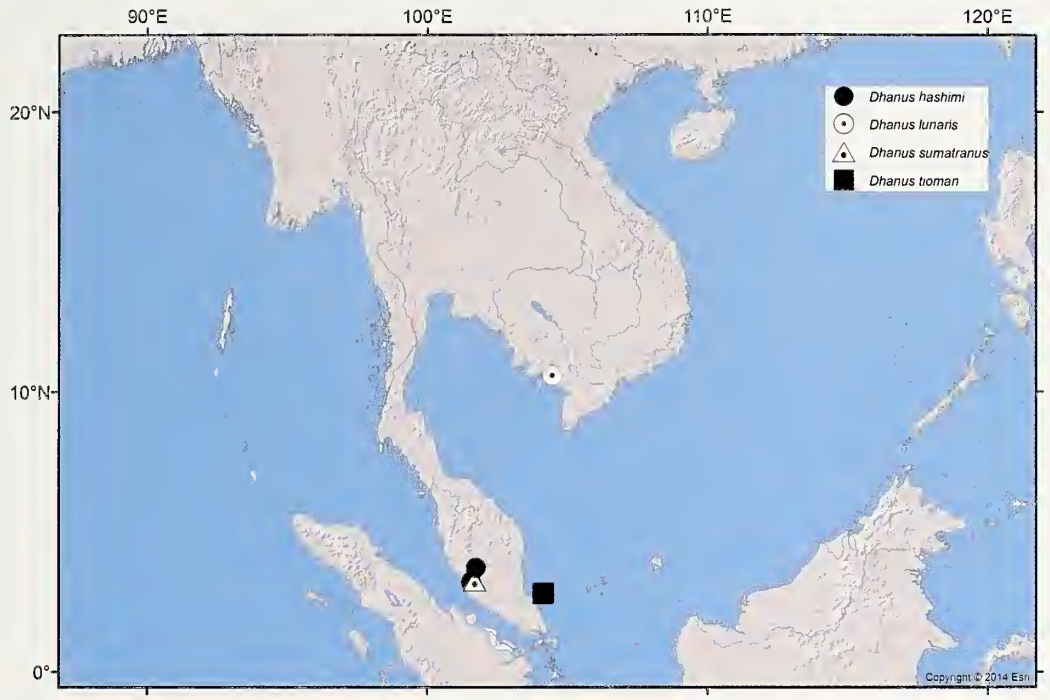

Figure 5.—Distribution of *Dhanus* species.

arolium. Examination of a wide range of ideoroncids from across the Asian region demonstrates that this feature is sufficiently constant to maintain both genera, with *Dhanus* restricted to *D. sumatranus* and three new species from Malaysa and Cambodia. As demonstrated elsewhere in this paper, *D. siamensis* lacks the cheliceral lamina interior found in all species of *Dhanus* and *Shravana*, and has a ventral hook on the arolium. Therefore, *D. siamensis* is transferred to a new genus, *Siroucus*.

Members of the genus *Dhanus* are found in peninsular Malaysia and southern Cambodia (Fig. 5). *Dhanus sumatranus* and *D. lunaris* are apparently restricted to cave ecosystems, but *D. hashimi* and *D. tioman* are found in tropical rainforest leaf litter.

Etymology.—The name *Dhanus* is most likely derived from Dhanus (or Dhanushya) which is a divine weapon in Hindu mythology.

KEY TO SPECIES OF *DHANUS*

1. Trichobothrium *ib* region extending only half-way along chelal hand (Fig. 8B, C); chelal hand with small patch of microsetae near *eb* and *esb* (Figs. 6D, 8C); fixed chelal finger and hand with 23–26 trichobothria (Fig. 3A, B); *eb* region with 1 trichobothrium (Fig. 3A, B); *b* region with 3 trichobothria (Fig. 3A, B) 2
   Trichobothrium *ib* region extending nearly full length of chelal hand (Figs. 7B, 9B); chelal hand without microsetae near *eb* and *esb* (Figs. 7D, 9C); fixed chelal finger and hand with 29–31 trichobothria (Fig. 3C,D); *eb* region with 2 trichobothria (Fig. 3A, B); *b* region with 4 trichobothria (Fig. 3A, B) 3
2. Trichobothria *eb*, *esb* and *isb* arranged in straight line (Fig. 6D); pedipalps larger and thinner [e.g., 1.46–1.53 (♂), 1.59–1.71 (♀) mm, 3.81–3.87 (♂), 3.57–3.61 (♀) x longer than broad] ..... *D. hashimi*
   Trichobothrium *esb* situated in advance of *eb* and *isb*, forming triangle (Fig. 8C); pedipalps larger and thinner [e.g., chela (with pedicel) 2.275–2.55 (♂), 2.37–2.59 (♀) mm, 4.35–4.85 (♂), 4.09–4.14 (♀) x longer than broad].... *D. sumatranus*
3. Fixed chelal finger and hand with 29 trichobothria, including 6 in the *ib* region (Fig. 3C); movable finger with 12 trichobothria, including 6 in *t* region (Fig. 3C); chela (with pedicel) 2.11 (♀) mm in length ..... *D. lunaris*
   Fixed chelal finger and hand with 31 trichobothria, including 7 in the *ib* region (Fig. 3D); movable finger with 13 trichobothria, including 7 in *t* region (Fig. 3D); chela (with pedicel) 1.34–1.495 (♂), 1.475–1.64 (♀) mm in length ..... *D. tioman*

Dhanus hashimi sp. nov.
http://zoobank.org/NomenclaturalActs/urn:lsid:zoobank.org:act:C83CEB48-DA1B-4E60-BAD7-8BF0DB32BA32
(Figs. 3A, 6)

Material examined.—*Holotype male*. MALAYSIA: *Pahang*: Jalan Lady Maxwell, 3°42′59″N, 101°44′19″E, 1281 m, 22 June 2009, sifting rainforest litter, M.S. Harvey, K.L. Edward, R. Hashim, S. Dzarawi (ZMUM, WAM T129592).

Paratypes. MALAYSIA: *Pahang*: 2 ♀, Bukit Fraser, Air Tejun Jeriau (Jeriau Waterfall), 3°43′34″N, 101°42′49″E, 938 m, 21 June 2009, sifting dry litter, M.S. Harvey, K.L. Edward, R. Hashim, S. Dzarawi (WAM T125646, T129593); 1 ♂, Bukit Fraser [3°43′N, 101°45′E], 4,200 feet, 17 September 1972, T. Jaccoud (MHNG); 3 ♂, 2 ♀, 1 deutonymph, Fraser's Hill [=

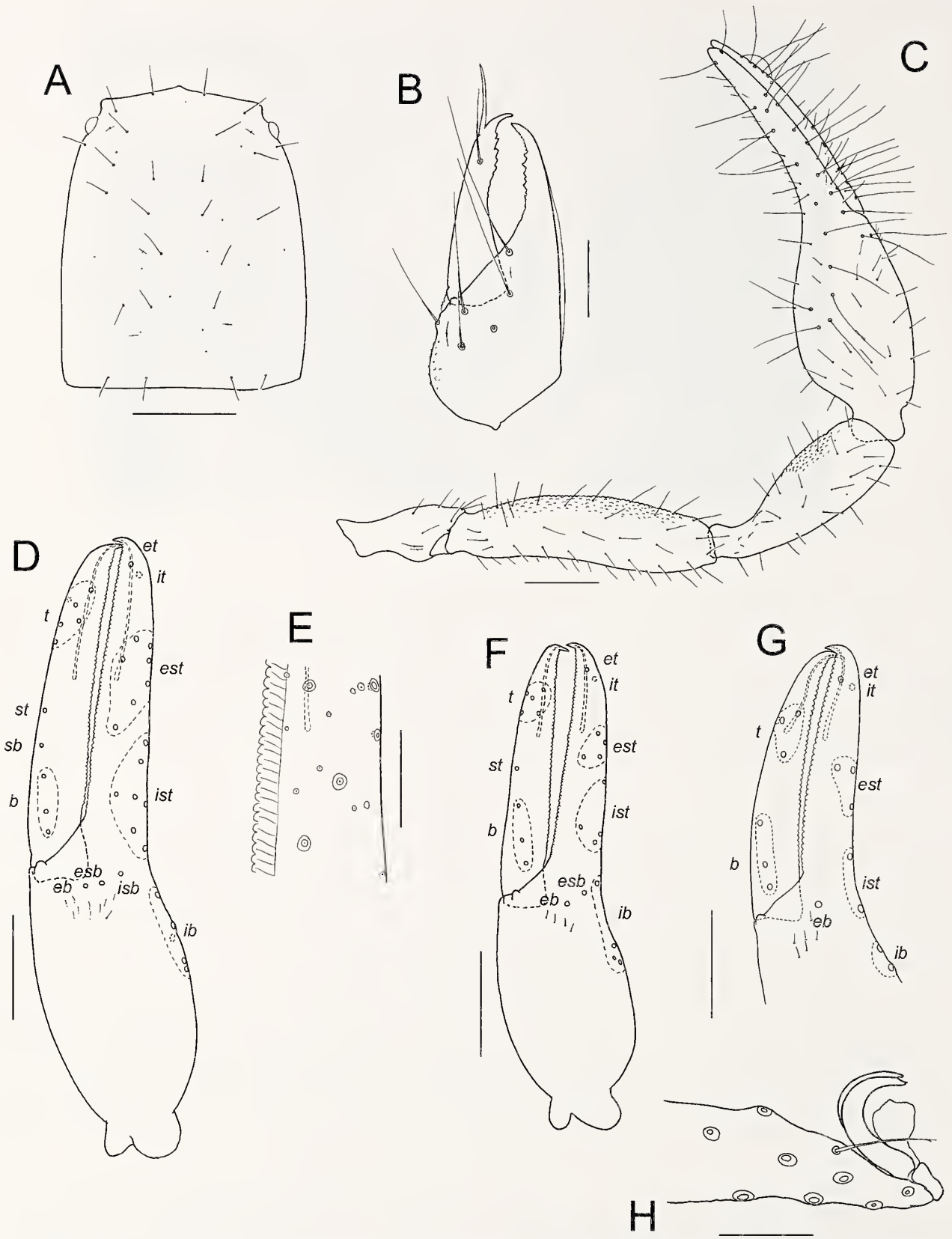

Figure 6.—*Dhanus hashimi* sp. nov., male holotype, unless stated otherwise: A. Carapace; B. Chelicera; C. Right pedipalp, dorsal; D. Left chela, lateral; E. Detail of fixed chelal finger; E. Left chela, lateral, tritonymph (MHNG, from Bukit Fraser); F. Left chela, lateral, deutonymph (SMNS, from Bukit Fraser); G. Distal end of tarsus IV showing arolium, claws and subterminal seta, other setae omitted. Scale lines = 0.25 mm (A, C, D, F); 0.2 mm (G); 0.1 mm (B, E); 0.05 mm (H).

Bukit Fraser] [3°43′N, 101°45′E], 17 April 1990, A. Riedel (SMNS); 1 ♂, 1 ♀, 1 tritonymph, Bukit Fraser, Maxwell Trail, 3°42′59.1″N, 101°44′18.9″E, 1350 m, evergreen hill forest, 12–16 May 2004, P. Schwendinger (MHNG); *Selangor*: 1 ♂, 2 ♀, The Gap [3°42′N, 101°44′E], 900 m, 14 March 1993, forêt dégradée (tamisage), I. Löbl, F. Calame (MHNG); 2 ♂, 1 ♀, 1 tritonymph, 1 km au-dessous de Fraser's Hill [3°42′N, 101°44′E], 1280 m, forêt dégradée (tamisage), 15 March 1993, I. Löbl, F. Calame (MHNG); 1 ♀, Sungei Buloh, near Kuala Lumpur [3°13′N, 101°34′E], 27 July 1972, T. Jaccoud (MHNG).

Diagnosis.—*Dhanus hashimi* is most similar to *D. sumatranus* as both have the trichobothria of the *ib* region restricted to the distal half of the chelal hand (Fig. 6C), several microsetae on the chelal hand near trichobothria *eb* and *esb* (Fig. 6D), and 23–26 trichobothria on the fixed chelal finger and hand (Fig. 3A). *Dhanus hashimi* differs from *D. sumatranus* by the smaller and stouter chelal and leg segments [e.g., chela (with pedicel) 1.46–1.53 (♂), 1.59–1.71 (♀) mm, 3.81–3.87 (♂), 3.57–3.61 (♀) x longer than broad in *D. hashimi*, and 2.275–2.55 (♂), 2.37–2.59 (♀) mm, 4.35–4.85 (♂), 4.09–4.14 (♀) x longer than broad in *D. sumatranus*], and by trichobothria *eb*, *esb* and *isb*, which are in a straight line in *D. hashimi* (Fig. 6D) but are arranged in a triangle in *D. sumatranus* (Fig. 6C).

Description (adult).—*Color:* pedipalps and carapace deep red-brown; chelicerae and legs yellow-brown; tergites and sternites pale yellow-brown.

Setae: generally long, straight or slightly curved, and acicular.

Chelicera (Fig. 6B): with 7–9 setae on hand; movable finger with 1 submedial seta; galea very slender and elongate; fixed finger with 9–11 (♂), 11–12 (♀) teeth; movable finger with 6 (♂), 6–7 (♀) teeth; rallum of 4 blades, each with 1–3 small serrations; lamina exterior present, very thin.

Pedipalp (Fig. 6C): prolateral faces of femur and patella coarsely rugose, trochanter and chela smooth; trochanter 2.03–2.39 (♂), 2.18–2.38 (♀), femur 3.70–4.14 (♂), 3.52–3.75 (♀), patella 2.76–3.19 (♂), 2.73–2.88 (♀), chela (with pedicel) 3.81–3.87 (♂), 3.53–3.61 (♀), chela (without pedicel) 3.61–3.68 (♂), 3.33–3.44 (♀), hand 1.59–1.66 (♂), 1.48–1.53 (♀) x longer than broad, movable finger 1.25–1.35 (♂), 1.28–1.33 (♀) x longer than hand. Fixed chelal finger with 23–24 trichobothria, movable chelal finger with 11 trichobothria (Figs. 3A, 6D): *eb*, *esb* and *isb* in straight row at base of finger; *eb*, *esb*, *et*, *isb* and *it* regions each with 1 trichobothrium; *ib* region with 5 trichobothria, and extending about half-way along chelal hand; *ist* region with 7 trichobothria; *est* region with 6–7 trichobothria; *et* slightly distal to *it*; *b* region with 3 trichobothria; *sb* and *st* regions each with 1 trichobothrium; *t* region with 6 trichobothria; 10 small, lanceolate setae situated proximal to *eb-esb-isb*. Venom apparatus present in both chelal fingers, venom duct terminating in nodus ramosus near *est* region in fixed finger and near basal section of *t* region in movable finger (Fig. 6D). Chelal hand with patch of microsetae basal to *eb* and *esb* (Fig. 6D). Chelal teeth flat topped, slightly retrorse, evenly spaced (Fig. 6E), fixed finger with 67 (♂), 69 (♀) teeth; movable finger with 63 (♂), 62 (♀) teeth.

Carapace (Fig. 6A): 1.17–1.23 (♂), 1.03–1.16 (♀) x longer than broad; lateral margins evenly convex; with 2 small bulging eyes; with small epistome; with 25 (♂), 28 (♀) setae, including 4 near anterior margin and 4 near posterior margin; with shallow posterior furrow.

Coxal region: manducatory process with 2 long apical setae, plus 10 (♂), 8 (♀) additional setae; chaetotaxy of coxae I–IV: ♂, 5: 8: 8: 9; ♀, 5: 6: 8: 7.

Legs: femur + patella 2.88–3.04 (♂), 2.92–3.13 (♀) x longer than deep; subterminal tarsal setae weakly bifurcate (Fig. 6H); arolium slightly shorter than claws (Fig. 6H).

Abdomen: tergites and sternites barely divided and uniseriate. Tergal chaetotaxy: ♂, 6: 7: 9: 11: 13: 14: 12: 13: 12: 11: 10 (including 4 tactile setae): 2; ♀, 4: 7: 9: 12: 12: 12: 12: 11: 12: 11: 8 (including 4 tactile setae): 2. Sternal chaetotaxy: ♂, 12: (1) 12 [3+3] (1): (1) 9 (1): 15: 14: 14: 14: 13: 12: 7 (including 4 tactile setae): 2; ♀, 6: (1) 5 (1): (1) 9 (1): 12: 13: 13: 13: 14: 13: 8 (including 4 tactile setae): 2. Setae of tergites and sternites IX-XI acuminate.

Genitalia: male with median genital sac deeply bipartite; female with large gonosac covered with pores.

Dimensions (mm): males: holotype followed by other males (when measured): Body length 2.02 (2.06–2.69). *Pedipalp*: trochanter 0.415/0.175 (0.375–0.43/0.175–0.20), femur 0.88/0.225 (0.85–0.91/0.22–0.23), patella 0.725/0.235 (0.69–0.765/0.235–0.26), chela (with pedicel) 1.465/0.375 (1.46–1.53/0.38–0.40), chela (without pedicel) 1.38 (1.38–1.47), hand length 0.63 (0.62–0.64), movable finger length 0.815 (0.785–0.86). Chelicera 0.395/0.17, movable finger length 0.255. Carapace 0.75/0.615 (0.74–0.80/0.63–0.665); eye diameter 0.055. Leg I: femur 0.46/0.10, patella 0.22/0.11, tibia 0.315/0.085, metatarsus 0.19/0.07, tarsus 0.31/0.065. Leg IV: femur + patella 0.69/0.24 (0.685–0.695/0.225–0.235), tibia 0.515/0.11, metatarsus 0.25/0.09, tarsus 0.44/0.075.

Females: paratype (WAM T125646) followed by other females (when measured): Body length 2.69 (2.00–3.09). *Pedipalp*: trochanter 0.44/0.185 (0.435–0.465/0.195–0.20), femur 0.915/0.24 (0.90–0.95/0.24–0.27), patella 0.79/0.265 (0.75–0.805/0.275–0.28), chela (with pedicel) 1.60/0.435 (1.59–1.71/0.44–0.485), chela (without pedicel) 1.505 (1.515–1.615), hand length 0.67 (0.675–0.72), movable finger length 0.835 (0.895–0.92). Chelicera 0.435/0.195, movable finger length 0.28. Carapace 0.755/0.705 (0.77–0.91/0.665–0.775); eye diameter 0.06. Leg I: femur 0.46/0.105, patella 0.215/0.115, tibia 0.31/0.08, metatarsus 0.175/0.07, tarsus 0.315/0.065. Leg IV: femur + patella 0.715/0.235 (0.72–0.745/0.23–0.255), tibia 0.515/0.11, metatarsus 0.255/0.095, tarsus 0.40/0.095.

Description (tritonymph).—*Chelicera:* galea long and slender, slightly curved; with 7 setae on hand; 1 on movable finger; fixed finger with 8 small teeth, movable finger with 4 small teeth; rallum composed of 4 blades, all serrate.

Pedipalp: trochanter 2.34, femur 3.41, patella 2.60, chela (with pedicel) 3.63, chela (without pedicel) 3.42, hand 1.43 x longer than broad; movable finger 1.35 x longer than hand (without pedicel). Fixed chelal finger with 16 trichobothria, movable chelal finger with 9 trichobothria (Fig. 6F); *isb* and *st* absent; *eb*, *esb*, *et* and *it* regions each with 1 trichobothrium; *eb* and *esb* at base of finger; *est* region with 4 trichobothria; *ib* region with 4 trichobothria; *ist* region with 4 trichobothria; *et* slightly distal to *it*; *b* region with 3 trichobothria; *sb* region with 1 trichobothrium; *t* region with 5 trichobothria.

Carapace: anterior margin medially prominent; with 2 small bulging eyes; with 20 setae including 4 setae near anterior margin and 4 near posterior margin.

Legs: much as in adult.

Dimensions (mm): Body length 1.97. *Pedipalp*: trochanter 0.34/0.145, femur 0.665/0.195, patella 0.56/0.215, chela (with pedicel) 1.18/0.325, chela (without pedicel) 1.11, hand length 0.465, movable finger length 0.63. Carapace 0.605/0.51.

Description (deutonymph).—*Chelicera:* galea long and slender, slightly curved; with 5 setae on hand; 1 on movable finger; rallum composed of 4 blades, all serrate.

Pedipalp: trochanter 2.29, femur 3.59, patella 2.19, chela (with pedicel) 3.55, chela (without pedicel) 3.39, hand 1.60 x longer than broad; movable finger 1.44 x longer than hand (without pedicel). Fixed chelal finger with 10 trichobothria, movable chelal finger with 7 trichobothria (Fig. 6G); *esb*, *isb*, *sb* and *st* absent; *eb*, *et* and *it* regions each with 1 trichobothrium; *eb* at base of finger; *est* region with 3 trichobothria; *ib* region with 2 trichobothria; *ist* region with 2 trichobothria; *et* slightly distal to *it*; *b* region with 3 trichobothria; *t* region with 4 trichobothria.

Carapace: anterior margin medially prominent; with 2 small bulging eyes; with 4 setae near anterior margin and 4 near posterior margin.

Legs: much as in adult.

Dimensions (mm): Body length 1.52. *Pedipalp*: trochanter 0.275/0.12, femur 0.52/0.145, patella 0.35/0.16, chela (with pedicel) 0.905/0.255, chela (without pedicel) 0.865, hand length 0.36, movable finger length 0.52. Carapace 0.52/0.425.

Remarks.—This species is known from south-western Malaysia in the states of Pahang and Selangor (Fig. 5). The specimens were collected from leaf litter.

Etymology.—This species is named for Professor Dr Rosli Hashim, University of Malaya, in recognition of his support for the field work conducted in Malaysia which resulted in the collection of specimens of this species.

Dhanus lunaris sp. nov.
http://zoobank.org/NomenclaturalActs/urn:lsid:zoobank.org:act:6072C16A-EB43-4366-AA75-01E8DE02AC11
(Figs. 3C, 7)

Material examined.—*Holotype female*. CAMBODIA: *Kampot*: Grotte de Kampong Trach [10°34′N, 104°28′E], sur les parois, relativement sèches, November 1967, Cl. Boutin (MNHN Ps-KH5).

Diagnosis.—*Dhanus lunaris* is most similar to *D. tioman* as both have the trichobothria of the chelal hand extending for most of the length of the hand (Figs. 7B, 9B) and they both lack microsetae on the chelal hand near trichobothria *eb* and *esb* (Figs. 7D, 9C). *Dhanus lunaris* has only 29 trichobothria on the fixed chelal finger and hand, including 6 in the *ib* region (Fig. 3C), whereas *D. tioman* has 31 trichobothria, with 7 in the *ib* region (Fig. 3D). *Dhanus lunaris* is larger than *D. tioman* and has thinner pedipalpal segments, e.g., chela (with pedicel) length 2.11 (♀) mm and 3.20 (♀) x longer than broad.

Description (adult).—*Color:* pedipalps and carapace red-brown; chelicerae and legs yellow-brown; tergites and sternites pale yellow-brown.

Setae: generally long, straight or slightly curved, and acicular.

Chelicera (Fig. 7C): with 7 setae on hand; movable finger with 1 submedial seta; galea very slender and elongate; fixed finger with 8 teeth; movable finger with 7 teeth; rallum of 4 blades, distal 3 with several small serrations, basal blade broken, not observed; lamina exterior present, very thin.

Pedipalp (Fig. 7B): prolateral faces of femur and patella coarsely rugose, prolateral face of chela slightly rugose, trochanter smooth; trochanter 1.98, femur 4.15, patella 3.35, chela (with pedicel) 3.20, chela (without pedicel) 3.03, hand 0.79 x longer than broad, movable finger 2.06 x longer than hand. Fixed chelal finger with 29 trichobothria, movable chelal finger with 12 trichobothria (Figs. 3C, 7D): *eb*, *esb* and *isb* in straight row at base of finger; *esb*, *et*, *isb* and *it* regions each with 1 trichobothrium; *eb* region with 2 trichobothria; *ib* region with 6 trichobothria, and extending nearly full length of chelal hand; *ist* region with 9 trichobothria; *est* region with 8 trichobothria; *et* slightly distal to *it*; *b* region with 4 trichobothria; *sb* and *st* regions each with 1 trichobothrium; *t* region with 6 trichobothria. Venom apparatus present in both chelal fingers, venom duct terminating in nodus ramosus near *est* region in fixed finger and near basal section of *t* region in movable finger (Fig. 7D). Chelal hand without microsetae near *eb* and *esb* (Fig. 7D). Chelal teeth slightly retrorse, pointed distally, becoming rounded basally, evenly spaced (Fig. 7E), fixed finger with ca. 80 teeth; movable finger with 69 teeth.

Carapace (Fig. 7A): 1.31 x longer than broad; lateral margins evenly convex; with 2 small bulging eyes; without epistome; with *ca.* 36 setae, including 4 near anterior margin and 6 near posterior margin; with shallow posterior furrow.

Coxal region: manducatory process with 2 long apical setae, plus 9 other setae; chaetotaxy of coxae I–IV: 6: 8: 8: 8.

Legs (Fig. 7F, G): femur + patella 2.85 x longer than deep; subterminal tarsal setae bifurcate (Fig. 7H); arolium slightly shorter than claws (Fig. 7H).

Abdomen: tergites and sternites apparently undivided, uniseriate. Tergal chaetotaxy: 6: 7: 8: 10: 12: 11: 12: 11: 12: 8: 8: 2. Sternal chaetotaxy: 4: (1) 4 (1): (1) 7 (1): 10: 12: 12: 11: 10: 10: 10: 2. Setae of tergites and sternites IX-XI acuminate.

Genitalia: with large gonosac covered with scattered pores.

Dimensions (mm), female: holotype: Body length 3.92. *Pedipalp*: trochanter 0.532/0.269, femur 1.31/0.316, patella 1.200/0.358, chela (with pedicel) 2.112, chela (without pedicel) 1.998, hand length 0.520, movable finger length 1.069. Chelicera 0.538/0.230, movable finger length 0.365. Carapace 1.091/0.832; eye diameter 0.052. Leg I: femur 0.624/0.158, patella 0.324/0.146, tibia 0.558/0.096, metatarsus 0.286/0.082, tarsus 0.418/0.058. Leg IV: femur + patella 1.008/0.354, tibia 0.778/0.149, metatarsus 0.352/0.130, tarsus 0.576/0.081.

Remarks.—*Dhanus lunaris* is known from a humid cave in southern Cambodia (Fig. 5). The holotype is slightly depigmented, and displays some troglomorphic adaptations such as large body size and slightly elongated legs.

Etymology.—This species is named for the local, unofficial name of the cave, which translates as Moon Cave (*lunaris*, Latin, of the moon) (Brown 1956).

Dhanus sumatranus (Redikorzev, 1922)
http://zoobank.org/NomenclaturalActs/urn:lsid:zoobank.org:act:2268091F-6C5A-431A-A590-70484F30CD0E
(Figs. 1, 3B, 4, 8)

Ideoroncus sumatranus Redikorzev 1922:545–550, figs. 1–4.

Dhanus sumatranus (Redikorzev): Chamberlin 1930:47, figs.

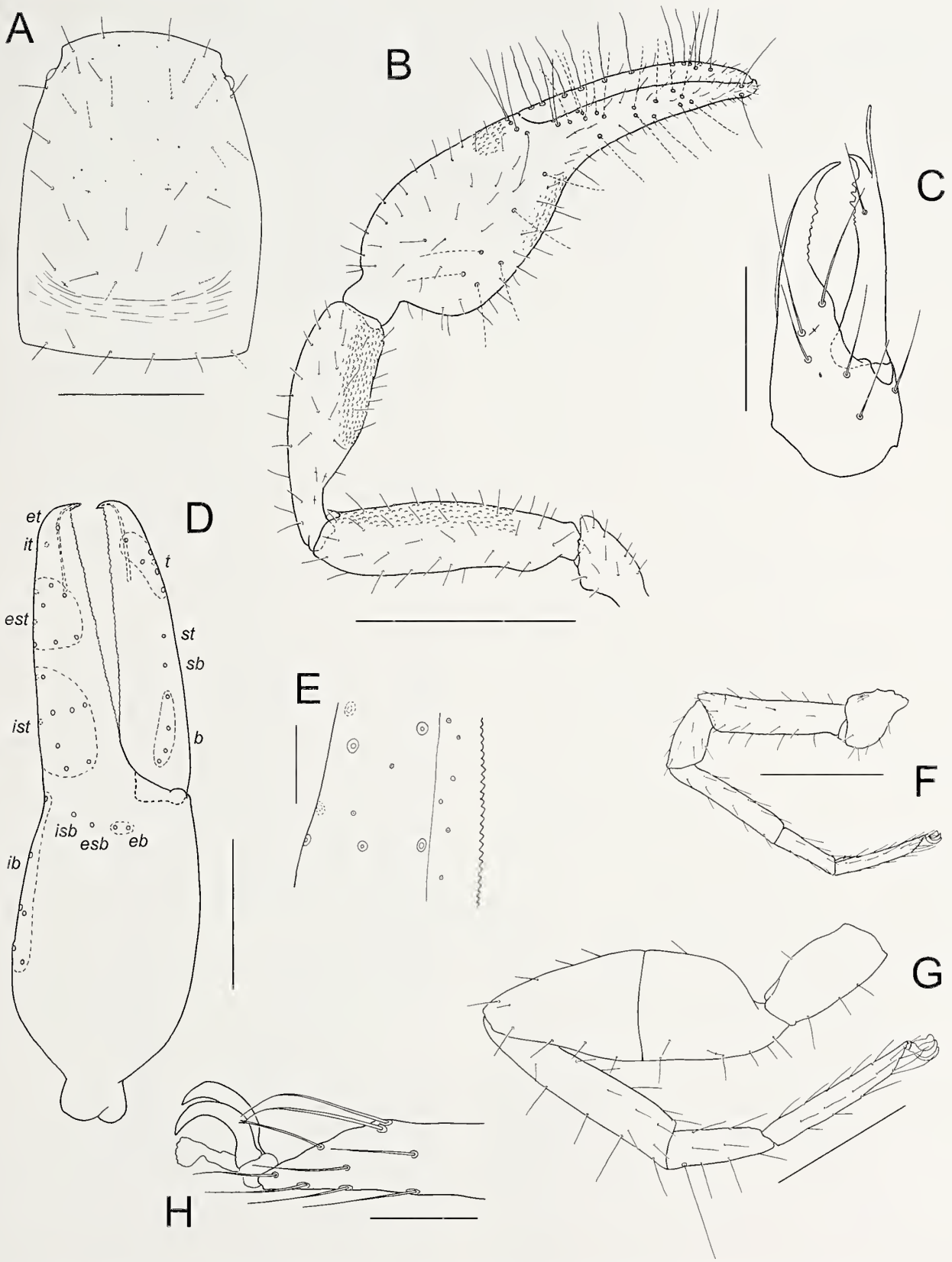

Figure 7.—*Dhanus lunaris* sp. nov., female holotype: A. Carapace; B. Left pedipalp, dorsal; C. Right chelicera; D. Right chela, lateral; E. Detail of fixed chelal finger; F. Left leg I; G. Left leg IV; H. Distal end of tarsus IV showing arolium, claws and subterminal seta, other setae omitted. Scale lines = 1.0 mm (B); 0.5 mm (A, D, F, G); 0.25 mm (C); 0.1 mm (E, H).

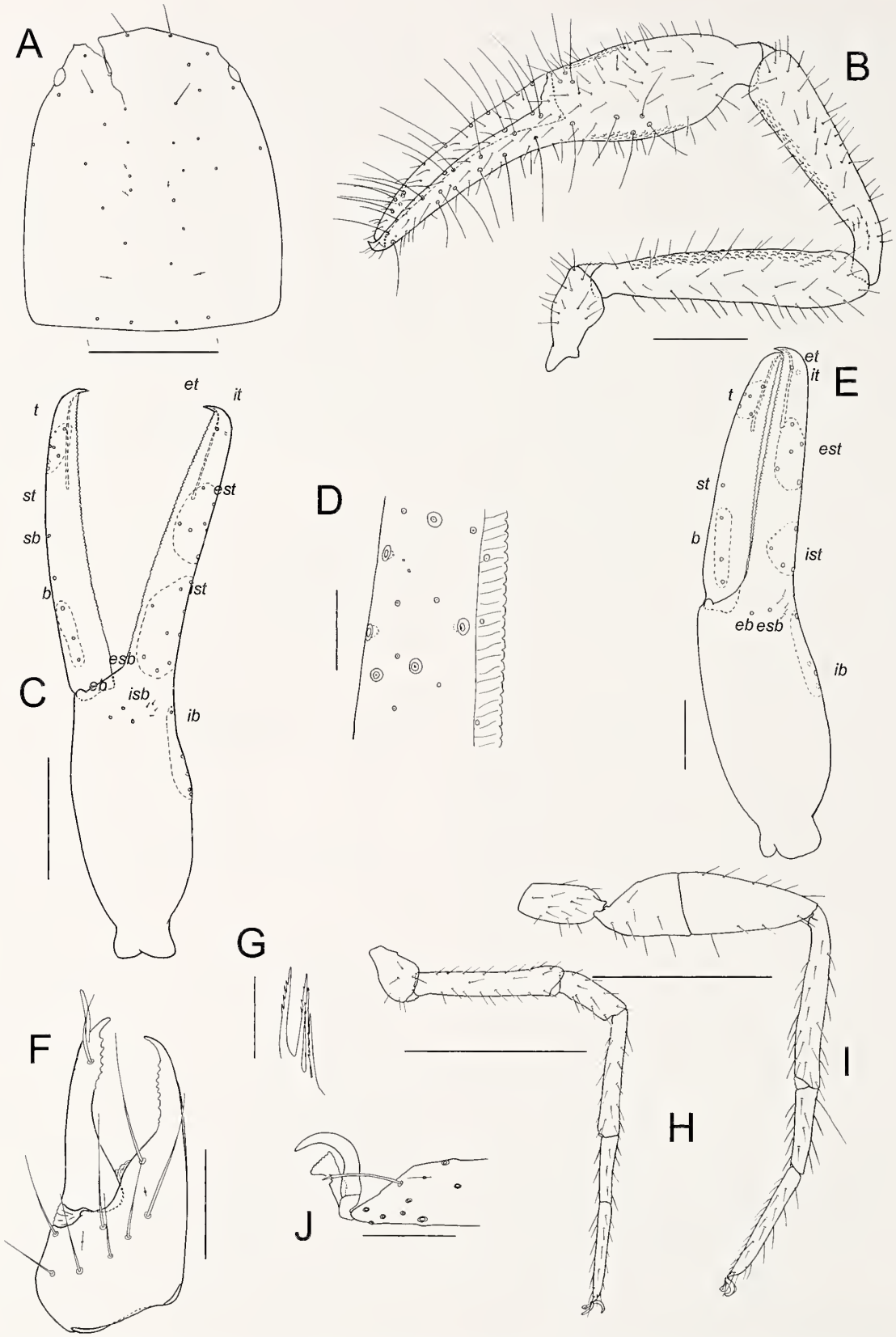

Figure 8.—*Dhanus sumatranus* (Redikorzev), male from Batu Cave, Malaysia (CAS, JC–103.01001), unless stated otherwise: A. Carapace; B. Right pedipalp, dorsal; C. Right chela, lateral; D. Detail of fixed chelal finger; E. Left chela, lateral, tritonymph (WAM T135077); F. Left chelicera, female (CAS, JC–103.01003); G. Rallum, female (CAS, JC–103.01003); H. Leg I (male, CAS, JC–103.01002); I. Leg IV (male, CAS, JC–103.01002). J. Distal end of leg IV, showing arolium, claws and subterminal seta, other setae omitted. Scale lines = 1.0 mm (H, I); 0.5 mm (A–C); 0.25 mm (E); 0.2 mm (F); 0.1 mm (D, F, J).

2ff, 3c; Chamberlin 1931:128, figs. 13n–p, 15j, 25i, 25m–n; Beier 1932a:174–175, fig. 203; Roewer 1936: fig. 30d; Roewer 1937: 257; Beier 1963:51; McClure 1965:71; McClure, Lim & Winn 1967:425; Harvey 1991:319; Harvey, Barba, Muchmore & Pérez 2007: fig. 6; Harvey & Volschenk 2007:368, figs. 1–4; Mosely, Lim & Lim 2012:89; Harvey 2013: unpaginated.

Dhanus doveri Bristowe 1952:699–700, figs. 3–5; McClure 1965:71; McClure, Lim & Winn 1967:425; Harvey 1991:318; Judson 1997:15; Mosely, Lim & Lim 2012:89; Harvey 2013: unpaginated. **Syn. nov.** [http://zoobank.org/NomenclaturalActs/urn:lsid:zoobank.org:act:7B200418-D767-43FD-BAB8-676399679524]

Dhanus sp.: Yussof 1988:figure on p. 29; Yussof 1997:plate 28.

Material examined.—*Syntype female*. MALAYSIA: *Selangor*: Batu Caves (as "Datu Caves") [3°14′N, 101°42′E], lover (=lower?) cave, dark (= Dark Cave), 25 January 1913, O. John (ZISP, no. 187).

Other material. MALAYSIA: *Selangor*: 2 ♂, 1 ♀, Batu Caves [3°14′N, 101°42′E], "dark places" and "permanent dark", E. Mjöberg (CAS, JC–103.01001–3); 10 ♂, 18 ♀, 1 tritonymph, Gua Pandan, Batu Caves, 3°14′28″N, 101°41′14″E, 19 January 2015, dark zone, under rocks and on cave wall, M.S. Harvey, T.W. Lim, Z.K. Hymeir, M.F. Azmi, J. Nordin, L.T. Tshen (ZMUM, WAM T135069–135077).

Diagnosis.—*Dhanus sumatranus* is most similar to *D. hashimi* as both have the trichobothria of the *ib* region restricted to the distal half of the chelal hand (Figs. 6C, 8B), several microsetae on the chelal hand near trichobothria *eb* and *esb* (Figs. 6D, 8C), and 23–26 trichobothria on the fixed chelal finger and hand (Fig. 3A, B). *Dhanus sumatranus* differs from *D. hashimi* by the larger and thinner pedipalpal and leg segments [e.g., chela (with pedicel) 2.275–2.55 (♂), 2.37–2.59 (♀) mm, 4.35–4.85 (♂), 4.09–4.14 (♀) x longer than broad in *D. sumatranus*, and 1.46–1.53 (♂), 1.59–1.71 (♀) mm, 3.81–3.87 (♂), 3.57–3.61 (♀) x longer than broad in *D. hashimi*], and by trichobothria *eb*, *esb* and *isb*, which are arranged in a triangle in *D. sumatranus* (Fig. 8C), but are in a straight line in *D. hashimi*.

Description (adult).—*Color* (Fig. 1): pedipalps and carapace deep red-brown; chelicerae and legs yellow-brown; tergites and sternites pale yellow-brown.

Setae: generally long, straight or slightly curved, and acicular.

Chelicera (Fig. 8F): with 6–8 (♂), 7–8 (♀) long, acuminate setae on hand; movable finger with 1 long subdistal seta; galea very slender and elongate, longer in the female; cheliceral teeth all small and of equal size, fixed finger with 9 (♂), 9 (♀) teeth, movable finger with 6 (♂), 9 (♀) teeth; rallum (Fig. 8G) of 4 thickened serrate blades; lamina exterior present.

Pedipalp (Fig. 8B): trochanter slightly scaly, femur and patella rugose, prolateral and retrolateral faces of chela rugose; trochanter 2.08–2.30 (♂), 2.00–2.31 (♀), femur 5.13–5.23 (♂), 4.86–5.01 (♀), patella 4.19–4.50 (♂), 3.74–4.16 (♀), chela (with pedicel) 4.35–4.85 (♂), 4.09–4.14 (♀), chela (without pedicel) 4.13–4.58 (♂), 3.88–3.98 (♀), hand 1.87–2.13 (♂), 1.81–2.26 (♀) x longer than broad, movable finger 1.20–1.33 (♂), 1.19–1.29 (♀) x longer than hand. Fixed chelal finger with 23–26 trichobothria, movable chelal finger with 11 trichobothria (Figs. 3B, 8C): *eb*, *esb* and *isb* forming a triangle at base of finger, with *isb* situated posterior to *esb*; *eb*, *esb*, *et*, *isb* and *it* regions each with 1 trichobothrium; *ib* region with 5 trichobothria, and extending about half-way along chelal hand; *ist* region with 7–9 trichobothria; *est* region with 6–8 trichobothria; *et* slightly distal to *it*; *b* region with 3 trichobothria; *sb* and *st* regions each with 1 trichobothrium; *t* region with 6 trichobothria. Venom apparatus present in both chelal fingers, venom duct terminating in nodus ramosus near *est* region in fixed finger and midway between *t* region and *st* in movable finger. Chelal hand with small patch of microsetae near *eb* and *esb* (Fig. 8C). Chelal teeth all closely spaced, rounded (Fig. 8D), fixed finger with 79 (♂), 80 (♀) teeth; movable finger with 75 (♂), 72 (♀) teeth.

Carapace (Fig. 8A): 1.16–1.31 (♂), 1.08–1.32 (♀) x longer than broad; lateral margins slightly convex; with 2 small, bulging eyes; small epistome present; with 32 (♂), 34 (♀) setae, including 4 near anterior margin and 4 near posterior margin; with shallow posterior furrow.

Coxal region (Fig. 4A): manducatory process with 2 long apical setae, plus 12 (♂), 10 (♀) additional setae; chaetotaxy of coxae I–IV: ♂, 10: 8: 8: 9; ♀, 7: 6: 7: 9.

Legs (Fig. 8H, I): femur + patella 3.66–4.11 (♂), 3.95–4.68 (♀) x longer than deep; subterminal tarsal setae with 2 small sub-distal denticles (Fig. 8J); arolium undivided and somewhat shorter than claws (Fig. 8J).

Abdomen: tergites and sternites undivided and uniseriate, all setae acuminate; tergal chaetotaxy: ♂, 5: 6: 10: 11: 11: 11: 11: 11: 12: 8 (including 4 tactile setae): 6 (including 4 tactile setae): 2; ♀, 5: 6: 7: 10: 12: 12: 11: 12: 12: 8 (including 4 tactile setae): 7 (including 4 tactile setae): 2; sternal chaetotaxy: ♂, 15: (1) 21 (1): (1) 8 [3 + 3] (1): 14: 13: 12: 12: 11: 10: 6 (including 2 tactile setae): 2; ♀, 11: (1) 10 (1): (1) 9 (1): 12: 13: 12: 12: 12: 11: 6 (including 2 tactile setae): 2.

Genitalia: male with median genital sac deeply bipartite (Fig. 4E); female with large gonosac covered with pores (Fig. 4G).

Dimensions (mm): Males: WAM T135077A followed by other males (when measured): Body length 3.62 (3.70). *Pedipalp*: trochanter 0.53/0.255 (0.58–0.62/0.26–0.27), femur 1.49/0.285 (1.48–1.54/0.285–0.30), patella 1.35/0.30 (1.34–1.41/0.32), chela (with pedicel) 2.255/0.465 (2.275–2.35/0.505–0.54), chela (without pedicel) 2.13 (2.15–2.23), hand length 0.99 (0.945–1.025), movable finger length 1.19 (1.255–1.31). Chelicera 0.48/0.205, movable finger length 0.31. Carapace 1.105/0.845 (1.15–1.155/1.00); eye diameter 0.075. Leg I: femur 0.78/0.135, patella 0.365/0.13, tibia 0.655/0.085, metatarsus 0.345/0.085, tarsus 0.51/0.075. Leg IV: femur + patella 1.15/0.28 (1.19–1.245/0.325–0.335), tibia 0.955/0.125, metatarsus 0.445/0.11, tarsus 0.655/0.09.

Females: WAM T135077F followed by other females (when measured): Body length 3.99 (4.38). *Pedipalp*: trochanter 0.625/0.27 (0.54–0.61/0.265–0.27), femur 1.56/0.315 (1.435–1.46/0.29–0.30), patella 1.435/0.345 (1.31–1.345/0.335–1.35), chela (with pedicel) 2.59/0.625 (2.37–2.42/0.58), chela (without pedicel) 2.43 (2.25–2.315), hand length 1.145 (1.05), movable finger length 1.36 (1.31–1.355). Chelicera 0.56/0.24, movable finger length 0.37. Carapace 1.215/0.92 (1.135–1.165/0.785–1.08); eye diameter 0.075. Leg I: femur 0.865/0.145, patella

0.405/0.14, tibia 0.73/0.115, metatarsus 0.385/0.09, tarsus 0.575/0.075. Leg IV: femur + patella 1.31/0.28 (1.245–1.31/0.27–0.315), tibia 1.05/0.14, metatarsus 0.51/0.115, tarsus 0.75/0.09.

Description (tritonymph).—*Chelicera:* galea long and slender, slightly curved; with 6 setae on hand; 1 on movable finger; fixed finger with 7 small teeth, movable finger with 6 small teeth; rallum composed of 4 blades, all serrate.

Pedipalp: trochanter 2.38, femur 4.50, patella 3.76, chela (with pedicel) 4.20, chela (without pedicel) 3.99, hand 1.85 x longer than broad; movable finger 1.20 x longer than hand (without pedicel). Fixed chelal finger with 17 trichobothria, movable chelal finger with 9 trichobothria (Fig. 8E); *isb* and *sb* absent; *eb* and *esb* at base of finger; *eb*, *esb*, *et* and *it* regions each with 1 trichobothrium; *ib* region with 4 trichobothria; *ist* region with 4 trichobothria; *est* region with 5 trichobothria; *et* slightly distal to *it*; *b* region with 3 trichobothria; *st* region with 1 trichobothrium; *t* region with 5 trichobothria.

Carapace: anterior margin medially prominent; with 2 small, bulging eyes; with 26 setae including 4 setae near anterior margin and 4 near posterior margin.

Legs: much as in adult.

Dimensions (mm) (WAM T135077U): Body length 2.43. *Pedipalp*: trochanter 0.475/0.20, femur 1.125/0.25, patella 1.015/0.27, chela (with pedicel) 1.825/0.435, chela (without pedicel) 1.735, hand length 0.805, movable finger length 0.97. Carapace 0.915/0.66.

Remarks.—Redikorzev (1922) described *Ideoroncus sumatranus* from two adult specimens (one male and one female), neither of which was apparently selected as the holotype. Only the female has been available for this study, which is in fair condition although the right chelicera and both first legs have been dissected from the specimen and are no longer included in the vial with the specimen. The type locality of *I. sumatranus* has been unclear. Redikorzev (1922) stated that the specimens were collected from "Sumatra, Datu Caves, lover cave, dark" in 1913 by O. John. The word "lover" appears to be a typographical error for "lower". Beier (1932b) recorded the locality as "Sumatra: Datu (Batu) Höhlen", and he later altered the type locality of *I. sumatranus* to Batu Caves, near Kuala Lumpur, in Malaysia (Beier 1963). Harvey (1991) tentatively implied that the type locality may be situated in Malaysia. The specimens, however, were definitely from Dark Cave, Batu Caves, Malaysia, and not from Sumatra, as outlined in an article by O. John, the collector of the specimens (John 1914), who even mentioned the collection of pseudoscorpions (p. 363). Therefore, the type locality of *I. sumatranus* is here amended to Dark Cave.

The three slide-mounted specimens recorded as *D. sumatranus* by Chamberlin (1930) are labelled "Batu Caves, peninsular Malaysia" but were reported by Chamberlin (1930) to be from Batu Caves, "Northern Sarawak"; the latter location was confirmed by E. Mjöberg in correspondence with Chamberlin (1930, p. 48). The female type specimen of *I. sumatranus* and the three Mjöberg specimens appear to represent the same species. The meristics of most segments are very similar and, most importantly, all four specimens display the unusual arrangement of trichobothria *eb*, *esb* and *isb* where *esb* is situated slightly in advance of the other two thus forming a triangular arrangement (Fig. 8C). In the other three species of *Dhanus* examined for this study, these three trichobothria are situated in a straight line (Figs. 6D, 7D, 9C). The recently collected specimens from Gua Pandan, a cave in the Batu Caves hill, are also conspecific with the type specimen and Mjöberg's specimens. Due to the morphological congruence, it is very likely that Mjöberg's specimens indeed came from Batu Caves, Kuala Lumpur, rather than from a cave in northern Sarawak. Mjöberg spent several years in south-east Asia, first at the Deli Experimental Station in Sumatra from 1919–1921, and then as curator of the Sarawak State Museum in Borneo 1922–1924. In an account of his experiences published in "Forest life and adventures in the Malay Archipelago" Mjöberg (1930), he does not mention the Batu Caves, but it is conceivable that he did indeed visit this iconic location during his time in Asia. He did indeed visit the Niah Caves in northern Sarawak (Mjöberg 1930), which is perhaps the source of any confusion that might have occurred.

Dhanus doveri was described from an unknown number of specimens collected in Dark Cave by W.S. Bristowe in 1930 and 1931 (Bristowe 1952). These specimens are not present in the BMNH (Judson 1997), and do not appear to have been among Bristowe's personal collection after his death in 1979 (A. Russell-Smith, in litt., 8 July 2013). The original description of *D. doveri* lacks sufficient detail to adequately characterize the species.

A search by the author in Dark Cave in May 2009 failed to locate any specimens of *Dhanus*, but a large population was subsequently found in the dark zone of Gua Pandan in January 2015. As this cave is also situated in the Batu massif, and is only 600 m from Dark Cave (Lim et al. 2010), there is little doubt that these specimens are conspecific with *D. sumatranus*. In particular, they share the triangular arrangement of *eb*, *esb* and *isb*. As *I. sumatranus* and *D. doveri* share the same type locality, I have no hesitation in placing *D. doveri* as a junior synonym of *D. sumatranus*. It is unfortunate that the name of this species, which thus far is known only from the Batu Caves, must be retained as "*sumatranus*". Article 18 of the International Commission on Zoological Nomenclature (1999) states that the original name must be retained, even if the name is inappropriate.

Some of the specimens collected in Gua Pandan were found under rocks, but most were found on the walls of the cave, particularly where the bat guano on the floor of the cave meets the wall. The pseudoscorpions were very abundant, and two were observed to feed on small cockroaches (Fig. 1B), most likely of the cave cockroach *Pycnoscelus striata* (Kirby, 1903) (T.W. Lim, in litt., 24 January 2015).

There is slight variation in the number and positions of the trichobothria of the fixed chelal finger. For example, the three adult specimens collected by Mjöberg have a total of 24–26 trichobothria; one male (JC–103.010001) has 7 trichobothria in the *est* region and 9 in the *ist* region on the left finger and has 6 trichobothria in the *est* region and 8 in the *ist* region on the right finger; the second male (JC–103.010002) has 7 trichobothria in the *est* region and 8 in the *ist* region on the left finger, with the right chela absent from the slide preparation; and the female (JC–103.010003) has 6 trichobothria in the *est* region and 9 in the *ist* region on the left finger, and 8 trichobothria in the *est* region and 7 in the *ist* region on the left finger.

Dhanus tioman sp. nov.
http://zoobank.org/NomenclaturalActs/urn:lsid:zoobank.org:act:59FF9BFF-D58A-4261-8A44-0D45BA84BFBF
(Figs. 3D, 9)

Material examined.—*Holotype male.* MALAYSIA: *Pahang*: Tioman Island, westside of Mount Kajang, 2 km E. of Kg. Genting, 2°47′N, 104°08′E, 24 June 2001, 100 m, M01–41, A. Schulz, K. Vock (MHNG).

Paratypes. MALAYSIA: *Pahang*: 1 ♀, 1 tritonymph, collected with holotype (MHNG); 1 ♂, Tioman Island, westside of Mount Kajang, 2 km E. of Kg. Genting, 2°47′N, 104°08′E, 2 July 2001, 400 m, M01–108, A. Schulz & K. Vock (MHNG); 1 ♀, Tioman Island, westside of Mount Kajang, 2 km E. of Kg. Genting, 2°47′N, 104°08′E, 24 June 2001, 100 m, M01–8, A. Schulz, K. Vock (MHNG); 1 ♀, same data except 25 June 2001, M01–36 (MHNG); 1 ♂, 1 ♀, same data except M01–37 (WAM T140743); 2 ♀, same data except 26 June 2001, M01–39 (MHNG); 2 ♂, 1 tritonymph, same data except M01–67 (MHNG); 1 ♂, 2 ♀, same data except M01–40 (MHNG); 3 ♂, 1 ♀, same data except M01–69 (MHNG); 2 ♂, 2 ♀, 1 tritonymph, 1 deutonymph, same data except 27 June 2001, M01–68 (MHNG); 2 ♂, 1 ♀, same data except 28 June 2001, M01–72 (MHNG); 1 ♀, Tioman Island, westside, 2 km E. of Kg. Tekek, 2°49′N, 104°11′E, 4 July 2001, 500 m, M01–142, A. Schulz, K. Vock (MHNG).

Diagnosis.—*Dhanus tioman* is most similar to *D. lunaris* as both have the trichobothria of the chelal hand extending for most of the length of the hand (Figs. 7D, 9B) and they both lack microsetae on the chelal hand near trichobothria *eb* and *esb* (Figs. 7D, 9B). *Dhanus tioman* has 31 trichobothria on the fixed chelal finger and hand, including 6 in the *ib* region (Fig. 3D), whereas *D. lunaris* has only 29 trichobothria, including 5 in the *ib* region (Fig. 3C). *Dhanus tioman* is smaller than *D. lunaris* and has stouter pedipalpal segments, e.g., chela (with pedicel) length 1.34–1.495 (♂), 1.475–1.64 (♀) mm and 3.29–3.36 (♂), 3.04–3.27 (♀) x longer than broad.

Description (adult).—*Color:* pedipalps and carapace deep red-brown; chelicerae and legs yellow-brown; tergites and sternites pale yellow-brown.

Setae: long, straight, acicular and generally quite slender.

Chelicera: with 7–8 (♂, ♀) setae on hand; movable finger with 1 subdistal seta; galea very slender and elongate; fixed finger with 7 (♂), 7 (♀) teeth; movable finger with 5 (♂), 6 (♀) teeth; rallum of 4 serrate blades; very slender lamina exterior present.

Pedipalp (Fig. 9B): prolateral faces of trochanter finely granulate, prolateral face of femur and patella and both prolateral and retrolateral faces of chela coarsely rugose; trochanter 2.34–2.46 (♂), 2.26–2.45 (♀), femur 3.27–3.52 (♂), 3.20–3.46 (♀), patella 2.44–2.54 (♂), 2.34–2.63 (♀), chela (with pedicel) 3.28–3.36 (♂), 3.04–3.27 (♀), chela (without pedicel) 3.00–3.13 (♂), 2.80–3.03 (♀), hand 1.32–1.56 (♂), 1.44–1.52 (♀) x longer than broad, movable finger 1.05–1.07 (♂), 0.95–1.12 (♀) x longer than hand. Fixed chelal finger with 31 trichobothria, movable chelal finger with 13 trichobothria (Figs. 3D, 9C): *eb*, *esb* and *isb* in straight row at base of finger; *esb*, *et*, *isb* and *it* regions each with 1 trichobothrium; *eb* region with 2 trichobothria; *ib* region with 7 trichobothria; *ist* region with 9 trichobothria; *est* region with 9 trichobothria; *et* slightly distal to *it*; *b* region with 4 trichobothria; *sb* and *st* regions each with 1 trichobothrium; *t* region with 7 trichobothria. Venom apparatus present in both chelal fingers, venom duct terminating in nodus ramosus near *est* region in fixed finger and near basal section of *t* region in movable finger (Fig. 9C). Chelal hand without microsetae near *eb* and *esb* (Fig. 9C). Chelal teeth very low, small and rounded, fixed finger with 73 (♂), 76 (♀) teeth; movable finger with 61 (♂), 64 (♀) teeth.

Carapace (Fig. 9A): 1.06–1.18 (♂), 0.94–1.16 (♀) x longer than broad; lateral margins slightly convex; with 2 small bulging eyes; without epistome; with 40 (♂), 35 (♀) setae, including 4 (♂, ♀) setae near anterior margin and 10 (♂, ♀) near posterior margin; with shallow posterior furrow.

Coxal region: manducatory process with 2 long apical setae, plus 11 (♂, ♀) other setae; chaetotaxy of coxae I–IV: ♂, 9: 8: 9: 11; ♀, 7: 8: 9: 10.

Legs: femur + patella 2.80 (♂), 2.88 (♀) x longer than deep; subterminal tarsal setae with 2–3 distal furcae (Fig. 9F); arolium slightly shorter than claws (Fig. 9F).

Abdomen: tergites and sternites undivided and uniseriate. Tergal chaetotaxy: ♂, 11: 10: 10: 10: 13: 14: 13: 14: 14: 10 (including 4 tactile setae): 10 (including 4 tactile setae): 2; ♀, 12: 10: 11: 11: 12: 12: 12: 11: 12: 9 (including 2 tactile setae): 8 (including 4 tactile setae): 2. Sternal chaetotaxy: ♂, 10: (1) 11 [3 + 3] (1): (1) 9 (1): 16: 14: 15: 15: 15: 11: 12 (including 4 tactile setae): 2; ♀, 8: (1) 8 (1): (1) 8 (1): 15: 15: 15: 16: 13: 13: 10 (including 4 tactile setae): 2. Setae of tergites and sternites IX–XI acuminate.

Genitalia: male with median genital sac deeply bipartite; female with large gonosac covered with pores.

Dimensions (mm): males: holotype followed by other males (when measured): Body length 2.76 (2.13–2.50). *Pedipalp*: trochanter 0.445/0.19 (0.43–0.45/0.175–0.19), femur 0.865/0.26 (0.80–0.88/0.235–0.25), patella 0.72/0.30 (0.67–0.75/0.275–0.295), chela (with pedicel) 1.495/0.455 (1.34–1.46/0.41–0.435), chela (without pedicel) 1.39 (1.27–1.36), hand length 0.675 (0.605–0.67), movable finger length 0.778 (0.68–0.725). Chelicera 0.415/0.20, movable finger length 0.28. Carapace 0.76/0.72 (0.69–0.735/0.59–0.64); eye diameter 0.035. Leg I: femur 0.425/0.125, patella 0.215/0.13, tibia 0.365/0.095, metatarsus 0.18/0.07, tarsus 0.325/0.06. Leg IV: femur + patella 0.685/0.245, tibia 0.52/0.125, metatarsus 0.43/0.095, tarsus 0.41/0.065.

Females: paratype (MHNG M01–08) followed by other females (when measured): Body length 3.38 (2.23–3.10). *Pedipalp*: trochanter 0.485/0.21 (0.43–0.49/0.19–0.205), femur 0.99/0.29 (0.80–0.95/0.25–0.275), patella 0.84/0.345 (0.70–0.815/0.28–0.33), chela (with pedicel) 1.64/0.52 (1.395–1.615/0.44–0.52), chela (without pedicel) 1.52 (1.29–1.49), hand length 0.79 (0.635–0.77), movable finger length 0.785 (0.70–0.805). Chelicera 0.485/0.225, movable finger length 0.31. Carapace 0.805/0.86 (0.67–0.85/0.64–0.74); eye diameter 0.045. Leg I: femur 0.455/0.12, patella 0.235/0.125, tibia 0.385/0.095, metatarsus 0.19/0.07, tarsus 0.335/0.06. Leg IV: femur + patella 0.75/0.26, tibia 0.545/0.14, metatarsus 0.255/0.10, tarsus 0.44/0.07.

Description (tritonymph).—*Chelicera:* galea long and slender, slightly curved; with 7 setae on hand; 1 on movable finger; fixed finger with 8 small teeth, movable finger with 9 small teeth; rallum composed of 4 blades, all serrate.

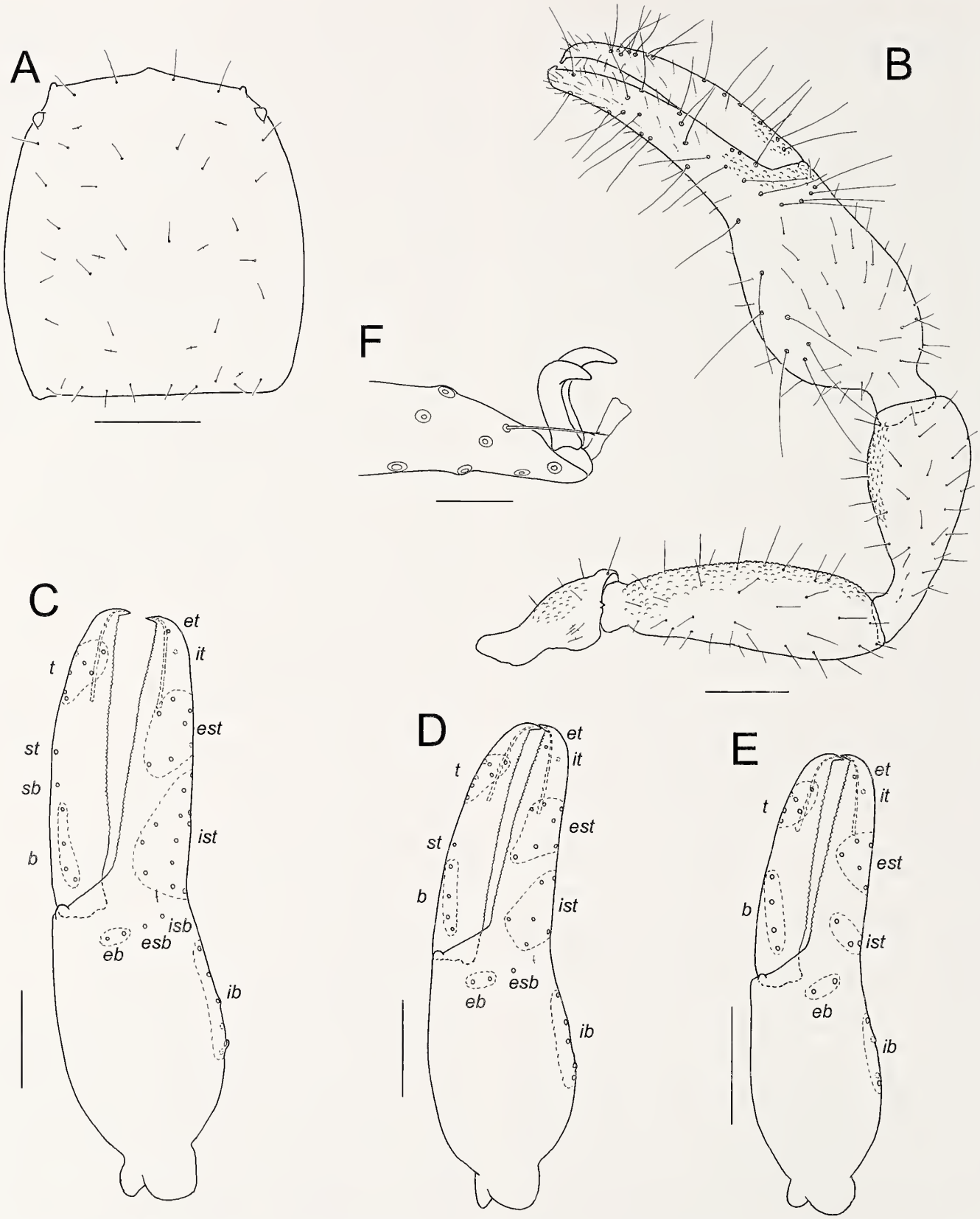

Figure 9.—*Dhanus tioman* sp. nov., male holotype, unless stated otherwise: A. Carapace; B. Right pedipalp, dorsal; C. Left chela, lateral; D. Left chela, lateral, tritonymph paratype; E. Left chela, lateral, deutonymph paratype; F. Distal end of tarsus IV showing arolium, claws and subterminal seta, other setae omitted. Scale lines = 0.25 mm (A–E); 0.1 mm (F).

Pedipalp: trochanter 2.27, femur 3.21, patella 2.40, chela (with pedicel) 3.19, chela (without pedicel) 2.98, hand 1.49 x longer than broad; movable finger 1.06 x longer than hand (without pedicel). Fixed chelal finger with 23 trichobothria, movable chelal finger with 12 trichobothria (Fig. 9D); *isb* and *sb* absent; *esb*, *et* and *it* regions each with 1 trichobothrium; *eb* and *esb* at base of finger; *eb* region with 2 trichobothria; *ib* region with 5 trichobothria; *ist* region with 6 trichobothria; *est* region with 7 trichobothria; *et* slightly distal to *it*; *b* region with 4 trichobothria; *st* region with 1 trichobothrium; *t* region with 6 trichobothria.

Carapace: anterior margin medially prominent; 1 pair of small eyes present; with 33 setae including 4 setae near anterior margin and 9 near posterior margin.

Legs: as in adult.

Dimensions (mm): Body length 2.56. *Pedipalp*: trochanter 0.384/0.169, femur 0.706/0.220, patella 0.621/0.259, chela (with pedicel) 1.25/0.392, chela (without pedicel) 1.170, hand length 0.583, movable finger length 0.618. Carapace 0.656/0.621.

Description (deutonymph).—*Chelicera:* galea long and slender, slightly curved; with 6 setae on hand; 1 on movable finger; fixed finger with 6 small teeth, movable finger with 4 small teeth; rallum composed of 4 blades, all serrate.

Pedipalp: trochanter 2.36, femur 3.61, patella 2.26, chela (with pedicel) 3.20, chela (without pedicel) 3.07, hand 1.51 x longer than broad; movable finger 1.02 x longer than hand (without pedicel). Fixed chelal finger with 16 trichobothria, movable chelal finger with 10 trichobothria (Fig. 9D); *isb* and *sb* absent; *esb*, *et* and *it* regions each with 1 trichobothrium; *eb* and *esb* at base of finger; *eb* region with 2 trichobothria; *ib* region with 4 trichobothria; *ist* region with 3 trichobothria; *est* region with 5 trichobothria; *et* slightly distal to *it*; *b* region with 4 trichobothria; *t* region with 6 trichobothria.

Carapace: anterior margin medially prominent; 1 pair of small eyes present; with 25 setae including 4 setae near anterior margin and 6 near posterior margin.

Legs: as in adult.

Dimensions (mm): Body length 1.41. *Pedipalp*: trochanter 0.295/0.125, femur 0.56/0.155, patella 0.44/0.195, chela (with pedicel) 0.945/0.295, chela (without pedicel) 0.905, hand length 0.445, movable finger length 0.455. Carapace 0.44/0.385.

Remarks.—*Dhanus tioman* has only been collected from rainforest leaf litter habitats on Pulau Tioman (Fig. 5) in southern Malaysia, where it occurs sympatrically with *Shravana withi*.

Etymology.—The specific epithet is a noun in apposition taken from the type locality, Pulau Tioman.

Shravana Chamberlin, 1930

http://zoobank.org/NomenclaturalActs/urn:lsid:zoobank.org:act:F041190B-270B-4B74-B0A1-DD3790C1CD78

Shravana Chamberlin, 1930:48; Beier, 1932a:175–176; Mahnert, 1984:679; Harvey, 1991:322; Harvey, 2013: unpaginated.

Nhatrangia Redikorzev, 1938:78–79; Mahnert, 1984:680–681; Harvey, 1991:321; Harvey, 2013: unpaginated. First synonymized by Beier (1967). [http://zoobank.org/NomenclaturalActs/urn:lsid:zoobank.org:act:6EA06891-2D6D-4342-A911-E422F11C73E5]

Type species.—*Shravana: Ideobisium (Ideoroncus) laminatus* With, 1906, by original designation. *Nhatrangia*: *Nhatrangia dawydoffi* Redikorzev, 1938, by monotypy.

Diagnosis.—Species of *Shravana* differ from all other genera except *Dhanus* and *Negroroncus* by the presence of a thin lamina exterior on the chelicera (Figs. 14D, 16B, 18B). They differ from *Dhanus* by the long arolium (e.g., Fig. 17E), and from *Negroroncus* by the lack of a ventral hooked process on the arolium (e.g., Fig. 17E).

Description (adult).—*Setae:* generally long, straight or slightly curved, and acicular.

Chelicera: hand with 6–8 (or occasionally 5) long, acuminate setae; movable finger with 1 long subdistal seta; rallum of 4 thickened blades, all blades serrate; lamina exterior present; galea long and slender.

Pedipalp: long and slender; patella with disto-prolateral excavation. Fixed chelal finger with 20–31 trichobothria, movable chelal finger with 10–14 trichobothria (Fig. 10): *esb*, *isb*, *et* and *it* regions each with 1 trichobothrium; *eb* region with 1–3 trichobothria; *est* region with 6–9 trichobothria; *ib* region with 4–6 trichobothria; *ist* region with 5–12 trichobothria; *b* region with 2–4 trichobothria; and *t* region with 6–8 trichobothria. Venom apparatus present in both chelal fingers, venom duct terminating in nodus ramosus near *est* region in fixed finger and near *t* region in movable finger. Chelal teeth juxtadentate; base of fixed chelal finger without small denticles; chelal hand with retrolateral condyle small and rounded; without patch of microsetae near *eb*, *esb* and *isb*.

Carapace (e.g., Fig. 17A): with 2 small, bulging eyes; epistome present; posterior furrow either absent or very shallow.

Coxal region (Fig. 17A): manducatory process with 2 long distal setae; median maxillary lyrifissure present and subbasally situated.

Legs: femur I and II without basal swelling; femur I much longer than patella I; suture line between femur IV and patella IV transverse; metatarsus shorter than tarsus; subterminal tarsal setae distally bifurcate or trifurcate; arolium undivided and longer than claws, without ventral hooked process; claws slender and simple.

Abdomen: tergites and sternites usually with indication of medial division, consisting of an anterior and posterior desclerotisation of the sclerite. Pleural membrane longitudinally striate. Each stigmatic sclerite with 1 seta; spiracles simple, with spiracular helix. Anal operculum not abutting sternite X (Fig. 11B).

Genitalia: male with median genital sac deeply bipartite (Fig. 11E); female with large gonosac covered with pores (Fig. 11G).

Description (tritonymph).—*Pedipalp:* fixed finger and hand with 16–25 trichobothria, movable finger with 8–12 trichobothria (Figs. 13E, 18F, 19F, 20E, 21E); *esb*, *it* and *et* regions each with 1 trichobothrium; *eb* region with 1–3 trichobothria; *ib* region with 4 trichobothria; *ist* region with 3–7 trichobothria; *est* region with 5–8 trichobothria; *et* slightly distal to *it*; *b* region with 3–4 trichobothria; *st* region with 1 trichobothrium; *t* region with 5–7 trichobothria; *isb* and *sb* absent.

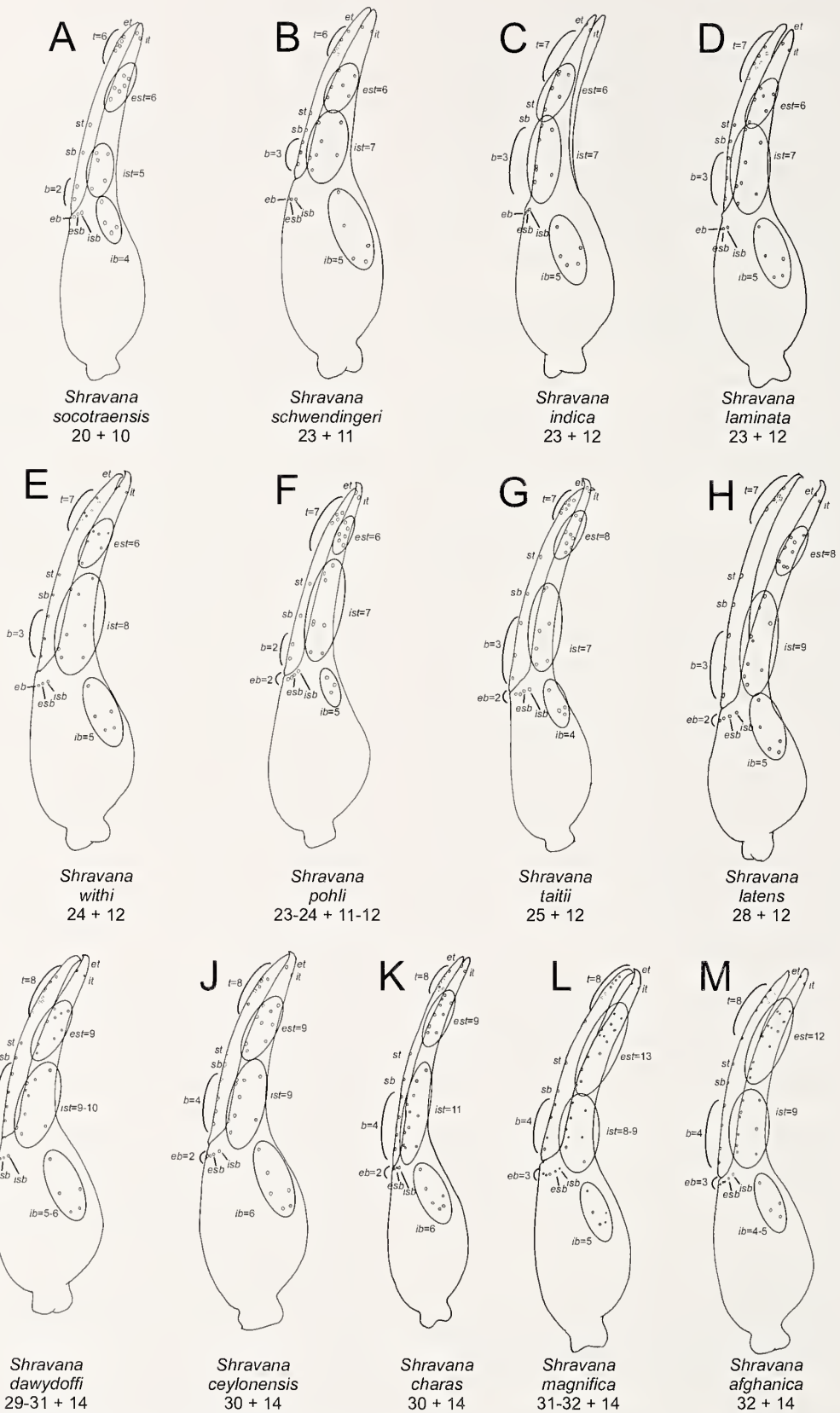

Figure 10.—Trichobothrial patterns of *Shravana* species, taken from left chela (or a mirror image of the right chela), arranged in order of increasing trichobothrial number.

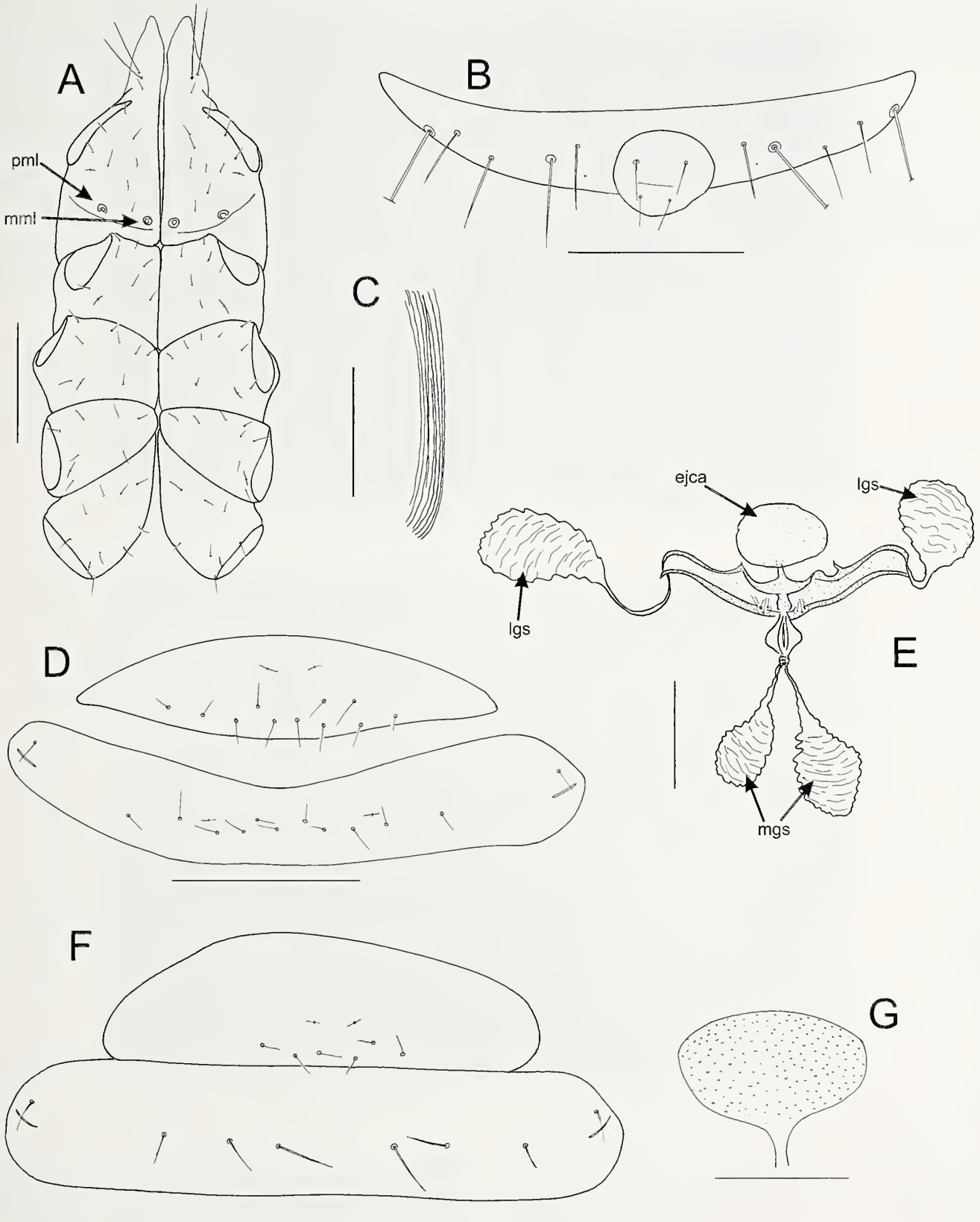

Figure 11.—*Shravana laminata* (With), male and female from Ko Chang, Thailand (MNHG), unless stated otherwise: A. Cephalothorax, ventral, male; B. Sternite XI and anal operculum, female; C. Pleural membrane, male; D. Sternites III and IV, ventral, male; E. Male genitalia, ventral; F. Sternites III and IV, female, ventral; G. Female genitalia, ventral. Abbreviations: ejca, ejaculatory canal atrium; lgs, lateral genital sac; mgs, median genital sac; mml, median maxillary lyrifissure; pml, posterior maxillary lyrifissure. Scale lines = 0.25 mm (A); 0.2 mm (B, D, F, G); 0.1 mm (E); 0.05 mm (C).

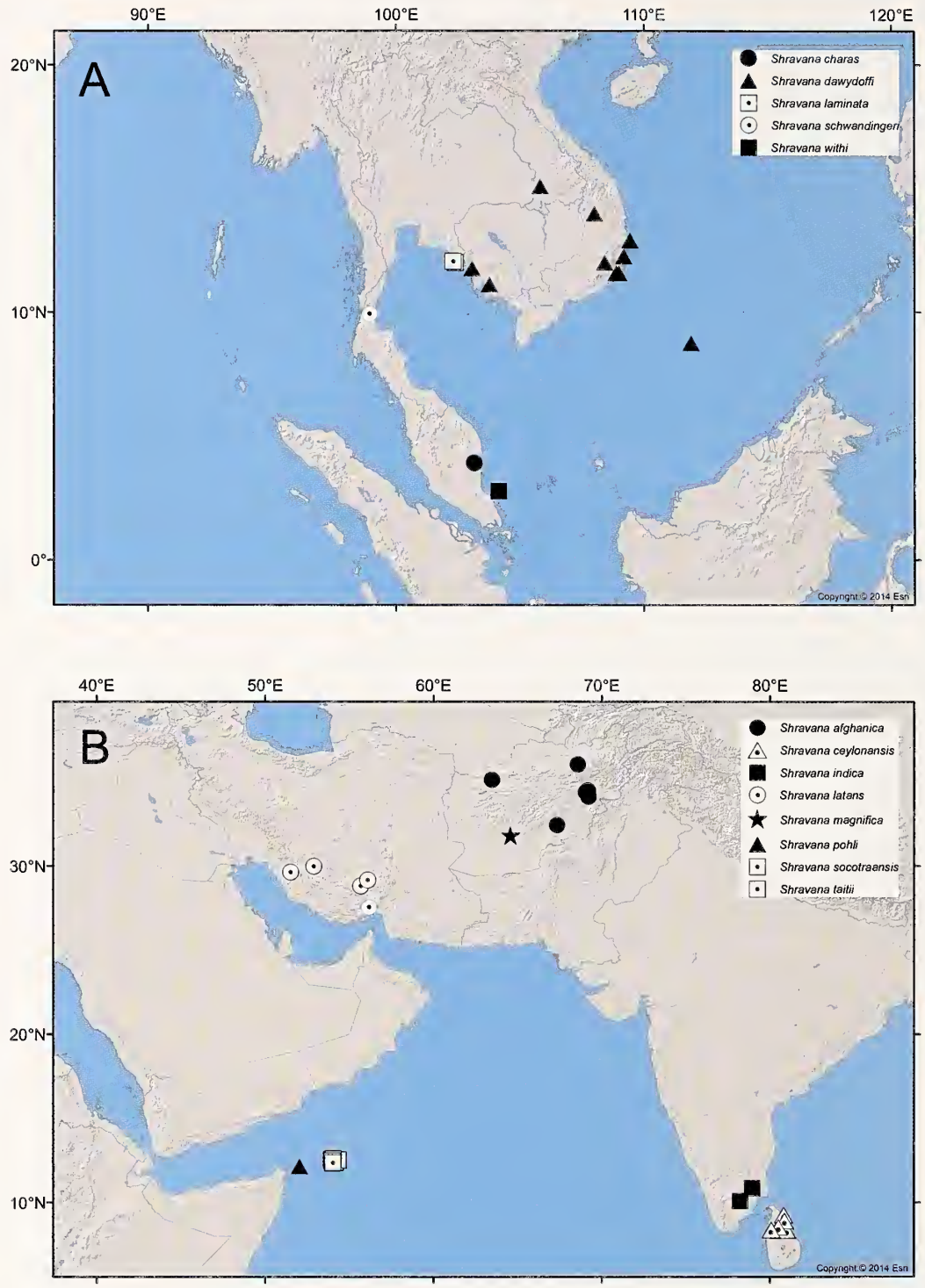

Figure 12.—Distribution of *Shravana* species.

Description (deutonymph).—*Pedipalp:* fixed finger and hand with 9–20 trichobothria, movable finger with 6–10 trichobothria (Figs. 13F, 14C, 19G, 20F); *it* and *et* regions each with 1 trichobothrium; *eb* region with 1–2 trichobothria; *ib* region with 2–4 trichobothria; *ist* region with 2–6 trichobothria; *est* region with 3–6 trichobothria; *et* slightly distal to *it*; *b* region with 4 trichobothria; *t* region with 6 trichobothria; *esb*, *isb*, *sb* and *st* absent.

Description (protonymph).—Unknown.

Remarks.—Mahnert (1984) separated *Nhatrangia* and *Shravana* based on the total number of trichobothria (30/14 and 31/14, including two in the *eb* group in *Nhatrangia*, and 23/12 including only one in the *eb* group in *Shravana*). With the discovery of species with patterns of 20/10, 23/12, 24/12, 25/12, 28/12, 30/14 and 31/14 trichobothria (Table 1), it suggests that basing generic concepts solely on trichobothrial number is fruitless. Therefore, the synonymy of *Nhatrangia* with *Shravana*, which was first proposed by Beier (1967), is

supported. The generic diagnosis proposed here entails the transfer to *Shravana* of several species that were previously included in *Dhanus*: *D. afghanicus*, *D. indicus*, *D. pohli*, *D. socotraensis* and *D. taitii*. All these species have a thin lamina exterior and long arolia that lack a ventral hook.

Members of the genus *Shravana* are found sporadically throughout Asia and the Socotran archipelago (Fig. 12), including Socotra (*S. pohli*, *S. taitii* and *S. socotraensis*), Iran (*S. latens*), Afghanistan (*S. afghanica* and *S. magnifica*), India (*S. indica*), Sri Lanka (*S. ceylonensis*), and south-eastern Asia (*S. charas*, *S. dawydoffi*, *S. laminata*, *S. schwendingeri* and *S. withi*).

Etymology.—The name *Shravana* is probably taken from the Hindu lunar mansion of the same name. The gender of the name was not specified by Chamberlin (1930), but his alteration of the species name *Ideobisium (Ideoroncus) laminatus* to *Shravana laminata* suggests that he considered the name to be feminine.

Nhatrangia is derived from the Vietnamese town of Nha Trang, one of the original localities from which the type species was collected. The gender of the name was not specified by Redikorzev (1938), and the only included species, *N. dawydoffi*, is a patronym and cannot be used to determine gender. The only other species included in the genus, *N. ceylonensis*, is an adjective and likewise does not indicate the gender of the genus.

KEY TO SPECIES OF *SHRAVANA*

1. Trichobothrium *b* region with 2 or 3 trichobothria (Fig. 10A–H) 2
   Trichobothrium *b* region with 4 trichobothria (Fig. 10I–M) 9
2. Trichobothrium *b* region with 2 trichobothria (Fig. 10A, F) 3
   Trichobothrium *b* region with 3 trichobothria (Fig. 10C–E, G, H) 4
3. Chela with 20 trichobothria on fixed finger and hand, and 10 trichobothria on movable finger (Fig. 10A) ... *S. socotraensis*
   Chela with 23–24 trichobothria on fixed finger and hand, and 11–12 trichobothria on movable finger (Fig. 10F) ..... *S. pohli*
4. Trichobothrium *eb* region with 1 trichobothrium (Fig. 10B–E) 5
   Trichobothrium *eb* region with 2 trichobothria (Fig. 10G, H) 8
5. Pedipalpal femur and patella rugose (Figs. 16B, 20B, 21B) 6
   All palpal segments completely smooth (Fig. 17B) ..... *S. laminata*
6. Prolateral face of chelal hand rugose (Fig. 16B) ..... *S. indica*
   Prolateral face of chelal hand smooth (Figs. 20B, 21B) 7
7. Chela with 24 trichobothria on fixed finger and hand, including *ist* region with 8 trichobothria (Fig. 10E); *ib* region situated in distal half of chelal hand (Fig. 10E); movable finger with 12 trichobothria, including *t* region with 7 trichobothria (Fig. 10E) ..... *S. withi*
   Chela with 23 trichobothria on fixed finger and hand, including *ist* region with 6 trichobothria (Fig. 10B); *ib* region situated in middle of chelal hand (Fig. 10B); movable finger with 11 trichobothria, including *t* region with 6 trichobothria (Fig. 10B) ..... *S. schwendingeri*
8. Chela with 25 trichobothria on fixed finger and hand, including *ist* region with 7 trichobothria (Fig. 10G) ..... *S. taitii*
   Chela with 28 trichobothria on fixed finger and hand, including *ist* region with 9 trichobothria (Fig. 10H) ..... *S. latens*
9. Trichobothrium *eb* region with 2 trichobothria (Fig. 10I–K) 10
   Trichobothrium *eb* region with 3 trichobothria (Fig. 10L, M) 12
10. Large troglobitic species, e.g., pedipalpal femur ca. 1.80 mm in length ..... *S. charas*
    Small epigean species, pedipalpal femur less than 1.10 mm in length 11
11. Pedipalpal femur 0.87–0.88 (♂), 0.88–1.05 (♀) mm in length ..... *S. dawydoffi*
    Pedipalpal femur 0.76–0.84 (♂), 0.82–0.91 (♀) mm in length ..... *S. ceylonensis*
12. Smaller in size, e.g., chela (with pedicel) 2.21–2.40 (♂), 2.275–2.475 (♀) mm in length ..... *S. afghanica*
    Larger in size, e.g., chela (with pedicel) 2.90 (♂), 3.25 (♀) mm in length ..... *S. magnifica*

Shravana afghanica (Beier, 1959), comb. nov.
http://zoobank.org/NomenclaturalActs/urn:lsid:zoobank.org:act:59AD1064-E54D-424D-9387-D5767737FA11
(Figs. 10M, 13)

Dhanus afghanicus Beier, 1959:264, fig. 6 (in part; see *Shravana magnifica* sp. nov.); Beier, 1960:41; Beier, 1961:1; Lindberg, 1961:31; Harvey, 1991:318; Harvey, 2013: unpaginated.

Not *Dhanus afghanicus* Beier: Beier, 1971:360–361 (misidentification; see *Shravana latens* sp. nov.).

Material examined.—*Lectotype male (present designation).* AFGHANISTAN: *Kabul*: Bagh-Chah Babar [34°30′N, 69°09′E], sous pierres dans le jardin, 21 June 1957, K. Lindberg (MZLU A.270).

Paralectotypes. AFGHANISTAN: *Baghlan*: 2 tritonymphs, a l'emplacement des fouilles Surkh-Kotal, near Chashmah-ye Shēr (as Tchachméh Cher) [17 km NW. of Pol-Khomri = Puli-Khumri) [36°04′N, 68°35′E], 610 m, 10 October 1957, K. Lindberg (MZLU, A.361); *Kabul*: 2 ♂, collected with lectotype, K. Lindberg (NHMW); 2 ♀, 5 tritonymphs, Kōh-e Shēr Darwāzah (as Mont Cher Dervazéh) [34°30′N, 69°10′E], sous pierres, 20–27 September 1957, K. Lindberg (MZLU, A.400, A.409); 1 deutonymph, Qal'-éh Omar Khan, Tangi Lalander (as Tang-Lalander) [34°24′N, 69°02′E], 1820 m, sous pierres, bord du la rivière, 28 June 1957, K. Lindberg (MZLU, A.252); *Lowgar*: 1 ♀, Surkh Āb (as Sorkhab) [34°08′N, 69°12′E], 2000 m, 10 July 1957, K. Lindberg

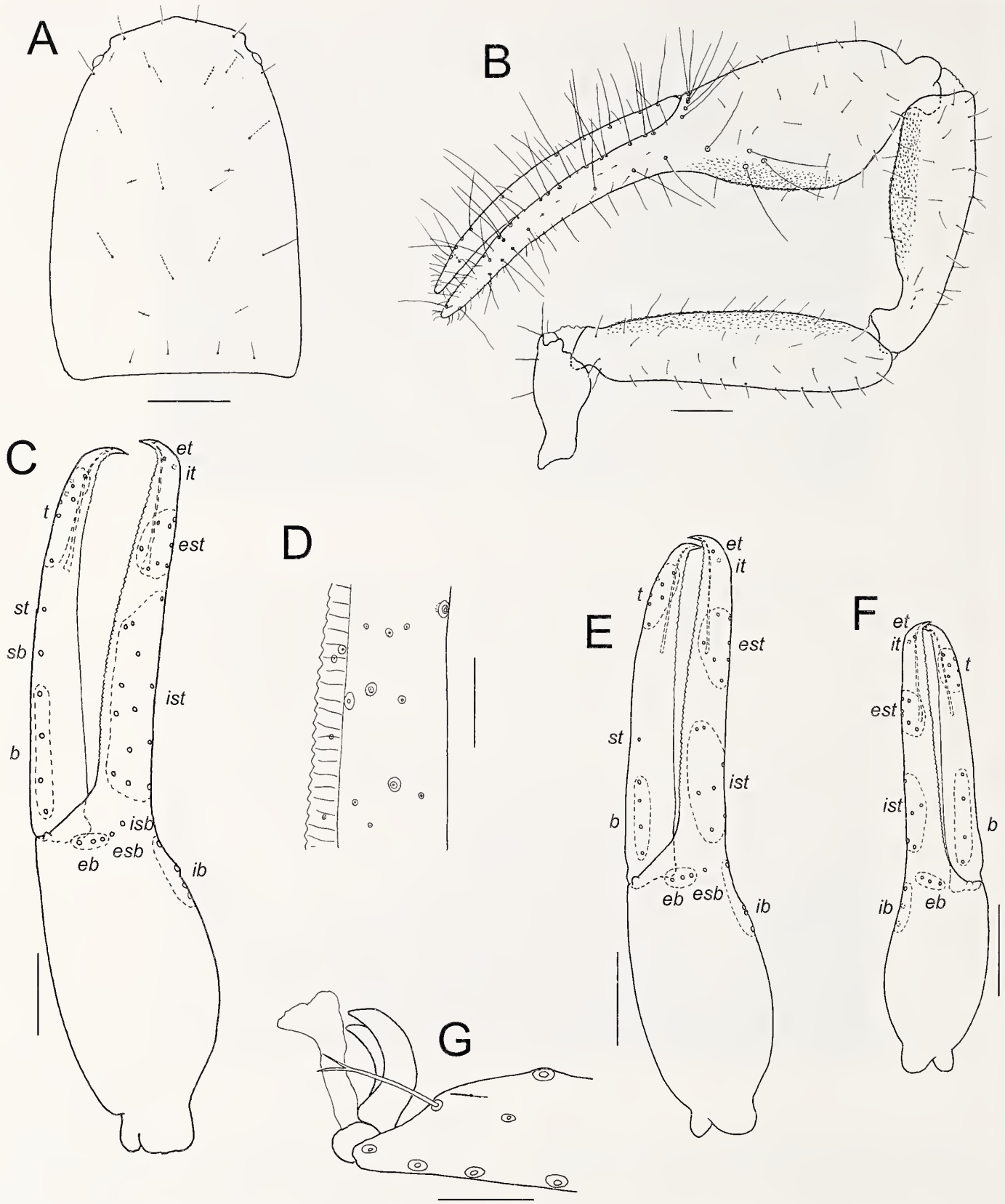

Figure 13.—*Shravana afghanica* (Beier), male lectotype, unless stated otherwise: A. Carapace; B. Right pedipalp, dorsal; C. Left chela, lateral; D. Detail of fixed chelal finger; E. Left chela, lateral, tritonymph (MZLU, A.409); F. Right chela, lateral, deutonymph (MZLU, A.252); G. Distal end of left leg IV showing arolium, claws and subterminal seta. Scale lines = 0.5 mm (A–C); 0.25 mm (E, F); 0.1 mm (D); 0.05 mm (G).

(MZLU, A.424); *Zabul*: 1 deutonymph, Gadzhoi (as Gadjoui) [32°27′N, 67°20′E], sous pierre, 10 September 1957, K. Lindberg (MZLU, A.318).

Other material. AFGHANISTAN: *Badghis*: 1 tritonymph, Darreh-ye Bum (as Darreh-Boum), between Bala Morghab and Qal'Eh-Naou [35°08′N, 63°28′E], 820 m, under stone, 3 July 1959, K. Lindberg (MZLU, A.681); *Vardak*: 1 ♂, 1 ♀, Kouh-Qorough near Tangī Sayyidān (as Tang-Saïdan), 20 km W. of Kabul [34°25′N, 69°07′E], 1820 m, under stone, 31 May 1960, K. Lindberg (MZLU).

Diagnosis.—*Shravana afghanica* differs from all other ideoroncids except *S. magnifica* by the presence of three trichobothria in the *eb* region of the chela (Figs. 10M, 13C). It differs from *S. magnifica* by its smaller size, e.g., chela (with pedicel) 2.21–2.40 (♂), 2.275–2.475 (♀) mm in length, compared with 2.90 (♂), 3.25 (♀) mm in *S. magnifica*.

Description (adult).—*Color:* pedipalps and carapace deep red-brown; chelicerae and legs yellow-brown; tergites and sternites pale yellow-brown.

Setae: generally long, straight or slightly curved, and acicular.

Chelicera: with 6–8 setae on hand; movable finger with 1 subdistal seta; galea very slender and elongate; fixed finger with 8 (♂), 9 (♀) teeth; movable finger with 5 (♂), 7 (♀) teeth; rallum of 4 blades, the 3 distal blades serrate, the basal blade with very small serrations; thin lamina exterior present.

Pedipalp (Fig. 13B): trochanter and femur entirely rugose, prolateral face of patella and chela rugose, remainder of patella and chela smooth or with faint striations; trochanter 2.53–2.62 (♂), 2.44–2.50 (♀), femur 4.10–4.45 (♂), 4.10–4.30 (♀), patella 3.03–3.45 (♂), 3.01–3.10 (♀), chela (with pedicel) 3.80–4.00 (♂), 3.55–3.66 (♀), chela (without pedicel) 3.64–3.80 (♂), 3.39–3.41 (♀), hand 1.54–1.69 (♂), 1.33–1.45 (♀) x longer than broad, movable finger 1.31–1.40 (♂), 1.42–1.58 (♀) x longer than hand. Fixed chelal finger with 32 trichobothria, movable chelal finger with 14 trichobothria (Fig. 13C): *eb*, *esb* and *isb* in straight row at base of finger; *esb*, *et*, *isb* and *it* regions each with 1 trichobothrium; *eb* region with 3 trichobothria; *ib* region with 4 (occasionally 5) trichobothria; *ist* region with 9 (occasionally 8) trichobothria; *est* region with 12 trichobothria; *et* slightly distal to *it*; *b* region with 4 trichobothria; *sb* and *st* regions each with 1 trichobothrium; *t* region with 8 trichobothria. Venom apparatus present in both chelal fingers, venom duct terminating in nodus ramosus near *est* region in fixed finger and near basal section of *t* region in movable finger (Fig. 13C). Chelal hand without microsetae near *eb* and *esb* (Fig. 13C). Chelal teeth juxtadentate, fixed finger with ca. 70 (♂), 71 (♀) small, retrorse teeth (Fig. 13D); movable finger with ca. 68 (♂), 69 (♀) very low teeth.

Carapace (Fig. 13A): 1.36–1.61 (♂), 1.44–1.53 (♀) x longer than broad; lateral margins slightly convex; with 2 small bulging eyes; with small but distinct epistome; with 21 setae including 4 near the anterior margin and 4 near the posterior margin; without furrows.

Coxal region: manducatory process with 2 long apical setae, plus 11 (♂, ♀) other setae; chaetotaxy of coxae I–IV: ♂, 8: 8: 10: 11; ♀, 7: 7: 10: 10.

Legs: femur + patella 2.90 (♂), 3.06 (♀) x longer than deep; subterminal tarsal setae deeply bifurcate (Fig. 13G); arolium longer than claws (Fig. 13G).

Abdomen: setae of tergites and sternites IX–XI faintly lanceolate. Tergites and sternites divided and uniseriate. Tergal chaetotaxy: ♂, 6: 6: 8: 9: 10: 9: 9: 9: 8: 8 (including 4 tactile setae): 6 (including 4 tactile setae): 2; ♀, 6: 6: 8: 9: 9: 11: 8: 9: 8: 8 (including 4 tactile setae): 6 (including 4 tactile setae): 2. Sternal chaetotaxy: ♂, 12: (1) 17 [3 + 3] (1): (1) 9 (1): 13: 12: 10: 9: 10: 9 (including 2 tactile setae): 8 (including 2 tactile setae): 2; ♀, 9: (1) 6 (1): (1) 9 (1): 12: 12: 12: 11: 9: 8: 8 (including 2 tactile setae): 2.

Genitalia: male with median genital sac deeply bipartite; female with large gonosac covered with scattered pores.

Dimensions (mm): males: lectotype followed by 3 other males (when measured): Body length 4.02 (ca. 3.48–3.63). *Pedipalp*: trochanter 0.57/0.225 (0.575–0.625/0.225–0.23), femur 1.28/0.305 (1.29–1.425/0.30–0.32), patella 1.105/0.32 (1.045–1.15/0.325–0.35), chela (with pedicel) 2.24/0.56 (2.21–2.40/0.575–0.61), chela (without pedicel) 2.13 (2.095–2.27), hand length 0.945 (0.90–1.00), movable finger length 1.265 (1.26–1.355). Chelicera 0.53/0.19, movable finger length 0.33. Carapace 1.14/0.79 (1.155–1.215/0.755–0.89); eye diameter 0.055. Leg I: femur 0.595/0.20, patella 0.49/0.14, tibia 0.48/0.09, metatarsus 0.245/0.07, tarsus 0.40/0.055. Leg IV: femur + patella 0.985/0.34, tibia 0.775/0.145, metatarsus 0.335/0.105, tarsus 0.485/0.065.

Females: paralectotype from Surkh Āb followed by 3 other females (when measured): Body length 4.24 (3.84–4.70). *Pedipalp*: trochanter 0.61/0.25 (0.585–0.60/0.24), femur 1.375/0.335 (1.32–1.355/0.315–0.385), patella 1.10/0.355 (1.04–1.07/0.345–0.405), chela (with pedicel) 2.475/0.68 (2.275–2.34/0.64), chela (without pedicel) 2.32 (2.17–2.185), hand length 0.965 (0.85–0.96), movable finger length 1.40 (1.275–1.345). Chelicera 0.505/0.225, movable finger length 0.31. Carapace 1.27/0.88 (1.18–1.23/0.805–0.815); eye diameter 0.065. Leg I: femur 0.65/0.15, patella 0.32/0.14, tibia 0.54/0.09, metatarsus 0.25/0.075, tarsus 0.41/0.055. Leg IV: femur + patella 1.01/0.33, tibia 0.77/0.14, metatarsus 0.33/0.11, tarsus 0.505/0.075.

Description (tritonymph).—*Chelicera:* galea long and slender, slightly curved; with 6 setae on hand; 1 on movable finger; fixed finger with 8 small teeth, movable finger with 5 small teeth; rallum composed of 4 blades, all serrate.

Pedipalp: trochanter 2.33, femur 4.21, patella 3.82, chela (with pedicel) 4.28, chela (without pedicel) 4.05, hand 1.63 x longer than broad; movable finger 1.49 x longer than hand (without pedicel). Fixed chelal finger with 24 trichobothria, movable chelal finger with 11 trichobothria (Fig. 13E); *isb* and *sb* absent; *eb* and *esb* at base of finger; *esb*, *et* and *it* regions each with 1 trichobothrium; *eb* region with 3 trichobothria; *ib* region with 4 trichobothria; *ist* region with 7 trichobothria; *est* region with 7 trichobothria; *et* slightly distal to *it*; *b* region with 4 trichobothria; *st* region with 1 trichobothrium; *t* region with 6 trichobothria.

Carapace: anterior margin medially prominent; with 2 small bulging eyes; with 19 setae including 4 setae near anterior margin and 4 near posterior margin.

Legs: much as in adult.

Dimensions (mm): Body length 3.55. *Pedipalp*: trochanter 0.42/0.18, femur 0.99/0.235, patella 0.935/0.245, chela (with pedicel) 1.71/0.40, chela (without pedicel) 1.62, hand length 0.65, movable finger length 0.97. Carapace 0.945/0.645.

Description (deutonymph).—*Chelicera:* galea long and slender, slightly curved; with 6 setae on hand; 1 on movable finger;

fixed finger with 5 small teeth, movable finger with 4 small teeth; rallum composed of 4 blades, all serrate.

Pedipalp: trochanter 2.38, femur 3.92, patella 2.79, chela (with pedicel) 4.03, chela (without pedicel) 3.75, hand 1.48 x longer than broad; movable finger 1.59 x longer than hand (without pedicel). Fixed chelal finger with 19 trichobothria, movable chelal finger with 10 trichobothria (Fig. 13F); *esb*, *isb* and *sb* and *st* absent; *eb* and *esb* at base of finger; *et* and *it* regions each with 1 trichobothrium; *eb* region with 3 trichobothria; *ib* region with 3 trichobothria; *ist* region with 5 trichobothria; *est* region with 6 trichobothria; *et* slightly distal to *it*; *b* region with 4 trichobothria; *t* region with 6 trichobothria.

Carapace: anterior margin medially prominent; with 2 small bulging eyes; with 14 setae including 4 setae near anterior margin and 4 near posterior margin.

Legs: much as in adult.

Dimensions (mm): Body length 2.89. *Pedipalp*: trochanter 0.31/0.13, femur 0.745/0.19, patella 0.545/0.195, chela (with pedicel) 1.29/0.32, chela (without pedicel) 1.20, hand length 0.475, movable finger length 0.755. Carapace 0.705/0.58.

Remarks.—Specimens of *D. afghanicus* have a lamina exterior on the chelicera and long arolia, and the species is therefore transferred to the genus *Shravana*. Beier (1959) selected three specimens from Bagh-Chah Babar as "Typen", of which one was lodged in MZLU and the other two in NHMW. The remaining specimens were regarded as "Paratypen". Beier's practice of not selecting a single specimen that could serve as the holotype was briefly discussed by Harvey (1991). One of the "Paratypen" vials contains specimens that are here considered to represent a different species, named below as *Shravana magnifica*. As the type series of *D. afghanicus* consists of more than one species, a lectotype has been selected from one of the three specimens from Bagh-Chah Babar.

Some of the vials have a differing number of specimens or incorrect sexes or stages than stated by Beier (1959): the two samples from Mont Cher Dervazéh (vials A.400 and A.409) have 4 tritonymphs and 2 ♀, 1 tritonymph, respectively, but Beier (1959) stated a total of 2 ♀, 7 tritonymphs; A.252 has 1 deutonymph, but Beier (1959) stated 2 deutonymphs; A.318 has 1 deutonymph, but Beier (1959) stated 1 tritonymph.

Shravana afghanica is known from central and northern Afghanistan (Fig. 12B), where it occurs under stones. The populations from Qal'-éh Omar Khan (Kabul Province), Surkh-Kotal (Baghlan Province), Gadzhoi (Zabul Province) and Darreh-ye Bum (Badghis Province) are only represented by nymphal specimens. Adult specimens from other sites in Kabul Province are confirmed as specimens of *S. afghanica*, so the identity of the Qal'-éh Omar Khan population seems certain. However, without adults from the other sites, their identification cannot be fully confirmed. The specimens from Iran identified as *D. afghanicus* by Beier (1971) are here considered to represent a separate species, which is described below as *S. latens*.

Shravana ceylonensis (Mahnert, 1984), comb. nov.
http://zoobank.org/NomenclaturalActs/urn:lsid:zoobank.org:act:478EF853-3D17-4EFC-8FF9-8B091C95DD3D
(Fig. 10J)

Shravana dawydoffi (Redikorzev): Beier, 1973:43 (misidentification).

Nhatrangia ceylonensis Mahnert, 1984:681–684, figs. 56–61; Harvey, 1991:322; Harvey, 2013:unpaginated; Batuwita & Benjamin, 2014:12, fig. 6A.

Material examined.—*Holotype male*. SRI LANKA: *North Central Province*: Medawachchiya [8°32′N, 80°29′E], 2 miles N. of Ort, forest litter, 6 February 1970, C. Besuchet, I. Löbl (MHNG).

Paratypes. SRI LANKA: *North Central Province*: 7 ♂, 2 ♀, 2 tritonymphs, same data as holotype (MHNG); 2 ♂, 2 tritonymphs, Mihintale [8°21′N, 80°30′E], 7 February 1970, C. Besuchet, I. Löbl (MHNG); *Eastern Province*: 3 ♂, 2 ♀, Kantalei [8°21′N, 81°00′E], 2 February 1970, C. Besuchet, I. Löbl (MHNG); *Northern Province*: 3 ♂, 1 deutonymph, Mullaittivu [9°16′N, 80°49′E], 6 February 1970, C. Besuchet, I. Löbl (MHNG); 2 ♂, 1 deutonymph, 2 miles NE. of Puliyan [8°55′N, 80°52′E], Waldstreu, 6 February 1970, C. Besuchet, I. Löbl (MHNG).

Diagnosis.—*Shravana ceylonensis* is most similar to *S. charas* and *S. dawydoffi* as all possess 2 trichobothria in the *eb* region and 4 in the *b* region (Fig. 10J). It differs from *S. dawydoffi* and *S. charas* by the dimensions of the pedipalps, e.g., pedipalpal femur 0.76–0.84 (♂), 0.82–0.91 (♀) mm in *S. ceylonensis*; 0.87–0.88 (♂), 0.88–1.05 (♀) mm in *S. dawydoffi*, and 1.945 (♂), 1.80–1.87 (♀) mm in *S. charas*.

Description (adult).—see Mahnert (1984).

Description (tritonymph).—see Mahnert (1984).

Description (deutonymph).—see Mahnert (1984).

Remarks.—This species has been thoroughly described and illustrated by Mahnert (1984). As it has a lamina exterior on the chelicera and long arolia (Mahnert 1984), it is transferred to the genus *Shravana*. *Shravana ceylonensis* is found throughout northern Sri Lanka (Fig. 12B) (Mahnert 1984; Batuwita & Benjamin 2014).

Shravana charas sp. nov.
http://zoobank.org/NomenclaturalActs/urn:lsid:zoobank.org:act:8D8A29B5-0AD1-4000-86DC-02CF274309AF
Figs. 10K, 14

Material examined.—*Holotype female*. MALAYSIA: *Pahang*: Gua Charas, ca. 3 km N. of Panching, 3°54′41.1″N, 103°08′50.2″E, 120 m, limestone cave, 7–8 July 2001, P. Schwendinger (MHNG).

Paratypes. MALAYSIA: *Pahang*: 1 ♀, same data as holotype (MHNG); 1 ♂, 1 ♀, same data except 1–2 June 2004 (MHNG); 1 deutonymph, Gua Charas, 25 km NW. of Kuantan, 3°54′28″N, 103°08′52″E, upper chamber, dark zone of cave, 27 June 2009, M.S. Harvey, K.L. Edward, R. Hashim, S. Dzarawi (WAM T129594).

Diagnosis.—*Shravana charas* most closely resembles *S. ceylonensis* and *S. dawydoffi* as all three species possess 2 trichobothria in the *eb* region and 4 in the *b* region (Fig. 10I–K). *Shravana charas* differs from both of these species by its larger size and very slender appendages, e.g., pedipalpal femur 1.945 (♂), 1.80–1.87 (♀) mm in length, and femur 6.17 (♂), 6.10–6.13 (♀) x longer than broad.

Description (adult).—*Color:* pedipalps and carapace deep red-brown; chelicerae and legs yellow-brown; tergites and sternites pale yellow-brown.

Setae: long, straight, acicular and generally quite slender.

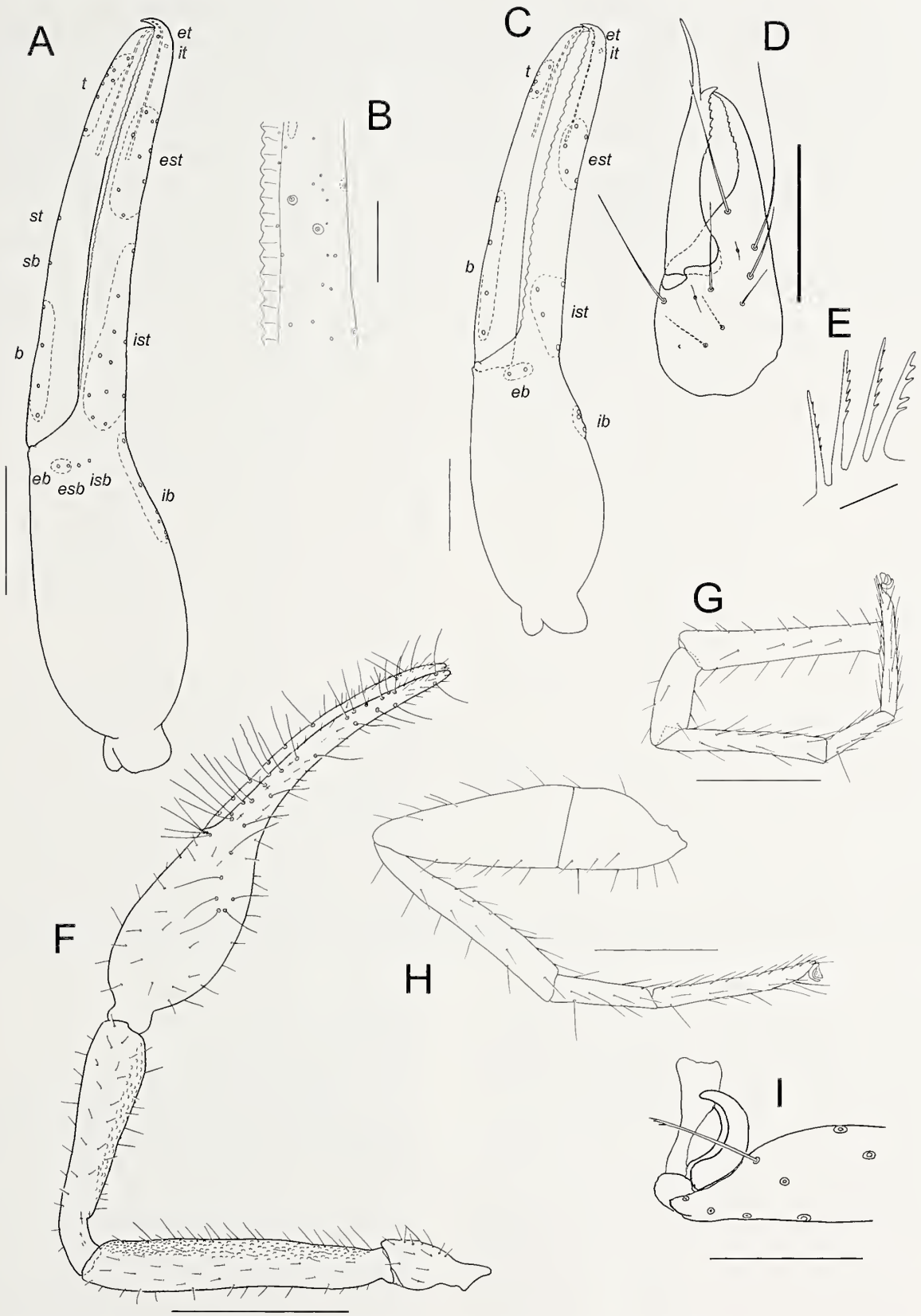

Figure 14.—*Shravana charas* sp. nov., female holotype, unless stated otherwise: A. Left chela, lateral; B. Detail of fixed chelal finger; C. Left chela, lateral, deutonymph paratype; D. Left chelicera; E. Rallum; F. Left pedipalp, dorsal; G. Left leg I; H. Left leg IV; I. Distal end of tarsus IV showing arolium, claws and subterminal seta, other setae omitted. Scale lines = 1.0 mm (F); 0.5 mm (A–C, G, H); 0.25 mm (B); 0.1 mm (I); 0.05 mm (E).

Chelicera (Fig. 14D): with 7 (♂), 8 (♀) setae on hand; movable finger with 1 subdistal seta; galea very slender and elongate; fixed finger with ca. 9 (♂), 8 (♀) teeth; movable finger with ca. 6 (♂), 7 (♀) teeth; rallum (Fig. 14E) of 4 serrate blades; lamina exterior present.

Pedipalp (Fig. 14F): femur and patella rugose on prolateral face, chela finely granulate on prolateral face; trochanter 2.42 (♂), 2.35–2.39 (♀), femur 6.17 (♂), 6.10–6.13 (♀), patella 5.00 (♂), 4.37–4.63 (♀), chela (with pedicel) 5.24 (♂), 4.64–4.70 (♀), chela (without pedicel) 5.00 (♂), 4.43–4.53 (♀), hand 2.17 (♂), 1.95 (♀) x longer than broad, movable finger 1.37 (♂), 1.29–1.39 (♀) x longer than hand. Fixed chelal finger with 32 trichobothria, movable chelal finger with 14 trichobothria (Fig. 14A): *eb*, *esb* and *isb* in straight row at base of finger; *esb*, *et*, *isb* and *it* regions each with 1 trichobothrium; *eb* region with 2 trichobothria; *ib* region with 6 trichobothria; *ist* region with 11 trichobothria; *est* region with 9 trichobothria; *et* slightly distal to *it*; *b* region with 4 trichobothria; *sb* and *st* regions each with 1 trichobothrium; *t* region with 8 trichobothria. Venom apparatus present in both chelal fingers, venom duct terminating in nodus ramosus near *est* region in fixed finger and near basal section of *t* region in movable finger (Fig. 14A). Chelal hand without microsetae near *eb* and *esb* (Fig. 14A). Chelal teeth very low, small and retrorse (Fig. 14B), fixed finger with ca. 52 (♂), 51 (♀) teeth; movable finger with 56 (♂), 49 (♀) teeth; movable chelal finger with several distal lanceolate setae.

Carapace: 1.65 (♂), 1.49 (♀) x longer than broad; lateral margins slightly convex; with 2 bulging eyes; with well developed epistome; with 25 (♂), 26 (♀) setae, including 4 setae near anterior margin and 4 near posterior margin; with single posterior transverse furrow.

Coxal region: manducatory process with 3 long apical setae, plus 13 (♂), 12 (♀) additional setae; chaetotaxy of coxae I–IV: ♂, 10: 7: 10: 8; ♀, 7: 10: 10: 9.

Legs (Fig. 14G, H): femur + patella 3.67 (♂), 3.79 (♀) x longer than deep; subterminal tarsal setae bifurcate (Fig. 14I); arolium longer than claws (Fig. 14I).

Abdomen: tergites and sternites uniseriate; some tergites with small anterior impressions suggesting rudimentary division. Tergal chaetotaxy: ♂, 4: 5: 6: 7: 8: 8: 8: 8: 8: 8 (including 4 tactile setae): 6 (including 2 tactile setae): 2; ♀, 6: 6: 8: 8: 8: 8: 8: 8: 8: 8 (including 4 tactile setae): 6 (including 4 tactile setae): 2. Sternal chaetotaxy: ♂, 12: (1) 6 [3 + 3] (1): (1) 8 (1): 12: 10: 11: 10: 10: 8 (including 2 tactile setae): 9 (including 4 tactile setae): 2; ♀, 6: (1) 6 (1): (1) 7 (1): 10: 9: 9: 9: 7: 6: 8 (including 4 tactile setae): 2. Setae of tergites and sternites IX–XI acuminate.

Genitalia: male with median genital sac deeply bipartite; female with large gonosac covered with pores.

Dimensions (mm): male: paratype: Body length 4.16. *Pedipalp*: trochanter 0.665/0.275), femur 1.945/0.315, patella 1.65/0.33, chela (with pedicel) 2.96/0.565, chela (without pedicel) 2.825, hand length 1.225, movable finger length 1.68. Chelicera 0.485/0.23, movable finger length 0.295. Carapace 1.375/0.835; eye diameter 0.09. Leg 1: femur 0.95/0.175, patella 0.43/0.145, tibia 0.795/0.105, metatarsus 0.39/0.09, tarsus 0.555/0.065. Leg IV: femur + patella 1.375/0.375, tibia 1.065/0.145, metatarsus 0.48/0.11, tarsus 0.755/0.075.

Females: holotype followed by other female (when measured): Body length ca. 4.00 (3.63). *Pedipalp*: trochanter 0.645/0.27 (0.625/0.27), femur 1.80/0.295 (1.87/0.305), patella 1.465/0.335 (1.505/0.325), chela (with pedicel) 2.775/0.59 (2.785/0.60), chela (without pedicel) 2.67 (2.655), hand length 1.15 (1.17), movable finger length 1.60 (1.505). Chelicera 0.49/0.205, movable finger length 0.28. Carapace 1.25/0.84; eye diameter 0.07. Leg I: femur 0.865/0.155, patella 0.385/0.15, tibia 0.705/0.085, metatarsus 0.325/0.08, tarsus 0.53/0.065. Leg IV: femur + patella 1.27/0.335, tibia 0.985/0.135, metatarsus 0.465/0.115, tarsus 0.845/0.075.

Description (deutonymph).—*Chelicera:* galea long and slender, slightly curved; with 6 setae on hand; 1 on movable finger; fixed finger with ca. 8 small teeth, movable finger with ca. 5 small teeth; rallum composed of 4 blades, all serrate.

Pedipalp: trochanter 2.21, femur 5.44, patella 3.57, chela (with pedicel) 4.71, chela (without pedicel) 4.51, hand 1.90 x longer than broad; movable finger 1.40 x longer than hand (without pedicel). Fixed chelal finger with 16 trichobothria, movable chelal finger with 10 trichobothria (Fig. 14C); *esb*, *isb*, *sb* and *st* absent; *eb* region with 2 trichobothria; *et* and *it* regions each with 1 trichobothrium; *eb* at base of finger; *ib* region with 3 trichobothria; *ist* region with 4 trichobothria; *est* region with 5 trichobothria; *et* slightly distal to *it*; *b* region with 4 trichobothria; *t* region with 6 trichobothria.

Carapace: anterior margin medially prominent; with 2 small bulging eyes; with 19 setae including 4 setae near anterior margin and 3 near posterior margin.

Legs: as in adult.

Dimensions (mm): Body length 2.92. *Pedipalp*: trochanter 0.365/0.165, femur 1.01/0.195, patella 0.75/0.21, chela (with pedicel) 1.65/0.35, chela (without pedicel) 1.58, hand length 0.665, movable finger length 0.93. Carapace 0.81/0.72.

Remarks.—*Shravana charas* is currently known only from Charas Cave, situated in the south-eastern region of peninsular Malaysia (Fig. 12A). Specimens of this species are quite large and display some clear troglomorphic features including elongate appendages (Fig. 14F). However, unlike other troglobitic ideoroncids such as *Albiorix anophthalmus* Muchmore, 1999 from Arizona (Muchmore & Pape 1999; Harvey & Muchmore 2013) and *Botswanoncus ellisi* Harvey and Du Preez, 2014 from Botswana (Harvey & Du Preez 2014), the eyes are not noticeably reduced.

Etymology.—The specific epithet is a noun in apposition taken from the type locality.

Shravana dawydoffi (Redikorzev, 1938)
http://zoobank.org/NomenclaturalActs/urn:lsid:zoobank.org:act:B8C63689-F88C-4EDC-94A4-FCFF2CAC5DE7
(Figs. 10I, 15)

Nhatrangia dawydoffi Redikorzev, 1938:79–81, figs. 6–9; Roewer, 1940:345; Beier, 1951:67; Mahnert, 1984a:681, fig. 55; Gao & Zhang, 2013:847–848, figs. 11, 12; Harvey, 2013: unpaginated.

Shravana dawydoffi (Redikorzev): Beier, 1967:343.

Not *Shravana dawydoffi* (Redikorzev): Beier, 1973:43 (misidentification; see *Nhatrangia ceylonensis* Mahnert).

Material examined.—VIETNAM: *Ninh Thuan Province*: 1 ♂, 1 ♀, 14 km W. of Phan Rang [11°34′N, 108°53′E], 21–22 June 1960, R.E. Leech (BPBM).

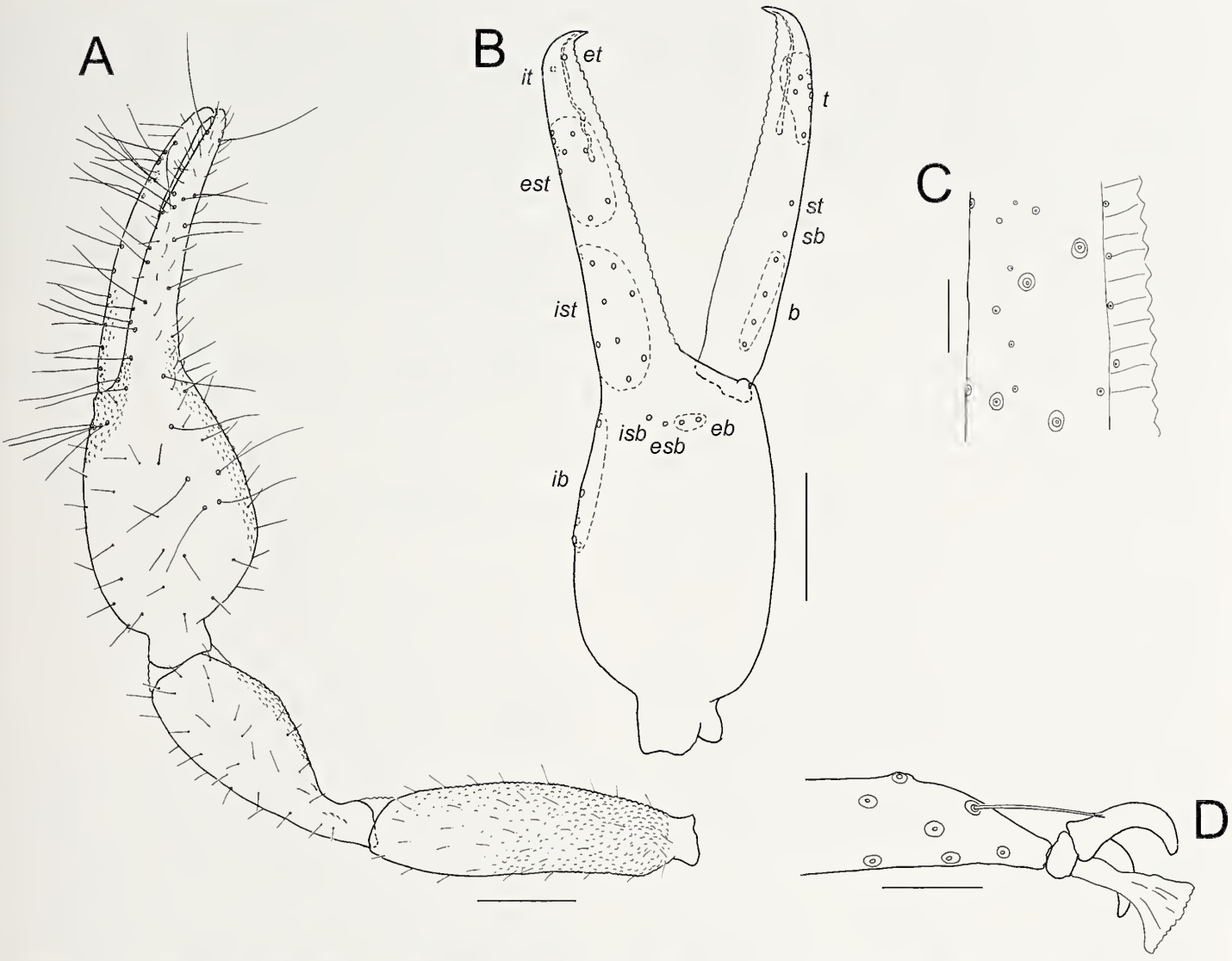

Figure 15.—*Shravana dawydoffi* (Redikorzev), male from 14 km W. of Phan Rang, Vietnam (BPBM): A. Left pedipalp, dorsal; B. Right chela, lateral; C. Detail of fixed chelal finger; E. Distal end of tarsus IV showing arolium, claws and subterminal seta, other setae omitted. Scale lines = 0.25 mm (A, B); 0.05 mm (C, D).

Diagnosis.—*Shravana dawydoffi* is most similar to *S. ceylonensis* and *S. charas*, as all possess 2 trichobothria in the *eb* region and 4 trichobothria in the *b* region (Fig. 10I–K). It differs from *S. ceylonensis* by the presence of 10 trichobothria in the *ist* region (Fig. 10I) (9 trichobothria in *S. ceylonensis*), and by the dimensions of the pedipalps [e.g., pedipalpal femur 0.87–0.88 (♂), 0.88–1.05 (♀) mm in *S. dawydoffi*, and 0.76–0.84 (♂), 0.82–0.91 (♀) mm in *S. ceylonensis*].

Description (adult).—*Color:* pedipalps and carapace deep red-brown; chelicerae and legs yellow-brown; tergites and sternites pale yellow-brown.

Setae: long, straight, acicular and generally quite slender.

Chelicera: with 8 (♂, ♀) setae on hand; movable finger with 1 subdistal seta; galea very slender and elongate; fixed finger with ca. 8 (♂, ♀) teeth; movable finger with ca. 5 (♂, ♀) teeth; rallum of 4 serrate blades; lamina exterior present.

Pedipalp (Fig. 15A): prolateral face of patella, and prolateral and retrolateral faces of femur and chelal hand coarsely rugose, trochanter and retrolateral face of chelal finger finely granulate; trochanter 2.41 (♂), 2.34 (♀), femur 3.78 (♂), 3.74 (♀), patella 2.68 (♂), 2.64 (♀), chela (with pedicel) 3.33 (♂), 3.22 (♀), chela (without pedicel) 3.11 (♂), 3.01 (♀), hand 1.45 (♂), 1.40 (♀) x longer than broad, movable finger 1.22 (♂), 1.27 (♀) x longer than hand. Fixed chelal finger with 29–30 trichobothria, movable chelal finger with 14 trichobothria (Fig. 15B): *eb*, *esb* and *isb* in straight row at base of finger; *esb*, *et*, *isb* and *it* regions each with 1 trichobothrium; *eb* region with 2 trichobothria; *ib* region with 5–6 trichobothria; *ist* region with 9 trichobothria; *est* region with 9 trichobothria; *et* slightly distal to *it*; *b* region with 4 trichobothria; *sb* and *st* regions each with 1 trichobothrium; *t* region with 8 trichobothria. Venom apparatus present in both chelal fingers, venom duct terminating in nodus ramosus near *est* region in fixed finger and basal to *t* region in movable

finger (Fig. 15B). Chelal hand without microsetae near *eb* and *esb* (Fig. 15B). Chelal teeth very low, small and retrorse (Fig. 15C), fixed finger with ca. 37 (♂), 38 (♀) teeth; movable finger with ca. 36 (♂), 30 (♀) teeth.

Carapace: 1.24 (♂), 1.26 (♀) x longer than broad; lateral margins slightly convex; with 2 bulging eyes; with well developed epistome; with ca. 24 (♂), 26 (♀) setae, including 4 setae near anterior margin and 4 near posterior margin; with very shallow posterior furrow.

Coxal region: manducatory process with 3 long apical setae, plus 10 (♂, ♀) additional setae; chaetotaxy of coxae I–IV: ♂, 5: 8: 8: 9; ♀, 7: 6: 8: 10.

Legs: femur + patella 2.18 (♂), 2.33 (♀) x longer than deep; subterminal tarsal setae trifurcate (Fig. 15D); arolium slightly longer than claws (Fig. 15D).

Abdomen: tergites and sternites undivided and uniseriate. Tergal chaetotaxy: ♂, 6: 6: 7: 8: 8: 8: 8: 8: 9: 8 (including 4 tactile setae): 9 (including 4 tactile setae): 2; ♀, 6: 6: 8: 8: 7: 8: 6: 6: 7: 7 (including 4 tactile setae): 8 (including 4 tactile setae): 2. Sternal chaetotaxy: ♂, 8: (1) 12 [4+4] (1): (1) 8 (1): 12: 14: 13: 14: 11: 10: 10 (including 4 tactile setae): 2; ♀, 7: (1) 8 (1): (1) 8 (1): 14: 15: 13: 14: 12: 11: 8 (including 4 tactile setae): 2. Setae of tergites and sternites IX–XI acuminate.

Genitalia: male with median genital sac deeply bipartite; female with large gonosac covered with pores.

Dimensions (mm): male: Body length 2.56. *Pedipalp*: trochanter 0.41/0.17, femur 0.87/0.23, patella 0.71/0.265, chela (with pedicel) 1.45/0.435, chela (without pedicel) 1.35, hand length 0.63, movable finger length 0.77. Chelicera 0.385/0.18, movable finger length 0.255. Carapace 0.755/0.61; eye diameter 0.055. Leg I: femur 0.38/0.115, patella 0.205/0.10, tibia 0.34/0.07, metatarsus 0.175/0.06, tarsus 0.28/0.145. Leg IV: femur + patella 0.71/0.325, tibia 0.53/0.14, metatarsus 0.23/0.095, tarsus 0.37/0.06.

Female: Body length 2.72. *Pedipalp*: trochanter 0.41/0.175, femur 0.88/0.235, patella 0.70/0.265, chela (with pedicel) 1.515/0.47, chela (without pedicel) 1.415, hand length 0.66, movable finger length 0.835. Chelicera 0.40/0.185, movable finger length 0.265. Carapace 0.78/0.62; eye diameter 0.06. Leg I: femur 0.405/0.115, patella 0.215/0.105, tibia 0.35/0.07, metatarsus 0.16/0.055, tarsus 0.26/0.04. Leg IV: femur + patella 0.71/0.305, tibia 0.52/0.15, metatarsus 0.23/0.095, tarsus 0.385/0.07.

Remarks.—*Nhatrangia dawydoffi* was described by Redikorzev (1938) based on numerous specimens collected from three localities in Vietnam: Nhatrang (now known as Nha Trang; 12°15′N, 109°11′E), Plei-Ku, Plateau de Kontum (now Plây Cu; 13°59′N, 108°00′E), and Phanrang (now Phan Rang; 11°34′N, 108°59′E). Mahnert (1984) examined two male and four female type specimens from 'Canda', which appear to be syntypes. This locality is probably a lapsus for Nhatrang, as the date of collection (October 1929) matches one of the Nha Trang collections (29 October 1929) mentioned by Redikorzev (1938). As *N. dawydoffi* has a lamina exterior on the chelicera and long arolia (Mahnert 1984) (Fig. 15D), it is here transferred to the genus *Shravana*, which renders *Nhatrangia* a junior synonym of *Shravana*, which was first proposed by Beier (1967).

The trichobothrial pattern of the syntypes is usually composed of 31 trichobothria on the fixed chelal finger and hand, and 14 on the movable finger, although one female syntype has a pattern of 30/14 with the *ib* region having only 5 trichobothria, and a male syntype also has 30/14 with the *ib* region having only 5 trichobothria on the left chela and the *ist* region having only 9 trichobothria (Mahnert 1984). The male from 14 km W. of Phan Rang examined in this study has a pattern of 29/14 with the *ib* region having 5 trichobothria and the *ist* region having 9 trichobothria (Fig. 15B), whereas the female had a pattern of 30/14 with the *ib* region having 6 trichobothria and the *ist* region having 9 trichobothria. The two specimens examined in this study were both thought to be females by Beier (1967), but are here confirmed as a male and a female.

Shravana dawydoffi is widespread in Vietnam, Cambodia and southern Laos, and also occurs on Spratly Island in the South China Sea (Fig. 12A).

Shravana indica (Murthy & Ananthakrishnan, 1977), comb. nov.
http://zoobank.org/NomenclaturalActs/urn:lsid:zoobank.org:act:693D9C96-47C1-41F0-B8F2-685980A2EEEE
(Figs. 10C, 16)

Dhanus indicus Murthy & Ananthakrishnan, 1977:26–28, fig. 7a, b; Harvey, 1991:318; Harvey, 2013: unpaginated.

Material examined.—INDIA: *Tamil Nadu*: 6 ♂, 3 ♀, Alagarkoil, 21 km NE. of Madurai [10°06′N, 78°13′E], 27–28 December 1989, B. & V. Roth (CAS).

Diagnosis.—*Shravana indica* is most similar to *S. laminata*, *S. schwendingeri* and *S. withi* as all possess only 1 trichobothrium in the *eb* region and 3 trichobothria in the *eb* region (Fig. 10B–E). *Shravana indica* has 1 or 2 small conical processes on the pedal coxae (Fig. 16F), carapace and pedipalps which are lacking in *S. laminata*, *S. schwendingeri* and *S. withi*, and the pedipalpal femur, patella and chelal hand are rugose (Fig. 16D), but are completely smooth in *S. laminata*, and only the femur and patella are rugose in *S. schwendingeri* and *S. withi*.

Description.—*Adults: Color:* pedipalps and carapace deep red-brown; chelicerae and legs yellow-brown; tergites and sternites pale yellow-brown.

Setae: generally long, straight or slightly curved, and acicular.

Chelicera (Fig. 16B): with 7 long, acuminate setae on hand; movable finger with 1 long subdistal seta; galea very slender and elongate, equal-sized in ♂ and ♀; cheliceral teeth generally small and sub-equal in size, fixed finger with 7–8 (♂), 5–7 (♀) teeth, movable finger with 5–6 (♂), 7–8 (♀) teeth; rallum (Fig. 16C) of 4 thickened blades, all blades serrate; lamina exterior present.

Pedipalp (Fig. 16D): prolateral faces of femur and patella strongly rugose, prolateral and retrolateral faces of chela rugose; trochanter 2.19–2.46 (♂), 2.19–2.41 (♀), femur 3.77–4.24 (♂), 3.78–3.90 (♀), patella 2.98–3.19 (♂), 2.72–2.91 (♀), chela (with pedicel) 3.62–3.89 (♂), 3.55–3.69 (♀), chela (without pedicel) 3.41–3.68 (♂), 3.26–3.44 (♀), hand 1.50–1.54 (♂), 1.46–1.53 (♀) x longer than broad, movable finger 1.28–1.34 (♂), 1.23–1.28 (♀) x longer than hand. Fixed chelal finger with 23 trichobothria, movable chelal finger with 12 trichobothria (Fig. 16E): *eb*, *esb* and *isb* in straight line; *eb*, *esb*,

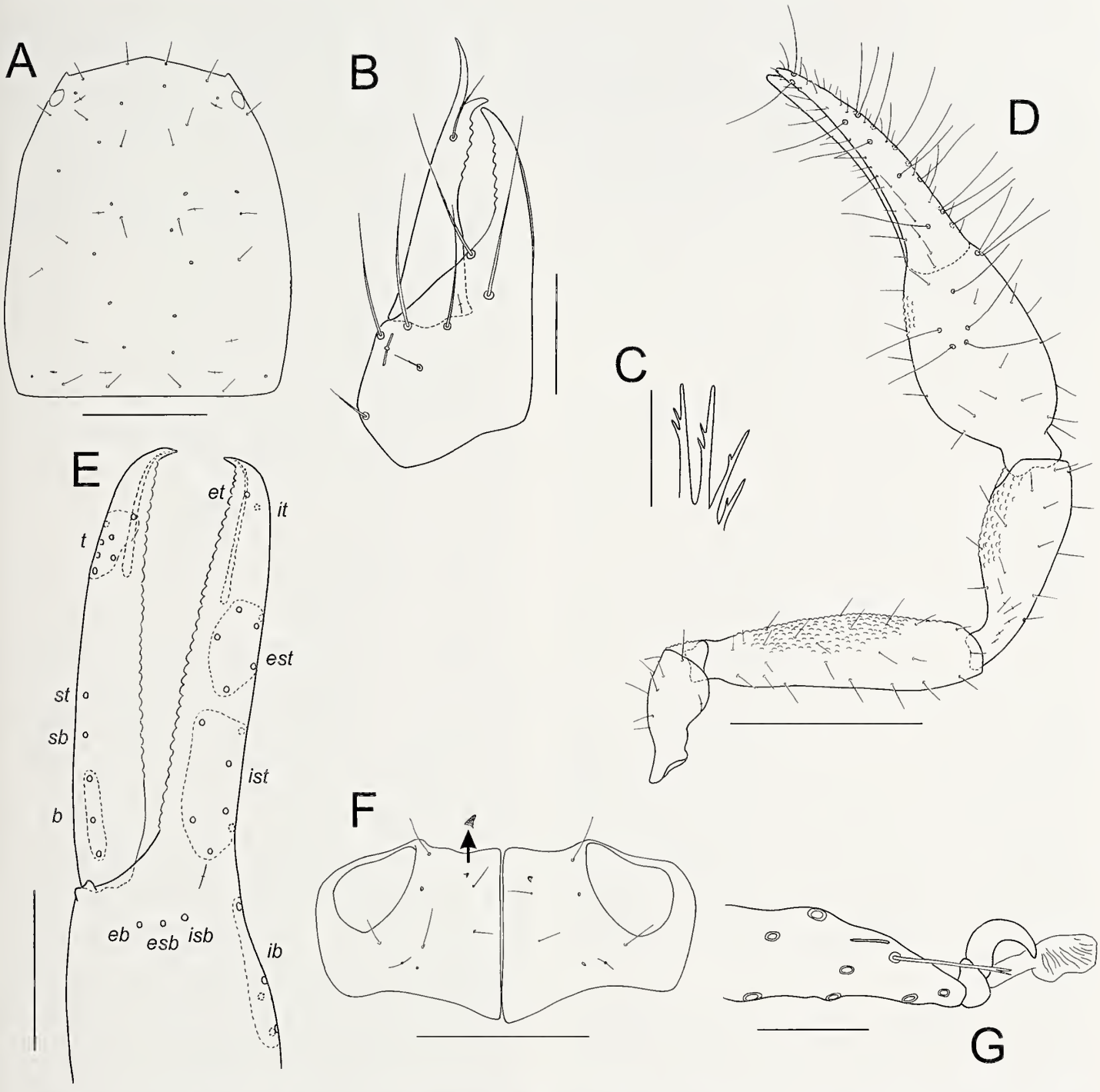

Figure 16.—*Shravana indica* (Murthy and Ananthakrishnan), male from Alagarkoil, India (CAS): A. Carapace; B. Left chelicera; C. Right rallum; D. Right pedipalp, dorsal; E. Left chela, lateral; F. Coxae I; G. Distal end of tarsus IV showing arolium, claws and subterminal seta, other setae omitted. Scale lines = 0.5 mm (D); 0.25 mm (A, E); 0.2 mm (F); 0.1 mm (B); 0.05 mm (C, G).

et, *isb* and *it* regions each with 1 trichobothrium; *ib* region with 5 trichobothria; *ist* region with 7 trichobothria; *est* region with 6 trichobothria; *et* slightly distal to *it*; *b* region with 3 trichobothria; *sb* and *st* regions each with 1 trichobothrium; *t* region with 7 trichobothria. Venom apparatus present in both chelal fingers, venom duct terminating in nodus ramosus near *est* region in fixed finger and near basal end of *t* region in movable finger (Fig. 16E). Chelal hand without microsetae near *eb* and *esb* (Fig. 16E). Chelal teeth all closely spaced, fixed finger with 32 (♂), 36–37 (♀) teeth; movable finger with 29 (♂), 30–32 (♀) teeth.

Carapace (Fig. 16A): 1.21–1.39 (♂), 1.20–1.22 (♀) x longer than broad; lateral margins slightly convex; with 2 small, bulging eyes; epistome absent; with 20 (♂, ♀) setae, including 4 near anterior margin and 4 near posterior margin; without furrows.

Coxal region: manducatory process with 2 long apical setae, plus 11 (♂), 12 (♀) other setae; chaetotaxy of coxae I–IV: ♂, 4: 7: 7: 6–7; ♀, 4: 5–6: 7–8: 8.

Legs: femur + patella 2.39 (♂), 2.75 (♀) x longer than deep; subterminal tarsal setae bifurcate (Fig. 16G); arolium undivided and longer than claws (Fig. 16G).

Abdomen: tergites and sternites divided and uniseriate, all setae acuminate; tergal chaetotaxy: ♂, 5–6: 6: 7: 8: 8: 8: 8: 8: 8: 8 (including 4 tactile setae): 8 (including 4 tactile setae): 2; ♀, 5–6: 6: 7–8: 8: 8–9: 7–8: 8: 8: 8: 8 (including 4 tactile setae): 8 (including 4 tactile setae): 2; sternal chaetotaxy: ♂, 6: (1) 8 [3 + 3] (1): (1) 6 (1): 10–13: 11–12: 10–12: 10–12: 9–10: 9–11: 8 (including 4 tactile setae): 2; ♀, 7–9: (1) 4–5 (1): (1) 6–7 (1): 11: 11: 10–12: 10: 8–10: 8–10: 8 (including 4 tactile setae): 2.

Genitalia: male with median genital sac deeply bipartite; female with large gonosac covered with pores.

Dimensions (mm): males: male from Alagarkoil, India (CAS), followed by other males (when measured): Body length 2.31 (2.16–2.44). *Pedipalp*: trochanter 0.35/0.15 (0.345–0.35/0.14–0.16), femur 0.735/0.195 (0.735–0.805/0.185–0.19), patella 0.625/0.21 (0.615–0.67/0.205–0.215), chela (with pedicel) 1.27/0.345 (1.23–1.29/0.325–0.355), chela (without pedicel) 1.185 (1.16–1.21), hand length 0.525 (0.51–0.545), movable finger length 0.705 (0.675–0.695). Chelicera 0.295/0.14, movable finger length 0.19. Carapace 0.70/0.58 (0.71–0.72/0.515–0.58); eye diameter 0.045. Leg I: femur 0.345/0.095, patella 0.18/0.09, tibia 0.275/0.065, metatarsus 0.135/0.05, tarsus 0.25/0.04. Leg IV: femur + patella 0.58/0.245, tibia 0.425/0.105, metatarsus 0.105/0.07, tarsus 0.315/0.05.

Females: female from Alagarkoil, India (CAS), followed by other females (when measured): Body length 2.99 (2.34–2.96). *Pedipalp*: trochanter 0.34/0.155 0.37–(0.385/0.155–0.16), femur 0.80/0.205 (0.775–0.815/0.205–0.215), patella 0.655/0.225 (0.625–0.67/0.23–0.235), chela (with pedicel) 1.33/0.36 (1.33–1.42/0.375–0.40), chela (without pedicel) 1.24 (1.25–1.305), hand length 0.55 (0.565–0.585), movable finger length 0.705 (0.705–0.72). Chelicera 0.317/0.154, movable finger length 0.200. Carapace 0.730/0.608 (0.72–0.76/0.59); eye diameter 0.045. Leg I: femur 0.36/0.09, patella 0.185/0.095, tibia 0.29/0.065, metatarsus 0.145/0.05, tarsus 0.25/0.045. Leg IV: femur + patella 0.615/0.225, tibia 0.44/0.095, metatarsus 0.20/0.07, tarsus 0.33/0.05.

Remarks.—Although the type specimens of *Dhanus indicus* have not been available for study, a series of specimens collected from Alagarkoil, also situated in Tamil Nadu, only 115 km from Pooindi (Fig. 12B), appear to represent this species as they closely match the original description. This species has a lamina exterior on the chelicera (Fig. 16B), and long arolia (Fig. 16G), and is therefore transferred to the genus *Shravana*.

Shravana indica is known only from Tamil Nadu in southern India (Fig. 12B).

Shravana laminata (With, 1906)
http://zoobank.org/NomenclaturalActs/urn:lsid:zoobank.org:act:7650DD9B-4A45-4AA5-86A2-D7747975BFE2
(Figs. 10D, 17)

Ideobisium (Ideoroncus) laminatus With, 1906:84–87, plate 1 fig. 5a–c.

Shravana laminata (With): Chamberlin, 1930:48; Chamberlin, 1931:75, 167, fig. 36g–h; Beier, 1932a:176; Roewer, 1937:257; Vachon, 1949:fig. 219b (as *Shrawana* [sic] *laminata*); Weygoldt, 1966:fig. 31b (as *Shrawana* [sic] *laminata*); Weygoldt, 1969:fig. 15b; Mahnert, 1984:679–680, figs. 52–54; Harvey, 1991:322; Harvey and Volschenk, 2007:369, figs. 1–4; Harvey, 2013:unpaginated.

Material examined.—*Lectotype female*. THAILAND: *Trat Province*: Ko Chang (as Koh Chang) [12°00′N, 102°23′E], under a stone, January 1900, T. Mortensen (ZMC, JC–445.01001).

Paralectotype. THAILAND: *Trat Province*: 1 ♂, same data as lectotype (ZMC).

Other material. THAILAND: *Trat Province*: 23 ♂, 22 ♀, Ko Chang, west side, 12°03′N, 102°18′E, 3–23 December 1999, A. Schulz (MHNG); 2 ♂, 2 ♀, same data (WAM T140761).

Diagnosis.—*Shravana laminata* is most similar to *S. indica*, *S. schwendingeri* and *S. withi* as all possess only 1 trichobothrium in the *eb* region and 3 trichobothria in the *eb* region (Fig. 10B–E). All pedipalpal segments of *S. laminata* are smooth (Fig. 17B), whereas at least the pedipalpal femur and patella are rugose in *S. indica*, *S. schwendingeri* and *S. withi*.

Description (adult).—*Color:* pedipalps and carapace deep red-brown; chelicerae and legs yellow-brown; tergites and sternites pale yellow-brown.

Setae: long, straight, acicular and generally quite slender.

Chelicera: with 7 (♂, ♀) setae on hand; movable finger with 1 subdistal seta; galea very slender and elongate; fixed finger with 7 (♂), 6 (♀) teeth; movable finger with 4 (♂), 4 (♀) teeth; rallum of 4 serrate blades; slender lamina exterior present.

Pedipalp (Fig. 17B): all pedipalpal segments completely smooth; trochanter 2.33–2.53 (♂), 2.00–2.50 (♀), femur 3.85–4.36 (♂), 3.70–4.04 (♀), patella 3.10–3.35 (♂), 2.90–3.25 (♀), chela (with pedicel) 3.65–4.21 (♂), 3.65–4.04 (♀), chela (without pedicel) 3.45–3.97 (♂), 3.43–3.81 (♀), hand 1.53–1.75 (♂), 1.44–1.66 (♀) x longer than broad, movable finger 1.28–1.42 (♂), 1.27–1.44 (♀) x longer than hand. Fixed chelal finger with 23 trichobothria, movable chelal finger with 12 trichobothria (Fig. 17C): *eb*, *esb* and *isb* in straight row at base of finger; *eb*, *esb*, *et*, *isb* and *it* regions each with 1 trichobothrium; *ib* region with 5 trichobothria; *ist* region with 7 trichobothria; *est* region with 6 trichobothria; *et* slightly distal to *it*; *b* region with 3 trichobothria; *sb* and *st* regions each with 1 trichobothrium; *t* region with 7 trichobothria. Venom apparatus present in both chelal fingers, venom duct terminating in nodus ramosus near *est* region in fixed finger and near basal section of *t* region in movable finger (Fig. 17C). Chelal hand without microsetae near *eb* and *esb* (Fig. 17C). Chelal teeth very low, small and retrorse (Fig. 17D), fixed finger with 34 (♂, ♀) teeth; movable finger with 29 (♂), 27 (♀) very low teeth.

Carapace (Fig. 17A): 1.16 (♂), 1.08 (♀) x longer than broad; lateral margins slightly convex; with 2 bulging eyes; with small epistome; with 22 (♂), 20 (♀) setae, including 4 setae near anterior margin and 4 near posterior margin; with very faint basal furrow.

Coxal region: manducatory process with 2 long apical setae, plus 9 (♂, ♀) other setae; chaetotaxy of coxae I–IV: ♂, 7: 8: 7: 9; ♀, 7: 8: 7: 9.

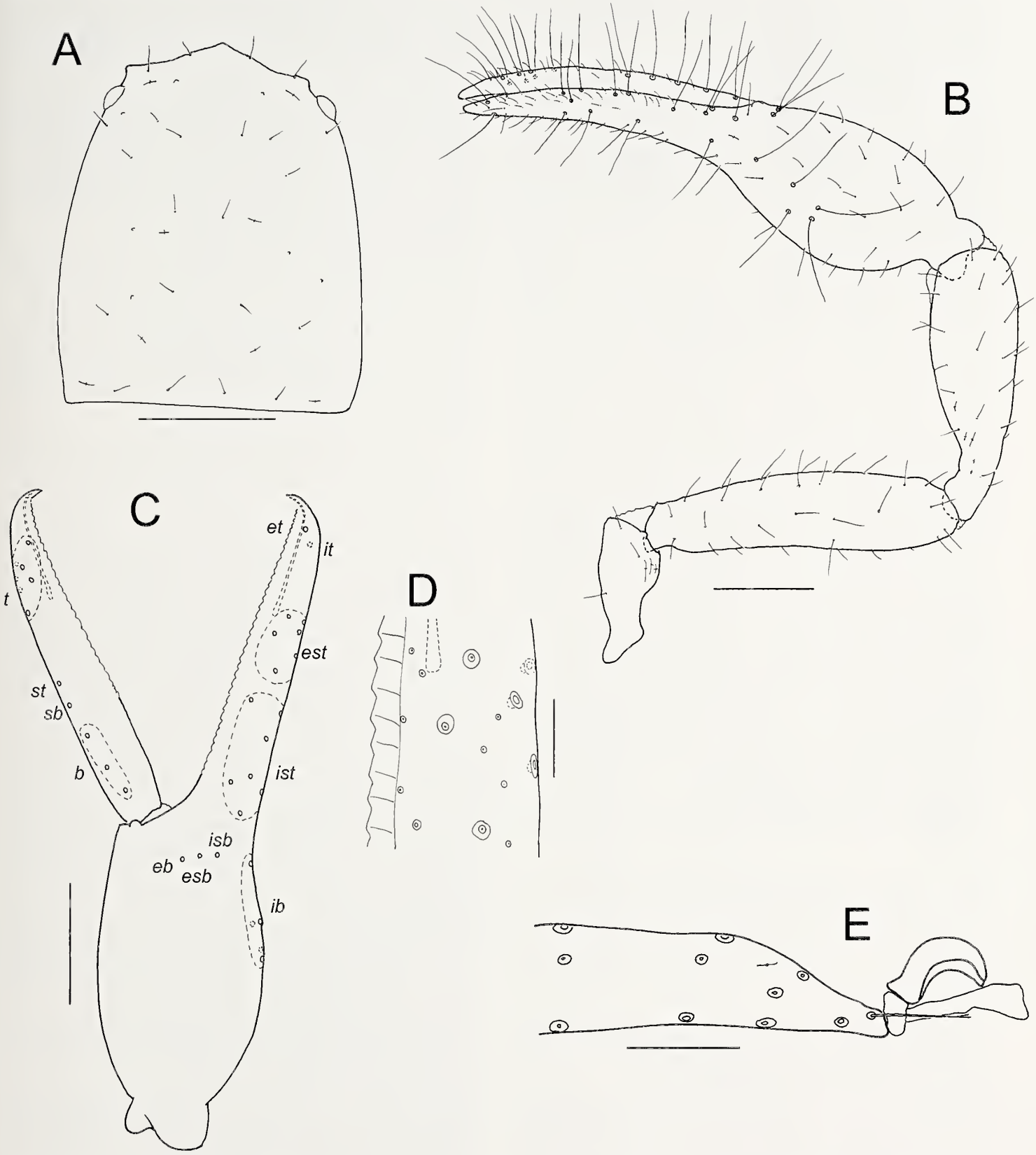

Figure 17.—*Shravana laminata* (With), female lectotype, unless stated otherwise: A. Carapace, male from Ko Chang (MHNG); B. Right pedipalp, dorsal, male from Ko Chang (MHNG); C. Left chela, lateral; D. Detail of fixed chelal finger; E. Distal end of tarsus IV showing arolium, claws and subterminal seta, other setae omitted. Scale lines = 0.25 mm (A–C); 0.05 mm (D, E).

Legs: femur + patella 3.05 (♂), 3.54 (♀) x longer than deep; subterminal tarsal setae bifurcate (Fig. 17E); arolium longer than claws (Fig. 17E).

Abdomen: tergites and most sternites divided and uniseriate. Tergal chaetotaxy: ♂, 3: 6: 8: 8: 10: 8: 8: 8: 9: 10 (including 4 tactile setae): 10 (including 4 tactile setae): 2; ♀, 5: 6: 9: 10: 10: 10: 9: 10: 9: 8 (including 4 tactile setae): 10 (including 4 tactile setae): 2. Sternal chaetotaxy: ♂, 11: (1) 11 [3 + 3] (1): (1) 6 (1): 14: 12: 12: 12: 10: 5 (including 2 tactile setae): 8 (including 4 tactile setae): 2; ♀, 6: (1) 6 (1): (1) 4 (1): 14: 12: 12: 10: 11: 12: 10 (including 4 tactile setae): 2. Setae of tergites and sternites IX–XI acuminate.

Genitalia: male with median genital sac deeply bipartite; female with large gonosac covered with pores.

Dimensions (mm): males: a male from Ko Chang (MHNG) followed by 6 other males (when measured): Body length 2.60. *Pedipalp*: trochanter 0.375/0.15 (0.345–0.385/0.145–0.165), femur 0.755/0.195 (0.75–0.85/0.18–0.215), patella 0.72/0.225 (0.635–0.77/0.20–0.23), chela (with pedicel) 1.365/0.345 (1.315–1.44/0.315–0.375), chela (without pedicel) 1.29 (1.25–1.36), hand length 0.55 (0.535–0.59), movable finger length 0.765 (0.75–0.815). Chelicera 0.325/0.15, movable finger length 0.185. Carapace 0.665/0.575; eye diameter 0.06. Leg I: femur 0.40/0.095, patella 0.195/0.09, tibia 0.30/0.06, metatarsus 0.175/0.05, tarsus 0.25/0.04. Leg IV: femur + patella 0.64/0.21, tibia 0.46/0.095, metatarsus 0.235/0.07, tarsus 0.335/0.05.

Females: a female from Ko Chang (MHNG) followed by 6 other females (when measured): Body length 2.90. *Pedipalp*: trochanter 0.375/0.15 (0.315–0.42/0.15–0.17), femur 0.785/0.205 (0.785–0.91/0.20–0.225), patella 0.715/0.22 (0.67–0.77/0.21–0.25), chela (with pedicel) 1.455/0.37 (1.35–1.595/0.37–0.42), chela (without pedicel) 1.36 (1.27–1.505), hand length 0.60 (0.57–0.655), movable finger length 0.815 (0.735–0.835). Chelicera 0.335/0.16, movable finger length 0.195. Carapace 0.69/0.64; eye diameter 0.055. Leg I: femur 0.415/0.095, patella 0.20/0.095, tibia 0.31/0.06, metatarsus 0.18/0.06, tarsus 0.25/0.055. Leg IV: femur + patella 0.655/0.185, tibia 0.46/0.09, metatarsus 0.245/0.065, tarsus 0.33/0.05.

Remarks.—*Shravana laminata* is currently known only from the island of Ko Chang in the Gulf of Siam (Fig. 12A).

Shravana latens sp. nov.
http://zoobank.org/NomenclaturalActs/urn:lsid:zoobank.org:act:169AE670-0A7C-4F4F-A2A8-FD85E0346237
(Figs. 10H, 18)

Dhanus afghanicus Beier: Beier, 1971:360–361 (misidentification).

Material examined.—*Holotype male*. IRAN: *Fārs*: 5 km NE. of Takht-e-Jamshīd (as Persepolis) [ca. 29°59′N, 52°52′E], under stone, 20 April 1970, F. Ressl (NHMW).

Paratypes. IRAN: *Fārs*: 3 ♂, 4 ♀, same data as holotype (NHMW); 2 ♂, 2 ♀, same data as holotype (WAM T62565); 2 ♂, 2 ♀, *ca.* 100 km W. of Shīrāz [*ca.* 29°38′N, 51°30′E], under stone, 18 April 1970, F. Ressl, K. Bilek (NHMW); 2 ♂, 2 ♀, 2 tritonymphs, 180 km S. of Ābādān [coordinates not calculated; see Remarks], under stone, 20 April 1970, K. Bilek, F. Ressl (NHMW); *Hormozgān*: 1 ♀, 40 km N. of Bandar-e 'Abbās [*ca.* 27°34′N, 56°10′E], under stone, 7 April 1972, K. Bilek (NHMW); *Kermān*: 1 ♀, 80 km S. of Sīrjān [Sa'īdābād] [*ca.* 28°49′N, 55°40′E], under stone, 9 April 1970, F. Ressl (NHMW); 1 ♂, 1 ♀, 52 km S. of Sīrjān [Sa'īdābād] [*ca.* 29°10′N, 56°05′E], under stone, 17 April 1972, F. Ressl (NHMW).

Diagnosis.—*Shravana latens* differs from all other *Shravana* species except *S. taitii* by the presence of 2 trichobothria in the *eb* region and 3 trichobothria in the *b* region (Fig. 10G, 10H). It differs from *S. taitii* by the presence of 28 trichobothria on the fixed chelal finger and hand, including 9 trichobothria in the *ist* region (Fig. 10H), whereas *S. taitii* has 25 trichobothria, including 7 in the *ist* region (Fig. 10G).

Description (adult).—*Color:* pedipalps and carapace deep red-brown; chelicerae and legs yellow-brown; tergites and sternites pale yellow-brown.

Setae: long, straight, acicular and generally quite slender.

Chelicera (Fig. 18B): with 6 (occasionally 5 or 7) setae on hand; movable finger with 1 subdistal seta; galea very slender and elongate; fixed finger with 7 (♂), 10 (♀) teeth; movable finger with 5 (♂), 5 (♀) teeth; rallum (Fig. 18C) of 4 serrate blades; very slender lamina exterior present.

Pedipalp (Fig. 18D): anterior faces of trochanter, femur and chela lightly rugose; trochanter 2.35–2.41 (♂), 2.19–2.53 (♀), femur 4.23–4.57 (♂), 4.17–4.51 (♀), patella 3.00–3.20 (♂), 3.08–3.41 (♀), chela (with pedicel) 3.70–4.48 (♂), 3.58–4.33 (♀), chela (without pedicel) 3.54–4.10 (♂), 3.58–4.16 (♀), hand 1.26–1.50 (♂), 1.29–1.38 (♀) x longer than broad, movable finger 1.76–2.06 (♂), 1.73–2.03 (♀) x longer than hand. Fixed chelal finger with 28 trichobothria, movable chelal finger with 12 trichobothria (Fig. 18E): *eb*, *esb* and *isb* in straight row at base of finger; *esb*, *et*, *isb* and *it* regions each with 1 trichobothrium; *eb* region with 2 trichobothria; *ib* region with 5 trichobothria; *ist* region with 9 trichobothria; *est* region with 8 trichobothria; *et* slightly distal to *it*; *b* region with 3 trichobothria; *sb* and *st* regions each with 1 trichobothrium; *t* region with 7 trichobothria. Venom apparatus present in both chelal fingers, venom duct terminating in nodus ramosus near *est* region in fixed finger and near basal section of *t* region in movable finger (Fig. 18E). Chelal hand without microsetae near *eb* and *esb* (Fig. 18E). Chelal teeth very low, small and retrorse (Fig. 18E), fixed finger with 43 (♂), 40 (♀) teeth; movable finger with several low (♂, ♀) teeth. Movable chelal finger with several distal lanceolate setae.

Carapace (Fig. 18A): 1.44–1.63 (♂), 1.42–1.59 (♀) x longer than broad; lateral margins slightly convex; with 2 bulging eyes; with well developed epistome; with 19 (♂), 24 (♀) setae, including 4 (♂, ♀) setae near anterior margin and 5 (♂), 6 (♀) near posterior margin; without furrows.

Coxal region: manducatory process with 2 long apical setae, plus 9 (♂), 10 (♀) other setae; chaetotaxy of coxae I–IV: ♂, 4: 8: 8: 10; ♀, 9: 8: 10: 10.

Legs (Fig. 18G, H): femur + patella 2.45 (♂), 2.65 (♀) x longer than deep; subterminal tarsal setae bifurcate (Fig. 18I); arolium longer than claws (Fig. 18I).

Abdomen: tergites and sternites undivided and uniseriate; some tergites with small anterior impressions suggesting rudimentary division. Tergal chaetotaxy: ♂, 7: 6: 7: 8: 8: 8: 8: 7: 6: 8 (including 4 tactile setae): 8 (including 4 tactile setae): 2; ♀, 6: 7: 8: 8: 8: 8: 8: 9: 6: 8 (including 4 tactile setae): 8 (including 4 tactile setae): 2. Sternal chaetotaxy: ♂, 6: (1) 10 [3

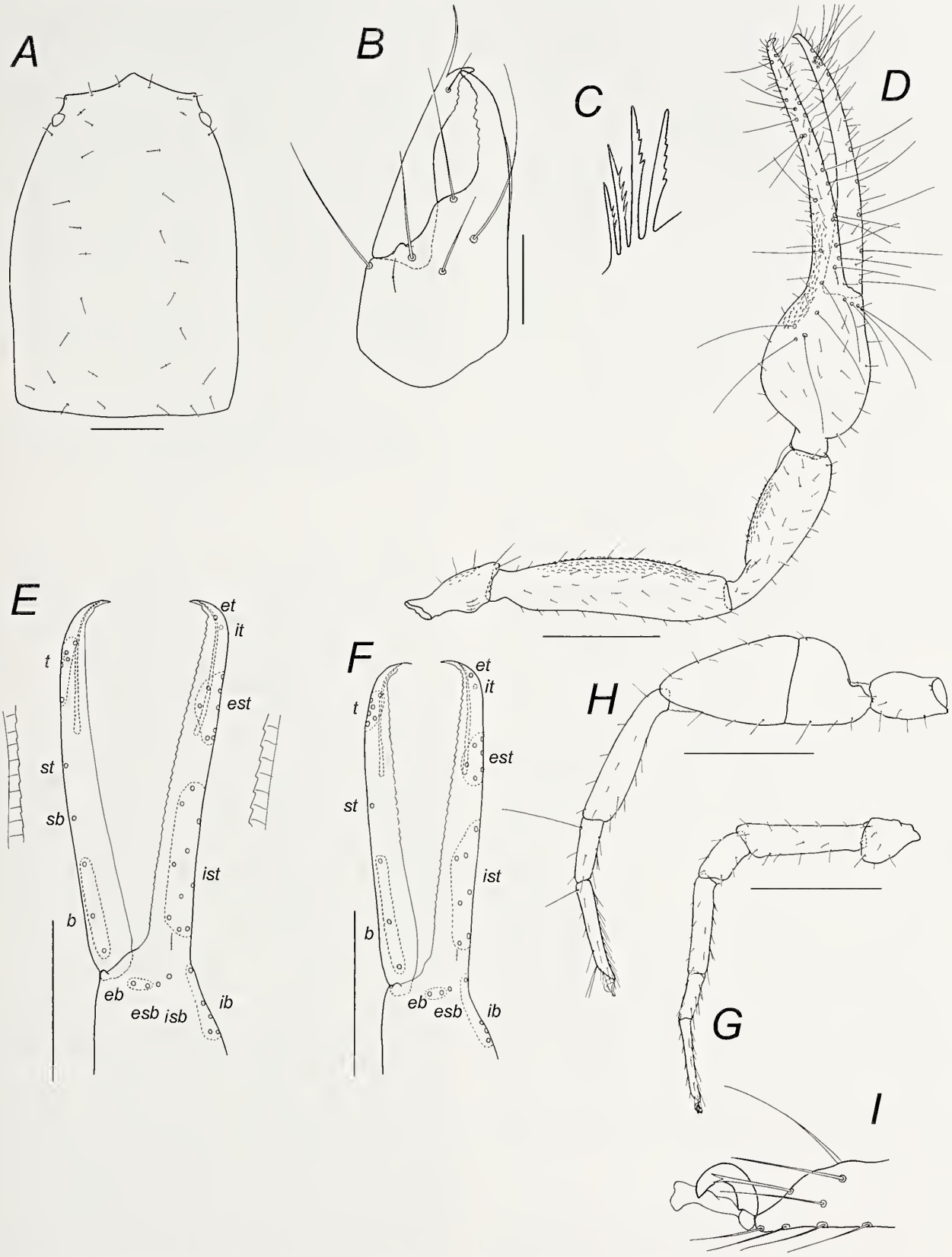

Figure 18.—*Shravana latens* sp. nov., male holotype, unless stated otherwise: A. Carapace; B. Left chelicera; C. Rallum; D. Right pedipalp, dorsal; E. Left chela, lateral; F. Left chela, lateral, tritonymph paratype from 180 km S. of Ābādān; F. Left leg I; G. Left leg IV; H. Distal end of tarsus IV showing arolium, claws and subterminal seta, other setae omitted. Scale lines = 0.5 mm (D—H); 0.2 mm (A); 0.1 mm (B).

+ 3] (1): (1) 10 (1): 12: 11: 9: 10: 7: 8: 10 (including 4 tactile setae): 2; ♀, 9: (1) 8 (1): (1) 8 (1): 12: 10: 10: 10: 6: 6: 8 (including 4 tactile setae): 2. Setae of tergites and sternites IX–XI moderately lanceolate.

Genitalia: male with median genital sac deeply bipartite; female with large gonosac covered with pores.

Dimensions (mm): males: holotype followed by other males (when measured): Body length 3.45 (2.5–3.3). *Pedipalp*: trochanter 0.44/0.185 (0.385–0.465/0.16–0.19), femur 1.045/0.245 (0.91–1.08/0.205–0.245), patella 0.785/0.255 (0.66–0.815/0.205–0.26), chela (with pedicel) 1.84/0.48 (1.62–1.93/0.39–0.47), chela (without pedicel) 1.75 (1.54–1.845), hand length 0.605 (0.545–0.66), movable finger length 1.17 (1.02–1.24). Chelicera 0.365/0.17), movable finger length 0.235. Carapace 0.945/0.655 (0.84–0.965/0.515–0.62); eye diameter 0.055 (0.045–0.055). Leg I: femur 0.48/0.125, patella 0.22/0.15, tibia 0.38/0.07, metatarsus 0.185/0.06, tarsus 0.315/0.045. Leg IV: femur + patella 0.81/0.33, tibia 0.57/0.13, metatarsus 0.265/0.08, tarsus 0.39/0.055.

Females: paratype (NHMW, Iran: 5 km NE. of Persepolis) followed by other females (when measured): Body length 3.7 (3.5–3.65). *Pedipalp*: trochanter 0.45/0.205 (0.45–0.49/0.18–0.21), femur 1.165/0.265 (1.06–1.28/0.235–0.275), patella 0.865/0.275 (0.77–0.955/0.24–0.28), chela (with pedicel) 2.035 (1.82–2.38/0.465–0.55), chela (without pedicel) 1.54–1.845 (1.82–2.29), hand length 0.695 (0.64–0.74), movable finger length 1.31 (1.14–1.50). Chelicera 0.42/0.175, movable finger length 0.26. Carapace 1.05/0.665 (0.91–1.08/0.60–0.66); eye diameter 0.05 (0.05–0.055). Leg I: femur 0.56/0.13, patella 0.24/0.115, tibia 0.43/0.075, metatarsus 0.19/0.045, tarsus 0.21/0.04. Leg IV: femur + patella 0.86/0.325, tibia 0.60/0.13, metatarsus 0.28/0.085, tarsus 0.40/0.065.

Description (tritonymph).—*Chelicera:* galea long and slender, slightly curved; with 6 setae on hand; 1 on movable finger; fixed finger with 5 small teeth, movable finger with 5 small teeth; rallum composed of 4 blades, all serrate.

Pedipalp: trochanter 2.12–2.19, femur 4.10–4.33, patella 2.98–3.09, chela (with pedicel) 4.05–4.16, chela (without pedicel) 3.85–3.95, hand 1.36–1.43 x longer than broad; movable finger 1.82–1.92 x longer than hand (without pedicel). Fixed chelal finger with 22 trichobothria, movable chelal finger with 10 trichobothria (Fig. 18H); *isb* and *sb* absent; *esb*, *et* and *it* regions each with 1 trichobothrium; *eb* and *esb* at base of finger; *eb* region with 2 trichobothria; *ib* region with 4 trichobothria; *ist* region with 7 trichobothria; *est* region with 6 trichobothria; *et* slightly distal to *it*; *b* region with 3 trichobothria; *st* region with 1 trichobothrium; *t* region with 6 trichobothria.

Carapace: anterior margin medially prominent; with 2 small bulging eyes; with 22 setae including 4 setae near anterior margin and 4 near posterior margin.

Legs: as in adult.

Dimensions (mm): Body length 2.89–3.42. *Pedipalp*: trochanter 0.34–0.35/0.155–0.165, femur 0.82–0.93/0.20–0.215, patella 0.595–0.665/0.20–0.215, chela (with pedicel) 1.56–1.66/0.375–0.41, chela (without pedicel) 1.48–1.58, hand length 0.51–0.585, movable finger length 0.98–1.005. Carapace 0.825/0.53.

Remarks.—*Shravana latens* is known only from Iran (Fig. 12B), where it has been collected from under stones in various locations. The locality "180 km S. of Ābādān" is not included on the map, as this would be situated in southern Kuwait. It is possible that an error was made when the label was prepared, and it might be possible that the locality is actually situated east of Ābādān. This would situate the locality to within about 250 km of the other localities sampled by the collectors on the same day, 20 April 1970, 5 km NE. of Persepolis, 160 km NE. of Shiraz and 160 km E. of Shiraz (Beier 1971).

Although several specimens of *S. latens* are substantially larger than the remaining specimens, they have not been conferred separate specific status due to the lack of differences in other morphological characters (e.g., trichobothriotaxy and number of cheliceral setae).

Etymology.—The specific epithet refers to the previous misidentification of these specimens as *Dhanus afghanicus* (*latens* Latin, concealed, hidden) (Brown 1956).

Shravana magnifica sp. nov.
http://zoobank.org/NomenclaturalActs/urn:lsid:zoobank.org:act:75B959C8-BE52-4FC8-9629-E27C728D21AA
(Figs. 10L, 19)

Dhanus afghanicus Beier, 1959:264, fig. 6 (misidentification, in part).

Material examined.—*Holotype male*. AFGHANISTAN: *Helmand*: Grotte Khvadjah (or Ghar-Khvadjah), north of Gereshk near the village of "Kouh-Siah Pochtéh" [Gereshk = 31°49′N, 64°34′E], 1150 m, 19 April 1958, K. Lindberg (NHMW) (also a paralectotype of *Dhanus afghanicus*).

Paratypes. AFGHANISTAN: *Helmand*: 1 ♀, 3 tritonymphs, 1 deutonymph, collected with holotype (NHMW) (also paralectotypes of *Dhanus afghanicus*).

Diagnosis.—*Shravana magnifica* differs from all other ideoroncids except *S. afghanica* by the presence of three trichobothria in the *eb* region of the chela (Fig. 10L, M). It differs from *S. afghanica* by its larger size, e.g., chela (with pedicel) 2.90 (♂), 3.25 (♀) mm in length, compared with 2.21–2.40 (♂), 2.275–2.475 (♀) mm in *S. afghanica*.

Description (adult).—*Color:* pedipalps and carapace deep red-brown; chelicerae and legs yellow-brown; tergites and sternites pale yellow-brown.

Setae: generally long, straight or slightly curved, and acicular.

Chelicera: with 8 (♂, ♀) setae on hand; movable finger with 1 subdistal seta; galea very slender and elongate; fixed finger with 8 (♂), 11 (♀) teeth; movable finger with 5 (♂), 8 (♀) teeth; rallum of 4 serrate blades; thin lamina exterior present.

Pedipalp (Fig. 19B): trochanter and femur entirely rugose, retrolateral face of patella rugose, and prolateral face of chelal hand and retrolateral face of fingers rugose, remainder of chela smooth; trochanter 2.41 (♂), 2.47 (♀), femur 4.67 (♂), 4.40 (♀), patella 3.48 (♂), 3.48 (♀), chela (with pedicel) 3.92 (♂), 3.59 (♀), chela (without pedicel) 3.72 (♂), 3.41 (♀), hand 1.71 (♂), 1.54 (♀) x longer than broad, movable finger 1.23 (♂), 1.31 (♀) x longer than hand. Fixed chelal finger with 31–32 trichobothria, movable chelal finger with 14 trichobothria (Fig. 19D): *eb*, *esb* and *isb* in straight row at base of finger; *esb*, *et*, *isb* and *it* regions each with 1 trichobothrium; *eb* region with 3 trichobothria; *ib* region with 5 trichobothria; *ist* region with 8–9 trichobothria; *est* region with 13 trichobothria; *et* slightly distal to *it*; *b* region with

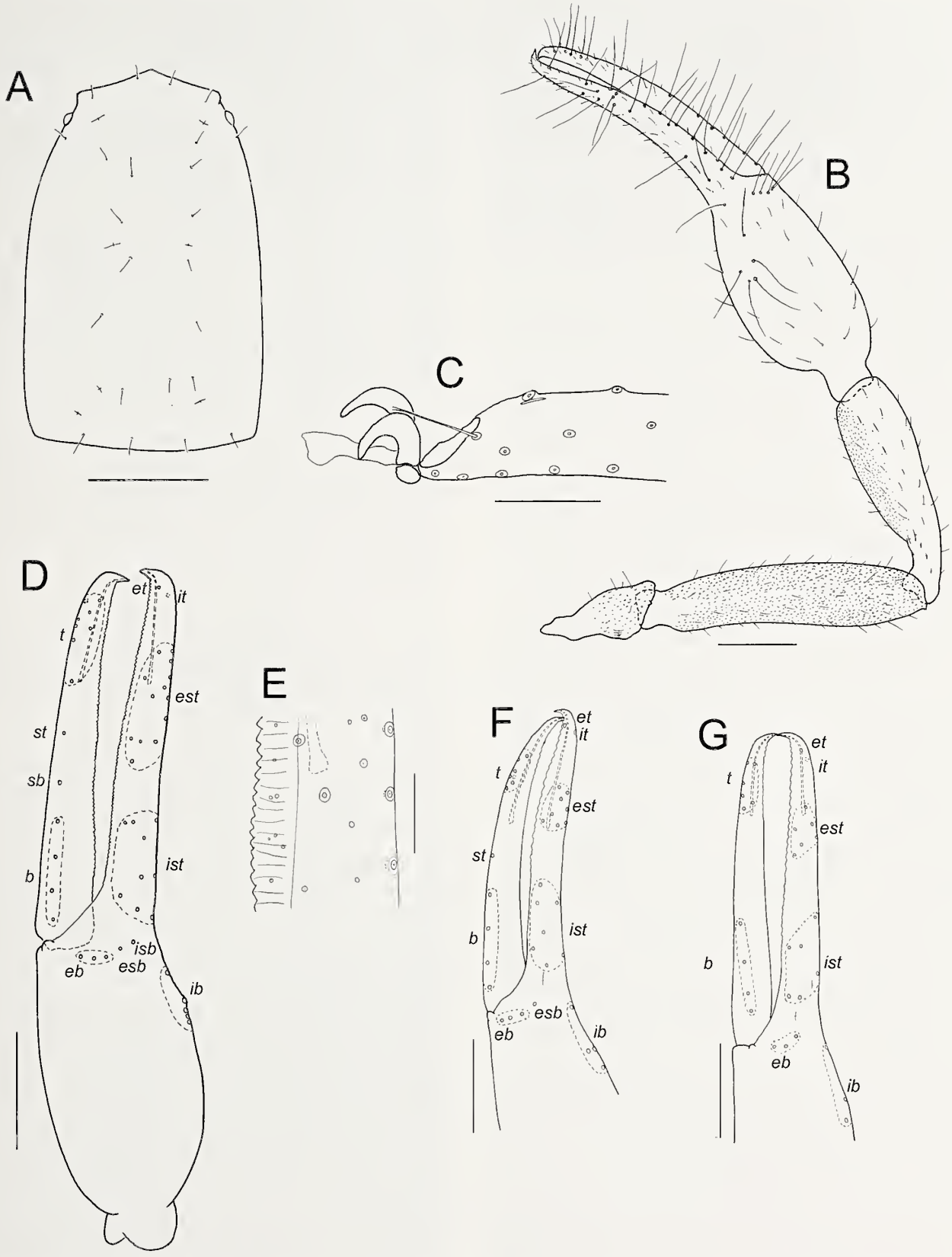

Figure 19.—*Shravana magnifica* sp. nov, male holotype, unless stated otherwise: A. Carapace; B. Right pedipalp, dorsal; C. Distal end of left leg IV showing arolium, claws and subterminal seta; D. Left chela, lateral; E. Detail of fixed chelal finger; F. Left chela, lateral, tritonymph paratype; G. Left chela, lateral, deutonymph paratype. Scale lines = 0.5 mm (A, B, D); 0.25 mm (F, G); 0.1 mm (E, C).

4 trichobothria; *sb* and *st* regions each with 1 trichobothrium; *t* region with 8 trichobothria. Venom apparatus present in both chelal fingers, venom duct terminating in nodus ramosus near *est* region in fixed finger and near basal section of *t* region in movable finger (Fig. 19D). Chelal hand without microsetae near *eb* and *esb* (Fig. 19D). Chelal teeth juxtadentate, fixed finger with ca. 87 (♂), 85 (♀) small, retrorse teeth (Fig. 19E); movable finger with ca. 72 (♂), 75 (♀) very low teeth.

Carapace (Fig. 19A): 1.55 (♂), 1.57 (♀) x longer than broad; lateral margins slightly convex; with 2 small bulging eyes; with small but distinct epistome; with 23 (♂), 25 (♀) setae including 4 near anterior margin and 4 (♂), 5 (♀) near posterior margin; without furrows.

Coxal region: manducatory process with 2 long apical setae, plus 14 (♂), 15 (♀) other setae; chaetotaxy of coxae I–IV: ♂, 11: 10: 10: 14; ♀, 12: 11: 10: 15.

Legs: femur + patella 3.04 (♂), 3.13 (♀) x longer than deep; subterminal tarsal setae deeply bifurcate (Fig. 19C); arolium longer than claws (Fig. 19C).

Abdomen: setae of tergites and sternites IX–XI acicular. Tergites and sternites divided and uniseriate. Tergal chaetotaxy: ♂, 8: 8: 10: 10: 11: 12: 12: 11: ?: ?: ?: 2; ♀, 6: 8: 12: 12: 12: 11: 11: 12: 11: 8 (including 4 tactile setae): ?: 2. Sternal chaetotaxy: ♂, 22: (1) 24 [3 + 3] (1): (1) 15 (1): 14: 12: 12: 11: ?: ?: ?: 2; ♀, 12: (1) 10 (1): (1) 9 (1): 11: 12: 11: 13: 13: 12 (including 4 tactile setae): 8 (including 4 tactile setae): 2.

Genitalia: male with median genital sac deeply bipartite; female with large gonosac covered with scattered pores.

Dimensions (mm): male: holotype: Body length ca. 4.08. *Pedipalp*: trochanter 0.70/0.295, femur 1.82/0.39, patella 1.445/0.415, chela (with pedicel) 2.90/0.74, chela (without pedicel) 2.75, hand length 1.265, movable finger length 1.55. Chelicera 0.59/0.255, movable finger length 0.335. Carapace 1.57/1.015; eye diameter 0.075. Leg I: femur 0.855/0.175, patella 0.40/0.165, tibia 0.705/0.12, metatarsus 0.315/0.12, tarsus 0.525/0.075. Leg IV: femur + patella 1.275/0.42, tibia 0.985/0.175, metatarsus 0.48/0.135, tarsus 0.645/0.085.

Female: paratype: Body length ca. 4.47. *Pedipalp*: trochanter 0.855/0.345, femur 1.89/0.43, patella 1.62/0.465, chela (with pedicel) 3.25/0.905, chela (without pedicel) 3.09, hand length 1.39, movable finger length 1.815. Chelicera 0.615/0.295, movable finger length 0.37. Carapace 1.73/1.10; eye diameter 0.09. Leg I: femur 0.945/0.195, patella 0.44/0.19, tibia 0.77/0.12, metatarsus 0.33/0.11, tarsus 0.60/0.08. Leg IV: femur + patella 1.41 /0.45, tibia 1.085 /0.19, metatarsus 0.555/0.14, tarsus 0.725/0.09.

Description (tritonymph).—*Chelicera:* galea long and slender, slightly curved; with 7 setae on hand; 1 on movable finger; fixed finger with 7 small teeth, movable finger with 5 small teeth; rallum composed of 4 blades, all serrate.

Pedipalp: trochanter 2.38, femur 4.73, patella 3.33, chela (with pedicel) 3.73, chela (without pedicel) 3.56, hand 1.41 x longer than broad; movable finger 1.56 x longer than hand (without pedicel). Fixed chelal finger with 25 trichobothria, movable chelal finger with 11 trichobothria (Fig. 19F); *isb* and *sb* absent; *eb* and *esb* at base of finger; *esb*, *et* and *it* regions each with 1 trichobothrium; *eb* region with 3 trichobothria; *ib* region with 4 trichobothria; *ist* region with 7 trichobothria; *est* region with 8 trichobothria; *et* slightly distal to *it*; *b* region with 4 trichobothria; *st* region with 1 trichobothrium; *t* region with 7 trichobothria.

Carapace: anterior margin medially prominent; with 2 small bulging eyes; with 16 setae including 4 setae near anterior margin and 4 near posterior margin.

Legs: much as in adult.

Dimensions (mm): Body length 2.56. *Pedipalp*: trochanter 0.38/0.16, femur 0.945/0.20, patella 0.665/0.20, chela (with pedicel) 1.456/0.39, chela (without pedicel) 1.39, hand length 0.55, movable finger length 0.856. Carapace 0.96/0.66.

Description (deutonymph).—*Chelicera:* galea long and slender, slightly curved; with 6 setae on hand; 1 on movable finger; fixed finger with 5 small teeth, movable finger with 4 small teeth; rallum composed of 4 blades, all serrate.

Pedipalp: trochanter 2.07, femur 3.63, patella 2.78, chela (with pedicel) 3.93, chela (without pedicel) 3.71, hand 1.39 x longer than broad; movable finger 1.73 x longer than hand (without pedicel). Fixed chelal finger with 20 trichobothria, movable chelal finger with 10 trichobothria (Fig. 19G); *esb*, *isb* and *sb* and *st* absent; *eb* and *esb* at base of finger; *et* and *it* regions each with 1 trichobothrium; *eb* region with 2 trichobothria; *ib* region with 3 trichobothria; *ist* region with 6 trichobothria; *est* region with 6 trichobothria; *et* slightly distal to *it*; *b* region with 4 trichobothria; *t* region with 6 trichobothria.

Carapace: anterior margin medially prominent; with 2 small bulging eyes; with 14 setae including 4 setae near anterior margin and 4 near posterior margin.

Legs: much as in adult.

Dimensions (mm): Body length 2.64. *Pedipalp*: trochanter 0.31/0.15, femur 0.745/0.205, patella 0.555/0.20, chela (with pedicel) 1.355/0.345, chela (without pedicel) 1.28, hand length 0.48, movable finger length 0.83. Carapace 0.72/0.55.

Remarks.—The specimens listed above were collected by Knut Lindberg of Lund University and were originally included as paratypes of *Dhanus afghanicus* by Beier (1959). However, they are much larger than typical specimens of that species and are here considered to represent a new species. Beier (1959) stated that the vial contained 1 ♂ and 1 ♀, but there are in fact 1 ♂, 1 ♀, 3 tritonymphs and 1 deutonymph. The collection data published by Beier (1959) stated "Grotte Khvadjah, Kouh-Siah Pochtéh, Farah, 19. 4. 1958″, which suggests that the site is located in Farah Province. However this cave was discussed by Lindberg (1961:19) under the name "Ghar-Khvadjah" or "Ghar-Bad Khaneh", in Naouzar District north of Guerechk in the Province of Qandahar. The cave opening was near a village called "Siah Pochtéh". Transliteration of Afghani place names is a difficult task, and identifying the localities listed by Beier (1959) and Lindberg (1961) has not always been possible. Guerechk is nowadays known as Gereshk and is located in Helmand Province at 31°49′N, 64°34′E. Naouzar (now known as Now Zād, 32°24′N, 64°28′E) is located 64 km north of Gereshk, but only about 30 km from the border with Farah Province. The village names "Kouh-Siah Pochtéh" or "Siah Pochtéh" could not be located definitively, but a village called "Poshteh" or "Pushtah" is located at 32°32′N, 63°36′E, which is 83 km WNW of Gereshk in Farah Province. Whether this represents the village mentioned by Beier (1959) and Lindberg (1961) might never be possible to determine. In the meantime, I treat the type locality as located somewhere north of Gereshk in Helmand Province.

Shravana magnifica is currently known from a single short cave in southern Afghanistan (Fig. 12B), although apart from

its large size it lacks any obvious modifications for cave life such as reduced eyes or elongated appendages.

Etymology.—The species epithet refers to the large size of this species (*magnificus*, Latin, noble, splendid, eminent).

Shravana pohli (Mahnert, 2007), comb. nov.
http://zoobank.org/NomenclaturalActs/urn:lsid:zoobank.org:act:D0F84D06-FCAC-4A18-92EF-8D4F466F65C6
(Fig. 10F)

Dhanus pohli Mahnert, 2007:277–279, figs. 7–10; Harvey, 2013: unpaginated.

Material examined.—None.

Diagnosis.—*Shravana pohli* differs from all other *Shravana* species except *S. socotraensis* by the presence of only 2 trichobothria in the *b* region (Fig. 10A, F). It differs from *S. socotraensis* by the presence of 23–24 trichobothria on the fixed chelal finger and hand (Fig. 10F), whereas *S. socotraensis* has only 20 trichobothria (Fig. 10A).

Description (adult).—See Mahnert (2007).

Remarks.—This species has a lamina exterior on the chelicera and long arolia (Mahnert 2007), and is therefore transferred to the genus *Shravana*. Dr. V. Mahnert (in litt., April 2016) confirmed the numbers of chelal trichobothria (Table 1).

Shravana pohli is known only from Samha Island, in the Socotran Archipelago (Fig. 12B).

Shravana schwendingeri sp. nov.
http://zoobank.org/NomenclaturalActs/urn:lsid:zoobank.org:act:3AD33F75-0A05-49E0-84F2-24FC3202547F
(Figs. 10B, 20)

Material examined.—*Holotype male*. THAILAND: *Chumphon Province*: male, Khao Kai Jae Waterfall, Lang Suan District, 9°55′04.6″N, 98°56′33.7″E, semi-evergreen rainforest, 17–18 July 2002, TH–02/08, P. Schwendinger (MHNG).

Paratypes. THAILAND: *Chumphon Province*: 1 ♀, 3 tritonymphs, collected with holotype (MHNG); 1 ♂, 1 deutonymph, same data as holotype except 5–8 May 2003, 80 m, TH–03/02 (MHNG).

Diagnosis.—*Shravana schwendingeri* is most similar to *S. indica*, *S. laminata* and *S. withi* as all possess only 1 trichobothrium in the *eb* region and 3 trichobothria in the *eb* region (Fig. 10B–E). *Shravana schwendingeri* differs from *S. laminata* by the rugose pedipalpal femur and patella (Fig. 20B), which are smooth in *S. laminata* (Fig. 17B), from *S. indica* by the smooth chelal hand (Fig. 20B), which is rugose in *S. indica* (Fig. 16D), and from *S. withi* by the medial position of the trichobothria of the *ib* region (Fig. 20B) which are in the distal half of the chelal hand in *S. withi* (Fig. 21B).

Description (adult).—*Color:* pedipalps and carapace deep red-brown; chelicerae and legs yellow-brown; tergites and sternites pale yellow-brown.

Setae: long, straight, acicular and generally quite slender.

Chelicera: with 7 (♂, ♀) setae on hand; movable finger with 1 subdistal seta; galea very slender and elongate; fixed finger with ca. 8 (♂), 9 (♀) teeth; movable finger with ca. 7 (♂), 6 (♀) teeth; rallum of 4 serrate blades; lamina exterior present.

Pedipalp (Fig. 20B): prolateral faces of femur and patella coarsely rugose, trochanter and chela smooth; trochanter 2.26–2.52 (♂), 2.27 (♀), femur 3.91–3.98 (♂), 3.66 (♀), patella 2.90–3.04 (♂), 2.80 (♀), chela (with pedicel) 3.59–3.72 (♂), 3.49 (♀), chela (without pedicel) 3.33–3.47 (♂), 3.26 (♀), hand 1.74–1.78 (♂), 1.62 (♀) x longer than broad, movable finger 1.04–1.08 (♂), 1.08 (♀) x longer than hand. Fixed chelal finger with 23 trichobothria, movable chelal finger with 11 trichobothria (Fig. 20C): *eb*, *esb* and *isb* in straight row at base of finger; *eb*, *esb*, *et*, *isb* and *it* regions each with 1 trichobothrium; *ib* region with 5 trichobothria; *ist* region with 7 trichobothria; *est* region with 6 trichobothria; *et* slightly distal to *it*; *b* region with 3 trichobothria; *sb* and *st* regions each with 1 trichobothrium; *t* region with 6 trichobothria. Venom apparatus present in both chelal fingers, venom duct terminating in nodus ramosus near *est* region in fixed finger and basal to *t* region in movable finger (Fig. 20C). Chelal hand without microsetae near *eb* and *esb* (Fig. 20C). Chelal teeth very low, small and retrorse (Fig. 20D), fixed finger with ca. 42 (♂), 43 (♀) teeth; movable finger with ca. 32 (♂), 28 (♀) teeth.

Carapace (Fig. 20A): 1.08–1.24 (♂), 1.11 (♀) x longer than broad; lateral margins slightly convex; with 2 bulging eyes; with well developed epistome; with 33 (♂), 32 (♀) setae, including 4 setae near anterior margin and 5 (♂), 4 (♀) near posterior margin; with very shallow posterior furrow.

Coxal region: manducatory process with 3 long apical setae, plus 11 (♂), 12 (♀) additional setae; chaetotaxy of coxae I–IV: ♂, 7: 7: 10: 11; ♀, 7: 10: 9: 9.

Legs: femur + patella 2.72 (♂), 2.94 (♀) x longer than deep; subterminal tarsal setae trifurcate (Fig. 20G); arolium slightly longer than claws (Fig. 20G).

Abdomen: tergites and sternites undivided and uniseriate. Tergal chaetotaxy: ♂, 6: 8: 9: 11: 12: 12: 12: 13: 12 (including 4 tactile setae): 11 (including 4 tactile setae): 7 (including 4 tactile setae): 2; ♀, 7: 7: 10: 10: 11: 11: 12: 13: 12: 11 (including 4 tactile setae): 10 (including 4 tactile setae): 2. Sternal chaetotaxy: ♂, 11: (1) 15 [3 + 3] (1): (1) 7 (1): 14: 14: 14: 13: 14: 10: 10 (including 4 tactile setae): 2; ♀, 5: (1) 6 (1): (1) 8 (1): 14: 13: 14: 13: 12: 11 (including 2 tactile setae): 6 (including 2 tactile setae): 2. Setae of tergites and sternites IX–XI acuminate.

Genitalia: male with median genital sac deeply bipartite; female with large gonosac covered with pores.

Dimensions (mm): males: holotype followed by other male (when measured): Body length 2.55 (2.13). *Pedipalp*: trochanter 0.395/0.175 (0.415/0.165), femur 0.90/0.23 (0.895/0.225), patella 0.755/0.26 (0.79/0.26), chela (with pedicel) 1.40/0.39 (1.45/0.39), chela (without pedicel) 1.30 (1.355), hand length 0.67 (0.68), movable finger length 0.70 (0.72). Chelicera 0.37/0.175, movable finger length 0.245. Carapace 0.725/0.67 (0.755/0.61); eye diameter 0.06. Leg I: femur 0.435/0.11, patella 0.265/0.105, tibia 0.335/0.075, metatarsus 0.19/0.06, tarsus 0.275/0.04. Leg IV: femur + patella 0.68/0.25, tibia 0.51/0.105, metatarsus 0.27/0.08, tarsus 0.37/0.06.

Females: paratype: Body length 2.44. *Pedipalp*: trochanter 0.43/0.19, femur 0.915/0.25, patella 0.77/0.275, chela (with pedicel) 1.50/0.43, chela (without pedicel) 1.40, hand length 0.695, movable finger length 0.75. Chelicera 0.41/0.19, movable finger length 0.27. Carapace 0.785/0.705; eye diameter 0.06. Leg I: femur 0.45/0.115, patella 0.32/0.155, tibia 0.32/0.075, metatarsus 0.19/0.06, tarsus 0.18/0.18. Leg IV: femur + patella 0.72/0.245, tibia 0.495/0.11, metatarsus 0.255/0.085, tarsus 0.37/0.06.

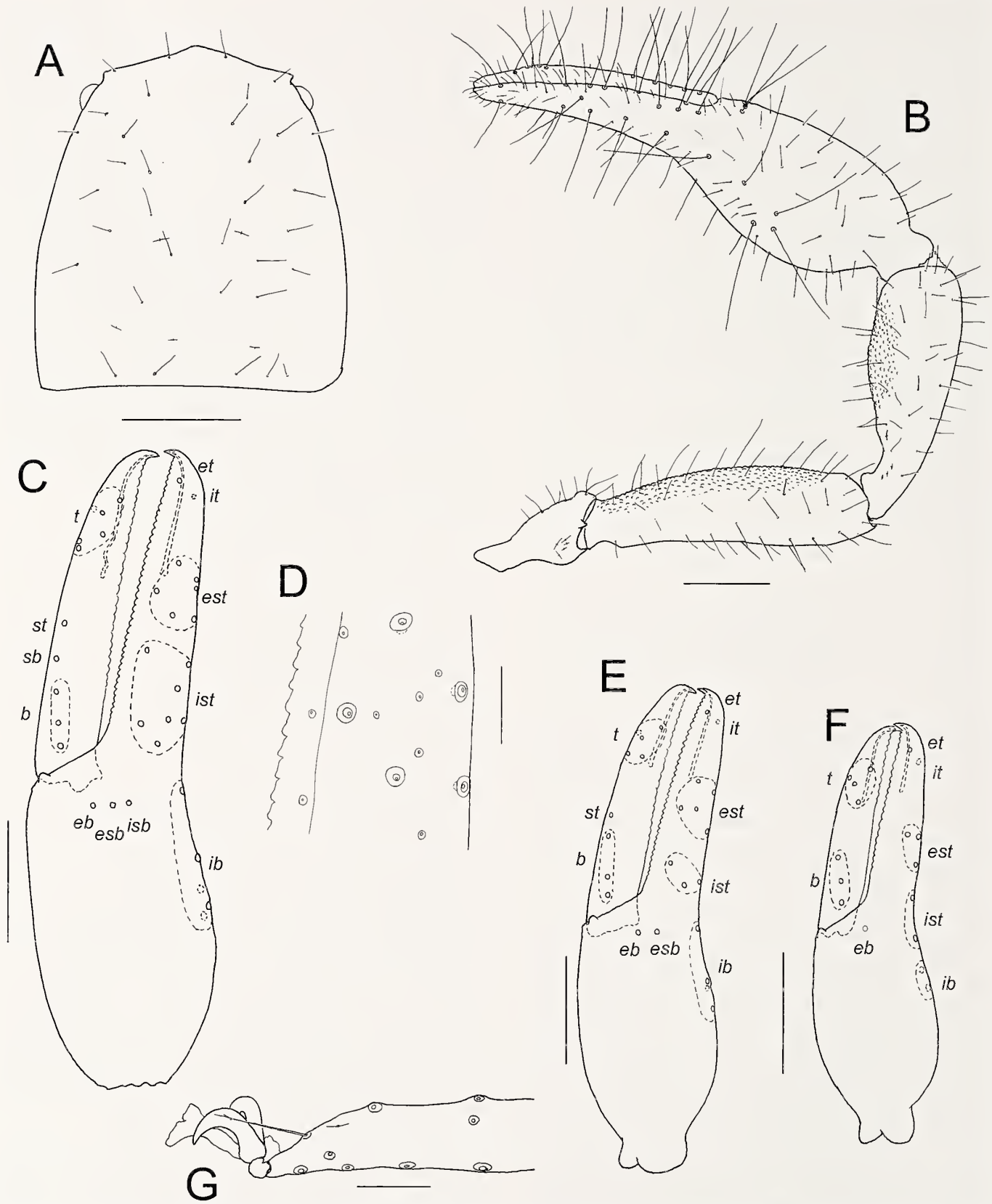

Figure 20.—*Shravana schwendingeri* sp. nov., male holotype, unless stated otherwise: A. Carapace; B. Right pedipalp, dorsal; C. Left chela, lateral; D. Detail of fixed chelal finger; E. Left chela, lateral, tritonymph paratype; F. Left chela, lateral, deutonymph paratype; G. Distal end of tarsus IV showing arolium, claws and subterminal seta, other setae omitted. Scale lines = 0.5 mm (B); 0.25 mm (A, C, E, F); 0.05 mm (D, G).

Description (tritonymph).—*Chelicera:* galea long and slender, slightly curved; with 6 setae on hand; 1 on movable finger; fixed finger with ca. 13 small teeth, movable finger with ca. 8 small teeth; rallum composed of 4 blades, all serrate.

Pedipalp: trochanter 2.38, femur 3.43, patella 2.70, chela (with pedicel) 3.48, chela (without pedicel) 3.23, hand 1.62 x longer than broad; movable finger 1.02 x longer than hand (without pedicel). Fixed chelal finger with 16 trichobothria, movable chelal finger with 8 trichobothria (Fig. 20E); *isb* and *sb* absent; *eb*, *esb*, *et* and *it* regions each with 1 trichobothrium; *eb* and *esb* at base of finger; *ib* region with 4 trichobothria; *ist* region with 3 trichobothria; *est* region with 5 trichobothria; *et* slightly distal to *it*; *b* region with 3 trichobothria; *st* region with 1 trichobothrium; *t* region with 5 trichobothria.

Carapace: anterior margin medially prominent; with 2 small bulging eyes; with 28 setae including 4 setae near anterior margin and 4 near posterior margin.

Legs: as in adult.

Dimensions (mm): Body length 2.03. *Pedipalp*: trochanter 0.345/0.145, femur 0.685/0.20, patella 0.58/0.215, chela (with pedicel) 1.15/0.33, chela (without pedicel) 1.065, hand length 0.535, movable finger length 0.545. Carapace 0.64/0.615.

Description (deutonymph).—*Chelicera:* galea long and slender, slightly curved; with 5 setae on hand; 1 on movable finger; fixed finger with ca. 8 small teeth, movable finger with ca. 5 small teeth; rallum composed of 4 blades, all serrate.

Pedipalp: trochanter 2.22, femur 3.47, patella 2.58, chela (with pedicel) 3.44, chela (without pedicel) 3.22, hand 1.56 x longer than broad; movable finger 1.06 x longer than hand (without pedicel). Fixed chelal finger with 10 trichobothria, movable chelal finger with 7 trichobothria (Fig. 20F); *esb*, *isb*, *sb* and *st* absent; *eb*, *et* and *it* regions each with 1 trichobothrium; *eb* at base of finger; *ib* region with 2 trichobothria; *ist* region with 2 trichobothria; *est* region with 3 trichobothria; *et* slightly distal to *it*; *b* region with 3 trichobothria; *t* region with 4 trichobothria.

Carapace: anterior margin medially prominent; with 2 small bulging eyes; with 20 setae including 4 setae near anterior margin and 4 near posterior margin.

Legs: as in adult.

Dimensions (mm): Body length 1.62. *Pedipalp*: trochanter 0.255/0.115, femur 0.52/0.15, patella 0.425/0.165, chela (with pedicel) 0.86/0.25, chela (without pedicel) 0.805, hand length 0.39, movable finger length 0.415. Carapace 0.415/0.42.

Remarks.—*Shravana schwendingeri* has only been collected from Khao Kai Jae Waterfall in Chumpon Province, Thailand (Fig. 12A), where it has been found in rainforest leaf litter.

Etymology.—This species is named for Peter Schwendinger, the collector of the type specimens and many other interesting pseudoscorpions from south-east Asia.

Shravana socotraensis (Mahnert, 2007), comb. nov.
http://zoobank.org/NomenclaturalActs/urn:lsid:zoobank.org:act:7DCD9B09-417B-4AA4-BDE7-717E7BD5D6E7
(Fig. 10A)

Dhanus socotraensis Mahnert, 2007:279–280, figs. 11–14; Harvey, 2013: unpaginated.

Material examined.—None.

Diagnosis.—*Shravana socotraensis* differs from all other *Shravana* species by the presence of only 20 trichobothria on the fixed chelal finger and 10 on the movable finger (Fig. 10A).

Description (adult).—See Mahnert (2007).

Description (deutonymph).—See Mahnert (2007).

Remarks.—This species has a lamina exterior on the chelicera, and long arolia (Mahnert 2007), and is therefore transferred to the genus *Shravana*.

Shravana socotraensis is widely distributed on Socotra (Fig. 12B).

Shravana taitii (Mahnert, 2007), comb. nov.
http://zoobank.org/NomenclaturalActs/urn:lsid:zoobank.org:act:E9F7415A-A4A9-425D-89C8-865436425671
(Fig. 10G)

Dhanus taitii Mahnert, 2007:280–282, figs. 15–22; Harvey, 2013: unpaginated.

Material examined.—None.

Diagnosis.—*Shravana taitii* differs from all other *Shravana* species except *S. latens* by the presence of 2 trichobothria in the *eb* region and 3 trichobothria in the *b* region (Fig. 10G, H). It differs from *S. latens* by the presence of only 25 trichobothria on the fixed chelal finger and hand, including 7 trichobothria in the *ist* region (Fig. 10G), whereas *S. latens* has 28 trichobothria, including 9 in the *ist* region (Fig. 10H).

Description (adult).—See Mahnert (2007).

Description (tritonymph).—See Mahnert (2007).

Remarks.—This species has a lamina exterior on the chelicera and long arolia (Mahnert 2007), and is therefore transferred to the genus *Shravana*. *Shravana taitii* is currently known from Dejub Cave, Socotra (Fig. 12B).

Shravana withi sp. nov.
http://zoobank.org/NomenclaturalActs/urn:lsid:zoobank.org:act:DE870D1C-F64C-43ED-ADC1-19736E027580
(Figs. 10E, 21)

Material examined.—*Holotype male.* MALAYSIA: *Pahang*: Pulau Tioman, pied du Gunung Kajang, 2°47.181′N, 104°07.892′E, 160 m, rainforest, 2 October 2001, L. Monod (MHNG).

Paratypes. MALAYSIA: *Pahang*: 1 ♀, collected with holotype (MHNG); 1 ♂, Tioman Island, westside of Mount Kajang, 2 km E. of Kg. Genting, 2°47′N, 104°08′E, 26 June 2001, M01–39, 100 m, A. Schulz, K. Vock (MHNG); 1 ♂, 1 ♀, same data except M01–67 (MHNG); 1 ♀, 1 tritonymph, same data except M01–41 (MHNG); 1 ♀, same data except 23 June 2001, 50 m, M01–2 (MHNG); 1 ♂, same data except 28 June 2001, M01–70 (WAM T140762).

Diagnosis.—*Shravana withi* is most similar to *S. indica*, *S. laminata* and *S. schwendingeri* as all possess only 1 trichobothrium in the *eb* region and 3 trichobothria in the *eb* region (Fig. 10B–E). *Shravana withi* differs from *S. laminata* by the rugose pedipalpal femur and patella (Fig. 20B), which are smooth in *S. laminata* (Fig. 17B), and from *S. indica* by the smooth chelal hand (Fig. 20B), which is rugose in *S. indica* (Fig. 16D). It differs from *S. schwendingeri* by the position of the trichobothria of the *ib* region in distal half of the chelal

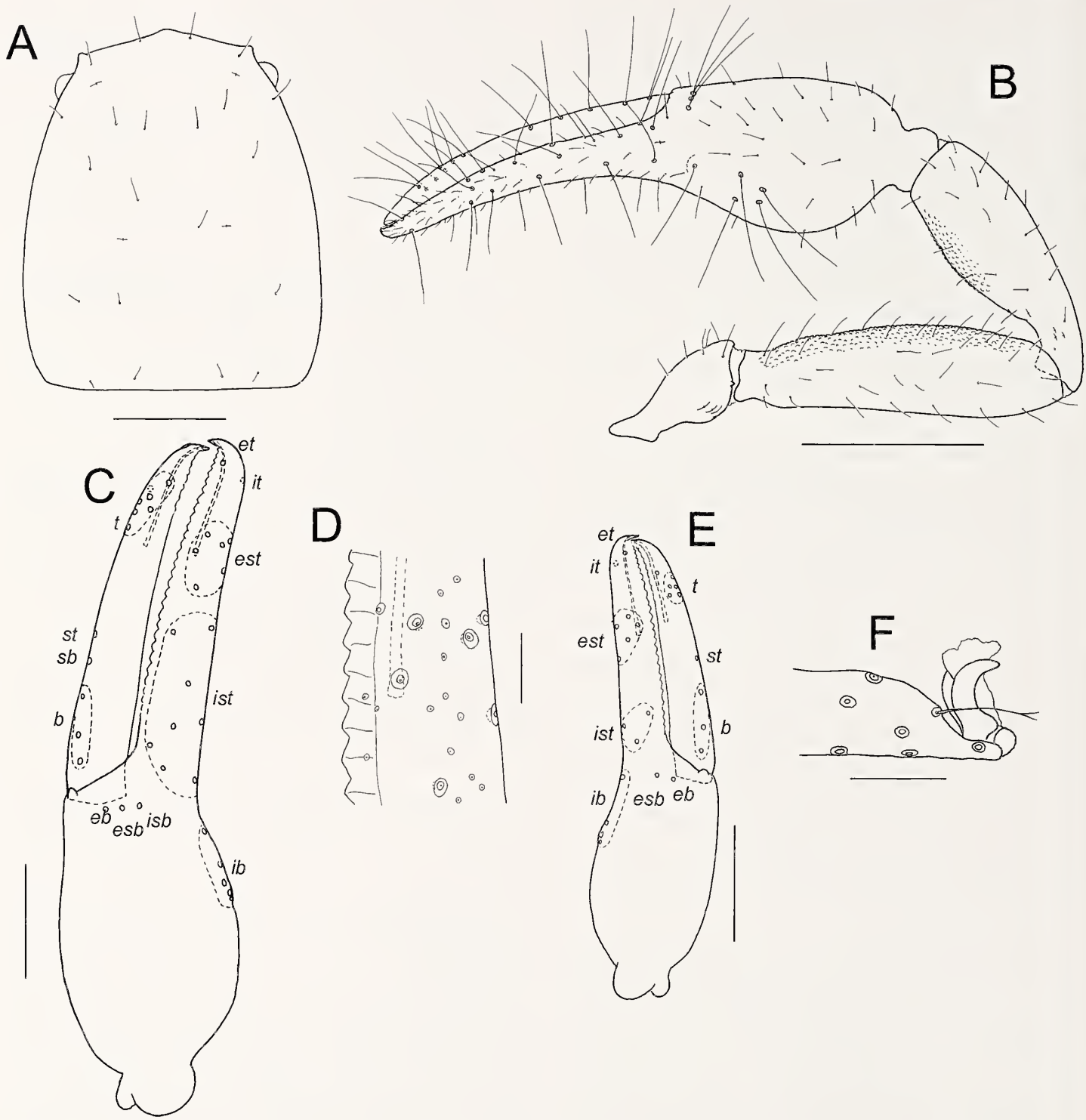

Figure 21.—*Shravana withi* sp. nov., male holotype, unless stated otherwise: A. Carapace; B. Right pedipalp, dorsal; C. Left chela, lateral; D. Detail of fixed chelal finger; E. Left chela, lateral, tritonymph paratype. F. Distal end of tarsus IV showing arolium, claws and subterminal seta, other setae omitted; Scale lines = 0.5 mm (B); 0.25 mm (A, C, E); 0.05 mm (D, F).

hand (Fig. 21B), which are situated medially in *S. schwendingeri* (Fig. 20B).

Description (adult).—*Color:* pedipalps and carapace deep red-brown; chelicerae and legs yellow-brown; tergites and sternites pale yellow-brown.

Setae: long, straight, acicular and generally quite slender.

Chelicera: with 7 setae on hand; movable finger with 1 subdistal seta; galea very slender and elongate; fixed finger with 8 (♂), 7 (♀) teeth; movable finger with 4 (♂), 6 (♀) teeth; rallum of 4 serrate blades; lamina exterior present.

Pedipalp (Fig. 21B): prolateral faces of femur and patella coarsely rugose, trochanter and chela smooth; trochanter 2.20–2.36 (♂), 2.28–2.36 (♀), femur 3.73–3.87 (♂), 3.58–3.80

(♀), patella 2.80–2.88 (♂), 2.75–2.91 (♀), chela (with pedicel) 3.51–3.61 (♂), 3.47–3.57 (♀), chela (without pedicel) 3.28–3.42 (♂), 3.28–3.39 (♀), hand 1.46–1.54 (♂), 1.42–1.53 (♀) x longer than broad, movable finger 1.25–1.41 (♂), 1.30–1.41 (♀) x longer than hand. Fixed chelal finger with 24 trichobothria, movable chelal finger with 12 trichobothria (Fig. 21C): *eb*, *esb* and *isb* in straight row at base of finger; *eb*, *esb*, *et*, *isb* and *it* regions each with 1 trichobothrium; *ib* region with 5 trichobothria; *ist* region with 8 trichobothria; *est* region with 6 trichobothria; *et* slightly distal to *it*; *b* region with 3 trichobothria; *sb* and *st* regions each with 1 trichobothrium; *t* region with 7 trichobothria. Venom apparatus present in both chelal fingers, venom duct terminating in nodus ramosus near *est* region in fixed finger and basal to *t* region in movable finger (Fig. 21C). Chelal hand without microsetae near *eb* and *esb* (Fig. 21C). Chelal teeth very low, small and retrorse (Fig. 21D), fixed finger with 32 (♂), 31 (♀) teeth; movable finger with 26 (♂), 29 (♀) teeth.

Carapace (Fig. 21A): 1.15–1.28 (♂), 1.06–1.22 (♀) x longer than broad; lateral margins slightly convex; with 2 bulging eyes; with well developed epistome; with 22 (♂), 20 (♀) setae, including 4 setae near anterior margin and 4 near posterior margin; with shallow posterior furrow.

Coxal region: manducatory process with 3 long apical setae, plus 9 (♂), 10 (♀) additional setae; chaetotaxy of coxae I–IV: ♂, 5: 7: 8: 10; ♀, 7: 8: 8: 9.

Legs: femur + patella 2.57 (♂), 2.60 (♀) x longer than deep; subterminal tarsal setae bifurcate (Fig. 21F); arolium longer than claws (Fig. 21F).

Abdomen: tergites and sternites undivided and uniseriate; some tergites with small anterior impressions suggesting rudimentary division. Tergal chaetotaxy: ♂, 4: 6: 8: 8: 8: 10: 8: 9: 8: 8 (including 4 tactile setae): 6 (including 4 tactile setae): 2; ♀, 4: 6: 8: 8: 8: 8: 8: 8: 8: 8 (including 4 tactile setae): 8 (including 4 tactile setae): 2. Sternal chaetotaxy: ♂, 10: (1) 7 [3 + 3] (1): (1) 6 (1): 12: 10: 13: 10: 10: 10: 11 (including 6 tactile setae): 2; ♀, 7: (1) 4 (1): (1) 5 (1): 12: 10: 11: 10: 8: 8: 8 (including 2 tactile setae): 2. Setae of tergites and sternites IX–XI acuminate.

Genitalia: male with median genital sac deeply bipartite; female with large gonosac covered with pores.

Dimensions (mm): males: holotype followed by other males (when measured): Body length 2.53 (2.23–3.25). *Pedipalp*: trochanter 0.425/0.18 (0.385–0.43/0.17–0.185), femur 0.945/0.245 (0.89–0.98/0.23–0.26), patella 0.745/0.26 (0.70–0.755/0.245–0.275), chela (with pedicel) 1.525/0.435 (1.44–1.63/0.41–0.47), chela (without pedicel) 1.435 (1.345–1.54), hand length 0.635 (0.61–0.69), movable finger length 0.845 (0.79–0.895). Chelicera 0.36/0.18, movable finger length 0.205. Carapace 0.845/0.66 (0.75–0.83/0.625–0.705); eye diameter 0.07. Leg I: femur 0.455/0.12, patella 0.225/0.11, tibia 0.33/0.08, metatarsus 0.195/0.065, tarsus 0.30/0.05. Leg IV: femur + patella 0.72/0.28, tibia 0.50/0.11, metatarsus 0.26/0.085, tarsus 0.365/0.06.

Females: paratype collected with holotype followed by other females (when measured): Body length 3.58 (2.59–2.73). *Pedipalp*: trochanter 0.445/0.195 (0.41–0.425/0.18), femur 0.97/0.255 (0.895–0.975/0.25–0.26), patella 0.80/0.275 (0.73–0.80/0.26–0.275), chela (with pedicel) 1.66/0.47 (1.56–1.64/0.45–0.46), chela (without pedicel) 1.56 (1.48–1.56), hand length 0.67 (0.64–0.705), movable finger length 0.93 (0.905–0.92). Chelicera 0.385/0.195, movable finger length 0.23. Carapace 0.825/0.78 (0.785–0.87/0.67–0.715); eye diameter 0.065. Leg I: femur 0.51/0.135, patella 0.24/0.12, tibia 0.40/0.085, metatarsus 0.21/0.07, tarsus 0.305/0.05. Leg IV: femur + patella 0.78/0.30, tibia 0.555/0.115, metatarsus 0.30/0.09, tarsus 0.41/0.065.

Description (tritonymph).—*Chelicera:* galea long and slender, slightly curved; with 6 setae on hand; 1 on movable finger; fixed finger with 5 small teeth, movable finger with 3 small teeth; rallum composed of 4 blades, all serrate.

Pedipalp: trochanter 2.32, femur 2.64, patella 2.97, chela (with pedicel) 3.64, chela (without pedicel) 3.45, hand 1.60 x longer than broad; movable finger 1.27 x longer than hand (without pedicel). Fixed chelal finger with 16 trichobothria, movable chelal finger with 10 trichobothria (Fig. 21E); *isb* and *sb* absent; *eb*, *esb*, *et* and *it* regions each with 1 trichobothrium; *eb* and *esb* at base of finger; *ib* region with 4 trichobothria; *ist* region with 3 trichobothria; *est* region with 5 trichobothria; *et* slightly distal to *it*; *b* region with 3 trichobothria; *st* region with 1 trichobothrium; *t* region with 6 trichobothria.

Carapace: anterior margin medially prominent; with 2 small bulging eyes; with 20 setae including 4 setae near anterior margin and 4 near posterior margin.

Legs: as in adult.

Dimensions (mm): Body length 1.72. *Pedipalp*: trochanter 0.29/0.125, femur 0.655/0.18, patella 0.475/0.16, chela (with pedicel) 1.055/0.29, chela (without pedicel) 1.00, hand length 0.465, movable finger length 0.59. Carapace 0.58/0.495.

Remarks.—*Shravana withi* has only been collected from Pulau Tioman (Fig. 12A), southern Malaysia, where it occurs in rainforest leaf litter, along with *Dhanus tioman*.

Etymology.—This species is named in honor of Danish zoologist Carl Johannes With (1877–1923) in recognition of his work on pseudoscorpions, and particularly for his description of the first Asian ideoroncids (With 1906).

Sironcus gen. nov.

http://zoobank.org/NomenclaturalActs/urn:lsid:zoobank.org:act:36CFD8EB-024C-410D-ACC0-401A3A8B3CCF

Type species.—*Ideobisium (Ideoroncus) siamensis* With, 1906.

Diagnosis.—Species of *Sironcus* bear a small hooked process on the ventral surface of the arolium (e.g., Fig. 27H), a structure that is present in only four other ideoroncid genera, *Mahnertius*, *Typhloroncus* and *Xorilbia* from central and South America, and *Negroroncus* from east Africa (Harvey & Muchmore 2013). It differs from *Negroroncus* by the absence of a lamina exterior on the chelicera (Figs. 25H, 27B), from *Mahnertius* by the lack of compressed and enlarged distal teeth on the fixed chelal finger (e.g., Fig. 27E), from *Typhloroncus* by having the anal operculum separate from sternite X (Fig. 23V), and from *Xorilbia* by the undivided arolium (e.g., Fig. 27H).

Description.—*Setae:* generally long, straight or slightly curved, and acicular.

Chelicera: with 6 or 7 long, acuminate setae on hand; movable finger with 1 long medial seta; rallum of 4 thickened

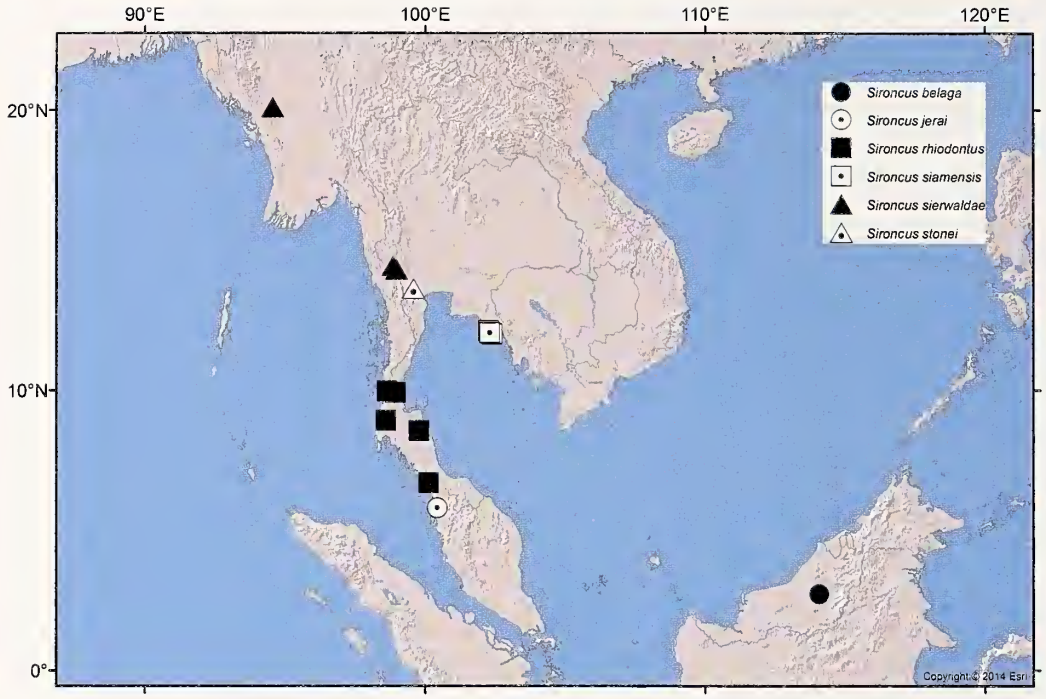

Figure 22.—Distribution of *Sironcus* species.

blades, all blades serrate; lamina exterior absent; galea long and slender.

Pedipalp: long and slender; patella with disto-prolateral excavation. Fixed chelal finger with 20 trichobothria, movable chelal finger with 10 trichobothria (Figs. 24C, 25C, 26D, 27E, 28C, 29C): *eb* region with 1 trichobothrium; *est* region with 6 trichobothria; *ib* region with 4 trichobothria; *ist* region with 5 trichobothria; *b* region with 2 trichobothria; and *t* region with 6 trichobothria. Venom apparatus present in both chelal fingers, venom duct terminating in nodus ramosus near *est* region in fixed finger and near *t* region in movable finger (Figs. 24C, 25C, 26D, 27E, 28C, 29C). Chelal teeth juxtadentate (Figs. 24D, 25D, 26E, 27F, 28D); base of fixed chelal finger without small denticles (e.g., Fig. 27E); chelal hand with retrolateral condyle small and rounded; without patch of microsetae near *eb*, *esb* and *isb* (e.g., Fig. 27E).

Carapace (Figs. 24A, 25A, 26A, 27A, 28A, 29A): with 2 small, bulging eyes; epistome either absent or very small; without furrows.

Coxal region (Fig. 23A): manducatory process with 2 long distal setae; median maxillary lyrifissure present and sub-basally situated.

Legs (Figs. 25J, K & 27G): femur I and II without basal swelling; femur I much longer than patella I; suture line between femur IV and patella IV transverse; metatarsus shorter than tarsus; metatarsal pseudotactile seta sub-proximal; subterminal tarsal setae with 2 small sub-distal denticles (Figs. 24E, 25L, 26C, 27H, 28E, 29F); arolium undivided and shorter than claws, always bearing a ventral hooked process (Figs. 24E, 25L, 26C, 27H, 28E, 29F); claws slender and simple.

Abdomen: tergites and sternites undivided. Pleural membrane longitudinally striate (Fig. 23C). Each stigmatic sclerite with 1 seta; spiracles simple, with spiracular helix. Anal operculum not abutting sternite X (Fig. 23B).

Genitalia: male median genital sac deeply bipartite; female with large gonosac covered with pores.

Remarks.—The type species of *Sironcus*, *S. siamensis*, was included in the genus *Dhanus* by Chamberlin (1930) who relied heavily on the arolium being shorter than the claws in both species to define the genus. However, as shown above, *S. siamensis* differs substantially from species of *Dhanus* in two significant features including the lack of a lamina exterior (Figs. 25H, 27B), and in the presence of a ventral hooked process on the arolium (Figs. 24E, 25L, 26C, 27H, 28E, 29F). The affinities of this genus may be with the three other ideoroncid genera with a hooked process, *Mahnertius*, *Negroroncus*, *Typhloroncus* and *Xorilbia*. It differs from each of them by the features outlined in the generic diagnosis.

The nymphal trichobothrial patterns (Fig. 25A–G) of *S. jerai* are identical to those of *Albiorix chilensis*, *Ideoroncus setosus*, *Pseudalbiorix reddelli*, *Xorilbia arboricola* and *X. gracilis*, which are the only other ideoroncids in which the complete post-embryonic trichobothrial pattern is known (Mahnert 1984; Harvey et al. 2007; Harvey & Muchmore 2013). The protonymph of *S. jerai* bears four unusual tactile setae near the *ib*, *ist*, *est* and *b* regions. The bases of these setae (8 μm) are larger than those of normal chelal setae (4–5 μm), but are smaller than the bothria (15 μm). Each seta is longer than a normal seta, but shorter than a trichobothrium. It is possible that they each represent the precursor to the trichobothrium that develops at the deutonymph stage.

Members of the genus *Sironcus* occur in Myanmar, Thailand, northern peninsular Malaysia and Sarawak (Figs. 2B, 22), where they inhabit leaf litter in rainforest ecosystems.

Etymology.—The generic name is a contraction of Siam and *Roncus*, a typical suffix within the Ideoroncidae.

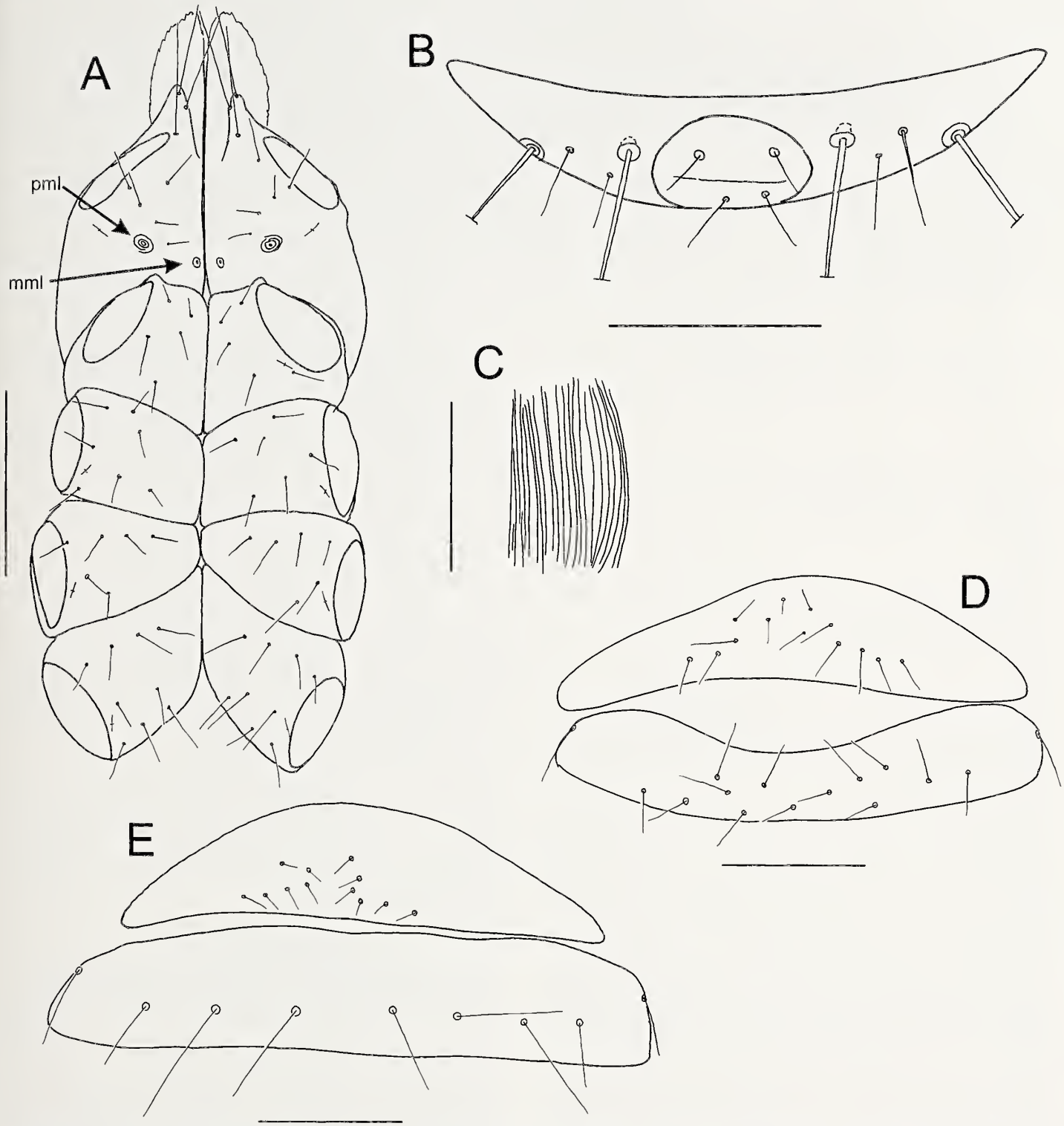

Figure 23.—*Sironcus siamensis* (With), male from Ko Chang, Thailand (MHNG), unless stated otherwise: A. Cephalothorax, ventral; B. Sternite XI and anal operculum; C. Pleural membrane; D. Sternites III and IV, male, ventral; E. Sternites III and IV, female, ventral. Abbreviations: ejca, ejaculatory canal atrium; lgs, lateral genital sac; mgs, median genital sac; mml, median maxillary lyrifissure; pml, posterior maxillary lyrifissure. Scale lines = 0.25 (B); 0.2 mm (A); 0.1 mm (C–E).

KEY TO SPECIES OF *SIRONCUS*

1. All pedipalpal segments smooth (Fig. 25B); carapace with 18 setae (Fig. 25A) ..... *S. jerai*
   At least some pedipalpal segments with fine granulations on prolateral face (Figs. 24B, 26B, 27D, 28B, 29B); carapace with 23–27 setae (Figs. 24A, 26A, 27A, 28A, 29A) 2
2. Pedipalpal segments slightly elongated (Fig. 29B), e.g., patella 3.45 (♂), 3.39 (♀) x longer than broad ..... *S. stonei*
   Pedipalpal segments less elongate (Figs. 24B, 26B, 27D, 28B), e.g., patella 2.69–3.08 (♂), 2.47–3.15 (♀) x longer than broad 3
3. Teeth of fixed chelal finger prominent, with basal face expanded (Fig. 26E) ..... *S. rhiodontus*
   Teeth of fixed chelal finger low, with basal face not expanded (Figs. 24D, 27F, 28D) 4
4. Teeth of the fixed chelal finger with rounded cusps (Fig. 24D) ..... *S. belaga*
   Teeth of the fixed chelal finger with triangular or pointed cusps (Figs. 27F, 28D) 5
5. Pedipalpal femur smooth (Fig. 27D) ..... *S. siamensis*
   Pedipalpal femur finely granulate on prolateral face (Fig. 28B) ..... *S. sierwaldae*

Sironcus belaga sp. nov.

http://zoobank.org/NomenclaturalActs/urn:lsid:zoobank.org:act:9E2DD215-FB61-48CF-BD68-836A4C4B7187

Fig. 24

Material examined.—*Holotype male*. MALAYSIA: *Sarawak*: Long Linau, Belaga District [2°44′N, 114°04′E], 17–21 March 1990, A. Riedel (SMNS).

Diagnosis.—*Sironcus belaga* differs from other species of the genus by the rounded teeth of the fixed chelal finger (Fig. 24D).

Description (male).—*Color:* pedipalps and carapace deep red-brown; chelicerae and legs yellow-brown; tergites and sternites pale yellow-brown.

Setae: generally long, straight or slightly curved, and acicular.

Chelicera: with 6 setae on hand; movable finger with 1 seta; galea very slender and elongate; fixed finger with ca. 8 teeth; movable finger with ca. 5 teeth; rallum of 4 blades, the 3 distal blades serrate, the basal blade with very small serrations; lamina exterior absent.

Pedipalp (Fig. 24B): prolateral face of femur and patella granulate, other segments smooth; trochanter 2.31, femur 3.62, patella 2.69, chela (with pedicel) 3.74, chela (without pedicel) 3.51, hand 1.58 x longer than broad, movable finger 1.28 x longer than hand. Fixed chelal finger with 20 trichobothria, movable chelal finger with 10 trichobothria (Fig. 24C): *eb*, *esb* and *isb* in straight row at base of finger; *eb*, *esb*, *et*, *isb* and *it* regions each with 1 trichobothrium; *ib* region with 4 trichobothria; *ist* region with 5 trichobothria; *est* region with 6 trichobothria; *et* slightly distal to *it*; *b* region with 2 trichobothria; *sb* and *st* regions each with 1 trichobothrium; *t* region with 6 trichobothria. Venom apparatus present in both chelal fingers, venom duct terminating in nodus ramosus near *est* region in fixed finger and near basal section of *t* region in movable finger (Fig. 24C). Chelal hand without microsetae near *eb* and *esb* (Fig. 24C). Chelal teeth juxtadentate, fixed finger with 48 teeth, mostly low and rounded (Fig. 24D); movable finger with 39 very low, rounded teeth.

Carapace (Fig. 24A): 0.84 x longer than broad; lateral margins slightly convex; with 2 small bulging eyes; epistome absent; with 27 setae, including 4 near anterior margin and 4 near posterior margin; without furrows.

Coxal region: manducatory process with 2 long apical setae, plus 6 additional setae; chaetotaxy of coxae I–IV: 4: 6: 5: 7.

Legs: femur + patella 2.56 x longer than deep; subterminal tarsal setae bifurcate (Fig. 24E); arolium undivided, shorter than claws, bearing a ventral hooked process (Fig. 24E).

Abdomen: tergites and sternites undivided and uniseriate. Tergal chaetotaxy: 4: 5: 10: 12: 13: 14: 14: 15: 15: 11 (including 4 tactile setae): 8 (including 4 tactile setae): 2. Sternal chaetotaxy: 10: (1) 17 [3 + 3] (1): (1) 13 (1): 14: 16: 16: 16: 15: 15: 8 (including 4 tactile setae): 2. Setae of tergites and sternites IX–XI acuminate.

Genitalia: male with median genital sac deeply bipartite.

Dimensions (mm): male: holotype: Body length 1.60. *Pedipalp*: trochanter 0.30/0.13, femur 0.615/0.17, patella 0.475/0.18, chela (with pedicel) 1.03/0.275, chela (without pedicel) 0.965, hand length 0.435, movable finger length 0.555. Chelicera 0.315/0.145, movable finger length 0.22. Carapace 0.48/0.57; eye diameter 0.035. Leg I: femur 0.315/0.09, patella 0.16/0.085, tibia 0.205/0.06, metatarsus 0.13/0.05, tarsus 0.20/0.05. Leg IV: femur + patella 0.50/0.195, tibia 0.34/0.09, metatarsus 0.17/0.07, tarsus 0.29/0.55.

Remarks.—*Sironcus belaga* has only been collected from Long Linu, in central Sarawak (Fig. 22). Long Linau is located a few km south and upstream of the Bakun Hydroelectric Dam, 2°44′N, 114°04′E (see Sagin et al. 2001).

Etymology.—The species epithet is a noun in apposition taken from Belaga District.

Sironcus jerai sp. nov.

http://zoobank.org/NomenclaturalActs/urn:lsid:zoobank.org:act:5CE9F81B-BFB6-4DD9-B8DC-21EEC1E3688A

Fig. 25

Dhanus siamensis (With): Harvey, 1992:figs. 58–67 (misidentification).

Material examined.—*Holotype female*. MALAYSIA: *Kedah*: Gunong Jerai, 5°48′N, 100°26′E, 550 m, rainforest berlesate, 12 September 1982, R.W. Taylor, R.A. Barrett (ANIC).

Paratypes. MALAYSIA: *Kedah*: 1 tritonymph, 1 deutonymph, 4 protonymphs, collected with holotype (ANIC); 1 tritonymph, 1 deutonymph, 1 protonymph, collected with holotype (WAM T91/1351–1353).

Diagnosis.—*Sironcus jerai* differs from other species of the genus by the smooth pedipalpal segments (Fig. 25B), and only 18 carapaceal setae (Fig. 25A). In all other species, at least the

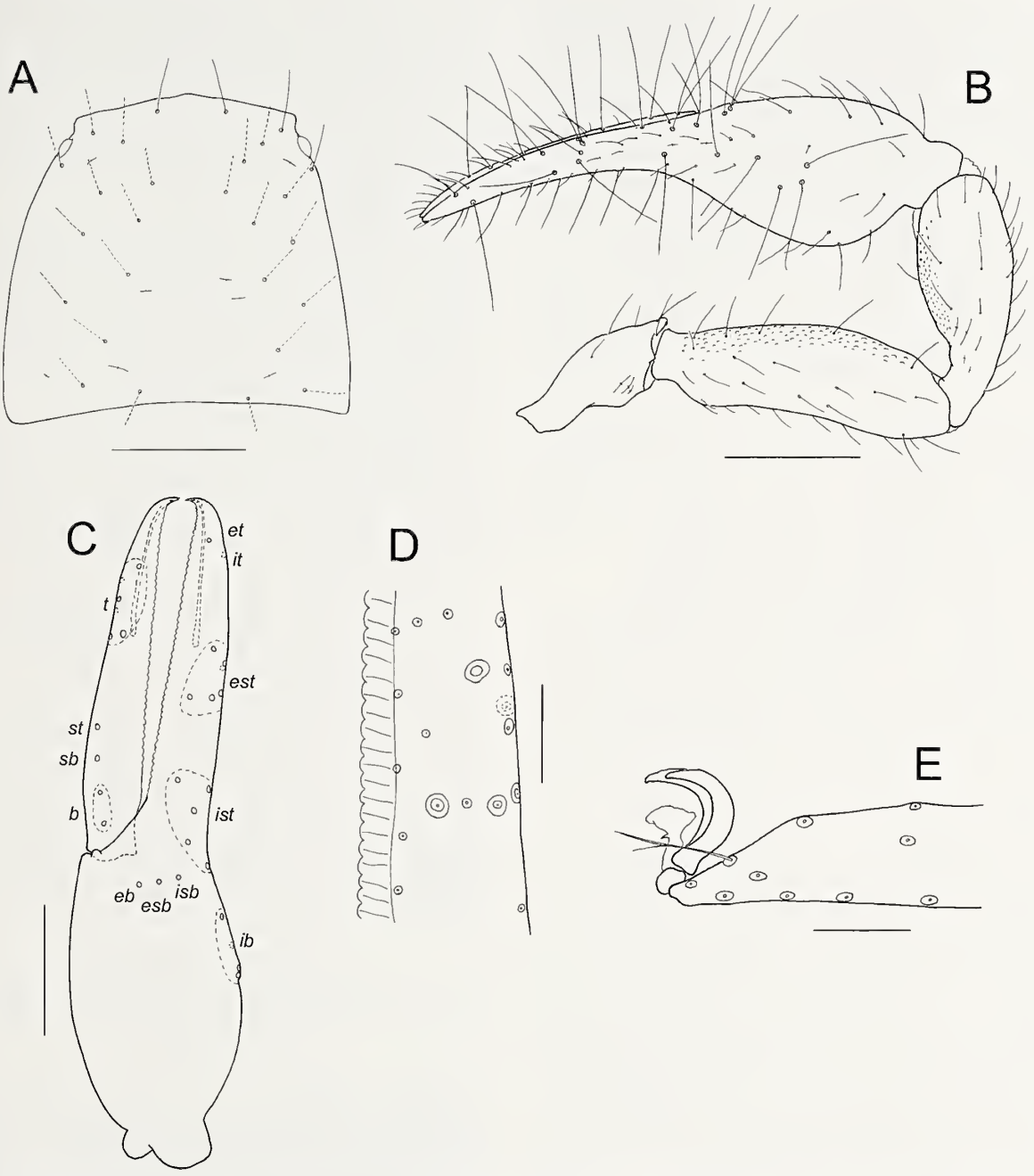

Figure 24.—*Sironcus belaga* sp. nov., male holotype: A. Carapace; B. Right pedipalp, dorsal; C. Left chela, lateral; D. Detail of fixed chelal finger; E. Distal end of tarsus IV showing arolium, claws and subterminal seta, other setae omitted. Scale lines = 0.25 mm (B); 0.2 mm (A, B); 0.05 mm (D, E).

femur and patella is granulate on the prolateral face, and the carapace bears 23–27 setae.

Description (female).—*Color:* pedipalps and carapace deep red-brown; chelicerae and legs yellow-brown; tergites and sternites pale yellow-brown.

Setae: generally long, straight or slightly curved, and acicular.

Chelicera (Fig. 25H): with 6 setae on hand; movable finger with 1 seta; galea very slender and elongate; fixed finger with 8 teeth; movable finger with 6 small teeth; rallum (Fig. 25I) of 4 blades, the 3 distal blades serrate, the basal blade with very small serrations; lamina exterior absent.

Pedipalp (Fig. 25B): segments smooth; trochanter 2.21, femur 3.42, patella 2.47, chela (with pedicel) 3.35, chela (without pedicel) 3.18, hand 1.47 x longer than broad, movable finger 1.20 x longer than hand. Fixed chelal finger with 20 trichobothria, movable chelal finger with 10 trichobothria (Fig. 25C): *eb*, *esb* and *isb* in straight row at base of finger; *eb*, *esb*, *et*, *isb* and *it* regions each with 1 trichobothrium; *ib* region with 4 trichobothria; *ist* region with 5 trichobothria; *est* region with 6 trichobothria; *et* slightly distal to *it*; *b* region with 2 trichobothria; *sb* and *st* regions each with 1 trichobothrium; *t* region with 6 trichobothria. Venom apparatus present in both chelal fingers, venom duct

terminating in nodus ramosus near *est* region in fixed finger and near basal section of *t* region in movable finger (Fig. 25C). Chelal hand without microsetae near *eb* and *esb* (Fig. 25C). Chelal teeth juxtadentate, fixed finger with 47 teeth, mostly truncate (Fig. 25D); movable finger with 37 very low teeth.

Carapace (Fig. 25A): 1.02 x longer than broad; lateral margins slightly convex; with 2 bulging eyes; with extremely small epistome; with 18 setae, including 4 near anterior margin and 2 near posterior margin; without furrows.

Coxal region: manducatory process with 2 long apical setae, plus 5 additional setae; chaetotaxy of coxae I–IV: 4: 5: 5: 5.

Legs (Fig. 25J, K): femur + patella 2.50 x longer than deep; subterminal tarsal setae bifurcate (Fig. 25L); arolium undivided, shorter than claws, bearing a ventral hooked process (Fig. 25L).

Abdomen: tergites and sternites undivided and uniseriate. Tergal chaetotaxy: 4: 4: 9: 9: 9: 10: 14: 11: 11: 12 (including 2 tactile setae): 12 (including 4 tactile setae): 2. Sternal chaetotaxy: 8: (1) 4 (1): (1) 5 (1): 8: 11: 11: 13: 12: 13 (including 2 tactile setae): 10 (including 4 tactile setae): 2. Setae of tergites and sternites IX–XI acuminate.

Genitalia: with large gonosac covered with pores.

Dimensions (mm): female: holotype: Body length 1.84. *Pedipalp*: trochanter 0.31/0.14, femur 0.65/0.19, patella 0.47/0.19, chela (with pedicel) 1.14/0.34, chela (without pedicel) 1.08, hand length 0.50, movable finger length 0.67. Chelicera 0.33/0.16, movable finger length 0.21. Carapace 0.54/0.53; eye diameter 0.05. Leg I: femur 0.34/0.10, patella 0.17/0.09, tibia 0.22/0.06, metatarsus 0.14/0.06, tarsus 0.20/0.04. Leg IV: femur + patella 0.55/0.22, tibia 0.38/0.10, metatarsus 0.19/0.08, tarsus 0.29/0.05.

Description (tritonymph).—*Chelicera:* galea long and slender, slightly curved; with 6 setae on hand; 1 on movable finger; rallum composed of 4 blades, all serrate.

Pedipalp: trochanter 2.30, femur 3.07, patella 2.25, chela (with pedicel) 3.43, chela (without pedicel) 3.21, hand 1.30 x longer than broad; movable finger 1.40 x longer than hand (without pedicel). Fixed chelal finger with 14 trichobothria, movable chelal finger with 8 trichobothria (Fig. 25E); *isb* and *sb* absent; *eb*, *esb*, *et* and *it* regions each with 1 trichobothrium; *eb* and *esb* at base of finger; *ib* region with 3 trichobothria; *ist* region with 4 trichobothria; *est* region with 3 trichobothria; *et* slightly distal to *it*; *b* region with 2 trichobothria; *st* region with 1 trichobothrium; *t* region with 5 trichobothria.

Carapace: anterior margin with very small epistome; with 2 small bulging eyes; with 18 setae including 4 setae near anterior margin and 2 near posterior margin.

Legs: much as in adult.

Dimensions (mm): Body length 1.50. *Pedipalp*: trochanter 0.23/0.10, femur 0.46/0.15, patella 0.36/0.16, ehela (with pedicel) 0.79/0.23, chela (without pedicel) 0.74, hand length 0.30, movable finger length 0.42. Carapace 0.41/0.48.

Description (deutonymph).—*Chelicera:* galea long and slender, slightly curved; with 5 setae on hand; 1 on movable finger; rallum composed of 4 blades, all serrate.

Pedipalp: trochanter 2.00, femur 3.67, patella 1.92, chela (with pedicel) 3.50, chela (without pedicel) 3.31, hand 1.44 x longer than broad; movable finger 1.39 x longer than hand (without pedicel). Fixed chelal finger with 9 trichobothria, movable chelal finger with 6 trichobothria (Fig. 25F); *esb*, *isb*, *sb* and *st* absent; *eb* at base of finger; *ib* region with 2 trichobothria; *ist* region with 2 trichobothria; *est* region with 2 trichobothria; *et* slightly distal to *it*; *b* region with 2 trichobothria; *t* region with 4 trichobothria.

Carapace: anterior margin with very small epistome; with 2 small bulging eyes; with 16 setae including 4 setae near anterior margin and 2 near posterior margin.

Legs: much as in adult.

Dimensions (mm): Body length 1.15. *Pedipalp*: trochanter 0.18/0.09, femur 0.33/0.09, patella 0.23/0.09, chela (with pedicel) 0.56/0.16, chela (without pedicel) 0.53, hand length 0.23, movable finger length 0.32. Carapace 0.33/0.33.

Description (protonymph).—*Chelicera:* galea long and slender, slightly curved; with 4 setae on hand; 0 on movable finger; rallum composed of 4 blades, all serrate.

Pedipalp: trochanter 1.88, femur 3.43, patella 1.90, chela (with pedicel) 3.83, chela (without pedicel) 3.58, hand 1.50 x longer than broad; movable finger 1.39 x longer than hand (without pedicel). Fixed chelal finger with 3 trichobothria, movable chelal finger with 1 trichobothrium (Fig. 25G); *eb*, *et*, *ist* and *t* present; single pseudo-trichobothria present near *ib*, *ist*, *est* and *b* region.

Carapace: anterior margin with very small epistome; with 2 small bulging eyes; with 14 setae including 4 setae near anterior margin and 2 near posterior margin.

Legs: much as in adult.

Dimensions (mm): Body length 0.79. *Pedipalp*: trochanter 0.15/0.08, femur 0.24/0.07, patella 0.19/0.10, ehela (with pedicel) 0.46/0.12, chela (without pedicel) 0.43, hand length 0.18, movable finger length 0.25. Carapace 0.275/0.245.

Remarks.—*Sironcus jerai* has only been collected from Gunong Jerai, in north-western Malaysia (Fig. 22).

Etymology.—The species epithet is a noun in apposition taken from the type locality, Gunong Jerai.

Sironcus rhiodontus sp. nov.
http://zoobank.org/NomenclaturalActs/urn:lsid:zoobank.org:act:C7C4D52A-EE54-459D-93D1-102A6CD8AF80
(Fig. 26)

Material examined.—*Holotype male.* THAILAND: *Chumphon Province*: near border Lang Suan - Phato Districts, Khao Kai Jae Waterfall, 9°55′04.6″N, 98°56′33.7″E, 5–8 May 2003, semi-evergreen rainforest, P. Schwendinger (MHNG).

Paratypes. THAILAND: *Chumphon Province*: 2 ♂, 3 ♀, collected with holotype (MHNG); 1 ♂, 1 ♀, collected with holotype (WAM T140763); 5 ♂, 3 ♀, 1 deutonymph, Lang Suan District, Khao Kai Jae Waterfall, 9°55′04.6″N, 98°56′33.7″E, 80 m, 17–18 July 2002, semi-evergreen rainforest, P. Schwendinger (MHNG).

Other material examined. THAILAND: *Nakhon Si Thammarat Province*: 1 ♂, Khao Luang National Park, Ay Khieo Waterfall, 8°33′25.0″N, 99°46′36.1″E, 25 November 2001, semi-evergreen rainforest, P. Schwendinger (MHNG); *Phangnga Province*: 2 ♂, 3 ♀, 1 tritonymph, Khao Sok National Park, 30 km E. of Takua Pa, 8°55′N, 98°36′E, 21–26 December 1997, secondary moist forest with primary spots, A. Schulz (MHNG); *Ranong Province*: 1 ♀, Ranong, outside town behind Jansom Thara Hotel [9°58′N, 98°38′E], 50 m, semi-evergreen rainforest, 18 September 1992, P. Schwen-

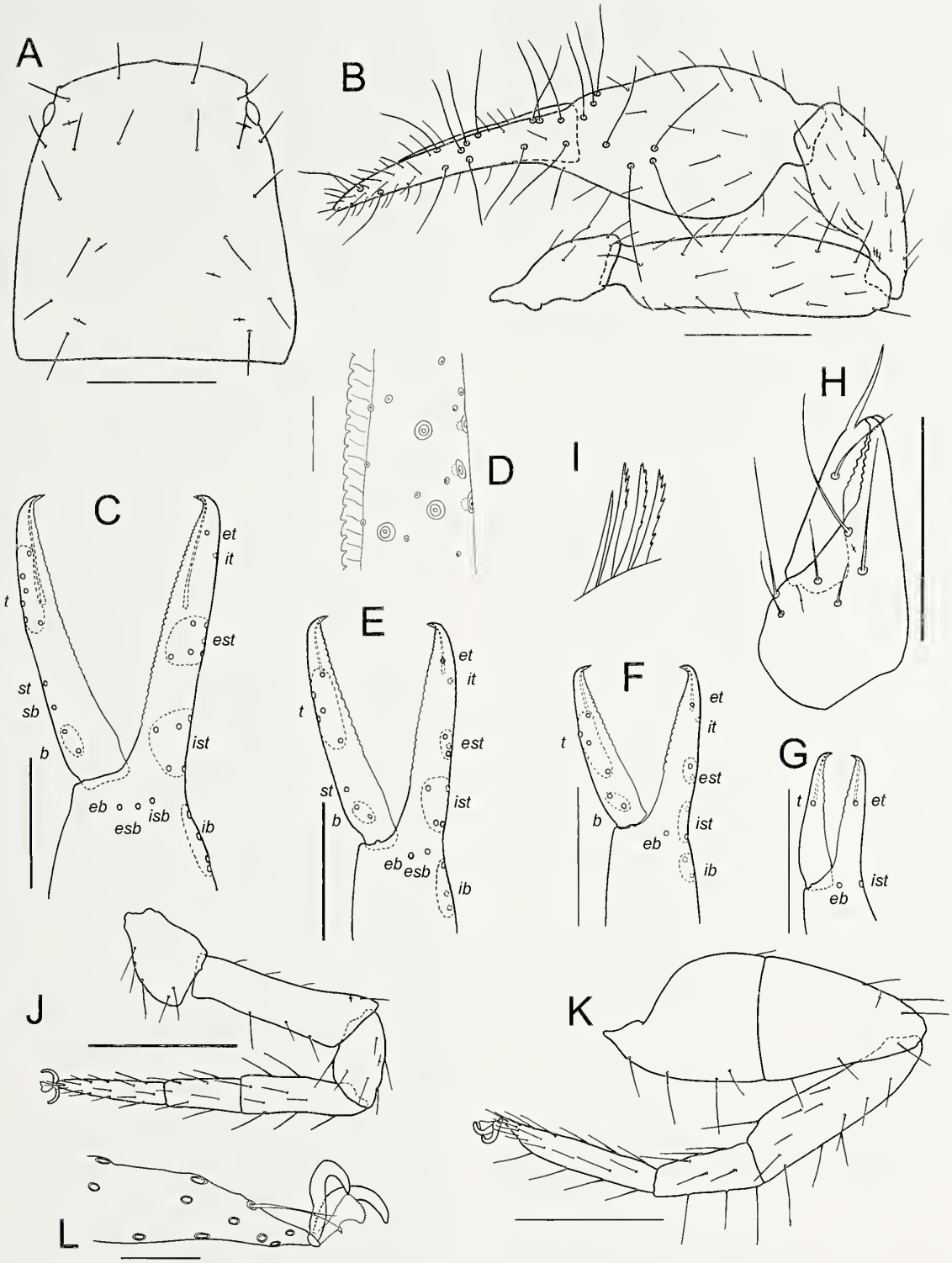

Figure 25.—*Sironcus jerai* sp. nov., female holotype, unless stated otherwise: A. Carapace; B. Right pedipalp, dorsal; C. Left chela, lateral; D. Detail of fixed chelal finger; E. Left chela, lateral, tritonymph; F. Left chela, lateral, deutonymph; G. Left chela, lateral, protonymph; H. Left chelicera; I. Rallum; J. Left leg I; K. Left leg IV; L. Distal end of tarsus IV showing arolium, claws and subterminal seta, other setae omitted. Scale lines = 0.25 mm (A–C, E–H, J, K); 0.05 mm (D, L).

dinger (MHNG); *Satun Province*: 3 ♂, 1 ♀, Thaleban National Park, 6°42′N, 100°07′E, 1–5 January 1998, primary moist forest, A. Schulz, K. Vock (MHNG).

Diagnosis.—*Sironcus rhiodontus* differs from all other species of the genus by the expanded basal face of the chelal teeth of the fixed finger (Fig. 26E).

Description (adult).—*Color:* pedipalps and carapace deep red-brown; chelicerae and legs yellow-brown; tergites and sternites pale yellow-brown.

Setae: generally long, straight or slightly curved, and acicular.

Chelicera: with 6–7 (♂), 7 (♀) setae on hand; movable finger with 1 seta; galea very slender and elongate; fixed finger with 7 (♂), 8 (♀) teeth; movable finger with 7 (♂, ♀) small teeth; rallum of 4 serrate blades; lamina exterior absent.

Pedipalp (Fig. 26B): femur and patella lightly granulate on prolateral surface, remaining segments smooth; trochanter 2.04–2.37 (♂), 2.19–2.39 (♀), femur 3.72–4.24 (♂), 3.93–4.04 (♀), patella 2.83–3.08 (♂), 2.81–2.97 (♀), chela (with pedicel) 3.88–4.14 (♂), 3.68–3.81 (♀), chela (without pedicel) 3.73–3.91 (♂), 3.45–3.64 (♀), hand 1.53–1.66 (♂), 1.47–1.62 (♀) x longer than broad, movable finger 1.35–1.50 (♂), 1.30–1.39 (♀) x longer than hand. Fixed chelal finger with 20 trichobothria, movable chelal finger with 10 trichobothria (Fig. 26D): *eb*, *esb* and *isb* in straight row at base of finger; *eb*, *esb*, *et*, *isb* and *it* regions each with 1 trichobothrium; *ib* region with 4 trichobothria; *ist* region with 5 trichobothria; *est* region with 6 trichobothria; *et* slightly distal to *it*; *b* region with 2 trichobothria; *sb* and *st* regions each with 1 trichobothrium; *t* region with 6 trichobothria. Venom apparatus present in both chelal fingers, venom duct terminating in nodus ramosus near *est* region in fixed finger and near basal section of *t* region in movable finger (Fig. 26D). Chelal hand without microsetae near *eb* and *esb* (Fig. 26D). Chelal teeth juxtadentate, fixed finger with 40 (♂), 39 (♀) teeth, most with expanded basal face (Fig. 26E); movable finger with 29 (♂, ♀) low teeth.

Carapace (Fig. 26A): 1.06–1.11 (♂), 0.90–0.97 (♀) x longer than broad; lateral margins slightly convex; with 2 bulging eyes; with small epistome; with 23 (♂), 26 (♀) setae, including 6 setae near the anterior margin and 4 near the posterior margin; without furrows.

Coxal region: manducatory process with 2 long apical setae, plus 7 (♂, ♀) additional setae; chaetotaxy of coxae I–IV: ♂, 7: 8: 7: 8; ♀, 5: 9: 8: 11.

Legs: femur + patella 2.44 (♂), 2.61 (♀) x longer than deep; subterminal tarsal setae bifurcate (Fig. 26C); arolium undivided, shorter than claws, bearing a ventral hooked process (Fig. 26C).

Abdomen: tergites and sternites undivided and uniseriate. Tergal chaetotaxy: ♂, 4: 4: 6: 8: 8: 9: 9: 12: 13 (including 4 tactile setae): 10 (including 4 tactile setae): 8 (including 4 tactile setae): 2; ♀, 4: 4: 7: 10: 10: 11: 11: 13: 13: 11 (including 4 tactile setae): 7 (including 4 tactile setae): 2. Sternal chaetotaxy: ♂, 8: (1) 12 [3 + 3] (1): (1) 13 (1): 13: 15: 14: 16: 14 (including 2 tactile setae): 8 (including 4 tactile setae): 8 (including 4 tactile setae): 2; ♀, 8: (1) 8 (1): (1) 11 (1): 17: 16: 18: 19: 20: 15 (including 4 tactile setae): 10 (including 4 tactile setae): 2. Setae of tergites and sternites IX–XI acuminate.

Genitalia: male with median genital sac deeply bipartite; female with large gonosac covered with pores.

Dimensions (mm): males: holotype followed by other males (when measured): Body length 1.55 (1.36–1.61). *Pedipalp*: trochanter 0.275/0.135 (0.29–0.32/0.135), femur 0.67/0.17 (0.67–0.72/0.165–0.18), patella 0.505/0.175 (0.50–0.555/0.175–0.18), chela (with pedicel) 1.16/0.29 (1.11–1.32/0.275–0.36), chela (without pedicel) 1.11 (1.065–1.12), hand length 0.445 (0.445–0.475), movable finger length 0.67 (0.61–0.67). Chelicera 0.315/0.15, movable finger length 0.20. Carapace 0.515/0.465 (0.51–0.535/0.45–0.50); eye diameter 0.505. Leg I: femur 0.36/0.10, patella 0.215/0.095, tibia 0.225/0.065, metatarsus 0.175/0.06, tarsus 0.235/0.045. Leg IV: femur + patella 0.585/0.24, tibia 0.39/0.105, metatarsus 0.215/0.075, tarsus 0.345/0.06.

Females: paratype followed by other females (when measured): Body length 2.36 (1.40–1.66). *Pedipalp*: trochanter 0.355/0.155 (0.34–0.37/0.155), femur 0.825/0.21 (0.805–0.83/0.20–0.21), patella 0.59/0.21 (0.58–0.605/0.195–0.205), chela (with pedicel) 1.39/0.365 (1.325–1.45/0.35–0.40), chela (without pedicel) 1.33 (1.26–1.33), hand length 0.58 (0.535–0.59), movable finger length 0.785 (0.74–0.785). Chelicera 0.41/0.19, movable finger length 0.26. Carapace 0.57/0.635 (0.55–0.56/0.565–0.59); eye diameter 0.06. Leg I: femur 0.45/0.11, patella 0.235/0.165, tibia 0.285/0.075, metatarsus 0.21/0.065, tarsus 0.26/0.045. Leg IV: femur + patella 0.705/0.27, tibia 0.475/0.11, metatarsus 0.265/0.085, tarsus 0.40/0.055.

Description (tritonymph).—*Chelicera:* galea long and slender, slightly curved; with 6 setae on hand; 1 on movable finger; rallum composed of 4 blades, all serrate.

Pedipalp: trochanter 2.26, femur 3.79, patella 2.76, chela (with pedicel) 3.89, chela (without pedicel) 3.70, hand 1.64 x longer than broad; movable finger 1.30 x longer than hand (without pedicel). Fixed chelal finger with 14 trichobothria, movable chelal finger with 8 trichobothria (Fig. 26F); *isb* and *sb* absent; *eb*, *esb*, *et* and *it* regions each with 1 trichobothrium; *eb* and *esb* at base of finger; *ib* region with 3 trichobothria; *ist* region with 4 trichobothria; *est* region with 3 trichobothria; *et* slightly distal to *it*; *b* region with 2 trichobothria; *st* region with 1 trichobothrium; *t* region with 5 trichobothria.

Carapace: anterior margin medially prominent; with 2 small bulging eyes; with 22 setae including 6 setae near anterior margin and 4 near posterior margin.

Legs: much as in adult.

Dimensions (mm): Body length 1.85. *Pedipalp*: trochanter 0.305/0.135, femur 0.625/0.165, patella 0.455/0.165, chela (with pedicel) 1.09/0.28, chela (without pedicel) 1.035, hand length 0.46, movable finger length 0.60. Carapace 0.485/0.46.

Description (deutonymph).—*Chelicera:* galea long and slender, slightly curved; with 5 setae on hand; 1 on movable finger; rallum composed of 4 blades, all serrate.

Pedipalp: trochanter 2.33, femur 3.77, patella 2.46, chela (with pedicel) 4.00, chela (without pedicel) 3.81, hand 1.59 x longer than broad; movable finger 1.39 x longer than hand (without pedicel). Fixed chelal finger with 9 trichobothria, movable chelal finger with 6 trichobothria (Fig. 26G); *esb*, *isb*, *sb* and *st* absent; *eb* at base of finger; *ib* region with 2 trichobothria; *ist* region with 2 trichobothria; *est* region with 2 trichobothria; *et* slightly distal to *it*; *b* region with 2 trichobothria; *t* region with 4 trichobothria.

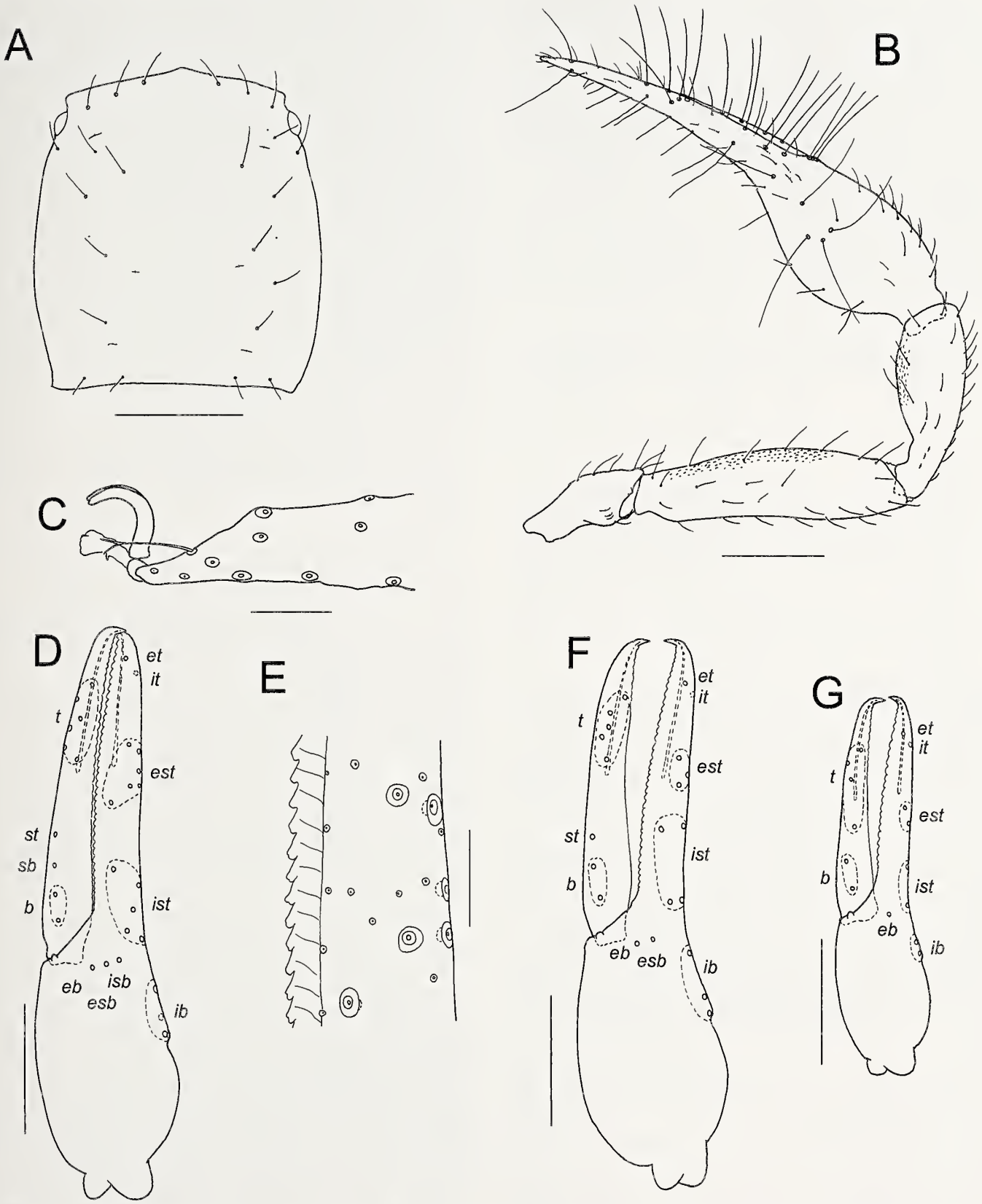

Figure 26.—*Sironcus rhiodontus* sp. nov., male holotype, unless stated otherwise: A. Carapace; B. Right pedipalp, dorsal; C. Distal end of tarsus IV showing arolium, claws and subterminal seta, other setae omitted; D. Left chela, lateral; E. Detail of fixed chelal finger; F. Left chela, lateral, tritonymph; G. Left chela, lateral, deutonymph. Scale lines = 0.25 mm (B, D, F, G); 0.2 mm (A); 0.05 mm (E, G).

Carapace: anterior margin medially prominent; with 2 small bulging eyes; with 17 setae including 5 setae near anterior margin and 2 near posterior margin.

Legs: much as in adult.

Dimensions (mm): Body length 1.20. *Pedipalp*: trochanter 0.21/0.09, femur 0.415/0.11, patella 0.295/0.12, chela (with pedicel) 0.74/0.185, chela (without pedicel) 0.705, hand length 0.295, movable finger length 0.41. Carapace 0.395/0.37.

Remarks.—*Sironcus rhiodontus* occurs in rainforest habitats in southern Thailand (Fig. 22).

Etymology.—The species epithet refers to the enlarged teeth of fixed chelal finger which bear a basal overhanging portion (*rhion*, Greek, a jutting part of a mountain, peak, headland; *odontos*, Greek, tooth) (Brown 1956).

Sironcus siamensis (With), comb. nov.
http://zoobank.org/NomenclaturalActs/urn:lsid:zoobank.org:act:1D51B4AF-ED7C-4587-953A-8C7AB2D71B65
(Figs. 23, 27)

Ideobisium (Ideoroncus) siamensis With, 1906:81–84, plate 1 fig. 4a–i.

Dhanus siamensis (With): Chamberlin, 1930:47; Beier, 1932a:174, fig. 8; Beier, 1932b:figs. 200c, 208; Roewer, 1936:figs. 37a–b, 83g, 86, 107a–b; Roewer, 1937:257; Harvey, 1991:318; Schawaller, 1994:737, fig. 33 (misidentification, in part); Judson, 1997:40; Harvey, 2013:unpaginated.

Not *Dhanus siamensis* (With): Harvey, 1992:figs. 58–67 (misidentification, see *Sironcus jerai*).

Material examined.—*Lectotype male (present designation).* THAILAND: *Trat Province*: Ko Chang [as Koh Chang] [*ca.* 12°00′N, 102°23′E], 6 January 1900, T. Mortensen (ZMC).

Paralectotypes. THAILAND: *Trat Province*: 1 ♀, same data as lectotype except 5 January 1900 (ZMC); 1 ♂, Khlong Salak Phet (as Klong Salakpet) [12°01′N, 102°22′E], 13 March 1900, T. Mortensen (ZMC, JC–446.01001).

Other material examined. THAILAND: *Trat Province*: 1 ♂, 2 ♀, Ko Chang National Park, Khlong Phrao Waterfall and hill near White Sand Beach [12°07′N, 102°16′E], 100 m, 23–25 August 1992, P. Schwendinger (MHNG); 36 ♂, 21 ♀, Ko Chang, west side, 12°03′N, 102°18′E, 3–23 December 1999, A. Schulz (MHNG); 2 ♂, 2 ♀, same data (WAM T140764).

Diagnosis.—*Sironcus siamensis* differs from all other species of the genus except *S. sierwaldae* by the triangular cusps of the teeth of the fixed chelal finger (Fig. 27F), and differs from *S. sierwaldae* by the completely smooth pedipalpal femur (Fig. 27D).

Description (adult).—*Color:* pedipalps and carapace deep yellow-brown; chelicerae and legs yellow-brown; tergites and sternites pale yellow-brown.

Setae: generally long, straight or slightly curved, and acicular.

Chelicera (Fig. 27B): with 6–7 (♂, ♀) setae on hand; movable finger with 1 seta; galea very slender and elongate; fixed finger with 11 (♂, ♀) teeth; movable finger with 7 (♂), 8 (♀) small teeth; rallum (Fig. 27C) of 4 blades, all serrate; lamina exterior absent.

Pedipalp (Fig. 27D): segments smooth, except for minute denticles on prolateral face of patella; trochanter 1.52–2.33 (♂), 2.00–2.38 (♀), femur 3.93–4.23 (♂), 3.60–4.03 (♀), patella 2.93–3.06 (♂), 2.65–2.83 (♀), chela (with pedicel) 3.85–4.00 (♂), 3.50–3.93 (♀), chela (without pedicel) 3.65–3.83 (♂), 3.33–3.75 (♀), hand 1.63–1.68 (♂), 1.48–1.69 (♀) x longer than broad, movable finger 1.26–1.36 (♂), 1.20–1.26 (♀) x longer than hand. Fixed chelal finger with 20 trichobothria, movable chelal finger with 10 trichobothria (Fig. 27E): *eb*, *esb* and *isb* in straight row at base of finger; *eb*, *esb*, *et*, *isb* and *it* regions each with 1 trichobothrium; *ib* region with 4 trichobothria; *ist* region with 5 trichobothria; *est* region with 6 trichobothria; *et* slightly distal to *it*; *b* region with 2 trichobothria; *sb* and *st* regions each with 1 trichobothrium; *t* region with 6 trichobothria. Venom apparatus present in both chelal fingers, venom duct terminating in nodus ramosus near *est* region in fixed finger and near basal section of *t* region in movable finger (Fig. 27E). Chelal hand without microsetae near *eb* and *esb* (Fig. 27E). Chelal teeth juxtadentate, fixed finger with 31 (♂, ♀) triangular teeth (Fig. 27F); movable finger with 24 (♂, ♀) very low, obsolete teeth.

Carapace (Fig. 27A): 1.08–1.12 (♂), 0.85–1.02 (♀) x longer than broad; lateral margins slightly convex; with 2 bulging eyes; with small epistome; with 26 (♂, ♀) setae, including 6 near the anterior margin and 4 near the posterior margin; without furrows.

Coxal region (Fig. 23A): manducatory process with 2 long apical setae, plus 7 (♂), 6 (♀) additional setae; chaetotaxy of coxae I–IV: ♂, 6: 8: 7: 9; ♀, 7: 8: 9: 10.

Legs (Fig. 27 G): femur + patella 2.45 (♂), 2.80 (♀) x longer than deep; subterminal tarsal setae bifurcate (Fig. 27H); arolium undivided, shorter than claws, bearing a ventral hooked process (Fig. 27H).

Abdomen: tergites and sternites undivided and uniseriate. Tergal chaetotaxy: ♂, 4: 4: 8: 11: 10: 13: 13: 12: 12: 10 (including 4 tactile setae): 9 (including 4 tactile setae): 2; ♀, 4: 4: 8: 11: 11: 11: 12: 13: 13: 12 (including 4 tactile setae): 7 (including 4 tactile setae): 2. Sternal chaetotaxy: ♂, 13: (1) 12 [3 + 3] (1): (1) 13 (1): 10: 14: 15: 15: 16: 13 (including 4 tactile setae): 8 (including 4 tactile setae): 2; ♀, 11: (1) 6 (1): (1) 11 (1): 13: 15: 16: 16: 18: 15 (including 4 tactile setae): 9 (including 4 tactile setae): 2. Setae of tergites and sternites IX–XI acuminate (Fig. 23B).

Genitalia: male with median genital sac deeply bipartite; female with large gonosac covered with pores.

Dimensions (mm): males: lectotype followed by 2 other males (when measured): Body length 1.51 (1.51–1.82). *Pedipalp*: trochanter 0.25/0.12 (0.19–0.245/0.105–0.125), femur 0.59/0.15 (0.565–0.635/0.14–0.15), patella 0.465/0.155 (0.41–0.475/0.14–0.155), chela (with pedicel) 1.00/0.25 (0.915–1.00/0.23–0.26), chela (without pedicel) 0.95 (0.88–0.95), hand length 0.42 (0.375–0.425), movable finger length 0.565 (0.51–0.535). Chelicera 0.20/0.135, movable finger length 0.175. Carapace 0.50/0.445 (0.465/0.43); eye diameter 0.04. Leg I: femur ? (0.285/0.085), patella ? (0.175/0.075), tibia ?, metatarsus ?, tarsus ?. Leg IV: femur + patella ? (0.47/0.185), tibia ? (0.315/0.08), metatarsus ? (0.18/0.065), tarsus ? (0.28/0.045).

Females: paralectotype followed by 2 other females (when measured): Body length 2.14 (1.63–1.77). *Pedipalp*: trochanter 0.26/0.13 (0.30–0.31/0.13–0.135), femur 0.64/0.17 (0.63–0.685/0.17–0.175), patella 0.48/0.17 (0.45–0.495/0.17–0.175), chela

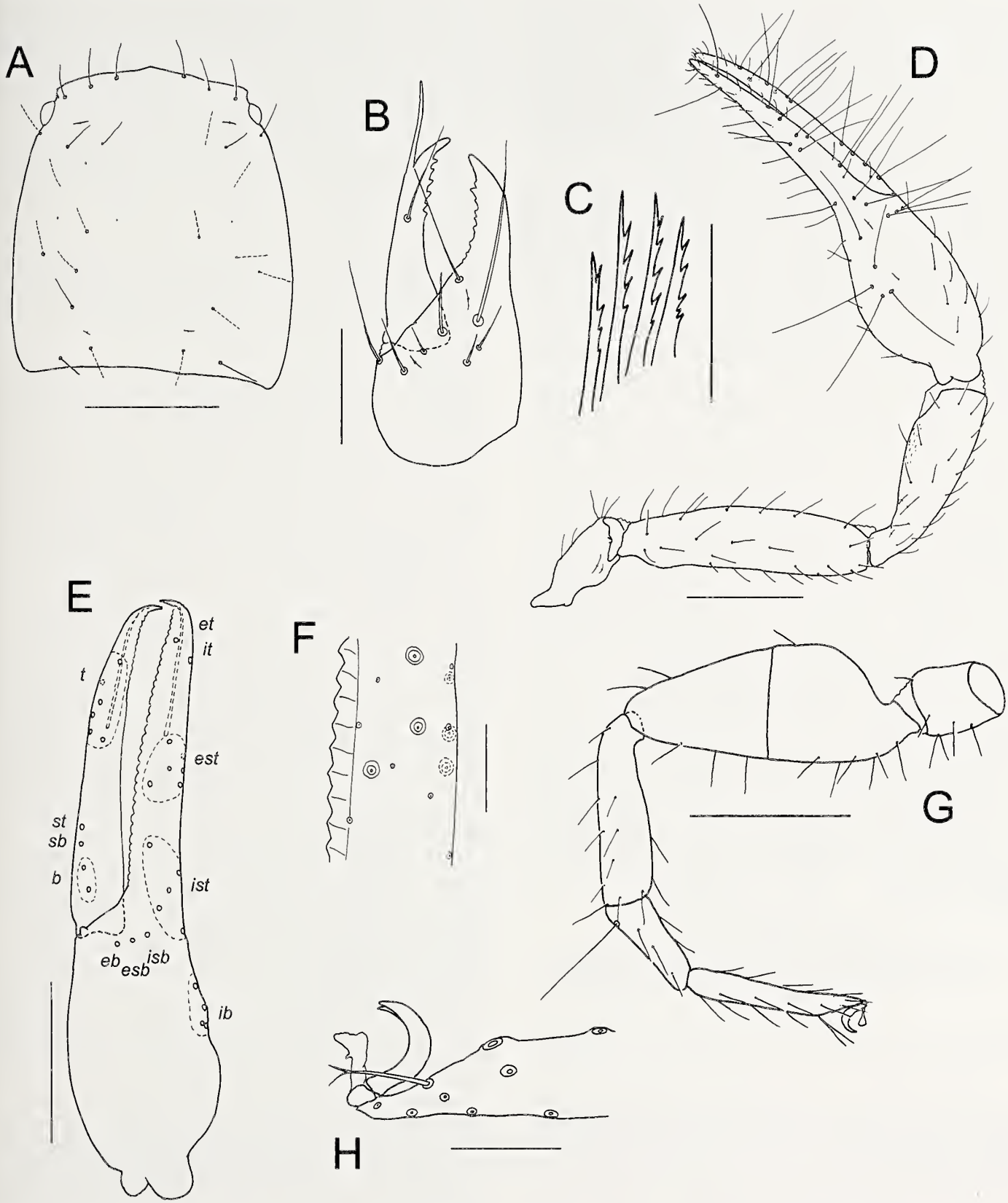

Figure 27.—*Sironcus siamensis* (With), male from Ko Chang, Thailand (MHNG), unless stated otherwise: A. Carapace; B. Left chelicera; C. Rallum; D. Right pedipalp, dorsal; E. Left chela, lateral; F. Detail of fixed chelal finger; G. Leg IV; H. Distal end of tarsus IV showing arolium, claws and subterminal seta, other setae omitted. Scale lines = 0.25 mm (D, E, G); 0.2 mm (A); 0.1 mm (B); 0.05 mm (F, C, H).

(with pedicel) 1.12/0.32 (1.11–1.16/0.295–0.30), chela (without pedicel) 1.065 (1.065–1.105), hand length 0.475 (0.47–0.50), movable finger length 0.585 (0.59–0.60). Chelicera 0.33/0.155, movable finger length 0.215. Carapace 0.56/0.55 (0.48–0.50/0.50–0.565); eye diameter 0.05. Leg I: femur 0.305/0.09, patella 0.18/0.09, tibia 0.215/0.065, metatarsus 0.16/0.05, tarsus 0.20/0.04. Leg IV: femur + patella ? (0.56/0.20), tibia ? (0.385/0.09), metatarsus ? (0.21/0.07), tarsus ? (0.315/0.05).

Remarks.—With (1906) described *Ideobisium (Ideoroncus) siamensis* from five adult specimens, including a female and two males from Koh Chang, and two males from Klong Salapket. One male and one female from Koh Chang, and one male from Klong Salakpet have been examined for this study. Other slide-mounted material in ZMC was not examined due to its extreme fragility (Dr. H. Enghoff, in litt.), and one male is also lodged in the Natural History Museum, London (Judson 1997) but not examined for this study. As With (1906) did not designate a holotype for this species, a male lectotype has been selected here to stabilize the type locality. The types that have been examined are bleached, but otherwise in good condition. Legs I and IV and the right pedipalp of the male from Klong Salakpet were mounted on a microscope slide by J.C. Chamberlin. The carapace and chelicerae of this specimen have been dissected from the specimen (presumably by With), but are missing from the vial. The measurements of this species provided by With (1906) and Beier (1932b) are at variance with those given here [e.g., pedipalpal femur length 0.70 (♂), 0.75 (♀) mm according to With; 0.70 mm according to Beier, but 0.63–0.635 (♂), 0.64 (♀) in this study], which is presumed to be due to differences in measurement technique.

Schawaller (1994) identified several specimens from Thailand as *D. siamensis* but based on their distribution, some most likely represent other species. In his illustration of the chelal trichobothrial pattern, Schawaller (1994, fig. 33) depicts 20 trichobothria on the fixed finger and hand, and 12 on the movable finger. This is slightly inaccurate, as no specimens of *Sironcus* examined for this study have such a pattern. Therefore, the only confirmed localities from which *S. siamensis* has been recorded are in Ko Chang, southern Thailand (Fig. 22).

Sironcus sierwaldae sp. nov.
http://zoobank.org/NomenclaturalActs/urn:lsid:zoobank.org:act:820F9A91-78FD-4856-9F8C-922B1B777BBD
(Fig. 28)

Dhanus siamensis (With): Kusch, 1982:66, fig. 2 (misidentification).

Material examined.—*Holotype male.* THAILAND: *Kanchanaburi Province*: Sai Yok National Park, near Headquarters [14°26′N, 98°51′E], 120 m, 14 November 2000, P. Schwendinger (MHNG).

Paratypes. THAILAND: *Kanchanaburi Province*: 1 ♀, collected with holotype (MHNG); 1 ♀, Tham Kung Lawa (= Tham Kaeng Lawa) [14°17′59″N, 98°58′58″E], 155 m, 11 April 1978, [H.] Kusch (NHMW). MYANMAR: *Magway Region*: 1 ♀, Shwesettaw Wildlife Reservation, 20°05′51.1″N, 94°33′24.5″E, 450 feet, 29 September 2003, deciduous forest, P. Sierwald (FMNH).

Diagnosis.—*Sironcus sierwaldae* differs from other species of the genus, except *S. stonei*, by the finely granulate prolateral faces of the pedipalpal femur and tibia (Fig. 28B). It differs from *S. stonei* by the less slender pedipalpal segments, e.g., patella 2.55 (♂), 2.79–2.89 (♀) x in *S. sierwaldae* and 3.45 (♂), 3.39 (♀) x longer than broad in *S. stonei*.

Description (adult).—*Color:* pedipalps and carapace red-brown; chelicerae and legs yellow-brown; tergites and sternites pale yellow-brown.

Setae: generally long, straight or slightly curved, and acicular.

Chelicera: with 7 (♂, ♀) setae on hand; movable finger with 1 seta; galea very slender and elongate; fixed finger with 7 (♂, ♀) small teeth; movable finger with 6 (♂), 8 (♀) small teeth; rallum of 4 blades, all blades serrate; lamina exterior absent.

Pedipalp (Fig. 28B): femur and patella lightly granulate on prolateral surface, remaining segments smooth; trochanter 2.29 (♂), 2.19–2.41 (♀), femur 3.69 (♂), 3.81–4.12 (♀), patella 2.55 (♂), 2.79–3.15 (♀), chela (with pedicel) 4.14 (♂), 3.58–3.98 (♀), chela (without pedicel) 3.76 (♂), 3.40–3.78 (♀), hand 2.25 (♂), 1.45–1.61 (♀) x longer than broad, movable finger 1.47 (♂), 1.37–1.40 (♀) x longer than hand. Fixed chelal finger with 20 trichobothria, movable chelal finger with 10 trichobothria (Fig. 28C): *eb*, *esb* and *isb* in straight row at base of finger; *eb*, *esb*, *et*, *isb* and *it* regions each with 1 trichobothrium; *ib* region with 4 trichobothria; *ist* region with 5 trichobothria; *est* region with 6 trichobothria; *et* slightly distal to *it*; *b* region with 2 trichobothria; *sb* and *st* regions each with 1 trichobothrium; *t* region with 6 trichobothria. Venom apparatus present in both chelal fingers, venom duct terminating in nodus ramosus near *est* region in fixed finger and near basal section of *t* region in movable finger (Fig. 28C). Chelal hand without microsetae near *eb* and *esb* (Fig. 28C). Chelal teeth juxtadentate, fixed finger with 34 (♂), 36 (♀) low, triangular teeth (Fig. 28D); movable finger with ca. 25 (♂), 27 (♀) teeth, but only the distal 8 or so with distinct crowns.

Carapace (Fig. 28A): 0.90 (♂), 0.66 (♀) x longer than broad; lateral margins convex; with 2 bulging eyes; epistome absent; with 27 (♂), 25 (♀) setae, including 6 near anterior margin and 4 near posterior margin; without furrows.

Coxal region: manducatory process with 2 long apical setae, plus 8 (♂, ♀) additional setae; chaetotaxy of coxae I–IV: ♂, 7: 7: 8: 9; ♀, 8: 7: 7: 11.

Legs: femur + patella 2.32 (♂), 2.64 (♀) x longer than deep; subterminal tarsal setae bifurcate (Fig. 28E); arolium undivided, shorter than claws, bearing a ventral hooked process (Fig. 28E).

Abdomen: tergites and sternites undivided and uniseriate. Tergal chaetotaxy: ♂, 4: 4: 8: 11: 11: 13: 14: 14: 13: 10 (including 4 tactile setae): 6 (including 4 tactile setae): 2; ♀, 4: 4: 8: 9: 10: 12: 13: 14: 14: 12 (including 4 tactile setae): 7 (including 4 tactile setae): 2. Sternal chaetotaxy: ♂, 11: (1) 10 [3 + 3] (1): (1) 8 (1): 16: 17: 18: 18: 19: 17: 8 (including 2 tactile setae): 2; ♀, 9: (1) 6 (1): (1) 8 (1): 15: 16: 17: 16: 17: 16: 7 (including 4 tactile setae): 2. Setae of tergites and sternites IX–XI acuminate.

Genitalia: male with median genital sac bifurcate; female with large gonosac covered with pores.

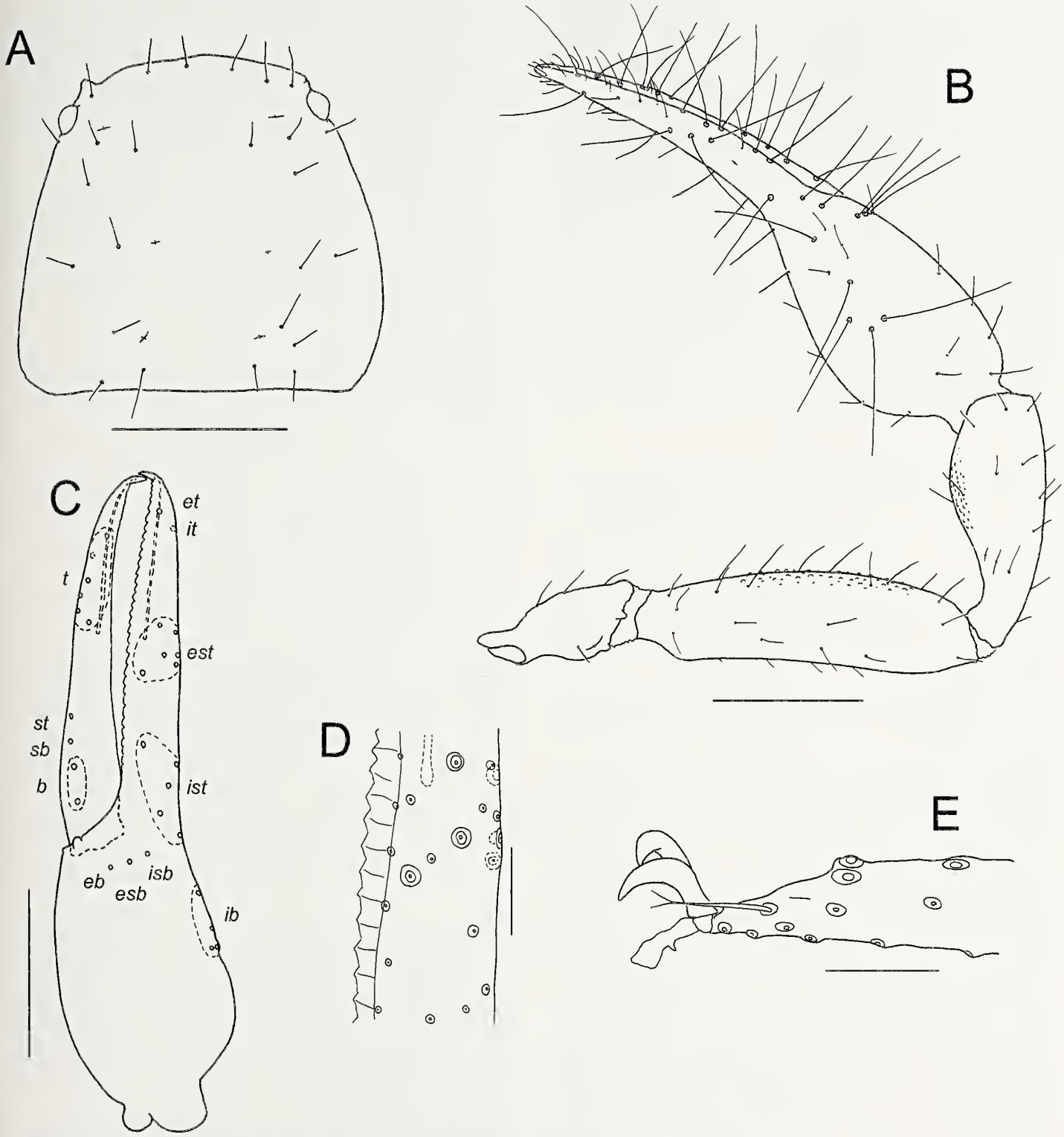

Figure 28.—*Sironcus sierwaldae* sp. nov., male holotype, unless stated otherwise: A. Carapace; B. Right pedipalp, dorsal; C. Left chela, lateral; D. Detail of fixed chelal finger; E. Distal end of tarsus IV showing arolium, claws and subterminal seta, other setae omitted. Scale lines = 0.25 mm (A–C); 0.05 mm (D, E).

Dimensions (mm): male: holotype: Body length 1.59. *Pedipalp*: trochanter 0.275/0.12, femur 0.59/0.16, patella 0.42/0.165, chela (with pedicel) 1.005/0.255, chela (without pedicel) 0.96, hand length 0.39, movable finger length 0.575. Chelicera 0.28/0.135, movable finger length 0.185. Carapace 0.47/0.52; eye diameter 0.05. Leg I: femur 0.32/0.085, patella 0.18/0.08, tibia 0.205/0.055, metatarsus 0.15/0.05, tarsus 0.24/0.04. Leg IV: femur + patella 0.51/0.22, tibia 0.34/0.09, metatarsus 0.205/0.065, tarsus 0.29/0.045.

Females: paratype from Sai Yok National Park followed by other female (when measured): Body length 1.87 (2.06–2.13). *Pedipalp*: trochanter 0.325/0.135 (0.285–0.31/0.12–0.13), femur 0.695/0.18 (0.61–0.64/0.155–0.16), patella 0.52/0.18 (0.46–0.505/0.16–0.165), chela (with pedicel) 1.165/0.325 (1.05–1.075/0.27–0.285), chela (without pedicel) 1.105 (0.985–1.02), hand length 0.47 (0.435), movable finger length 0.66 (0.595–0.605). Chelicera 0.34/0.17, movable finger length 0.225. Carapace 0.385/0.58; eye diameter 0.05. Leg I: femur 0.37/0.095, patella 0.185/0.09, tibia 0.225/0.065, metatarsus 0.155/0.055, tarsus 0.23/0.04. Leg IV: femur + patella 0.58/0.22, tibia 0.395/0.095, metatarsus 0.23/0.07, tarsus 0.345/0.05.

Remarks.—*Sironcus sierwaldae* has been found in rainforest habitats in western Thailand (Kanchanaburi Province) and south-western Myanmar (Magway Region) (Fig. 22). The female specimen from Tham Kung Lawa was identified by Max Beier as *Dhanus siamensis* and listed by Kusch (1982).

Etymology.—This species is named for the collector of one of the paratypes, Petra Sierwald.

Sironcus stonei sp. nov.
http://zoobank.org/NomenclaturalActs/urn:lsid:zoobank.org:act:7520A67D-6B74-433B-BCAE-7B614D2B07E9
(Fig. 29)

Material examined.—*Holotype male*. THAILAND: *Ratchaburi Province*: Amphoe Chom Bung, Tham Chom Phon (label uses the alternative term "Tham Chom Phol") [13°37′N, 99°35′E], 25 August 1981, F.D. Stone (BPBM, WM6120.01002).

Paratypes. THAILAND: *Ratchaburi Province*: 1 ♀, 1 tritonymph, collected with holotype (BPBM, WM6120.01002–3).

Diagnosis.—The pedipalpal segments of *Sironcus stonei* are slightly more elongated that those of other species of *Sironcus* (Fig. 29B), especially the patella which is 3.45 (♂), 3.39 (♀) x longer than broad, but is 2.69–3.08 (♂), 2.47–2.97 (♀) in the other species.

Description (adult).—*Color:* pedipalps and carapace red-brown; chelicerae and legs yellow-brown; tergites and sternites pale yellow-brown.

Setae: generally long, straight or slightly curved, and acicular.

Chelicera: with 7 (♂), 6–7 (♀) setae on hand; movable finger with 1 seta; galea very slender and elongate; fixed finger with 8 (♂), 9 (♀) teeth; movable finger with 4 (♂), 6 (♀) small teeth; rallum of 4 blades, all blades serrate; lamina exterior absent.

Pedipalp (Fig. 29B): femur and patella lightly granulate on prolateral surface, remaining segments smooth; trochanter 2.32 (♂, ♀), femur 4.31 (♂), 4.44 (♀), patella 3.45 (♂), 3.39 (♀), chela (with pedicel) 4.30 (♂), 4.12 (♀), chela (without pedicel) 4.11 (♂), 4.12 (♀), hand 1.67 (♂), 1.62 (♀) x longer than broad, movable finger 1.49 (♂, ♀) x longer than hand. Fixed chelal finger with 20 trichobothria, movable chelal finger with 10 trichobothria (Fig. 29C): *eb*, *esb* and *isb* in straight row at base of finger; *eb*, *esb*, *et*, *isb* and *it* regions each with 1 trichobothrium; *ib* region with 4 trichobothria; *ist* region with 5 trichobothria; *est* region with 6 trichobothria; *et* slightly distal to *it*; *b* region with 2 trichobothria; *sb* and *st* regions each with 1 trichobothrium; *t* region with 6 trichobothria. Venom apparatus present in both chelal fingers, venom duct terminating in nodus ramosus near *est* region in fixed finger and near basal section of *t* region in movable finger (Fig. 29C). Chelal hand without microsetae near *eb* and *esb* (Fig. 29C). Chelal teeth juxtadentate, fixed finger with 38 (♂), 40 (♀) low, triangular teeth with the highest point in the distal half (Fig. 29D); movable finger with ca. 30 (♂), 32 (♀) teeth, but only the distal 10 or so with distinct crowns.

Carapace (Fig. 29A): 1.13 (♂), ? (♀) x longer than broad; lateral margins slightly convex; with 2 bulging eyes; with small epistome; with 24 (♂, ♀) setae, including 6 near anterior margin and 4 near posterior margin; without furrows.

Coxal region: manducatory process with 2 long apical setae, plus 7 (♂, ♀) additional setae; chaetotaxy of coxae I–IV: ♂, 5: 7: 6: 8; ♀, 6: 7: 6: 8.

Legs: femur + patella 2.36 (♂), 2.72 (♀) x longer than deep; subterminal tarsal setae bifurcate (Fig. 29F); arolium undivided, shorter than claws, bearing a ventral hooked process (Fig. 29F).

Abdomen: tergites and sternites undivided and uniseriate. Tergal chaetotaxy: ♂, 4: 4: 7: 9: 9: 9: 10: 9: 10: 9 (including 4 tactile setae): 10 (including 2 tactile setae): 2; ♀, 4: 5: 7: 9: 9: 11: 10: 11: 13: 10 (including 4 tactile setae): 7 (including 4 tactile setae): 2. Sternal chaetotaxy: ♂, 11: (1) 9 [3 + 2] (1): (1) 6 (1): 9: 10: 11: 14: 12: 12 (including 2 tactile setae): 6 (including 2 tactile setae): 2; ♀, 11: (1) 7 (1): (1) 6 (1): 12: 14: 12: 12: 12: 11: 6 (including 4 tactile setae): 2. Setae of tergites and sternites IX–XI acuminate.

Genitalia: male with median genital sac not visible in slide preparation; female with large gonosac covered with pores.

Dimensions (mm): male: holotype: Body length ? (damaged). *Pedipalp*: trochanter 0.325/0.14, femur 0.755/0.175, patella 0.57/0.165, chela (with pedicel) 1.225/0.285, chela (without pedicel) 1.17, hand length 0.475, movable finger length 0.71. Chelicera 0.305/0.145, movable finger length 0.195. Carapace 0.565/0.50; eye diameter 0.05. Leg I: femur 0.365/0.095, patella 0.19/0.085, tibia 0.23/0.065, metatarsus 0.16/0.055, tarsus 0.225/0.05. Leg IV: femur + patella 0.59/0.25, tibia 0.40/0.095, metatarsus 0.225/0.065, tarsus 0.345/0.05.

Female: paratype: Body length ca. 2.42. *Pedipalp*: trochanter 0.36/0.155, femur 0.865/0.195, patella 0.61/0.18, chela (with pedicel) 1.34/0.325, chela (without pedicel) 1.28, hand length 0.525, movable finger length 0.78. Chelicera 0.27/0.175, movable finger length 0.225. Carapace 0.57/? (flattened); eye diameter 0.04. Leg I: femur 0.415/0.10, patella 0.21/0.09, tibia 0.28/0.06, metatarsus 0.185/0.055, tarsus 0.25/0.04. Leg IV: femur + patella 0.64/0.235, tibia 0.45/0.10, metatarsus 0.245/0.085, tarsus 0.37/0.065.

Description (tritonymph).—*Chelicera:* galea long and slender, slightly curved; with 6 setae on hand; 1 on movable finger; rallum composed of 4 blades, all serrate.

Pedipalp: trochanter 2.33, femur 4.30, patella 2.85, chela (with pedicel) 4.21, chela (without pedicel) 4.00, hand 1.60 x longer than broad; movable finger 1.51 x longer than hand (without pedicel). Fixed chelal finger with 16 trichobothria, movable chelal finger with 8 trichobothria (Fig. 29E); *isb* and *sb* absent; *eb*, *esb*, *et* and *it* regions each with 1 trichobothrium; *eb* and *esb* at base of finger; *ib* region with 4 trichobothria; *ist* region with 4 trichobothria; *est* region with 3 trichobothria; *et*

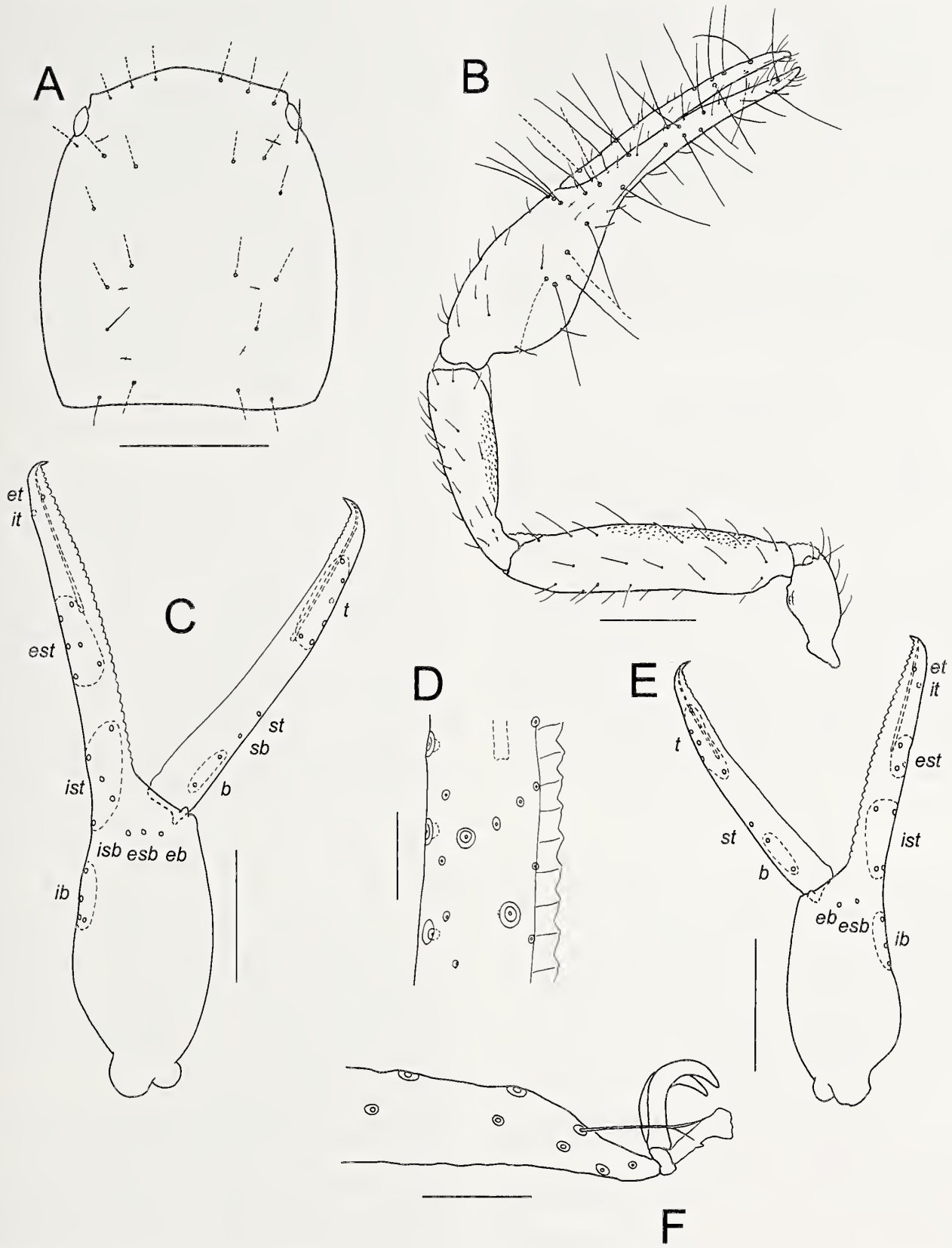

Figure 29.—*Sironcus stonei* sp. nov., male holotype, unless stated otherwise: A. Carapace; B. Left pedipalp, dorsal; C. Right chela, lateral; D. Detail of fixed chelal finger; E. Left chela, lateral, tritonymph paratype; F. Distal end of tarsus IV showing arolium, claws and subterminal seta, other setae omitted. Scale lines = 0.25 mm (A–C, E); 0.1 mm (D); 0.05 mm (F).

slightly distal to *it*; *b* region with 2 trichobothria; *st* region with 1 trichobothrium; *t* region with 5 trichobothria.

Carapace: anterior margin slightly medially prominent; with 2 small bulging eyes; with 19 setae including 5 setae near anterior margin and 4 near posterior margin.

Legs: much as in adult.

Dimensions (mm): Body length ? (damaged). *Pedipalp*: trochanter 0.245/0.105, femur 0.58/0.135, patella 0.385/0.135, chela (with pedicel) 0.905/0.215, chela (without pedicel) 0.86, hand length 0.345, movable finger length 0.52. *Carapace* 0.435/0.445.

Remarks.—*Sironcus stonei* has been found inside Tham Chom Phon, a cave set in a small limestone hill on the western outskirts of Chom Bueng.

Etymology.—This species is named for the collector of the type specimens, Fred Stone.

ACKNOWLEDGMENTS

The specimens used in this study were kindly loaned by Henrik Enghoff and Nikolai Scharff (ZMC), Charles Griswold and Vincent Lee (CAS), Jürgen Gruber and Christoph Hörweg (NHMW), Bruce Halliday (ANIC), Mark Judson (MNHN), Lars Lundqvist and Jonas Ekström (MZLU), Volker Mahnert and Peter Schwendinger (MHNG), Vladimir Ovtsharenko (ZISP), Wolfgang Schawaller (SMNS) and Sabina Swift (BPBM). Mark Judson kindly provided valuable information regarding the types of *Dhanus doveri* and *Ideoroncus siamensis*, and Tony Russell-Smith informed me that no pseudoscorpion specimens could be located in the late W.S. Bristowe's collection. Jürgen Gruber and Peter Schwendinger supplied information and literature on Thai localities. I am also very grateful to Rosli Hashim and Teck Wyn Lim for facilitating field work in Malaysia, and to Syud Dzarawi and Karen Edward for their assistance in the field.

LITERATURE CITED

Batuwita, S. & S.P. Benjamin. 2014. An annotated checklist and a family key to the pseudoscorpion fauna (Arachnida: Pseudoscorpiones) of Sri Lanka. Zootaxa 3814:37–67.

Beier, M. 1932a. Pseudoscorpionidea - Afterskorpione. Pp. 117–192. *In* Handbuch der Zoologie. (W. Kükenthal & T. Krumbach eds.). Vol. 3 (2) (5). Walter de Gruyter & Co., Berlin and Leipzig.

Beier, M. 1932b. Pseudoscorpionidea I. Subord. Chthoniinea et Neobisiinea. Tierreich 57:i–xx, 1–258.

Beier, M. 1951. Die Pseudoscorpione Indochinas. Mémoires du Muséum National d'Histoire Naturelle, Paris, nouvelle série 1:47–123.

Beier, M. 1959. Zur Kenntnis der Pseudoscorpioniden-Fauna Afghanistans. Zoologische Jahrbücher, Abteilung für Systematik, Ökologie und Geographie der Tiere 87:257–282.

Beier, M. 1960. Pseudoscorpionidea. Contribution à l'étude de la faune d'Afghanistan. 27. Förhandlingar vid Kungliga Fysiografiska Sällskapets i Lund 30:41–45.

Beier, M. 1961. Pseudoscorpionidea II. Contribution à l'étude de la faune d'Afghanistan 56. Förhandlingar vid Kungliga Fysiografiska Sällskapets i Lund 31:1–4.

Beier, M. 1963. Pseudoscorpione von den Batu-Höhlen in Malaya. Pacific Insects 5:51–52.

Beier, M. 1967. Pseudoscorpione vom kontinentalen Südost-Asien. Pacific Insects 9:341–369.

Beier, M. 1971. Pseudoskorpione aus dem Iran. Annalen des Naturhistorischen Museums in Wien 75:357–366.

Beier, M. 1973. Pseudoscorpionidea von Ceylon. Entomologica Scandinavica, Supplement 4:39–55.

Bristowe, W.S. 1952. The arachnid fauna of the Batu Caves in Malaya. Annals and Magazine of Natural History (12) 5:697–707.

Brown, R.W. 1956. Composition of scientific words. Revised edition. Smithsonian Institution Press, Washington, D.C.

Chamberlin, J.C. 1930. A synoptic classification of the false scorpions or chela-spinners, with a report on a cosmopolitan collection of the same. Part II. The Diplosphyronida (Arachnida-Chelonethida). Annals and Magazine of Natural History (10) 5:1–48, 585–620.

Chamberlin, J.C. 1931. The arachnid order Chelonethida. Stanford University Publications, Biological Sciences 7(1):1–284.

Gao, Z. & F. Zhang. 2013. Pseudoscorpions from Laos: description of a new species and new records (Arachnida: Pseudoscorpiones). Archives of Biological Sciences, Belgrade 65:839–850.

Harvey, M.S. 1991. Catalogue of the Pseudoscorpionida. Manchester University Press, Manchester.

Harvey, M.S. 1992. The phylogeny and classification of the Pseudoscorpionida (Chelicerata: Arachnida). Invertebrate Taxonomy 6:1373–1435.

Harvey, M.S. 2013. Pseudoscorpions of the World, version 3.0. Western Australian Museum, Perth. Accessed 4 February 2016. Online at http://museum.wa.gov.au/catalogues-beta/pseudoscorpions

Harvey, M.S. & G. Du Preez. 2014. A new troglobitic ideoroncid pseudoscorpion (Pseudoscorpiones: Ideoroncidae) from southern Africa. Journal of Arachnology 42:106–110.

Harvey, M.S. & K.L. Edward. 2007. A review of the pseudoscorpion genus *Ideoblothrus* (Pseudoscorpiones, Syarinidae) from western and northern Australia. Journal of Natural History 41:445–472.

Harvey, M.S. & W.B. Muchmore. 2013. The systematics of the pseudoscorpion family Ideoroncidae (Pseudoscorpiones, Neobisioidea) in the New World. Journal of Arachnology 41:229–290.

Harvey, M.S. & E.S. Volschenk. 2007. The systematics of the Gondwanan pseudoscorpion family Hyidae (Pseudoscorpiones: Neobisioidea): new data and a revised phylogenetic hypothesis. Invertebrate Systematics 21:365–406.

Harvey, M.S., R. Barba D., W.B. Muchmore & A. Peréz G. 2007. *Pseudalbiorix*, a new genus of Ideoroncidae (Pseudoscorpiones, Neobisioidea) from central America. Journal of Arachnology 34:610–626.

Harvey, M.S., P.B. Ratnaweera, P.V. Udagama & M.R. Wijesinghe. 2012. A new species of the pseudoscorpion genus *Megachernes* (Pseudoscorpiones: Chernetidae) associated with a threatened Sri Lankan rainforest rodent, with a review of host associations of *Megachernes*. Journal of Natural History 46:2519–2535.

International Commission on Zoological Nomenclature. 1999. International code of zoological nomenclature, fourth edition. International Trust for Zoological Nomenclature, London.

John, O. 1914. ["Batu" Caves of the Malayan Peninsula]. Lyubitel' Prirody 12:353–365. (in Russian)

Judson, M.L.I. 1997. Catalogue of the pseudoscorpion types (Arachnida: Chelonethi) in the Natural History Museum, London. Occasional Papers on Systematic Entomology 11:1–54.

Judson, M.L.I. 2007. A new and endangered species of the pseudoscorpion genus *Lagynochthonius* from a cave in Vietnam, with notes on chelal morphology and the composition of the Tyrannochthoniini (Arachnida, Chelonethi, Chthoniidae). Zootaxa 1627:53–68.

Kusch, H. 1982. Ergebnisse speläologischer Forschungen in Thailand (Stand 1978). Die Höhle 33:59–69.

Lim, T.K., S.S. Yussof & M. Ashraf. 2010. The caves of Batu Caves: a toponymic revision. Malaysian Nature Journal 62:335–348.

Lindberg, K. 1961. Recherches biospéléologiques en Afghanistan. Acta Universitatis Lundensis, nova series 57:1–39.

Mahnert, V. 1981. Die Pseudoskorpione (Arachnida) Kenyas. I. Neobisiidae und Ideoroncidae. Revue Suisse de Zoologie 88:535–559.

Mahnert, V. 1984. Beitrag zu einer besseren Kenntnis der Ideoroncidae (Arachnida: Pseudoscorpiones), mit Beschreibung von sechs neuen Arten. Revue Suisse de Zoologie 91:651–686.

Mahnert, V. 1985. Pseudoscorpions (Arachnida) from the lower Amazon region. Revista Brasileira de Entomologia 29:75–80.

Mahnert, V. 2007. Pseudoscorpions (Arachnida: Pseudoscorpiones) of the Socotra Archipelago, Yemen. Fauna of Arabia 23:271–307.

McClure, H.E. 1965. Microcosms of Batu Caves and a list of species collected at Batu Caves. Malayan Nature Journal 19:65–74.

McClure, H.E., B.-L. Lim & S.E. Winn. 1967. Fauna of the Dark Cave, Batu Caves, Kuala Lumpur, Malaysia. Pacific Insects 9:399–428.

Mjöberg, E. 1930. Forest life and adventures in the Malay Archipelago. (Translated from the Swedish by A. Barwell). William Morrow & Company, New York.

Mosely, M., T.K. Lim & T.T. Lim. 2012. Fauna reported from Batu caves, Selangor, Malaysia: annotated checklist and bibliography. Cave and Karst Science 39:77–92.

Muchmore, W.B. & R.B. Pape. 1999. Description of an eyeless, cavernicolous *Albiorix* (Pseudoscorpionida: Ideoroncidae) in Arizona, with observations on its biology and ecology. Southwestern Naturalist 44:138–147.

Murthy, V.A. & T.N. Ananthakrishnan. 1977. Indian Chelonethi. Oriental Insects Monograph 4:1–210.

Redikorzev, V. 1922. Two new species of pseudoscorpion from Sumatra. Ezhegodnik Zoologicheskago Muzeya 23:545–554.

Redikorzev, V. 1938. Les pseudoscorpions de l'Indochine française recueillis par M. C. Dawydoff. Mémoires du Muséum National d'Histoire Naturelle, Paris 10:69–116.

Roewer, C.F. 1936. Chelonethi oder Pseudoskorpione. Pp. 1–160. *In* Bronn's Klassen und Ordnungen des Tierreichs. (H.G. Bronns ed.). Vol. 5(IV)(6)(1). Akademische Verlagsgesellschaft M.B.H., Leipzig.

Roewer, C.F. 1937. Chelonethi oder Pseudoskorpione. Pp. 161–320. *In* Bronn's Klassen und Ordnungen des Tierreichs. (H.G. Bronns ed.). Vol. 5(IV)(6)(1). Akademische Verlagsgesellschaft M.B.H., Leipzig.

Roewer, C.F. 1940. Chelonethi oder Pseudoskorpione. Pp. 321–354. *In* Bronn's Klassen und Ordnungen des Tierreichs. (H.G. Bronns ed.). Vol. 5(IV)(6)(1). Akademische Verlagsgesellschaft M.B.H. Leipzig.

Sagin, D.D., G. Ismail, J.N. Fui & J.J. Jok. 2001. *Schistosomiasis malayensis*-like infection among the Penan and other interior tribes (Orang Ulu) in upper Rejang River Basin Sarawak Malaysia. Southeast Asian Journal of Tropieal Medicine and Public Health 32:27–32.

Schawaller, W. 1994. Pseudoskorpione aus Thailand (Arachnida: Pseudoscorpiones). Revue Suisse de Zoologie 101:725–759.

Vachon, M. 1949. Ordre des Pseudoscorpions. Pp. 437–481. *In* Traité de Zoologie. (P.-P. Grassé, ed.). Vol. 6. Masson, Paris.

Vachon, M. 1958. Sur deux Pseudoscorpions nouveaux des cavernes de l'Afrique équatoriale [Ideoroncidae]. Notes Biospéologiques 13:57–66.

Vachon, M. 1964. Sur l'établissement de formules précisant l'ordre d'apparition des trichobothries au cours du développement postembryonnaire chez les Pseudoscorpions (Arachnides). Comptes Rendus Hebdomadaires des Séances de l'Académie des Sciences, Paris 258:4839–4842.

Weygoldt, P. 1966. Moos- und Bücherskorpione. A. Ziemsen Verlag, Wittenberg Lutherstadt.

Weygoldt, P. 1969. The Biology of Pseudoscorpions. Harvard University Press, Cambridge, Massachusetts.

With, C.J. 1906. The Danish expedition to Siam 1899–1900. III. Chelonethi. An account of the Indian false-scorpions together with studies on the anatomy and classification of the order. Oversigt over det Konigelige Danske Videnskabernes Selskabs Forhandlinger (7) 3:1–214.

Yussof, S. 1988. Some invertebrates from Batu Caves, Selangor. Nature Malaysiana 13(2):24–31.

Yussof, S. 1997. The Natural and Other Histories of Batu Caves. Malaysian Nature Society, Kuala Lumpur.

Manuscript received 21 June 2016, revised 11 August 2016.

2016. Journal of Arachnology 44:330–346

Changes in nymphal morphometric values and tarsal microstructures during postembryonic development in the Neotropical harvestman *Heteromitobates albiscriptus* (Opiliones: Gonyleptidae)

Alessandra Z. Ramin[1], **Rodrigo H. Willemart**[2,3,4] and **Pedro Gnaspini**[1,4]: [1]Departamento de Zoologia, Instituto de Biociências, Universidade de São Paulo, Rua do Matão, travessa 14, 321, 05508-090, São Paulo, SP, Brazil; E-mail: gnaspini@ib.usp.br; [2]Laboratório de Ecologia Sensorial e Comportamento de Artrópodes, Escola de Artes, Ciências e Humanidades, Universidade de São Paulo, Rua Arlindo Béttio, 1000, Ermelino Matarazzo, São Paulo – SP, 03828-000 Brazil; [3]Programa de Pós Graduação em Ecologia e Evolução, Universidade Federal de São Paulo, Campus Diadema, Rua Professor Artur Riedel, 275, Jardim Eldorado, Diadema – SP, 09972-270 Brazil; [4]Programa de Pós Graduação em Zoologia, Instituto de Biociências, Universidade de São Paulo, Rua do Matão, 321, Travessa 14, Cidade Universitária, São Paulo – SP, 05508-090 Brazil

Abstract. The postembryonic development of Opiliones (Arachnida) includes three phases: larval, nymphal (with four to eight instars), and adult (when molts cease). The present study aimed to describe the postembryonic development of *Heteromitobates albiscriptus* (Mello-Leitão, 1932) (Gonyleptidae) including both a morphometric study and SEM analysis of two structures present in the tarsus of nymphs and adults: the "tarsal aggregate pores" (TAPs) and the "tarsal perforated organ" (TPO). The nymphal phase includes five stages, which can be easily recognized by morphometric values. In contrast to the pectinate tarsal claws found in legs III–IV of adults (the main synapomorphy of the genus *Heteromitobates* in the subfamily Goniosomatinae), nymphs bear smooth claws. First nymphs lack TAPs and TPOs. TAPs seem to have a precisely defined position in both prolateral and retrolateral faces of the tarsus. The number of pores in TAPs grows from three or four among second nymphs to around 20 among adults, and measure around 2.15 μm in diameter with no clear difference between ages. An additional field of pores on legs III–IV ("ventral tarsal aggregate pores", vTAPs) was detected only among adults. The plates at the base and the apex of the TPOs differ from the ones in between. The length of the TPO and its number of plates increase with each molt. However, there is no discernible pattern of growth throughout the postembryonic development when taking into account both the average size of the plates (ranging between ~7–11 μm) and the ratio of TPO length to tarsus length.

Keywords: Morphology, glandular opening, Gonyleptidae, Goniosomatinae, ontogeny

After hatching, arthropods pass through successive molts to achieve adulthood, defining a postembryonic developmental phase. The postembryonic development of arachnids of the order Opiliones (harvestmen) includes three phases: larval, nymphal, and adult (e.g., Juberthie 1964; Gnaspini 2007). The larva hatches and molts to the first nymphal instar; after a variable number of nymphal molts, usually four to eight (mostly, six), the adult stage is reached (Gnaspini 2007). The duration of each phase varies among the suborders Cyphophthalmi, Eupnoi, Dyspnoi, and Laniatores (reviewed by Gnaspini 2007): whereas the larva of a sironid specimen of Cyphophthalmi takes four to seven days before molting into the first nymph, the larvae of the remaining suborders usually molt into the first nymph within less than an hour (e.g., Juberthie 1964; Gnaspini 2007). During postembryonic development each molt results in a larger animal. Because total body length and width may vary with the amount of food in the gut, these measurements are unsuitable for documenting growth, but the appendages seem to be more appropriate structures and have been used in most comparative studies (e.g., Table 2 in Gnaspini 2007).

According to Juberthie (1964), sexual characters usually appear in the penultimate instar (i.e., the last nymphal stage), but Muñoz-Cuevas (1971a) and Gnaspini (1995) have shown that, in the studied neotropical Laniatores, sexual characters appear in the antepenultimate instar. In many Laniatores, males can often be distinguished from females by enlarged armature of the body, but especially in legs IV (trochanter, femur and/or tibia) (e.g., from several chapters in Pinto-da-Rocha et al. 2007), and these apophyses already appear in penultimate nymphal instars (e.g., Muñoz-Cuevas 1971b; Gnaspini 1995). Especially considering Muñoz-Cuevas's (1971b) statement that sexual maturity is achieved in the penultimate stage (i.e., the last nymphal instar), this stage is frequently treated as "subadult" stage. In addition, based on the assumption that both subadults and adults were sexually mature, Gnaspini et al. (2004) suggested that the adult phase of laniatoreans included two stages, contrary to the general rule among arachnids, except for some mygalomorph spiders (in which some females may molt after sexual maturity), molts cease with adulthood. The presence of two adult stages among harvestmen was shown to be wrong and the variation observed among sexually mature males was recognized as profound differences related to sexual selection (e.g., DaSilva & Gnaspini 2009; Zatz et al. 2010; Munguía-Steyer et al. 2012).

Among Grassatores (an infraorder of Laniatores), there are typical morphological features that aid in distinguishing between nymphs and adults. All legs of Cyphophthalmi, Eupnoi, and Dyspnoi as well as legs I and II of Laniatores bear only one claw. Among "Insidiatores" (a non-monophyletic infraorder of Laniatores), legs III and IV have a complex and usually trifid claw. In Grassatores, legs III and IV have two single claws, independently inserted in the tarsus, although the claws may be fused at the base (e.g., Gnaspini 2007). In Grassatores, nymphs and adults differ in the

Table 1.—Summary of leg measurements (length, in mm) for the available material of *Heteromitobates albiscriptus* (see complete list in Appendix 1), reported as the range of values observed in each stage. The number of specimens analyzed [N] of each age is given between square brackets. The average growth of each leg (percentage) relative to the previous stage is given in parentheses.

	Nymph 1 [N=8]	Nymph 2 [N=5] (% growth)	Nymph 3 [N=11] (% growth)	Nymph 4 [N=14] (% growth)	Nymph 5 [N=3] (% growth)	Adult [N=15] (% growth)
Leg I	7.71–8.75	10.60–10.87 (29)	13.12–14.73 (31)	17.13–19.55 (33)	23.74–24.36 (27)	30.20–36.53 (35)
Leg II	19.64–23.33	26.78–28.73 (25)	34.02–39.05 (29)	43.70–48.45 (27)	57.32–58.70 (25)	73.43–84.08 (37)
Leg III	11.19–13.89	16.30–17.60 (27)	20.72–24.66 (31)	26.42–30.90 (34)	38.33–39.18 (30)	49.73–58.65 (35)
Leg IV	16.11–19.58	23.29–25.26 (26)	28.36–33.00 (30)	38.46–42.43 (29)	51.42–52.19 (28)	67.84–79.77 (39)

structures found between the two tarsal claws (e.g., Muñoz-Cuevas 1971a, b). In this group, all nymphal stages bear two typical "juvenile" structures ventrally in both third and fourth leg tarsi: one projection similar to a third tarsal claw, called a 'pseudonychium', and a "fleshy" projection, called an 'arolium'. These structures grow during nymphal development, but are not observed in adults (Muñoz-Cuevas 1971a, b; Gnaspini 1995, 2007). On the other hand, there is a third structure in most Gonyleptoidea (Cosmetidae, Cranaidae, Gonyleptidae, Manaosbiidae, Stygnidae), called a 'tarsal process', which may grow gradually with each molt, but which is fully developed only in adults (Muñoz-Cuevas 1971a, b). It is a dorsal projection on the apex of the last tarsomere, which usually bears a long and unusual seta.

Although studies concerning Eupnoi and Dyspnoi have shown that many structures develop or increase in size and/or complexity during post-embryonic development (e.g., setae of the appendages, shape of the eyemound, pseudoarticulation of femora, and the shape and size of the hood among some Dyspnoi; see review in Gnaspini 2007), studies concerning Laniatores have focused mainly on the armature of pedipalps and legs and the increase in the number of tarsomeres (Gnaspini 2007), except for the work of Townsend et al. (2009), who also added some information on body tubercles and color.

Recent studies by Willemart & Gnaspini (2003), Willemart et al. (2007, 2009, 2010), Willemart & Giribet (2010), Wijnhoven (2013) and Rodriguez et al. (2014) have reviewed the knowledge about sensory structures and glandular openings on the integument of harvestmen. Willemart et al. (2007) described six glandular openings in the articulations, trochanter, metatarsus and tarsus of the legs and one that occurs all over the body. Among them are the tarsal aggregate pores (TAPs) that were first recognized at the retrolateral and prolateral faces of the distal end of legs III and IV, close to the tarsal process (among adults), as in figs 8, 9 from Willemart et al. (2007), in both sexes. Gainett et al. (2014) showed the large morphological variation of these structures in all families of Laniatores. Another conspicuous structure on all legs is the tarsal perforated organ (TPO), which is located on the ventral surface of the most proximal tarsomere, as in figs 11, 12 from Willemart et al. (2007) and is composed of two parallel rows of allegedly perforated plates. Because of its external appearance, TPO was thought to be glandular but has recently been suggested to be a region of attachment of muscles (Proud & Felgenhauer 2013).

So far, no studies have dealt with the ontogeny and phylogenetic distribution, as well as sexual dimorphism of glandular openings, and such studies are important because they provide indirect functional evidence. Cuticular structures that only appear in adults or late instars and sexually dimorphic structures usually have a sexual function, being a product of sexual selection (Andersson 1994; Willemart et al. 2006; Buzatto et al. 2014; Fowler-Finn et al. 2014). Therefore, morphology is very important in giving clues that help to explain typical behaviors of a species.

Thus the present study aimed to describe the postembryonic development of *Heteromitobates albiscriptus* (Mello-Leitão, 1932) (Laniatores: Gonyleptidae), including a morphometric study and analysis of two common structures (tarsal aggregate pores and tarsal perforated organ) present in the tarsus in all nymphal stages as well as in adults of both sexes.

METHODS

Species studied.—Males and females for each developmental stage of the species *Heteromitobates albiscriptus* (Laniatores: Gonyleptidae: Goniosomatinae) were examined. The animals analyzed were collected previously in Gruta da Quarta Divisão, Ribeirão Pires, São Paulo, during the study by Willemart & Gnaspini (2004a, b) and preserved in 70% ethanol. See also DaSilva & Gnaspini (2009) for a redescription and taxonomic discussion.

Morphometric and meristic analysis.—Based on the methodology described by Gnaspini (1995) when studying another goniosomatine harvestman and on structures that have been used in the study of the postembryonic development of harvestmen (as listed in Gnaspini 2007), we measured the

Table 2.—Summary of the counts of tarsomeres (number of articles in tarsi) in the available material of *Heteromitobates albiscriptus* (see complete list in Appendix 1), reported as the range of values observed in each stage. The number of specimens analyzed [N] of each age is given between square brackets.

	Nymph 1 [N=8]	Nymph 2 [N=5]	Nymph 3 [N=11]	Nymph 4 [N=14]	Nymph 5 [N=3]	Adult [N=15]
Leg I	1	2	2	2	2	9–12
Leg II	1	2	2	2	2	20–27
Leg III	2	2	2	2	3	10–14
Leg IV	2	2	2	2	3	13–15

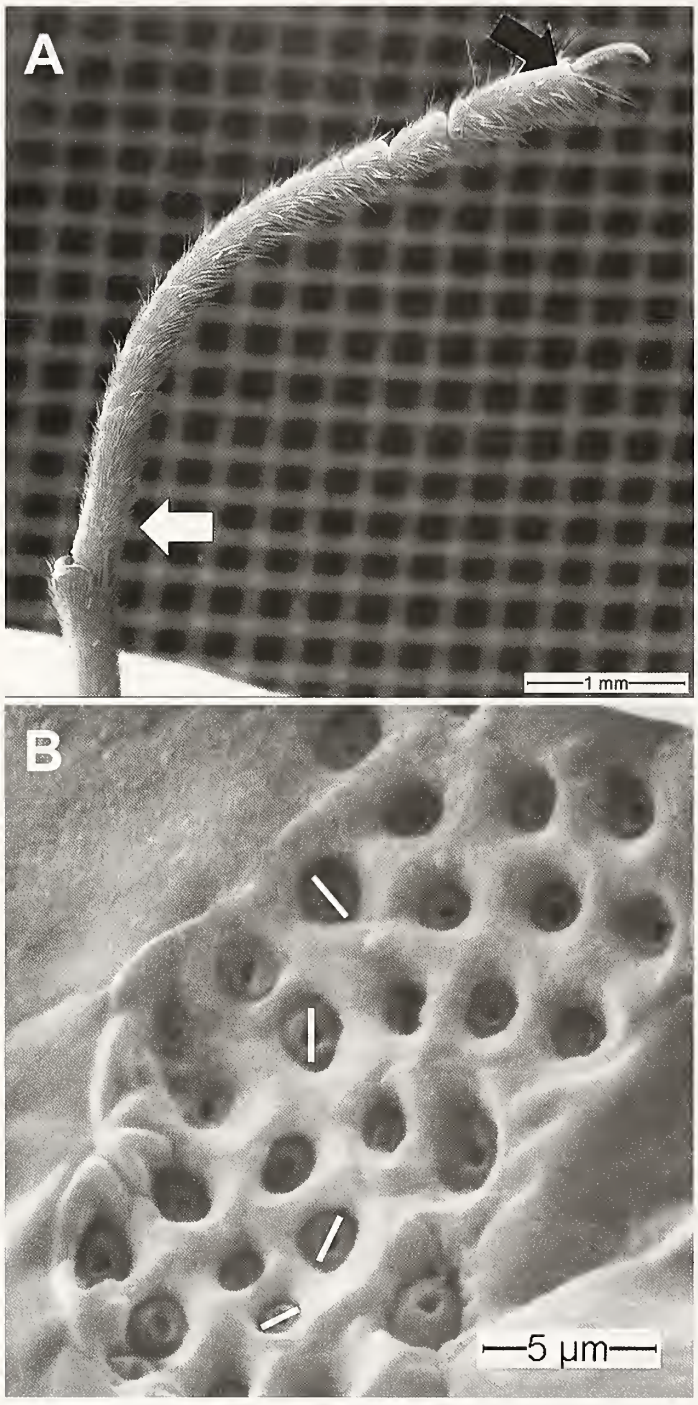

Figure 1.—**A.** Right tarsus of leg III of an adult male of *Heteromitobates albiscriptus*, showing the location of the tegumental structures studied herein under SEM. The black arrow shows the region where TAPs ("tarsal aggregate pores") are located, and the white arrow shows the position of TPO ("tarsal perforated organ"). Retrolateral view. **B.** Retrolateral view of right tarsus of leg IV of an adult male of *Heteromitobates albiscriptum*, showing measurements of the diameter taken in some pores of TAPs (white lines).

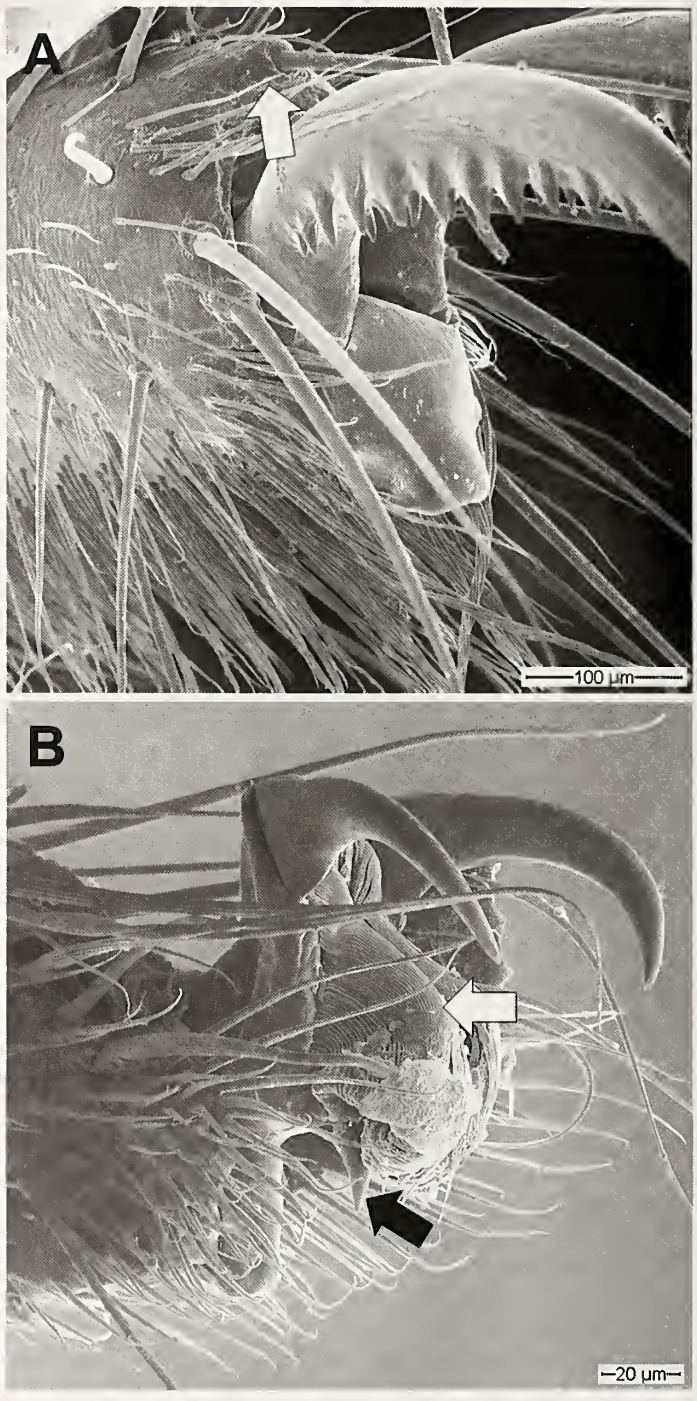

Figure 2.—**A.** Right leg IV of an adult male of *Heteromitobates albiscriptus*, showing the pectinate tarsal claws typical of the genus *Heteromitobates* and the tarsal process (arrow) typical of the adult tarsus of some gonyleptoid Laniatores. **B.** Right leg IV of a first nymph of *Heteromitobates albiscriptus*, showing the smooth tarsal claws, the arolium (white arrow) and the pseudonychium (black arrow). Retrolateral views.

following structures of all 56 individuals available: body length (from the base of chelicerae to the end of the abdomen) and width (at the widest point), total length and number of tarsal segments of each leg. Measurements were taken with a digital caliper and when necessary under a stereomicroscope. Measurements were taken on the right appendages; when a leg was missing or incomplete, the corresponding left appendage was measured. Measurements are herein expressed as the average measure ± standard deviation. Since we noticed, during the study, that sex could be recognized both in adults and last instar nymphs, we identified the sex when taking the

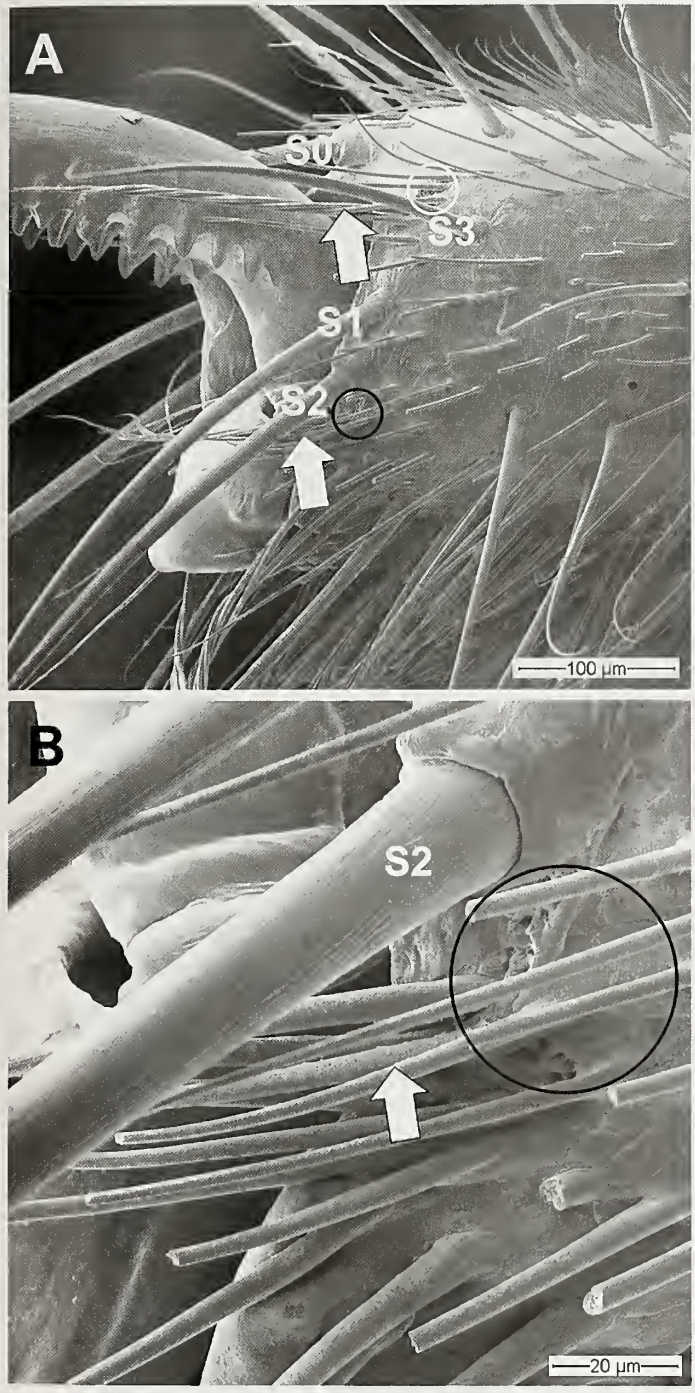

Figure 3.—**A.** Right leg III of an adult male of *Heteromitobates albiscriptus*, showing the TAPs (white circle) and vTAPs (black circle). **B.** Detail showing vTAPs. S0-S3 = setae (see text for description); arrows = associated trichomes (see text). Prolateral views.

measurements that were used in tarsal microstructural analyses, but the reduced number of females available did not allow comparisons between sexes in the morphometric analysis. Therefore, results are reported for all adults combined.

Morphological analysis of tarsal structures under SEM.—For SEM analysis, we followed the procedures described in Willemart et al. (2007, 2009, 2010). The legs were removed, cleaned ultrasonically and then mounted on a stub using silver glue. The stubs were sputter coated with gold using a Balzer SCD 50 sputter coater and then examined under the Zeiss DSM 940 SEM of the Electronic Microscope Laboratory of IBUSP. We used the right leg when available; otherwise, we used the left leg. For this study we used at least one specimen of each nymphal stage and at least one male and one female specimen for the last nymphal and the adult stages. Unfortunately, all available second nymphs had dirt adhered to their legs, hampering optimal analyses and micrographs.

In order to analyze the ontogenetic changes of the TAPs (Fig. 1A, black arrow) and TPO (Fig. 1A, white arrow) during the postembryonic development, we made a series of measurements and counts, as described below. We then compared the number and size of the studied structures in relation to the length of the tarsus along the postembryonic stages.

In the case of the TAPs, we used the micrographs to count the number of pores and to measure their diameter, in both prolateral and retrolateral groups. The numbers given here are an estimate of the real number of pores, because in some cases we could not properly see all pores due to the presence of the typical trichomes covering the group of pores. Therefore, we made several micrographs from different angles in order to allow precise counts of pores. In the case of the diameter, for comparisons among ontogenetic stages, we used the average diameter of the pores in the group; we measured as many pores as possible in each group (Fig. 1B), directly on the micrograph, using the scale bar as a reference. Although these pores were only previously detected on legs III and IV (Willemart et al. 2007), we analyzed all four legs in our study to check this information, especially considering that we included juveniles, not studied before.

In the case of the TPO, we photographed with high magnification and analyzed only one of the rows of all legs; we used the retrolateral row whenever possible, but we used the prolateral row when needed and also for comparison of structures between the two rows. We measured the total length of the organ and counted the number of plates included in the organ. Since the plates have an irregular shape, we measured the longest length of three randomly selected plates and used the mean length to make comparisons among stages.

We also observed the structures located between the two tarsal claws of legs III and IV and previously known to be exclusive of nymphs (arolium and pseudonychium) or adults (fully developed tarsal process), and looked for additional structures that could help in the recognition of ontogenetic stages and/or sexes.

RESULTS

Morphometric analysis of the postembryonic stages.—We herein recognized five stages in the nymphal phase. Tables 1 and 2 summarize the data collected in this study (Appendix 1 shows all measurements collected for all specimens studied). Clearly there is no overlap between the measured values of successive stages, which can therefore be easily recognized by morphometric values. The number of tarsomeres is initially small in nymphs and increases among adults, with a major saltational change between the two phases. Sex cannot be recognized in the first four nymphal stages. Males can be distinguished from females by the presence of an apophysis on

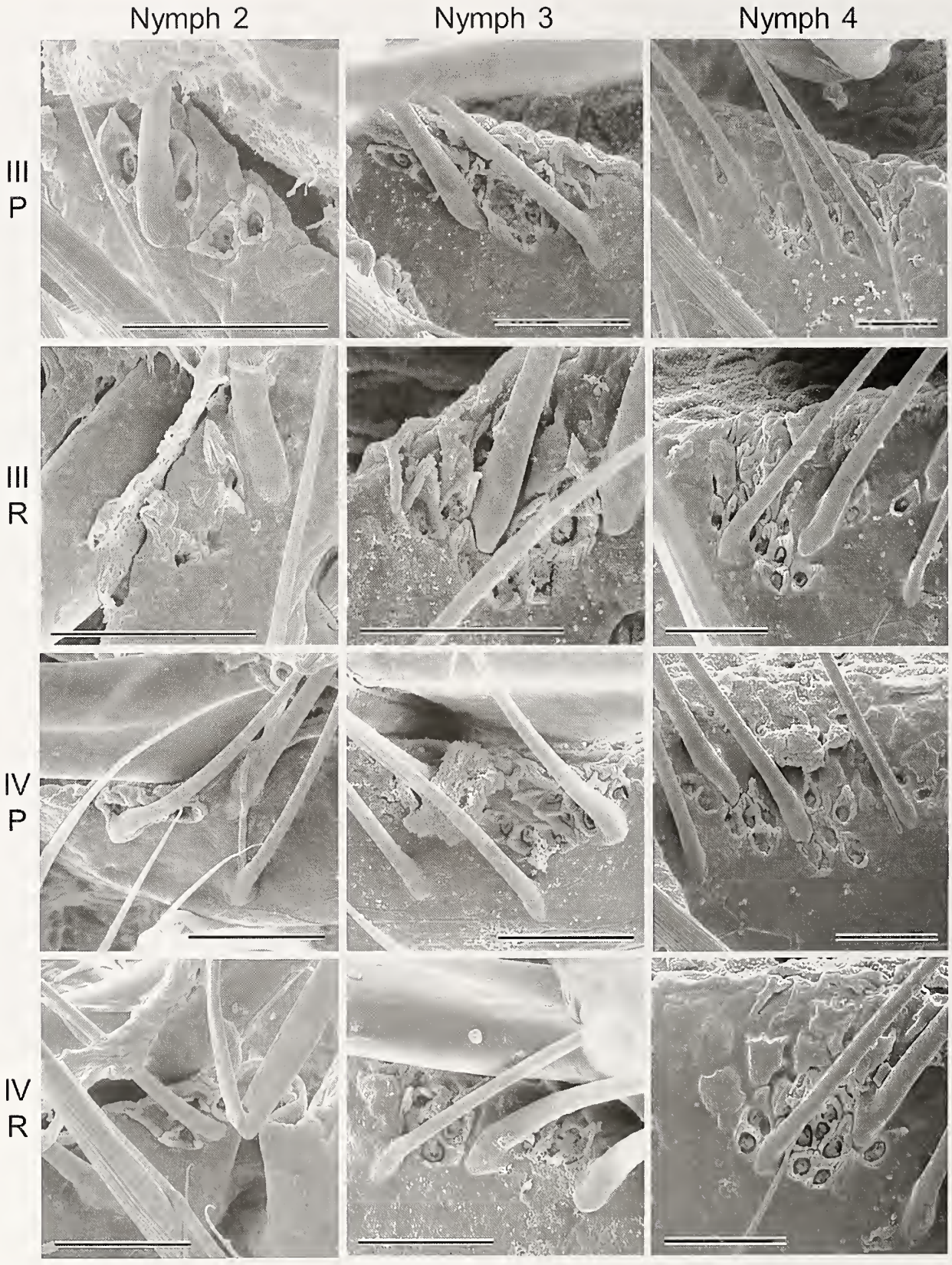

Figure 4.—Comparative plate of TAPs in both prolateral (P) and retrolateral (R) margins of legs III and IV during the postembryonic development of *Heteromitobates albiscriptus*. Nymphs 2–4 (compare to Figs. 5, 6). Scale = 20μm.

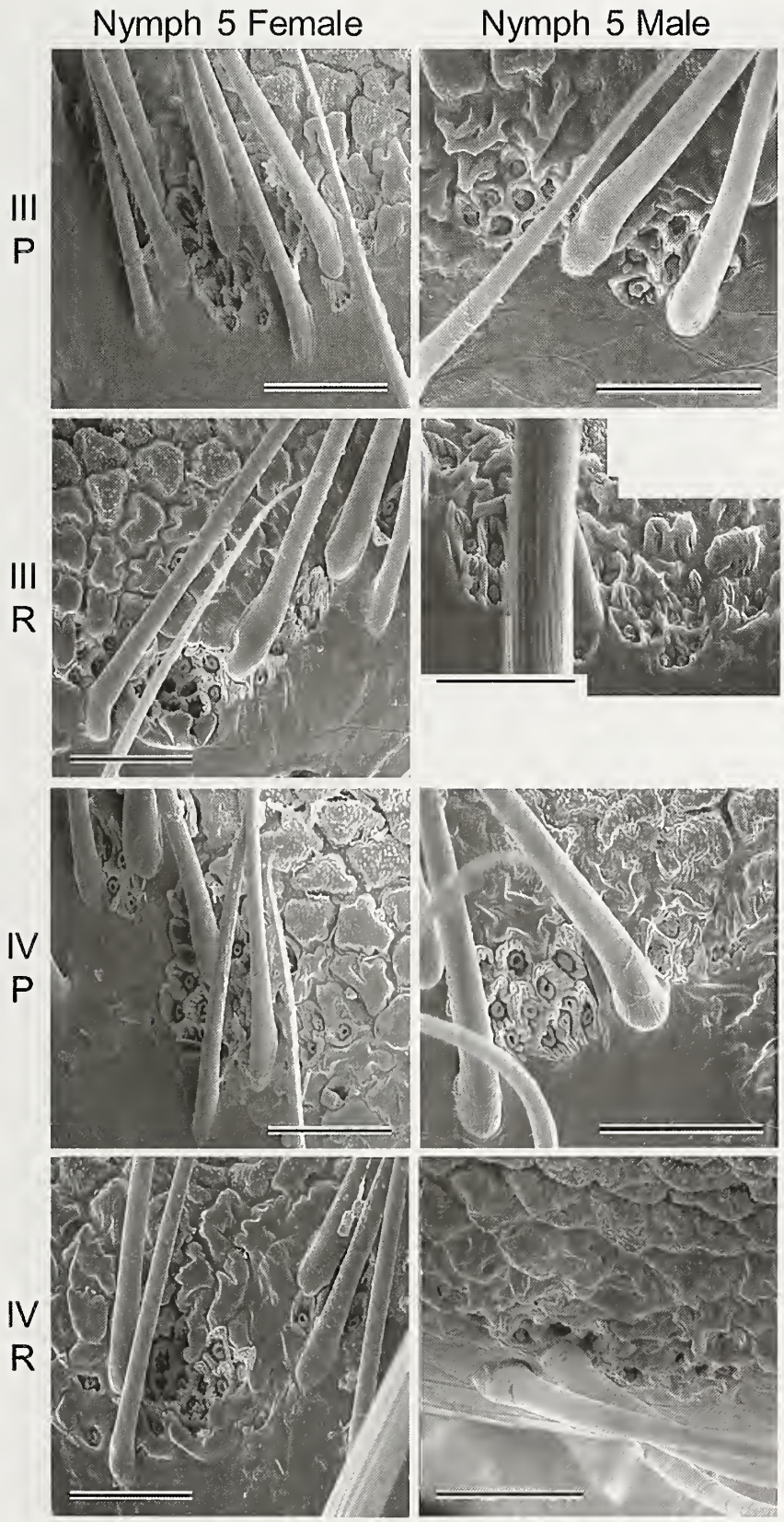

Figure 5.—Comparative plate of TAPs in both prolateral (P) and retrolateral (R) margins of legs III and IV during the postembryonic development of *Heteromitobates albiscriptus*. Nymphs 5 (compare to Figs. 4, 6). Scale = 20μm.

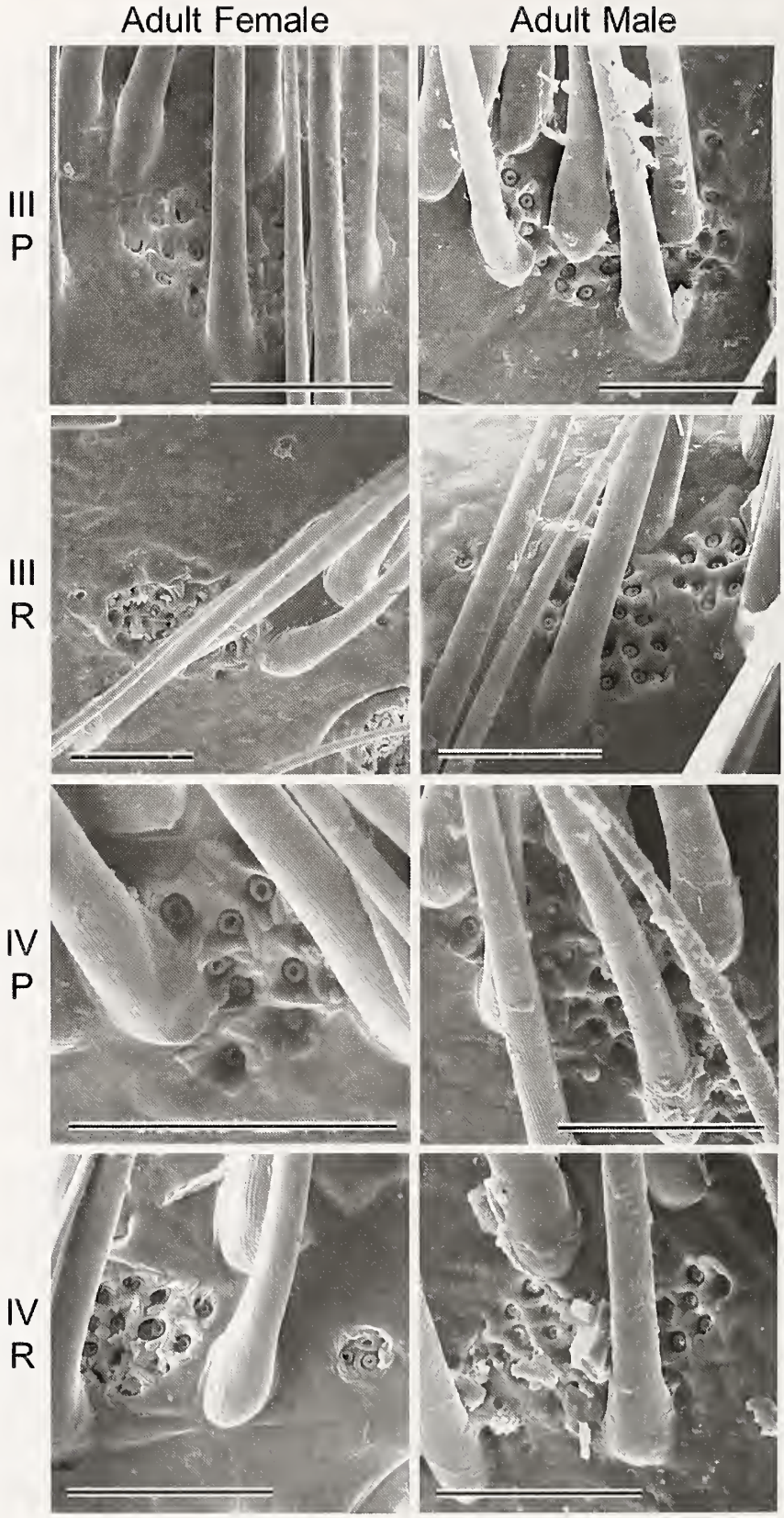

Figure 6.—Comparative plate of TAPs in both prolateral (P) and retrolateral (R) margins of legs III and IV during the postembryonic development of *Heteromitobates albiscriptus*. Adults (compare to Figs. 4, 5). Scale = 20μm.

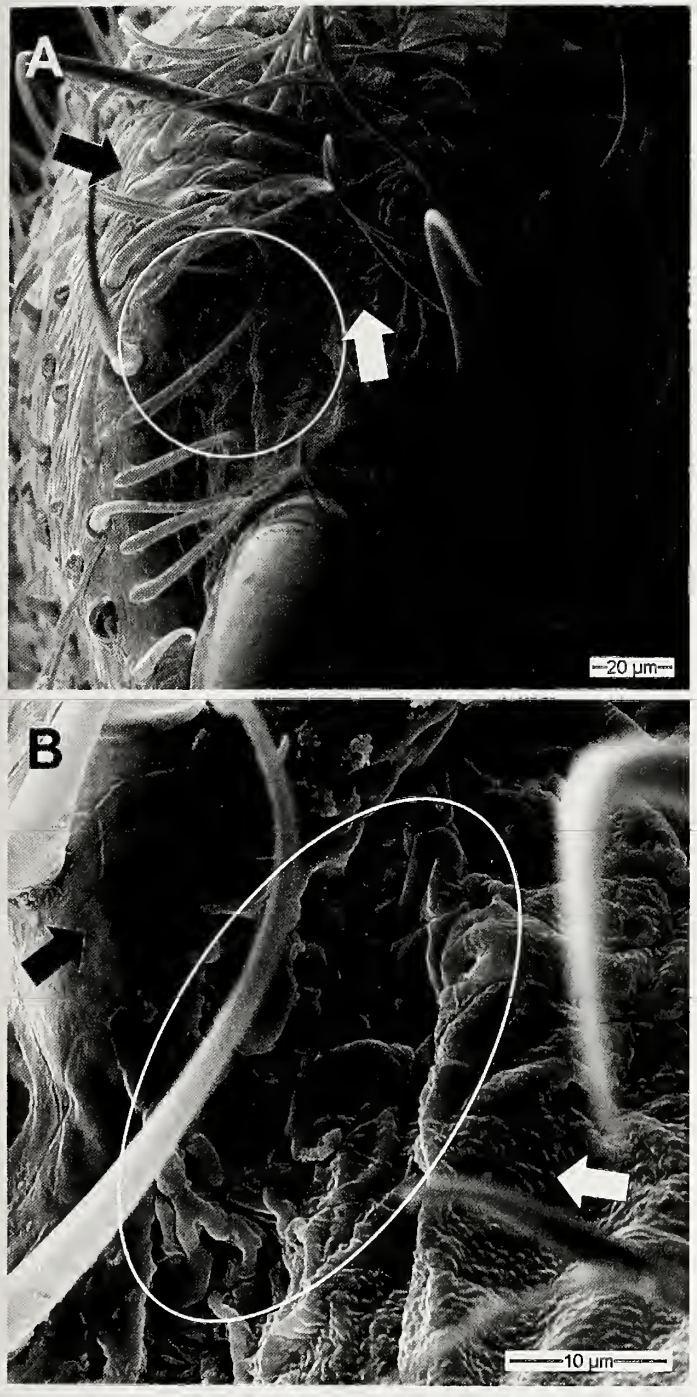

Figure 7.—**A.** Frontal view of tarsus I of an adult female of *Heteromitobates albiscriptus*, showing the different integument between the distal pleura around the articulation of the tarsal claw (white arrow) and the regular integument (black arrow). **B.** Detail of the circle in **A**, showing FAPs ("frontal tarsal aggregate pores") (ellipse); arrows show difference in integument, as in **A**.

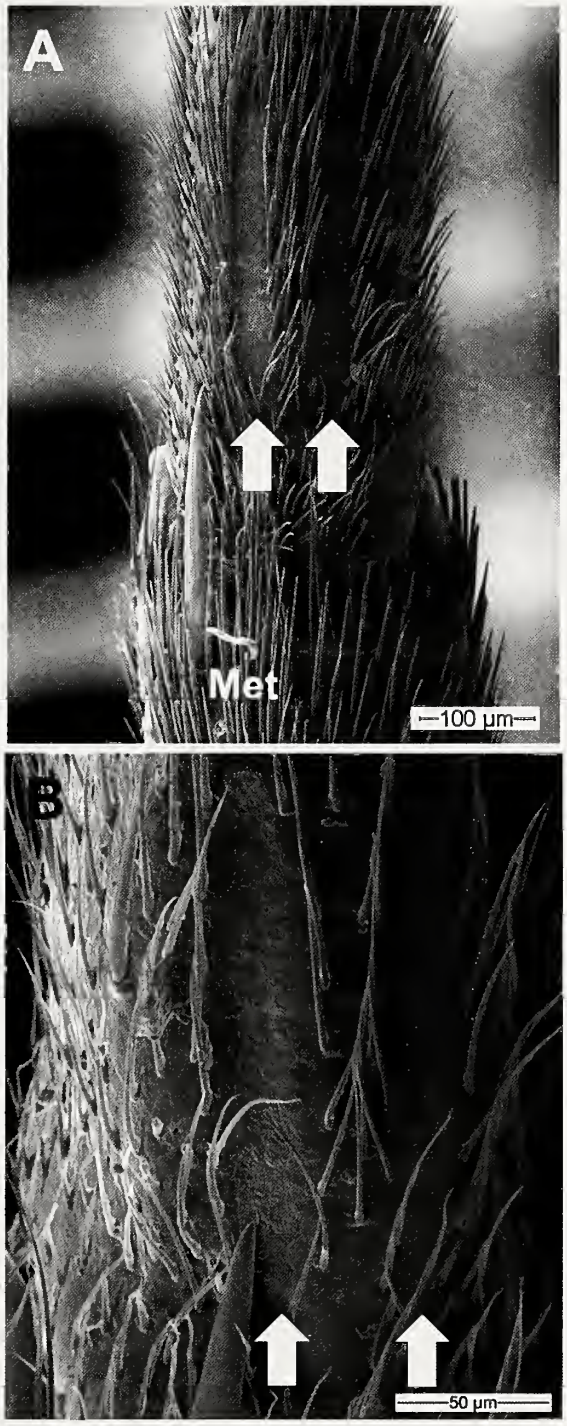

Figure 8.—Ventral view of the first tarsomere showing the pair of TPOs (arrows) running along the base of the tarsomere of *Heteromitobates albiscriptus*. **A.** Left fourth leg of an adult female. **B.** Right fourth leg of a fourth instar nymph. Met = apex of metatarsus.

trochanter IV both in the last nymphal stage and, more pronouncedly, in adults.

Additional taxonomic description of *H. albiscriptus* concerning nymphal features.—In addition to the description of *Heteromitobates albiscriptus* provided by DaSilva & Gnaspini (2009), our data allowed the recognition of important information related to nymphs. First, the color of the body and legs of nymphs is a patchy mixture of green and light grey, in both preserved and live specimens. Second, in contrast to the pectinate tarsal claws in legs III and IV of adults (Fig. 2A), nymphs bear smooth claws (Fig. 2B).

Tarsal aggregate pores: additional description and ontogenetic analysis.—Willemart et al. (2007) described the TAPs as "an aggregation of glandular openings that is always close to

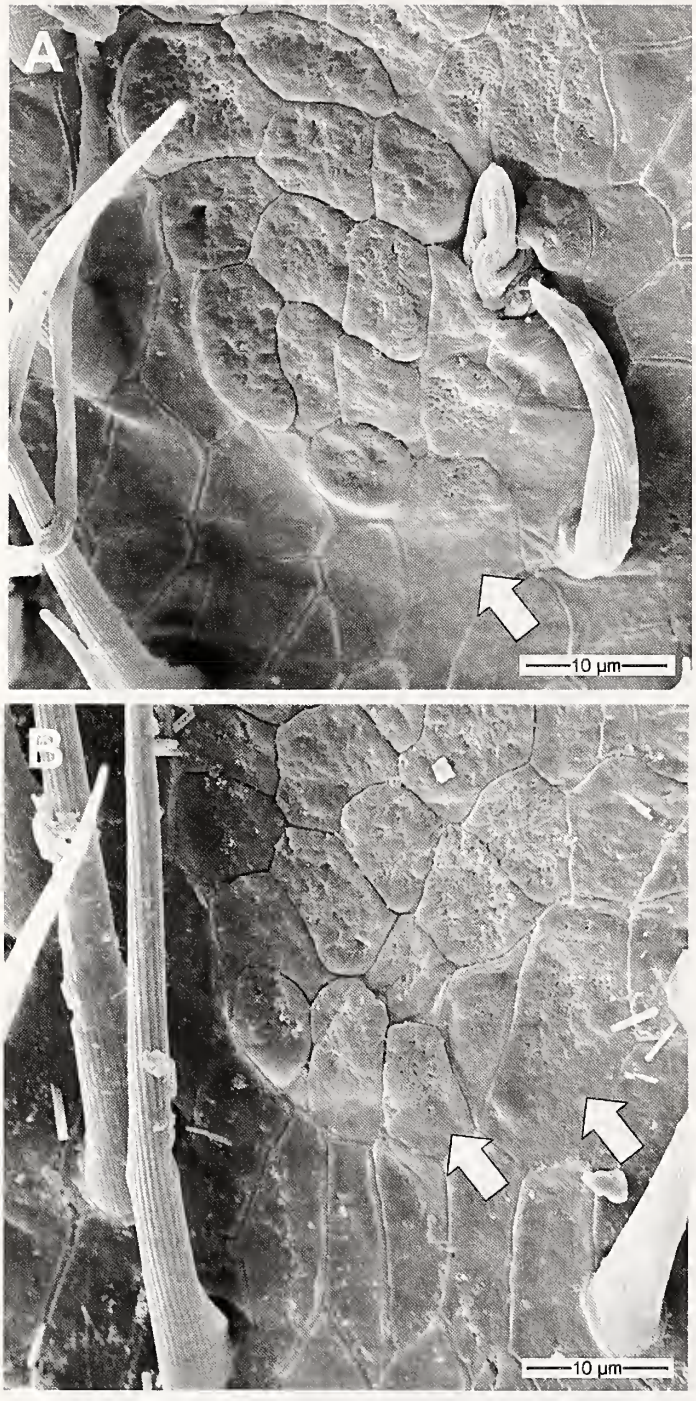

Figure 9.—Detail of the proximal portion of TPOs of *Heteromitobates albiscriptus*, showing the partially perforated nature of some of the proximally placed plates (arrows) as well as the more elongate shape of some proximal plates (both from the TPO and the surrounding integument). **A.** Leg III. **B.** Leg IV. Both are prolateral rows on the right legs from an adult female.

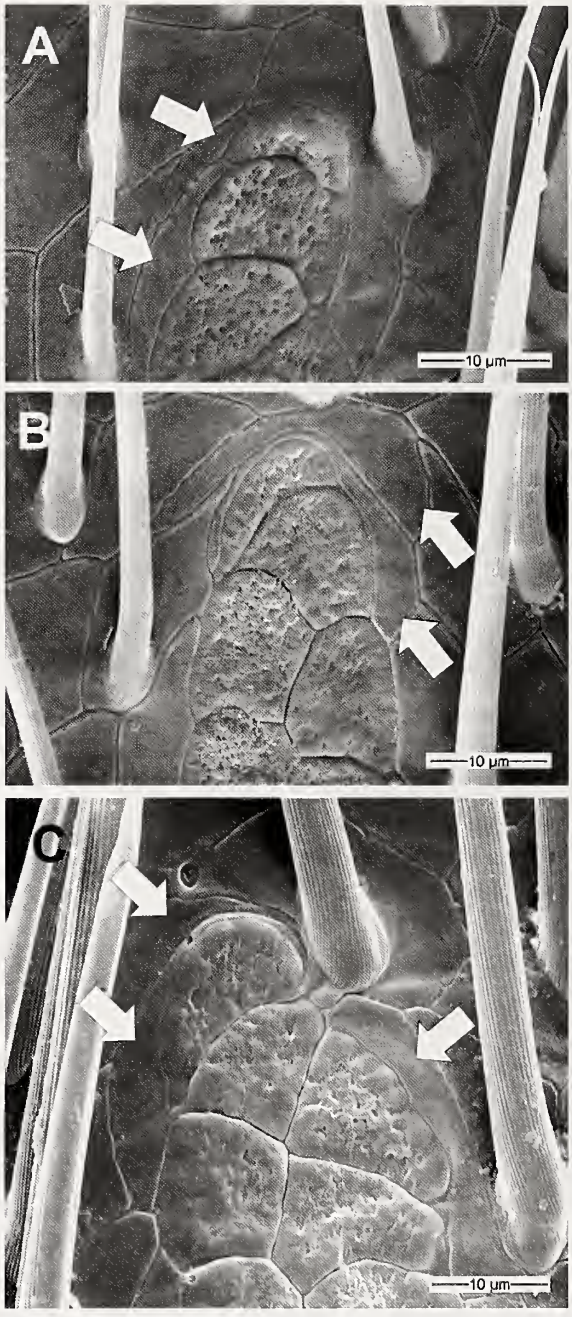

Figure 10.—Detail of the distal portion of TPOs of *Heteromitobates albiscriptus*, showing that the single cell or group of distal cells form a round margin frequently surrounded by very narrow and elongate curved tegumental plate(s) (arrows), very different from the other tegumental plates. **A, B.** Male 5th nymph, retrolateral row of left leg II and prolateral plate of right leg IV, respectively. **C.** Retrolateral row of right leg IV of an adult male.

the base of an aggregation of trichomes." They observed ~15 openings with a ca. 1 mm diameter. These associated trichomes are located at a specific position on the tarsus and are frequently twisted together (Fig. 3, arrows), so that this group of trichomes can be promptly recognized and could help to locate the TAPs. TAPs from each side of the tarsus may form a single group or they can be split into two groups located on either side of the associated trichomes. We observed up to 25 pores in total among adult males, either on a single group or split into two groups.

In addition, TAPs seem to have a precisely defined position in both prolateral and retrolateral faces of the tarsus (Fig. 3A, white circle), close to the distal margin surrounding the insertion of the tarsal claws, and close to the dorsal face of the tarsus, on both sides of a large seta (part of the tarsal process of adults but also present among nymphs; Fig. 3A, "S0"). In

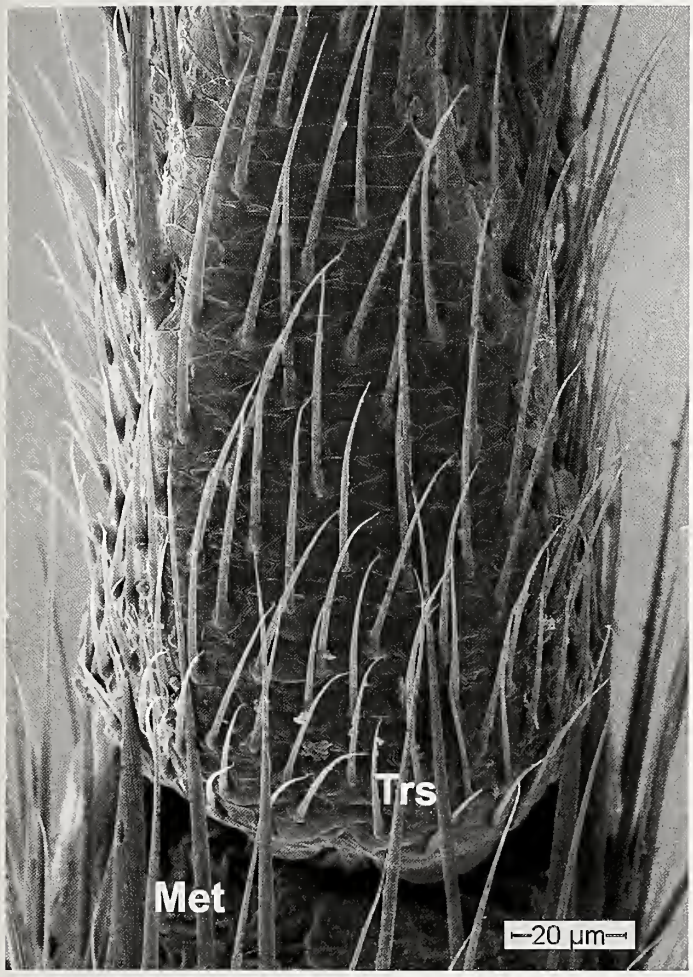

Figure 11.—Proximal region of the proximal tarsomere (Trs) of right leg IV of a first nymph of *Heteromitobates albiscriptus*, ventral view, showing the absence of TPOs. Met = apex of metatarsus.

both prolateral and retrolateral faces of legs III and IV, it is possible to recognize the following group of setae (Fig. 3A): "S0" is dorsally placed and it is attached to the tarsal process among adults or, among nymphs, it represents the position where the tarsal process will later develop, and it is placed close to the distal margin of the tarsomere; two additional large setae, "S1" and "S2", are also located close to the distal margin of the tarsomere, but are more ventral than "S0"; "S3" is located between setae "S0" and "S1" in a position somewhat displaced from the distal margin of the tarsomere. TAPs are placed inside the triangle formed by setae "S0-S1-S3", usually close to the distal margin of the tarsomere, but at a variable distance from "S0".

TAPs appear in legs III and IV of all stages except among the first nymphs, and grow in number from three or four among second nymphs to around 20 among adults (Table 3 and Figs. 4–6). The individuals analyzed usually had similar numbers of pores both on prolateral and retrolateral regions, as well as when both legs III and IV were compared. The diameter of the pores did not show a clear difference among ages, and measured 2.15 ± 0.46 µm (N = 174) (Table 3).

In our study, we identified an additional field of tarsal aggregate pores, placed more ventrally, just below "S2" (Fig. 3A, B), with similar structure to the group described above, also associated with the same kind of typical trichomes. We herein refer to this newly discovered group as the "ventral tarsal aggregate pores" (vTAPs). These groups of pores were observed only among adults (in both males and females), and usually have a smaller number of pores when compared to the "regular" TAPs. Although a similar group of the typical associated trichomes could be observed among the last instar nymphs (though less conspicuous than those of adults), the pores were absent.

Pores on the distal pleura of legs I & II.—By analyzing the distal region of the tarsi of legs I and II, which bear only one tarsal claw and lack TAPs, we recognized an additional group of pores, herein detected for the first time and informally named "frontal tarsal aggregate pores" (FAPs) in order to facilitate communication in the present text. They are placed on the distal pleura of the tarsus, around the articulation of the tarsal claw, on both sides of the tarsal claw (Fig. 7). The integument of the distal pleura (Fig. 7, white arrows) can be easily recognized from the integument of the rest of the tarsus (which is composed of smooth plates and bears trichomes and setae, as in Fig. 7, black arrows). In the material examined, we could clearly observe FAPs on legs I of males and females of both fifth nymph and adult stages; and FAPs were clearly absent on legs III of female fifth nymphs and adults and on legs IV of adult females. The rest of the material herein analyzed did not allow us to precisely identify the presence or absence of FAPs.

Tarsal perforated organ (TPO): additional description and ontogenetic analysis.—As described by Willemart et al. (2007), the "tarsal perforated organ" (TPO) is composed of a pair of rows of perforated plates located on the ventral side of the first tarsomere of all legs (Fig. 8A, B). We herein observed typical features that are frequently found in the TPOs analyzed.

Concerning the proximal portion of the rows of plates, it is common to find longitudinally elongate tegumental plates just proximally to the TPO (Fig. 9A, B), and some of the proximal plates of the TPO may also be more elongate than the others (Fig. 9A, arrow). In addition, the more proximal plates of the TPO are very frequently only perforated on their distal portion and their proximal portion is smooth, resembling the surrounding tegumental plates (Fig. 9, arrows).

Concerning the distal portion of the TPO, it is very common that the distal plate(s) has (have) a round distal margin (Fig. 10). This shape is not frequently observed among the other plates of the TPO, which are usually sub-rectangular in shape (i.e., opposed sides are frequently straight lines parallel to each other). In addition, the tegumental plates that surround the apex of the TPO are frequently narrow and very elongated when compared to the other tegumental plates, and usually contour the apex of the TPO (Fig. 10, arrows).

TPOs appear in all legs of all stages except among the first nymphs (Table 4, Figs. 11–15). Except for the second nymph, which showed lower values when compared to the other stages, there is no clear growth during the postembryonic development when both the average size of the plates (ranging between 7–11 µm) and the percentile relation between the length of TPO and the total length of the tarsus are concerned

Table 3.—Number and diameter of pores in the TAPs ("tarsal aggregate pores") during the postembryonic development of *Heteromitobates albiscriptus*. TAPs were not observed in nymphs 1. Right legs were used in the study (when they were not available, left legs were used, marked with an *). Tarsus = length of tarsus (mm); Total = total length of leg (mm); #prol = number of pores in the prolateral group; #retrol = number of pores in the retrolateral group; Φprol/Φretrol = diameter (average ± std dev., in μm) of pores in prolateral and retrolateral groups respectively (N is given in parentheses).

Instar	Leg	Tarsus	Total	# prol	# retrol	Φ prol	Φ retrol
Nymph 2	III	2.11	16.35	4	4	2.20±0.30 (3)	1.49±0.14 (3)
	IV*	2.84	24.74	3	4	2.56±0.35 (2)	1.87±0.21 (3)
Nymph 3	III	2.96	22.67	8	9	2.28±0.27 (4)	2.29±0.24 (4)
	IV	3.47	32.54	8	8	2.50±0.15 (4)	2.51±0.51 (4)
Nymph 4	III	3.57	29.28	11	12	2.31±0.23 (5)	2.41±0.22 (6)
	IV	4.65	42.48	13	11	2.74±0.44 (7)	2.65±0.45 (7)
Nymph 5 female	III	4.75	37.58	18	20	2.38±0.19 (5)	2.34±0.22 (9)
	IV	6.14	50.99	18	15	2.53±0.32 (9)	2.51±0.32 (9)
Nymph 5 male	III	4.81	38.17	16	17	2.27±0.38 (9)	2.21±0.34 (6)
	IV	5.77	51.65	15	15	2.20±0.35 (9)	2.29±0.20 (5)
Adult female	III	6.08	47.42	14	19	1.94±0.19 (5)	1.41±0.06 (5)
	IV*	7.20	65.01	15	17	1.67±0.14 (5)	1.50±0.20 (7)
Adult male	III	7.04	55.65	20	25	1.88±0.24 (9)	1.85±0.24 (16)
	IV	8.46	75.74	19	20	1.73±0.29 (5)	1.80±0.26 (9)

(Table 4). In turn, as expected based on the information above, there is a clear growth in the number of plates per TPO, as well as the length of TPO, throughout the ontogeny. Yet, the length of the TPOs is often greater among males, which usually have longer legs than females.

TPOs may be formed by one single row of cells (which is common among early stages [except first nymphs, which lack TPOs] and/or in legs I–II) or by more than one (up to four or five), which is common among the older stages and/or in legs III–IV (Figs. 12–15).

Table 4.—Morphometric analysis of TPO ("tarsal perforated organ") during the postembryonic development of *Heteromitobates albiscriptus*. Right legs were used in the study (when they were not available, left legs were used, marked with an *). Leg Total = total length of leg (mm); Tarsus = length of tarsus (mm); TPO = length of the TPO (mm); TPO/Tarsus = length of the TPO as a proportion of the length of the tarsus, expressed as a percentage; Plate = average length of single plates of the TPO (μm); #Plates = number of plates that composed the TPO.

Instar	Leg	Leg Total	Tarsus	TPO	TPO/Tarsus (%)	Plate	#Plates
Nymph 2	I	11.11	1.99	0.056	2.8	6.45	9
	II	26.02	5.10	0.056	1.1	9.06	7
	III	16.35	2.11	0.103	4.9	6.67	28
	IV*	24.74	2.84	0.063	2.2	7.11	16
Nymph 3	I	13.32	2.25	0.068	3.0	8.19	9
	II	37.31	6.58	0.063	1.0	7.62	10
	III	22.67	2.96	0.144	4.9	10.43	32
	IV	32.54	3.47	0.108	3.1	7.46	30
Nymph 4	I	18.46	2.69	0.105	3.9	8.19	16
	II	45.63	8.53	0.068	0.8	8.16	12
	III	29.28	3.57	0.201	5.6	10.11	43
	IV	42.48	4.65	0.163	3.5	10.37	36
Nymph 5 female	I	26.64	3.22	0.130	4.0	8.39	25
	II	56.88	10.39	0.093	0.9	8.71	19
	III	37.58	4.75	0.189	4.0	10.58	47
	IV	50.99	6.14	0.218	3.6	11.74	37
Nymph 5 male	I	24.43	3.15	0.139	4.4	8.33	26
	II*	59.03	10.40	0.137	1.3	8.42	26
	III	38.17	4.81	0.247	5.1	9.03	66
	IV	51.65	5.77	0.251	4.4	11.95	62
Adult female	I	30.32	4.05	0.180	4.4	9.72	36
	II	72.60	12.03	0.134	1.1	9.22	30
	III	47.42	6.08	0.249	4.1	10.00	82
	IV*	65.01	7.20	0.262	3.6	10.87	84
Adult male	I	33.96	4.30	0.226	5.3	10.71	41
	II	81.58	13.12	0.148	1.1	9.33	28
	III	56.00	7.02	0.232	3.3	10.18	81
	IV	74.57	8.12	0.301	3.7	11.67	91

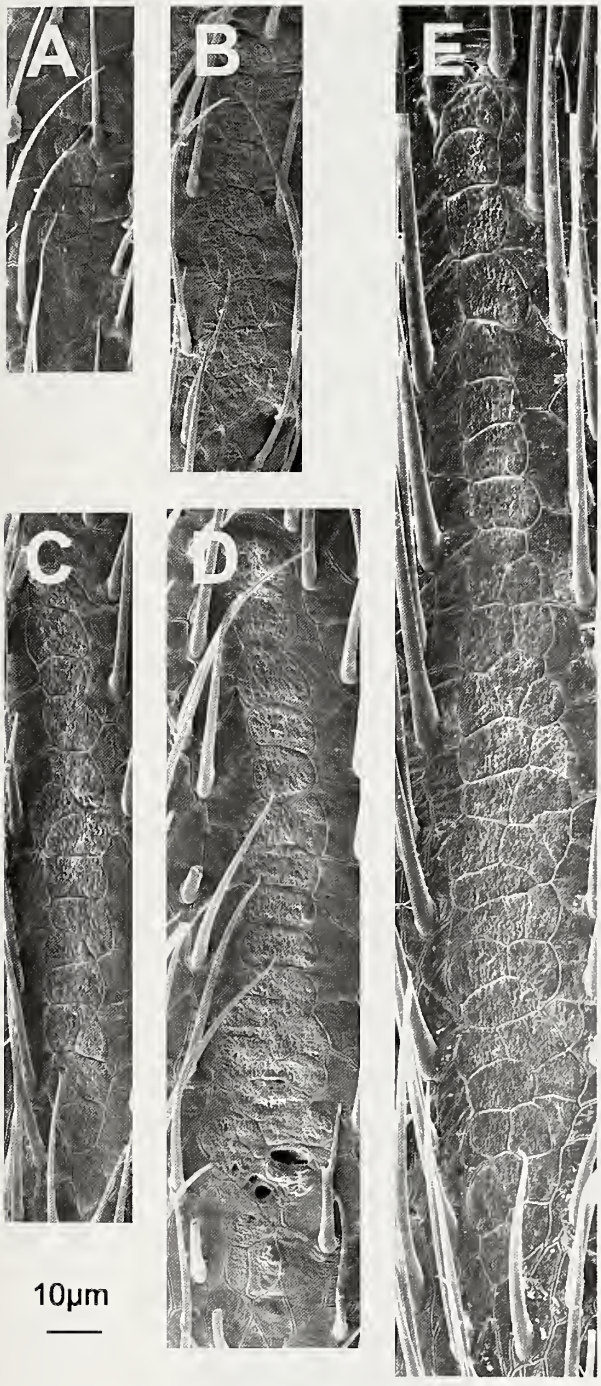

Figure 12.—Ontogenetic modification of TPOs of leg I, from 2nd nymph to the adult of *Heteromitobates albiscriptus* (**A–E**, respectively; **D** male 5th nymph and **E** adult male). All figures to the same scale (same as in Figs. 13–15).

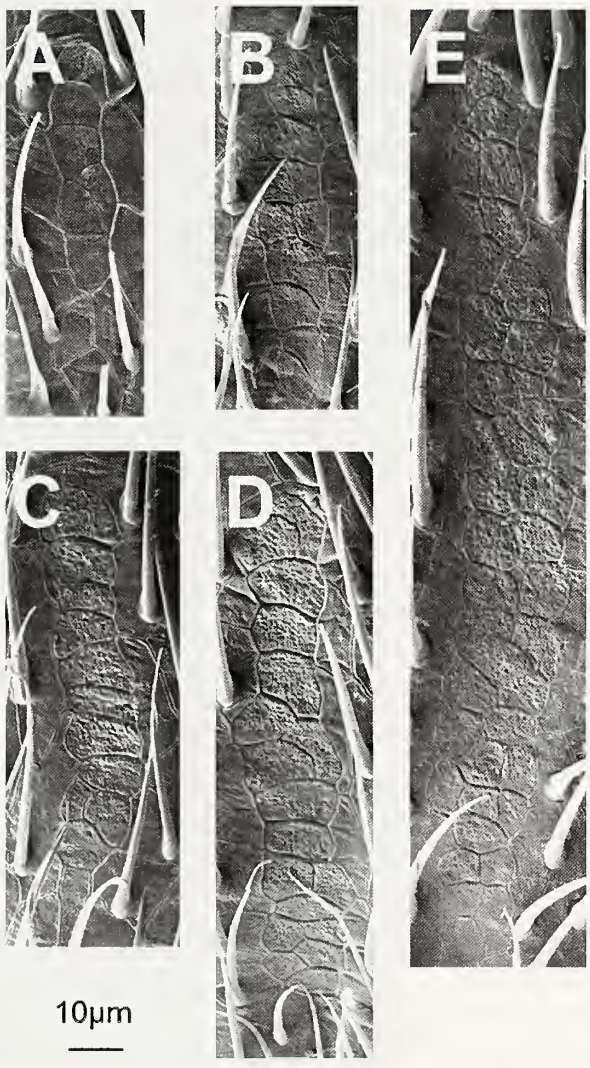

Figure 13.—Ontogenetic modification of TPOs of leg II, from 2nd nymph to the adult of *Heteromitobates albiscriptus* (**A–E**, respectively; **D** female 5th nymph and **E** adult male). All figures to the same scale (same as in Figs. 12, 14, 15).

DISCUSSION

Taxonomic remark: juvenile stages should be taken into consideration in taxonomic studies.—The fact that nymphs bear simple tarsal claws in legs III and IV (Fig. 2B) instead of the pectinate claws of adults (Fig. 2A) is important information for taxonomists, since the genus *Heteromitobates* is characterized by the presence of pectinate tarsal claws, contrasting to the other genera in the subfamily Goniosomatinae (DaSilva & Gnaspini 2009), which all bear smooth claws. In other words, if one has in hand nymphs of *Heteromitobates* with no knowledge of this information, one may describe or try to identify the species in a different (and incorrect) genus, creating a taxonomic confusion. The importance of ontogeny in taxonomy is recognized in other groups, including extant and fossil animals, as, for instance, in the controversy around pachycephalosaurid dinosaurs (e.g., Horner & Goodwin 2009).

Recognition of the postembryonic stages.—Considering that the stage recognized in previous publications as the "subadult" should be considered part of a single adult stage (as discussed by DaSilva & Gnaspini 2009; see also Zatz et al. 2010; Munguía-Steyer et al. 2012) and not the last nymphal instar (see discussion in Gnaspini et al. 2004), the number of nymphal stages herein observed (five) agrees with other goniosomatines (e.g., Gnaspini 1995, 2007), when the previous publications numbers are corrected. In contrast, the larger growth detected by Gnaspini (1995) for the molt between the first and the second nymph was not detected here; in our case,

Figure 14.—Ontogenetic modification of TPOs of leg III, from 2nd nymph to the adult of *Heteromitobates albiscriptus* (**A–E**, respectively; **D** male 5th nymph and **E** adult male). All figures to the same scale (same as in Figs. 12, 13, 15).

there is no difference detected between subsequent stages (Table 1), which seems to be the case also with cranaids (Townsend et al. 2009; although the lack of information for some nymphal stages do not allow precise conclusions) and most Eupnoi and Dyspnoi studied (as summarized in Gnaspini 2007). Yet, in contrast with Gnaspini (1995), the developmental stages of *H. albiscriptum* can be easily recognized by morphometric data, with no overlap between successive stages (Table 3). Our data agreed with Gnaspini (1995) concerning the increase in the number of tarsomeres that occurs in legs III–IV in the last nymphal instar and in all legs in the molt to the adult phase. The only difference

Figure 15.—Ontogenetic modification of TPOs of leg IV, from 2nd nymph to the adult of *Heteromitobates albiscriptus* (**A–E**, respectively; **D** female 5th nymph and **E** adult male). All figures to the same scale (same as in Figs. 12–14).

detected is the number of tarsomeres in legs I–II among the first nymphs, being one tarsomere in *H. albiscriptum* in contrast to the two tarsomeres detected in *Serracutisoma spelaeum* (Mello-Leitão, 1933). Therefore, the number of tarsomeres tend to be conservative among nymphs of Laniatores, based on studies focusing on Gonyleptidae (with differences possibly occurring in the first and/or last nymphs, e.g., Muñoz-Cuevas 1971b; Gnaspini 1995, 2007; Gnaspini et

al. 2004; this study) and Cranaidae (Townsend et al. 2009; although the variation is not clear due to the lack of information for some nymphal stages); in contrast with one studied species of the suborder Dyspnoi, in which the number of tarsomeres tend to increase with each molt (Avram 1973).

In addition to morphometric values, the last nymphal instar (5^{th} instar, in our case) can also be recognized by the increase in the number of tarsomeres in relation to the previous instars, although this is a much smaller increase when compared to the molt to the adult tarsus.

In addition to the well-known presence of a full grown tarsal process, our study detected one additional tarsal structure typical of the adult phase: vTAPs (on legs III–IV; Fig. 3), as well as the presence of pectinate claws, which is probably restricted to species of the genus *Heteromitobates* Roewer, 1913, as discussed above. Moreover, the number of pores in TAPs as well as the number of plates in TPOs increase with age and can also be used to recognize the ontogenetic stage of an individual.

FAPs: frontal tarsal aggregate pores on the distal pleura of legs I–II.—Glandular pores are widespread all over the integument of harvestmen (e.g., Willemart et al. 2007) and FAPs may simply be "regular" pores, and, for this reason, we preferred to use FAP as an informal term at the present time. Although we clearly detected their presence in some legs of some stages and their absence in other legs, our data are inconclusive with respect to their presence throughout postembryonic development, and, therefore, FAPs deserve a more specific approach.

TAPs: tarsal aggregate pores.—The morphology of TAPs observed herein agreed with their original description (Willemart et al. 2007) and their association with typical trichomes which frequently twist together was also commented on by Gainett et al. (2014). Here we described their specific position in the tarsus and recorded a second group of TAPs located more ventrally (vTAPs), only among adults. Although no clear difference could be detected among the different stages considering the diameter of the pores, adults seem to have smaller pores when compared to the previous instars (except for the second nymphs), which may be related to the larger number of pores in the TAPs among adults (Table 3). Having found no clear distinction between TAPs in immatures and adults or between adult males and females, we have no evidence of sexual selection influencing the development of TAPs (Andersson 1994). If histological studies confirm that they are in fact glandular as their external morphology suggests, they might therefore be used for a non-sexual purpose such as leaving chemical trails used for navigation. Chemicals left on the substrate have indeed been shown to be used in a variety of contexts in harvestmen (Willemart & Hebets 2011; Teng et al. 2012; Fernandes & Willemart 2014).

TPO: tarsal perforated organ.—Although the number of plates (and consequently the total length of TPO) and also the number of rows of plates in the TPO grow with age, the ratio of TPO length to tarsus length does not show a clear growth with age (Table 4). It is also worth noting that some unusual features may be observed in TPOs, and may represent anomalies during the integument formation. For instance, both rows of plates of the TPO usually form a single group, but in a few cases we observed gaps within them (as in the distal portion in Fig. 14E). Other types of unusual features observed in TPOs were holes (Fig. 12D; which are clearly not pores) and intrusions (Fig. 9A). These features were rarely observed and could not be related to age or to specific legs.

When the four legs are compared, the absolute number of plates in the TPO as well as the TPO absolute and percentile length in relation to the length of the tarsus of leg II are smaller when compared to the other legs, despite the fact that leg II is the longest leg. In all legs, TPOs have multi-porous plates, with no obvious difference between legs or sexes. We therefore have no evidences of any sexual role for such an organ. When Willemart et al. (2007) described the TPOs, they suggested that TPOs were the openings of contact glands. However, the recent study published by Proud & Felgenhauer (2013) provided evidence against the "contact gland" hypothesis. Those authors related the TPO to internal attachments of muscles to the inner surface of the exoskeleton. More specifically, they related TPO to the first internal pulley detected in a series of pulleys located along the tarsomeres. They could not explain why only the first pulley had external reflections in the integument, and suggested this was related to the molting process when the first pulley would be the one to maintain connection with muscles. The irregular external surface of the tegumental plates would represent scars related to the microtubules and tonofibrillae that were extended throughout the cuticular matrix. Based on our results, we would add more questions to this scenario. First, the internal connection to a pulley and the "scar nature" of TPOs may explain their irregular integument (as well as the "mistakes" observed in the integument, as described above) but do not explain the specific shape of the surrounding anterior and posterior tegumental plates, which differ from the other plates in the legs. Second, especially considering that leg II is the longest leg, the scenario does not explain why the TPO is the shortest both in absolute and in relative values (in this case 1% of the tarsus length against 4% in the other legs) on this leg. Third, we observed the absence of the TPO in first nymphs. It is known that harvestmen hatch in the form of larvae that molt into a first nymphal stage (e.g., Gnaspini 2007). Therefore, we would expect to find TPOs among first instar nymphs if they are the results of the molting process. Gnaspini & Lerche (2010) noticed that the molting process starts already inside the egg, during embryonic development. This premature molting process may explain the absence of TPO in first nymphs if TPO is actually related to molting. Although they are clear structures on the tarsus of all legs, and in spite of the great advances provided by the work of Proud & Felgenhauer (2013), there are still unanswered questions about the TPOs.

ACKNOWLEDGMENTS

The authors thank Dr. A.A.G.F.C. Ribeiro, E. Mattos, P. Lenktaitis and M.V. Cruz, from the Electronic Microscope Laboratory of IBUSP, for the use of the SEM facilities. We also thank the owner of the land, Mr. Almeida, for allowing access to the cave, and the several friends that helped in the field, particularly M.C.C. da Inês and M.V. Nakamura. This study was funded by Fundação de Amparo à Pesquisa do Estado de São Paulo (FAPESP) #2010/08630-5 (AZR) and #1999/07943-9 (RHW); Conselho Nacional de Desenvolvi-

mento Científico e Tecnológico (CNPq) #304534/2007-2, 304272/2010-8 (PG).

LITERATURE CITED

Andersson, M. 1994. Sexual Selection. Princeton University Press, Princeton.

Avram, S. 1973. Contribution a la connaisance du developpement embryonaire et postembryonnaire chez *Nemastoma* cf. *sillii* Herman (Opiliones, Nemastomatidae). Pp. 269–303. *In* Livre de Cinquantenaire de l'Institut de Spéologie "Emile Racovitza". (T. Orghidan, ed.). Academia Republicii Socialiste Romania, Bucharest.

Buzatto, B.A., J.L. Tomkins, L.W. Simmons & G. Machado. 2014. Correlated evolution of sexual dimorphism and male dimorphism in a clade of neotropical harvestmen. Evolution 68:1671–1686.

DaSilva, M.B. & P. Gnaspini. 2009. A systematic revision of Goniosomatinae (Arachnida: Opiliones: Gonyleptidae), with a cladistic analysis and biogeographical notes. Invertebrate Systematics 23:530–624.

Fernandes, N.S. & R.H. Willemart. 2014. Neotropical harvestmen (Arachnida, Opiliones) use sexually dimorphic glands to spread chemicals in the environment. Comptes Rendus Biologies 337:269–275.

Fowler-Finn, K.D., E. Triana & O.G. Miller. 2014. Mating in the harvestman *Leiobunum vittatum* (Arachnida: Opilionidae): from premating struggles to solicitous tactile engagement. Behaviour 151:1663–1686.

Gainett, G., P.P. Sharma, R. Pinto-da-Rocha, G. Giribet & R.H. Willemart. 2014. Walk it off: predictive power of appendicular characters toward inference of higher-level relationships in Laniatores (Arachnida: Opiliones). Cladistics 30:120–138.

Gnaspini, P. 1995. Reproduction and postembryonic development of *Goniosoma spelaeum*, a cavernicolous harvestman from southeastern Brazil (Arachnida: Opiliones: Gonyleptidae). Invertebrate Reproduction & Development 28:137–151.

Gnaspini, P. 2007. Development. Pp. 455–472. *In* Harvestmen: The Biology of Opiliones. (R. Pinto-da-Rocha, G. Machado & G. Giribet, eds.). Harvard University Press, Cambridge.

Gnaspini, P. & C.F. Lerche. 2010. Embryonic development of *Ampheres leucopheus* and *Iporangaia pustulosa* (Arachnida: Opiliones: Gonyleptidae). Journal of Experimental Zoology B Molecular and Developmental Evolution 314B:489–502.

Gnaspini, P., M.B. DaSilva & F.C. Pioker. 2004. The occurrence of two adult instars among Grassatores (Arachnida: Opiliones) – A new type of life cycle in arachnids. Invertebrate Reproduction & Development 45:29–39.

Horner, J.R. & M.B. Goodwin. 2009. Extreme cranial ontogeny in the Upper Cretaceous dinosaur *Pachycephalosaurus*. Plos One 4:e7626.

Juberthie, C. 1964. Recherches sur la biologie des opilions. Annales de Spéléologie 19:1–244.

Munguía-Steyer, R., B.A. Buzatto & G. Machado. 2012. Male dimorphism of a neotropical arachnid: harem size, sneaker opportunities, and gonadal investment. Behavioral Ecology 23:827–835.

Muñoz-Cuevas, A. 1971a. Étude du tarse, de l'apotele et de la formation des griffes au cours du développement postembryonnaire chez *Pachylus quinamavidensis* (Arachnida. Opilions, Laniatores). Bulletin du Museum National d'Histoire Naturelle 42:1027–1036.

Muñoz-Cuevas, A. 1971b. Contribution à l'étude du développement postembryonnaire chez *Pachylus quinamavidensis* Muñoz Cuevas (Arachnida. Opilions, Laniatores). Bulletin du Museum National d'Histoire Naturelle 12:629–641.

Pinto-da-Rocha, R., G. Machado & G. Giribet. 2007. Harvestmen: The Biology of Opiliones. Harvard University Press, Cambridge.

Proud, D.N. & B.E. Felgenhauer. 2013. The harvestman tarsus and tarsal flexor system with notes on appendicular sensory structures in Laniatores. Journal of Morphology 274:1216–1229.

Rodriguez, A.L., V.R. Townsend Jr. & D.N. Proud. 2014. Comparative study of the microanatomy of four species of harvestmen (Opiliones, Eupnoi). Annals of the Entomological Society of America 107:496–509.

Teng, B., S. Dao, Z.R. Donaldson & G.F. Grether. 2012. New communal roosting tradition established through experimental translocation in a Neotropical harvestman. Animal Behaviour 84:1183–1190.

Townsend Jr., V.R., N.J. Rana, D.N. Proud, M.K. Moore, P. Rock & B.E. Felgenhauer. 2009. Morphological changes during postembryonic development in two species of Neotropical harvestmen (Opiliones, Laniatores, Cranaidae). Journal of Morphology 270:1055–1068.

Willemart, R.H. & G. Giribet. 2010. A scanning electron microscopic survey of the cuticle in Cyphophthalmi (Arachnida, Opiliones) with the description of novel sensory and glandular structures. Zoomorphology 129:175–183.

Willemart, R.H. & P. Gnaspini. 2003. Comparative density of hair sensilla on the legs of cavernicolous and epigean harvestmen (Arachnida, Opiliones). Zoologischer Anzeiger 242:353–365.

Willemart, R.H. & P. Gnaspini. 2004a. Breeding biology of the cavernicolous harvestman *Goniosoma albiscriptum* (Arachnida, Opiliones, Laniatores): sites of oviposition, egg batches characteristics and subsocial behaviour. Invertebrate Reproduction & Development 45:15–28.

Willemart, R.H. & P. Gnaspini. 2004b. Spatial distribution, mobility, gregariousness, and defensive behavior in the Brazilian cave harvestman *Goniosoma albiscriptum* (Arachnida, Opiliones, Laniatores). Animal Biology 54:221–235.

Willemart, R.H. & E.A. Hebets. 2011. Sexual differences in the behavior of the harvestman *Leiobunum vittatum* (Opiliones, Sclerosomatidae) towards conspecific cues. Journal of Insect Behavior 25:12–23.

Willemart, R.H., M.C. Chelini, R. Andrade & P. Gnaspini. 2007. An ethological approach to a SEM survey on sensory structures and tegumental gland openings of two neotropical harvestmen (Arachnida. Opiliones). Italian Journal of Zoology 74:39–54.

Willemart, R.H., J.P. Farine & P. Gnaspini. 2009. Sensory biology of Phalangida harvestmen (Arachnida, Opiliones): a review, with new morphological data on 18 species. Acta Zoologica 90:209–227.

Willemart, R.H., J.P. Farine, A.V. Peretti & P. Gnaspini. 2006. Behavioral roles of the sexually dimorphic structures in the male harvestman, *Phalangium opilio* (Opiliones, Phalangiidae). Canadian Journal of Zoology 84:1763–1744.

Willemart, R.H., A. Pérez-González, J.P. Farine & P. Gnaspini. 2010. Sexually dimorphic tegumental gland openings in Laniatores (Arachnida, Opiliones), with new data on 23 species. Journal of Morphology 271:641–653.

Wijnhoven, H. 2013. Sensory structures and sexual dimorphism in the harvestman *Dicranopalpus ramosus* (Arachnida: Opiliones). Arachnologische Mitteilungen 46:27–46.

Zatz, C., R.M. Werneck, R. Macías-Ordoñez & G. Machado. 2010. Alternative mating tactics in dimorphic males of the harvestman *Longiperna concolor* (Arachnida: Opiliones). Behavioral Ecology and Sociobiology 65:995–1005.

Manuscript received 1 December 2015, revised 14 June 2016.

Appendix 1.—Measurements (mm) of body length and width and total length of right appendages (L1–L4 = leg I to leg IV), and number of articles in the tarsus of each leg (T1–T4). * indicates a measurement made on a left appendage.

	Body length	Body width	L1	T1	L2	T2	L3	T3	L4	T4
1st nymph	2.28	1.59	7.71	1	19.64	1	11.19	2	16.11	2
	1.88	1.30	8.33	1	22.29	1	12.18	2	18.24	2
	2.15	1.73	8.24	1	21.79	1	13.65	2	18.91	2
	2.47	1.83	8.48	1	23.33	1	13.31	2	19.24	2
	2.35	1.62	8.47	1	23.06	1	13.40	2	19.24	2
	2.12	1.72	8.42	1	22.75	1	13.29	2	19.08	2
	2.27	1.90	8.21	1	22.88	1	13.50	2	19.44	2
	2.33	1.84	8.75	1	22.63	1	13.89	2	19.58	2
2nd nymph	2.19	1.49	10.85	2	26.78	2	16.52	2	23.29	2
	3.07	2.46	10.87	2	27.90	2	16.30	2	23.31	2
	2.77	1.90	10.82	2	28.73	2	17.00	2	24.10	2
	2.9	2.06	10.60	2	28.47	2	17.34	2	24.54	2
	3.12	2.49	10.78	2	28.34	2	17.60	2	25.26	2
3rd nymph	3.45	2.99	13.12	2	34.02	2	21.20	2	28.36	2
	2.89	2.42	13.12	2	35.24	2	20.72	2	30.14	2
	3.3	2.42	14.26	2	35.00	2	22.28*	2	30.35	2
	3.71	3.16	13.82	2	36.44	2	21.44	2	31.08	2
	3.02	2.49	14.07	2	36.01*	2	22.09	2	31.28*	2
	3.63	3.31	14.21	2	36.55	2	22.24	2	31.32	2
	3.67	2.99	14.04	2	37.06	2	23.43	2	31.40	2
	3.6	3.09	14.56	2	36.55	2	22.02	2	31.70	2
	3.47	3.09	14.49	2	39.45	2	24.66	2	32.84	2
	3.42	3.01	14.73	2	38.19	2	22.80	2	32.89	2
	3.47	2.94	14.41	2	37.64	2	23.62	2	33.00	2
4th nymph	4.08	3.79	17.13	2	43.70	2	26.42	2	38.46	2
	4.21	4.26	18.26	2	45.06	2	27.76	2	38.71	2
	3.83	3.53	18.01	2	44.66	2	29.00	2	39.28	2
	3.95	3.59	18.12	2	44.59	2	28.19	2	39.75	2
	4.27	4.00	18.34	2	45.51	2	29.29	2	39.76	2
	4.54	4.11	19.03	2	43.90	2	29.66	2	40.44	2
	4.13	3.60	19.02	2	46.43	2	30.32	2	40.47	2
	4.22	4.10	18.87	2	46.43	2	29.70	2	40.54	2
	4.16	3.84	19.21	2	48.45	2	30.15	2	40.59	2
	3.77	4.16	19.00	2	46.64	2	29.86	2	40.91	2
	4.3	4.24	19.55	2	46.91	2	30.20	2	41.24	2
	4.66	3.84	18.49	2	46.85	2	29.89	2	41.56	2
	3.81	3.73	19.35	2	47.94	2	30.90	2	42.39	2
	4.34	4.21	18.84	2	47.66	2	30.13	2	42.43	2
5th nymph female	5.69	5.31	23.98	2	57.32	2	38.33	3	51.42	3
	5.23	5.36	23.74	2	58.26	2	38.76	3	52.19	3
5th nymph male	5.21	5.04	24.36	2	58.70	2	39.18	3	51.98	3
Adult female	7.2	8.03	30.20	11	73.43	26	50.09	12	67.84	14
	7.87	7.91	36.53	9	84.08	20	58.65	11	79.77	14
Adult male	6.55	6.72	31.36	12	77.94	27	50.25	13	68.22	14
	6.86	7.04	31.89	11	75.97	20	51.26	11	68.50	13
	6.53	6.14	30.69	11	76.35	26	49.73	11	68.57	13
	6.67	6.32	31.69	12	-	-	49.84	14	69.08	15
	6.66	6.90	32.35	12	76.98	22	50.44	11	69.95	15
	6.62	6.66	31.66	11	76.30	24	51.33	12	70.29	15
	7.34	7.35	32.60	10*	79.17	25	53.89	12	72.34	15
	7.64	7.74	31.97	10	79.97	26	54.04	13	73.60	15
	7.68	7.69	33.18	11	80.58	25	54.21	13	74.02	15
	7.89	8.53	32.55	10	81.81	26	55.16	12	75.11	15
	7.93	7.98	33.17	11	82.08	21	52.28	10	75.17	15
	7.67	7.92	34.55	12	83.19	25	55.94	12	75.26	15
	7.79	8.24	34.50	11	83.13	25	56.68	12	76.40	14

2016. Journal of Arachnology 44:347–358

Aerial dispersal activity of spiders sampled from farmland in southern England

Christopher Woolley[1,2], **C. F. George Thomas**[2], **Rod P. Blackshaw**[2] and **Sara L. Goodacre**[3]: [1]Evolutionary Studies Institute, University of the Witwatersrand, Johannesburg, Gauteng, Wits 2050, South Africa. Email: christopher.woolley@wits.ac.za; [2]School of Biological Sciences, Portland Square, Plymouth University, Drake Circus, Plymouth, Devon, PL4 8AA, UK; [3]School of Life Sciences, University of Nottingham, University Park, Nottingham, NG7 2RD, UK

Abstract. Spiders can suppress populations of some important crop pests. Although dispersal is essential to their survival in the disturbed farmland environment, accounts of their dispersal activity over several seasons are few. Spiders dispersing across a landscape of mixed farmland were sampled over an 18-month period using Stick, Net and Bottle traps (SNB traps). Traps were located in a two year old grass ley where ground densities of spiders and wind speed data were also recorded. SNB traps were effective at sampling large numbers of dispersers; Linyphiidae were the most abundant family sampled (93%). Numbers of adult linyphiids dispersing were found to increase in autumn and winter with dispersal activity occurring frequently throughout the study period. Dispersal patterns were similar for congeners (*Erigone* spp., *Oedothorax* spp.) although differences were evident between common agrobiont species. Weather conditions associated with stable high-pressure systems appeared important for stimulating mass dispersal in *Oedothorax* Bertkau, 1883 species. *Erigone atra* Blackwall, 1833 dispersed more frequently and under more variable conditions. Winter and spring dispersal was low for adult *Tenuiphantes tenuis* (Blackwall, 1852) and *Bathyphantes gracilis* (Blackwall, 1841) compared to common erigonids. Ground populations correlated positively with dispersing spiders for some species indicating that dispersal activity was in part a function of population size. For *Oedothorax fuscus* (Blackwall, 1834) it is suggested that life history traits and weather conditions may interact to influence the sex ratio of dispersers over time.

Keywords: Linyphiidae, ballooning, *Erigone*, *Oedothorax*, *Tenuiphantes*

In the British Isles, only a few species of spider typically complete their life-cycles within the open field environment. Linyphiids (sheet weavers, money or dwarf spiders) account for the majority of these, possessing traits particularly suited to the repeated disturbance brought about by modern farmland management. Rapid development in warmer seasons and the potential to increase the number of generations in favourable years (De Keer & Maelfait 1987a; Thorbek et al. 2003) enable agrobiont linyphiids to achieve high densities in crops (Topping & Sunderland 1994), increasing their potential as useful predators of pest species (Nyffeler & Sunderland 2003). Field conditions vary temporally and spatially over the agricultural landscape, and aerial dispersal using silk (termed 'ballooning') enables spiders to disperse repeatedly over landscape-scale distances to exploit resources and escape hazards (Thomas & Jepson 1999).

To disperse by ballooning, a spider releases silk from the spinnerets into moving air. The silk affects a frictional drag which, in exceeding the gravitational pull on the spider, enables it to become airborne. The spider gains height when the upwards vertical movement of the air exceeds the terminal velocity of the spider (Suter 1991). Ballooning occurs at wind speeds below 3 m s^{-1} (Vugts & Van Wingerden 1976). Low wind speeds, together with non-ideal convection, are thought to represent conditions where a balance between convective and lateral air movement exists such that a spider's gain in height is more effectively translated into distance travelled from the take-off point (Reynolds et al. 2007). Spiders can potentially balloon over large distances. Modelling has indicated that given suitable weather conditions a spider can travel 30 km in six hours (Thomas & Brain 2003). The probability of travelling such distances is, however, relatively small and most flights are thought to occur near to the ground and cover only a few metres (Thorbek et al. 2002).

The majority of ballooning spiders comprise individuals of small mass which are either immature or adults of small species (e.g., many of the Linyphiidae). Larger individuals are also observed to balloon. While Greenstone et al. (1987) typically recorded ballooning spiders of 0.2–1.0 mg, the largest was 25.5 mg. Sex ratios of linyphiids sampled in studies are inconsistent with reports of male-bias (Thomas & Jepson 1999), female-bias (Duffey 1956) and approximately equal ratios (Greenstone et al. 1987). Factors influencing ballooning frequency and motivation are reviewed by Weyman et al. (2002) and Bell et al. (2005). Some examples include food deprivation (Weyman et al. 1994), changes in habitat quality (Thomas & Jepson 1999), temperatures experienced during development (Bonte et al. 2003), infection by bacterial endosymbionts (Goodacre et al. 2009) and meteorological conditions (Vugts & Van Wingerden 1976).

Differences in life history, behavior, and the means by which species perceive and respond to environmental stimuli may result in specific patterns of dispersal activity. To date, relatively few studies have been carried out in the British Isles where species-specific dispersal activity has been compared over several seasons. The work described here constitutes an 18 month sampling program utilizing a novel and highly effective trapping method (Woolley et al. 2007). Emphasis is placed on the dispersal patterns of common agrobiont linyphiids (e.g., *Erigone* spp., *Oedothorax* spp., *Tenuiphantes tenuis* (Blackwall, 1852) and *Bathyphantes gracilis* (Blackwall, 1841)). The hypotheses the study addresses are: i) whether agrobiont spiders display differential patterns of dispersal; ii) whether the patterns observed are a function of ground population densities; and iii) whether a differential response in

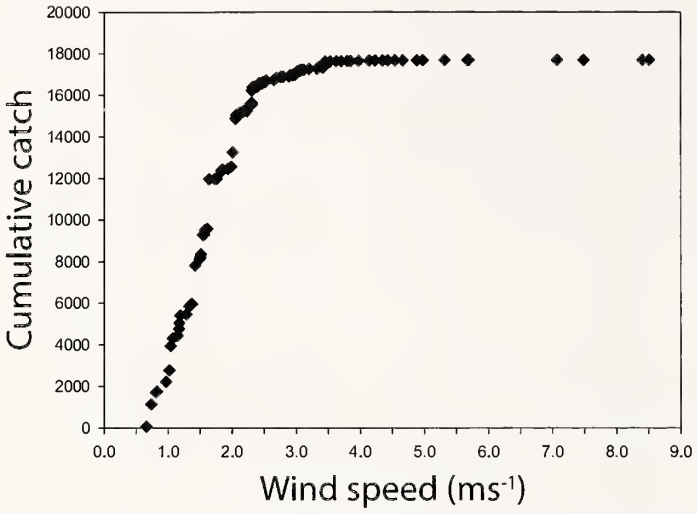

Figure 1.—Relationship between cumulative catch based on catches from single days (averages over several days removed) and the corresponding average wind speed recorded for each single day (between sunrise and sunset).

dispersal activity is observed with respect to meteorological conditions. Results are also discussed in relation to life histories, sex ratios and sampling performance.

METHODS

The work was conducted on the estate farm of the former Seale-Hayne Faculty of Agriculture, Food and Land Use, Plymouth University, now owned by the Dame Hannah Rodgers Trust. The farm is located near the market town of Newton Abbot, Devon, in the southwestern peninsula of the British Isles. This is the most rural region of England with approximately 80% of land in agricultural use (Ministry of Agriculture, Fisheries and Food 2000). At the time of sampling, fields were either in fodder crops (wheat, barley and maize) or grass leys.

Dispersing spiders were sampled from an 8-hectare, 2-year-old grass ley (50.544458°N 3.662869°W) between September 2003 and February 2005. The sampling method using 'climbing-stick traps with integral nets' (referred to here as Stick, Net and Bottle traps or SNB traps), works by intercepting dispersing spiders which are then trapped in an apical collecting vessel as they climb to re-attempt ballooning. The effective interception height of the traps is from ground level to approximately 1.3 m. A validation of this method is described in Woolley et al. (2007). Ten SNB traps were set at 10 m intervals in a straight line transect running north to south. The transect was protected by an electric fence to prevent disturbance by livestock. The ungrazed area within was managed by occasional trimming. Operations in the field included a silage harvest in May followed by periodic grazing by cattle and sheep. Grazing intensity was typically low with adjoining fields being accessible to livestock.

Over the 18-month sampling period, SNB traps were emptied daily from Monday to Friday at approximately 18:00; extracted spiders were preserved in ethanol. Traps were kept open over the duration of the weekend and for longer periods when daily collections were not possible. Samples of spiders taken over two or more days were divided by the number of days in order to give an average daily catch for that period. Ground populations were sampled monthly between February and November 2004 using a modified garden vacuum suction sampler (Flymo BVL-320, Husqvarna). Each sample consisted of 54 random placements of a 0.1 m^2 quadrat within the grass ley, this number being based on moving averages calculated prior to the study.

Owing to the large numbers of dispersing spiders caught, SNB samples identified were limited to weeks in which ground sampling also occurred. The number of SNB samples identified per month varied in accordance with the number of ground population samples which were timed to coincide with field operations. Altogether SNB samples from 22 sampling periods were identified, each representing a period of daily catches averaging 8.59 days (± 0.98). The interval between sampling periods averaged 15.14 days (± 3.14) with the maximum interval being 27 days. As the sampling period for dispersing spiders exceeded that for ground populations, the first week in the month of SNB trap samples was chosen where a corresponding ground population sample wasn't available. Over the 18-month study, the 22 sampling periods comprised 149 collections of the traps from the field. Of these, 113 represented single days, 32 were 2-day periods (mostly weekends), 3 were 3-day periods and 1 was a 4-day period. The number of days in the 22 sampling periods was 190 representing approximately one third of the total number of days sampled during the study.

All adult spiders were identified to species. Immature spiders were identified where possible to family with lycosid and thomisid immatures being distinctive. Immatures of other families such as theridiids and araneids were only distinguished when diagnostic features could be easily discerned, usually at a late developmental or sub-adult stage.

Wind speed data were recorded at a height of five metres using an A100R reed switch anemometer (Vector Instruments, Denbighshire) sited in the same field as the traps and connected to a DL2e data logger (Delta-T, Cambridge).

To assess whether numbers of dispersing adult spiders are a function of changes in the ground population, the influence of daily variation in wind speed was minimized by only considering days with similar average wind speeds. Days or periods with an average wind speed above the median value of 2.36 m s^{-1} were discarded because this approximated to the point on the accumulation curve (Fig. 1) where a clear change in the accumulation rate was evident. For linyphiid species (males, females and the eombined total), correlations (Pearson product moment) were performed on total numbers sampled per month in ground samples (or the average where more than one sample was taken per month) and the daily average caught in SNB traps for the corresponding months. A log (n+1) transformation was applied prior to performing correlations to reduce the negative influence of high counts on the linearity of the data.

RESULTS

Of the SNB samples identified, a total of 22,719 spiders were collected over an 18-month period between September 2003 and February 2005. From suction samples a total of 2930 spiders were collected between February 2004 and November

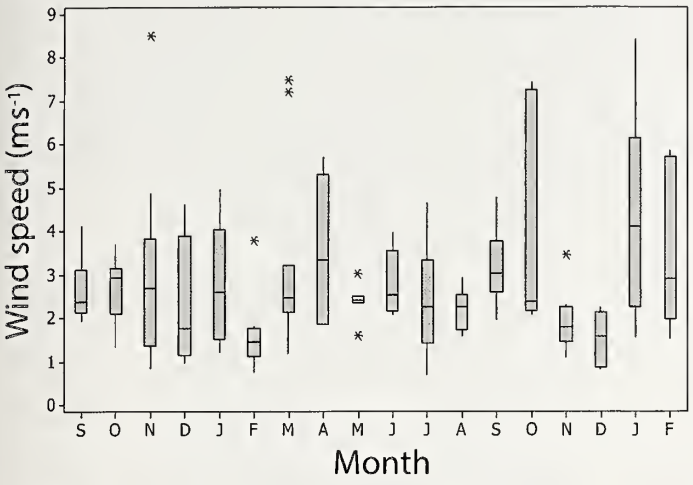

Figure 2.— Box plot of wind speeds for the subset of samples selected each month between September 2003 and February 2005. The box represents the interquartile range (the middle 50% of the data); horizontal bar is the median. Upper and lower whiskers represent the upper 25% and lower 25% of the distribution respectively. Asterisks represent outliers.

2004. The SNB samples comprised 38 species of linyphiids and 24 species from nine other families excluding lycosids which were not identified to species (Table 1, where taxonomic citations are also given). From ground samples, 19 species of linyphiids were identified as were five species from four other families. The most abundant disperser was *Oedothorax fuscus* (N = 6732) followed by *Erigone atra* (N = 4502). The most frequent disperser was *E. atra* (found in 111 of the 149 samples) followed by *O. fuscus* (N = 86), although immature linyphiids were as a group more frequent (N = 88). The most abundant non-linyphiid in the traps was the theridiid *Robertus arundineti* (N = 450) followed by the tetragnathid *Pachygnatha degeeri* (N = 351). *Robertus arundineti* was also the most frequent non-linyphiid disperser (N = 58) and thomisids, comprising immature *Xysticus cristatus*, were the second most frequent (N = 43). Spiders were found in traps in 140 of the 149 samples which represented a maximum of 180 of the 190 days when dispersal activity could have occurred. Of the samples representing single days, dispersal activity was recorded from 104 of the 112 days.

Wind speed and dispersal activity.—The number of dispersing spiders sampled became increasingly limited between wind speeds of 2 and 3 m s^{-1} (Fig. 1), accounting for a progressively smaller increment of the cumulative catch. Using the median wind speed of sample days (2.36 m s^{-1}) as a reference, the average catch of spiders per day below the median was 293. Above the median, the average catch decreased to 20 spiders per day. Median wind speeds (Fig. 2) relative to the samples selected each month showed no obvious seasonality although differences between the 1st and 3rd quartiles tended to be smaller during the summer months. Relatively low median wind speeds were recorded in the months of February, November and December, 2004.

Oedothorax fuscus.—*Oedothorax fuscus* (Fig. 3a, b) was the most abundant species in ground and SNB samples. Large peaks in female dispersal activity occurred in February/March and in November/December of 2004. Lower numbers of dispersing males were sampled compared to females. During the autumn/winter period of 2003/04, the dispersal periods of males and females were noticeably separated with males dispersing earlier in October/November 2003. For females, dispersal peaks corresponded to higher ground densities while generally lower densities were recorded during summer for both sexes.

Oedothorax retusus.—The dispersal of female *Oedothorax retusus* (Fig. 3c, d) was similar to that of *O. fuscus* with peaks in February/March 2004 and November/December 2004 although ground densities were far lower. Compared to *O. fuscus*, no distinct dispersal peak was evident for males in 2003 and, therefore, differences in the timing of dispersal between sexes were not apparent. Changes in ground densities were broadly comparable to *O. fuscus* although numbers remained low until the end of ground sampling in November.

Erigone atra.—In contrast to *O. fuscus* females, the dispersal of *E. atra* males and females (Fig. 3e, f) followed a similar pattern in both autumn/winter periods. *Erigone atra* was the most frequent disperser of all the species sampled and both males and females displayed a rather prolonged period of relatively higher dispersal throughout autumn/winter with smaller numbers dispersing during spring/summer. Changes in ground density were similar to those observed for *Oedothorax* spp., although a brief increase was observed for females in April.

Erigone dentipalpis.—A similar dispersal pattern to *E. atra* was observed for male and female *Erigone dentipalpis* (Fig. 3g, h) with a relatively prolonged period of higher dispersal in autumn/winter and lower but frequent dispersal during spring/summer. Changes in ground densities of females were similar to those of *E. atra* females. An increase in density was observed for *E. dentipalpis* males in April.

Collinsia inerrans.—Dispersal occurred between November and March with a distinct but shorter period of lower activity in May/June (Fig. 4a, b). Peaks in dispersal activity were similar to those of female *Oedothorax* spp. Males and females displayed very similar dispersal patterns in timing and numbers dispersing. Changes in ground densities were similar to those of *O. retusus*.

Savignia frontata.—This species occurred more commonly as a disperser than in ground samples (Fig. 4c, d). Numbers in SNB traps increased in autumn/winter of both years although dispersal activity took place earlier compared to other erigonids (e.g., *Erigone* spp., *Oedothorax* spp.) with little activity beyond January.

Tenuiphantes tenuis.—The dispersal of male and female *T. tenuis* (Fig. 4e, f) peaked in the autumn of both years and corresponded closely in timing. Between February and May, males and females were absent from SNB traps although low numbers were caught frequently from May onwards. In contrast to the erigonids, low ground densities were recorded in February and these generally persisted until the peak observed in July/August. This peak was not reflected in the SNB traps where numbers remained low. Ground densities declined in August/September with only small numbers recorded in samples thereafter.

Bathyphantes gracilis.—The pattern of dispersal of *B. gracilis* males and females (Fig. 4g, h) were similar to that of *T. tenuis* with peak dispersal occurring in autumn/winter and a

Table 1.—List of species, number collected and months recorded by SNB traps (Linyphiidae and other families). *Species that were collected during testing phase of SNB traps.

family	species	males	females	imm.	total	months recorded											
						J	F	M	A	M	J	J	A	S	O	N	D
Linyphiidae	*Bathyphantes gracilis* (Blackwall 1841)	632	900		1532	•	•	•	•	•	•	•	•	•	•	•	•
	Centromerita bicolor (Blackwall 1833)	9	8		17										•	•	
	Centromerita concinna (Thorell 1875)	13	26		39									•	•	•	•
	Centromerus dilutus (O. P.-Cambridge 1875)		1		1												•
	Cnephalocotes obscurus (Blackwall 1834)	1			1		•										
	Collinsia inerrans (O. P.-Cambridge 1885)	1735	2016		3751	•	•	•	•	•	•	•	•		•	•	•
	Dicymbium nigrum (Blackwall 1834)		1		1							•					
	Diplostyla concolor (Wider 1834)	1	7		8	•										•	•
	Erigone atra Blackwall 1833	2594	1908		4502	•	•	•	•	•	•	•	•	•	•	•	•
	Erigone dentipalpis (Wider 1834)	507	390		897	•	•	•	•	•	•	•	•	•	•	•	•
	Erigone promiscua (O. P.-Cambridge 1873)		1		1										•		
	Gongylidiellum vivum (O. P.-Cambridge 1875)	4	3		7		•									•	•
	Hypomma bituberculatum (Wider 1834)	12			12					•	•						
	Lepthyphantes minutus (Blackwall 1833)	1			1												•
	Meioneta rurestris (C.L. Koch, 1836)	23	24		47	•	•	•	•	•	•	•	•	•	•	•	•
	Micrargus subequalis (Westring 1851)	5	1		6					•	•						
	Microctenonyx subitaneus (O. P.-Cambridge 1875)	1			1											•	
	Microlinyphia pusilla (Sundevall 1830)	1			1									•			
	Mioxena blanda (Simon 1884)		9		9	•	•									•	
	Monocephalus castaneipes (Simon 1884)	1	1		2	•											•
	Monocephalus fuscipes (Blackwall 1836)		1		1					•							
	Neriene clathrata (Sundevall 1830)	2	2		4											•	
	Oedothorax fuscus (Blackwall 1834)	713	6019		6732	•	•		•	•	•	•			•	•	•
	Oedothorax retusus (Westring 1851)	226	221		447	•	•	•	•	•	•	•	•		•	•	•
	Ostearius melanopygius (O. P.-Cambridge 1879)		3		3				•						•		
	Palliduphantes ericaeus (Blackwall 1853)	4			4		•									•	
	Pelecopsis parallela (Wider 1834)	23	56		79	•	•	•							•	•	•
	Porhomma pygmaeum (Blackwall 1834)	2			2	•									•		
	Porrhomma microphthalmum (O. P.-Cambridge 1871)	10	33		43	•		•		•	•				•	•	•
	Savignia frontata Blackwall 1833	73	79		152	•	•		•	•		•			•	•	•
	Styloctetor stativus (Simon 1881)		2		2						•						
	Taranucnus setosa (O. P.-Cambridge 1863)		1		1					•							
	Tenuiphantes flavipes (Blackwall 1854)	5	1		6										•	•	
	Tenuiphantes mengei (Kulczyński 1887)		1		1							•					
	Tenuiphantes tenuis (Blackwall 1852)	660	1165		1825	•	•	•		•	•	•	•	•	•	•	•
	Tenuiphantes zimmermanni (Bertkau 1890)		4		4	•										•	
	Walckenaeria antica (Wider 1834)	2	3		5											•	
	Walckenaeria vigilax (Blackwall 1853)	18	26		44		•								•	•	•
Tetragnathidae	*Pachygnatha clercki* Sundevall 1823	3	7		10										•	•	•
	Pachygnatha degeeri Sundevall 1830	141	210	6	357									•	•	•	•
	Tetragnatha obtusa C.L. Koch 1837	1			1				•								
	not identified to species			9	9		•	•							•	•	

Table 1.—Continued.

family	species	males	females	imm.	total	months recorded											
						J	F	M	A	M	J	J	A	S	O	N	D
Araneidae	*Araneus angulatus* Clerck 1757*			1	1	not recorded											
	Larinioides cornutus (Clerck 1757)	2		2	4			•	•		•		•				
	Nuctenea umbractica (Clerck 1757)			1	1									•			
	Zygiella x-notata (Clerck 1757)		1	1	2							•					
	not identified to species			85	85	•	•	•	•	•		•	•	•	•	•	•
Uloboridae	*Hyptiotes paradoxus* (C.L. Koch 1834)*	1			1								•				
Theridiidae	*Auelosinus vittatus* (C.L. Koch 1836)	2			2					•	•						
	Enoplognatha ovata (Clerek 1757)		2		2							•	•				
	Episinus sp.			1	1										•		
	Kochiura aulicus (C.L. Koch 1836)	1			1					•							
	Paidiscura pallens (Blackwall 1834)	6	2		8					•	•	•					
	Parasteatoda simulans (Thorell 1875)	2			2						•						
	Phylloneta sisyphia (Clerck 1757)	1			1						•						
	Robertus arundineti (O. P.-Cambridge 1871)	134	316		450	•	•	•	•	•	•	•			•	•	•
	Robertus neglectus (O. P.-Cambridge 1871)	5	16		21							•	•	•	•	•	•
	Theridion mystaceum C.L. Koch 1870	1			1					•							
	Theridion varians Hahn 1833	1			1						•						
Lycosidae	not identified to species	9		107	116	•	•	•	•	•	•	•	•	•	•	•	•
Pisauridae	*Pisaura mirabilis* (Clerck 1757)			2	2										•	•	
Dictynidae	*Dictyna uncinata* Thorell 1856		1		1						•						
	Nigma puella (Simon 1870)	1			1						•						
Thomisidae	*Xysticus cristatus* (Clerck 1757)	1	3	207	211	•		•		•		•	•	•	•	•	•
Philodromidae	*Philodromus albidus* Kulczyński 1911	3			3						•	•					
	Philodromus collinus C.L. Koch 1835	1			1							•					
Clubionidae	*Clubiona diversa* O. P.-Cambridge 1862		3		3				•			•					
Mimetidae	*Ero cambridgei* Kulczyński 1911	2	2	1	5										•	•	•

near absence of spiders caught in traps between February and May, although low but frequent dispersal was recorded thereafter. An increase in ground densities was observed for males in April and the largest peak for both sexes in July/August corresponded to that observed for *T. tenuis*.

Immature linyphiids.—Immature linyphiids (Fig. 5a) were caught frequently in traps throughout the sampling period but were generally less numerous than adults. Numbers in traps declined from October 2003 to March 2004 before increasing from April to June. The smaller catches that were again recorded from July to October coincided with a large increase in ground densities representing the emergence of the overwintering generation. Dispersal activity increased markedly between November 2004 and January 2005 despite ground densities showing a substantial decline since August.

Adult linyphiids.—The majority of dispersal activity of adult linyphiids occurred during autumn/winter (Fig. 5b). Lower numbers were observed dispersing in spring/summer although frequent dispersal continued. High ground densities over the winter of 2003/2004 reflected the more abundant erigonids although the sharp decline in May/June, possibly due to the grass having been cut for silage, was observed for most species. Ground densities generally increased thereafter although peaks in density were variable and many species, particularly the less abundant *T. tenuis* and *B. gracilis*, declined in density after August/September.

Robertus arundineti.—Dispersal of male and female *R. arundineti* was synchronous and frequent (Fig. 5c, d) starting from November and continuing into spring and early summer although at a lower intensity. No dispersal was evident between late June and late October. Ground densities were low although this species had previously been sampled from several locations on the farm. *Robertus neglectus* was sampled in smaller numbers from July to September.

Pachygnatha degeeri.—Dispersal activity, which appeared to be well defined in both sexes, occurred in late October and November in 2003 and 2004 (Fig. 5e, f). No dispersal was recorded in the intervening period despite relatively high ground densities in winter/spring.

Xysticus cristatus.—Thomisids caught by SNB traps (Fig. 5g) were exclusively immature *X. cristatus*. In both years, they mainly dispersed between September and December with little activity recorded outside this period. Ground samples were small with a few immatures recorded from June to September, mostly before the dispersal period.

Lycosidae.—Immature lycosids far outnumbered adults caught in traps and ground samples (Fig. 5h). April and November/December were the periods of greatest dispersal activity although numbers dispersing in 2003 were comparatively low. Both dispersal peaks in 2004 were preceded by increases in the ground density in March, and June to August respectively. The highest proportion of adults in ground

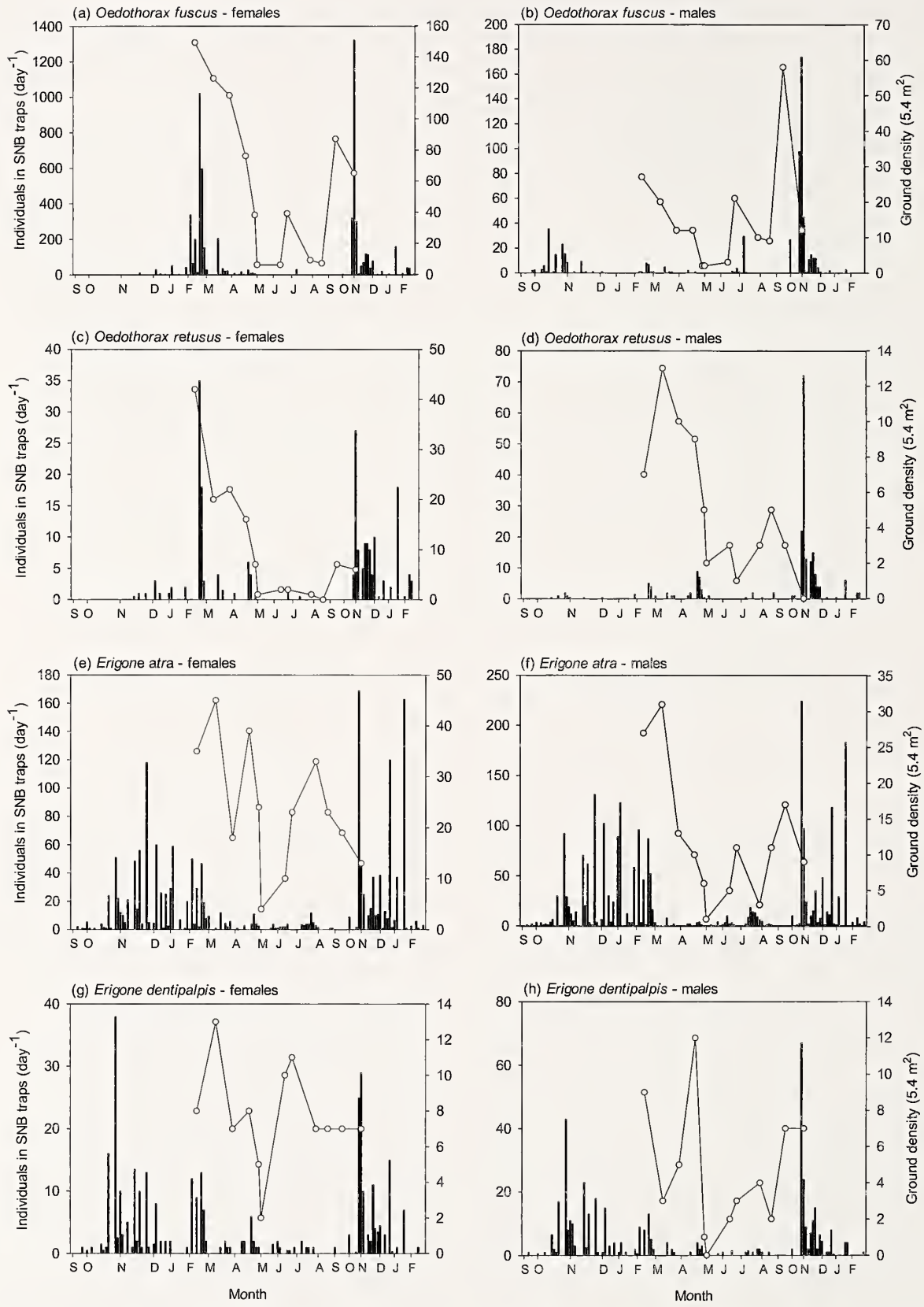

Figure 3.—Barplots of daily catches from SNB traps of females and males of *O. fuscus* (a,b), *O. retusus* (c,d), *E. atra* (e,f), and *E. dentipalpis* (g,h) over 18 months. Sample days vary per month according to the number of corresponding suction samples. Ground densities (line) were sampled over 10 months.

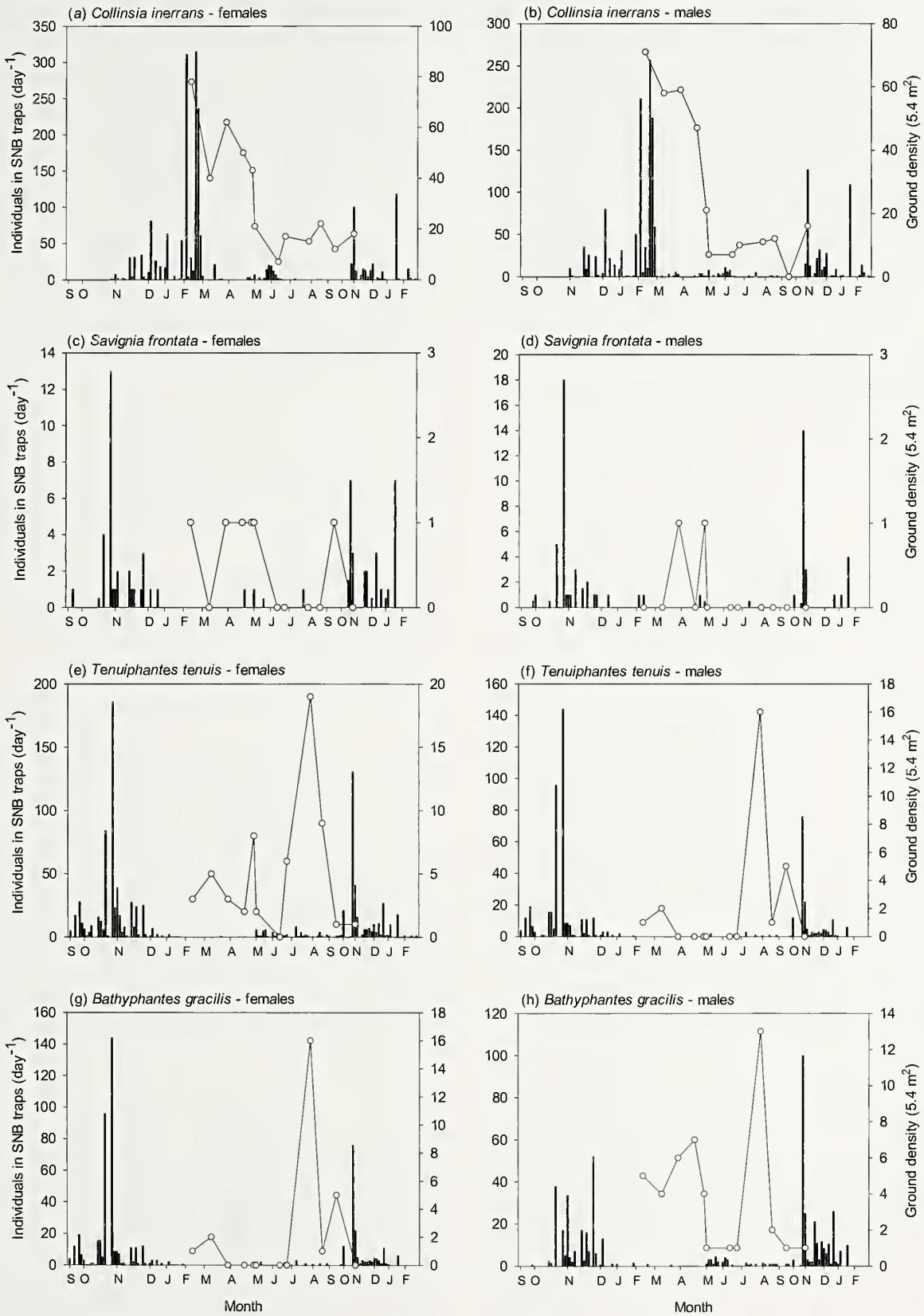

Figure 4.—Barplots of daily catches from SNB traps of females and males of *C. inerrans* (a,b), *S. frontata* (c,d), *T. tenuis* (e,f) and *B. gracilis* (g,h) over 18 months. Sample days vary per month according to the number of corresponding suction samples. Ground densities (line) were sampled over 10 months.

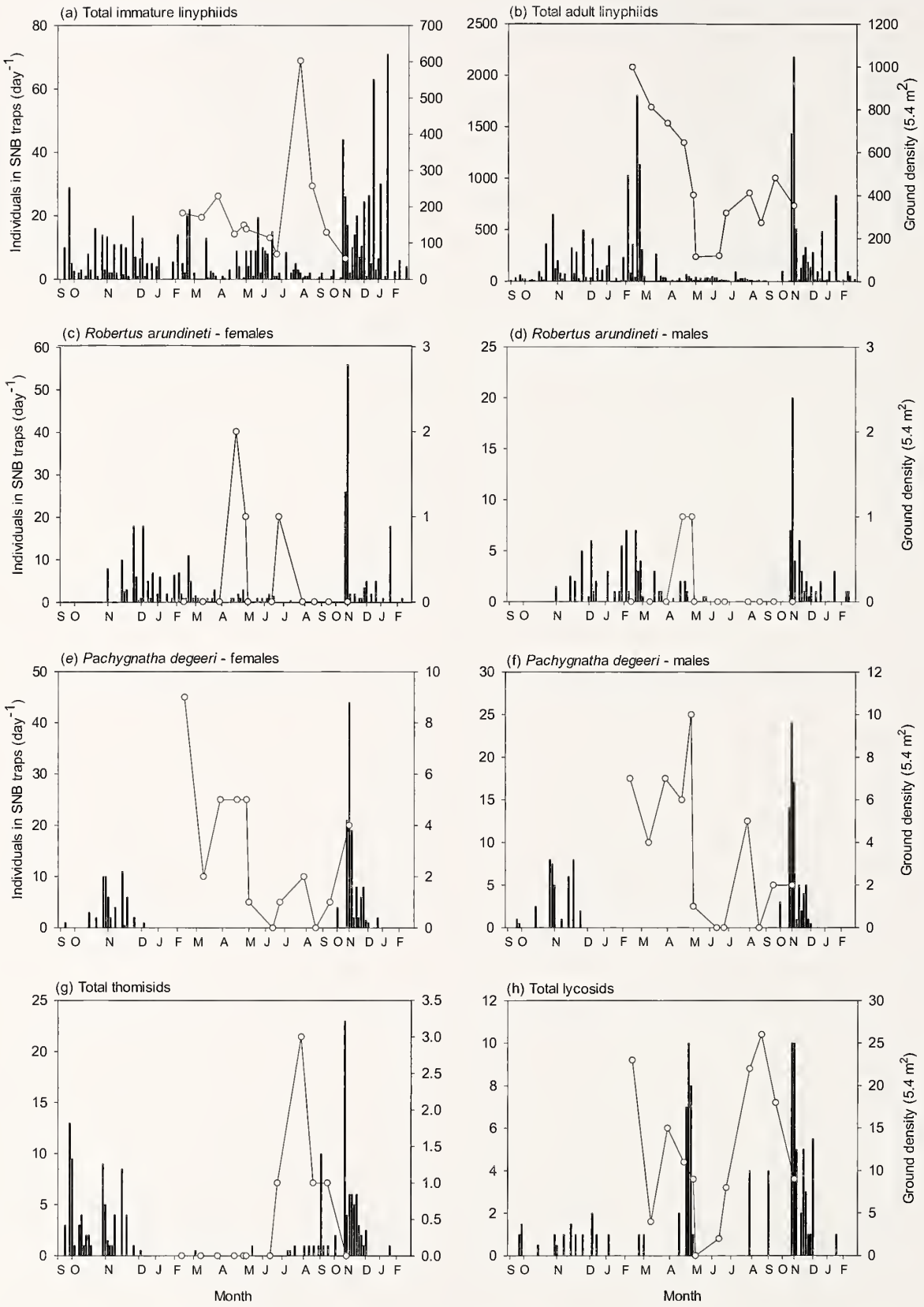

Figure 5.—Barplots of daily catches from SNB traps of total immature linyphiids (a), total adult linyphiids (b), females and males of *P. degeeri* (c,d) and *R. arundineti* (e,f) and total thomisids (g) and lycosids (h) over 18 months. Sample days vary per month according to the number of corresponding suction samples. Ground densities (line) were sampled over 10 months.

Table 2.—Total numbers of males and females sampled by SNB traps and suction samples, and corresponding ratios of males to females.

	SNB traps			Suction samples		
species	males	females	ratio	males	females	ratio
Bathyphantes gracilis	632	900	0.70	79	125	0.63
Collinsia inerrans	1735	2016	0.86	319	385	0.83
Erigone atra	2594	1908	1.36	144	286	0.50
Erigone dentipalpis	507	390	1.30	55	92	0.60
Oedothorax fuscus	713	6019	0.12	188	723	0.26
Oedothorax retusus	226	221	1.02	61	126	0.48
Pachygnatha degeeri	141	210	0.67	44	35	1.26
Robertus arundineti	134	316	0.42	4	6	0.67
Savignia frontata	73	79	0.92	2	6	0.33
Tenuiphantes tenuis	660	1165	0.57	25	59	0.42

samples was recorded during the first peak in March with the later peak comprising mostly immatures. The highest proportion of adults dispersing was during the later dispersal period in November/December. Samples may have included several species as adults and immatures were not specifically identified.

Correlations between dispersers and ground populations.—Significant positive correlations were observed in three species; *O. fuscus* females ($r = 0.881$, $P = 0.004$) and total numbers ($r = 0.901$, $P = 0.002$), *O. retusus* females ($r = 0.719$, $P = 0.045$) and *E. dentipalpis* males ($r = 0.786$, $P = 0.021$). A significant negative correlation was observed for *B. gracilis* males ($r = -0.732$, $P = 0.039$).

Sex ratios of dispersers and ground populations.—Ground populations of all frequently sampled species were strongly dominated by females apart from *P. degeeri* and *C. inerrans* for which numbers of both sexes were comparable (Table 2). For most species, female dominance was reflected in SNB samples with the exception of *E. atra*, *E. dentipalpis* and *O. retusus* where male dispersers were more numerous. Sex ratios of the *Erigone* spp. were very similar in both SNB and ground samples. *Oedothorax* spp. were in contrast dissimilar with *O. retusus* having relatively more dispersing males. *Oedothorax fuscus* numbers were heavily dominated by females in both ground and SNB samples. Females of *B. gracilis* and *T. tenuis* also dominated in both samples but to a lesser degree.

DISCUSSION

Adult agrobiont linyphiids sampled by SNB traps were found to disperse in greatest numbers in autumn and winter. These results agree with accounts from northern temperate regions that periods of more intense dispersal activity tend to occur during colder months (Bristowe 1929; Duffey 1956, 1998; Parker 1974; Sunderland & Dalingwater 1986; Bennett 2003). There were positive correlations between dispersal activity and ground populations for *O. fuscus* females (the most abundant species found in the grass ley), *O. retusus* females, and males of *E. dentipalpis*. While this is a small proportion, it does partially support the findings of Weyman et al. (1995) that dispersal activity in *E. atra* reflected changes in the ground population rather than seasonal variation in motivation. Populations increasing in late summer and autumn (Duffey 1998) may then broadly enhance numbers dispersing in colder months. However, for most species, no positive correlations were found. While this may suggest that population size was less influential, the relative height of the traps, the integral net (equivalent to 2.24 m^2 for ten traps) and the number of SNB traps deployed may have increased the interception of dispersing spiders from outside the field compared to the deposition (water tray) traps used by Weyman et al. (1995). SNB traps may then have had limited accuracy in determining the relationship between dispersal activity and local ground density.

Immature linyphiids exhibited less seasonal variation in dispersal activity than adults. Peaks in ground density, representing emergence of summer and over-wintering generations, were not reflected in increased numbers found in SNB traps. By sampling grass and cereal fields using deposition traps, Thomas & Jepson (1999) collected large numbers of dispersing immatures in August. This peak corresponds to the August ground density peak observed in this study and suggests that early instar spiders may be under-represented possibly because very small spiders were able to disperse without climbing to the height of the traps (1.3 m).

Erigone atra was found to disperse more frequently than *O. fuscus*, (111 versus 86 days) supporting findings from previous studies (Weyman et al. 2002). In respect to the proportion of spiders dispersing during certain periods, dispersal patterns of *E. atra* and *O. fuscus* appeared similar to their congeners, *E. dentipalpis* and *O. retusus*. Although ground densities differed considerably between congeners, they were comparable between *E. dentipalpis* and *O. retusus*, with a similar difference in dispersal frequency (82 versus 54 days). To this extent, the deterministic processes governing initiation of dispersal may then be common for closely related species. However, ballooning motivation in *E. atra* has been shown to be a highly individual-specific behavior (Bonte et al. 2009). Higher dispersal frequency may then only be exhibited by a proportion of the *Erigone* population. The impetus for dispersal in these spiders may be the result of positive stimulation by shorter periods of light wind conditions which *Oedothorax* spp. do not typically exploit. The normal diurnal cycle of wind speed at low levels frequently produces a short-lived wind speed minimum in the early morning (Brunt 2002) which may provide a suitable stimulus for dispersal in *Erigone* species. *Oedothorax* spp. may instead respond to longer periods of settled weather and low wind speeds such as those brought about by slow moving, anticyclonic weather systems in autumn and winter. In this study, a particularly strong dispersal response was observed for the more abundant *Oedothorax* females in February 2003 and November/December 2004 when these conditions prevailed and relatively low wind speeds were recorded. In contrast, relatively little activity was observed during periods of more unsettled weather. This difference in dispersal frequency between *Oedothorax* spp. and *Erigone* spp. supports life history strategies outlined by Thorbek et al. (2004); *E. atra* spreads risks to progeny by producing a large number of egg sacs with a small clutch size, which are oviposited across a wide area by frequent dispersal, thereby minimizing the probability that all egg sacs will succumb to local disturbance or parasitism. In contrast *Oedothorax* spp. produce a smaller number of egg sacs with

a larger clutch size which, because of less frequent dispersal, are oviposited more locally. However unlike *E. atra*, *Oedothorax* spp. invest time in protecting individual egg sacs by egg guarding thus reducing the risk of parasitism to all clutches (Baarlen et al. 1994).

The dispersal patterns of two common agrobiont spiders, *T. tenuis* and *B. gracilis*, were similar in respect to the near absence of adult dispersal between February and May. Relatively small numbers were recorded dispersing thereafter until November. The lack of dispersal activity in *T. tenuis* corresponds with very low ground densities of adults recorded by Topping & Sunderland (1998) prior to May in winter wheat and may be due to the low dispersal activity of adults in spring. Indeed, it may be that autumn and early winter dispersal of *T. tenuis* is largely 'one way', with only their offspring entering into crops the following year. *Bathyphantes gracilis* is also known to be a late colonizer of winter wheat indicating that the first generation of this species may remain in permanent habitats (Thorbek et al. 2004). The peak dispersal activity of *B. gracilis* and *T. tenuis* in November/December 2004 was consistent with low wind speeds recorded during this period. However, in the previous year peak dispersal occurred earlier in October/November when wind speeds were relatively higher. The cause of this is unknown but poor habitat quality in relation to the very dry conditions in 2003 may be of significance. Apart from the population peak in July/August, which was observed for both *T. tenuis* and *B. gracilis*, ground densities were not especially high throughout the year compared to the common erigonids. That both species construct relatively large webs (compared with *Erigone* spp.), supported by surrounding vegetation (Sunderland et al. 1986), may suggest that the partially disturbed, grazed ley was not a preferred habitat particularly for the larger *T. tenuis*.

Linyphiids accounted for the vast majority of dispersing spiders identified, with other families making up 7% of the total. The most abundant of the non-linyphiid speeies, the theridiid *R. arundineti*, appears to be a common but transient species with higher numbers dispersing than in ground samples. Locket & Millidge (1953) describe *R. arundineti* as a 'rare' spider frequenting "heather and grass on open moor and mountain sides". The proximity of Dartmoor, an upland moor area to the west, and lowland heaths to the north, could account for a local abundance of this species, however, Samu & Szinetar (2002) found *R. arundineti* frequently in arable situations suggesting that farmland in other localities may support higher ground densities.

The dispersal pattern observed for the tetragnathid, *P. degeeri*, is notable in that it is consistent for both years, occurring in late October and November. That almost all dispersers sampled were adults is unusual in that most documented dispersal in spiders usually occurs as immatures, or in both the immature and adult stages (Bell et al. 2005). From the development times given by Alderweireldt & De Keer (1990), much of the later brood whose egg sacs were laid in July, may be expected to have already reached maturity and, therefore, the final molt is probably not a stimulus for dispersal. The specificity of the dispersal period could perhaps point to a precise deterministic cue such as photoperiod. Blandenier et al. (2013) recorded a bimodal pattern for *P. degeeri* with a similarly discrete period of dispersal in October/November but also a dispersal peak in early spring. It may be relevant that this corresponds with the beginning of the reproductive period and increased ground activity (Alderweireldt & De Keer 1990), although relatively high adult ground densities were not synchronous with dispersal activity in this study.

The later dispersal peak in lycosids recorded in November/December 2004 followed the emergence of immatures in June to August and coincided with favourable weather for dispersal. While other species also dispersed during this period, the earlier dispersal peak in late April was restricted to the lycosids. Members of the genus *Pardosa*, account for the commonest and most widely distributed lycosids in the British Isles (Richter 1970) and it is likely these made up the greater part of those sampled. Common species of *Pardosa* are univoltine and typically produce egg sacs in May (Den Hollander 1971). The April dispersal peak would therefore have consisted of immature spiders having overwintered from the previous year. A stimulus for this dispersal could be a decrease in insolation caused by increasing grass height prior to the silage cut in May. This may have reduced the habitat suitability for these ground dwelling spiders, many of which are thermophilic in habit (Büchs 2003). Both lycosids and thomisids dispersed in increased numbers in colder months. Because aerial dispersal in these families occurs more commonly in the immatures, the fact that the majority of spiders overwinter in this stage is likely to have also increased the proportion dispersing.

Whereas ground populations of most linyphiid species were dominated by females, sex ratios of dispersing spiders varied between species. Dispersing *T. tenuis* and *B. gracilis* were found to be predominately female although the proportion of dispersing males was slightly greater compared to ground samples. Topping & Sunderland (1998) and Meijer (1977) also found catches of *T. tenuis* and *B. gracilis* to be female dominated, although unlike the present study, these occurred in proportionally greater numbers compared to ground samples. In this study, very similar sex ratios were observed for both *Erigone* species with ground samples being female dominated and samples of dispersing spiders being male dominated. Overall for *Erigone* spp. there was little consistency in the sex ratios between this and previous studies (Duffey 1956; Meijer 1977; Blandenier & Fürst 1997).

Several studies have documented female biased populations of *O. fuscus* (Meijer 1977; De Keer & Maelfait 1987b; Alderweireldt & De Keer 1988). In this study, ground samples of *O. fuscus* were also heavily female biased (4:1) and this proportion was seen to increase twofold in samples of dispersing spiders (8:1). Why the proportion of dispersing females increased in *O. fuscus* and not in *O. retusus* is partially a result of *O. fuscus* males dispersing earlier than females in 2003. This earlier dispersal appears to be a consequence of mating aetivity which takes place in the autumn (Alderweireldt & De Keer 1988) with most males dying soon after (De Keer & Maelfait 1987a,b). Dispersal activity of males was likely limited by marginal weather conditions whereas female dispersal was delayed until high pressure brought fine weather in February. The high abundance and exclusivity of overwintering females, together

with favourable weather, therefore resulted in far larger numbers of females dispersing compared to males. Sex-specific traits and behavior in response to meteorological conditions arguably then have the potential to skew sex ratios of dispersers recorded in field studies. Female-biased ground populations, and in particular the highly skewed ratio exhibited by *O. fuscus*, could be the result of infection by one or more endosymbiotic bacteria which, through a self-propagating process of 'male killing', are known to produce female-biased sex ratios (Goodacre et al. 2006, Vanthournout et al. 2014). With respect to altering the sex ratio of dispersers, the relationship may however be more complicated in that endosymbiont infection (*Rickettsia*) has been demonstrated to reduce long-distance dispersal tendency in *E. atra* (Goodacre et al. 2009).

A contributing factor to the large number of spiders sampled by SNB traps is that most dispersal is thought to constitute short, low-level flights covering only a few metres (Thorbek et al. 2002; Thomas & Brain 2003). The low interception height of the traps (ground level to approximately 1.3 m) is therefore likely to sample more dispersal activity than traps operating at greater heights (e.g., Rothamsted suction traps). There is also evidence to suggest that spiders disperse closer to ground level in colder months owing to shallow surface-based inversions suppressing lift (Toft 1995), or through spiders being preconditioned to ground-based rappelling instead of ballooning (Bonte et al. 2008). Further work is needed to determine the validity of low level dispersal for agrobiont species.

In summary, colder months, particularly during winter, are often thought of as periods of inactivity and refuge. The prevalence of dispersal during autumn and winter found in this study demonstrates that agrobiont species readily disperse during colder months given favourable conditions.

ACKNOWLEDGEMENTS

This work was funded through BBSRC grants D14032, D20476 and D14036. We would like to thank the technical and farm staff at Seale-Hayne for their assistance.

LITERATURE CITED

Alderweireldt, M. & R. De Keer. 1988. Comparison of the life cycle history of three *Oedothorax*-species (Arancae, Linyphiidae) in relation to laboratory observations. Pp. 169–177. *In* XI. Europäisches Arachnologisches Colloquium. (J. Haupt, ed.). Technische Universität Berlin, Berlin.

Alderweireldt, M. & R. De Keer. 1990. Field and laboratory observations on the life cycle of *Pachygnatha degeeri* Sundevall, 1830 and *Pachygnatha clercki* Sundevall, 1823 (Araneae, Tetragnathidae). Acta Zoologica Fennica 190:35–39.

Baarlen, P.V., K.D. Sunderland & C.J. Topping. 1994. Eggsac parasitism of money spiders (Araneae, Linyphiidae) in cereals, with a simple method for estimating percentage parasitism of *Erigone* spp. eggsacs by Hymenoptera. Journal of Applied Entomology 118:217–223.

Bell, J.R., D.A. Bohan, E.M. Shaw & G.S. Weyman. 2005. Ballooning dispersal using silk: world fauna, phylogenies, genetics and models. Bulletin of Entomological Research 95:69–114.

Bennett, R. 2003. Mass dispersal of erigonine spiders from a clover field in British Columbia, Canada. Newsletter of the British Arachnological Society 97:2–3.

Blandenier, G. & P.-A. Fürst. 1997. Ballooning spiders caught by a suction trap in an agricultural landscape in Switzerland. Pp. 177–186. *In* 17th European Colloquium of Arachnology. (P.A. Selden, ed.). British Arachnology Society, Edinburgh.

Blandenier, G., O.T. Bruggisser, R.P. Rohr & L.-F. Bersier. 2013. Are phenological patterns of ballooning spiders linked to habitat characteristics? Journal of Arachnology 41:126–132.

Bonte, D., I. Deblauwe & J.-P. Maelfait. 2003. Environmental and genetic background of tiptoe-initiating behaviour in the dwarf spider *Erigone atra*. Animal Behaviour 66:169–174.

Bonte, D., N. De Clercq, I. Zwertvaegher & L. Lens. 2009. Repeatability of dispersal behaviour in a common dwarf spider: evidence for different mechanisms behind short- and long-distance dispersal. Ecological Entomology 34:271–276.

Bonte, D., J.M.J. Travis, N. De Clercq, I. Zwertvaegher & L. Lens. 2008. Thermal conditions during juvenile development affect adult dispersal in a spider. Proceedings of the National Academy of Sciences 105:17000–17005.

Bristowe, W.S. 1929. The distribution and dispersal of spiders. Proceedings of the Zoological Society of London 99:633–657.

Brunt, D. 2002. Physical and Dynamical Meteorology. Cambridge University Press, Cambridge.

Büchs, W. 2003. Predators as biocontrol agents of oilseed rape pests. Pp. 279–298. *In* Biocontrol of Oilseed Rape Pests. (D.V. Alford, ed.). Blackwell Science Ltd, Oxford.

De Keer, R. & J.-P. Maelfait. 1987a. Laboratory observations on the development and reproduction of *Oedothorax fuscus* (Blackwall, 1834) (Araneida, Linyphiidae) under different conditions of temperature and food supply. Revue Ecologie & Biologie du Sol (Fr) 24:63–73.

De Keer, R. & J.-P. Maelfait. 1987b. Life history of *Oedothorax fuscus* (Blackwall 1834) (Araneida, Linyphiidae) in a heavily grazed pasture. Revue Ecologie & Biologie du Sol (Fr) 24:171–185.

Den Hollander, J. 1971. Life-history of species of the *Pardosa pullata* group, a study of ten populations in the Netherlands (Araneae, Lycosidae). Tijdschrift voor Entomologie 114:255–281.

Duffey, E. 1956. Aerial dispersal in a known spider population. Journal of Animal Ecology 25:85–111.

Duffey, E. 1998. Aerial dispersal in spiders. Pp. 187–191. *In* 17th European Colloquium of Arachnology. (P.A. Selden, ed.). British Arachnological Soeiety, Edinburgh.

Goodacre, S., O. Martin, D. Bonte, L. Hutchings, C. Woolley, K. Ibrahim et al. 2009. Microbial modification of host long-distance dispersal capacity. BMC Biology 7:32.

Goodacre, S.L., O.Y. Martin, C.F.G. Thomas & G.M. Hewitt. 2006. *Wolbachia* and other endosymbiont infections in spiders. Molecular Ecology 15:517–527.

Greenstone, M.H., C.E. Morgan & A.-L. Hultsch. 1987. Ballooning spiders in Missouri, USA, and New South Wales, Australia: family and mass distributions. Journal of Arachnology 15:163–170.

Locket, G.H. & A.F. Millidge. 1953. British Spiders Vol. II. The Ray Society, London.

Meijer, J. 1977. The immigration of spiders (Araneida) into a new polder. Ecological Entomology 2:81–90.

Ministry of Agriculture, Fisheries and Food. 2000. England Rural Development Programme 2000–2006, Appendix A9, South West Region. The Stationery Office, London.

Nyffeler, M. & K.D. Sunderland. 2003. Composition, abundance and pest control potential of spider communities in agroecosystems: a comparison of European and US studies. Agriculture and Forest Entomology 95:579–612.

Parker, J.R. 1974. Observations on gossamer and the aerial dispersal of spiders. Newsletter of the British Arachnological Society 10:1–3.

Reynolds, D.R., D.A. Bohan & J.R. Bell. 2007. Ballooning dispersal in arthropod taxa: conditions at take-off. Biology Letters 3:237–240.

Richter, C.J.J. 1970. Aerial dispersal in relation to habitat in eight wolf spider species (*Pardosa*, Araneae, Lycosidae). Oecologia 5:200–214.

Samu, F. & C. Szinetar. 2002. On the nature of agrobiont spiders. Journal of Arachnology 30:389–402.

Sunderland, K.D. & J.E. Dalingwater. 1986. The 1985 Spider Ballooning Survey. Newsletter of the British Arachnological Society 46:5.

Sunderland, K.D., A.M. Fraser & A.F.G. Dixon. 1986. Distribution of linyphiid spiders in relation to capture of prey in cereal fields. Pedobiologia 29:367–375.

Suter, R.B. 1991. Ballooning in spiders: results of wind tunnel experiments. Ethology, Ecology and Evolution 3:13–25.

Thomas, C.F.G. & P. Brain. 2003. Aerial activity of linyphiid spiders: modelling dispersal distances from meteorology and behaviour. Journal of Applied Ecology 40:912–927.

Thomas, C.F.G. & P.C. Jepson. 1999. Differential aerial dispersal of linyphiid spiders from a grass and a cereal field. Journal of Arachnology 27:294–300.

Thorbek, P., K.D. Sunderland & C.J. Topping. 2003. Eggsac development rates and phenology of agrobiont linyphiid spiders in relation to temperature. Entomologia Experimentalis et Applicata 109:89–100.

Thorbek, P., K.D. Sunderland & C.J. Topping. 2004. Reproductive biology of agrobiont linyphiid spiders in relation to habitat, season and biocontrol potential. Biological Control 30:193–202.

Thorbek, P., C.J. Topping & K.D. Sunderland. 2002. Validation of a simple method for monitoring aerial activity of spiders. Journal of Arachnology 30:57–64.

Toft, S. 1995. Two functions of gossamer dispersal in spiders. Acta Jutlandica 2:257–268.

Topping, C.J. & K.D. Sunderland. 1994. Methods for quantifying spider density and migration in cereal crops. Bulletin of the British Arachnological Society 9:209–213.

Topping, C.J. & K.D. Sunderland. 1998. Population dynamics and dispersal of *Lepthyphantes tenuis* in an ephemeral habitat. Entomologia Experimentalis et Applicata 87:29–41.

Vanthournout, B., V. Vandomme & F. Hendrickx. 2014. Sex ratio bias caused by endosymbiont infection in the dwarf spider *Oedothorax retusus*. Journal of Arachnology 42:24–33.

Vugts, H.F. & W.K.R.E. Van Wingerden. 1976. Meteorological aspects of aeronautic behaviour of spiders. Oikos 27:433–444.

Weyman, G.S., P.C. Jepson & K.D. Sunderland. 1995. Do seasonal-changes in numbers of aerially dispersing spiders reflect population density on the ground or variation in ballooning motivation? Oecologia 101:487–493.

Weyman, G.S., K.D. Sunderland & J.S. Fenlon. 1994. The effect of food deprivation on aeronautic dispersal behaviour (ballooning) in *Erigone spp.* spiders. Entomologia Experimentalis et Applicata 73:121–126.

Weyman, G.S., K.D. Sunderland & P.C. Jepson. 2002. A review of the evolution and mechanisms of ballooning by spiders inhabiting arable farmland. Ethology, Ecology and Evolution 14:307–326.

Woolley, C., C.F.G. Thomas, L. Hutchings, S. Goodacre, G.M. Hewitt & S.P. Brooks. 2007. A novel trap to capture ballooning spiders. Journal of Arachnology 35:307–312.

Manuscript received 27 July 2015, revised 23 May 2016.

2016. Journal of Arachnology 44:359–366

Diet of the ladybird spider *Eresus kollari* (Araneae: Eresidae) in an arid system of southeastern Spain

Laura Pérez Zarcos and **Francisco Sánchez Piñero**: Dpto. Biología Animal, Facultad de Ciencias, Universidad de Granada, 18071 Granada, Spain. E-mail: perez.zarcos@gmail.com

Abstract. Spiders are a diverse and abundant group of predaceous arthropods in arid environments. Spiders in the genus *Eresus* Walckenaer, 1805 are widely distributed in mesic and arid regions of the Palaearctic, but data on their diet are scarce. The goal of this study was to analyze the diet of *Eresus kollari* Rossi, 1846 in an arid habitat of the southeastern Iberian Peninsula. A total of 64 webs of *Eresus kollari* with prey remnants were collected in a field site at the Guadix-Baza Basin, and prey were identified to species or the lowest possible taxonomic level, and counted. Prey size was estimated based on remains from the webs and voucher specimens from the study area. In addition, laboratory observations of prey capture were made. The results showed that *E. kollari* has a broad diet, including prey from a total of 106 taxa. Prey included large arthropods (mostly tenebrionids) as well as relatively small insects (e.g., ants, which constituted a high proportion of prey). Laboratory observations showed that adult *E. kollari* actively captured tenebrionid beetles crawling on silk threads around the web, and ants moving on the surface of the web sheets. The high proportion of large-size prey in the webs studied, especially tenebrionids, indicate that this spider has a diet similar to that of *Latrodectus lilianae* Melic, 2000 in the study area, but the different hunting techniques used by the two spiders probably account for the dissimilar proportion of ants and predacious arthropods in the two diets.

Keywords: Prey composition, prey size, hunting technique, Coleoptera, Tenebrionidae, Formicidae

Predaceous arthropods constitute a key component of terrestrial ecosystems able to affect prey abundance and distribution (e.g., Symondson et al. 2002; Cronin et al. 2004; Woltz & Landis 2013). Spiders, a diversified and abundant group in most terrestrial ecosystems, are predatory arthropods with a relevant role in the food web of many habitats, where they are involved in an array of direct and indirect interactions, including cannibalism and intraguild predation (Wise 1993; Schmitz 1998; Denno et al. 2004). Due to the importance of spiders in food webs of arid ecosystems (Louw & Seely 1982; Polis & Yamashita 1991), studies focusing on their diet are pivotal in understanding the role of desert spiders as predators.

Spiders of the family Eresidae inhabit a variety of habitats in the Palaearctic, Afrotropical, Indomalaian, and Neotropical regions (Jocqué & Dippenaar-Schoeman 2006; Miller et al. 2012; Platnick 2013), including arid and semiarid ecosystems of the Old World (Ergashev 1979; Kuznetsov 1985; Henschel & Lubin 1992; Ward & Lubin 1993), where they may constitute abundant, albeit usually inconspicuous, predators. Several species of the genus *Eresus* Walckenaer, 1805, a Palaearctic genus with a complex taxonomy (Řezáč et al. 2008), inhabit steppe and desert ecosystems of the Palaearctic region (Ergashev 1979; Kuznetsov 1985; El-Hennawy 2004a, b). Despite being a frequent and widely distributed genus in Europe, Central Asia, North Africa, and the Middle East, studies on the biology of *Eresus*, and particularly on its diet, are very scarce (Ergashev 1979, 1983; Baumann 1997; Wisniewski & Hughes 1998; Walter 1999a, b). Although some authors have provided accounts of the prey captured by *Eresus* species, mentioning that it includes highly mobile (e.g., cicindelid beetles) and large prey (e.g., Geotrupidae and, principally, Tenebrionidae beetles) species (Berland 1932; Jones 1985; Kuznetsov 1985; Whitehead 2000), few studies have exhaustively analysed the composition of the diet of *Eresus* species (Ergashev 1979; Baumann 1997; Walter 1999a). The results of these studies, conducted in contrasting habitats, a desert in Uzbekistan (Ergashev 1979), and pastures in Germany (Baumann 1997) and Switzerland (Walter 1999a), showed that the diet of *Eresus* spiders included large prey (mainly beetles) as well as small prey (mostly ants). However, Ergashev (1979) provided only a qualitative description of the diet, categorizing prey as rare, frequent or very abundant, while Baumann (1997) and Walter (1999a) gave quantitative data on the diet composition of *Eresus* spiders. In addition, no precise information about the hunting technique used by the spiders is available and only Ergashev (1979) provided a very general description of prey capture, indicating that after prey are caught in the web they are removed by the spider, which carries prey inside its burrow to feed on them.

In this study, we analyse the diet of *Eresus kollari* Rossi, 1846 (Fig. 1) in an arid zone of southeastern Spain. To describe the diet, we report 1) the taxonomic and size composition of the prey captured in adult female webs and 2) laboratory observations of prey capture using the two main taxa found in the webs (small ants and large tenebrionid beetles).

METHODS

Study area.—The study was conducted at Barranco del Espartal (37.53° N, 2.69° W), a site in the arid Guadix-Baza Basin (southeastern Spain). The site is an occasional watercourse (*rambla*) with a gypsum loam soil. The climate is Mediterranean continental and highly seasonal, characterized by cool winters, hot summers and short springs. Rain falls mainly during the winter season (annual rainfall: 250–300 mm). Potential evapotranspiration is 3-fold the amount of precipitation. The vegetation is an open shrub-steppe (58% bare soil, 40% shrub cover) dominated by *Artemisia* (*A. herba-alba* Asso, *A. barrelieri* Besser) and *Salsola vermiculata* L. shrubs, *Macrochloa tenacissima* (L.) Kunth tussock grasses and *Retama sphaerocarpa* L. brushes. A more detailed

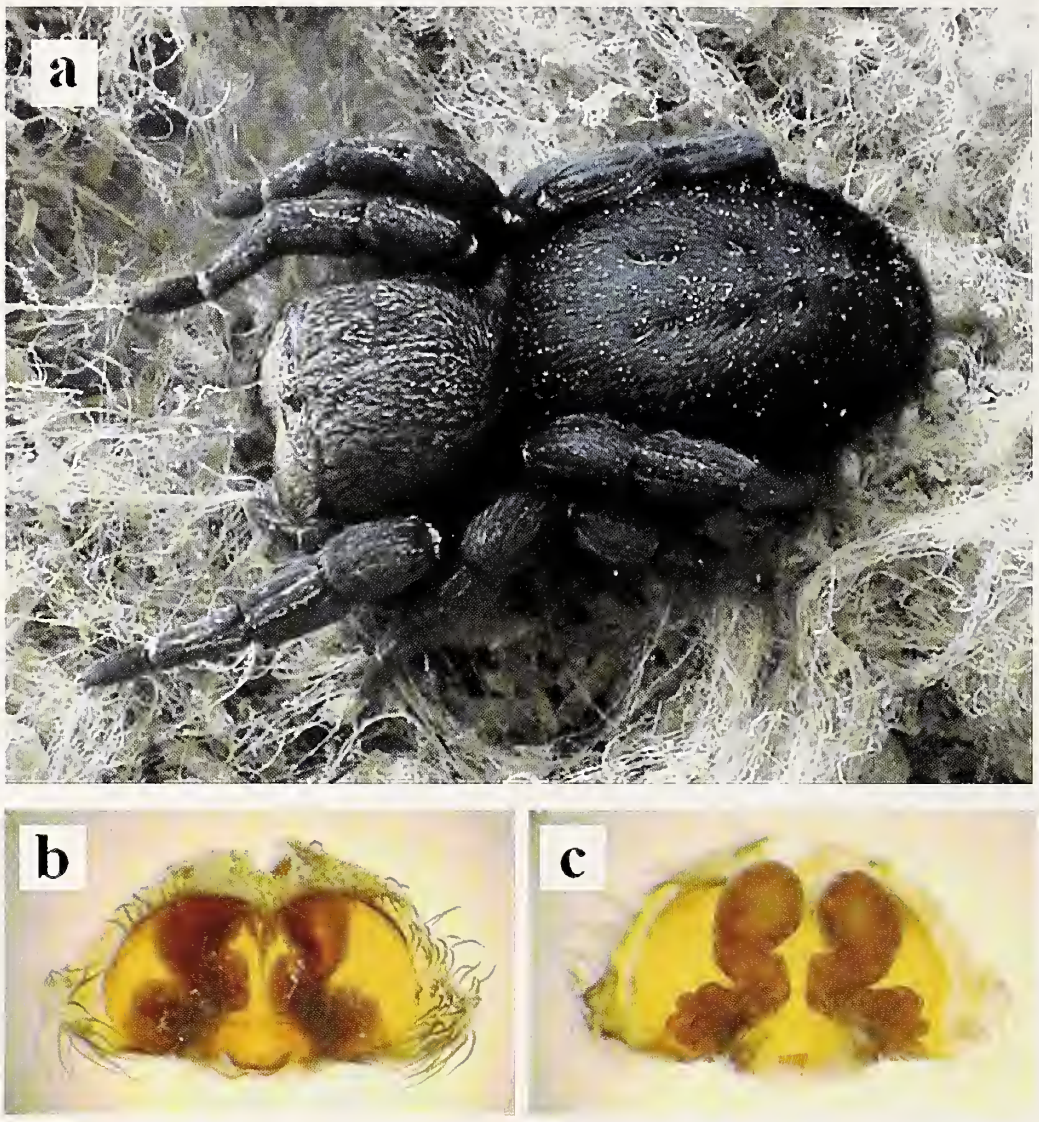

Figure 1.—Habitus (a), epigyne (b) and vulva (c) of female *Eresus kollari* from the study site. Notice that one fissure of the epigyne (the left one in this case) is deformed, a feature of the epigyne of female remains found in the nests.

description of the study site can be found elsewhere (Doblas et al. 2009).

Natural history of *Eresus* spiders.—*Eresus kollari* is a robust spider, prosomal length of females from central Europe ranging from 3.6 to 6.1 mm (Řezáč et al. 2008), and total body length ranging from 8.5 to 20 mm (Melic 1992; Baumann 1997). Spiders in the study area reached 10.4 ± 0.6 mm (mean ± S.E.) prosomal length and 17.6 ± 1.5 mm total body length. The life cycle of the ladybird spider is completed in 3–4 years (Kuznetsov 1985; Wisniewski & Hughes 1998; Walter 1999b). After dispersal, juveniles construct simple, superficial webs and become predators (Kuznetsov 1985). Webs of older juveniles and adults have a large vertical burrow (1.5–3 cm diameter, up to 40 cm deep in our study site), sometimes including lateral branches 5–7 cm long, covered by normal silk (Jones 1985; Kuznetsov 1985; Melic 1992; Wisniewski & Hughes 1998; L. Pérez-Zarcos & F. Sánchez-Piñero, pers. obs.). The web continues with a thick mass of cribellate silk, forming a cover (Jones 1985; Kuznetsov 1985; Melic 1992; Wisniewski & Hughes 1998). The spiders keep the remains of their prey stacked in the web (Jones 1985; Wisniewski & Hughes 1998). Since females can use the same burrow through their entire life (Jones 1985), prey contained in the webs of adult females may provide information on the prey captured by an individual over its life.

Web collecting, prey sorting, and measurement.—Webs of *E. kollari* were collected from November 2005 to March 2006. Because *E. kollari* webs are usually difficult to find (they are covered by sand and debris, and camouflaged with the substrate), webs were collected looking within 50 × 50 cm quadrats randomly placed following transects previously established at the study site. Within each quadrat, we searched for webs using a small gardening rake. Webs were collected and placed in a container. In the laboratory, prey remains from each web were carefully separated from the silk, sorted, identified to the lowest taxonomic level possible (in large beetles and most ants to species or genus level), and counted. To analyse prey-size composition, we measured the total body length excluding appendages (rostrum, antennae, ovipositor, wings, etc.) by means of a binocular microscope equipped with

an ocular micrometer (± 0.1 mm) or a digital calliper (in the case of large specimens). Size was measured in well-preserved prey remains or 3–10 voucher specimens per taxon from the study site kept in the collection of the Zoology Department (University of Granada, Spain).

Laboratory observations of prey capture.—Because previous studies (Ergashev 1983; Baumann 1997; Walter 1999a) and webs from the study site revealed that both large beetle and small ant remains were numerous in webs of adult *E. kollari*, we made laboratory observations in order to 1) determine the hunting technique used by the spider to capture prey, mainly represented by *Messor* ants and tenebrionid beetles at the study site; and 2) establish whether ants and other small prey were actual prey of adult females and not only remains from prey captured by small juveniles occurring in the webs, given that *Eresus* rarely changes burrows (see Walter 1999a). For the observations, four spiders were kept in individual terraria in the laboratory. The small number of adult spiders collected was due to the low abundance of the species in the fall 2006 and the following year, because of the large interannual variations of species abundance occurring in these arid areas (Sánchez-Piñero et al. 2011) and/or due to long life cycle in *Eresus* spiders (Walter 1999b). Each terrarium was a 25 cm length x 10 cm width x 25 cm height glass container filled with soil from the study site to a height of 18 cm and provided with a hole 10 cm deep in its centre for the spider to construct its burrow. When the spiders were placed in the containers, they occupied the burrows and built webs. For two weeks before the observations, the spiders were satiated by feeding twice a week on tenebrionid beetles (*Pimelia monticola* Rosenhauer, 1856, and *Akis discoidea* Quensel, 1806) to ensure that all the spiders had the same level of hunger.

Ant predation by adult females was observed from mid-March to late April 2008. Observations were made considering two different levels of hunger. In a first set of observations, after a week without feeding, each spider was first fed with one tenebrionid (*Pimelia monticola*) from the study site, and then three and five days later, respectively, one ant (*Messor bouvieri* Bondroit, 1918) was offered to each spider. Two rounds of this set of observations were conducted consecutively. Then, a second set of observations were conducted feeding each spider with one *P. monticola* twice per week, and then offering one ant, *M. bouvieri*, to each spider three days later. Two consecutive rounds of this set of observations were also conducted. In each observation, one ant was carefully placed in one terrarium, recording whether the ant crawled on the spider web or not, and whether the ant was captured by the spider or not after 5 min of observation (because the spiders usually did not try to capture the ant after this time). In the few cases in which the ant did not crawl on the spider web, the ant was taken out of the terrarium and the trial was not considered; then, another ant was introduced in the terrarium to start a new observation 10 min later, to avoid any potential disturbance of the spider when the observer removed the ant. If the ant crawled on the web but was not captured by the spider after the five min of observation, a second trial with a different ant was carried out about 30–60 min later. Thus, a total of 16 observations were made when spiders were fed with two tenebrionids/week and 29 trials when the spiders were fed with one tenebrionid/week (3 in which the spider captured the first ant provided, and 13 with two consecutive trials).

RESULTS

Prey in the webs.—A total of 64 webs were collected, with 2033 prey found. The webs of *E. kollari* contained prey belonging to a total of 106 taxa of 11 different Orders of arthropods, including insects (Coleoptera, Dermaptera, Dictyoptera, Hemiptera, Hymenoptera, Lepidoptera, Orthoptera), crustaceans (Isopoda), myriapods (Diplopoda) and arachnids (Solifugae, Araneae) (Appendix 1). The number of prey in the webs averaged 31.8 ± 2.8 prey/web (mean ± S.E.) ranging from zero in one web to over 100 prey in two webs (103 and 106 prey).

The diet of *E. kollari* at the study site was dominated by Coleoptera (63.11% of the prey), mostly Tenebrionidae (69.52% of the beetles), although Carabidae, Curculionidae, and Chrysomelidae were also relatively numerous in *E. kollari* webs. The other dominant prey were Formicidae (mainly *Messor bouvieri* and *M. barbarus* (Linnaeus, 1767); Appendix 1), comprising 32.96% of the prey. There was a slightly positive correlation between the number of remains of tenebrionids and ants in the webs (Pearson correlation, $r = 0.25$, $P = 0.046$, $n = 64$). By contrast, the correlations between the number of carcasses of the remaining prey taxa as a whole and the number of remains of tenebrionids ($r = 0.12$, $P = 0.34$, $n = 64$) and ants ($r = 0.17$, $P = 0.18$, $n = 64$) in the webs were non-significant.

Webs of *E. kollari* showed that the diet of the spider includes a small proportion (0.64%) of predatory arthropods, most of them of relatively large size: Solifugae [*Gluvia dorsalis* (Latreille, 1817)], Araneae (Lycosidae, Gnaphosidae), predatory beetles [*Carabus lusitanicus* (Fabricius, 1801), *Cymindis lineola* Dufour, 1820, *Ocypus ophtalmicus* (Scopoli, 1763), *Pactolinus major* (Linnaeus, 1767), *Hister grandicollis* Illiger, 1807] and assassin bugs [*Reduvius personatus* (Linnaeus, 1758)].

Prey size showed a very wide distribution, from 1.9 mm of small ants and some Curculionidae to 32.5 mm of *Blaps* tenebrionid beetles, and up to 45 mm of Julida (Fig. 2; see also Appendix 1). The prey-size distribution showed a peak occurring at 5.0–7.5 mm (corresponding to *Messor* harvester ants) and two other peaks at 12.5–15.0 mm and 17.5–22.5 mm [corresponding to the most abundant species of Tenebrionidae in the spider webs, i.e., *Sepidium bidentatum* Solier, 1844, *Pimelia baetica* Solier, 1836, *Morica hybrida* (Charpentier, 1825), and *Alphasida oberthueri* (Escalera, 1801); Appendix 1].

Laboratory observations.—The spiders in the terraria captured and fed on large tenebrionids as well as ants. However, the technique used for each type of prey was different. In the case of tenebrionids, the spiders captured the prey in the surroundings of the webs when the beetles walked on the peripheral strings of the web. The spiders exited the web, caught the beetles and bit them in one of the fore coxae. Large tenebrionid beetles actively fought against the spider for 30 to 60 min before the effects of the venom were noted in the prey. Then, the spiders dragged the prey into their burrows. The spiders captured ants by following the prey from under the web. Spiders would bite the web and usually it took the spiders several attempts to capture an ant. In most instances

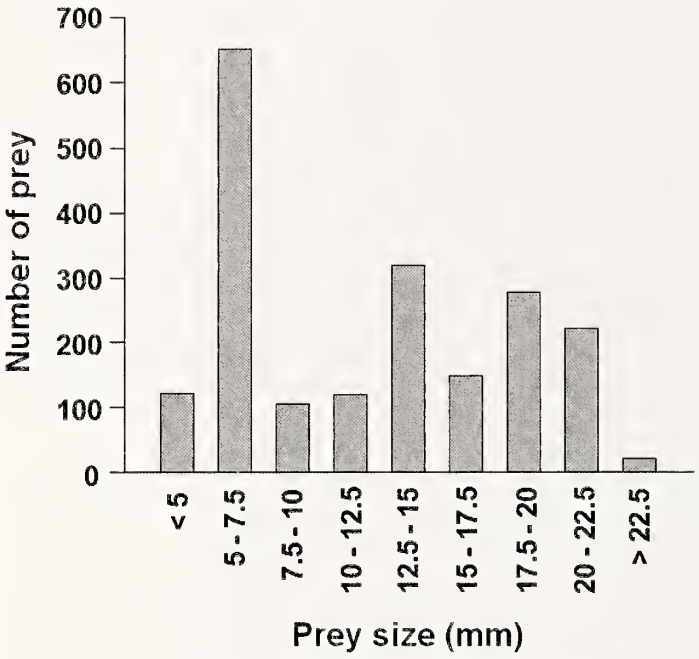

Figure 2.—Number of prey in each size category found in the webs of *E. kollari*.

(21 out of 29 trials in which the spider attempted to capture the ant, i.e., about 3/4 of the attempts), the spiders were unable to catch the ants.

The capture of prey, especially ants, depended on hunger level of the spiders, as spiders did not respond to prey (large or small) if they had previously been satiated. Also, when regularly fed with tenebrionids (twice a week), spiders did not respond to ants and only attempted to capture ants when tenebrionids were offered less frequently (once a week). In this case, only about 1/4 of the ants (8 out of 29 ant trials) were captured by the spider.

DISCUSSION

Eresus kollari from arid zones of the Guadix-Baza Basin kept in the laboratory actively captured prey crawling on silk threads around the web (in the case of tenebrionids) or tried to capture prey moving on the web sheet by biting along the web sheet from below (in the case of ants). For large tenebrionids, it was surprising to observe the fierce fighting of the spider with the beetle for a relatively long time before the predator was able to drag the almost paralyzed prey inside the web. These observations contrast with the hunting technique of capturing prey caught in the web reported by Ergashev (1979). Whether the two hunting techniques observed are used to capture small and large prey in general and whether entanglement in the web constitutes a further mechanism to capture other prey types remain open questions.

Our results reveal that *E. kollari* in arid zones of the Guadix-Baza Basin feeds on a wide range of prey, from large arthropods, such as most tenebrionids, to small insects, such as ants. The diet was amply dominated by Tenebrionidae and Formicidae, which comprised more than 75% of the number of remains found in the spider webs. The fact that these prey had a relatively thick cuticle and their remains were well preserved in the webs may lead to an overestimation of these taxa in the diet of *E. kollari*. However, the potential degradation of prey remains in the webs did not appear to constitute an important bias in our results. Firstly, only remains exposed on the surface of the webs showed some decoloration by sun bleaching, but all these remains were unequivocally identifiable. Secondly, soft-bodied insect larvae and invertebrates in arid systems are primarily belowground dwellers to avoid desiccation and exposure to extreme temperatures (Wallwork 1982), and thus are not preyed upon by *E. kollari*. In addition, most soft-bodied insect larvae in the study area (mainly Coleoptera and Lepidoptera; Sánchez-Piñero 1994; Doblas et al. 2007) were easily identified in the webs by the well-preserved sclerotized cephalic capsules, although in most cases there were also remains of the body cuticle (making it possible even to identify tenebrionid larvae to the genus level). Furthermore, on the soil surface and in the litter, the very low abundance of lightly sclerotized Diptera larvae lacking a cephalic capsule (< 1% in litter; Doblas et al. 2007), and the absence in superficial soil levels of the scarce *Allolobophora caliginosa* (Savigny, 1826) earthworms (Doblas et al. 2007) makes the potential bias provoked by the degradation of their remains likely unimportant. Finally, most larvae are not very vagile animals, reducing their probability of being preyed upon by *E. kollari*. Thus, the proportion of larvae collected in pitfall traps in the study area (0.5–0.9%; Sánchez-Piñero 1994) was similar to the proportion of larvae found in *E. kollari* webs (0.54%). Nonetheless, an experimental assessment of the degradation of prey remains in the webs would enhance the accuracy of diet information gathered from studying the spider webs.

Although our results cannot be easily compared to the data provided by previous studies (Ergashev 1979; Baumann 1997; Walter 1999a), there are some remarkable similarities in the diet of *Eresus* spiders. On one hand, the most abundant remains in the webs were beetles and ants. Ants occurred not only in similar proportions in the webs of the spider both in Switzerland (36.6%) and southeastern Iberian Peninsula (33%), but were also very abundant items in Uzbekistan, although they constituted only some 10% of the remains found in the webs in Germany. Tenebrionid beetles constituted the main prey in the present study and were also reported as very abundant prey in the central Asian desert by Ergashev (1979), although this author did not specify whether these beetles were the most abundant prey in the spider webs. However, in central Europe the most abundant beetle prey were Carabidae (21% to >40% of prey), a group found in a much lower proportion in the diet of *Eresus* in arid areas of Spain (5.5% of the total number of prey) and Uzbekistan (recorded as frequent prey). On the other hand, there were some differences, as the high abundance of orthopterans and sphecid wasps in the spider webs analyzed by Ergashev (1979), and the frequent occurrence of honey bees both in Uzbekistan and Switzerland. These differences can be explained by the contrasting prey availability among sites, as suggested by the generalist diet of *E. kollari*.

The high proportion of Tenebrionidae and Formicidae in the webs of *E. kollari* in the Baza Basin would be related to the fact that these are the dominant groups in the study area (Sánchez-Piñero 1994; Sánchez-Piñero et al. 2011), indicating

the generalist character of *E. kollari* diet. This is also corroborated by the fact that the most abundant remains in the webs (the tenebrionids *Pimelia baetica*, *Sepidium bidentatum*, *Alphasida oberthueri*, and *Morica hybrida*, and the ants *Messor bouvieri* and *M. barbarus*) coincide with the most abundant taxa in the study area (Sánchez-Piñero 1994; Sánchez-Piñero et al. 2011). The slightly positive correlation between the number of remains of tenebrionids and ants in the webs is presumably related to the fact that tenebrionid beetles in the study area aggregate in ant-nest mounds (Sánchez-Piñero & Gómez 1995). Nevertheless, the percentage of tenebrionids preyed upon by the spider (43.62%) is much higher than the percentage of these beetles captured in pitfall traps reported in previous studies at the study site (3.3–16.9% of all arthropods captured; Sánchez-Piñero et al. 2011). By contrast, ants, the numerically dominant taxa at the study site, appeared in the webs of *E. kollari* in a lower proportion (33.7%) than in the pitfall-trap data (49.1–57.1% of the total number of arthropods collected; Sánchez-Piñero et al. 2011). Although these data could be interpreted as a preference of *E. kollari* for large prey, our observations suggest that the lower proportion of ants in the webs in comparison to their abundance at the study site is also probably related to the limited success of the spiders in capturing ants crawling on the web sheets, although the proportion of ants captured by spiders in the laboratory may differ from the proportion captured under natural conditions.

Besides the preference and/or higher capture success of *E. kollari* for large prey, ants (mainly *Messor bouvieri* and *M. barbarus*) still constitute a dominant item in the diet of this spider in the study area. Ants could be so abundant in webs because: 1) they were preyed upon only when the spiders were small juveniles, and remains occurred in the webs because *Eresus* rarely changed their burrows; or 2) ants are actually preyed by adult females (see Walter 1999a). Our laboratory observations showed that adult *E. kollari* actually captured and fed on ants, although they preferred large prey. Surprisingly, five webs of spiders of 5–6 mm in body length (difficult to find, because the small, flat webs were usually concealed in minor cracks or depressions in the soil) collected showed a high proportion of large tenebrionids (31 individuals, 32% of prey) and ants (33 individuals, 34% of prey), indicating that both small and large *E. kollari* were able to capture prey in a similar size range. A plausible explanation for the high number of ants in *E. kollari* webs is that ants are not only the numerically dominant taxon at the study site, but also they remain active year round in the area and may constitute the staple food for the spider in winter and early spring, when tenebrionid beetles are practically inactive and ants and small insects are the main prey available (Sánchez-Piñero 1994; L. Pérez-Zarcos & F. Sánchez-Piñero pers. obs.). The importance of ants in the diet of ground spiders during the winter has been indicated for large trap-door spiders (Buchli 1969; Bradley 1996; Decay et al. 2007; Pérez-Zarcos, pers. obs.). Ants are also important food items during the winter in the study area for sedentary birds, such as *Oenanthe leucura* (Gmelin, 1789) (Muscicapidae) and *Galerida theklae* (Brehm, 1858) (Alaudidae) (Hódar 1993, 1995). Thus, ants may be important prey for the long-lived *E. kollari*, which have to survive for several winters in a habitat where ants are among the few arthropods able to forage during the cold months.

The high proportion of large arthropods (especially tenebrionids), the presence of predatory arthropods in webs, and the potential predation of *Eresus* spiders on lizards, as recorded in the desert systems of Uzbekistan (Ergashev 1979), reveal that this species has a diet similar to that of the black widow spider *Latrodectus lilianae* Melic, 2000 in the Guadix-Baza Basin (Hódar & Sánchez-Piñero 2002). The similarity of the diet of both spiders is also corroborated by the fact that the same tenebrionid species (*Pimelia* spp., *Sepidium bidentatum* and *Alphasida oberthueri* – recorded as *A. clementei* in Hódar & Sánchez-Piñero 2002) were the main prey items in the webs of both *L. lilianae* and *E. kollari* (Hódar & Sánchez-Piñero 2002). However, there are two important differences between the diets of these two spiders. First, although the diet of *E. kollari* at the study site included large predatory arthropods, intraguild predation appears less relevant in the diet of *E. kollari* (0.6%) than in the black widow (4–14%; Hódar & Sánchez Piñero 2002) in the study area. Second, there was a lower proportion of ants in the diet of *L. lilianae* (0.2–8.7% of the prey). The difference in the relative proportions of ants in the diets of these two spiders can be explained by the fact that prey captured by *L. lilianae* are constrained by the size of the prey able to break the strings of the web (Hódar & Sánchez-Piñero 2002), while *E. kollari* appears to be limited only by the ability of the spider to capture the prey while moving on the web surface.

In conclusion, the diet of *E. kollari* showed a wide variety of prey both taxonomically and in terms of prey size, and it is dominated by large tenebrionid beetles and formicids, the two dominant taxa in the study area. The potential role of ants as an important resource for winter survival in these spiders is a question requiring further investigation.

ACKNOWLEDGMENTS

We thank José Antonio Hódar, Adela González Megías, Antonio Abril, and Enrique Doblas for their assistance during the field work and comments on the manuscript. José Manuel Vidal a.k.a. "Er Jota" identified the ant remains from the spider webs and the ant species used in the laboratory, and also helped to carry out the laboratory trials. Manuel Baena kindly identified the Heteroptera. The owners of Barranco del Espartal allowed us to conduct this study on their property. We thank two anonymous reviewers for comments on the manuscript and David Nesbitt for improving the English. This work was funded by research project CGL2005-05890/BOS of Ministerio de Educación y Ciencia.

LITERATURE CITED

Baumann, T. 1997. Populationsökologische und zönotische Untersuchungen zur Bedeutung von Habitatqualität und Habitatfragmentierung für Spinnenpopulationen auf Trokenrasen am Beispiel von *Eresus cinnaberinus* (Oliv. 1789). Wissenschaft und Technik Verlag, Berlin.

Berland, L. 1932. Les Arachnides. Paul Lechevalier et fils, Paris.

Bradley, R.A. 1996. Foraging activity and burrow distribution in the Sydney brown trapdoor spider (*Misgolas rapax* Karsch: Idiopidae). Journal of Arachnology 24:58–67.

Buchli, H.H.R. 1969. Hunting behavior in the Ctenizidae. American Zoologist 9:175–193.

Cronin, J.T., K.J. Haynes & F. Dillemuth. 2004. Spider effects on planthopper mortality, dispersal, and spatial population dynamics. Ecology 85:2134–2143.

Decay, A., P. Cardoso & P. Selden. 2007. Taxonomic review of the Portuguese Nemesiidae (Araneae, Mygalomorphae). Revista Ibérica de Aracnología 14:1–18.

Denno, R.F., M.S. Mitter, G.A. Langellotto, C. Gratton & D.L. Finke. 2004. Interaetions between a hunting spider and a web builder: Consequences of intraguild predation and cannibalism for prey suppression. Ecological Entomology 29:566–577.

Doblas, E., F. Sánchez-Piñero & A. González-Megías. 2007. Soil macroinvertebrate fauna of a Mediterranean arid system: Composition and temporal changes in the assemblage. Soil Biology and Biochemistry 39:1916–1925.

Doblas, E., F. Sánchez-Piñero & A. González-Megías. 2009. Different structuring factors but connected dynamics shape litter and belowground macrofaunal food webs. Soil Biology and Biochemistry 41:2543–2550.

El-Hennawy, H.K. 2004a. Review of spiders of genus *Eresus* in Egypt (Araneida: Eresidae). Serket 9:25–35.

El-Hennawy, H.K. 2004b. A new species of genus *Eresus* from Algeria (Araneida: Eresidae). Serket 9:1–4.

Ergashev, N.E. 1979. The trophic relations of the spider *Eresus niger* Pet. Uzbekskii Biologicheskii Zhurnal 5:60–62.

Ergashev, N.E. 1983. An interesting phenomenon in the reproduction of spiders *Eresus niger* Pet., *Stegodiphus lineatus* Latr. (family Eresidae). Doklady Akademii Nauk Uzbekskoi SSR 10:51–52.

Henschel, J.R. & Y.D. Lubin. 1992. Environmental factors affecting the web and activity of a psammophilous spider in the Namib Desert. Journal of Arid Environments 22:173–189.

Hódar, J.A. 1993. Relaciones tróficas entre los Passeriformes insectívoros en dos zonas semiáridas del sureste peninsular. PhD Thesis. Universidad de Granada, Granada.

Hódar, J.A. 1995. Diet of the black wheatear *Oenanthe leucura* in two shrubsteppe zones of southeastern Spain. Alauda 63:229–235.

Hódar, J.A. & F. Sánchez-Piñero. 2002. Feeding habits of the blackwidow spider *Latrodectus lilianae* (Araneae: Theridiidae) in an arid zone of south-east Spain. Journal of Zoology 257:101–109

Jocqué, R. & A.S. Dippenaar-Sehoeman. 2006. Spider Families of the World. Royal Museum for Central Africa, Tervuren, Belgium.

Jones, D. 1985. Guía de campo de los arácnidos de España y Europa. Omega, Barcelona.

Kuznetsov, G.T. 1985. [On the ecology of spiders *Eresus niger* Pet. and *Lithyphantes paykullionus* Walck. (Aranei, Eresidae, Theridiidae) in south Turkmenistan.]

Izvestiya Akademii Nauk Turkmenskoi SSR Seriya Biologicheskikh Nauk 1985 (6):70–72 (in Russian).

Louw, G. & M. Seely. 1982. Ecology of Desert Organisms. Longman, London.

Melic, A. 1992. La familia Eresidae (Arachnida: Araneae) en Aragón. Notas aracnológicas aragonesas, 4. Boletín de la Sociedad Entomológica Aragonesa 11:7–12.

Miller, J.A., C.E. Griswold, N. Scharff, M. Řezáč, T. Szűts & M. Marhabaie. 2012. The velvet spiders: an atlas of the Eresidae (Arachnida, Araneae). ZooKeys 195:1–144.

Platnick, N. I. 2013. The world spider catalog, version 14.0. American Museum of Natural History, online at http://research.amnh.org/iz/spiders/catalog/

Polis G.A. & T. Yamashita. 1991. The ecology and importance of predaceous arthropods in desert communities. Pp. 180–222. *In* The Ecology of Desert Communities. (G.A. Polis, ed.). University of Arizona Press, Tucson, Arizona.

Řezáč, M., S. Pekár & J. Johannesen. 2008. Taxonomic review and phylogenetic analysis of central European *Eresus* specics (Araneae: Eresidae). Zoologica Scripta 37:263–287.

Sánchez-Piñero, F. 1994. Ecología de las comunidades de coleópteros en zonas áridas de la Depresión de Guadix-Baza (sureste de la Península Ibérica). Ph.D Thesis, University of Granada.

Sánchez-Piñero, F. & J.M. Gómez. 1995. Use of ant-nest debris by darkling beetles and other arthropod specics in an arid system in South Europe. Journal of Arid Environments 31:91–104.

Sánchez-Piñero, F., A. Tinaut, A. Aguirre-Segura, J. Miñano, J.L. Lencina, F.J. Ortiz-Sánchez et al. 2011. Terrestrial arthropod fauna of arid areas of SE Spain: Diversity, biogeography, and conservation. Journal of Arid Environments 75:1321–1332.

Schmitz, O.J. 1998. Direct and indirect effects of predation and predation risk in old-field interaction webs. American Naturalist 151:327–342.

Symondson, W.O.C., K.D. Sunderland & M.H. Greenstone. 2002. Can generalist predators be effective biocontrol agents? Annual Review of Entomology 47:561–594.

Wallwork, J.A. 1982. Desert Soil Fauna. Praeger, New York.

Walter, J.E. 1999a. Durer's rhinoceros and the prey of *Eresus cinnaberinus* (Olivier) (Araneae: Eresidae). Arachnologischc Mitteilungen 17:11–19.

Walter, J.E. 1999b. Lebenszyklus von *Eresus cinnaberinus* (Olivier, 1789) (Araneae: Eresidae) in der Schweiz. Mitteilungen der Entomologischen Gesellschaft Basel 49:2–7.

Ward, D. & Y. Lubin. 1993. Habitat selection and the life history of a desert spider, *Stegodyphus lineatus* (Eresidae). Journal of Animal Ecology 62:353–363.

Whitehead, P.F. 2000. Coleoptera in the diet of *Eresus walckenaeri* Brulle (Araneae, Eresidae) in Zakynthos, Ionian Islands, Greece. Entomologist's Monthly Magazine 136:205–206.

Wise, D.H. 1993. Spiders in Ecological Webs. Cambridge University Press, Cambridge.

Wisniewski, P.J. & 1. Hughes 1998. The ladybird spider *Eresus cinnaberinus* rearing project. International Zoo Yearbook 36:158–162.

Woltz, M. & D.A. Landis. 2013. Coccinellid immigration to infested host patches influences suppression of *Aphis glycines* in soybean. Biological Control 64:330–337.

Manuscript received 2 November 2015, revised 4 May 2016.

Appendix 1.—Prey taxa, number of individuals for each taxon, and prey size (mean ± S.E.) collected from webs of *E. kollari*.

Taxa	Number of prey	Prey size (mm)
CHELICERIFORMES		
Solifugae		
Daesiidae		
Gluvia dorsalis (Latreille, 1817)	1	20.0
Araneae		
Lycosidae	1	15.0
Gnaphosidae	1	10.0
CRUSTACEA		
Isopoda		
Oniscidae	4	16.5
HEXAPODA		
Blattodea		
Blattellidae		
Ectobius sp.	3	7.5 ± 0.6
Coleoptera		
Anthicidae		
Notoxus sp.	2	4.5 ± 0.1
Buprestidae		
Julodis onopordi (Fabricius, 1787)	7	25.1 ± 1.1
Acmaeoderella moroderi (Reitter, 1906)	1	7.1
Carabidae		
Acinopus picipes (Olivier, 1795)	10	13.5 ± 0.5
Carabus lusitanicus (Fabricius, 1801)	3	24.3 ± 0.8
Cymindis lineola Dufour, 1820	1	11
Dixus capito (Serville, 1821)	46	13.5 ± 0.3
Dixus sphaerocephalus (Olivier, 1795)	25	8.7 ± 0.1
Eriotomus villosulus (Reiche, 1859)	1	6.9
Harpalus tenebrosus Dejean, 1829	1	9.7
Orthomus barbarus Dejean, 1828	21	9.85 ± 0.2
Poecilus cupreus (Linnaeus, 1758)	1	13.5
Carabidae larvae	4	-
Unidentified Carabidae	2	-
Cerambycidae		
Iberodorcadion fuliginator (Dalman, 1817)	5	22.4 ± 0.9
Chrysomelidae		
Chrysolina banksii (Fabricius, 1775)	3	10.4 ± 0.2
Chrysolina affinis (Fabricius, 1787)	2	8.1 ± 0.1
Chrysolina diluta (Germar, 1824)	13	7.0 ± 0.2
Chrysolina jan-bechynei Cobos, 1953	4	8.1 ± 0.5
Coptocephala scopolina (Linnaeus, 1767)	1	7.3
Cyrtonus plumbeus Fairmaire, 1850	7	8.1 ± 0.9
Galeruca augusta (Küster, 1849)	46	10.4 ± 0.1
Unidentified Chrysomelidae	2	-
Curculionidae		
Aspidiotes westringii Schoenherr, 1847	10	7.0 ± 0.2
Brachycerus pradieri Fairmaire, 1856	8	9.3 ± 1.8
Coniocleonus tabidus (Olivier, 1790)	36	11.7 ± 0.8
Cycloderes glabratus (Gyllenhal, 1833)	14	8.0 ± 0.1
Larinus flavescens Germar, 1824	1	15.45
Ocladius grandii Osella & Meregalli, 1987	1	5.3
Rhytirhinini	4	5.1 ± 0.6
Sibinia iberica Hoffmann, 1959	3	2.2 ± 0.2
Trachyphloenini	2	3.5 ± 0.5
Xanthochelus cinctiventris (Fahaeus, 1842)	1	16.0
Unidentified Curculionidae	24	4.1 ± 1.7
Elateridae		
Cebrio spp.	1	14.1 ± 0.6
Cardiophorus sp.	6	7.0 ± 0.2
Melanotus sp.	4	12.7 ± 0.6

Appendix 1.—Continued.

Taxa	Number of prey	Prey size (mm)
Histeridae		
Hister grandicollis Illiger, 1807	1	10.5
Pactolinus major (Linnaeus, 1767)	1	13.0
Melyridae		
Graellsinus praticola (Waltl, 1835)	3	5.4 ± 0.2
Malachiinae	2	4.6 ± 0.1
Unidentified Melyridae	1	4.8 ± 0.2
Scarabaeidae		
Aphodius baeticus (Mulsant & Rey, 1869)	17	6.8 ± 0.2
Bolbelasmus bocchus (Erichson, 1841)	3	14.0 ± 0.5
Rhizotrogus toletanus Báguena, 1955	15	11.5 ± 0.5
Staphylinidae		
Ocypus ophthalmicus (Scopoli, 1763)	3	26.5 ± 1.2
Tenebrionidae		
Akis discoidea Quensel, 1806	2	22.0 ± 2.0
Alphasida oberthueri (Escalera, 1901)	124	20.0 ± 0.5
Alphasida rectipennis (Escalera, 1906)	26	18.8 ± 0.5
Alphasida sp. larvae	1	-
Asida oblonga frigida Escalera, 1905	55	13.4 ± 0.5
Asida sp.	1	12.8
Blaps lusitanica Herbst, 1799	2	28.8 ± 0.5
Blaps nitens brachyura Küster, 1848	2	27.0 ± 0.5
Blaps waltli Seidlitz, 1893	1	32.5
Crypticus antoinei Español, 1950	2	7.1 ± 0.2
Leptoderis collaris (Linnaeus, 1767)	1	20.0
Morica hybrida (Charpentier, 1825)	87	20.2 ± 0.5
Phylan gibbulus (Motschoulsky, 1849)	2	9.1 ± 0.1
Pimelia baetica Solier, 1836	251	17.9 ± 0.4
Pimelia monticola Rosenhauer, 1856	66	16.6 ± 0.3
Pimelia sp. larvae	1	-
Probaticus interstitialis (Küster, 1850)	7	13.4 ± 0.9
Scaurus rugulosus Solier, 1838	5	15.6 ± 1.4
Scaurus uncinus (Forster, 1771)	65	15.7 ± 0.8
Sepidium bidentatum Solier, 1844	164	14.1 ± 0.4
Tentyria laevis Solier, 1835	27	14.3 ± 2.3
Unidentified Coleoptera	22	-
Dermaptera		
Forficulidae		
Forficula auricularia Linnaeus, 1758	3	17.0 ± 2.0
Hemiptera		
Cercopidae		
Cercopis sp.	1	10.3 ± 0.8
Dyctiopharidae	2	3.6 ± 0.1
Cydnidae		
Aethus pilosus (Herrich-Schaeffer, 1834)	1	6.5
Legnotus fumigatus (A. Costa, 1853)	1	4.0
Tritomegas cf. *theryi* (Lindberg, 1932)	1	6.3
Lygaeidae		
Plinthisus cf. lepineyi Vidal, 1940	1	4.2
Pentatomidae		
Aelia sp.	2	15.0 ± 0.3
Aelia cribrosa Fieber, 1868	10	9.9 ± 1,0
Aucyrosoma lencogrammes (Gmelin, 1790)	1	6.5
Carpocoris cf. *fuscipinus* (Boheman, 1849)	1	10.1
Irochrotus maculiventris (Germar, 1839)	2	8.8
Unidentified Pentatomidae	1	-
Pyrrocoridae		
Codophila varia (Fabricius, 1787)	1	11.1
Pyrrocoris apterus (Linnaeus, 1758)	1	11.0

Appendix 1.—Continued.

Taxa	Number of prey	Prey size (mm)
Reduviidae		
Reduvius personatus (Linnaeus, 1758)	1	10.0
Scutelleridae		
Psacasta sp.	1	8.8
Stenocephalidae		
Dicranocephalus sp.	1	14.0
Hymenoptera		
Formicidae		
Aphaenogaster ibérica Emery, 1908	14	6.5 ± 0.7
Camponotus sp.	23	6.0 ± 2.8
Cataglyphis ibérica Emery, 1906	18	5.5 ± 2.1
Crematogaster sp.	23	3.5 ± 0.7
Goniomma sp.	3	3.9 ± 0.6
Messor spp.	529	5.6 ± 0.9
Pheidole pallidula (Nylander, 1848)	1	2.1
Proformica sp.	2	6.0 ± 2.8
Tapinoma sp.	44	1.9 ± 0.5
Tetramorium spp.	13	3.5 ± 0.7
Sphecidae	1	14.5
Bethylidae	2	9.9 ± 1.0
Unidentified Hymenoptera	26	-
Lepidoptera (larvae)	6	-
Orthoptera		
Acrididae		
Mioscirtus wagneri (Kittary, 1859)	1	15.6 ± 0.2
MYRIAPODA		
Julida		
Julidae	2	33.3 ± 1.8

2016. Journal of Arachnology 44:367–379

Pleistocene refugia and their effects on the phylogeography and genetic structure of the wolf spider *Pardosa sierra* (Araneae: Lycosidae) on the Baja California Peninsula

Ricardo González-Trujillo[1], **Miguel M. Correa-Ramírez**[2], **Eduardo Ruiz-Sanchez**[3], **Emiliano Méndez Salinas**[4], **María Luisa Jiménez**[5] and **Francisco J. García-De León**[1]: [1]Laboratorio de Genética para la Conservación, Centro de Investigaciones Biológicas del Noroeste (CIBNOR), Ave. Instituto Politécnico Nacional 195, Col. Playa Palo Santa Rita, 23096, La Paz, Baja California Sur, México; E-mail: fgarciadl@cibnor.mx; [2]Centro Interdisciplinario de Investigación para el Desarrollo Integral Regional (CIIDIR), Unidad Durango, Instituto Politécnico Nacional, Durango 34220, México; [3]Escuela Nacional de Estudios Superiores Unidad Morelia (UNAM), Antigua Carretera a Pátzcuaro 8701, Col. Ex Hacienda de San José de la Huerta 58190, Pátzcuaro, Michoacán, México; [4]Instituto de la Patagonia, Universidad de Magallanes, Ave. Bulnes 01855, Punta Arenas, Chile; [5]Laboratorio de Aracnología, Centro de Investigaciones Biológicas del Noroeste (CIBNOR), Ave. Instituto Politécnico Nacional 195, Col. Playa Palo Santa Rita, CP 23096, La Paz, Baja California Sur, México

Abstract. The phylogeographic structure of some species distributed across the Baja California Peninsula has been traditionally hypothesized as resulting from vicariant events thought to have occurred between 1–3 Mya. Climatic fluctuations during the Pleistocene have also been shown to influence the distribution patterns of species, and vicariant patterns may have been erased as a consequence of population contractions or expansions into or out of refugia generated during the last glacial maximum ca. 21,000 years ago. Thus, there is still some uncertainty regarding the relative role of vicariance in shaping the modern biota of Baja California. To understand the evolutionary history of the wolf spider *Pardosa sierra* Banks, 1898 on the peninsula, a phylogeny of this species and closely related taxa was generated using a fragment of the mitochondrial gene cytochrome c oxidase subunit I (CO1). Sequences of a fragment of the CO1 gene for 38 individuals from 14 sampling sites along the entire distribution range of *P. sierra* were used to infer phylogeographic patterns, and five nuclear microsatellite loci were also used to genotype 296 individuals from seven of these 14 locations. The current and past potential distributions from two Pleistocene periods were estimated using niche-based distribution modeling, and scenarios of colonization from detected refugia were simulated. We found that Californian populations of *P. sierra* diverged from peninsular populations 4 Mya, this divergence coinciding with the northern-gulf split. However, we did not detect genetic breaks in regions where the mid-peninsular and Isthmus of La Paz canals were presumably formed, either with mitochondrial DNA sequences or microsatellite loci. Two refugia were further detected at the geographic ends of the peninsula, these likely preceding subsequent habitat expansion.

Keywords: Mitochondrial DNA, microsatellite, vicariance, climate change, niche modeling

The Baja California Peninsula (BCP; Fig. 1) has been a model landscape for phylogeographic studies due to its geographic isolation, landscape heterogeneity and high levels of endemism (Jezkova et al. 2009; Wilson & Pitts 2012; Graham et al. 2014; Dolby et al. 2015). In several studies, population divergences or phylogeographic breaks have been detected in a diversity of taxa (Upton & Murphy 1997; Riddle et al. 2000; Murphy & Aguirre-León 2002; Nason et al. 2002; Zink 2002a; Crews & Hedin 2006; Lindell et al. 2006; Graham et al. 2014; Lira-Noriega et al. 2015). To explain the causes of such phylogeographic breaks, hypotheses that include vicariance events have been proposed, with the most important being these: (1) the marine transgression of the Gulf of California in the northern-gulf region (south of California and Arizona), with separation from the rest of the BCP occurring 3 million years ago (Mya) (Riddle et al. 2000; Hafner & Riddle 2005); (2) the mid-peninsular channel, which formed approximately 1 to 1.6 Mya in the nearby Vizcaíno Desert (Upton & Murphy 1997; Hafner & Riddle 2005; Crews & Hedin 2006; Lindell et al. 2006); and (3) the Isthmus of La Paz Channel, which separated the Cape Region of the BCP 3 Mya (Riddle et al. 2000; Hafner & Riddle 2005; Garrick et al. 2013).

Alternative non-vicariant biogeographic hypotheses have also been proposed, most of these highlighting the potential effects of cyclic climatic changes during Pleistocene glacial and interglacial periods (Hewitt 1996, 2004; Hafner & Riddle 2005; Lindell et al. 2006; Riddle & Hafner 2006; Leaché & Mulcahy 2007; Garrick et al. 2009, 2013). In particular, the Last Glacial Maximum (LGM) ca. 21,000 years ago (Dansgaard et al. 1993) may have forced many species from the deserts of the Northern Hemisphere to find refuge south of their previous distributions (Hewitt 1996, 2000, 2004; Van Devender 2002; Graham et al. 2013; Harl et al. 2014). The Cape Region, at the southern tip of the BCP, was likely used as a refugium for species that could not tolerate cold (Murphy & Aguirre-León 2002; Garrick et al. 2013). However, the number and location of refugia is species dependent, as each likely responded differently to climatic events (Harl et al. 2014). Similarly, it is also probable that cycles of range contraction and range expansion generated by climatic oscillations (Grismer 2002) may have erased the genetic fingerprints produced by earlier vicariance events (Crews & Hedin 2006). This raises uncertainty about whether the phylogeographic patterns observed are due to hypothesized vicariance events or climatic changes or both.

Pardosa sierra Banks, 1898 is a species of wolf spider (Lycosidae) that is endemic to the BCP (Correa-Ramírez et al. 2010); it is intolerant of cold temperatures (Van Dyke & Lowrie 1975) and strongly dependent on water bodies (Punzo & Farmer 2006; Correa-Ramírez 2010; Jiménez et al. 2015).

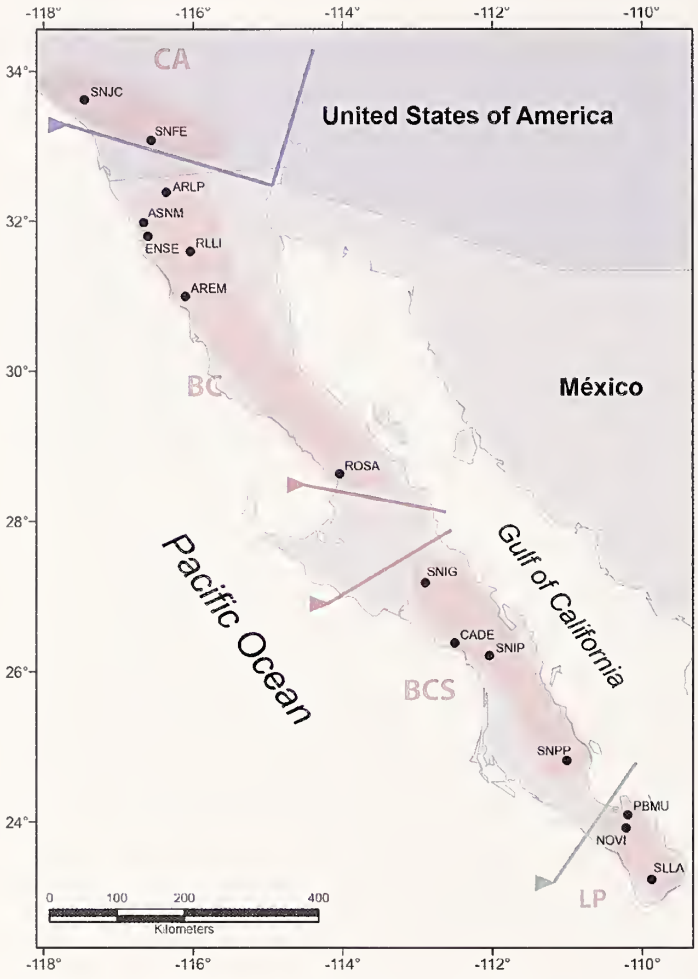

Figure 1.—*Pardosa sierra* collection sites in the Baja California Peninsula. For the acronyms of each collecting site refer to Table 1. Lines indicate the hypothetical vicariance events of the northern-gulf (*blue*), the Vizcaíno mid-peninsular channel (*red*) and the Isthmus of La Paz (*green*). CA = California; BC = Baja California; BCS = South Baja California; LP = La Paz.

Given these biological constraints, it is expected that populations of *P. sierra* would have been affected by changes to their habitat due to climatic variations during the Pleistocene, as has been shown for other desert species of Rodentia (Jezkova et al. 2009), Hymenoptera (Wilson & Pitts 2012), and Scorpiones (Graham et al. 2013), among others (Van Devender 2002).

In this study, mitochondrial DNA sequences and nuclear microsatellites were used to analyze the phylogeographic patterns and genetic structure of *P. sierra* populations across the BCP, with the aim of addressing the following questions: What is the phylogeographic pattern of *P. sierra* along the BCP? How and when did current distribution patterns potentially originate? Does the genetic structure inferred using microsatellite loci coincide with phylogeographic patterns detected using mtDNA sequences? Did *P. sierra* use refugia in more than one climatically suitable area during the LGM? If so, where were these refugia? We expect that any genetic signal resulting from potential vicariance events that occurred before or during the Pleistocene were erased due to refuge-colonization processes caused by climatic changes after the LGM. Finally, if *P. sierra* expanded its distribution from southern refugia after the LGM, we predict a decreasing gradient of microsatellite genetic diversity from the south region to the north of the BCP.

METHODS

Samples and study locations.—Between 2006 and 2011, 296 adult *P. sierra* specimens were hand collected from the margins of rivers, ponds and other suitable habitats along the BCP and southwestern United States (Fig. 1; Table 1). We collected 38 specimens from 14 localities throughout the range of the species for mitochondrial DNA sequence analysis, and 296 specimens were sampled from only seven locations along the BCP for microsatellite genotyping (Table 1). The specimens were preserved in 95% ethanol and deposited in the Colección Aracnológiea y Entomológica del Centro de Investigaciones Biológicas del Noroeste (CAECIB).

DNA extraction and genetic characterization using mitochondrial markers and microsatellites.—Total genomic DNA was extracted from the legs of each specimen as reported by Aljanabi & Martinez (1997). DNA quality was verified on 1% agarose gels (buffer TAE 1x, GelRed 10x), and DNA concentration (ng/μl) was quantified with a NanoDrop 8000 (Thermo Fisher Scientific, Wilmington, DE). A mitochondiral fragment of the cytochrome c oxidase subunit I (CO1) gene was amplified by polymerase chain reaction (PCR) and sequenced using the primers CO1P- L and CO1P-R (Correa-Ramírez et al. 2010). PCR reactions were performed with a PTC-200 DNA Engine Thermal Cycler (BioRad Laboratories, Hercules, CA) in a total reaction volume of 15 μl (~50 ng genomic DNA, 0.40 mM each primer, 2.5 mM mM $MgCl_2$, 0.2 mM each dNTP, 1x PCR buffer and 0.5 U Taq polymerase (Invitrogen, Carlsbad, CA)). A total of 35 temperature cycles were performed, each cycle consisted of denaturation for 30 seconds at 94°C, annealing for 30 seconds at 52°C, extension for 30 seconds at 72°C, and included an initial denaturation step for 4 minutes at 94°C, and a final extension step for 10 minutes at 72°C. PCR products were visualized using electrophoresis in 1.5% agarose gels. The sequencing of PCR products was performed using the BigDye Terminator sequencing method in an ABI PRISM 3730XL sequencer (PE Applied Biosystems; Macrogen, Seoul, Korea).

Five microsatellite loci previously described for *P. sierra* in Molecular Ecology Resources Primer Development Consortium et al. (2010) were used. The final PCR reaction volume was 15 μl with ~30 ng genomic DNA, 1x PCR buffer (20 mM Tris-HCl, pH 8.4, 50 mM KCl), 200 μM each dNTP, 0.4 μM each primer, 1.5–2.5 mM MgCl2 and 0.15 U Taq DNA Polymerase (Invitrogen, Carlsbad, CA). The PCR conditions were 95°C for 5 min, followed by 35 cycles of 95°C for 30 sec, annealing at 52°C for 30 sec, 72°C for 30 sec, and a final extension of 72°C for 5 min. PCR reactions were performed in an MJ Research PTC-200 thermal cycler. PCR products were visulaized by electrophoresis on 6% polyacrylamide gels with 7.5 M urea. Gels were silver-stained according to Benbouza et al. (2006). The allele size was determined by their relative position on the gel compared to the molecular marker (nucleotide ladders of 10 and 50 bp, Invitrogen).

Phylogeography and population genetic structure.—To assess whether the phylogeographic pattern of *P. sierra* along the

Table 1.—Sampling locations of *Pardosa sierra* in the Baja California Peninsula and frequency of haplotypes of mitochondrial gene CO1. n^a = number of individuals analyzed for each microsatellite locus.

Location	ID	Lat (°N)	Long (°W)	n^a	Haplotypes CO1 (*n*)
USA, CA, Sn. Juan Creek	SNJC	33.638	−117.421	-	*Hap3* (4)
USA, CA, Sn. Felipe	SNFE	33.066	−116.553	-	*Hap*3 (1), *Hap*7 (3)
Mexico, BC, Arroyo Las Palomas	ARLP	32.373	−116.354	-	*Hap*1 (2), *Hap*6 (2)
Mexico, BC, Arroyo Sn. Antonio Minas	ASNM	31.968	−116.658	-	*Hap*1 (4)
Mexico, BC, Ensenada	ENSE	31.783	−116.6	26	*Hap*1 (1), *Hap*5 (3)
Mexico, BC, Rancho Las Liebres	RLLI	31.584	−116.03	-	*Hap*2 (2)
Mexico, BC, Arroyo El Mejin	AREM	30.980	−116.094	-	*Hap*6 (1)
Mexico, BC, El Rosarito	ROSA	28.616	−114.033	10	*Hap*1 (1), *Hap*5 (1)
Mexico, BCS, Sn. Ignacio	SNIG	27.174	−112.869	-	*Hap*1 (1)
Mexico, BCS, Cadejé	CADE	26.366	−112.5	52	*Hap*1 (2), *Hap*4 (2)
Mexico, BCS, Sn. Isidro-La Purísima	SNIP	26.2	−112.033	52	*Hap*1 (1)
Mexico, BCS, Sn. Pedro de la Presa	SNPP	24.833	−110.983	52	-
Mexico, BCS, Presa de la Buena Mujer	PBMU	24.088	−110.191	-	*Hap*1 (2)
Mexico, BCS, El Novillo	NOVI	23.916	−110.216	52	*Hap*1 (3)
Mexico, BCS, Sierra de la Laguna	SLLA	23.233	−109.866	52	*Hap*1 (2)

Baja California peninsula was correlated with geological vicariance events, the 14 locations were clustered *a priori* into four groups, California (CA), Baja California (BC), Baja California Sur (BCS) and La Paz (LP), based on the positions of the hypothetical trans-peninsular channels (Fig. 1). An analysis of molecular variance (AMOVA) was performed using CO1 sequences among these groups. Additionally, genetic differentiation values (F_{ST}) were estimated by applying 10,000 permutations using ARLEQUIN 3.5 (Excoffier & Lischer 2010).

To determine the genetic structure of *P. sierra*, microsatellite loci were analyzed using STRUCTURE 2.3.4 software (Pritchard et al. 2000). First, we performed an analysis without the LOCPRIOR option to obtain an initial K, and afterwards we ran it again using this K value as LOCPRIOR. In both analyses the admixture model was used, with a burn-in period of 100,000 and $1x10^6$ MCMC repetitions thereafter. The number of populations was estimated using the ΔK value using Evanno's method (Evanno et al. 2005) in STRUCTURE HARVESTER Web v0.6.94 (Earl & VonHoldt, 2012). The results of 15 independent runs were processed and visualized using CLUMPP 1.1.2 (Jakobsson & Rosenberg 2007) and DISTRUCT 1.1 (Rosenberg 2004) respectively. Finally, the genetic differentiation values (F_{ST}) were evaluated using the infinite allele model (Weir & Cockerham 1984) in ARLEQUIN, using the Bonferroni correction to adjust the significance level for multiple tests (Rice 1989).

Genetic diversity.—To observe haplotype diversity, haplotype frequencies from the CO1 sequences were calculated using DnaSp 5.10 (Librado & Rozas 2009). To estimate population growth of *P. sierra*, the R2 test was performed (Ramos-Onsins & Rozas 2002), with 10,000 coalescence simulations using DnaSP v5 (Librado & Rozas 2009). To detect potential relationships among haplotypes, a statistical parsimony network was estimated for CO1 with a 95% confidence criterion, using TCS 1.13 software (Clement et al. 2000).

To detect a genetic diversity gradient along the peninsula, we calculated the Pearson correlation coefficient between the latitude of each location with its corresponding heterozygosity (H_E) and allelic diversity (A/L) of microsatellites previously obtained from GENEPOP 4.0.7. (Rousset 2008). To observe if there is a relationship between distance and genetic identity between populations, we tested for isolation-by-distance, using the Mantel test (Slatkin 1993) with 10,000 permutations in IBDWSin v3.23 (Jensen et al. 2005). Recent population bottleneck analysis was performed with a two-tailed Wilcoxon sign-rank test for heterozygosity excess under a two-phased mutation model (TPM; Di Rienzo et al. 1994; Miller et al. 2012), using the program BOTTLENECK 1.2.02 (Piry et al. 1999).

Phylogenetic analysis.—In addition to the newly-generated CO1 sequences from this study, additional sequences were obtained from GenBank (http://www.ncbi.nlm.nih.gov/genbank/; accessed April 2014) for another 28 taxa, these included different species of *Pardosa* C.L. Koch, 1847 and closely related genera (Appendix 1). For Bayesian phylogenetic inference we used MRBAYES 3.2.2 (Ronquist & Huelsenbeck 2003), and JMODELTEST 2.1.6 software (Darriba et al. 2012) was used to identify an optimal GTR+I+G model of molecular evolution for the un-partitioned CO1 matrix under the Akaike Information Criterion (AIC). Bayesian analysis was performed using two independent runs consisting of $10x10^6$ MCMC generations, with sampling every 1,000 generations. A 50% majority-rule consensus tree was generated after 10% burn-in.

Estimation of divergence time.—To test whether phylogeographic patterns detected were temporally concordant with hypothetical vicariance events, interspecific and population divergence times were estimated in BEAST 1.8 (Drummond et al. 2012), using both fossil and rate calibration methods with CO1. The first analysis included individuals of *P. sierra*, plus other *Pardosa* species and related genera. The GTR+I+G substitution model was used based on the results of JMODELTEST 2.1.6, along with a lognormal relaxed clock model and Yule speciation process to model the tree prior. The Yule process evaluates the relative ages of nodes contributing to the prior distribution of nodal ages (Ho & Phillips 2009). A lycosid macrofossil from the Miocene found in Dominican amber (Penney 2001) was used as a root calibration point, with a minimum age constraint of 20 Mya. We implemented a hard minimum bound (Ho & Phillips 2009)

to a well-identified macrofossil with a lognormal distribution (mean 0, SD 1.0, offset 20). The fossil specimen used here is considered the first representative of the family Lycosidae from the fossil record (Penney 2001); previously recorded fossils from the Carboniferous, Tertiary, Miocene, or Pliocene assigned to genera of Lycosidae were likely misidentified species that correspond to other families (Penney 2001).

We also performed a second BEAST analysis including only *P. sierra* specimens, using the Coalescent constant size to model the tree prior. The tree was rate calibrated using the substitution rate of 0.0115 substitutions per site per million years for CO1, proposed for insects by Brower (1994) and also used for spiders in phylogeographic studies (e.g., Chang et al. 2007). For both BEAST analyses, two independent runs of $40x10^6$ generations were performed, sampling every 2,000 generations. The results were analyzed in TRACER 1.5 (Rambaut & Drummond 2007). To ensure parameter convergence and the effective sampling size (ESS), all parameters and trees for both independent runs were combined in LOGCOMBINER 1.8 (Rambaut & Drummond 2007) with a burn-in of 25% for the first trees in TREEANNOTATOR 1.8 (Rambaut & Drummond 2007). Finally, the results were summed up in a single tree (maximum clade credibility tree) and visualized in FIGTREE 1.4 (http://tree.bio.ed.ac.uk/software/figtree/).

Niche-based distribution model.—To identify geographic areas that might have served as refugia for *P. sierra* during and after the LGM, we generated a niche-based distribution model (NBDM; Segurado et al. 2006) using records of *P. sierra* collected for this study at 31 localities in the States of Baja California and Baja California Sur in Mexico, and California in the United States of America (Appendix 2). To infer the NBDMs the records were loaded into the 'maximum entropy machine-learning algorithm' MAXENT 3.2.2 (Phillips et al. 2006). Current bioclimatic variables used (BIO 1–19) were downloaded from WorldClim (Hijmans et al. 2005; www.worldclim.org) with a resolution of 1 km^2 using 75% of the records for training and the remaining 25% for validation of the model. To run MAXENT, default parameters were used with 1,000 iterations. The models were evaluated with the area under the curve (AUC) method. The algorithm compensates for co-linearity between variables using a method for regularization that deals with feature selection. There is thus less of a need to remove correlated variables (Elith et al. 2011), as the algorithm ranks the contribution of each during the analysis. The results were projected in QUANTUM GIS 2.2 Valmiera software. To explore the potential occurrence of a species in the past, the models generated under current climatic conditions were projected onto the LGM (21,000 years ago) and interglacial (140,000–120,000 years ago) scenarios. The climatic layers from the past were downloaded from WorldClim for LGM scenarios developed by the Paleoclimate Modelling Intercomparison Project Phase II (Braconnot et al. 2007), the Community Climate System Model (CCSM; Collins et al. 2004), the Model for Interdisciplinary Research on Climate (MIROC; Hasumi & Emori 2004) and, for the interglacial period, we used the layers developed by Otto-Bliesner et al. (2006). The CCSM and MIROC models simulate climatic conditions that were calculated as prevailing during the LGM, however a stronger decrease in temperature is assumed for the CCSM compared to the MIROC model (Otto-Bliesner et al. 2006). For assessing variable importance in each model a jackknife test was performed in MAXENT.

RESULTS

Phylogeography and population genetic structure.—The mitochondrial CO1 gene studied had 630 base pairs, and in the sample of 38 specimens, 7 unique haplotypes were detected (Fig. 2a, b; Table 1; GenBank accession numbers in Appendix 1). No population expansion was detected with the CO1 gene ($R2=0.099$; $P=0.239$). The haplotype network shows that the haplotypes tend to be grouped according to their geographical regions. Haplotype 1 (*Hap1*) was the most abundant in the southern region of the BCP, whereas *Hap2* and *Hap6* were only detected in the northern region of the BCP. Additionally, *Hap3* and *Hap7* were only observed in California (USA), seven mutational steps apart with respect to the remaining haplotypes (Fig. 2a, b; Table 1); this coincides with the geographical separation of clades detected in the phylogenetic analysis (Fig. 3). The AMOVA detected that the Californian locations are different from all the BCP locations ($F_{CT}=0.7$, $P = 0.001$), whereas inside the BCP using another test, no differences were observed between the BC, BCS and LP groups ($F_{CT} = 0.1$, $P = 0.07$) (results not shown). STRUCTURE clustered the seven locations of the BCP into five populations, although genetic mixing exists between them (Fig. 2 c, d), which in north-south latitudinal order are I (Ensenada), II (El Rosarito and Cadejé), III (San Isidro La Purísima and El Novillo), IV (San Pedro de La Presa) and V (Sierra de La Laguna). Pairwise F_{ST} values showed genetic differences between BCP populations (F_{ST} varied from 0.01 to 0.04, $P < 0.001$, Table 2).

Using microsatellite data, the genetic diversity detected was 9.4–17.6 for A/L and between 0.81–0.84 for H_E (Table 2). The Mantel test for the microsatellites ($r = 0.36$, $P = 0.9$), and correlation analyses between latitude and the population heterozygosity ($r = -0.64$, $P = 0.2$), and between latitude and A/L ($r = -0.82$, $P = 0.08$) were not significant. The bottleneck analysis was significant for the Wilcoxon sign-rank test only for northern populations I ($P = 0.03$) and II ($P = 0.03$).

Phylogenetic relationships.—The Bayesian 50% majority-rule consensus tree (Fig. 3) recovered the samples of *P. sierra* as monophyletic ($PP = 1.0$), and sister to *P. atromedia* Banks, 1904 (but with low nodal support; $PP = 0.69$). The sister-groups to *P. sierra* + *P. atromedia* were a polytomic assemblage of taxa including *P. valens* Barnes, 1959, *P. steva* Lowrie & Gertsch, 1955, *P. sura* Chamberlin & Ivie, 1941, and *P. vadosa* Barnes, 1959. Within the *P. sierra* lineage, only two subclades were detected: the California clade (CA) from the USA, and the Baja California Peninsula (BCP) clade from Mexico, each reciprocally monophyletic. This analysis did not detect divergence among populations of *P. sierra* from the BCP (Fig. 3).

Estimation of divergence times.—BEAST analysis using a fossil calibration inferred a divergence date for the separation of the CA clade from the BCP clade of ca. 4 Mya (95% HPD 8.52–1.65 Mya; Fig. 4). The CA clade started diversifying around 1.6 Mya (95% HDP 5.9–0.76 Mya) and the BCP clade around 2.4 Mya (95% HDP 4.3–0.3 Ma). Alternatively, for the

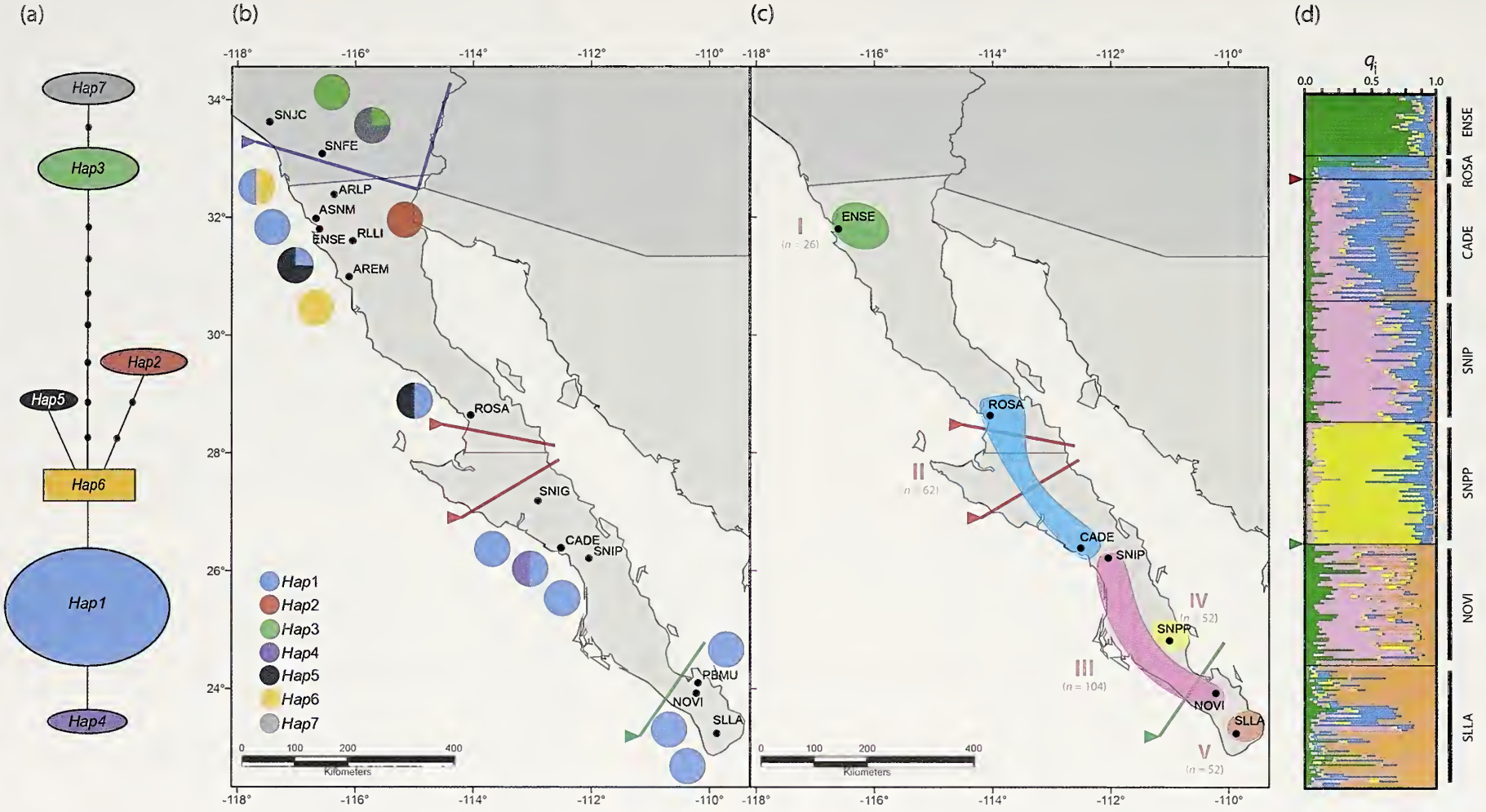

Figure 2.—Phylogeographic pattern and genetic structure of *Pardosa sierra* in the Baja California Peninsula. (a) Statistical parsimony network based on 38 CO1 sequences. The areas of the box and circles are proportional to the haplotype frequency, and each nucleotide substitution between haplotypes is represented by a dot. (b) Latitudinal distribution of seven haplotypes of the mtDNA gene CO1. The acronyms of each collecting site are described in Table 1. (c) Number of genetically homogeneous populations (I–V) detected, using five microsatellite loci in STRUCTURE. Abbreviation (*n*) indicates sample size per population. (d) In the diagram, each horizontal bar represents an individual and each color represents the membership proportion (*qi*) corresponding to each population defined by STRUCTURE. Lines and arrows on the maps indicate the putative channel transgressions of the northern-gulf (*blue* in b), the mid-peninsular Vizcaíno channel (*red* in b, c, and d) and the Isthmus of La Paz (*green* in b, c, and d).

Figure 3.—Bayesian 50% majority-rule consensus tree of mitochondrial CO1 sequences, for populations of *Pardosa sierra* and related Lycosidae. Numbers below the nodes indicate the posterior probability values. BCP = Baja California Peninsula, MEX = Mexico, CA = California, USA. For acronyms of the location of each specimen see Table 1.

Table 2.—Values of genetic differentiation (F_{ST}) estimated by pairs of populations, allelic diversity (A/L), expected (H_E) and observed (H_O) heterozygosity, based on the allelic frequencies of five microsatellite loci of *Pardosa sierra* from the Baja California Peninsula. Values below the diagonal show the pairwise F_{ST} values and above the diagonal are shown the corresponding probability (values *** $P < 0.0001$). I (Ensenada), II (Rosarito-Cadejé), III (San Isidro La Purisima and El Novillo), IV (San Pedro de la Presa), V (Sierra de La Laguna).

	Locations							
	I	II	III	IV	V	*A/L*	H_O	H_E
I	-	***	***	***	***	9.4	0.55	*0.81*
II	0.033	-	***	***	***	13.6	0.58	*0.84*
III	0.044	0.012	-	***	***	17.6	0.62	*0.83*
IV	0.035	0.025	0.037	-	***	14	0.46	*0.82*
V	0.038	0.012	0.020	0.039	-	14.8	0.57	*0.84*

rate-calibrated BEAST analysis, the split between both clades (CA and BCP) was inferred as being much more recent (0.6 Mya; 95% HPD 1.04–0.22 Mya; tree not shown), with diversification from 0.1 Mya (95% HDP 0.23–0.007 Ma) and 0.2 Mya (95% HDP 0.37–0.06 Ma) for the CA and BCP clades, respectively.

Niche-based distribution modeling.—The model projected for the interglacial period (140,000–120,000 years ago) indicated expanded areas of potential habitat in the northern and southern BCP (Fig. 5a). The models CCSM and MIROC projected for the LGM (21,000 years ago) revealed that the potential habitat of *P. sierra* was concentrated in the latitudinal geographic ends of the BCP and that an important wide band of inadequate habitat was projected in the center of the BCP (AUC = 0.75–0.99 for both models; Fig. 5b, c). Currently, the distribution predicted by MAXENT agrees with the known distribution of *P. sierra* (AUC = 0.945; Fig. 5d). The most important climatic variables identified by the

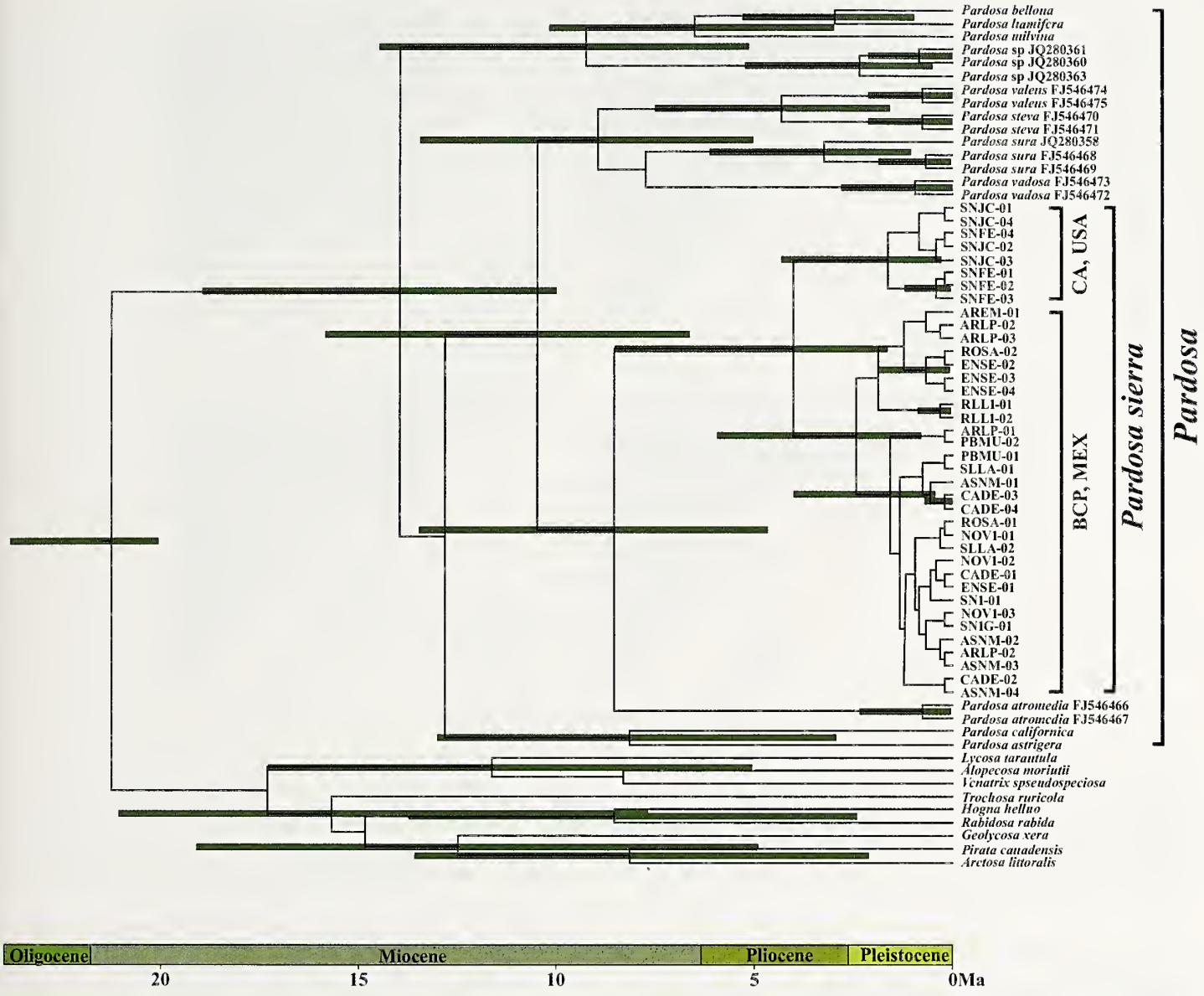

Figure 4.—Fossil calibrated BEAST chronogram of mitochondrial CO1 sequences, for populations of *Pardosa sierra* and related Lycosidae. Green bars indicate the 95% highest posterior density estimates of divergence time for each node. BCP = Baja California Peninsula, MEX = Mexico, CA = California, USA. For acronyms of the location of each specimen see Table 1.

jackknife test (by percentage contribution to the generation of the model) were annual temperature range ($Pc = 58$), precipitation in the driest month ($Pc = 12.8$) and mean diurnal range ($Pc = 8.2$).

DISCUSSION

Phylogeography and population genetic structure.—The observed mitochondrial genetic differentiation of *Pardosa sierra* populations from California versus the rest of the Baja California Peninsula coincides with the occurrence of the alleged vicariance event known as the northern-gulf (Riddle et al. 2000). Similar phylogenetic patterns have also been detected in this region in several vertebrate species, e.g., the toad *Bufo punctatus* (Riddle et al. 2000), the rodent *Thomomys bottae* (Alvarez-Castañeda & Patton 2004), the lizard *Xantusia* sp. (Sinclair et al. 2004) and the boa *Lichanura trivirgata* (Wood et al. 2008). The concordance in phylogeographic signal among these different taxa suggests that they may have responded in parallel to the same underlying process/es (Arbogast & Kenagy 2001; Zink 2002a). Therefore, it is probable that in this region, the northern-gulf vicariance event has influenced the genetic architecture of *P. sierra*. Both clades are reciprocally monophyletic (Avise 2000), and this is most likely due to the occurrence of an ancient barrier (Zink 2002a). However, low migration rate and reinforcement could be alternative explanations for this phylogeographic pattern (Munguía-Vega 2011; Dolby et al. 2015). Another explanation for reciprocal monophyly between clades would be that clade CA constitutes a cryptic species. The morphological characteristics of Californian specimens from this study (color pattern, size and male pedipalp) do not differ from those reported for *P. sierra* (Correa-Ramírez et al. 2010), however the female epigynum shows some variation in its internal

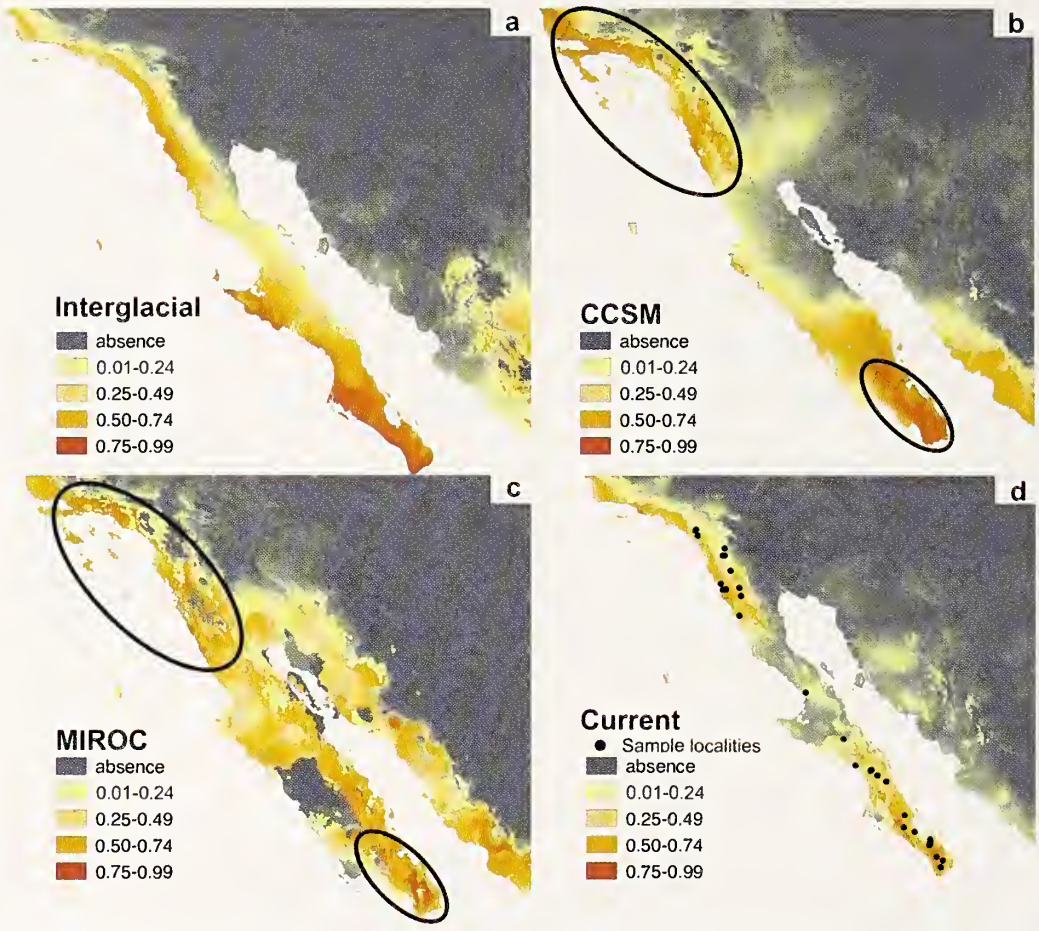

Figure 5.—Niche-based distribution models of *Pardosa sierra*. (a) Model for the last interglacial period (140,000–120,000 years ago). (b) Community Climate System Model corresponding to the last glacial maximum (LGM) 21,000 years ago. (c) Model for Interdisciplinary Research on Climate during the LGM. (d) Actual time model. Colored bars indicate the probability of a favorable habitat for *P. sierra*, with red indicating the highest value. Points in actual model (d) indicate the locations used to generate ENMs, and circles (b and c) indicate potential refugia during the LGM according to AUC = 0.75–0.99 range.

anatomy (i.e., structure of the spermathecae and copulatory ducts); the latter provides some support for a possible cryptic complex, with diversification during the Late Miocene/Early Pliocene (Starrett & Hedin 2006) in *P. sierra*. Indeed, cryptic speciation in spiders has been detected in the same region (Ramirez & Chi 2004), and is potentially explained by high rates of diversification in spiders more generally (Starrett & Hedin 2006). To better delimit species we need to include more individuals and additional molecular markers (i.e., unlinked nuclear genes), perform detailed morphological analyses, and reconcile multiple gene trees (Starret & Hedin 2006) using new statistical methods based as coalescent-theory (Yang & Rannala 2010; Ence & Carstens 2011; Fujita et al. 2012).

Although a phylogeographic break was observed around the mid-peninsular channel and Isthmus of La Paz (Crews & Hedin 2006) in spiders of the genus *Homalonychus* Marx, 1891 (Homalonychidae), in our study phylogeographic breaks were not detected among *P. sierra* populations along the BCP (Fig. 3). These results and a paucity of geological evidence refute the hypothesis of the occurrence of a mid-peninsular channel (Grismer 2002; Murphy & Aguirre-León 2002; Crews & Hedin 2006; Garrick et al. 2009), or if it did exist, it did not have a lasting impact on the genetic structure of *P. sierra* in this region. Indeed, although the signal from the CO1 data did not reveal population expansion, the wide distribution of a single haplotype (*Hap1*), the few haplotypes with restricted distribution (Fig. 2b) and the divergence time inferred (Fig. 4) all suggest that *P. sierra* populations were already present along the BCP at least 2.4 Mya.

Fossil and rate calibrations for divergence date estimation using BEAST resulted in unsurprisingly different estimates of divergence times. We used a relaxed molecular clock model for both analyses, with the fossil calibrated analysis estimating much deeper ages for all nodes. Each method has its limitations, and using substitution rates alone has been criticized due to relaxation of the strict molecular clock in many taxa (Ho & Larson 2006; Ho 2007), and the problems posed by applying substitution rates from other species (Zink 2002b). Meanwhile, the use of fossils to calibrate trees can be erroneous given the uncertainty of geological dating (Magallón 2004) and the incomplete nature of the geological record. In this study, we focus on the results of our fossil calibrated BEAST analysis, which are concordant with phylogeographic splits inferred for other vertebrate taxa (i.e., *Peromyscus eremicus*, *Chaetodipus baileyi*, *Bufo punctatus*) in the northern-gulf around 3 Mya (Riddle et al. 2000).

The genetic structure of *P. sierra*, as detected by microsatellite markers (Fig. 2c, d; Table 2), was not concordant with geographic breaks expected under a model of vicariance along the BCP. Despite the difference in mutation rates between microsatellite molecular markers and CO1 (Hedrick 1999), in this study both markers failed to detect phylogeographic signals related to the mid-peninsular and Isthmus of La Paz channels. This evidence could support the hypothesis that climatic phenomena configured the current genetic architecture of *P. sierra* populations, or that these phenomena erased any mitochondrial genetic signal that might have originated from these vicariance events.

Pleistocene refugia.—The location of Pleistocene refugia depends on how each species responded to the cyclic climate oscillations of this period (Harl et al. 2014). This is evident in the few studies that have focused on identifying potential refugia during the Pleistocene in the Baja California Peninsula. For some plant species, such as totem pole cactus (*Lophocereus schottii*; Nason et al. 2002) and cardon (*Pachycereus pringlei*; Gutiérrez 2015), and some animal species, such as the gnatcatcher *Polioptila californica* (Zink et al. 2000), refugia have been observed towards the south of the peninsula. In contrast, for some arthropod species, the peninsula's central region acted as a refugium (Wilson & Pitts 2012; Graham et al. 2014). In the case of *P. sierra*, two geographic areas located in the north and south end of the peninsula most likely acted as separate refugia (Fig. 5b, c), and these areas coincide with the refugia suggested by Hafner & Riddle (1997). According to the niche-based distribution modeling analysis, *P. sierra* probably occupied a greater geographic range along the BCP during the last interglacial period (140,000–120,000 years ago; Fig. 5a). However, according to the simulation results, when the temperature decreased during the LGM (21,000 years ago), its potential habitat became fragmented. The lack of a relationship between latitude and microsatellite heterozygosity and between latitude and allelic diversity supports the presence of two refugia, because if only one had existed in the south, more genetic diversity would be expected in this region and there would be a gradient of decreasing genetic diversity towards the north (as has been suggested for other species in the BCP; Riddle & Hafner 2006; Valdivia 2014; Gutiérrez 2015). Moreover, the existence of two populations of origin in opposing regions of the BCP could be the reason that a distance isolation structure was not detected.

The presence of greater haplotype diversity in the populations of the north and absence of exclusive haplotypes in the south (Fig. 2b), suggests that southern populations originated from those in the north before the refugia fragmented them. This is consistent with northern haplotypes of CA (*Hap7* and *Hap3*), which are more divergent relative to the other haplotypes (Fig. 2a). The wide distribution of only a single haplotype (*Hap1*) across the peninsula suggests that this could be considered an ancestral haplotype (Avise 2000; Cuenca et al. 2003), derived from northern populations. The fact that *Hap1* is present on opposite sides of the BCP (Fig. 2b) supports the hypothesis that *P. sierra* took refuge in these locations on the peninsula. Likewise, the bottleneck detected using microsatellite loci in populations I and II (Fig. 2c) could explain the low CO1 diversity in the southern populations, given that this region coincides geographically with the area where CO1 transitions to a single haplotype (*Hap1*) from the north toward the south of the peninsula. However the window of time detected by BOTTLENECK software using microsatellite loci is only about ~25–250 generations in accordance with Cornuet & Luikart (1996) and Luikart et al. (1998), therefore it is necessary to analyze genetic markers with low mutation rates to test if a bottleneck could be related to the middle peninsular vicariant event. Finally, the intolerance of *P. sierra* to cold and its sensitivity to changes in rainfall or humidity (Van Dyke & Lowrie 1975) are constraits that limit these spiders to preferentially inhabit areas surrounding water bodies and oases (Punzo & Farmer 2006; Correa-Ramírez 2010; Jiménez et al. 2015). Interestingly, variation in sea levels could be related to changes in the variables that most influenced the potential niche of the species during the Pleistocene (e.g., temperature and humidity), and may therefore be implicated in refugia occurring in more than one area of the BCP. Certainly, if cold intolerance forced *P. sierra* to occupy those disparate areas (Fig. 5b, c), as is likely, then it is plausible that postglacial recolonization processes were accountable for erasing the genetic signal that may have been produced by other vicariance events in the central and southern regions of the Baja California Peninsula.

Based on these data, the northern-gulf channel appears to be the only vicariance event that left a lasting phylogeographic signal in *P. sierra*. This conclusion is supported by strong genetic differentiation between California (USA) populations and those from the Baja California Peninsula. The genetic differentiation patterns revealed by mitochondrial sequences and microsatellites failed to detect genetic breaks in regions where the mid-peninsular and Isthmus of La Paz canals were presumably formed. Two refugia were detected at both ends of the Baja California peninsula during the Pleistocene, specifically between the last interglacial period (140,000–120,000 years ago) and the last glacial maximum period (21,000 years ago).

ACKNOWLEDGMENTS

This work was supported by the Consejo Nacional de Ciencia y Tecnología, México (CONACyT project CB-2008-01-106925) granted to FJGdL. This study was conducted with the partial support of the postdoctoral grant by CONACyT (Agreement 290885) to RGT. Ira Fogel of CIBNOR provided final editing services. The collecting permits were obtained from SEMARNAT: SGPA/DGVS/08331, 2010 and SGPA/DGVS/10182, 2011. We thank Dr. Marshall Hedin for the donation of specimens and field work support, and Dr. Michael Rix and two anonymous reviewers for providing comments that greatly improved the manuscript.

LITERATURE CITED

Aljanabi, S.M. & I. Martinez. 1997. Universal and rapid salt-extraction of high quality genomic DNA for PCR-based techniques. Nucleic Acids Research 25:4692–4693.

Alvarez-Castañeda, S.T. & J.L. Patton. 2004. Geographic genetic architecture of pocket gopher (*Thomomys bottae*) populations in Baja California, Mexico. Molecular Ecology 13:2287–2301.

Arbogast, B.S. & G.J. Kenagy. 2001. Comparative phylogeography as an integrative approach to historical biogeography. Journal of Biogeography 28:819–825.

Avise, J.C. 2000. Phylogeography: The History and Formation of Species. Harvard University Press, Cambridge, Massachusetts.

Benbouza, H., J.M. Jacquemin, J.P. Baudoin & G. Mergeai. 2006. Optimization of a reliable, fast, cheap and sensitive silver staining method to detect SSR markers in polyacrylamide gels. Biotechnology Agronomy Society & Environment 10:77–81.

Braconnot, P., B. Otto-Bliesner, S. Harrison, S. Joussaume, J.Y. Peterschmitt & A. Abe-Ouchi. 2007. Results of PMIP2 coupled simulations of the Mid-Holocene and Last Glacial Maximum – Part 2, feedbacks with emphasis on the location of the ITCZ and mid- and high latitudes heat budget. Climate of the Past 3:279–296.

Brower, A.V.Z. 1994. Rapid morphological radiation and convergence among races of the butterfly *Heliconius erato* inferred from patterns of mitochondrial DNA Evolution. Proceedings of the National Academy of Sciences of the United States of America 91:6491–6495.

Chang, J., D. Song and K. Zhou. 2007. Incongruous nuclear and mitochondrial phylogeographic patterns in two sympatric lineages of the wolf spider *Pardosa astrigera* (Araneae: Lycosidae) from China. Molecular Phylogenetics and Evolution 42:104–121.

Clement, M., D. Posada & K.A. Crandall. 2000. TCS: A computer program to estimate gene genealogies. Molecular Ecology 9:1657–1659.

Collins, W.D., C.M. Bitz, M.L. Blackmon, G.B. Bonan, C.S. Bretherton & J.A. Carton. 2004. The community climate system model, CCSM3. Journal of Climatology 19:2122–2143.

Cornuet, J.M. & G. Luikart. 1996. Description and power analysis of two tests for detecting recent population bottlenecks from allele frequency data. Genetics 144:2001–2014.

Correa-Ramírez, M.M. 2010. Análisis de la diversidad genética de *Pardosa sierra* Banks, 1898 (Araneae, Lycosidae) en la península de Baja California, México. Doctoral thesis, Centro de Investigaciones Biológicas del Noroeste, La Paz, BCS, Mexico.

Correa-Ramírez, M.M., M.L. Jiménez & García-De León. F.J. 2010. Testing species boundaries in *Pardosa sierra* (Araneae, Lycosidae) using female morphology and CO1 mtDNA. Journal of Arachnology 38:538–554.

Crews, S. & M. Hedin. 2006. Studies of morphological and molecular phylogenetic divergence in spiders (Araneae, Homalonychus) from the American southwest, including divergence along the Baja California Peninsula. Molecular Phylogenetics & Evolution 38:470–487.

Cuenca, A., A.E. Escalante & D. Piñero. 2003. Long-distance colonization, isolation by distance, and historical demography in a relictual Mexican pinyon pine (*Pinus nelsonii* Shaw) as revealed by paternally inherited genetic markers (cpSSRs). Molecular Ecology 12:2087–2097.

Dansgaard, W., S.J. Johnsen, H.B. Clausen, D. Dahl-Jensen, N.S. Gundestrup & C.U. Hammer. 1993. Evidence for general instability of past climate from a 250-kyr ice-core record. Nature 364:218–220.

Darriba, D., G.L. Taboada, R. Doallo, R. & D. Posada. 2012. jModelTest 2, more models, new heuristics and parallel computing. Nature Methods 9:772.

Di Rienzo, A., A.C. Peterson, J.C. Garza, A.M. Valdes, M. Slatkin & N.B. Freimer. 1994. Mutational processes of simple-sequence repeat loci in human populations. Proceedings of the National Academy of Sciences of the United States of America 91:3166–3170.

Dolby, G.A., S.E.K. Bennett, Lira-Noriega, A. B.T. Wilder & A. Munguía-Vega. 2015. Assessing the geological and climatic forcing of biodiversity and evolution surrounding the Gulf of California. Journal of the Southwest 57:391–455.

Drummond, A.J., M.A. Suchard, D. Xie & A. Rambaut. 2012. Bayesian phylogenetics with BEAUti and the BEAST 1.7. Molecular Biology & Evolution 29:1969–1973.

Earl, D.A. & B.M. VonHoldt. 2012. STRUCTURE HARVESTER, a website and program for visualizing STRUCTURE output and implementing the Evanno method. Conservation Genetic Resoureres 4:359–361.

Elith, J., S.J. Phillips, T. Hastie, M. Dudík, Y.E. Chee & C.J. Yates. 2011. A statistical explanation of MaxEnt for ecologists. Diversity and Distributions 17:43–57.

Ence, D.D. & B.C. Carstens. 2011. SpedeSTEM: a rapid and accurate method for species delimitation. Molecular Ecology Resourses 11:473–480.

Evanno, G., S. Regnaut & J. Goudet. 2005. Detecting the number of clusters of individuals using the software STRUCTURE: a simulation study. Molecular Ecology 14:2611–2620.

Excoffier, L. & H.E.L. Lischer. 2010. Arlequin suite ver 3.5: A new series of programs to perform population genetics analyses under Linux and Windows. Molecular Ecology Resources 10:564–567.

Fujita, M.K., A.D. Leaché, F.T. Burbrink, J.A. McGuire & C. Moritz. 2012. Coalescent-based speeies delimitation in an integrative taxonomy. Trends in Ecology and Evolution 27:480–488.

Garrick, R.C., J.D. Nason, J.F. Fernández-Manjarrés & R.J. Dyer. 2013. Ecological coassociations influence species' responses to past climatic change, an example from a Sonoran Desert bark beetle. Molecular Ecology 22:3345–3361.

Garrick, R.C., J.D. Nason, C.A. Meadows & R.J. Dyer. 2009. Not just vicariance: phylogeography of a Sonoran Desert euphorb indicates a major role of range expansion along the Baja peninsula. Molecular Ecology 18:1916–1931.

Graham, M.R., R.W. Bryson & B.R. Riddle. 2014. Late Pleistocene to Holocene distributional stasis in scorpions along the Baja California Peninsula. Biological Journal of the Linnean Society 111:450–461.

Graham, M.R., J.R. Jaeger, L. Prendini & B.R. Riddle. 2013. Phylogeography of Beck's desert scorpion, *Paruroctonus becki*, reveals Pliocene diversification in the Eastern California Shear Zone and postglacial expansion in the Great Basin Desert. Molecular Phylogenetics & Evolution 69:502–513.

Grismer, L.L. 2002. A re-evaluation of the evidence for a Mid-Pleistocene Mid-Peninsular seaway in Baja California: A reply to Riddle et al. Herpetological Review 33:15–16.

Gutiérrez, F.C. 2015. Filogeografía y estructura genética poblacional del cardón *Pachycereus pringlei* en el noroeste de México. Doctoral thesis, Centro de Investigaciones Biológicas del Noroeste, La Paz, BCS, Mexico.

Hafner, D.J. & B.R. Riddle. 1997. Biogeography of Baja California peninsular desert mammals. Pp. 39–68. *In* Life Among the Muses: Papers in Honor of James S. Findley. (T.L. Yates, W.L. Gannon, D.E. Wilson, eds.). The Museum of Southwestern Biology. The University of New Mexico, Albuquerque.

Hafner, D.J. & B.R. Riddle. 2005. Mammalian phylogeography and evolutionary history of northern Mexico's deserts. Pp. 225–245. *In* Biodiversity, Ecosystems, and Conservation in Northern Mexico. (J.L.E. Cartron, G. Ceballos, R.S. Felger, eds.). Oxford University Press, Oxford.

Harl, J., M. Duda, L. Kruckenhauser, H. Sattmann & E. Haring. 2014. In search of glacial refuges of the land snail *Orcula dolium* (Pulmonata, Orculidae) — An integrative approach using DNA sequence and fossil data. PLOS ONE 9:e96012. doi:10.1371/journal.pone.0096012.

Hasumi, H. & S. Emori. 2004. K-1 coupled GCM (MIROC) description. Center for Climate System Research, University of Tokyo, Japan.

Hedrick, P.W. 1999. Highly variable loci and their interpretation in evolution and conservation. Evolution 53:313–318.

Hewitt, G.M. 1996. Some genetic consequences of ice ages, and their role in divergence and speciation. Biological Journal of the Linnean Society 58:247–276.

Hewitt, G.M. 2000. The genetic legacy of the Quaternary ice ages. Nature 405:907–913.

Hewitt, G.M. 2004. Genetic consequences of climatic oscillations in the Quaternary. Philosophical Transactions of the Royal Society Series B 359:183–195.

Hijmans, R.J., S.E. Cameron, J.L. Parra, P.G. Jones & A. Jarvis. 2005. Very high resolution interpolated climate surfaces for global land areas. International Journal of Climatology 25:1965–1978.

Ho, S.Y.W. 2007. Calibrating molecular estimates of substitution rates and divergence times in birds. Journal of Avian Biology 38:409–414.

Ho, S.Y.W. & G. Larson. 2006. Molecular clocks: when times are a-changin'. TRENDS in Genetics 22:79–83.

Ho, S.Y.W. & M.J. Phillips. 2009. Accounting for calibration uncertainty in phylogenetic estimation of evolutionary divergence times. Systematic Biology 58:367–380.

Jakobsson, M. & N.A. Rosenberg. 2007. CLUMPP, a cluster matching and permutation program for dealing with label switching and multimodality in analysis of population structure. Bioinformatics 23:1801–1806.

Jensen, L.J., A.J. Bohonak & S.T. Kelley. 2005. Isolation by distance, web service. V3.23. BMC Genetics 6:13. Online at http://ibdws.sdsu.edu/

Jezkova, T., J.R. Jaeger, Z.L. Marshall & B.R. Riddle. 2009. Pleistocene impacts on the phylogeography of the desert pocket mouse (*Chaetodipus peuicillatus*). Journal of Mammalogy 90:306–320.

Jiménez, M.L., I.G. Nieto-Castañeda, M.M. Correa-Ramírez & C. Palacios-Cardiel. 2015. Spiders of the oases in the southern region of Baja California Peninsula, Mexico. Revista Mexicana de Biodiversidad 86:319–331.

Leaché, A.D. & D.G. Mulcahy. 2007. Phylogeny, divergence times and species limits of spiny lizards (*Sceloporus magister* species group) in western North American deserts and Baja California. Molecular Ecology 16:5216–5233.

Librado, P. & J. Rozas. 2009. DnaSP v5, A software for comprehensive analysis of DNA polymorphism data. Bioinformaties 25:1451–1452.

Lindell, J., A. Ngo & R. Murphy. 2006. Deep genealogies and the mid peninsular seaway of Baja California. Journal of Biogeography 33:1327–1331.

Lira-Noriega, A., O. Toro-Núñez, J.R. Oaks & M.E. Mort. 2015. The roles of history and ecology in chloroplast phylogeographic patterns of the bird-dispersed plant parasite *Phoradendron californicum* (Viscaceae) in the Sonoran Desert. American Journal of Botany 102:149–164.

Luikart, G., F.W. Allendorf, J.M. Cornuet & W.B. Sherwin. 1998. Distortion of allele frequency distributions provides a test for recent population bottlenecks. Journal of Heredity 89:238–247.

Magallón, S. 2004. Dating lineages: molecular and paleontological approaches to the temporal framework of clades. International Journal of Plant Sciences 165:S7–S21.

Miller, M.P., S.M. Haig, T.D. Mullins, K.J. Popper & M. Green. 2012. Evidence for population bottlenecks and subtle genetic structure in the yellow rail. Condor 114:100–112.

Molecular Ecology Resources Primer Development Consortium, Abdoullaye, D., I. Acevedo, A.A. Adebayo, J. Behrmann-Godel, et al.2010. Permanent genetic resources added to molecular ecology resources database 1 August 2009–30 September 2009. Molccular Ecological Resources 10:232–236.

Munguía-Vega, A. 2011. Habitat fragmentation in small vertebrates from the Sonoran Desert in Baja California. Ph.D. dissertation, University of Arizona, Tucson.

Murphy, R.W. & G. Aguirre-León. 2002. Nonavian reptiles, origins and evolution. Pp. 181–220. *In* A New Island Biogeography of the Sea of Cortés (T.J. Case, M.L. Cody, E. Ezcurra, eds.). Oxford University Press, Oxford. UK.

Nason, J.D., J.L. Hamrick & T.H. Fleming. 2002. Historical vicariance and postglacial colonization effects on the evolution of genetic structure in *Lophocereus*, a Sonoran desert columnar cactus. Evolution 56:2214–2226.

Otto-Bliesner, B.L., S.J. Marshall, J.T. Overpeck, G.H. Miller & A. Hu. 2006. Simulating Arctic climate warmth and icefield retreat in the Last Interglaciation. Science 311:1751–1753.

Penney, D. 2001. Advances in the taxonomy of spiders in Miocene amber from the Dominican Republic (Arthropoda, Araneae). Palaeontology 44:987–1009.

Phillips, S.J., R.P. Anderson & R.E. Schapire. 2006. Maximum entropy modeling of species geographic distributions. Ecological Modelling 190:231–259.

Piry, S., G. Luikart & J.M. Cornuet. 1999. BOTTLENECK: a computer program for detecting recent reductions in the effective population size using allele frequency data. Journal of Heredity 90:502–503.

Pritchard, J.K., M. Stephens & P. Donnelly. 2000. Inference of population structure using multilocus genotype data. Genetics 155:945–959.

Punzo, F. & C. Farmer. 2006. Life history and ecology of the wolf spider *Pardosa sierra* Banks (Araneae, Lycosidae) in southeastern Arizona. Southwestern Naturalist 51:310–319.

Rambaut, A. & A.J. Drummond. 2007. Tracer v1.5. Online at http://beast.bio.ed.ac.uk/Tracer

Ramirez, M.G. & B. Chi. 2004. Cryptic speciation, genetic diversity and gene flow in the California turret spider *Atypoides riversi* (Araneae: Antrodiaetidae). Biological Journal of the Linnean Society 82:27–37.

Ramos-Onsis, S.E. & J. Rozas. 2002. Statistical properties of new neutrality tests against population growth. Molecular Biology & Evolution 19:2092–2100.

Rice, W.R. 1989. Analysis tables of statistical tests. Evolution 43:223–225.

Riddle, B.R. & D.J. Hafner. 2006. A step-wise approach to integrating phylogeographic and phylogenetic biogeographic perspectives on the history of a core North American warm deserts biota. Journal of Arid Environments 66:435–461.

Riddle, B.R., D.J. Hafner, L.F. Alexander & R.J. Jaeger. 2000. Cryptic vicariance in the historical assembly of a Baja California peninsular desert biota. Proceedings of the National Academy of Sciences of the United States of America 96:14438–14443.

Ronquist, F. & J.P. Huelsenbeck. 2003. MrBayes 3: Bayesian phylogenetic inference under mixed models. Bioinformatics 19:1572–1574.

Rosenberg, N.A. 2004. DISTRUCT: a program for the graphical display of population structure. Molecular Ecology Notes 4:137–138.

Rousset, F. 2008. Genepop'007: a complete reimplementation of the Genepop software for Windows and Linux. Molecular Ecology Resources 8:103–106.

Segurado, P., M.B. Araújo & W.E. Kunin. 2006. Consequences of spatial autocorrelation for niche-based models. Journal of Applied Ecology 43:433–444.

Sinclair, E., R. Bezy, K. Bolles, J. Camarillo, K. Crandall & J. Sites. 2004. Testing species boundaries in an ancient species complex with deep phylogeographic history, genus *Xantusia* (Squamata, Xantusiidae). American Naturalist 164:396–414.

Slatkin, M. 1993. Isolation by distance in equilibrium and non-equilibrium populations. Evolution 47:264–279.

Starret, J. & M. Hedin. 2006. Multilocus genealogies reveal multiple cryptic species and biogeographical complexity in the California turret spider *Antrodiaetus riversi* (Mygalomorphae, Antrodiactidae). Molecular Ecology 16:583–604.

Upton, D. & R. Murphy. 1997. Phylogeny of the side blotched lizards (Phrynosomatidae: *Uta*) based on mtDNA sequences, support for

a midpeninsular seaway in Baja California. Molecular Phylogenetics & Evolution 8:104–113.

Valdivia, C.T. 2014. Filogeografía y modelación de nicho ecológico en la iguana del desierto *Dipsosaurus dorsalis* (Baird y Girard, 1852) en la Península de Baja California. Master's thesis, Centro de Investigaciones Biológicas del Noroeste, La Paz, BCS, Mexico.

Van Devender, T.R. 2002. Deep history of immigration in the Sonoran Desert region. Pp. 5–24. *In* Invasive Exotic Species in the Sonoran Region. (B. Tellman, ed.). The University of Arizona Press, Tucson.

Van Dyke, D. & D.C. Lowrie. 1975. Comparative life histories of the wolf spiders *Pardosa ramulosa* and *P. sierra* (Araneae, Lycosidae). Southwestern Naturalist 20:29–44.

Weir, B.S. & C.C. Cockerham. 1984. Estimating F-statistics for the analysis of population structure. Evolution 38:1358–1370.

Wilson, J.S. & J.P. Pitts. 2012. Identifying Pleistocene refugia in North American cold deserts using phylogeographic analyses and ecological niche modeling. Diversity & Distributions 18:1139–1152.

Wood, D.A., R.N. Fisher & T.W. Reeder. 2008. Novel patterns of historical isolation, dispersal, and secondary contact across Baja California in the rosy boa (*Lichanura trivirgata*). Molecular Phylogenetics & Evolution 46:484–502.

Yang, Z. & B. Rannala. 2010. Bayesian species delimitation using multilocus sequence data. Proceedings of the National Academy of Sciences of the United States of America 107:9264–9269.

Zink, R.M. 2002a. Methods in comparative phylogeography, and their application to studying evolution in the North American aridlands. Integrative & Comparative Biology 42:953–959.

Zink, R.M. 2002b. A new perspective on the evolutionary history of Darwin's finches. The Auk 119:864–871.

Zink, R.M., G.F. Barrowclough, J.L. Atwood & R.C. Blackwell-Rago. 2000. Genetics, taxonomy, and conservation of the threatened California gnatcatcher. Conservation Biology 14:1394–1405.

Manuscript received 2 December 2015, revised 22 June 2016.

Appendix 1.—GenBank accesion numbers of mitochondrial (COI) marker. The species listed were used in phylogenetic analysis for Lycosidae.

Species	GenBank Accesion number
Alopecosa moriutii	AB564729
Arctosa littoralis	JQ280374
Geolycosa xera	DQ151816
Hogna helluo	JQ280373
Lycosa tarantula	KC550668
Pardosa astrigera	AY836055
Pardosa atromedia	FJ546466
Pardosa atromedia	FJ546467
Pardosa bellona	JQ280362
Pardosa californica	JQ280357
Pardosa hamifera	JQ280364
Pardosa milvina	JQ280356
Pardosa sierra Hap1	FJ546464
Pardosa sierra Hap2	JQ280371
Pardosa sierra Hap3	JQ280366
Pardosa sierra Hap4	Fj546465
Pardosa sierra Hap5	KT364484
Pardosa sierra Hap6	JQ280372
Pardosa sierra Hap7	JQ280367
Pardosa steva	FJ546470
Pardosa steva	FJ546471
Pardosa sura	FJ546468
Pardosa sura	FJ546469
Pardosa sura	JQ280358
Pardosa vadosa	FJ546472
Pardosa vadosa	FJ546473
Pardosa valens	FJ546474
Pardosa valens	FJ546475
Pardosa sp	JQ280361
Pardosa sp	JQ280360
Pardosa sp	JQ280363
Pirata canadensis	KF368671
Rabidosa rabida	DQ029232
Trochosa ruricola	AB564731
Venatrix pseudospeciosa	JQ240195

Appendix 2.—Records of *Pardosa sierra* used to generate potential refuges for the Interglacial and during and after the Last Glacial Maximum periods. All data were collected for this study in the states of Baja California and Baja California Sur in Mexico and California in the United States of America.

Location	Lat	Long
USA, CA, Sn. Juan Creek	33.639	−117.422
USA, CA, Sn. Juan Creek 1	33.607	−117.444
USA, CA, Sn. Juan Creek, LakeLand Ville	33.607	−117.444
USA, CA, Margarita Truck Trail	33.454	−117.377
USA, CA, Sn. Felipe Creek	33.066	−116.553
USA, CA, Descanso Town	32.843	−116.605
USA, CA, Pine Creek	32.838	−116.538
México, BC, Arroyo Las Palomas	32.374	−116.355
México, BC, Arroyo Sn. Antonio Minas	31.969	−116.659
México, BC, Arroyo Sn. Salvado	31.853	−116.078
México, BC, Arroyo Sn. Carlos I	31.793	−116.501
México, BC, Arroyo Sn. Carlos II	31.786	−116.505
México, BC, Ensenada	31.783	−116.600
México, BC, Rancho Las Liebres	31.584	−116.033
México, BC, Arroyo El Mejín	30.980	−116.095
México, BC, El Rosarito	28.617	−114.033
México, BCS, Sn Ignacio	27.175	−112.869
México, BCS, Cadejé	26.367	−112.500
México, BCS, Carambuche-Sn. Isidro	26.237	−112.002
México, BCS, Sn. Isidro-La Purísima	26.200	−112.033
México, BCS, Arroyo Sn. José	26.059	−111.820
México, BCS, Arroyo Sn. Javier	25.871	−111.546
México, BCS, Sn. Pedro de la Presa	24.833	−110.983
México, BCS, El Pilar-Las Pocitas	24.472	−111.001
México, BCS, Rancho Camarón	24.320	−110.669
México, BCS, Presa de la Buena Mujer	24.088	−110.191
México, BCS, Playitas	23.986	−110.187
México, BCS, El Novillo	23.917	−110.217
México, BCS, Camino a Sierra de La Laguna	23.550	−109.984
México, BCS, El Chorro, Santiago	23.439	−109.804
México, BCS, Sierra de la Laguna	23.233	−109.867

2016. Journal of Arachnology 44:380–387

The effects of male competition on the expression and success of alternative mating tactics in the wolf spider *Rabidosa punctulata*

Sean De Young and **Dustin J. Wilgers**: Natural Sciences Department, McPherson College, 1600 E. Euclid, McPherson, KS 67460. E-mail: wilgersd@mcpherson.edu

Abstract. Alternative mating tactics are often expressed differentially based on a variety of factors associated with each mating context in order to maximize a male's reproductive success. In particular, males of many species attempt to reduce competition with males in the surrounding environment by altering their mating behaviors. In the wolf spider *Rabidosa punctulata* (Hentz, 1844), males exhibit two distinct mating tactics: 1) courtship—comprised of visual and seismic signals or 2) direct mount—involving males grappling with females for copulation. In natural environments, these spiders are relatively dense. Competing males are often close by and could potentially intercept courtship displays, locate the nearby female and steal the copulation. Here we investigate whether males adjust their mating tactic expression in response to indirect and directly competing males, and whether these decisions affect their likelihood to copulate. In both experiments, the actions of a competing male did not affect the expression of any male mating behaviors in the other, suggesting a lack of an effect of scramble competition on tactic expression. Evidence from our triad mating experiment suggests a mating advantage for males that adopt the direct mount tactic when in direct competition with other males. In particular, direct mounts were most successful when multiple males were actively pursuing a female and when adopted first among the competitors. Additionally, we observed direct male mating interference whereby the copulating pair was broken up. Following these breakups, females were observed to mate multiply, often as a result of a direct mount. This new observation may provide a context in which males benefit through additional copulations by adopting the direct mount tactic.

Keywords: Behavioral plasticity, social environment, intrasexual selection, multiple mating, male interference

Variation in factors intrinsic and extrinsic to the individuals involved has been found to affect female choice and mating probabilities (e.g., female/male age and condition, predators, environment, mate density; Jennions & Petrie 1997). This context-related variable reproductive success has favored the evolution of variable male mating behaviors (i.e., alternative mating tactics) that often vary considerably in form within a species (e.g., court vs. sneak, territorial vs. satellite). In many species, alternative mating tactic expression 1) depends on the context of the mating interaction, and 2) increases a male's reproductive success under these specific situations (reviews in Gross 1996; Brockman 2001). Specifically, tactic expression has been shown to be sensitive to variation in factors that are both intrinsic (e.g., condition, size, age) and extrinsic (e.g., predation, habitat, social environment) to individuals (e.g., Reynolds et al. 1993; Godin 1995; Rezucha & Reichard 2014; Sato et al. 2014; Brockmann et al. 2015). The context(s) that may have shaped the evolution and expression of mating tactics likely varies across species. Thus, in order to understand the conditions that may have favored the evolution of alternative mating tactics, it is important to understand the natural history of a species and the variety of context-specific reproductive benefits of each tactic.

One particularly influential context with regards to mating probabilities is the social environment. When attempting to find a mate, males often find themselves in competition with other males in their immediate vicinity. Male competition for fertilization of limited female eggs can occur at all points during the reproductive process, including pre-copulation scrambles for first access to mate with females, more direct agonistic behaviors and contests, mating interference of copulating pairs, and finally even post-copulation as the sperm collected by females from mating with multiple males compete to fertilize her eggs (Andersson 1994). This intense form of sexual selection has been an important driver of evolution of mating systems and a variety of traits related to reproduction (e.g., male size, ornamentation, weapons, sperm, behavior; Andersson 1994; Shuster & Wade 2003). How and whether this selection will manifest in mating behaviors will depend on when male competition is acting in each system, which will vary based on a species' natural history.

Pre-copulatory male competition for access to females often results in the evolution of variable mating behaviors due to the fitness benefits associated with this plasticity. Males commonly use broadcast courtship displays during courtship (Andersson 1994). The use of these broadcast displays, while known to attract the females they are directed toward, tend to also attract eavesdropping males, thus increasing competition (i.e., social facilitation; Balsby & Dabelsteen 2005; Milner et al. 2010; Clark et al. 2012). Selection should favor any alteration in male behaviors that reduces competition and thus enhances the likelihood of mating. We know that in many cases, males across the animal kingdom alter mating behaviors in response to the social environment in efforts to reduce competition with surrounding males. The presence of competing males is known to alter male courtship activity (reduce: e.g., Cade & Cade 1992; Barnett & Pankhurst 1996; Wong 2004; increase: e.g., Ridgeway & McPhail 1987; Sadowski et al. 2002; Desjardins et al. 2012), match their rival's displays (e.g., Clark et al. 2012), change display location (Dzieweczynski & Rowland 2004), or move to less competitive social networks (Bel-Venner et al. 2008; Oh & Badyaev 2010; Jordan et al. 2014). Across several taxa, males often adopt alternative mating tactics (e.g., sneaker, satellite, female mimic) that circumvent competition with rivals for access to females (e.g., Christenson & Goist 1979; Wagner 1992; Emlen 1997; Evans & Magurran 1999;

Correa et al. 2003; Auld et al. 2015). For example, in the redback spider, *Latrodectus hasselti* Thorell, 1870, when in the presence of rival males, inferior males forgo courtship and aggressive interactions to attempt sneak copulations with females (Stoltz et al. 2008; 2009). While these alternative tactics often achieve lower levels of reproductive success compared to other males (e.g., Christenson & Goist 1979; Whitehouse 1991; Brockman et al. 1994; but see Rowell & Cade 1993; Gress et al. 2014), this behavioral alteration increases individual fitness given the mating context (e.g., male condition, social environment) when compared to other alternatives (i.e., best of a bad job; Dawkins 1980; Gross 1996; examples: Berard et al. 1994; Oh & Badyaev 2010; Jordan et al. 2014). These alternative tactics are a successful strategy as they reduce costs associated with intrasexual competition while gaining copulations with females. The reproductive benefits associated with these behavioral alterations in response to the social environment could have been an important driver in the evolution of alternative mating tactics in many systems (Shuster & Wade 2003; Taborsky et al. 2008).

The mating systems of many wolf spider species are characterized as polygynous scramble competition (Roberts & Uetz 2005), whereby males are competing to locate and mate with relatively monandrous females first (Norton & Uetz 2005). In the wolf spider, *Rabidosa punctulata* (Hentz, 1844) (Araneae: Lycosidae), populations are often quite dense in their grassland habitats, with multiple males often seen in close proximity to a female, suggesting the potential for strong pre-mating scramble competition (Wilgers, pers. obs.). Upon detection of female silk (i.e., a female is/has been in the area), male *R. punctulata* often use a multimodal courtship display, which could increase mate competition if nearby males are eavesdropping. However, male *R. punctulata* are known to adopt alternative mating tactics, forgoing courtship by directly grabbing females and often grappling with them for copulation (Nicholas 2007). Direct mounts achieve copulation faster than courtship without broadcasting the presence of a female first (Wilgers et al. 2009), which could benefit males if competitors are nearby. The expression of these mating tactics has been found to be dependent on other variables, as their expression is sensitive to the male's condition (Wilgers et al. 2009) and the proximity of a predator (Wilgers et al. 2014). In each case, a male expresses the tactic that increases his chance at copulation while limiting the costs associated with that scenario, reducing the risk of cannibalism or potential detection by nearby predators. The potential tactic-specific costs and benefits associated with male-male competition suggest that mating tactic expression should be responsive to the social context of mating encounters as well. Use of the direct mount tactic should increase a male's reproductive success when faced with competing males in the environment by increasing his chance to copulate. Thus, upon detection of rivals, males would be predicted to adopt a direct mount tactic more frequently than courtship.

Here we test these hypotheses by investigating how 1) the social environment influences the mating tactics used during mating interactions, and 2) these mating tactic decisions affect a male's chances to copulate. The results from this study may shed light on how different types of male competition may have played a role in the evolution of alternative mating tactics in *R. punctulata*.

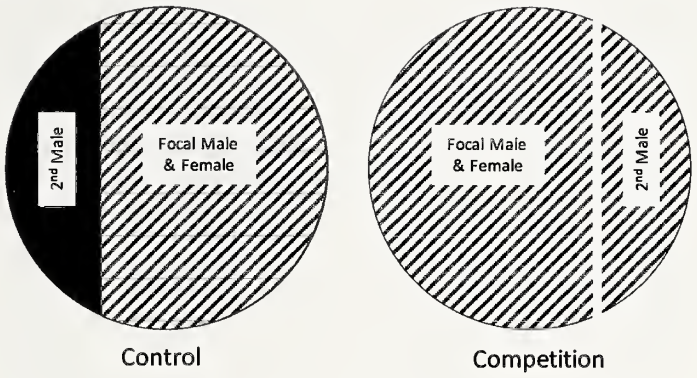

Figure 1.—Trial arenas used to investigate the effects of the presence of competing males on mating tactic expression in *Rabidosa punctulata*. Regions of arena with diagonal pattern indicate areas of floor covered with female-silk laden filter paper. Black regions of the arena indicate a granite arena floor. The barrier between the focal and secondary male compartments did not allow visual contact in either treatment. Arena dimensions: diameter = 20.2 cm, height = 7.3 cm.

METHODS

Spider collection and maintenance.—We collected over 300 immature *R. punctulata* on 23–24 August 2013 from Lancaster County, Nebraska. Upon collection, the spiders were taken to the lab and individually housed in plastic containers (8.4 × 8.4 × 11.0 cm) and were visually isolated from other conspecifics. Spiders were provided with water *ad libitum* and were fed 2–3 body-size matched crickets per week. All crickets were supplemented with Flukers® cricket feed (Port Allen, LA). We placed all spiders in a climate-controlled room (21–24° C) under a 14:10 light-dark cycle. Spiders were checked every 2–3 days for molts until maturation.

Experiment 1: Detection of competing male.—In order to examine how scramble competition may affect mating tactic expression, we tested whether the detection of a courting male alters a male's mating tactic expression when interacting with a female. To do this, we exposed males to one of two treatments: 1) Competition, where a courting male could be detected in the arena, or 2) Control, where no other male was detected. All trials were conducted in circular plastic arenas (Fig. 1; diameter = 20.2 cm, height = 7.3 cm; Pioneer Plastics) with granite floors. Trial arenas were split into two compartments, one for the interacting focal male and female, and the second for a secondary male. The structure of both the competition and control arenas were identical with the exception of the presence of filter paper connecting the focal male and secondary male compartments (Fig. 1). In the control treatment, there was no filter paper on the floor of the secondary male compartment; while in the competition treatment, filter paper (Whatman #1, 185 mm) with female silk cues (see below) lined the entire arena floor. Female silk is known to elicit male courtship displays even in the absence of females (Tietjen 1977). This setup induced the secondary male to court, allowing the focal males in the competition group to detect courting secondary males via seismic cues, but not visual cues, thanks to a connected substrate and opaque arena

walls. Males in the control group could not detect a second male present because the granite substrate effectively ablates the seismic cues caused by male movement, including courtship (Elias et al. 2004; Wilgers & Hebets 2011). Trials were always performed in pairs, consisting of a competition and control trial run simultaneously.

Prior to trials, we weighed all spiders to the nearest .001 g on an electronic scale (Denver Instruments Company, TR-603D). Females were then placed in a container to allow them to acclimate and deposit pheromone-laden silk onto filter paper for at least one hour before the experiment began. After this time period, the filter paper (of appropriate treatment size) was laid in the trial arena and the secondary males were introduced to their arena compartment. Once the competition secondary male began courting, the focal male and female for both treatments were placed into their respective arenas and the trial began.

Trials lasted 30 minutes, or until copulation occurred. If copulation occurred, that individual trial was done, but the other of the pair continued until 30 minutes or copulation occurred. The following behaviors were recorded for every trial: tactic used by the focal male (courtship, direct mount, or mixed tactic where both were used in a trial), latency (s) to each tactic, number of courtship bouts of the focal male, number of courtship bouts of the secondary male (competition treatment only), number of attacks by the female, copulation (yes, no), and latency (s) to copulation. All individuals used in each trial were virgins and had not come into contact with a mature individual of the opposite sex. All individuals were only used once. After each trial, the filter paper was disposed of and the arenas were cleaned with ethanol to remove silk cues and excreta.

Data analysis: We used likelihood ratio tests to analyze the effects of our treatments (competition vs. control) on several categorical response variables, including the overall mating tactic (courtship, direct mount, mixed), the first tactic used (courtship, direct mount), copulation success (yes, no), and the tactic used to gain copulation (courtship, direct mount). We used non-parametric tests to compare the control and experimental groups for the following continuous variables: female age & weight, focal male age & weight, courtship latency, number of courts, and copulation latency. Statistical tests were performed in JMP (version 6.0, SAS Institute). All results are reported as mean ± standard error.

Experiment 2: Direct male competition.—In order to examine how both scramble and direct competition with other males may affect male mating behaviors, tactic expression and mating success, we used a triad mating experiment and observed the mating success of each male based on his expressed tactic. The triad (i.e., 2-choice) mating experiment allowed two males and one female to directly interact. This experimental design has been used in other spider studies that explore mating success based on a variety of male attributes (e.g., size, ornamentation; Hebets et al. 2008; Shamble et al. 2009). Unlike other studies, we did not manipulate male characters or intentionally set up dichotomous males; instead we allowed males to naturally express a mating tactic based on the context and we then observed their success in acquiring the copulation with the sole female. Male ages ranged from 29–54 days post maturation ($\bar{x} = 36.4$ days), and only differed in age in four pairings ($\bar{x} = 0.56$ days). Males were generally the same size, on average only being 0.027 g different, and these differences did not influence mating success (Likelihood ratio, $\chi^2_1 = 0.4$, $P = 0.85$).

All trials were conducted in a circular plastic arena (diameter = 20.2 cm, height = 7.3 cm; Pioneer Plastics) with a floor lined with filter paper (Whatman #1, 185 mm). Prior to trials, all individuals were weighed to the nearest 0.001g on an electronic scale (Denver Instruments Company, TR-603D). Both males were marked with a dot on the dorsal surface of the cephalothorax with either a yellow or white painter's pen (Elmer's® Painters marker) to facilitate individual identification and tracking throughout the trial. Males were gently restrained in a resealable food storage bag and marked through a hole in the bag. Females were introduced to the arena one hour prior to the trial in order to acclimate and deposit pheromone-laden silk. Males were introduced to the trial arena in separate opaque glass vials. After one minute for acclimation, both vials were removed simultaneously and the trial began.

Trials lasted 30 minutes unless copulation occurred. We found interesting interactions after copulation during the first 7 trials, so for the final 20 trials we extended these trials for 10 minutes beyond a copulation to allow the second male to interact with the copulating pair (19/20 copulated). The following behaviors were reeorded for every trial: tactic used by each male, latency (s) to each tactic, number of courtship bouts by each male, number of attempted mounts by each male, number of attacks by the female on each male, copulation (yes/no), and latency (s) to copulation. After a copulation occurred, we recorded the number of break up attempts by the second male, if and when the eopulation was successfully broken up, and if broken up, whether a second copulation occurred, which male acquired this copulation, and the tactic used to gain the second copulation. All individuals used in each trial were naïve virgins. All individuals were used in trials only once. After each trial, the filter paper was disposed of and the arenas and glass vials were cleaned with ethanol to remove silk cues and excreta.

Data analysis: Because we were examining how differences in behaviors of competing males resulted in copulation success, we only included in our analyses trials that resulted in copulation. We used separate likelihood ratio tests to analyze the effects of expressed tactic and competing male behaviors on male copulation success. All other tests were nonparametric. Statistical tests were performed in SPSS (version 21, IBM®). All results are reported as mean ± standard error.

RESULTS

Experiment 1: Detection of competing male.—In total, 36 trials were conducted ($N = 18$/treatment). The focal males used in our experiment were similar across both of the treatment groups in age (Control: $\bar{x} = 36.3 \pm 1.5$ days; Competition: $\bar{x} = 36.0 \pm 1.7$ days; Wilcoxon 2-sample test, $Z = 0.64$, $P = 0.52$) and weight (Control: $\bar{x} = 0.127 \pm 0.007$ g; Competition: $\bar{x} = 0.119 \pm 0.005$ g; Wilcoxon 2-sample test, $Z = 0.32$, $P = 0.75$). Likewise, the secondary males used in each treatment were similar in both age (Control: $\bar{x} = 38.9 \pm 2.8$ days; Competition: $\bar{x} = 37.1 \pm 1.6$ days; Wilcoxon 2-sample test, $Z = 0.24$, $P =$

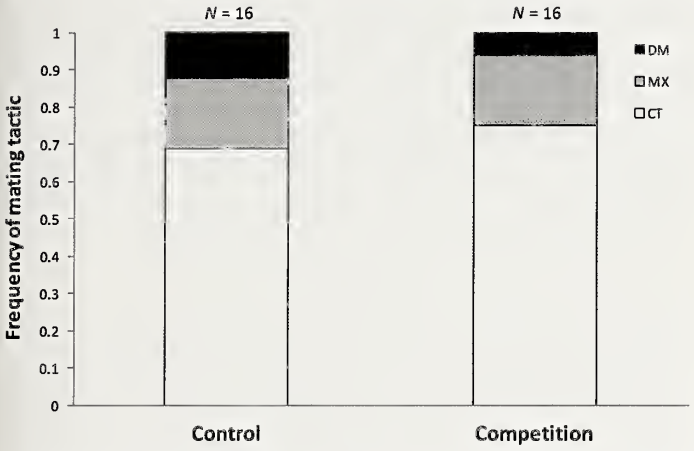

Figure 2.—The effects of competing males on mating tactic expression by male *R. punctulata*. There was no significant difference in the mating tactics expressed between the control and competition treatments ($P = 0.83$). CT= Courtship, DM= Direct Mount, MX= Mixed Tactic.

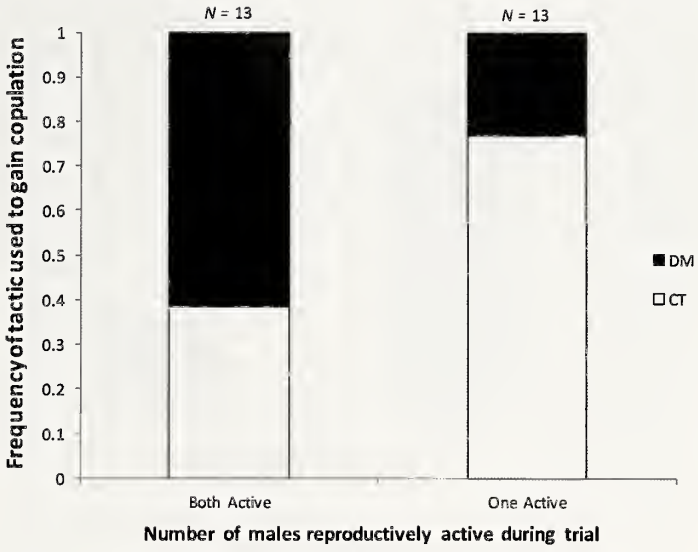

Figure 3.—Mating success of male mating tactics during triad mating trials based on the number of males that were reproductively active. The most successful mating tactic during trials was dependent on the number of males active during the trial ($P = 0.04$). CT= Courtship, DM= Direct Mount.

0.815) and weight (Control: $\bar{x} = 0.115 \pm 0.005$ g; Competition: $\bar{x} = 0.133 \pm 0.008$ g; Wilcoxon 2-sample test, $Z = 1.72$, $P = 0.09$). The females were also similar across both of the treatment groups in age (Control: $\bar{x} = 33.11 \pm 1.54$ days; Competition: $\bar{x} = 32.83 \pm 1.63$ days; Wilcoxon 2-sample test, $Z = 0.19$, $P = 0.85$) but not weight as control females were heavier (Control: $\bar{x} = 0.223 \pm 0.0071$ g; Exposed: $\bar{x} = 0.200 \pm 0.0079$ g; Wilcoxon 2-sample test, $Z = 2.03$, $P = 0.04$).

Exposure to a courting male in the environment did not affect the mating tactic expression of focal males; the frequencies of mating tactics witnessed were similar across our two treatments (Fig. 2; Likelihood ratio, $\chi^2_2 = 0.38$, $P = 0.83$). In four trials, males did not express a mating tactic during the trial. Exposure to a courting male did not affect this non-activity, as they were equally distributed between both treatments ($N = 2$ for control and experimental groups). Similarly, exposing a courting male in the environment did not affect which mating tactic was used first by the focal males; the frequencies of mating tactics witnessed were similar across both treatments (Likelihood ratio, $\chi^2_1 = 0$, $P = 1.0$). Variation in secondary male courtship effort did not affect the mating tactic expression of the focal males in the competition group, as no relationship was detected (Logistic regression; $\chi^2_3 = 2.10$, $P = 0.55$). In addition, both the focal male's latency to courtship (Control: $\bar{x} = 306 \pm 72.22$; Competition: $\bar{x} = 519 \pm 124.6$; Wilcoxon 2-sample test, $Z = 1.00$, $P = 0.32$) and the focal male's number of courtship bouts were similar across both treatments (Control: $\bar{x} = 21.64 \pm 3.97$; Competition: $\bar{x} = 23.53 \pm 15.11$; Wilcoxon 2-sample test, $Z = 0.24$, $P = 0.81$).

The presence of an additional courting male did not affect the likelihood or latency of copulation by the focal male. Both mating frequencies (Control: 61%; Competition: 50%; Likelihood ratio, $\chi^2_1 = 0.45$, $P = 0.50$) and latency to copulate were similar across both treatments (Control: $N = 11$, $\bar{x} = 797 \pm 167$; Competition: $N = 9$, $\bar{x} = 980 \pm 149$; Wilcoxon 2-sample test, $Z = 0.99$, $P = 0.32$). The mating tactics used by the focal males to successfully gain copulations were also similar across both treatments (Control: courtship = 82%, direct mount = 18%; Competition: courtship = 78%, direct mount = 22%; Likelihood ratio, $\chi^2_1 = 0.05$, $P = 0.82$).

Experiment 2: Direct male competition.—In total, 27 trials were conducted, of which 96% resulted in copulation. Males directly interacted with each other during 62% of trials. Male attacks on the other male were common (30% of trials), but not as common as males attempting to mount the other male (42% of trials).

Males expressed some reproductive behaviors in all trials. The frequencies of tactics that were expressed first were not equal ($\chi^2_1 = 15.39$, $P < 0.001$). The most common first tactic used during a trial was courtship ($N = 23/26$). The tactic expressed by the first male did not significantly influence the behavior of the second male (Likelihood ratio, $\chi^2_2 = 4.55$, $P = 0.10$). However, the frequency of male's not adopting a mating tactic tended to be higher following a direct mount (2^{nd} male tactic, $N = 3$: None 100%, Courtship = 0%, Direct Mount = 0%) when compared to after courtship (2^{nd} male tactic, $N = 23$: None = 43.4%, Courtship = 39.1%, Direct Mount = 17.4%). Both males expressed a mating tactic during the trial in 50% of trials ($N = 13$). The most successful tactic at gaining the copulation during a trial depended on how many males were reproductively active (Likelihood ratio, $\chi^2_1 = 4.06$, $P = 0.04$). When only one male was active, courtship was the most successful tactic, as it gained copulations more often; however, when both males were active, the direct mount tactic was more commonly used to acquire the copulation (Fig. 3).

Being the first male to express a tactic affected copulation success in different ways depending on the tactic being expressed. Males that were the first to adopt the direct mount tactic were significantly more likely than their competitor to gain the copulation in the trial (Fig. 4a; $\chi^2_1 = 5.56$, $P = 0.02$). However, males that were the first to adopt courtship were no more likely than their competitor to gain the copulation in the trial (Fig. 4b; Likelihood ratio, $\chi^2_1 = 1.53$, $P = 0.22$). Likewise, differential courtship intensity did not affect mating success,

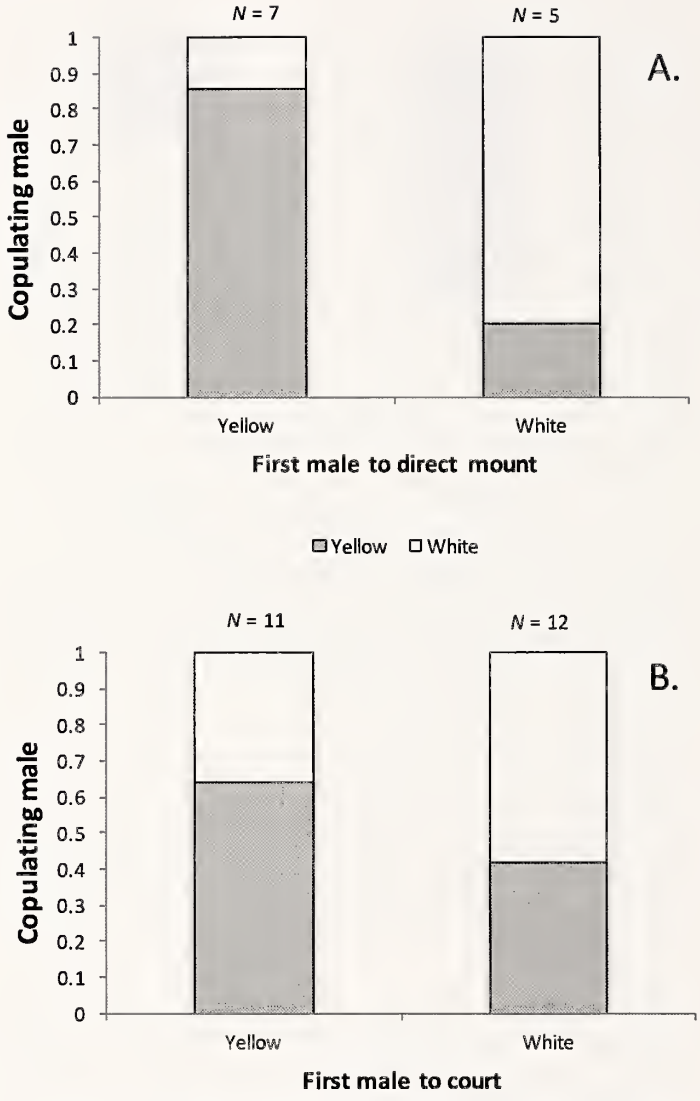

Figure 4.—Mating success of male mating tactics during triad mating trials based on the first male to adopt (A) the direct mount tactic or (B) courtship. The x-axis groups are based on the identification color randomly assigned to each male (yellow or white). The color inside the bars represents the proportion of males in each color that copulated under each circumstance. If order of action affects mating success, one would expect the color of the copulating male to match the color of the first male to act. This occurred in the direct mount tactic ($P = 0.02$), but not in the courtship tactic ($P = 0.22$).

as males that courted more intensely were no more likely to copulate than the other male in the trial (Court More-Copulate Match: 4/7, Court More-Copulate No Match: 3/7; Goodness of Fit, $\chi^2_1 = 0.14$, $P = 0.71$).

Of the 19 trials we observed following copulation, the second male attempted to directly break up the trial in 63% of them, often attempting to break up the pair multiple times ($\bar{x} = 1.89$ / trial overall). Males that attempted to break up the pair were successful in 50% of trials (6/12), with one of those break ups occurring before the initial copulating male inserted a pedipalp for sperm transfer (18 s post 1st male mount). After the pair was broken up, females were remounted for a 2nd copulation 83% (5/6 trials) of the time, with three of those 2nd copulations occurring with the other male in the trial. The tactic used for the first copulation was similar across the females that accepted a second copulation ($N = 3$ courtship, $N = 2$ direct mount). The direct mount tactic was the most successful tactic at gaining the 2nd copulation (80% of attempts; 4/5 trials). The only time a female accepted a courting male for a 2nd mounting was after the mating attempt that was broken up prior to pedipalp insertion.

DISCUSSION

In this study, we found differing effects of indirect and direct male competition on tactic-specific copulation success in *R. punctulata*. Despite this tactic-specific success, males did not alter their mating tactic expression in response to competing males in the environment. We found evidence that when males avoided courtship and took a more direct mating tactic, they had a mating advantage when directly competing with males in the environment, but not when courting males were simply nearby. Using the direct mount tactic increased the likelihood of gaining copulations over the courtship tactic when 1) multiple males in the surrounding environment had expressed some mating behaviors, and 2) when the male was the first one to attempt it. Additionally, we witnessed direct male interference during our trials. In some trials, competing males not only broke up copulating pairs, but would then gain copulations with females, most often by using a direct mount.

When multiple *R. punctulata* males are in close proximity and directly competing for a female, it is clear that engaging the female and using a direct mount tactic offers mating advantages. When directly competing with another male, no aspect of the courtship tactic that we measured increased a male's chance at copulation when competing with other males either indirectly or directly. In other wolf spider species, both the latency to begin courtship (negative relationship) and courtship intensity (positive relationship) have been linked with copulation success (e.g., Scheffer et al. 1996: Shamble et al. 2009). The direct mount tactic appears to be successful at achieving copulations by eliminating one variable that males cannot control, female approach. In *R. punctulata* and another closely related species, *R. rabida* (Walckenaer, 1837), females will approach courting males and often settle receptively (Rovner 1968; Wilgers pers. obs.). By approaching and grabbing females upon detection, males can ensure other males in the surrounding environment will not find her first. This conclusion is supported by the observations that courtship is only successful when one male is reproductively active, allowing more time for the courtship process. Instead, when both males were active, direct mounts were more successful and the male to adopt the direct mount tactic first more often gained the copulation.

The mating advantage associated with direct mounts when in competition with other males does not appear to be a strong enough source of selection to have affected tactic-expression patterns. Across both experiments, we found no evidence of pre-mating male-male competition. Males that were both directly and indirectly competing with males in their environment did not adjust their pre-mating behaviors. This absence of a response to competing males has also been seen in the wolf spider *Schizocosa ocreata* (Hentz, 1844) (Roberts et al. 2006). We also found no evidence of consistent agonistic

behaviors between males. Instead, we found that males mistakenly mounted the competing male as often as they attacked them. In other spider species, males often engage competing males directly with agonistic behaviors (Aspey 1977a, b; Christenson & Goist 1979; Rovner 1996; Uetz et al. 1996); however, evidence that outcomes of these aggressive encounters result in copulation is lacking (Kotiaho et al. 1997; Delaney et al. 2007).

Instead, in *R. punctulata* it appears that male competition comes in the form of male interference during copulations and sperm competition from multiple mating. Interference competition is prevalent in the animal kingdom and males of other spider species have been witnessed to disrupt copulating pairs (e.g., Lubin 1986; Foellmer & Fairbairn 2005). When detected, male *R. punctulata* clearly disrupted the copulating pair and then attempted to mate with the female afterwards. While 80% of second matings during the trial came from direct mounts, due to a limited sample size we were unable to statistically test the differential success of the mating tactics following mating interference. Future studies should more explicitly test the benefits of direct mounts following mating interference. While copulation interference is a striking behavior, it is not clear how common it is in nature, as copulating pairs are not nearly as obvious in their natural environment. In order to estimate its importance in sexual selection, it will be necessary to estimate rates of mating interference in the field.

Our limited results suggest that it may be beneficial for males to adjust their tactic and increase the use of direct mounts following mating pair breakups or already mated females. The only trial in which a female receptively approached a courting male was after a copulation attempt was broken up prior to sperm transfer. Interestingly, females of a closely related species, *R. rabida*, are not only unreceptive to courting males as well, but often very aggressive after mating once (D. Wilgers, unpub. data). Males that are able to assess the mating status of females could benefit from adjusting their mating tactic accordingly by direct mounting already mated and potentially unreceptive females. In the wolf spider *Schizocosa ocreata*, the limited rematings observed often came from more coercive male behaviors (Norton & Uetz 2005). Males of other spider species have been shown to be able to assess female mating status through chemical cues in her silk (e.g., Roberts & Uetz 2005; Stoltz et al. 2007). Future research should investigate if male *R. punctulata* are sensitive to this information during their mating interactions and if they adjust their mating tactic expression accordingly to maximize fitness.

In our study, if given the opportunity to copulate again shortly after mating the first time, females often (> 80%) copulated again. The observation that females will mate multiply is new to the species. Future studies should investigate female mating rates with longer periods of time between mating interactions. When females mate multiply, the scramble competition between males for the only copulation with a female is relaxed, but multiple mating by females introduces another form of male competition, post-copulatory sperm competition, where sperm from multiple males compete to fertilize a limited number of female eggs (Shuster & Wade 2003; examples in spiders: Schneider et al. 2000; Snow et al. 2006). In female spiders, male sperm is stored in the spermethecae, and in some species, females often store sperm from each mating separately, leaving the ability to control sperm release from these independent compartments (Eberhard 2004; Snow & Andrade 2005; Useta et al. 2007). By controlling sperm use post-mating, this more cryptic form of female choice could have dramatic consequences for the fitness of each male she has mated with (Eberhard 1996; examples in spiders: Welke & Schneider 2009; Peretti & Eberhard 2010). Male mating behaviors prior to copulation are known to affect female storage and use of their sperm (Watson 1991). In fact, in other taxa, the use of coercive tactics by males often leads to low fertilization success (e.g., fowl: Pizarri & Birkhead 2000; guppies: Evans & Magurran 2001). However, given the interesting condition-dependent expression and intimate nature of the direct mount tactic (i.e., good-condition males tend to direct mount; Wilgers et al. 2009), female *R. punctulata* could use the direct mounts as a form of assessment in determining the father of her offspring and we may expect a reversal in this sperm use pattern. First male sperm precedence is suggested in wolf spiders (Austad 1984; Rypstra et al. 2003); however, the determinants (e.g., mating order, male qualities) of sperm precedence in this species, which have yet to be determined, may result in reduced benefits of being the first mate (Eberhard 1996). Thus, the benefits of gaining that first mating may no longer outweigh the potential costs of grappling with a cannibalistic female for some males. While this paper only followed copulation success due to tactic-expression, which limits our discussion of tactic-related fitness consequences, it is clear that this mating system has many more questions to answer after the observations suggest more promiscuity than once thought. Investigations into the determinants of cryptic female choice (sperm precedence, male mating behavior, size, etc.) may provide considerable insight into the evolution of these mating behaviors. It is possible the optimal tactic may not depend on the social context, and may instead reflect some other factor associated with the mating interaction (e.g., male condition, female mating status), potentially explaining the lack of males adjusting their mating tactic to a more successful one based on the presence of direct competitors.

ACKNOWLEDGMENTS

Thanks to the Natural Sciences Department of McPherson College for funding this project. Thanks to Jonathan Frye, Allan Ayella, Allan van Asselt, Manjula Koralegedara, Kasey Fowler-Finn, Steven Schwartz and two anonymous reviewers for comments on earlier versions of this manuscript. Thanks to Eileen Hebets for allowing us to collect spiders on her property and to Christian Rodriguez for help in collecting the spiders.

LITERATURE CITED

Andersson, M. 1994. Sexual Selection. Princeton University Press. Princeton.

Aspey, W.P. 1977a. Wolf spider sociobiology. I. Agonistic display and dominance-subordinance relations in adult male *Schizocosa crassipes*. Behaviour 62:103–141.

Aspey, W.P. 1977b. Wolf spider sociobiology. II. Density parameters

influencing agonistic behavior in *Schizocosa crassipes*. Behaviour 62:143–162.

Auld, H.L., S.B. Jeswiet & J.G.J. Godin. 2015. Do male Trinidadian guppies adjust their mating tactics in the presence of a rival male audience? Behavioral Ecology and Sociobiology 69:1191–1199.

Austad, S.N. 1984. Evolution of sperm priority patterns in spiders. Pp. 223–249. *In* Sperm Competition and the Evolution of Animal Mating Systems. (R.L. Smith, ed.). Academic Press, New York.

Balsby, T.J.S. & T. Dabelsteen. 2005. Simulated courtship interactions elicit neighbor intrusions in the whitethroat, *Sylvia communis*. Animal Behaviour 69:161–168.

Barnett, C.W. & N.V. Pankhurst. 1996. Effect of density on the reproductive behaviour of the territorial demoiselle *Chromis dispulis* (Pisces: Pomacentridae). Environmental Biology of Fishes 46:343–349.

Bel-Venner, M.C., S. Dray, D. Allaine, F. Menu & S. Venner. 2008. Unexpected male choosiness for mates in a spider. Proceedings of the Royal Society B 275:77–82.

Berard, J.D., P. Nurnberg, J.T. Epplen & J. Schmidtke. 1994. Alternative reproductive tactics and reproductive success in male rhesus macaques. Behaviour 129:177–201.

Brockman, H.J. 2001. The evolution of alternative strategies and tactics. Advances in the Study of Behavior 30:1–51.

Brockman, H.J., T. Colson & W. Potts. 1994. Sperm competition in horseshoe crabs (*Limulus polyphemus*). Behavioral Ecology and Sociobiology 35:153–160.

Brockmann, H.J., S.L. Johnson, M.D. Smith & D. Sasson. 2015. Mating tactics of the American horseshoe crab. Pp. 321–351. *In* Changing Global Perspectives on Horseshoe Crab Biology, Conservation, and Management. (R. H. Carmichael, M. L. Botton, P. K. S. Shin, S. G. Cheung, eds.). Springer International Publishing, Heidelberg.

Cade, W.H. & E.S. Cade. 1992. Male mating success, calling and searching behaviour at high and low densities in the field cricket, *Gryllus integer*. Animal Behaviour 43:49–56.

Christenson, T.E. & K.C. Goist Jr. 1979. Costs and benefits of male-male competition in the orb-weaving spider, *Nephila clavipes*. Behavioral Ecology and Sociobiology 5:87–92.

Clark, D.L, J. A. Roberts & G.W. Uetz. 2012. Eavesdropping and signal matching in visual courtship displays of spiders. Biology Letters 8:375–378.

Correa, C., J.A. Baeza, I.A. Hinojosa & M. Thiel. 2003. Male dominance hierarchy and mating tactics in the rock shrimp *Rhynchocinetes typus* (Decapoda: Caridea). Journal of Crustacean Biology 23:33–45.

Dawkins, R. 1980. Good strategy or evolutionary stable strategy. Pp. 331–367. *In* Sociobiology: Beyond Nature/Nurture. (G. W. Barlow, J. Silverberg, eds.). Westview Press, Boulder, Colorado.

Delaney, K.J., J.A. Roberts & G.W. Uetz. 2007. Male signaling behavior and sexual selection in a wolf spider (Araneae: Lycosidae): a test for dual functions. Behavioral Ecology and Sociobiology 62:67–75.

Desjardins, J.K., H.A. Hofmann & R.D. Fernald. 2012. Social context influences aggressive and courtship behavior in a cichlid fish. PLoS One 7:e32781.

Dzieweczynski, T.L. & W.J. Rowland. 2004. Behind closed doors: use of visual cover by courting male three-spined stickleback, *Gasterosteus aculeatus*. Animal Behaviour 68:465–471.

Eberhard, W.G. 1996. Female Control: Sexual Selection by Cryptic Female Choice. Princeton University Press. Princeton.

Eberhard, W.G. 2004. Why study spider sex: special traits of spiders facilitate studies of sperm competition and cryptic female choice. Journal of Arachnology 32:545–556.

Elias, D.O., A.C. Mason & R.R. Hoy. 2004. The effect of substrate on the efficacy of seismic courtship signal transmission in the jumping spider *Habronattus dossenus* (Araneae: Salticidae). Journal of Experimental Biology 207:4105–4110.

Emlen, D.J. 1997. Alternative reproductive tactics and male-dimorphism in the horned beetle *Onthophagus acuminatus* (Coleoptera: Scarabacidae). Behavioral Ecology and Sociobiology 41:335–341.

Evans, J.P. & A.E. Magurran. 1999. Male mating behaviour and sperm production characteristics under varying sperm competition risk in guppies. Animal Behaviour 58:1001–1006.

Evans, J.P. & A.E. Magurran. 2001. Patterns of sperm precedence and predictors of paternity in the Trinidadian guppy. Proceedings of the Royal Society B 268:719–724.

Foellmer, M.W. & D.J. Fairbairn. 2005. Competing dwarf males: sexual selection in an orb-weaving spider. Journal of Evolutionary Biology 18:629–641.

Godin, J.G.J. 1995. Predation risk and alternative mating tactics in male Trinidadian guppies (*Poecilia reticulata*). Oecologia 103:224–229.

Gress, B.E., R.J. Waltzer, S. Lupold, E.M. Droge-Young, M.K. Manier & S. Pitnick. 2014. Alternative mating tactics in the yellow dung fly: resolving mechanisms of small male advantage off pasture. Proceedings of the Royal Society B 281: 20132164

Gross, M.R. 1996. Alternative reproductive strategies and tactics: diversity within sexes. Trends in Ecology and Evolution 11:92–98.

Hebets, E.A., J. Wesson & P.S. Shamble. 2008. Diet influences mate choice selectivity in adult female wolf spiders. Animal Behaviour 76:355–363.

Jennions, M.D. & M. Petrie. 1997. Variation in mate choice and mating preferences: a review of causes and consequences. Biological Review 72:283–327.

Jordan, L.A., H. Kokko & M. Kasumovic. 2014. Reproductive foragers: male spiders choose mates by selecting among competitive environments. American Naturalist 183:638–649.

Kotiaho, J., R.V. Alatalo, J. Mappes & S. Parri. 1997. Fighting success in relation to body mass and drumming activity in the male wolf spider *Hygrolycosa rubrofasciata*. Canadian Journal of Zoology 75:1532–1535.

Lubin, Y.D. 1986. Courtship and alternative mating tactics in a social spider. Journal of Arachnology 14:239–257.

Milner, R.N.C., M.I.D. Jennions & P.R.Y. Backwell. 2010. Eavesdropping in crabs: an agency for lady detection. Biology Letters 6:755–757.

Nicholas, A.C. 2007. The evolution of maternal investment among Lycosid spiders and mating behaviors in *Rabidosa punctulata*. Dissertation. University of Mississippi, Oxford.

Norton, S. & G.W. Uetz. 2005. Mating frequency in *Schizocosa ocreata* (Hentz) wolf spiders: evidence for a mating system with female monandry and male polygyny. Journal of Arachnology 33:16–24.

Oh, K.P. & A.V. Badyaev. 2010. Structure of social networks in a passerine bird: consequences for sexual selection and the evolution of mating strategies. The American Naturalist 176:E80–E89.

Peretti, A.V. & W.G. Eberhard. 2010. Cryptic female choice via sperm dumping favours male copulatory courtship in a spider. Journal of Evolutionary Biology 23:271–281.

Pizarri, T. & T.R. Birkhead. 2000. Female feral fowl eject sperm of subdominant males. Nature 405:787–789.

Reynolds, J.D., M.D. Gross & M.J. Coombs. 1993. Environmental conditions and male morphology determine alternative mating behaviour in Trinidadian guppies. Animal Behaviour 45:145–152.

Rezucha, R. & M. Reichard. 2014. The effect of social environment on alternative mating tactics in male Endler's guppy, *Poecilia wingei*. Animal Behaviour 88:195–202.

Ridgeway, M.S. & J.D. McPhail. 1987. Rival male effects on courtship behavior in the Enos Lake species pair of sticklebacks (*Gasterosteus*). Canadian Journal of Zoology 65:1951–1955.

Roberts, J.A. & G.W. Uetz. 2005. Information content of female chemical signals in the wolf spider, *Schizocosa ocreata*: male discrimination of reproductive state and receptivity. Animal Behaviour 70:217–223.

Roberts, J.A., E. Galbraith, J. Milliser, P.W. Taylor & G.W. Uetz. 2006. Absence of social facilitation of courtship in the wolf spider, *Schizocosa ocreata* (Araneae: Lycosidae). Acta Ethologica 9:71–77.

Rovner, J.S. 1968. An analysis of display in the lycosid spider *Lycosa rabida* Walckenaer. Animal Behaviour 16:358–369.

Rovner, J.S. 1996. Conspecific interactions in the lycosid spider *Rabidosa rabida*: the roles of different senses. Journal of Arachnology 24:16–23.

Rowell, G.A. & W.H. Cade. 1993. Simulation of alternative male reproductive behavior: calling and satellite behavior in field crickets. Ecological Modeling 65:265–280.

Rypstra, A.L., C. Wieg, S.E. Walker & M.H. Persons. 2003. Mutual mate assessment in wolf spiders: Differences in the cues used by males and females. Ethology 109:315–325.

Sadowski, J.A., J.L. Grace & A.J. Moore. 2002. Complex courtship behavior in the striped ground cricket, *Allonemobius socius* (Orthoptera: Gryllidae): Does social environment affect male and female behavior? Journal of Insect Behavior 15:69–84.

Sato, Y., M.W. Sabelis & M. Egas. 2014. Alternative mating behavior in the two-spotted spider mite: dependence on age and density. Animal Behaviour 92:125–131.

Scheffer, S.J., G.W. Uetz & G.E. Stratton. 1996. Sexual selection, male morphology, and the efficacy of courtship signaling in two wolf spiders (Araneae: Lycosidae). Behavioral Ecology and Sociobiology 38:17–23.

Schneider, J.M., M.E. Herberstein, F.C. De Crespigny, S. Ramamurthy & M.A. Elgar. 2000. Sperm competition and small size advantage for males of the golden orb-web spider *Nephila edulis*. Journal of Evolutionary Biology 13:939–946.

Shamble, P.S., D.J. Wilgers, K.A. Swoboda & E.A. Hebets. 2009. Courtship effort is a better predictor of mating success than ornamentation for male wolf spiders. Behavioral Ecology 20:1242–1251.

Shuster, S.M. & M.J. Wade. 2003. Mating Systems and Strategies. Princeton University Press. Princeton.

Snow, L.S.E. & M.C.B. Andrade. 2005. Multiple sperm storage organs facilitate female control of paternity. Proceedings of the Royal Society B 272:1139–1144.

Snow, L.S.E., A. Abdel-Mesih & M.C.B. Andrade. 2006. Broken copulatory organs are low cost adaptations to sperm competition in redback spiders. Ethology 112:1–11.

Stoltz, J.A., D.O. Elias & M.C.B. Andrade. 2008. Females reward courtship by competing males in a cannibalistic spider. Behavioral Ecology and Sociobiology 62:689–697.

Stoltz, J.A., D.O. Elias & M.C.B. Andrade. 2009. Male courtship effort determines female response to competing rivals in redback spiders. Animal Behaviour 77:79–85.

Stoltz, J.A., J.N. McNeil & M.C.B. Andrade. 2007. Males assess chemical signals to discriminate just-mated females from virgins in redback spiders. Animal Behaviour 74:1669–1674.

Taborsky, M., R.F. Oliveira & H.J. Brockmann. 2008. The evolution of alternative reproductive tactics: concepts and questions. Pp. 1–22. *In* Alternative Reproductive Tactics: An Integrative Approach. (R. F. Oliveira, M. Taborsky, H. J. Brockmann, eds.). Cambridge University Press. Cambridge, United Kingdom.

Tietjen, W.J. 1977. Dragline-following by male lycosid spiders. Psyche 84:165–178.

Uetz, G.W., W.J. McClintock, D. Miller, E.I. Smith & K.K. Cook. 1996. Limb regeneration and subsequent asymmetry in a male secondary sexual character influences sexual selection in wolf spiders. Behavioral Ecology and Sociobiology 38:253–257.

Useta, G., B.A. Huber & F.G. Costa. 2007. Spermathecal morphology and sperm dynamics in the female *Schizocosa malitiosa* (Araneae: Lycosidae). European Journal of Entomology 104:777–785.

Wagner Jr., W.E. 1992. Deceptive or honest signaling of fighting ability? A test of alternative hypotheses for the function of changes in call dominant frequency by male cricket frogs. Animal Behaviour 44:449–462.

Watson, P.J. 1991. Multiple paternity as genetic bet-hedging in female sierra dome spiders, *Linyphia litigiosa* (Linyphiidae). Animal Behaviour 41:343–360.

Welke, K. & J.M. Schneider. 2009. Inbreeding avoidance through cryptic female choice in the cannibalistic orb-web spider *Argiope lobata*. Behavioral Ecology 20:1056–1062.

Whitehouse, M.E.A. 1991. To mate or fight? Male-male competition and alternative mating strategies in *Argyrodes antipodiana* (Theridiidae, Araneae). Behavioural Processes 23:163–172.

Wilgers, D.J. & E.A. Hebets. 2011. Complex courtship displays facilitate male reproductive success and plasticity in signaling across variable environments. Current Zoology 57:175–186.

Wilgers, D.J., A.C. Nicholas, D.H. Reed, G.E. Stratton & E.A. Hebets. 2009. Condition-dependent alternative mating tactics in a sexually cannibalistic wolf spider. Behavioral Ecology 20:891–900.

Wilgers, D.J., D. Wickwire & E.A. Hebets. 2014. Detection of predator cues alters mating tactics in male wolf spiders. Behaviour 151:573–590.

Wong, B.B.M. 2004. Male competition is disruptive to courtship in the Pacific blue-eye. Journal of Fish Biology 65:333–341.

Manuscript received 17 December 2015, revised 17 June 2016.

2016. Journal of Arachnology 44:388–396

Exceptionally short-period circadian clock in *Cyclosa turbinata*: regulation of locomotor and web-building behavior in an orb-weaving spider

Darrell Moore[1], **J. Colton Watts**[1,2], **Ashley Herrig**[1] and **Thomas C. Jones**[1]: [1]Department of Biological Sciences, East Tennessee State University, Box 70703, Johnson City, TN 37614 USA. E-mail: jonestc@etsu.edu; [2]School of Biological Sciences, University of Nebraska, Lincoln, NE 68588-0118 USA

Abstract. A major advantage of having behavior controlled by a circadian clock is that the organism may be able to anticipate, rather than respond to, important daily events in its environment. Here, we describe the behavioral rhythms of locomotor activity and web building in the orb-weaving spider *Cyclosa turbinata* (Walckenaer, 1841). Web building occurs late in the scotophase, in absolute darkness, and is initiated and completed before lights-on under light:dark cycles in the laboratory. This scheduling presumably enables web-building to occur under the cover of darkness, thereby avoiding visual predators. Locomotor activity occurs predominantly in the dark with a sharp peak within one hour after lights-off and a broader peak occurring before lights-on. The locomotor activity rhythm free runs under constant dark and constant temperature conditions, thus indicating endogenous circadian control. Evidence from the free running rhythm suggests that the first peak under light:dark cycles is a result of masking but that the second peak is attributable to the endogenous circadian oscillator. The period of the free run is exceptionally short, about 19 hours. In comparison with locomotor activity, web building is quite sporadic under constant dark conditions, making detection of periodicities difficult and, therefore, whether web-building is under endogenous circadian control or is driven by exogenous factors remains unresolved.

Keywords: Behavioral rhythm, chronoecology, locomotor activity, adaptation

It is commonly assumed that circadian rhythms are adaptive, enabling the organism to perform each of its various functions, including behavior, at the most appropriate time of day with respect to its environment. In many cases, the possession of a circadian clock empowers the organism with the ability to anticipate important daily events in its ecosystem, such as the occurrences of food, potential mates, and predators. In the flying squirrel, for example, the circadian clock controls the emergence of this nocturnal animal from its den shortly before dark, allowing the squirrel to begin its activity in accord with a particular light intensity after sunset (DeCoursey 1989). Forager honey bees rely on a continuously-consulted circadian clock that allows them to remember the time of day of previously productive floral food sources (Beling 1929; Wahl 1932), thereby providing a mechanism to match foraging behavior with nectar secretion rhythms. A prominent feature of this honey bee 'time memory' is that foragers typically anticipate the previously rewarded time of day by making reconnaissance flights to the food source (Moore & Doherty 2009). Because the initial encounter of a forager with a new nectar source may not occur at the onset of a particular flower species' nectar availability, early investigative flights on subsequent days may be adaptive by scheduling foragers to arrive earlier within the window of opportunity (Van Nest & Moore 2012). More direct support for the adaptive significance of circadian rhythms is provided by Spoelstra et al. (2016) who showed that mice with short period circadian rhythms (via the *tau* mutation) released into outdoor enclosures showed reduced survivorship and reproduction relative to wild-type animals and Woelfle et al. (2004) who demonstrated that cyanobacterial strains with functioning circadian clocks outcompeted clock-disrupted strains in rhythmic environments.

For any spider, there is a precarious balancing act between the need to be aggressive enough to capture prey, yet wary enough to avoid predation. The relative expression of these two opposing behavioral states is expected to vary in accordance with daily changes in environmental conditions. Orb-weaving spiders are well-established models for ecological studies including consequences of habitat choice (reviewed by Riechert & Gillespie 1986), prey capture efficiency (reviewed by Eberhard 1986), and group foraging (reviewed by Uetz & Hieber 1997). Orb-weaving spiders have different temporal foraging patterns across species. Most are nocturnal, building their webs in the evening and foraging through the night, then leaving the web for a hideaway during the day. In *Larinioides cornutus* (Clerck, 1757), a night-foraging orb-weaver, there is a circadian clock-controlled partitioning of the antipredator 'huddle response' such that spiders are significantly more defensive during the day than during the night (Jones et al. 2011). Some species build webs and forage diurnally, while other species forage continuously around-the-clock. However, it is widely believed that the reason most orb-weaving species are nocturnal is to avoid diurnal predators such as birds and wasps (Cloudsley-Thompson 1958). In fact, many of the relatively few diurnal species have adaptations to avoid bird predation, such as abdominal spines or foul-tasting guanine deposits (Cloudsley-Thompson 1995). While reduced exposure to predators may be an advantage to the nocturnal behavioral phenotype, there may be associated costs including reduced prey density at night, shortened foraging periods in summer months, and increased competition with other spiders (Wise 1993). Continuous foragers perhaps may be so prey-limited that they are forced to forage around-the-clock.

Cyclosa turbinata (Walckenaer, 1841) is a small (4–7 mm) orb-weaving spider which forages in its web both day and night. Prey carcasses are incorporated into the web, forming a "trashline" which functions as daytime camouflage to avoid visual predators such as birds and wasps (Tseng & Tso 2009; Gan et al. 2010). While the trashline attracts attacking wasps,

they are usually unable to locate the spider resting upon it (Chou et al. 2005). For orb-weaving spiders, the timing of daily web-replacement is particularly important because the web's prey capture effectiveness declines with the passage of time after construction (Foelix 1996) and movements associated with web replacement may attract visual predators (Rypstra 1982). Although prey may land on the web at all times of day, data from lakeside habitats suggest that prey abundance increases over the course of the afternoon and peaks early in the night (Watts et al. 2015). In webs constructed under laboratory conditions, *C. turbinata* individuals exhibit the highest levels of foraging aggression during the night and early morning. Surprisingly, this behavioral state coincides with the time of day in which the spider has the highest probability of retreating from simulated predator attacks (Watts et al. 2014). The lowered probability of retreating during most of the daylight hours suggests a greater reliance on a passive antipredator strategy (remaining immobile, using the trashline as camouflage) compared to the more active strategy of fleeing from the web hub or dropping from the web. Taking into account all of these behavioral tendencies, we hypothesize that *C. turbinata* schedules its daily routine so as to replace its web under the cover of darkness, allowing enough time for completion of the building process before dawn, yet close enough to dawn so as to maintain the web's capture effectiveness as prey density increases over the course of the day.

The primary objective of the present study is to describe the exact timing of web replacement behavior in *C. turbinata* with respect to light:dark cycles and then to determine the mechanism by which this temporal phasing is controlled. Spiders have been shown to rely on circadian clocks to regulate a variety of behaviors and physiological processes (Seyfarth 1980; Schmitt et al. 1990; Suter 1993; Yamashita & Nakamura 1999; Ortega-Escobar 2002; Jones et al. 2011). However, current evidence from nocturnal orb-weavers under laboratory (Ramousse & Davis 1976) and natural (Ceballos et al. 2005) conditions as well as from a diurnal orb-weaver during a total solar eclipse (Uetz et al. 1994) suggests that web-building may respond directly to light conditions, rather than be controlled by an endogenous, light-entrainable circadian rhythm. If the phasing of web replacement behavior is under circadian clock control, then the diel behavioral rhythm should continue (free run) with the period of the underlying clock under constant conditions. Alternatively, if web replacement behavior is controlled exogenously (i.e., it responds directly to changes in light levels), then web-building behavior should occur immediately (or shortly) after dusk or dawn, and the diel rhythm, absent the need for circadian control, should not persist under constant dark conditions. In order to interpret these patterns in an ecological context, we also quantify diel patterns of prey and threat abundance in typical *Cyclosa* habitat.

METHODS

Study species.—Adult female *Cyclosa turbinata* (Araneae: Araneidae), commonly found along the edges of forested areas in the southeastern United States, were collected in Washington County, Tennessee in 2012, 2013, and 2015. Spiders were collected with their webs and trashlines and maintained in plastic deli containers. Care of the animals followed ASAB/ABS guidelines, and the animals were released following experiments.

Locomotor activity.—Locomotor activity was recorded continuously. Individual spiders were placed in 25 mm diameter X 100 mm length, clear plastic tubes and inserted into a locomotor activity monitor (model LAM) from Trikinetics, Inc. (Waltham, Massachusetts). Activity within each tube was measured via interruption of three infrared beams transmitting through the center of the tube: each interruption was registered as an event. To minimize possible visual interactions among the spiders placed in close or adjoining positions, the tubes containing the spiders were painted opaque white along their lengths, except for a small, central band allowing for transmission of the infrared light. Screen was fastened to each end of the tube and, on one end, water was available ad libitum via a cotton-plugged, flexible tube (10 mm diameter) projecting through the screen. Events were counted in 6-min bins and analyzed using Clocklab Analysis Software (Actimetrics, Wilmette, IL, U.S.A.). Activity was depicted graphically by double-plotted actograms to facilitate visual recognition of periods. Significant periods were detected using two different periodogram analyses, chi-square and Lomb-Scargle. The chi-square periodogram (Sokolove & Bushell 1978) is broadly applicable for analyzing circadian data. The Lomb-Scargle periodogram, using a form of Fourier spectral analysis, is better suited to analyze records with large or frequent gaps (Van Dongen et al. 1999). The use of these two complementary methods, rather than just one, provides additional support for determinations of period. Because of the sparse nature of activity bouts exhibited by the spiders, especially with respect to web-building behavior, we accepted circadian periodicities only if indicated by both methods.

Two different sets of spiders were tested. The first set was captured in August 2012. These spiders were monitored in a temperature-controlled environmental chamber (25 ± 0.5 °C) under a light-dark cycle containing 12 hours of light and 12 hours of dark (LD 12:12) for five days and then under constant darkness (DD) thereafter. Lights-on occurred at 08:00 h and lights-off at 20:00 h. Light during photophase was provided by four vertically mounted, 32 W fluorescent tubes and the illuminance was approximately 1400–1600 lux at the level of the activity monitor. Spiders from the second set were captured in August 2015, entrained under a ramping light:dark cycle (see below) for two weeks in the laboratory at 25 °C, the last two days of which were in the activity monitor. Recordings started on day 2 of constant dark conditions. Unlike the spiders from the 2012 collection, these spiders were not provisioned individually with water tubes but were housed in a laboratory room under high humidity conditions.

Web-building activity.—To determine the phasing of web-building behavior with respect to a light:dark cycle, individuals were maintained in 30 × 30 x 10 cm wooden frames (Watts et al. 2014) in the laboratory under either a hard (N = 8) or ramping (N = 10) LD 12:12 h cycle. The ramping cycle was employed as a more accurate simulation of natural conditions. For the hard LD 12:12 cycle, lights-on occurred at 07:00 h and lights-off at 19:00 h. For the ramping LD cycle, the dark-to-light transition began at 07:00 h and was

completed at 08:00 h; the light-to-dark transition likewise took place over one hour and began at 19:00 h. Therefore, in the hard LD cycle, spiders were exposed to light (at a continuous 1000–1200 lux) for 12 hours. In the ramped LD cycle, spiders were exposed to continuous light (1000–1200 lux) for 11 hours, flanked at the beginning and end with 1-hour periods of gradually increasing or decreasing light levels.

Spiders used in the hard LD 12:12 cycle were collected in August 2012 and maintained individually in 110 ml plastic "deli" containers for 5 days under LD 12:12 conditions. They were then moved to the wooden frames and the frames were wrapped in clear plastic food wrap, enabling web construction to occur overnight. On the day after transfer to the frames, the plastic wrap was removed and each spider was fed two *Drosophila hydei*. Behavior was then video-recorded at 6 frames/s for the next 5 days under the same light:dark cycle at 23 °C using surveillance cameras equipped with infrared night vision (Q-SEE QT9316 and Defender SP-301).

Spiders used in the ramping LD 12:12 cycle were collected in July and August of 2013 and were transferred directly to the wooden frames or kept in deli containers. Spiders not building a web within two days were replaced with spiders from the deli containers. All web-building spiders were acclimated to the ramping LD 12:12 cycle for at least 5 days and then tested in their webs for their foraging and antipredator behavior (Watts et al. 2014) from 11–21 August 2013. On 21 August, the spiders were misted with water and fed two termites. On the following day, they were misted but not fed. Then, on 23 August (day 1 of the experiment), the behavior was video-recorded at 6 frames/s under the ramping LD 12:12 cycle at 23 °C for 5 days and then for 12 days under constant dark conditions. The spiders were misted and fed two termites every three days (thereby preventing entrainment to the feeding event), beginning on day 4. Web-building aetivity (either present or absent) was binned in 6-min increments and analyzed, as with locomotor activity, with ClockLab Analysis Software.

Diel patterns of prey and threat density.—We used a malaise trap (Bugdorm SLAM Trap- Standard 110x110x110 cm) to sample flying insect densities over the diel cycle. The trap was placed in typical *Cyclosa* habitat along a mowed path between an old field and shrubline, in Washington County, Tennessee, USA. The contents of the trap were emptied every three hours, and trapping continued for three consecutive days in June 2014 during which there was no rain. Between 24-hour cycles, the trap was moved to a new location 25 m along the path. The collected insects were identified to order, and their body lengths were measured to the nearest mm. While there are no data on specific predators of *C. turbinata*, Chou et al. (2005) found that wasps frequently attack other species of *Cyclosa*. Thus, we considered wasps to be potential threats, and non-wasp insects under 15 mm to be potential prey.

RESULTS

Locomotor activity.—Thirteen *C. turbinata*, captured in 2012, performed locomotor activity though all 5 days of the LD 12:12 cycle. We calculated DiNoc ratios as: daytime activity – nighttime activity/ total activity (Suter & Benson 2014). All of the spiders' ratios were below 0 (mean = –0.79, SD = 0.26) indicating predominantly nighttime activity, with

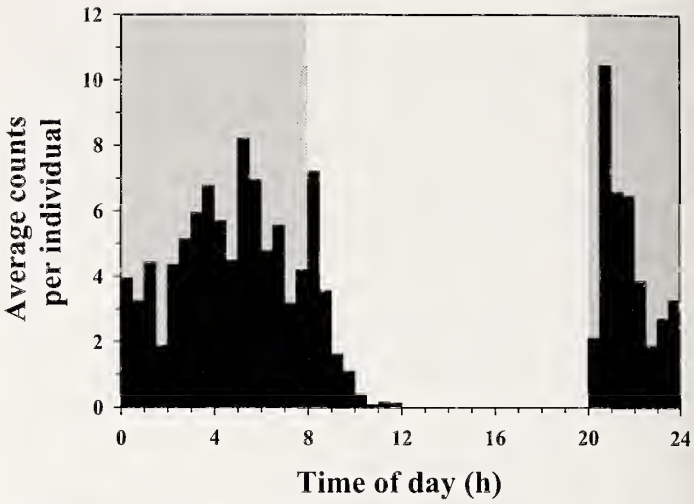

Figure 1.—Entrainment profile for locomotor activity in *C. turbinata*, illustrating average counts (interruptions of the infrared beam) per individual throughout the day, in 30-min intervals, for the last four days of the LD 12:12 h cycle. Dark background indicates dark portion of LD cycle.

two showing exclusively nighttime activity. The entrainment profile (Fig. 1) illustrates this nocturnality plus several additional trends. First, locomotor activity had a prominent peak occurring within one hour after lights-off, followed by a gradual build-up in activity through the scotophase, reaching a second, broader peak at about 05:00. The activity then declined through the remainder of the scotophase, extending into the first 4 h of the photophase, interrupted briefly by a sharp peak occurring immediately after lights-off. There was absolutely no activity during the last 8 hours of the photophase.

Ten spiders continued to show locomotor activity under constant dark conditions for at least 5 days after discontinuation of the LD cycle. Nine of these exhibited a robust, free-running rhythm with a significant and consistent period as revealed by chi-square and Lomb-Scargle periodogram analyses (Table 1). The mean free-running period, based on the chi-square periodograms, was 18.74 ± 0.13 h (SEM) for these spiders. In one case (Ct-10, Table 1), the periodogram analyses yielded significant, but different periods and, therefore, this individual was not used in the determination of mean free-running period. In another individual (Ct-13, Table 1), the chi-square periodogram indicated two significant periods (28.8 and 19 h) and the Lomb-Scargle identified only one (19.1 h). Because it was detected by both analyses, we accepted the 19 h rhythm in our calculation of mean free-running period.

Actograms and accompanying periodograms (Fig. 2) illustrate the nocturnality under the LD 12:12 h cycle and the extremely short endogenous periodicities of locomotor activity expressed by individual spiders under DD conditions. In individual Ct-17 (Fig. 2a), there is a predominance of activity during the scotophase of the LD cycle, especially during the second half of the night. Under DD, this spider exhibited a very short circadian rhythm of about 18.8 h, confirmed by the chi-square periodogram (Fig. 2a). The activity performed during each circadian cycle was restricted

Table 1.—Chi-square and Lomb-Scargle periodogram analyses of locomotor activity rhythms under DD. Indicated are the free-running periods under DD conditions (τ_{DD}), in hours, that were significant at $\alpha = 0.001$ (with two exceptions at $\alpha = 0.05$, indicated in parentheses). The first 10 individuals were captured in 2012; the last 5 in 2015.

	τ_{DD}	
Identity	chi-square	Lomb-Scargle
Ct-03	19	18.75
Ct-06	18.9	19.1
Ct-07	17.8	18.1
Ct-08	19	19.55
Ct-10	31.2	15.7
Ct-13	19, 28.8	19.15
Ct-14	18.4	18.65
Ct-16	18.8	18.75
Ct-17	18.8	18.8
Ct-19	19	18.7
CtF15-M1	19.8, 26.6	27.2 (0.05)
CtF15-M2	17.9	18.4
CtF15-M3	19	—
CtF15-M4	20	—
CtF15-M7	17.5	18.85 (0.05)

to short bouts of activity, ranging from about 1–4 h in duration. Individual Ct-14 exhibited sporadic, predominantly nocturnal activity under the LD 12:12 h cycle and a very short circadian rhythm of about 18.4 h in DD (Fig. 2b). Extrapolation back from the sequential onsets of activity in both actograms indicates that the free-running activity originated in late scotophase, suggesting that the nocturnal activity during this phase is under circadian control.

The free-running locomotor rhythms of an additional five *C. turbinata*, captured in August 2015, were recorded in the activity monitors under constant dark conditions at 25 °C in the laboratory (Table 1). Although all five showed significant periods in the range of 17.5 to 20 h according to chi-square periodograms, only two (CtF15-M3 at 17.9 h and CtF15-M7 at 17.5 h) were confirmed as significant by similar periods (18.4 and 18.85 h, respectively) according to the Lomb-Scargle method (Table 1).

Web-replacement behavior.—The mean onset time for the first component of web-building behavior, radial thread maintenance, occurred at 03:58 h ± 8 min (SEM) under the hard LD 12:12 cycle and 04:41 h ± 16 min (SEM) under the ramping LD 12:12 cycle (Fig. 3). These onset times were significantly different (T-test, $t = -2.31$, $df = 28$, $P = 0.029$). For the second component of web building, sticky spiral replacement, the mean start times under the hard (04:55 h ± 7 min) and ramping (04:59 h ± 11 min) LD cycles were not significantly different (T-test, $t = -0.32$, $df = 31$, $P = 0.751$).

The length of time required to complete both components of web building, for individuals that completed both components, was 118.9 ± 9.5 min (SEM) and 84.5 ± 7.9 min (SEM) under the hard and ramping LD cycles, respectively. Overall, the mean duration of web-building behavior was 103.6 ± 6.9 min (SEM).

Analyses of web-building behavior at the level of the individual spider were accomplished by the use of actograms depicting the occurrence or absence of web-building behavior (both radial thread maintenance and sticky spiral replacement) compiled in 6-min bins throughout the day for the duration of the experiment. Of the eight spiders exhibiting web-building behavior during DD, five performed this behavior only twice during the 12 days of DD and, therefore, were not used for determinations of circadian period. The remaining three individuals provided temporally sparse records under both LD and DD, illustrated by the actograms. For example, spider Ct-web 5 rebuilt its web (in late scotophase) only on days 2 and 3 during the five days of LD entrainment but reconstructed its web on all but one day under DD (Fig. 4a). This activity showed three significant periods (19.6, 26.1, and 29.2 h) according to the chi-square periodogram during the 12 days of DD but different periods were indicated by the Lomb-Scargle method (Table 2). Similarly, spider Ct-web 8 rebuilt its web only once during LD entrainment (again, during late photophase) but skipped only two days during its 12-day tenure under DD (Fig. 4b). Periodogram analyses (Table 2) confirmed three significant periods (18.5, 23.8, and 27.8 h). A third individual, Ct-web 7 (not shown), in accord with the previous two examples, showed web-building behavior on just one day under LD but on 10 days under DD. Periodogram analyses indicated two (chi-square) or three (Lomb-Scargle) significant periods for this activity under DD (Table 2).

Diel patterns of prey and threat density.—In the pooled three days of malaise trap sampling of potential prey and threats (Fig. 5), the distributions of trapped insects were clearly not random and were concentrated in the photophase (prey Chi-square = 131.2, d.f. = 7, $P < 0.001$; wasp Chi-square = 20.5, d.f. = 7, $P = 0.005$). In general, there were more potential prey trapped than potential threats. Also, the diel pattern of prey trapped showed a smooth oscillation over the diel cycle being lowest in the 3 hrs before and after dawn and peaking in late afternoon. There were no potential threats trapped between midnight and dawn and the majority were trapped between 0900 and dusk.

DISCUSSION

Observations under both hard and ramped LD cycles confirm that web-building behavior (consisting typically of both radial thread maintenance and sticky spiral replacement) is accomplished in complete darkness. Initiation of the behavior occurs approximately three hours before lights-on in the hard LD cycle and about two hours, 20 min before the beginning of the upward ramp in the ramped LD cycle (Fig. 4). The significantly later onset of activity in the ramped compared to the hard LD cycle suggests that entrainment of the daily rhythm of web replacement may be accomplished by exposure to a relatively high light level associated with 'dawn'. This exposure presumably would occur toward the end of the upward ramp (near 08:00 h) in the ramped LD cycle and at the lights-on transition (07:00 h) in the hard LD cycle. Because the behavior lasted, on average, about 119 min in the hard LD cycle and 85 min in the ramped LD cycle, the spider's web-building activity is completed before dawn. This scheduling in anticipation of sunrise ensures that movements associated with web-replacement are completed before visual predators are able to detect them (Fig. 5b). During the day, it remains motionless on its web, camouflaged by its trashline. This has

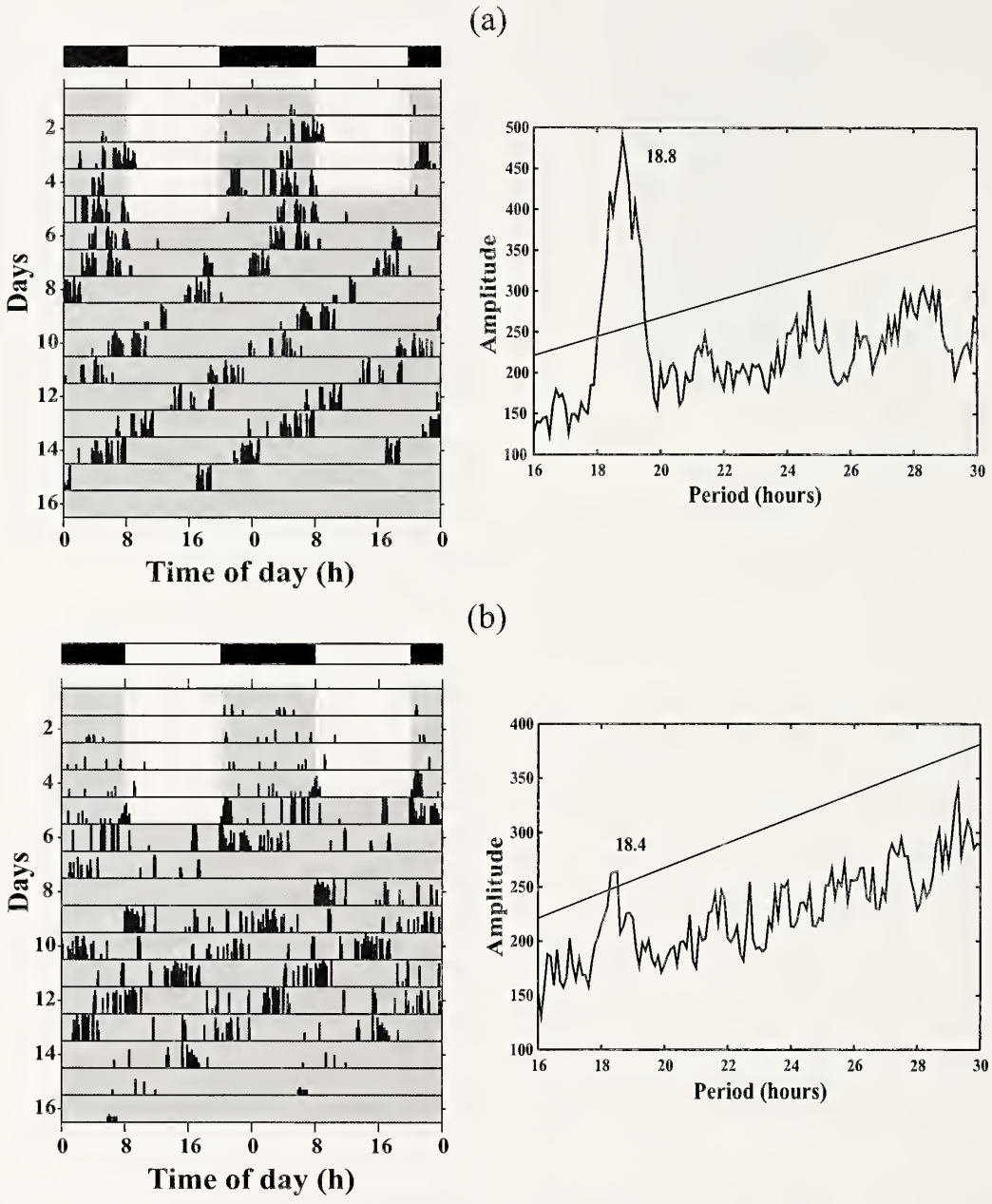

Figure 2.—Double-plotted actograms (left panels) depicting timing of locomotor activity for two individuals (a & b) under hard LD 12:12 h cycle for five days, followed by constant darkness. Dark periods are indicated by gray background. Chi-square periodograms (right panels) indicate significant ($P < 0.001$) periodicities in locomotor activity in constant darkness.

been demonstrated to be an effective antipredator strategy in other *Cyclosa* species (Chou et al. 2005; Tseng & Tso 2009). Its total behavioral commitment to visual crypsis is further supported by experiments showing that its lowest probability of retreating from a predator, as well as its lowest levels of foraging aggression, occur during the daylight hours (Watts et al. 2014). In contrast, another nocturnal orb-weaving spider, *Eriophora edax* (Blackwall, 1863), spins its web immediately after sunset, captures and feeds on its prey exclusively during the night, and dismantles its web just before dawn (Ceballos et al. 2005). Furthermore, because sticky spiral replacement in *C. turbinata* occurs near the very end of the night before sunrise, the web is able to retain its effectiveness (Foelix 1996) through the course of the daylight hours and, therefore, the spiders take advantage of increasing prey density over the course of the day, as found in this study (Fig. 5a) and a previous study (Watts et al. 2015). An additional potential advantage of scheduling web replacement before dawn is that this allows *C. turbinata* to forage in the hours immediately after dusk when prey are still relatively abundant (an advantage not available to spiders which use dusk as a cue to replace the web).

Although web-building behavior under LD conditions occurs during the late scotophase, in complete darkness and in anticipation of dawn (Fig. 3), the sparse actogram records during DD (Fig. 4) provide limited evidence that the behavior is under circadian control. Only three of eight spiders subjected to 12 days of DD performed web-building behavior more than twice. All three of these individuals built webs on at

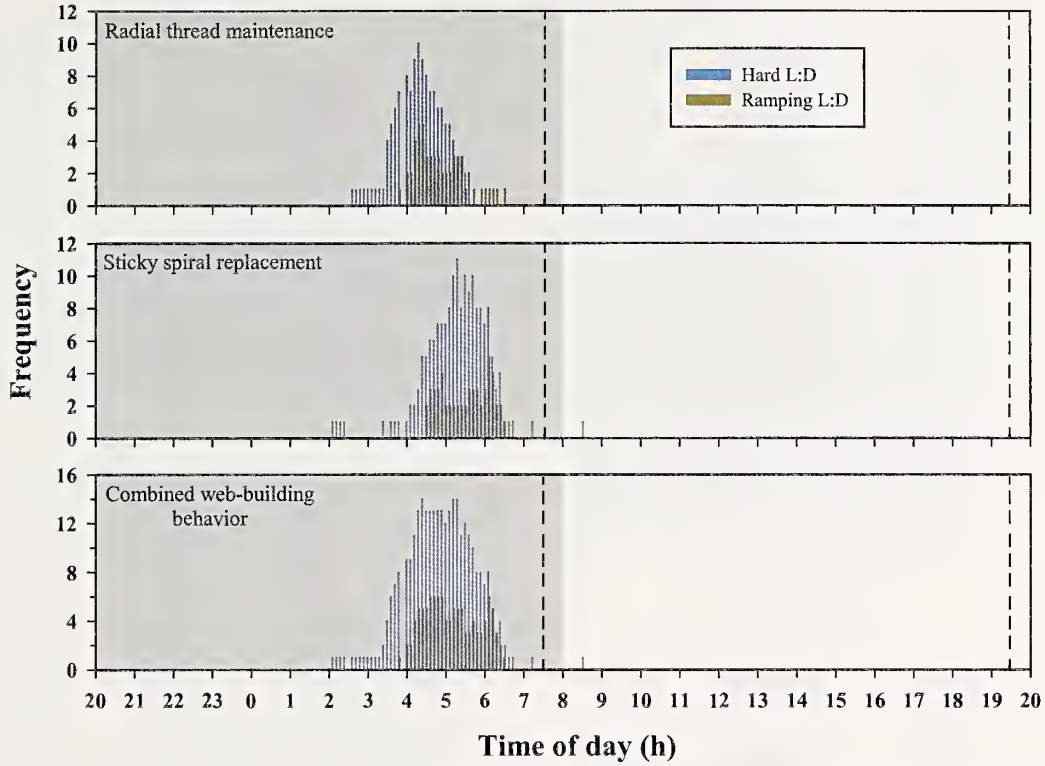

Figure 3.—Histograms depicting pooled frequencies of web-replacement behaviors across times of day for spiders observed under hard and ramping LD 12:12 h cycles. Top panel: radial thread maintenance; middle panel: sticky spiral replacement; bottom panel: combined web-building behavior. Vertical dashed lines indicate the beginning of the light ramp under ramped LD conditions.

least 10 days during DD. For each of these individuals, the chi-square and Lomb-Scargle periodogram analyses revealed at least two different significant periods for the behavior. Agreement between the two periodogram methods was achieved for only two individuals, Ct-web 7 and Ct-web 8 (Table 2). However, one of the significant periods indicated by the periodogram analyses for each of these two spiders (18.1 and 18.5 h, respectively) was in close agreement with the mean period of about 18.7 h exhibited by the locomotor activity rhythms. The absence of a consistent web-building rhythm under DD in *C. turbinata* is not understood. Although the results from two individuals suggest control by a circadian oscillator with a period similar, if not equal, to that controlling locomotor activity, there are other possibilities. For example, coupling of the behavior to the circadian oscillator may exist but be relatively weak. Perhaps many individuals are not inclined to perform web-building activities unless there is some damage to the web. These two possibilities are not necessarily mutually exclusive. Long-term video recordings over a span of several weeks, using a large number of spiders, may be necessary to confirm (or reject) the existence of circadian control of web-building behavior.

The pattern of locomotor activity elicited by *C. turbinata* in response to LD 12:12 conditions (Fig. 1) appears roughly bimodal with a sharp peak occurring within about 1 h after the lights-off transition followed by a more gradual build-up in activity that peaks about 3 h before the lights-on transition. Activity gradually declines from this second peak, except for a sharp increase in activity immediately after the lights-on transition, until terminating completely within the first 4 h of the photophase. Actograms depicting locomotor activity under LD 12:12 followed by DD show a free-running rhythm for which the activity onsets extrapolate back to the end of the scotophase (Fig. 2). These results suggest that the activity at the end of the scotophase may be under circadian control but the activity at the beginning of the scotophase may be the result of extensive masking in direct response to the LD cycle rather than entrainment of the endogenous oscillator. This phenomenon is reminiscent of the locomotor activity rhythm in *Drosophila pseudoobscura* in which there is both a dawn and a dusk peak of activity under LD cycles (Engelmann & Mack 1978). However, under DD, only the dusk peak persists and the resulting free-running rhythm extrapolates back to the phase of the dusk activity peak under LD. The dawn peak presumably is an exogenous response to lights-on. Similarly, the early scotophase peak of locomotor activity in *C. turbinata* may be an exogenous response to the lights-off transition. Further experiments with *C. turbinata* are planned to better characterize the mechanism of entrainment in this nocturnal spider, including determinations of the relative influences of the dawn and dusk transitions, the limits of entrainment, and the relationship between the free running period and phase angle.

The exceptionally short period (about 19 h) of the free-running rhythm of locomotor activity in *C. turbinata* is remarkable. The 19-h period is comparable to the *tau* mutant in hamsters, with a period of about 20 h (Ralph & Menaker 1988), the per^S mutant in *Drosophila*, with a period of about 19 h (Konopka & Benzer 1971), and the "super duper" mutant in hamsters, showing a period of about 18 h (Monecke et al.

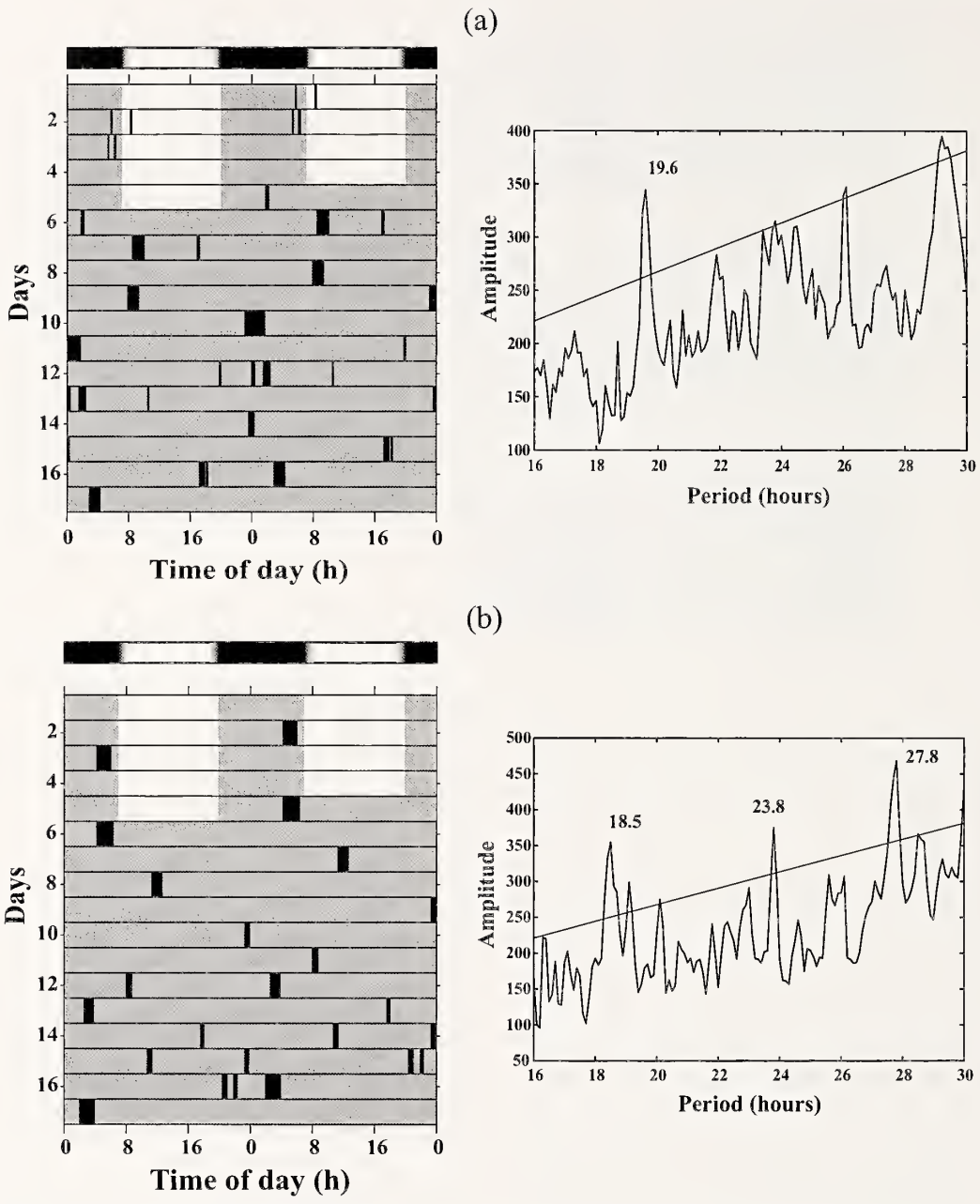

Figure 4.—Double-plotted actograms (left panels) depict timing of web-replacement behavior for two individuals (a & b) under ramping LD 12:12 h cycles for five days, followed by constant darkness. Dark periods are indicated by gray background. Chi-square periodograms (right panels) indicate significant ($P < 0.001$) periodicities in web-building activity in constant darkness.

Table 2.—Chi-square and Lomb-Scargle periodogram analyses for web-building behavior under DD. Indicated are the periods of web-building behavior (τ_{DD}), in hours, that were detected as significant at $\alpha = 0.001$.

	τ_{DD}	
Identity	chi-square	Lomb-Scargle
Ct-web 5	19.6, 26.1, 29.2	16.8, 23.3
Ct-web 7	18.1, 25.8	18, 22.9, 25.9
Ct-web 8	18.5, 23.8, 27.8	18.5, 23.8, 27.8

2011). In all three cases, the short-period mutant animals entrain to LD cycles with a significantly earlier phase angle compared to the wild type (which in all cases is close to 24-h). For example, heterozygous *tau* mutant hamsters, with a free-running period of 22 h under DD, exhibit activity onsets that are about 4 h early in 24-h LD cycles (Ralph & Menaker 1988). The 19-h Drosophila per^S mutant has an evening activity peak that occurs about 3 h earlier than normal (Hamblen-Coyle et al. 1992). The correlation between short circadian period and early phasing during entrainment also has been shown in humans (Duffy et al. 2001; Eastman et al. 2015). In fact, advanced sleep-phase syndrome, a rare disorder characterized by very early sleep onset and offset, has been

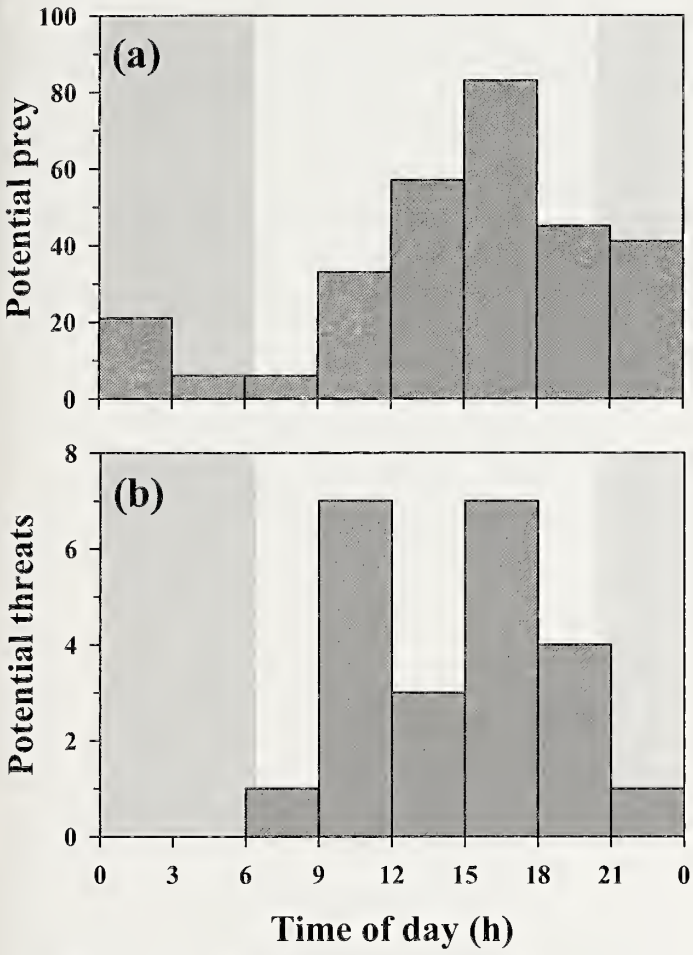

Figure 5.—Data from malaise trap sampling of flying insects in old field *Cyclosa* habitat. Traps were emptied every 3 hours for three consecutive days. Data shown are the combined captures for given time intervals including (a) potential *Cyclosa* prey non-wasp flying insects between 1–15 mm long, and, (b) potential *Cyclosa* threats (wasps). Transitions between shaded and light areas of the graph indicate the time of sunrise and sunset.

attributed to abnormally short-period circadian clocks (Jones et al. 1999). Future experiments are planned to test whether there is a correlation, using a large number of individuals, between the short-period circadian oscillator in *C. turbinata* and phase angle of locomotor and web-building behavior.

Does the short-period clock in *C. turbinata* provide any selective advantage? In most scenarios, one might expect that an extremely short circadian period would be selected against. For example, recent studies suggest, in organisms as diverse as mice (Spoelstra et al. 2016) and cyanobacteria (Woelfle et al. 2004), that natural selection eliminates genotypes with endogenous circadian periods that do not "resonate" with the natural 24-h light/dark cycle. Stringent evidence for adaptiveness of circadian clocks, however, is relatively rare (Johnson 2005). With respect to *C. turbinata*, direct confirmation of adaptive significance may require field experiments in which the period of the clock is manipulated, such that the phase relationship between web-building and the natural day:night cycle is advanced or delayed. For example, deuterium oxide in the drinking water is known to slow the free-running period of the clock in rodents (Suter & Rawson 1968) and cockroaches (Caldarola & Pittendrigh 1974). One might predict that such period lengthening in *C. turbinata* would result in a delay in web-building behavior, causing it to occur later in the scotophase, perhaps intruding into daylight hours. A possible consequence of such phase-shifting of web-building behavior would include greater predation by visual hunters.

ACKNOWLEDGMENTS

We gratefully acknowledge support from the National Science Foundation (IOS grant no. 1257133). We thank the ETSU Department of Biological Sciences for logistical support. We also thank E. Jakob, R. Vetter, R. Suter, and two anonymous reviewers for very constructive criticisms of the manuscript.

LITERATURE CITED

Beling, I. 1929. Über das Zeitgedächtnis der Bienen. Zeitschrift für Vergleichende Physiologie 9:259–338.

Caldarola, P.C. & C.S. Pittendrigh. 1974. A test of the hypothesis that D_20 affects circadian oscillations by diminishing the apparent temperature. Proceedings of the National Academy of Sciences, USA 71:4386–4388.

Ceballos, L., Y. Hénaut & L. Legal. 2005. Foraging strategies of *Eriophora edax* (Araneae, Araneidae): A nocturnal orb-weaving spider. Journal of Arachnology 33:509–515.

Chou, I., P. Wang, P. Shen & I. Tso. 2005. A test of prey-attracting and predator defense functions of prey carcass decorations built by *Cyclosa* spiders. Animal Behaviour 69:1055–1061.

Cloudsley-Thompson, J.L. 1958. Spiders, Scorpions, Centipedes and Mites. Pergamon Press, London.

Cloudsley-Thompson, J.L. 1995. A review of the anti-predator devices of spiders. Bulletin of the British Arachnological Society 10: 81–96.

DeCoursey, P.J. 1989. Photoentrainment of circadian rhythms: An ecologist's viewpoint. Pp. 187–206. *In* Circadian Clocks and Ecology. (T. Hiroshige & K.-I. Honma, eds.). University of Hokkaido Press, Sapporo.

Duffy, J.F., D.W. Rimmer & C.A. Czeisler. 2001. Association of intrinsic circadian period with morningness-eveningness, usual wake time, and circadian phase. Behavioral Neuroscience 115: 895–899.

Eastman, C.I., C. Suh, V.A. Tomaka & S.J. Crowley. 2015. Circadian rhythm phase shifts and endogenous free-running circadian period differ between African-Americans and European Americans. Scientific Reports doi:10.1.1038/srep08381

Eberhard, W.G. 1986. Effects of orb-web geometry on prey interception and retention. Pp. 70–100. *In* Spiders: Webs, Behavior and Evolution. (W.A. Shear, ed.). Stanford University Press, Redwood City, California.

Engelmann, W. & J. Mack. 1978. Different oscillators control the circadian rhythm of eclosion and activity in *Drosophila*. Journal of Comparative Physiology 127:229–237.

Foelix, R.F. 1996. Biology of Spiders, 2nd Ed. Oxford University Press, Oxford.

Gan, W., F.X. Liu, Y. Ren, J. Chen & D. Li. 2010. The effects of abiotic and biotic factors on web-decorating behaviour of an orb-weaving spider, *Cyclosa octotuberculata* Karsch (Araneae: Araneidae). Journal of Natural History 45:35–53.

Hamblen-Coyle, M.J., D.A. Wheeler, J.E. Rutila, M. Rosbash & J.C. Hall. 1992. Behavior of period-altered circadian rhythm mutants of

Drosophila in light: dark cycles (Diptera: Drosophilidae). Journal of Insect Behavior 5:417–446.

Johnson, C.H. 2005. Testing the adaptive value of circadian systems. Methods in Enzymology 393:818–837.

Jones, C.R., S.S. Campbell, S.E. Zone, F. Cooper, A. DeSano, P.J. Murphy et al. 1999. Familial advanced sleep-phase syndrome: A short-period circadian rhythm variant in humans. Nature Medicine 5:1062–1065.

Jones, T.C., T.S. Akoury, C.K. Hauser & D. Moore. 2011. Evidence of circadian rhythm in antipredator behavior in the orb-weaving spider *Larinioides cornutus*. Animal Behaviour 82:549–555.

Konopka, R.J. & S. Benzer. 1971. Clock mutants of *Drosophila melanogaster*. Proceedings of the National Academy of Sciences U.S.A. 68:2112–2116.

Monecke, S., J.M. Brewer, S. Krug & E.L. Bittman. 2011. Duper: A mutation that shortens hamster circadian period. Journal of Biological Rhythms 26:283–292.

Moore, D. & P. Doherty. 2009. Acquisition of a time-memory in forager honey bees. Journal of Comparative Physiology A 195:741–751.

Ortega-Escobar, J. 2002. Circadian rhythms of locomotor activity in *Lycosa tarantula* (Araneae, Lycosidae) and the pathways of ocular entrainment. Biological Rhythms Research 33:561–576.

Ralph, M.R. & M. Menaker. 1988. A mutation of the circadian system in golden hamsters. Science 241:1225–1227.

Ramousse, R. & F. Davis. 1976. Web-building time in a spider: preliminary applications of ultrasonic detection. Physiology & Behavior 17:997–1000.

Riechert, S.E. & R.G. Gillespie. 1986. Habitat choice and utilization in web-building spiders. Pp. 23–28. *In* Spiders: Webs, Behavior, and Evolution. (W.A. Shear, ed.). Stanford University Press, Redwood City, California.

Rypstra, A.L. 1982. Building a better insect trap: an experimental investigation of prey capture in a variety of spider webs. Oecologia 52:31–36.

Seyfarth, E.A. 1980. Daily patterns of locomotor activity in a wandering spider. Physiological Entomology 5:199–206.

Schmitt, A., R.M. Schuster & F.G. Barth. 1990. Daily locomotor patterns in three species of *Cupiennius* (Araneae, Ctenidae): the males are the wandering spiders. Journal of Arachnology 18:248–255.

Sokolove, P.G. & W.N. Bushell. 1978. The chi square periodogram: its utility for analysis of circadian rhythms. Journal of Theoretical Biology 72:131–160.

Spoelstra, K., M. Wikelski, S. Daan, A.S.I. Loudon & M. Hau. 2016. Natural selection against a circadian clock gene mutation in mice. Proceedings of the National Academy of Sciences, USA 113:686–691.

Suter, R.B. 1993. Circadian rhythmicity and other patterns of spontaneous motor activity in *Frontinella pyramitela* (Linyphiidae) and *Argyrodes trigonum* (Theridiidae). Journal of Arachnology 21:6–22.

Suter, R.B. & K. Benson. 2014. Nocturnal, diurnal, crepuscular: activity assessments of Pisauridae and Lycosidae. Journal of Arachnology 42:178–191.

Suter, R.B. & K.S. Rawson. 1968. Circadian activity rhythm of the deer mouse, *Peromyscus*: effect of deuterium oxide. Science 160:1011–1014.

Tseng, L. & I. Tso. 2009. A risky defence by a spider using conspicuous decoys resembling itself in appearance. Animal Behaviour 78:425–431.

Uetz, G.W. & C.S. Hieber. 1997. Colonial web-building spiders: balancing costs and benefits of group-living. Pp. 476–498. *In* Evolution of Social Behaviour in Insects and Arachnids. (J. Choe & B. Crespi, eds.). Cambridge University Press, Cambridge.

Uetz, G.W., C.S. Hieber, E.M. Jakob, S. Wilcox, D. Kroeger, A. McCrate et al. 1994. Behavior of colonial orb-weaving spiders during a solar eclipse. Ethology 96:24–32.

Van Dongen, H.P.A., E. Olofsen, J.H. Van Hartevelt & E.W. Kruyt. 1999. A procedure for multiple period searching in unequally spaced time-series with the Lomb-Scargle method. Biological Rhythm Research 30:149–177.

Van Nest, B.N. & D. Moore. 2012. Energetically optimal foraging strategy is emergent property of time-keeping behavior in honey bees. Behavioral Ecology 23:649–658.

Wahl, O. 1932. Neue Untersuchungen über das Zeitgedächtnis der Bienen. Zeitschrift für Vergleichende Physiologie 16:529–589.

Watts J.C., A. Herrig, W.D. Allen & T.C. Jones. 2014. Diel patterns of foraging aggression and antipredator behaviour in the trashline orb-weaving spider, *Cyclosa turbinata*. Animal Behaviour 94:79–86.

Watts, J.C., C.R. Ross & T.C. Jones. 2015. Diel and life-history characteristics of personality: consistency versus flexibility in relation to ecological change. Animal Behaviour 101:43–49.

Wise, D.H. 1993. Spiders in Ecological Webs. Cambridge University Press, Cambridge.

Woelfle, M.A., Y. Ouyang, K. Phanvijhitsiri & C.H. Johnson. 2004. The adaptive value of circadian clocks: an experimental assessment in cyanobacteria. Current Biology 14:1481–1486.

Yamashita, S. & T. Nakamura. 1999. Circadian oscillation of sensitivity of spider eyes: diurnal and nocturnal spiders. Journal of Experimental Biology 202:2539–2542.

Manuscript received 19 February 2016, revised 11 July 2016.

2016. Journal of Arachnology 44:397–400

SHORT COMMUNICATION

Leaf masquerade in an orb web spider

Matjaž Kuntner[1,2,4], **Matjaž Gregorič**[1], **Ren-Chung Cheng**[1] and **Daiqin Li**[3]: [1]Evolutionary Zoology Laboratory, Biological Institute ZRC SAZU, Ljubljana, Slovenia; E-mail: kuntner@gmail.com; [2]National Museum of Natural History, Smithsonian Institution, Washington, DC, USA; [3]Department of Biological Sciences, National University of Singapore, Singapore; [4]College of Life Sciences, Hubei University, Wuhan 430062, Hubei, China

Abstract. Leaf masquerade—an animal resembling leaves that are inedible for predators or innocuous for prey—is well known in insects but less so in arachnids. We report a case of a striking morphological and behavioral adaptation that can be labeled as leaf masquerade in an undescribed spider species (*Poltys* C.L. Koch, 1843, Araneidae) from southwest China. The female abdomen has anatomical analogues of a leaf pedicel and venation, and its color is both green and brown, thus resembling both live and dry leaves. The spider camouflages itself with pulled dead leaves among live ones. This novel natural history in a spider adds an arachnid model to the growing literature on animal masquerade.

Keywords: Passive defenses, anachoresis, crypsis, *Poltys*, Araneidae

Masquerade, the resemblance to uninteresting objects, is a fascinating product of natural selection that deceives predators or helps gain access to prey (Skelhorn et al. 2010). Better known in insects, plants, birds, and fish (Nel et al. 2008), masquerade in arachnids involves only a handful of spider genera with phenotypes that resemble flowers, dead twigs, plant detritus, buds, bark, or bird droppings (Foelix 2011; Liu et al. 2014; Pekar 2014). However, genuine leaf masquerade has not been known in arachnids. Here, we provide anecdotal evidence for such masquerade in a spider from southwest China and Southeast Asia belonging to a taxonomically and biologically unstudied species group within the genus *Poltys* C. L. Koch, 1843 (Araneidae). We show that females easily blend into live and dead leaf surroundings through color, morphological, and behavioral adaptation. The former involve shades of green and brown on the same animal, and, morphologically, the abdomen resembles a pedicel and leaf venation. Behavioral adaptation most likely involves the spider pulling and anchoring dead leaves amongst live ones, for the ultimate visual deception (Fig. 1).

We observed a *Poltys* species in Xishuangbanna, Yunnan, China, in January 2011. A female, deposited at National Museum of Natural History, Smithsonian Institution, Washington DC, USA (NMNH; accession number 2076621), was found in a rainforest near Mengla (21.54069444°N, 101.4907778°E, at 962 m) with no web, but rather with hung dead leaves on a twig, and her abdomen resembled a dead leaf ventrally and a live green leaf dorsally with an apical, pedicel-like abdominal projection (Fig. 1). During two weeks of searching only a single additional (juvenile) was found in its orb web in Baka forest (21.713675°N, 100.783023°E, at 695 m) (Fig. 2), and only one additional sample from Vietnam was discovered in museums (a female RMNH.ARA.12114, made available by J. Miller). This suggests that this form of *Poltys* is rare in tropical rain forests of southwest China and Southeast Asia.

Poltys research contains no reference to leaf masquerade, however, old descriptions depict this very shape of abdomen (Günther 1862; Ausserer 1871; Simon 1895; Hogg 1919; Grassé 1949). These shaped females are only known in three species, *P. mouhoti* (Günther, 1862) from Vietnam, *P. idae* (Ausserer, 1871) from Borneo, and *P. longitergus* Hogg, 1919 from Sumatra. To facilitate future identification of our samples, we provide their DNA barcodes (Appendix 1); the barcode from the Vietnam sample is available on BOLD (as an unidentified araneid: SVN03312). The two DNA barcodes from Yunnan are nearly identical (K2P distance between these sequences is only 0.2%), so these samples are clearly conspecific (Čandek & Kuntner 2014). However, K2P distances ranged 5.7–5.9% between the samples from Yunnan and Vietnam, falling into the lower range of interspecific mean distances reported for araneids (8.8 ± 4.2%; Čandek & Kuntner 2014). If the Vietnam population is about 6% different from the Yunnan one, then we find it likely that other Southeast Asian populations (see below) are also genetically distinct. We find it likely that the Vietnam sample belongs to *P. mouhoti* and that our samples from Yunnan belong to an undescribed species. More material and taxonomic studies are needed to confirm this.

In spite of the rarity of leaf masquerading *Poltys* spp., these spiders, judging from online photo repositories, can be found all over Southeast and East Asia (Taiwan; Vietnam; Malaysia; Borneo; Hong Kong), but have so far not been recorded in mainland China. While Chinese *Poltys* records exist from Hainan, species that occur there (*P. ellipticus* Han, Zhang & Zhu, 2010, *P. hainanensis* Han, Zhang & Zhu, 2010, and *P. pygmaeus* Han, Zhang & Zhu, 2010) do not mimic leaves (Han et al. 2010; World Spider Catalog 2016). We have examined other *Poltys* species from Yunnan (Gregorič et al. 2015a; unpublished data), but again, these are not leaf mimics.

Our juvenile was found at night in its aerial orb web with a tight mesh architecture, as is typical of *Poltys* (Fig. 2; compare with fig. 3 in Blackledge et al. 2011). The female, on the other hand, was found in early evening hiding among leaves on a tree and without a functional web. These spiders probably hide in camouflage during the day and only build webs at night, as is typical in *Caerostris* Thorell, 1868 and other *Poltys* (Smith 2006; Kuntner & Agnarsson 2010; Gregorič et al. 2015b). The observed female must have actively lifted dead leaves from the forest floor to attach them to a twig about 2.5 meters high up on a tree prior to positioning herself on a thread of silk amidst live and dead leaves (Fig. 1A–D). Lifting dead leaves is not uncommon in araneoid spiders; several species decorate their webs with lifted and folded leaves that function as retreats (Kuntner et al. 2008; Gregorič et al. 2015a). However, the speculated attaching of leaves to vegetation to match the spider body form is a novel behavior in orb web spiders. Such a manipulated scene blends the motionless spider perfectly with its surroundings to protect it from visual predators and/or gain access to prey by being mistaken for innocuous objects.

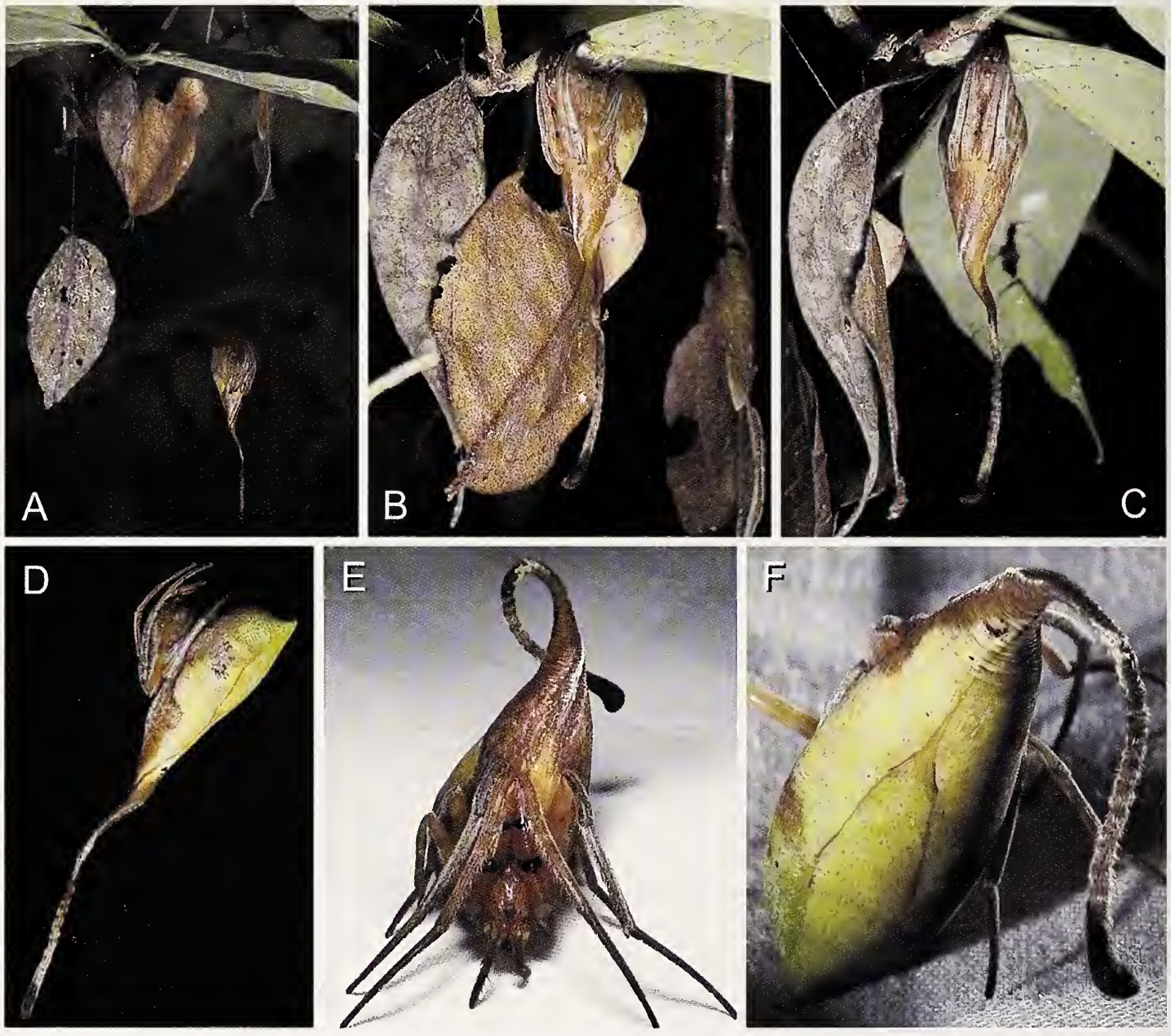

Figure 1.—The ultimate leaf masquerade in an orb web spider, an undescribed species of *Poltys* (Araneidae) from Yunnan. A–C, A female had hung dead leaves from a twig that also included live leaves to masquerade itself from visual predators (A). Upon slight disturbance, she withdrew higher onto the twig (B, C) where it remained motionless; D, lateral view of female pose in nature, note her abdomen resembling a dead leaf ventrally and a live, green leaf dorsally, both parts extending into a long and straight, apical abdominal hairy pedicel; E, female placed on a flat surface, showing her flexible abdominal pedicel, now curved; F, same, dorsal close up, note "leaf venation" and long hairy pedicel.

Distinguishing true masquerade (avoiding predation by being misidentified) from various types of erypsis (blending in with background not to be detected at all) is difficult with many cases falling in between well-defined extremes (Cuthill et al. 2005; Ruxton et al. 2005; Stevens & Merilaita 2009). Some grasshoppers and katydids (Orthoptera), stick and leaf insects (Phasmatodea), praying mantises (Mantodea), and moths and butterflies (Lepidoptera) are textbook examples of plant masquerade (Wedmann 2010). However, reviews on the topics of spider disguise and deceptive coloration do not account for leaf masquerade on a par with our reported example (Thery & Casas 2009; Foelix 2011; Nelson & Jackson 2011), and only anecdotal evidence exists for *Romphaea* L. Koch, 1872 and *Arachnura* Vinson 1863 to resemble dead leaves (Marson 1945; Whitehouse 1987).

True masquerade is rare in spiders being described in only about 100 of the 45,945 known species of spiders (Pekar 2014; World Spider Catalog 2016). In spiders, masquerade is mostly confined to the family Araneidae, with spider resemblance to twigs, debris, fruits, or bird droppings (Liu et al. 2014; Pekar 2014), and as we report here, leaves. Thomisid genera resemble flowers and plant detritus, *Deinopis* MacLeay 1839 (Deinopidae), *Tetragnatha* Latreille 1804 (Tetragnathidae) and *Miagrammopes* O. Pickard-Cambridge 1870 (Uloboridae) resemble dead twigs, *Portia* Karsch, 1878 (Salticidae), *Cyclosa* Menge, 1866 (Araneidae) and *Neospintharus* Exline, 1950 (Theridi-

Figure 2.—Juvenile *Poltys*, conspecific with female in Fig. 1, on a vertical orb web (web width 10.5 cm, height 12 cm, distance from top spiral to hub 6 cm). This typical *Poltys* web contained primary (and no secondary) radii and a dense mesh of sticky spiral.

idae) mimic plant detritus, whereas *Caerostris* and some other *Poltys* (Araneidae) mimic plant buds or bark (Grasshoff 1984; Smith 2006; Gregorič et al. 2015b). Among orb web spiders, masquerade typically occurs in nocturnal species and at intermediate phylogenetic levels within families (Pekar 2014).

Our discovery adds an arachnid model, *Poltys*, to the growing literature on animal passive defenses. We hope it will facilitate new research into masquerade and deceptive mimicry in arachnids, where leaf masquerade has not been known. One serious hindrance to this, however, is the apparent rarity of this enigmatic *Poltys*, confined to rainforests of southwest China, Southeast Asia, and East Asia where its cryptic habits and nocturnal lifestyle help evade not only predators, but also researchers.

ACKNOWLEDGMENTS

We thank Wenjin Gan and Liu Shengjie for help in the field, and Nikolaj Scharff, Jeremy Miller, Ingi Agnarsson and Helen Smith for useful comments on our discovery, and the identity of the spiders. Two anonymous reviewers helped us reshape our report.

LITERATURE CITED

Ausserer, A. 1871. Neue Radspinnen. Verhandlungen der Kaiserlich-Königlichen Zoologisch-Botanischen Gesellschaft in Wien 21:815–832.

Blackledge, T.A., M. Kuntner & I. Agnarsson. 2011. The form and function of spider orb webs: Evolution from silk to ecosystems. Pp. 175–262. *In* Advances in Insect Physiology, Vol 41: Spider Physiology and Behaviour—Behaviour. (J. Casas, ed.). Academic Press, Burlington, Massachusetts.

Čandek, K. & M. Kuntner. 2014. DNA barcoding gap: Reliable species identification over morphological and geographical scales. Molecular Ecology Resources 15:268–277.

Cuthill, I.C., M. Stevens, J. Sheppard, T. Maddocks, C.A. Parraga & T.S. Troscianko. 2005. Disruptive coloration and background pattern matching. Nature 434:72–74.

Foelix, R.F. 2011. Biology of Spiders. 3rd ed. Oxford University Press, Oxford.

Grassé, P.P. 1949. Traité de zoologie: anatomie, systématique, biologie. Tome VI. Masson, Paris.

Grasshoff, M. 1984. Die Radnetzspinnen-Gattung *Caerostris* (Arachnida: Araneae). Revue Zoologique Africaine 98:725–765.

Gregorič, M., I. Agnarsson, T.A. Blackledge & M. Kuntner. 2015a. Phylogenetic position and composition of Zygiellinae and *Caerostris*, with new insight into orb-web evolution and gigantism. Zoological Journal of the Linnean Society 175:225–243.

Gregorič, M., T.A. Blackledge, I. Agnarsson & M. Kuntner. 2015b. A molecular phylogeny of bark spiders reveals new species from Africa and Madagascar (Araneae: Araneidae: *Caerostris*). Journal of Arachnology 43:293–312.

Günther, A. 1862. On an apparently undescribed spider from Cochin China. Annals and Magazine of Natural History 10:299–300.

Han, G.X., F. Zhang & M.S. Zhu. 2010. Three new species of the genus *Poltys* from Hainan Island, China (Araneae: Araneidae). Acta Arachnologica 59:51–55.

Hogg, H.R. 1919. Spiders collected in Korinchi, West Sumatra by Messrs H. C. Robinson and C. Boden Kloss. Journal of the Federated Malay States Museums 8:81–106.

Kuntner, M. & I. Agnarsson. 2010. Darwin's bark spider: Web gigantism in a new species of bark spiders from Madagascar (Araneidae: *Caerostris*). Journal of Arachnology 38:346–356.

Kuntner, M., J.A. Coddington & G. Hormiga. 2008. Phylogeny of extant nephilid orb-weaving spiders (Araneae, Nephilidae): testing morphological and ethological homologies. Cladistics 24:147–217.

Liu, M.-H., S.J. Blamires, C.-P. Liao & I.-M. Tso. 2014. Evidence of birddropping masquerading by a spider to avoid predators. Scientific Reports 4:5058; DOI:10.1038/srep05058.

Marson, J.E. 1945. Two Burmese spiders which mimic scorpiones. Journal of the Bombay Natural History Society 45:616–617.

Nel, A., J. Prokop & A.J. Ross. 2008. New genus of leaf-mimicking katydids (Orthoptera: Tettigoniidae) from the late eocene - Early oligocene of France and England. Comptes Rendus Palevol 7:211–216.

Nelson, X.J. & R.R. Jackson. 2011. Flexible use of anti-predator defences. Pp. 99–126. *In* Spider Behaviour: Flexibility and Versatility. (M.E. Herberstein, ed.). Cambridge University Press, Cambridge.

Pekar, S. 2014. Comparative analysis of passive defences in spiders (Araneae). Journal of Animal Ecology 83:779–790.

Ruxton, G.D., T.N. Sherratt & M.P. Speed. 2005. Avoiding Attack: The Evolutionary Ecology of Crypsis, Warning Signals and Mimicry. Oxford University Press, Oxford.

Simon, E. 1895. Histoire naturelle des araignées. Paris 1:761–1084.

Skelhorn, J., H.M. Rowland, M.P. Speed & G.D. Ruxton. 2010. Masquerade: camouflage without crypsis. Science 327:51.

Smith, H.M. 2006. A revision of the genus *Poltys* in Australasia (Araneae: Araneidae). Records of the Australian Museum 58:43–96.

Stevens, M. & S. Merilaita. 2009. Animal camouflage: current issues and new perspectives. Philosophical Transactions of the Royal Society B-Biological Sciences 364:423–427.

Théry, M. & J. Casas. 2009. The multiple disguises of spiders: web colour and decorations, body colour and movement. Philosophical Transactions of the Royal Society B-Biological Sciences 364:471–480.

Wedmann, S. 2010. A brief review of the fossil history of plant masquerade by insects. Palaeontographica Abteilung B 283:175–182.

Whitehouse, A.E.A. 1987. Spider eat spider: the predatory behavior

of *Rhomphaea* sp. from New Zealand. Journal of Arachnology 15:355–362.
World Spider Catalog 2016. Version 17.0. Accessed 6 April 2016. Natural History Museum Bern. Online at http://wsc.nmbe.ch

Manuscript received 6 April 2016, revised 27 April 2016.

APPENDIX 1

DNA barcodes of the studied specimens.

Poltys sp. female from Yunnan, China (Genbank accession code KX231812):

GACATTATATTTAATGTTTGGGGCATGGGCTTCTATAGTA
GGGACAGCAATAAGAGTTTTAATTCGAATTGAATTAGGT
CAACCTGGGAGATTTATTGGGGATGATCAGTTATATAAT
GTTATTGTAACGGCACATGCTTTTGTTATAATTTTTTTTAT
AGTGATACCTATTTTAATTGGGGGGTTTGGAAATTGGTT
AGTTCCATTAATGTTAGGAGCTCCGGATATAGCTTTTCCT
CGAATAAATAATTTAAGATTTTGGTTGCTTCCTCCATCTTT
ATTTCTTTTATTAATTTCTTCTATAGTAGAAGTAGGAGTG
GGAGCAGGGTGGACAGTTTATCCTCCTTTAGCAAGATTA
GAGGGGCATGCTGGAAGATCTATAGATTTTGCAATTTTTT
CTCTTCATTTAGCAGGGGCTTCATCAATTATAGGGGCAAT
TAATTTTATTTCAACTATTATTAATATACGATTTTATGGGA
TATCTATGGAGAAAGTTTCATTGTTTGTTTGATCAGTTTT
AATTACTGCTGTATTATTATTATTATCTTTACCTGTATTGG
CAGGAGCTATTACCATATTATTAACAGATCGAAATTTTAA
TACTTCATTTTTTGATCCTTCAGGGGGAGGGGATCCAATT
TTATTTCAA

Poltys sp. juvenile from Yunnan, China (Genbank accession code KX231813):

GACATTATATTTAATGTTTGGGGCATGGGCTTCTATAGTA
GGGACAGCAATAAGAGTTTTAATTCGAATTGAATTAGGT
CAACCTGGGAGATTTATTGGGGATGATCAGTTATATAAT
GTTATTGTAACGGCACATGCTTTTGTTATAATTTTTTTTAT
AGTGATACCTATTTTAATTGGGGGGTTTGGAAATTGGTT
AGTTCCATTAATGTTAGGAGCTCCGGATATAGCTTTTCCT
CGAATAAATAATTTAAGATTTTGGTTGCTTCCTCCATCTTT
ATTTCTTTTATTAATTTCTTCTATAGTAGAAGTAGGAGTG
GGAGCAGGGTGGACAGTTTATCCTCCTTTAGCAAGATTA
GAGGGGCATGCTGGAAGATCTATAGATTTTGCAATTTTT
TCTCTTCATTTAGCAGGGGCTTCATCAATTATAGGGGCAA
TTAATTTTATTTCAACTATTATTAATATACGATTTTATGGG
ATATCTATGGAGAAAGTTTCATTGTTTGTTTGATCAGTTT
TAATTACTGCTGTATTATTATTATTATCTTTACCTGTATTG
GCA----------
----------TTCTTTTTTTGATCCTTCAGGGGGAG
GGGATCCAATTTTATTTCAA

2016. Journal of Araehnology 44:401–404

SHORT COMMUNICATION

The impact of UVA on the glycoprotein glue of orb-weaving spider capture thread from a diurnal and a nocturnal species (Araneae: Araneidae)

Sarah D. Stellwagen, Brent D. Opell and **Mary E. Clouse**: Department of Biological Sciences, Virginia Tech, Blacksburg, Virginia 24061, USA; E-mail: sstellw@vt.edu

Abstract. We compared the effect of Ultraviolet A radiation on the adhesive droplets of the diurnal orb-web weaver *Argiope trifasciata* Forskaal, 1775 and the nocturnal orb-web weaver *Neoscona crucifera* (Lucas, 1838). We hypothesized that glycoprotein glue within *A. trifasciata* droplets will either be unaffected or will benefit from UVA exposure, whereas the glycoprotein of *N. crucifera* will be degraded by UVA. In both species, the volume of fresh droplets did not differ from that of droplets that were exposed to UVA for four hours, or from the volume of droplets kept in the dark for four hours. This documented that UVA did not affect compounds that confer droplet hygroscopicity. Both dark and UVA treatments reduced the relative toughness of droplet glycoprotein, though the reductions were not statistically significant, with the dark treatment exhibiting a greater decrease in relative toughness. This study suggests that ecologically relevant levels of UVA exposure do not affect the glycoprotein glue of orb-weaver capture silk.

Keywords: Adhesion, biomaterials, toughness, silk, ultraviolet

Ultraviolet radiation (UVR) comes in several forms including UVA and UVB, the latter of which is more damaging, although more UVA enters the atmosphere than the other forms of UVR (Rizzo et al. 2011). Ultraviolet radiation induces cross-linking in proteins (Bhat & Karim 2009; Hu et al. 2013), and low doses may enhance spider silk performance by further aligning proteins, similar to the "improvement phase", during which molecule alignment is hypothesized to continue after a silk strand is extruded (Agnarsson et al. 2008). Non-adhesive major ampullate spider silk continues to improve mechanically after several hours of natural UVA exposure, hypothesized to be the result of free radical generation that induces cross-linking, however longer exposures do eventually result in degradation (Osaki 2004; Osaki & Osaki 2011; Perea et al. 2015). UVA at ~700 W/m^2 reduces the molecular weight of spider dragline silk from *Nephila clavipes* Linnaeus, 1767 more than 30% during the first hour, and more than 80% after 5 hours (Matsuhira et al. 2013). However the radiation intensity used was more than 20x the natural incident UVA striking spider webs in the summer. Osaki & Osaki (2011) demonstrated that ecologically relevant doses of UVA actually serve to mechanically strengthen dragline silk of *Argiope bruennichi* (Scopoli, 1772) while weakening that of *Neoscona nautica* (L. Koch, 1875).

The capture spiral threads of araneoid orb weaver webs differ from the dragline threads that form their radial and frame threads. These adhesive threads are composed of a pair of supporting axial flagelliform fibers that are covered by aqueous aggregate gland material. Originally deposited as a cylinder of dope, this material coalesces into regularly spaced droplets, each containing a glycoprotein glue core (Sahni et al. 2010, 2014). Inorganic salts and low molecular mass organic (LMMC) compounds within the aqueous layer that surrounds this glycoprotein core attract atmospheric moisture, causing droplet volume to fluctuate with environmental humidity (Edmonds & Vollrath 1992; Opell et al. 2013; Townley & Tillinghast 2013). We have shown that diurnal species preferring habitats that expose their webs to full or partial sun produce viscous threads with droplets that are not only resistant to degradation, but also contain glycoprotein that exhibits an increase in relative toughness when exposed to UVB (Stellwagen et al. 2015). This results in more work being required to extend these UVB exposed droplets. Species of the genus *Argiope* Audouin, 1826 (Orbiculariae), including *A. trifasciata* Forskaal, 1775, are found in habitats where their webs are exposed to full sun. Others, such as *Neoscona crucifera* (Lucas, 1838), are nocturnal and forage from the center of their webs at night and monitor their webs from an adjacent cryptic retreat during the day. The web's radial threads extend from the center like the spokes of a wheel and are largely responsible for absorbing the force of prey impact (Sensenig et al. 2012), whereas the prey capture spiral retains flying insects (Apstein 1889; Sekiguchi 1952; Sahni et al. 2014). The measure of a capture thread's ability to overcome the efforts of a prey struggling to escape is the droplet's toughness, the work required to extend a droplet (Sensenig et al. 2012). This is determined by the extent of droplet stretching (the droplet's extensibility) and the force required to extend the droplet until it pulls from a surface, that is, to overcome the droplet's adhesion.

To complement our previous UVB study (Stellwagen et al. 2015), we investigated the effects of UVA radiation on the performance of viscous glue droplets from *A. trifasciata* and *N. crucifera* (family Araneidae). We tested the hypothesis that the performance of droplets from the webs of the full-sun diurnal species, *A. trifasciata*, is enhanced by UVA exposure; whereas that of droplets from webs of the primarily nocturnal *N. crucifera*, is either not affected or is degraded by UVA. We did this by comparing several performance metrics. First, the duration of droplet extension before droplet pull-off, a measure of the time over which the work of extension occurs, and second, the angle of axial line deflection, a measure of the force on an extending droplet. Together, these metrics can be used to compute relative toughness, a measure of the energy required to extend a droplet to pull-off.

Fresh threads collected in the early morning (*A. trifasciata*) or late evening (*N. crucifera*), soon after they were spun, were compared with those that were aged in the dark for 4 hours and droplets that were exposed to 4 hours of UVA. We photographed each thread droplet prior to extension, permitting us to compare the effect of aging and UVA on droplet volume. This allowed us to test a contending hypothesis that differences observed in droplet performance can be explained by the impact of UVA on droplet hygroscopicity through its effect on LMMC and salts in a droplet's aqueous layer, a conclusion that would make it more difficult to ascribe UVA action to its effect on the droplet's glycoprotein core.

Table 1.—Droplet length (μm), width (μm), volume (μm^3), extension phase times (seconds), relative toughness (N/m^3), and log relative toughness for both species and treatments (n = 13; mean ± 1 standard deviation; MP = matched pair, WP = Wilcoxon pair). Droplet volume was computed as described in Liao et al. (2015).

	Length	Width	Volume	MP Volume	Total Loaded Time	Pre-Extension	Droplet Extension (DE)	MP DE	Relative Toughness (RT)	Log RT	Test (Log RT)
A. trifasciata											
Fresh	47.7 ± 8.0	33.5 ± 6.2	24,707 ± 13,183		32.5 ± 8.2	24.0 ± 7.3	8.5 ± 6.3		99.1 ± 106.8	3.5 ± 1.4	
UVA	48.1 ± 7.3	33.6 ± 6.1	24,760 ± 12,031	$P = 0.9812$	29.5 ± 7.1	23.5 ± 7.7	6.0 ± 5.2	$P = 0.0015$	52.5 ± 60.1	3.3 ± 1.2	$P = 0.5475$ (MP)
Dark	48.1 ± 7.3	34.6 ± 6.1	26,006 ± 12,071	$P = 0.4901$	28.4 ± 5.9	20.2 ± 7.7	8.3 ± 6.2	$P = 0.8457$	45.2 ± 37.1	2.9 ± 1.7	$P = 0.4418$ (WP)
N. crucifera											
Fresh	32.0 ± 10.8	23.4 ± 7.8	10,211 ± 11,940		28.2 ± 11.0	23.7 ± 11.3	24.2 ± 10.6		819 ± 524	6.4 ± 0.73	
UVA	31.3 ± 9.5	23.1 ± 6.8	9,237 ± 9,513	$P = 0.2931$	40.2 ± 11.4	20.0 ± 6.8	20.3 ± 12.7	$P = 0.2849$	566 ± 627	5.8 ± 1.1	$P = 0.1496$ (MP)
Dark	30.9 ± 9.0	22.8 ± 6.8	8,690 ± 8,142	$P = 0.2492$	41.4 ± 5.7	22.0 ± 7.9	19.4 ± 7.8	$P = 0.1363$	469 ± 242	6.0 ± 0.5	$P = 0.1083$ (MP)

Thread samples from webs constructed by 13 adult female *A. trifasciata* and 11 adult female *N. crucifera* were collected on and near the Virginia Tech campus in Blacksburg, Montgomery County, Virginia, USA, from 15 August to 25 September 2014. Each *A. trifasciata* web sample was collected between 05:30h and 08:30h and all images and videos captured by 16:00h the same day. Threads of *N. crucifera* webs were collected between 21:30h and 23:00h and their study was completed by 16:00h on the following day. Except for differences in irradiance described below, all methods and analyses are those described by Stellwagen et al. (2015).

Two 15.0 watt, 352 nm spectral peak UVA fluorescent tubes (F15T8BL; 440.4 mm length, 25.4 mm diameter; USHIO Inc., Cypress, CA, USA) were used to irradiate samples. Irradiance was measured using a photometer radiometer (Solar Light Co., Inc. PMA2200) equipped with a UVA detector (PMA2110, Glenside, Pennsylvania, USA) with a spectral sensitivity from 320–400 nm, calibrated traceable to the National Institute of Standards and Technology (NIST) on 18 August 2014. Threads were irradiated for 4 hours at ~13 W/m^2 (the maximum level produced by the UVA lamps), which is two-thirds the maximum level of full sunlight received in Blacksburg in late summer. Conditions in the dark treatment cylinder and the UV cabinet were recorded every 30 seconds for two hours by temperature/relative humidity data loggers (Hobo® model U23-002, Onset Computer Corp., Bourne, Massachusetts, USA). The dark treatment cylinder maintained ambient temperature at 24°C ± 0.13°C (mean ± SD) and relative humidity at 55% ± 1.3%; for the UV cabinet, the corresponding values were 24°C ± 0.08°C and 55% ± 1.7%.

We used JMP (SAS Institute, Cary, North Carolina) to analyze data and considered comparisons with $P \leq 0.05$ as significant. Shapiro-Wilk W tests were used to determine normality of the data ($P \geq 0.05$). Normally distributed values were compared with matched pair t-tests. Non-normal values were log-transformed, and again tested for normality. Remaining non-normal values were compared using Wilcoxon pair tests. Each treatment value was compared to the fresh thread value, which served as the control. Our best gauge of similarity of control and treatment droplets was droplet length and width, which, within each species, were quite similar (Table 1).

Neither the dark nor the UVA exposure treatments had an effect on the droplet volumes of either species (Table 1). This failed to support the contending hypothesis that salts and LMMC in a droplet's outer aqueous layer are affected by UVA exposure and indicate that any observed effect of aging or UVA exposure on droplet performance must be attributed to the effects of these treatments on the glycoprotein core within each droplet.

Total loaded time began when an axial line was at 180° and experienced no pull from a droplet, and ended when the droplet had extended and had either released from the contacting probe or had become so thin that it no longer exerted a measurable force on the axial line, which had returned to a 180° configuration. This time was divided into the pre-extension phase, before force on the droplet was sufficient to extend the droplet's glycoprotein core, and the extension phase, during which the glycoprotein elongated (fig. 2 in Stellwagen et al. 2015). Extension times provided an index of the extensibility of the glycoprotein within droplets (Table 1). For the full sun species, *A. trifasciata*, droplet extension time was reduced by 29% after UVA exposure. For *N. crucifera*, extension time was unaffected by UVA exposure.

Plotting the force on an extending droplet against extension time depicts the performance of an extended droplet. The area under this curve represents relative toughness and is an index of the energy required to extend a droplet (Table 1, Fig. 1). Compared with fresh threads, the energy absorbed by threads of *A. trifasciata* and *N. crucifera* decreased 55% and 43%, respectively, after dark treatments and 45% and 31%, respectively, after UVA exposure. Neither treatment difference wass significant and, although both treatment

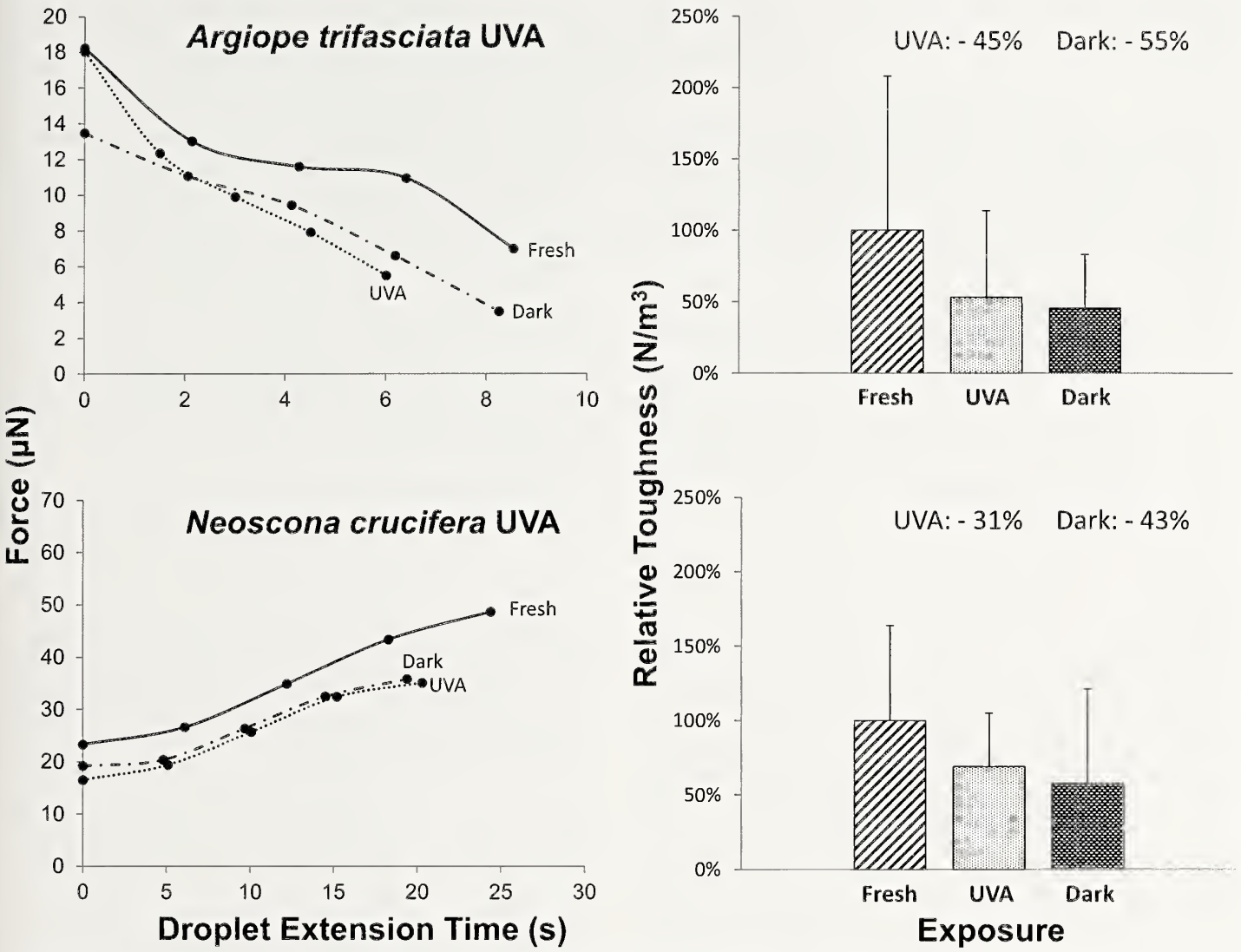

Figure 1.—Force/extension time plots for viscous droplets and corresponding histograms of relative toughness for droplets in each treatment, as determined from areas under these curves. Points in force/extension time plots are mean values and are connected by smoothed lines. Relative toughness values are mean + standard deviation.

values were less than the control, there was no evidence to suggest that that UVA exposure degraded droplet performance beyond the aging that occurred during this time.

Retention time is important for prey capture success, and a reduction of only a few seconds can mean a lost feeding opportunity for an orb-weaving spider (Blackledge & Zevenbergen 2006). This study hypothesized that droplets from webs of the diurnal, full sun species *A. trifasciata* would be more likely to be positively affected by UVA than those from the nocturnal species *N. crucifera*, or at least would be more resistant to UVA degradation. However, although droplets from *A. trifasciata* webs showed a reduction in droplet extension time after exposure to UVA, this did not affect the overall energy absorption of the droplet during its extension.

Interestingly, the relative toughness of both species' droplets decreased more after dark exposure than after UVA exposure, although these differences were not statistically significant. Threads of both species experienced a 4-hour, dark aging treatment, however, for *A. trifasciata* this occurred approximately 3 hours after a web was constructed, but for *N. crucifera* it occurred approximately 11 hours after a web was constructed. This difference may explain the smaller decrease in energy absorption by *N. crucifera* droplets. This decrease in toughness with aging may indicate that the chemical cross-linking mechanism hypothesized to strengthen dragline silk (Osaki 2004) either does not affect the glycoprotein, or that higher doses of UVA not typically experienced by spider threads are needed to see this effect and sufficiently counteract the effect of aging. Similar to UVB, UVA does not appear to impact the LMMC in droplets, which supports the observation that these compounds resist degradation (Opell et al. 2015). Thus, our study suggests that ecologically relevant doses of UVA have little impact on spider capture spiral thread function.

ACKNOWLEDGEMENTS

Carlyle C. Brewster assisted with statistical analyses. Author contributions: S.D.S. collected and prepared thread samples, performed droplet extensions and image measurements, analyzed data, and prepared the manuscript and figures. B.D.O. designed and constructed the instrumentation used in this study, collected and helped prepare thread samples, and contributed to data analysis, and manuscript and figure preparation. M.E.C. assisted with droplet extension, image measurements, and data entry. Funding: Funds from the State Council for Higher Education for Virginia provided

the digital camera used in this study. This study was supported by National Science Foundation grant IOS-1257719.

LITERATURE CITED

Agnarsson, I., C. Boutry & T.A. Blackledge. 2008. Spider silk aging: initial improvement in a high performance material followed by slow degradation. Journal of Experimental Zoology, Part A: Ecological Genetics and Physiology 309A:494–504.

Apstein, C.H. 1889. Bau und Function der Spinnendrusen der Araneida. Archiv fur Natur- geschichte 29–40.

Bhat, R. & A.A. Karim. 2009. Ultraviolet irradiation improves gel strength of fish gelatin. Food Chemistry 113:1160–1164.

Blackledge, T.A. & J.M. Zevenbergen. 2006. Mesh width influences prey retention in spider orb webs. Ethology 112:1194–1201.

Edmonds, D.T. & F. Vollrath. 1992. The contribution of atmospheric water vapour to the formation and efficiency of a spider's capture web. Proceedings of the Royal Society B: Biological Scienees 248:145–148.

Hu, X., W.K. Raja, B. An, O. Tokareva, P. Cebe & D.L. Kaplan. 2013. Stability of silk and collagen protein materials in space. Scientific Reports 3:3428.

Liao, C., S.J. Blamires, M.L. Hendricks & B.D. Opell. 2015. A re-evaluation of the formula to estimate the volume of orb web glue droplets. Journal of Arachnology 43:97–100.

Matsuhira, T., K. Yamamoto & S. Osaki. 2013. Effects of UV irradiation on the molecular weight of spider silk. Polymer Journal 45:1167–1169.

Opell, B.D., S.F. Andrews, S.E. Karinshak & M.A. Sigler. 2015. The stability of hygroscopic compounds in orb-web spider viscous thread. Journal of Arachnology 43:152–157.

Opell, B.D., S.E. Karinshak & M.A. Sigler. 2013. Environmental response and adaptation of glycoprotein glue within the droplets of viscous prey capture threads from araneoid spider orb-webs. Journal of Experimental Biology 216:3023–3034.

Osaki, S. 2004. Ultraviolet rays mechanically strengthen spider's silks. Polymer Journal 36:657–660.

Osaki, S. & M. Osaki. 2011. Evolution of spiders from nocturnal to diurnal gave spider silks mechanical resistanee against UV irradiation. Polymer Journal 43:200–204.

Perea, G.B., C. Solanas, G.R. Plaza, G.V. Guinea, I. Jorge, J. Vazquez et al. 2015. Unexpected behavior of irradiated spider silk links conformational freedom to mechanical performance. Soft Matter 11:4868–4878.

Rizzo, J.L., J. Dunn, A. Rees & T.M. Runger. 2011. No formation of DNA double-strand breaks and no activation of recombination repair with UVA. Journal of Investigative Dermatology 131:1139–1148.

Sahni, V., T.A. Blackledge & A. Dhinojwala. 2010. Viscoelastic solids explain spider web stickiness. Nature Communications 1:1–4.

Sahni, V., A. Dhinojwala, B.D. Opell & T.A. Blackledge. 2014. Prey capture adhesives produced by orb-weaving spiders. Pp. 203–217. *In* Biotechnology of Silk. (T. Asakura & T. Miller, eds.). Springer, Netherlands.

Sekiguchi, K. 1952. On a new spinning gland found in geometric spiders and its function. Annotationes Zoologicae Japonenses 25:394–399.

Sensenig, A.T., K.A. Lorentz, S.P. Kelly & T.A. Blackledge. 2012. Spider orb webs rely on radial threads to absorb prey kinetic energy. Journal of The Royal Society Interface 9:1880–1891.

Stellwagen, S.D., B.D. Opell & M.E. Clouse. 2015. The impact of UVB radiation on the glycoprotein glue of orb-weaving spider capture thread. Journal of Experimental Biology 218:2675–2684.

Townley, M. & E. Tillinghast. 2013. Aggregate silk gland secretions of araneoid spiders. Pp. 283–302. *In* Spider Ecophysiology. (W. Nentwig, ed.). Springer, Heidelberg.

Manuscript received 13 November 2015, revised 25 April 2016.

2016. Journal of Arachnology 44:405–407

SHORT COMMUNICATION

Dispersal behavior in agrobiont spiders (Linyphiidae) — differential response to a wind chamber

Christopher Woolley[1,2]: [1]Evolutionary Studies Institute, University of the Witwatersrand, Johannesburg, Gauteng, Wits 2050, South Africa. E-mail: christopher.woolley@wits.ac.za; [2]School of Biological Sciences, Plymouth University, Drake Circus, Plymouth, Devon, PL4 8AA, United Kingdom

Abstract. Two species of common, farmland-inhabiting money/dwarf spider, *Erigone atra* Blackwall, 1833 and *Oedothorax fuscus* (Blackwall, 1834), were exposed to light wind conditions within a wind chamber to determine their propensity to exhibit dispersal behaviors over a nine-month period. A novel design of wind chamber, incorporating two tangential fans, produced a wide outflow thereby allowing behaviors to be expressed over a relatively large test area (1 m × 0.65 m). Sticks placed at 3 cm intervals in an undulating foam surface structurally mimicked a natural field setting. Whereas the majority of *E. atra* expressed dispersal and related behaviors (tiptoe and drop posture and ballooning) in every month testing occurred, corresponding behaviors were rarely recorded in *O. fuscus*. Results are discussed in relation to knowledge of the dispersal activity of *O. fuscus* in the field and factors which may influence dispersal frequency and initiation.

Keywords: Ballooning, *Erigone*, *Oedothorax*

Erigone atra Blackwall, 1833 and *Oedothorax fuscus* (Blackwall, 1834) are two common species of money/dwarf spider (Linyphiidae) occurring in abundance on agricultural land in the British Isles. The survival of agrobiont spiders in the disturbed farmland environment is relevant from an agro-ecological perspective as evidence suggests that pest populations may be suppressed by farmland inhabiting linyphiids (Nyffeler & Sunderland 2003). Dispersal through the air by means of silk (ballooning) is thought to promote survival by spreading the risk of mortality-causing disturbance and by enabling spiders to quickly relocate should habitat quality decline (Weyman et al. 1994; Thomas & Jepson 1999). Although *E. atra* and *O. fuscus* are known to balloon, data from field studies suggests that *E. atra* is a more frequent disperser than *O. fuscus* (Weyman et al. 2002). In this study, spiders collected from the field over the course of nine months were exposed to light air currents within a wind chamber to determine: i) the proportion of spiders expressing dispersal behavior (ballooning and related behaviors) in a controlled environment; and ii) whether seasonal influence on dispersal motivation is a factor in the duration spent in dispersal behaviors and latency (i.e., the time taken to express dispersal behavior). The study was carried out at the former Seale-Hayne Faculty of Agriculture, Food and Land Use, Plymouth University, Devon, UK (now owned by the Dame Hannah Rodgers Trust).

The novel design of the wind chamber incorporated a large test area relative to a vertical air flow design (Weyman 1995), together with naturalistic structure with the intention of eliciting the fullest range of natural behaviors in test subjects. The wind chamber (Fig. 1) comprised a box made from 4 mm clear acrylic sheeting measuring 29 cm in height, 65 cm in width and 100 em in length. An air flow was generated by two tangential (cross-flow) fans mounted at one end (total fan length 60 cm, fan diameter 6 cm). This type of fan was chosen because the outflow of the air was even across the width of the fan's surface. Each fan was driven by an AC single-phase induction motor which allowed for a triac (triode for AC) based speed control. A domestic lighting dimmer switch was adequate for this purpose, enabling a wide degree of speed control down to very low fan speeds (the resistance rating being high enough for the inductive loading of the motor). The fans' outflow across the sticks (see below) produced a light, turbulent wind current throughout the chamber. A hot-wire anemometer recorded wind speeds 15 cm from the fan fluctuating between 0.10-0.46 m s^{-1}, and 15 cm from outflow end, between 0.09-0.42 m s^{-1}. Wind speeds also fluctuated between the top and bottom of the sticks with no clear differentiation in strength. On the floor of the wind chamber, a layer of 'egg-box' foam was fitted, into which sticks, 16 cm and 5 cm in length, were placed alternately at the top of each prominence. This created a lattice arrangement with a distance between each stick of 3 cm. The regular undulating surface allowed spiders on the ground to locate a stick at any point by following the surface inclines. The foam was raised slightly at the outflow end to preserve the direction of airflow over the back wall.

Spiders were collected from nearby fields using a modified garden vacuum suction sampler (Flymo BVL-320, Husqvarna) between February and October 2005. Species were identified and placed separately into clear plastic pots 46 mm in height and 90 mm in diameter. The bottom of each pot contained a 10 mm layer of moist Plaster of Paris to prevent dehydration. Spiders were kept outside in a sheltered area and were brought into the laboratory for testing within two days of collection.

Individual spiders were released onto the upper portion of the same stick, situated near the mid line of the chamber, approximately 20 cm from the outflow end. The duration of expressed behaviors were recorded over a three-minute period using *Etholog*, a behavioral transcription program (Ottoni 1999). The behavioral states recorded were as follows: i) tiptoe: spider rears up on the ends of the tarsi in a 'tiptoe stance', a precursor to the release of ballooning silk; ii) drop: spider drops on a short length of silk, a precursor to the release of ballooning silk; iii) non tiptoe/drop: release of silk when not in the previous positions; iv) balloon: spider becomes airborne after releasing silk; v) rig: spider traverses silk between sticks above the ground; vi) haul: silk released by the spider (or other spiders) is gathered by the forelegs while the spider is above the ground; vii) climb: spider climbs vertically up or down sticks; viii) lower: spider lowers itself on a length of silk but does not assume the 'drop' posture and continues to the ground; ix) ground active: spider is active on the ground; x) inactive: spider is inactive either above or on the ground; xi) groom: spider displays grooming behavior, usually while stationary.

The average number of spiders tested each month was 22.1 ± 6.1 *E. atra* females ($n = 161$), 20.6 ± 7.2 *E. atra* males ($n = 103$), 17.9 ± 1.1 *O. fuscus* females ($n = 143$) and 14.6 ± 3.1 *O. fuscus* males ($n = 44$). Insufficient numbers for testing ($n \leq 5$) were collected in some

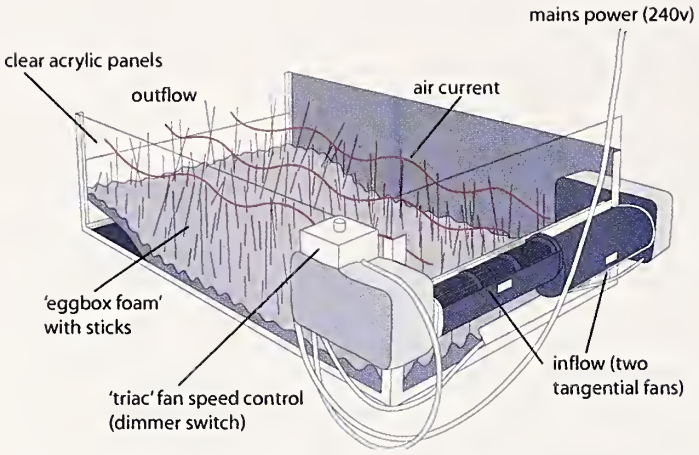

Figure 1.—Diagram of the wind chamber depicting tangential fans and the test area with egg-box foam and wooden sticks positioned at the top of each prominence. The intakes of the fans are reversed (one up, one down) to allow the fans to abut. The motors being on the same side prevented this arrangement when the intakes were in the same direction.

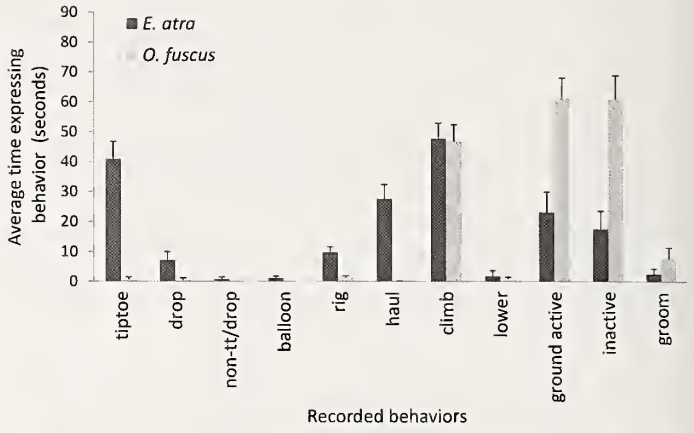

Figure 2.—Average time expressing recorded behaviors for *E. atra* ($n = 270$) and *O. fuscus* ($n = 188$) collected between February and October 2005. Error bars are 95% confidence intervals.

months. Between February and October *E. atra* females were not tested in April and August, *E. atra* males were not tested in March, April, May and August, and *O. fuscus* females were not tested in August. Males of *O. fuscus* were collected infrequently and only tested in February, July and October.

Dispersal behavior (tiptoe, drop, non-tiptoe drop and balloon) was recorded in all months for *E. atra* females and males. The total proportion of *E. atra* exhibiting dispersal behavior was 83% for females and 69% for males. Average time spent in dispersal behavior for *E. atra* females was higher for specimens collected in July, September and October than in earlier months. A Tukey HSD test revealed significant differences between March and July ($Q = 4.966$, $P < 0.001$), March and September ($Q = 4.906$, $P < 0.001$), May and July ($Q = 4.616$, $P = 0.019$) and May and September ($Q = 4.556$, $P = 0.022$). A significantly lower latency was recorded in October compared to May ($Q = 4.362$, $P = 0.033$). For *E. atra* males, average time spent in dispersal behavior was not significantly different between individual months although a one-way ANOVA (Welch's test for unequal variances) was significant for all months ($F = 2.576_{102}$, $P = 0.042$). Similarly, latency was not significantly different between individual months although a one-way ANOVA (Welch's test for unequal variances) was significant for all months ($F = 3.292_{41.28}$, $P = 0.02$).

The total proportion of *O. fuscus* exhibiting dispersal behavior was 1.4% for females and 11.4% for males. Dispersal behavior was recorded in five *O. fuscus* males, two in July and three in October. Only two spiders, both in October, displayed sustained dispersal-related activity (over one minute), with others showing very brief activity (less than ten seconds). Two *O. fuscus* females displayed very brief dispersal activity (less than ten seconds). Further statistical analysis between months was not performed owing to the small number of individuals expressing dispersal behavior.

Differences in time spent expressing behaviors between *E. atra* and *O. fuscus* was analysed for the behaviors, tiptoe, drop, balloon, climb and ground active. A General Linear Mixed Model (GLMM) analysis was performed using SAS/STAT® software using the 'GLIMMIX' procedure with 'Month' selected as a random factor. A negative binomial distribution was selected for the response distribution. Fit statistics (AIC) were comparable to those for the Tweedie distribution commonly fitted to data with a high proportion of zero counts (but not available in GLIMMIX). Time spent in 'tiptoe' was significantly higher for *E. atra* than *O. fuscus* ($F = 277.42_{448}$, $P < 0.001$), time spent in 'drop' was significantly higher for *E. atra* than *O. fuscus* ($F = 48.16_{448}$, $P < 0.001$), time spent in 'balloon' was significantly higher for *E. atra* than *O. fuscus* ($F = 15.79_{448}$, $P < 0.001$), time spent in 'climb' was non-significant ($F = 0.91_{448}$, $P = 0.34$) and time spent in 'ground active' was significantly higher for *O. fuscus* than *E. atra* ($F = 37.56_{448}$, $P < 0.001$).

Whereas dispersal related behaviors made up almost a third of all activity in *E. atra* females, these behaviors were almost absent in *O. fuscus* females. The majority of *O. fuscus* males were similarly unresponsive compared to *E. atra* males. 'Inactive' averaged one third of total time in *O. fuscus*, however, approximately 60% of total time was spent in active behaviors (Fig. 2). Spiders which were active tended to move along the ground but also frequently climbed to the top of sticks before rapidly descending and moving to another. In this manner, some *O. fuscus* climbed numerous sticks in the three minute period. The act of climbing is seen as a prelude to ballooning behavior (Weyman 1995), however, the lack of ballooning related activity, even in individuals that climbed, suggests that a different set of prerequisite conditions are necessary to elicit ballooning compared to *E. atra*. Possible explanations for the lack of dispersal related activity would appear to exclude seasonal influence, none of which was observed for *O. fuscus* (although this cannot be discounted until the appropriate conditions to initiate dispersal are known). Light wind conditions simulated by the wind chamber were within the 3 m s^{-1} threshold above which ballooning is limited (Vugts & Van Wingerden 1976). The character of the airflow was also investigated with spiders being placed in a chamber similar to that used by Weyman et al. (1995) with a vertical airflow. Dispersal behavior was also not elicited under these conditions (C. Woolley, unpublished data). Some indication as to the nature of the necessary conditions comes from dispersal activity monitored in the field. Females of *O. fuscus* were found to disperse in large numbers during sustained light wind conditions (lasting several days) associated with the passage of high pressure systems in autumn and winter (Woolley et al. 2016). Covariation under such conditions makes it difficult to implicate a specific variable as the cause (should just one exist). Changes in temperature, light, humidity, wind, vibration and atmospheric pressure, as has been found initiating dispersal in the twospotted spider mite (Li & Margolies 1994), have been suggested as possible stimuli (Weyman 1993); duration of conditions and rate of change may also be relevant.

Certain aspects of behavior and physiology appear to correspond with differences in dispersal frequency. The cursorial hunting habit observed for *O. fuscus* (Thornhill 1983) could compensate for local variations in prey density, reducing the need to balloon to higher density patches. Egg-guarding by female *O. fuscus* (Baarlen et al. 1994) could be inhibitory to dispersal, although male spiders would

not be similarly restricted. Interestingly, 'male-only' dispersal activity has been observed in autumn (Woolley et al. 2016) which may be related to reproductive activity and could account for the only sustained dispersal activity observed for *O. fuscus* males in October. For *E. atra*, where egg-guarding behavior is limited or does not occur (Baarlen et al. 1994), frequent dispersal could allow eggsacs to be dispersed over a wider area thereby reducing the probability that all eggsacs succumb to parasitism by spreading the risk across multiple locations. The physiology of *E. atra* also appears better adapted to perturbations in prey intake (De Keer & Maelfait 1988) which may be a consequence of frequent passive dispersal and greater exposure to habitats of varying quality.

In the locality where *O. fuscus* was collected, the population was found to be heavily female dominated. This could be the result of infection by a sex-ratio altering endosymbiont such as *Wolbachia*, which is known to manipulate sex ratios in congener *O. gibbosus* (Blackwall, 1841) (Vanthournout 2012). Individuals of *E. atra* infected by the endosymbiont *Rickettsia* have been shown to exhibit lower dispersal motivation compared with those receiving antibiotic treatment (Goodacre et al. 2009). Life history traits outlined above might suggest that endosymbiont infection is not a major determinant in dispersal frequency, at least not to the extent that it might account for the lack of dispersal motivation compared to *E. atra*. It has been suggested though that species which display pronounced phenotypic effects might be 'deeply modified organisms' (Thomas et al. 2005), with multiple traits arising under the influence of infection.

Compared to the findings of Weyman et al. (1995), *E. atra* females did not show a seasonally consistent ballooning response over the study period. More time spent in pre-ballooning behavior and lower latencies (although these variables are not independent) were observed in later months, although no clear pattern was discernible for males. That spiders were kept outside in a sheltered area could be of significance. Without radiative warming by the sun, spiders may not have been sufficiently warmed before being placed in the wind chamber. In warmer months, spiders were consequently more active which may have resulted in a greater propensity to display dispersal behavior.

Weyman et al. (2002), in their review of the evolution and mechanisms of ballooning, recognised the difficulty in unravelling the potential factors responsible for its initiation. With evidence that *O. fuscus* displays pronounced, although infrequent, dispersal in the field, this study suggests that *O. fuscus*, or one of its congeners (e.g., *O. apicatus* (Blackwall, 1850), a common agrobiont species which also shows infrequent dispersal (Blandenier 2009; Thomas et al. 1990), may be worthy of further investigation into ballooning initiation. Discovering the parameters under which *Oedothorax* spp. will disperse may have relevance to long-standing questions regarding conditions which give rise to the large and congruent dispersal of spiders, so called 'mass dispersal events' (Bennett 2003). Models to determine population persistence in the agricultural environment (Halley et al. 1996) may also benefit from such data.

This work was funded through BBSRC grants D14032, D20476 and D14036. I would like to thank the technical and farm staff at Seale-Hayne for their assistance.

LITERATURE CITED

Baarlen, P.V., K.D. Sunderland & C.J. Topping. 1994. Eggsac parasitism of money spiders (Araneae, Linyphiidae) in cereals, with a simple method for estimating percentage parasitism of *Erigone* spp. eggsacs by Hymenoptera. Journal of Applied Entomology 118:217–223.

Bennett, R. 2003. Mass dispersal of erigonine spiders from a clover field in British Columbia, Canada. British Arachnological Society Newletter 97:2–3.

Blandenier, G. 2009. Ballooning of spiders (Araneae) in Switzerland: general results from an eleven-year survey. Bulletin of the British Arachnological Society 14:308–316.

De Keer, R. & J.-P. Maelfait. 1988. Laboratory observations on the development and reproduction of *Erigone atra* Blackwall, 1833 (Araneae, Linyphiidae). Bulletin of the British Arachnological Society 7:237–242.

Goodacre, S., O. Martin, D. Bonte, L. Hutchings, C. Woolley, K. Ibrahim, et al. 2009. Microbial modification of host long-distance dispersal capacity. BMC Biology 7:1–8. Online at http://dx.doi.org/10.1186/1741-7007-7-32

Halley, J.M., C.F.G. Thomas & P.C. Jepson. 1996. A model for the spatial dynamics of spiders in farmland. Journal of Applied Ecology 33:471–492.

Li, J. & D.C. Margolies. 1994. Barometric pressure influences initiation of aerial dispersal in the twospotted spider mite. Journal of the Kansas Entomological Society 67:386–393.

Nyffeler, M. & K.D. Sunderland. 2003. Composition, abundance and pest control potential of spider communities in agroecosystems: a comparison of European and US studies. Agriculture and Forest Entomology 95:579–612.

Ottoni, E.B. 1999. Etholog—behavioural observation transcription tool, 2.2.5 edn. Bottoni, E.B., São Paulo.

Thomas, C.F.G. & P.C. Jepson. 1999. Differential aerial dispersal of linyphiid spiders from a grass and a cereal field. Journal of Arachnology 27:294–300.

Thomas, F., S. Adamo & J. Moore. 2005. Parasitic manipulation: where are we and where should we go? Behavioural Processes 68:185–199. Online at http://dx.doi.org/10.1016/j.beproc.2004.06.010

Thomas, C.F.G., E.H.A. Hol & J.W. Everts. 1990. Modelling the diffusion component of dispersal during recovery of a population of linyphiid spiders from exposure to insecticide. Functional Ecology 4:357–368.

Thornhill, W.A. 1983. The distribution and probable importance of linyphiid spiders living on the soil surface of sugar-beet fields. Bulletin of the British Arachnological Society 6:127–136.

Vanthournout, B. 2012. Sex ratio distortion in the male dimorphic dwarf spider *Oedothorax gibbosus*: mechanisms and the role of endosymbiont bacteria. PhD dissertation, Faculty of Sciences, Ghent University, Ghent, Belgium.

Vugts, H.F. & W.K.R.E. Van Wingerden. 1976. Meteorological aspects of aeronautic behaviour of spiders. Oikos 27:433–444.

Weyman, G.S. 1993. A review of the possible causative factors and significance of ballooning in spiders. Ethology Ecology and Evolution 5:279–291.

Weyman, G.S. 1995. Laboratory studies of the factors stimulating ballooning behaviour by linyphiid spiders (Araneae, Linyphiidae). Journal of Arachnology 23:75–84.

Weyman, G.S., P.C. Jepson & K.D. Sunderland. 1995. Do seasonal-changes in numbers of aerially dispersing spiders reflect population density on the ground or variation in ballooning motivation? Oecologia 101:487–493.

Weyman, G.S., K.D. Sunderland & J.S. Fenlon. 1994. The effect of food deprivation on aeronautic dispersal behaviour (ballooning) in *Erigone spp.* spiders. Entomologia Experimentalis et Applicata 73:121–126.

Weyman, G.S., K.D. Sunderland & P.C. Jepson. 2002. A review of the evolution and mechanisms of ballooning by spiders inhabiting arable farmland. Ethology Ecology and Evolution 14:307–326.

Woolley, C., C.F. George Thomas, R.P. Blackshaw & S.L. Goodacre. 2016. Aerial dispersal activity of spiders sampled from farmland in southern England. Journal of Arachnology 44:347–358.

Manuscript received 14 September 2015, revised 27 May 2016.

2016. Journal of Arachnology 44:408–411

SHORT COMMUNICATION

Resource allocation in food-restricted male *Physocyclus mexicanus* Banks, 1898 spiders does not favor proportionally larger testes (Araneae: Pholcidae)

Diane E. Wilson[1], Kristen D. Felt[1], Emily N. Campbell[1], Olivia R. Cohen[1], Lauren E. Geisel[1], Jove Graham[2] and Leocadia V. Paliulis[1]: [1]Biology Department, Bucknell University, Lewisburg, PA 17837; [2]Geisinger Center for Health Research, Danville, PA 17822. E-mail: le.paliulis@bucknell.edu

Abstract. The physiological effects of resource allocation due to dietary restriction in spiders are poorly understood; in fact, the system-wide effects of any environmental stresses on spider physiology remain relatively unstudied. The aim of this study was to show the consequences of dietary restriction in the pholcid spider *Physocyclus mexicanus* Banks, 1898. Male spiders were fed either a high (*ad libitum*) diet (n = 43) or low (5–8 *Drosophila melanogaster*/week) diet (n = 32) through their penultimate instar. We found significant differences in testis volume, body mass, and tibia-patella length [TPL] between the two groups. Linear regression analysis reveals that the differences in testis volume between the two groups are not solely due to differences in body mass; for any given body mass, the low diet group has a smaller mean testis size than the high diet group. Our results suggest that *P. mexicanus* males allocate resources away from testis volume in times of scarcity.

Keywords: Dietary restriction, testes size, body mass

Organisms maximize fitness for their expected reproductive lifespan by dynamically allocating available energy to growth, maintenanee, and reproduction depending on environmental and physical conditions (Sibly & Calow 1986; Stearns 1992). Increased allocation toward one of these three key components necessarily means deprivation to the other two (Stearns 1992; Reznick et al. 2000; Roff & Fairbairn 2001). Resource (energy) allocation is the study of the relative importance of these three at different times in the life history of a species and how changes in allocation depend on the amount of resources available (Jokela & Mutikainen 1995). As has been observed in the male redback spider *Latrodectus hasselti* Thorell, 1870, allocation patterns can shift depending on the environmental context (Kasumovic & Andrade 2006). Resource allocation has been studied in many taxa. For example, wolf spiders that were fed only a limited diet of crickets took longer to reach sexual maturity, were smaller in size, and had higher mortality rates than those fed a well-balanced diet of insects (Uetz et al. 1992). This not only suggests that life cycle readjustments occur in times of famine, but also that life extension as a result of a restricted diet could be an adaptation to dealing with the famine itself (Uetz et al. 1992; Kirkwood & Shanley 2005).

We studied testis size and body size to determine whether metabolic energy was being preferentially used to favor reproduction. Sperm production in spiders, like most investments in reproduction, is a considerable energy cost in males of reproductive age (Greenstone & Bennett 1980; Anderson 1996; Olsson et al. 1997; Hayward & Gilloly 2011). While testis size does not completely correlate with sperm production, larger testes typically correspond to higher levels of sperm production (Schärer et al. 2004; Schärer & Vizoso 2007) or the production of longer sperm (Pitnick 1996). Males with larger testis size can experience greater reproductive success as a result (Schulte-Hostedde & Millar 2004). If an organism were to favor reproduction over survival during times of food restriction, the animal would likely be smaller in size, but its testes would be proportionally larger.

Testis size is correlated to sperm competition between males in species where females mate with more than one male (Gage 1994; Gay et al. 2009; Vrech et al. 2014). Female polygamy acts as the driving force for sperm competition in many spider species, with males partaking in longer copulations, guarding of females, and the production of copulatory plugs in order to prevent the female from mating with other males (Huber 2005). In many cases, these adaptations arose as a result of the behaviors of female spiders and the morphology of their reproductive tracts (Elgar 1998; Eberhard 2005). In more monogamous species, such as the Australian golden orb-web spider *Nephila plumipes* (Latreille, 1804), the males do not adjust their sperm investment based upon sperm competition, and they instead protect their paternity through mate guarding (Schneider et al. 2008). Furthermore, in *Tidarren argo* Knoflach & van Harten, 2001, male spiders abandon spermiogenesis and undergo testes atrophy after their one mating event (Michalik et al. 2010). In more polyandrous species, such as the pholcid spider *Pholcus phalangioides* (Fuesslin, 1775), males spend more time mating with virgin females than already-mated females in order to try and overcome last-male sperm priority and guarantee their parentage (Yoward 1998). Different species of fruit flies (genus *Drosophila*) have varied testis size and sperm lengths, which are due to selective pressures they experience through their environment, life cycle, and mating habits (Pitnick 1996). Scorpion species that experience higher levels of sperm competition have a higher testes mass than their monogamous relatives (Vrech et al. 2014). In yellow dung flies, testis size is influenced not only by sperm competition but also by the number of expected mates, as predicted by the size of the male (Blanckenhorn et al. 2004).

In general, genital size is positively correlated with body size in spiders, though there is little information specifically on testis size in spiders. However, genital size and body size have negative allometry in spiders; i.e., genitals are disproportionally larger in smaller spiders. (Eberhard 2009 and the references therein). Testis size has also been correlated with body size in other arthropods. Butterflies, yellow dung flies, and fruit flies all exhibit positive allometry of testes mass and body size.

Limited resources may lead to increased allocation of resources to survival, reproduction, or growth (Sibly & Calow 1986; Stearns 1992). This can be seen in many different spider species. For example, food-restricted *Latrodectus pallidus* O. P-Cambridge, 1872 males live longer than males fed *ad libitum*, which may be an evolutionary mechanism to ensure survival in order to maximize chances of reproductive success before death (Segoli et al. 2007). This could also result from

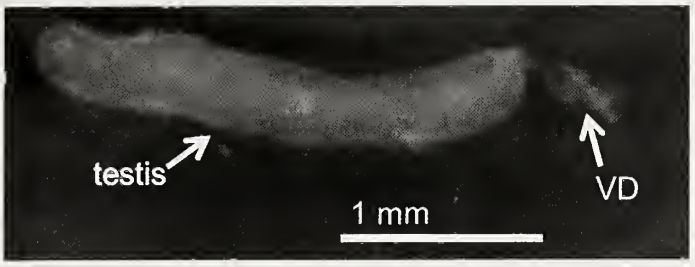

Figure 1.—Testis morphology in *P. mexicanus*, showing both testis and vas deferens (VD). Bar = 1 mm.

the possibility that lab feeding *ad libitum* may be overfeeding; individuals with restricted diets may actually be on a feeding regimen that more closely imitates their foods levels in the wild (Kirkwood & Shanley 2005). Extension of life span has been observed in many other species of spider (Austad 1989; Kleinteich et al. 2015); however, it is not true for all, as redback spiders do not show increased longevity under a restricted diet (Kasumovic et al. 2009). On the other hand, a restricted diet caused female *Tigrosa helluo* (Walckenaer, 1837) to seek mates less and to move to actively seek food more, a shift away from reproduction to survival (Walker et al. 1999). The shift away from reproduction has also been observed in water mites, minnows, and other species (Proctor 1992; Pyron 2000). In the conflict between investment in reproduction and survival, many diverse evolutionary strategies have evolved.

This study focuses on *Physocyclus mexicanus* Banks, 1898, a pholcid spider that can live more than one year (C. Kristensen, pers. comm.). We have observed that *P. mexicanus* continue to produce sperm through adulthood (data not shown), similar to previous observations of the pholcid *Pholcus phalangioides* (Michalik & Uhl 2005). *P. mexicanus* males are iteroparous and typically encounter many reproductive opportunities once they reach sexual maturity (C. Kristensen, pers. comm.). Thus, we hypothesized that they would not divert extra resources to reproduction during times of limited resources due to the likelihood that they would encounter a reproductive opportunity in the future when more resources become available again. As a result, we propose that *P. mexicanus*, like other iteroparous species, is likely to shift resource allocation in a restricted diet away from reproduction in order to prolong survival (Nakatsuru & Kramer 1982). We used testes size to estimate the allocation of resources to reproduction in male *P. mexicanus* spiders under dietary restriction.

Juvenile pre-penultimate-molt *Physocyclus mexicanus* males were collected and identified by C. Kristensen (Spider Pharm) in Yarnell, AZ. One male and one female specimen are deposited in the National Museum of American History, Smithsonian Institution. Spiders were kept individually in 1-pint (470-ml) deli containers with cheesecloth lids. Containers were stacked in aquarium tanks with standard aquarium heaters at approximately 25°C and exposed to natural light and dark cycles. Spiders were randomly assigned to high and low diet groups. A spider in the low diet group was fed 5–8 *Drosophila melanogaster* once per week through its penultimate instar. A spider in the high diet group was fed *ad libitum*, and was provided more than 100 *Drosophila melanogaster* per week through its penultimate instar. We do not have sufficient observations of feeding and life history to determine whether the low diet group represents a near-starvation diet, but food quantity for the low diet spiders was considerably less than individuals in the high diet group received, and led to differences in body mass, tibia-patella length, and testis volume relative to individuals receiving an *ad libitum* diet (see below).

Both treatment groups remained unfed for 5 days after their final molt before dissection to allow the high diet spiders to digest the contents of the gut (Nentwig 2013). Five days after the final molt,

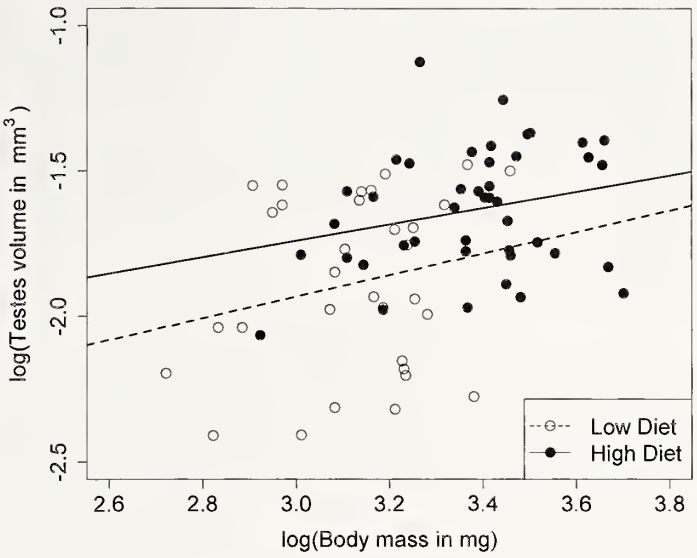

Figure 2.—Allometric relation between log testis volume (in mm^3) and log body mass (in mg) in low and high diet groups. Predicted log(testes volume) at body mass 27 mg = −1.82, slope of low diet group = 0.37 (95% CI = −0.14 to 0.88, P = 0.15), difference in predicted testes volume at body mass 27 mg = 0.166 (95% CI = 0.017 to 0.31, P = 0.029), slope of high diet group = 0.459. Difference in slopes = −0.089 (95% CI = −0.75 to 0.57, P = 0.79). R^2 = 0.21.

spiders were cold-anesthetized for 30 minutes, weighed, and dissected. The front leg was reserved for tibia-patella length measurements. Testes were removed in phosphate buffered saline and imaged using a Nikon (model C-DS) dissecting microscope with a Nikon Coolpix P6000 camera and an eyepiece adapter. Curve analyzing software, Image J 1.48 (Glyn II, 2011) was used to measure testis length and width compared to a ruler. Because *P. mexicanus* testes are nearly cylindrical (Fig. 1), testis volume was estimated using the formula for the volume of a cylinder ($V = \pi r^2 h$).

We compiled the results and used two tailed t-tests to determine whether there was a difference in resource allocation between the low diet (n = 32) and high diet (n = 43) groups. T-tests that yielded results with $P < 0.05$ were considered to show significant differences. The high and low diet groups had significant differences in mean tibia-patella length (TPL—high diet mean = 1.04 cm, low diet mean = 0.85 cm, t = 2.76, P = 0.0066), body mass (high diet mean = 29.75 mg, low diet mean = 23.13 mg, t = 5.78, $P = 7.7\times10^{-8}$), and testis volume (high diet mean = 0.199 mm^3, low diet mean = 0.158 mm^3, t = 4.04, P = 0.00013).

We fit a log-log regression model to the data, using both body mass and diet group as predictors of testis volume (Fig. 2). Our data show that both the low and high diet groups have low allometric slopes and display negative allometry (both slopes <1), as has been demonstrated for male genitalia in other spiders and insects (Eberhard 2009). While our data show that mean testis volume and mean body mass are both higher in the high diet group than in the low diet group, our analysis shows that the differences in testis volume between the two groups are not due solely to differences in body mass; i.e., for any given body mass, individuals in the low diet group will have a lower testis volume on average than individuals in the high diet group (Fig. 2). These data suggest that *P. mexicanus* invests more heavily in testis size when consuming an *ad libitum* diet than when consuming a restricted diet.

Because the male reproductive physiology of spiders is complex, diet could impact the size of more than one reproductive structure. Sperm are transferred from testes and vasa deferentia to pedipalps prior to mating (Huber & Eberhard 1997; Eberhard 2005). Because

the pedipalps play such a critical role in storage and transfer of sperm, it is likely that diet could impact pedipalp volume as well. While we did not measure the impact of diet on pedipalp size in *P. mexicanus*, this could be an interesting future study.

In conclusion, the results above suggest that in times of scarcity, *P. mexicanus* males will allocate resources away from reproduction. This makes sense, because they are iteroparous and can have a long lifespan (more than one year) (C. Kristensen, pers. comm.), allowing for opportunities to reallocate resources to reproduction when food supply improves.

ACKNOWLEDGMENTS

Many thanks to Chuck Kristensen (Spider Pharm, Yarnell, Arizona) for providing us with spiders and with information about their life history. We greatly appreciate our discussions with Tristan Stayton, without which this paper would never have been eompleted. We thank Amy Wendt for her eareful reading of the manuscript. We also thank two anonymous reviewers for their excellent advice on revising this manuscript.

LITERATURE CITED

Anderson, J.F. 1996. Metabolic rates of resting salticid and thomisid spiders. Journal of Arachnology 24:129–134.

Austad, S.N. 1989. Life extension by dietary restriction in the bowl and doily spider, *Frontinella pyramitela*. Experimental Gerontology 24:83–92.

Blanckenhorn, W.U., B. Hellriegel, D.J. Hosken, P. Jann, R. Altwegg & P.I. Ward. 2004. Does testis size track expected mating success in yellow dung flies? Functional Ecology 18:414–418.

Eberhard, W.G. 2005. Why study spider sex: Special traits of spiders facilitate studies of sperm competition and cryptic female choice. Journal of Arachnology 32:545–556.

Eberhard, W.G. 2009. Statie allometry and animal genitalia. Evolution 63:48–66.

Elgar, M.A. 1998. Sperm competition and sexual selection in spiders and other arachnids. Pp. 307–339. *In* Sperm Competition and Sexual Selection. (T.R. Birkhead, A.P. Møller, eds.). Aeademic Press, San Diego, California.

Gage, M.J.G. 1994. Associations between body size, mating pattern, testis size and sperm lengths across butterflies. Proceedings of the Royal Society B 258:247–254.

Gay, L., P.J. Hosken, R. Vasudev, T. Tregenza & P.E. Eady. 2009. Sperm competition and maternal effects differentially influence testis and sperm size in *Callosobruchus maculatus*. Journal of Evolutionary Biology 22:1143–1150.

Greenstone, M.H. & A.F. Bennett. 1980. Foraging strategy and metabolic rate in spiders. Ecology 61:1255–1259.

Hayward, A. & J.F. Gillooly. 2011. The cost of sex: quantifying energetic investments in gamete production by males and females. PLoS ONE 6(1): e16557.

Huber, B.A. 2005. Sexual selection research on spiders: progress and biases. Biological Reviews 80:363–385.

Huber, B.A. & W.G. Eberhard. 1997. Courtship, copulation, and genital mechanics in *Physocyclus globosus* (Araneae, Pholcidae). Canadian Journal of Zoology 74:905–918.

Jokela, J. & P. Mutikainen. 1995. Phenotypic plasticity and priority rules for energy allocation in a freshwater clam: a field experiment. Oecologia 104:122–132.

Kasumovic, M.M. & M.C.B. Andrade. 2006. Male development tracks rapidly shifting sexual versus natural selection pressures. Current Biology 16:R242–R243.

Kasumovic, M.M., R.C. Brooks & M.C.B. Andrade. 2009. Body condition but not dietary restriction prolongs lifespan in a semelparous capital breeder. Biology Letters 5:636–638.

Kirkwood, T.B.L. & D.P. Shanley. 2005. Food restriction, evolution and ageing. Mechanisms of Ageing and Development 126:1011–1016.

Kleinteich, A., S.M. Wilder & J.M. Schneider. 2015. Contributions of juvenile and adult diet to the lifetime reproductive success and lifespan of a spider. Oikos 124:130–138.

Michalik, P. & G. Uhl. 2005. The male genital system of the cellar spider *Pholcus phalangioides* (Fuesslin, 1775) (Pholcidae, Araneae): development of spermatozoa and seminal secretion. Frontiers in Zoology 2:12.

Michalik, P, B. Knoflach, K. Thaler & G. Alberti. 2010. Live for the moment—Adaptations in the male genital system of a sexually cannibalistic spider (Theridiidae, Araneae). Tissue Cell 42:32–36.

Nakatsuru, K. & D.L. Kramer. 1982. Is sperm cheap? Limited male fertility and female choiee in the lemon tetra (Pisces, Characidae). Science 216:753–755.

Nentwig, W. 2013. Spider Ecophysiology. Springer, New York.

Olsson, M., T. Madsen & R. Shine. 1997. Is sperm really so cheap? Costs of reproduction in male adders, *Vipera berus*. Proceedings of the Royal Society of London B 264:455–459.

Pitnick, S. 1996. Investment in testes and the cost of making long sperm in *Drosophila*. American Naturalist 148:57–80.

Proctor, H.C. 1992. Effect of food deprivation on mate searching and spermatophore production in male water mites (Acari: Unionicolidae). Functional Ecology 6:661–665.

Pyron, M. 2000. Testes mass and reproduetive mode of minnows. Behavioral Ecology and Sociobiology 48:132–136.

Rezniek, D., L. Nunney & A. Tessier. 2000. Big houses, big cars, superfleas and the costs of reproduction. Trends in Ecology & Evolution 15:421–425.

Roff, D.A. & D.J. Fairbairn. 2001. The genetic basis of dispersal and migration, and its consequences for the evolution of correlated traits. Pp. 191–202. *In* Consequences and Mechanisms of Dispersal at the Individual, Population and Community Level. (C. Clobert, J. Nichols, J. D. Danchinm, A. Dhondt, eds.). Oxford University Press, Oxford.

Schärer, L. & D.B. Vizoso. 2007. Phenotypic plasticity in sperm production rate: there's more to it than testis size. Evolutionary Ecology 21:295–306.

Schärer, L., P. Laduerner & R.M. Rieger. 2004. Bigger testes do more work: experimental evidence that testis size reflects testicular cell proliferation activity in the marine invertebrate, the free-living flatworm *Macrostromum sp*. Behavioral Ecology and Sociobiology 56:420–425.

Schneider, J.M., M.E. Herberstein, M.J. Bruce, M.M. Kasumovic, M.L. Thomas & M.A. Elgar. 2008. Male copulation frequency, sperm competition and genital damage in the golden orb-web spider (*Nephila plumipes*). Australian Journal of Zoology 56:233–238.

Schulte-Hostedde, A.I. & J.S. Millar. 2004. Intraspeeific variation of testis size and sperm length in the yellow-pine chipmunk (*Tamiasamoenus*): implications for sperm competition and reproductive suecess. Behavioral Ecology and Sociobiology 55:272–277.

Segoli, M., Y. Lubin & A.R. Harari. 2007. The effect of dietary restriction on the lifespan of males in a web-building spider. Evolutionary Ecology Research 9:697–704.

Sibly, R.M. & P. Calow. 1986. Physiological Ecology of Animals: An Evolutionary Approach. Blackwell Scientific Publications, Oxford.

Stearns, S.C. 1992. The Evolution of Life Histories. Oxford University Press, New York.

Uetz, G.W., J. Bischoff & J. Raver. 1992. Survivorship of wolf spiders (Lycosidae) reared on different diets. Journal of Arachnology 20:207–211.

Vrech, D.E., P.A. Olivero, C.I Mattoni & A.V. Peretti. 2014. Testes mass, but not sperm length, increases with higher levels of polyandry in an ancient sex model. PLoS ONE 9(4): e94135.

Walker, S.E., S.D. Marshall, A.L. Rypstra & D.H. Taylor. 1999. The effects of hunger on locomotory behavior in two species of wolf spider (Araneae, Lycosidae). Animal Behaviour 58:515–520.

Yoward, P.J. 1998. Sperm competition in *Pholcus phalangioides* (Fuesslin, 1775) (Araneae, Pholcidae)—shorter second copulations gain a higher paternity reward than first copulations. Pp. 167–170. *In* Proceedings of the 17th European Colloquium of Arachnology. (P.A. Selden ed.). British Arachnological Society. Edinburgh.

Manuscript received 30 June 2015, revised 22 July 2016.

2016. Journal of Arachnology 44:412–416

SHORT COMMUNICATION

Description of the sexual behavior of the Neotropical wolf spider *Pavocosa gallopavo* (Araneae: Lycosidae), with comments on sexual cannibalism

Carlos A. Toscano-Gadea and **Fernando G. Costa**: Laboratorio de Etología, Ecología y Evolución, IIBCE, Av. Italia 3318, CP: 11600 Montevideo, Uruguay. E-mail: ctoscanogadea@gmail.com

Abstract. We describe for the first time the sexual behavior of *Pavocosa gallopavo* (Mello-Leitão, 1941) (Lycosidae), analyzing encounters between 25 pairs of virgin adult individuals. Both courtship and copulation were brief, averaging 3.66 min and 1.74 min respectively. Males showed a very conspicuous and vigorous courtship, with Leg Shaking and Palpal Drumming as the most noticeable displays. Females were also active during courtship, performing Leg Waving as well as showing some level of aggression by displaying Cheliceral Opening and Pushes against males. The males mounted the females in the typical position of wolf spiders, and females initially performed intense body shakes (Bucking). The copulatory pattern consisted of alternating single insertions of both palps, with a unique hematodochal expansion by insertion. Females cannibalized males three times, two of them before copulation and the third after copulation. Copulation was brief with respect to other wolf spiders, and females were unusually active during copulation. The species would be suitable for further studies of multimodal communication and the sexual inhibition of female aggression.

Keywords: Courtship behavior, copulatory pattern, Uruguay

Sexual behavior is largely unknown for Neotropical spiders. Moreover, in small countries like Uruguay, with a long tradition of ethological studies of wolf spiders, sexual behavior has been described for only six of the thirty species recognized by Castro-O'Neil (2010) in the country. These six species belong to three subfamilies: *Schizocosa malitiosa* (Tullgren, 1905), *Lycosa thorelli* (Keyserling, 1877), and *L. carbouelli* (Costa & Capocasale, 1984) to Lycosinae; *Allocosa brasiliensis* (Petrunkevitch, 1910) and *A. alticeps* (Mello-Leitão, 1944) to Allocosinae; and *Aglaoctenus lagotis* (Holmberg, 1876) to Sosippinae (Costa 1975, 1979, 1991; Costa & Capocasale 1984; Aisenberg & Costa 2008; González et al. 2013, 2014). Here we present data on *Pavocosa gallopavo* (Mello-Leitão, 1941), a medium-sized Lycosinae occurring in southern Brazil, northern and central Argentina and throughout Uruguay (Murphy et al. 2006; Aisenberg et al. 2011b; World Spider Catalog 2015). The species is characterized by moderate sexual dimorphism, with an average body length of 11.3 mm in males and 15.1 mm in females. Males have a whitish ventral surface, whereas females may be whitish or have a small or large dark pigmented area on their venters.

The taxonomic status of the species is in doubt. For example, Castro-O'Neil (2010) examined the taxonomy and distribution of Uruguayan wolf spiders and considered *P. gallopavo* as a junior synonym of *Molitorosa molitor* (Bertkau, 1880). The genus *Pavocosa* (Roewer, 1960) is also controversial because it has only five species living in countries far from one another: Argentina, Brazil, Uruguay, Thailand, and the Caroline Islands. Murphy et al. (2006) included Brazilian specimens of *P. gallopavo* in their comprehensive phylogenetic analysis of wolf spiders and found affinities between the species and an Australasian clade of species, suggesting a Gondwanan origin of the group. Piacentini (2014), using morphological characters, found significant support for the hypothesis that *P. gallopavo* specimens from Argentina form a single clade with the Nearctic burrowing species *Geolycosa missouriensis* (Banks, 1895).

Until recently, *P. gallopavo* had been found only in very low density in Uruguay, preventing quantitative studies of its reproductive behavior. However, in 2014 we found high density populations in two open areas of the Departments of Canelones and San José. Using molecular techniques based on individuals from San José (close to our site of collection), Lacava (2014) found that this spider consumes mainly crickets, lepidopterans, and ants. Murphy et al. (2006), in a phylogenetic study of wolf spiders, considered *P. gallopavo* as a permanent inhabitant of burrows. However, nothing else is known about the biology of the species, and little is known about the entire genus. Our study of the reproductive behavior of *P. gallopavo* will provide new taxonomic characters useful for constructing the phylogeny of wolf spiders and will form the foundation for future behavioral studies.

We collected fifty juveniles of *P. gallopavo* during March 2013 and 2014, in the Department of Canelones, Uruguay (34°48′50.52″S, 55°58′16.18″W) and in the Department of San José, Uruguay (34°19′13.4″S, 56°43′06.5″W). All the spiders were collected at night, using headlamps. The habitat where *P. gallopavo* was found is open dry areas, with soil as substratum, small stones, and little or no grass. In the laboratory, the spiders were housed individually in Petri dishes (diameter 9.5 cm, height 1.5 cm) with a thin layer of sand as substrate, and a piece of cotton embedded in water. We fed all of the individuals twice a week with a mixed diet of mealworm larvae, *Tenebrio molitor* Linnaeus, 1758 (Coleoptera; Tenebrionidae), and juvenile stages of cockroaches, *Blaptica dubia* Serville, 1839 (Blattodea; Blattellidae). The individuals were monitored daily to determine the exact date that they reached adulthood. We used only virgin males and females of three or more days after last molt and did not reuse individuals. Room temperature and humidity averaged 21.6 ± 3.7 °C (mean ± SD) and 67.4 ± 10.4 %, respectively, and the photoperiod was 12:12 h light:dark.

Thirty-two trials were conducted during April and May of both 2013 and 2014. We used cylindrical glass arenas of 20 cm diameter and 10 cm height, with sand as substrate with very small pebbles (≤ 1 cm) to recreate the microhabitat where they were collected and to provide potential refuges. Females and males were randomly selected and males were removed after 30 min if they did not copulate. Females were placed in the arenas 48 hours before each trial for the deposition of draglines. Males were carefully placed in the arena on the opposite side from the females. Because this species is most active at night (Lacava 2014), all trials were performed at night, between 20:30 and 22:00. We illuminated the test arena from above with a 40-watt red light located 50 cm away. We video-recorded all the trials with a Sony DCR-SR45 video camera with a night shot mode. The

Table 1.—Description of the behaviors performed by *Pavocosa gallopavo*, during courtship and copulation.

Behavior	Description
Male behaviors	
Locomotion	Slow walking movements, with forelegs raised or directed forward, and palps contacting the substrate. Locomotion alternates with being motionless.
Palpal drumming	Quick and alternate pedipalps knocking on the substrate. Initially the drumming is of low intensity, but intensifies when approaching the female.
Leg shaking	Sudden and simultaneous movements, backward and forward, of both extended forelegs, creating an approximate angle of 45°–80° with respect to the substrate surface, usually with short advances. When the male is near the female, forelegs shake in vertical position and the second pair of legs can also raise and shake. When walking, one or few shakes occur consecutively, but near the female, the male performs a series of intense shakings (up to five times). In this last case, the male accompanies shakings with forward and backward movements, as well as with palpal drumming.
Rubbing	Alternate scraping of one leg against another ipsilateral leg, usually the first against the second leg, or the second against the third.
Tapping	Vibration of the extended first and second pair of legs on the frontal area of the carapace and forelegs of the female, with the concomitant raising of the male body when extending third and fourth legs. Simultaneously, he tries to separate the female's forelegs.
Retreat	Backwards movements of the male without stopping courting, when the female pushes him.
Mounting	Male climbing on the female's back, placing himself in the typical copulatory position of wolf spiders. It occurs when the male separates the raised forelegs of the female and achieves the simultaneous hyper-flexion of his palps against the clypeus.
Palpal insertion	Introduction of the embolus of one palpal bulb into one of the female genital openings. During each insertion, the hematodocha of the used palp expands once (ejaculation) and the leg spines become erect.
Side change	Change of the male position, allowing alternate palpal insertion. When inserting left embolus, male leans towards his right side, surrounding the female abdomen with his left foreleg and separating female fourth leg with the other foreleg. When inserts the right embolus, the reverse arrangement occurs.
Dismounting	Descent of the male from the female's back, followed by a quick escape.
Female behaviors	
Locomotion	Slow walking movements, in alternation with motionless.
Turn	Female rotation towards the approaching male.
Leg raising	Foreleg elevation (the first and sometimes also the second pair) facing the male, exposing to him the fully pigmented ventral surface of legs.
Cheliceral opening	Exposure of the dark opened chelicerae (basal segments and fangs) to the male. This behavior usually occurs during Leg raising.
Pushes	Shoving the male with forelegs with the front part of the body raised, when the partner is facing her.
Leg waving	Alternate movements of forelegs towards the courting male.
Lowering body	Female lowers her body and touches the substrate, allowing the male to mount.
Abdominal twists	Rotations of the abdomen side to side. These twists occur both during courtship (when the male shakes close to the female and touches her) and during copulation (accompanying male side changes).
Bucking	Intense body shaking during mounting, apparently trying to dislodge the male.
Attack and cannibalism	Attacks and attempts to kill the male, when male and female are facing or when the male dismounts.

trials ended after the male dismounted. We used JWatcher software (Blumstein et al. 2000) to analyze the occurrences and durations of the behavioral units. The male age during the trials averaged 10.8 ± 8.7 days (mean ± SD) after last molt, whereas the corresponding female age was 13.9 ± 11.0 days; the room temperature averaged 20.5 ± 1.5 °C and humidity 72.5 ± 9.7 %. We registered courtship latency (period from male deposition to first courtship unit), courtship duration (from first courtship behavior to mounting), copulation duration (from mounting to dismounting), number of palpal insertions and number of side changes. We immediately removed the male when the female attacked him. Voucher specimens were deposited at the Arachnological Collection of the Facultad de Ciencias, Montevideo.

We performed 32 trials and observed 25 copulations. Four trials ended after 30 min without mounting, and three led to cannibalism. We analyzed the sexual behaviors of the 25 successful couples and recognized 19 behavioral units. A catalog of the most relevant units is shown in Table 1, and an ethogram of sexual behavior of *P. gallopavo* is shown in Fig. 1.

The sexual behavior of *P. gallopavo* was very brief (5.41 ± 4.18 min, mean ± SD, range 1.34–21.47 min) and was divided into courtship (3.66 ± 3.88 min, range 0.69–18.49 min) and copulation (1.74 ± 0.82 min, range 0.40 – 3.07 min). During the copulation, males of *P. gallopavo* performed on average 12.56 ± 3.88 palpal insertions (range: 3–17) and 12.04 ± 3.87 side changes (range: 3–17). Once inside the arena, males usually remained stationary for several minutes (Motionless) prior to initiating Locomotion. In all trials, males began courtship after finding female draglines and touching them with their legs or palps. Females appeared able to perceive the male's display at a distance of 5–6 cm, when they turned and usually slowly walked towards the males. Males oriented towards females only after they perceived female movements. Some females (7 in 25 cases) performed Leg Waving. When the male was close to the female, she could stay still or performed short Pushes against the male, raising her forelegs. Female Leg Raising was accompanied by Cheliceral Opening in half of the cases. Once the males assumed the copulatory position, all females shook their bodies intensely up to nine times

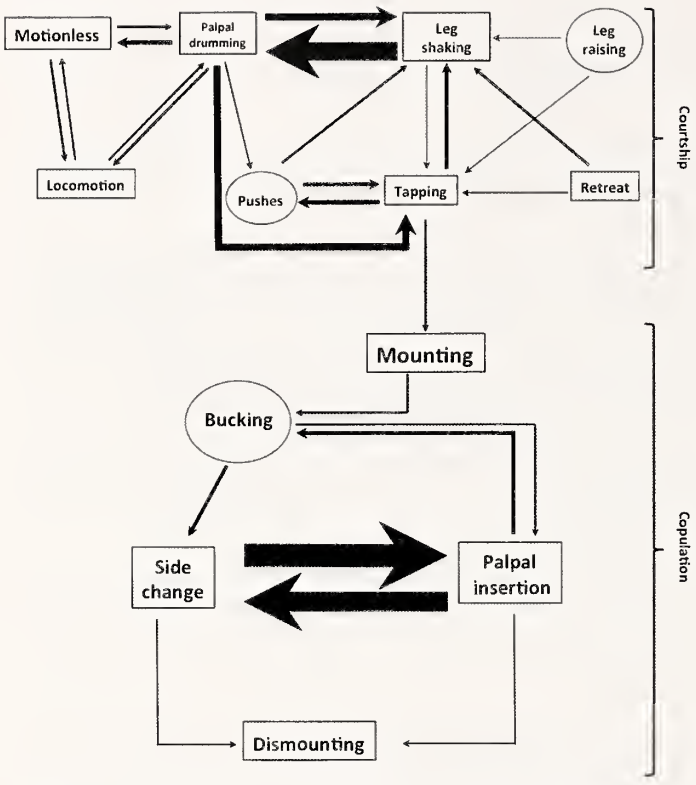

Figure 1.—Ethogram of courtship and copulation behaviors in *Pavocosa gallopavo*. Males performed the behavioral units within boxes and females performed the behavioral units within ovals. Behavioral acts that occurred less than ten times were not included in this diagram.

(Bucking). Males usually resisted being dislodged, but in two cases they were displaced, although were able to re-mount.

The eopulatory pattern consisted of a strict alternation of a single insertion of each embolus of the palpal bulb, with a single hematodochal expansion (ejaculation) per insertion. Meanwhile, the female rotated her abdomen allowing embolus introduction into each genital opening of her epigynum (right embolus into the right female genital opening, and the left into the left). Initially, the male changed sides several times before performing the first insertion with sperm transfer. Palpal insertion was evidenced by the expansion of the hematodocha and by the erection of spines of male hind legs, both due to the increase of hemolymph pressure. Each insertion was mediated by a change in the use of each palp (Palpal Change). Ending copulation, the male touched the female abdomen alternately with his forelegs and quickly dismounted.

Females cannibalized males three times in 32 trials, twice before copulation and once after copulation. In the first two cases, males performed courtship after contacting female silk and females approached them. When they faced each other, the males performed Leg Shaking and Palpal Drumming but immediately tried to mount instead of continuing with courtship while the female gave threat displays. In the postcopulatory case, the male reached the typical copulatory position but could not perform palpal insertions, failing several attempts (flubs) in one or the other side. When the male tried to dismount, the female immediately attacked and cannibalized him.

Pavocosa gallopavo females were active during courtship, performing their own receptive display but simultaneously showing clear symptoms of aggression. While the copulatory position was typical of wolf spiders, intense female mobility and brief copulation were atypical (Stratton et al. 1996; González et al. 2013; García-Diaz et al. 2015). The observed copulatory pattern (alternated single insertions of both palps, performing a unique hematodochal expansion by insertion) was also infrequent for the family (Stratton et al. 1996).

The meeting of both sexes seems to be mediated by female contact sex pheromones, because males initiate searching and courtship behaviors prior to locating the female but after finding female silken threads. This type of chemical communication is well known in other wandering wolf spiders (Tietjen & Rovner 1982; Gaskett 2007; Baruffaldi et al. 2010; Uhl & Elias 2011; Dolejš et al. 2012). The conspieuousness of male Leg Shaking in *P. gallopavo* is extreme for the family, involving not only the first pair of legs raised but also frequently the second pair when the male is facing the female; we did not find in the literature other lycosids that shake their front four legs. This striking display may have increased energetic costs and predatory risks for the male. Furthermore, Leg Shaking involving four legs also implies that all the legs are in good condition because the remaining four hind legs must firmly maintain the male equilibrium during the display. In other words, it seems to be an honest display (Zahavi 1975). Considering that *P. gallopavo* is a nocturnal species (Lacava 2014), we suggest that the conspicuousness of this display allows the male to compensate for the difficulties of visual communication under low light conditions.

As occurs in other Lycosinae (Hebets et al. 1996; Foelix 2011), small stridulatory organs are present at the tibiotarsal joint of the pedipalps of *P. gallopavo* males (Piacentini, pers. comm.). Males articulate this joint during palpal drumming, and they also hit the palps with intensity on the substrate, generating small holes in the sand surface. These observations suggest the occurrence of both stridulation and percussion during sexual communication (Uetz & Stratton 1982). These types of signal production could involve both acoustic and seismic channels, which seem to be particularly useful to communicate at short distances and during the nighttime. We are now studying these behaviors in more detail.

When a male and a female were facing each other, and the male increased the courtship intensity, we observed that the female always pushes the male, simulating attacks. A similar behavior ("lunge") was usually performed by unreceptive female wolf spiders, according to Hebets et al. (1996), Scheffer et al. (1996) and Brown (2006) in *Schizocosa retrorsa* (Banks, 1911), *S. ocreata* (Hentz, 1844), and *Rabidosa santrita* (Chamberlin & Ivie, 1942), respectively. These pushes suggest that the female is testing the male's abilities. The female may also test male vigor and persistence by rejecting several male mount attempts, maintaining both the body and the forelegs raised. However, this hypothesis remains to be tested.

During mount attempts, females usually perform abdominal twists, which are similar to the ones performed by other wolf spider females during copulation, facilitating palpal insertion (Rovner 1971; Stratton et al. 1996). Rovner (1971) mentioned that abdominal rotation in *Rabidosa rabida* (Walckenaer, 1837) was experimentally elicited by touching the carapace of females that were in a cataleptic state. In *P. gallopavo*, this rotation is the rule and apparently is elicited by the male tapping on the forelegs and the front of the carapace of the female. Abdomen rotation seems to be a clear indicator of female receptivity (all females that performed abdominal shift mated). This receptive behavior contrasts with her threatening displays with raised body and forelegs as well as Cheliceral Opening, which the female displays simultaneously. More studies are needed to understand these behaviors.

During mounting, the male hyper-flexes his palps, suggesting that at the time of maximum danger he moves away his copulatory organs to avoid being bitten by the female. Female Bucking, which occurs with the male in copulatory position, is other behavior may be a test of male quality. Shakes of females in copula were observed in some wolf spiders such as *Aglaoctenus lagotis*, *Allocosa brasiliensis*, and *Hogna vivittata* Yin, Bao & Zhang, 1995, which are restless during copulation (González et al. 2013; García-Díaz et al. 2015; González

pers. comm.). However, the body shakes of those species are not as violent as in *P. gallopavo*, where the female can force the male to dismount.

Stratton et al. (1996) state that a few species of wolf spiders (in the genera *Arctosa* C.L. Koch, 1847 and *Geolycosa* Montgomery, 1904) mate for a few seconds or minutes, whereas the majority mate for several minutes up to eight hours. In contrast, copulation duration of *P. gallopavo* (1.7 min) is relatively brief, and is the shortest known in the wolf spiders of Uruguay. Accordingly, palpal insertions (12.6 in average) are few despite the intense male activity. Brief copulation with few insertions would be frequent in burrowing wolf spiders according to Stratton et al. (1996) and Dolejš et al. (2010). We hypothesized it is possible that predation avoidance determines these short copulations because generally mating takes place at the burrow entrance where they are exposed to this danger. On the other hand, the copulatory pattern of *P. gallopavo* (alternation of single insertions with a unique hematodochal expansion) occurs only within Lycosinae subfamily and was described for many species of *Rabidosa* Roewer, 1960 and for some species of *Hogna* Simon, 1885, *Gladicosa* Brady, 1897, *Arctosa, Pardosa* C.L. Koch, 1847 and *Geolycosa* (see Stratton et al. 1996 for review). Finally, *P. gallopavo* also shows other copulatory singularities; males do not perform either abdominal vibrations or palpal moistening, two maneuvers which are usual during copulation of wolf spiders.

Sexual cannibalism is infrequent in wolf spiders, perhaps due to their moderate sexual dimorphism and their secure copulatory position. However, high rates of sexual cannibalism have been indicated by Rabaneda-Bueno et al. (2008, 2014) for females of *Lycosa hispanica* (formerly *L. tarantula*) (33% of the cases). In addition, males in the sex-role reversed lycosid *Allocosa brasiliensis* frequently cannibalize females (30% of interactions) (Aisenberg et al. 2011a). In comparison, despite the aggressive behavior of females, *P. gallopavo* has a moderate rate of sexual cannibalism (9%). This rate is comparable to that performed by *Schizocosa ocreata*, according to Seheffer et al. (1996) and Persons & Uetz (2005) (between 5–11.5%), but higher than the sporadic cases observed in *S. malitiosa, L. thorelli*, and *L. carbonelli*, according to Costa (1979) and Costa & Capocasale (1984). The single case of postcopulatory cannibalism we observed in this study coincided with the occurrence of frequent flubs of the male intromittent organ when he tried to insert.

This species is well suited to further studies of multimodal communication during sexual encounters and the inhibition of female aggression. These would provide useful new characters in phylogenetic studies of the family.

ACKNOWLEDGMENTS

We are grateful to Mariángeles Lacava and Alicia Postiglioni for their help in collecting specimens. We are indebted to Macarena González and María José Albo for critically reading the first draft of the manuscript. Special thanks to Macarena González for his help in preparing the Ethogram. We also would like to thank Anita Aisenberg and J. Henderson for revising the English. We thank two anonymous reviewers for their critical reading and valuable comments on the manuscript.

LITERATURE CITED

Aisenberg, A. & F.G. Costa. 2008. Reproductive isolation and sex role reversal in two sympatric sand-dwelling wolf spiders of the genus *Allocosa*. Canadian Journal of Zoology 86:648–658.

Aisenberg, A., F.G. Costa & M. González. 2011a. Male sexual cannibalism in a sand-dwelling wolf spider with sex role reversal. Biological Journal of the Linnean Society 103:68–75.

Aisenberg, A., C.A. Toscano-Gadea & S. Ghione. 2011b. Guía de Arácnidos del Uruguay. Ediciones de la Fuga, Montevideo.

Baruffaldi, L., F.G. Costa, A. Rodríguez & A. González-Ritzel. 2010. Chemical communication in *Schizocosa malitiosa*: evidence of a female contact sex pheromone and persistence in the field. Journal of Chemical Ecology 36:759–767.

Blumstein, D.T., C.S. Evans & J.C. Daniel. 2000. JWatcher. (Accessed 2009 March 13). Online at http://galliform.psy.mq.edu.au/jwatcher/

Brown, C.A. 2006. Observations on courtship and copulation of the wolf spider *Rabidosa santrita* (Araneae, Lycosidae). Journal of Arachnology 34:476–479.

Castro-O'Neil, M. 2010. Las arañas lobo en Uruguay: taxonomía y distribución (Araneae, Lycosidae). Degree Thesis, Facultad de Ciencias, Universidad de la República, Montevideo.

Costa, F.G. 1975. El comportamiento precopulatorio de *Lycosa malitiosa* Tullgren (Araneae: Lycosidae). Revista Brasileira de Biologia 35:359–368.

Costa, F.G. 1979. Análisis de la cópula y de la actividad postcopulatoria de *Lycosa malitiosa* Tullgren (Araneae: Lycosidae). Revista Brasileira de Biologia 39:361–376.

Costa, F.G. 1991. Fenología de *Lycosa malitiosa* Tullgren (Araneae, Lycosidae) como componente del criptozoos en Marindia, localidad costera del sur del Uruguay. Boletín de la Sociedad Zoológica del Uruguay (2a época) 6:8–21.

Costa, F.G. & R.M. Capocasale. 1984. *Lycosa carbonelli* sp. nov., una etoespeciegemela, simpátrida de *Lycosa thorelli* (Keyserling) (Araneae, Lycosidae). Journal of Arachnology 11:423–431.

Dolejš, P., L. Kubcova & J. Buchar. 2010. Courtship, mating, and cocoon maintenance of *Tricca lutetiana* (Araneae: Lycosidae). Journal of Arachnology 38:504–510.

Dolejš, P., L. Kubcova & J. Buchar. 2012. Reproduction of *Arctosa alpigena lamperti* (Araneae: Lycosidae) – where, when, how, and how long? Invertebrate Reproduction & Development 56:72–78.

Foelix, R.F. 2011. Biology of Spiders, 3rd ed. Oxford University Press, New York.

García-Díaz, V., A. Aisenberg & A.V. Peretti. 2015. Communication during copulation in the sex-role reversed wolf spider *Allocosa brasiliensis*: Female shakes for soliciting new ejaculations? Behavioural Processes 116:62–68.

Gaskett, A.C. 2007. Spider sex pheromones: emission, reception, structures, and functions. Biological Reviews 82:27–48.

González, M., F.G. Costa & A.V. Peretti. 2014. Strong phenological differences between two populations of a Neotropical funnel-web wolf spider. Journal of Natural History 48:2183–2197.

González, M., A.V. Peretti, C. Viera & F.G. Costa. 2013. Differences in sexual behavior of two distant populations of the funnel-web wolf spider *Aglaoctenus lagotis*. Journal of Ethology 31:175–184.

Hebets, E., G.E. Stratton & G. Miller. 1996. Habitat and courtship behavior of the wolf spider *Schizocosa retrorsa* (Banks) (Araneae, Lycosidae). Journal of Arachnology 24:141–147.

Lacava, M. 2014. Versatilidad predadora de las arañas lobo (Araneae, Lycosidae) y su efecto sobre insectos de importancia económica en soja. MsC Thesis, PEDECIBA—Universidad de la República, Uruguay.

Murphy, N.P., V.W. Framenau, S.C. Donellan, M.S. Harvey, Y.C. Park & A.D. Austin. 2006. Phylogenetic reconstruction of the wolf spiders (Araneae: Lycosidae) using sequences from the 12S rRNA, 28S rRNA, and NADH1 genes: implications for classification, biogeography, and the evolution of web building behavior. Molecular Phylogenetics and Evolution 38:583–602.

Persons, M.H. & G.H. Uetz. 2005. Sexual cannibalism and mate choice decisions in wolf spiders: influence of male size and secondary sexual characters. Animal Behaviour 69:83–94.

Piacentini, L.N. 2014. Análisis filogenético de las arañas lobo (Araneae: Lycosidae) utilizando caracteres morfológicos y moleculares. PhD Thesis, Universidad de Buenos Aires, Buenos Aires.

Rabaneda-Bueno, R., S. Aguado, C. Fernández-Montraveta & J.

Moya-Laraño. 2014. Does female personality determine mate choice through sexual cannibalism? Ethology 120:238–248.

Rabaneda-Bueno, R., M.A. Rodríguez-Gironés, S. Aguado-de-la-Paz, C. Fernández-Montraveta, E. De-Mas, D.H. Wise et al. 2008. Sexual cannibalism: high incidence in a natural population with benefits to females. PLoS ONE 3:1–10.

Rovner, J.S. 1971. Mechanisms controlling copulatory behavior in wolf spiders (Araneae: Lycosidae). Psyche 78:150–165.

Scheffer, S. J., G.W. Uetz & G.E. Stratton. 1996. Sexual selection, male morphology, and the efficacy of courtship signaling in two wolf spiders (Araneae: Lycosidae). Behavioral Ecology and Sociobiology 38:17–23.

Stratton, G.E., E.A. Hebets, P.R. Miller & G.L. Miller. 1996. Pattern and duration of copulation in wolf spiders (Araneae, Lycosidae). Journal of Arachnology 24:186–200.

Tietjen, W.J. & J.S. Rovner. 1982. Chemical communication in lycosids and other spiders. Pp. 249–279. *In* Spider Communication: Mechanisms and Ecological Significance. (P.N. Witt, J.S. Rovner, eds.). Princeton University Press, Princeton.

Uetz, G.W. & G.E. Stratton. 1982. Acoustic communication and reproductive isolation in spiders. Pp. 123–159. *In* Spider Communication: Mechanisms and Ecological Significance. (P.N. Witt, J.S. Rovner, eds.). Princeton University Press, Princeton.

Uhl, G. & D.O. Elias. 2011. Communication. Pp. 127–189. *In* Spider Behavior: Flexibility and Versatility. (M.E. Herberstein, ed.). Cambridge University Press, Cambridge.

World Spider Catalog. 2015. Natural History Museum Bern. Version 16.5. Online at http://wsc.nmbe.ch

Zahavi, A. 1975. Mate selection – a selection for a handicap. Journal of Theoretical Biology 57:205–214.

Manuscript received 5 November 2015, revised 5 July 2016.

2016. Journal of Arachnology 44:417–418

INSTRUCTIONS TO AUTHORS

(revised October 2016)

All manuscripts are submitted online at
http://www.editorialmanager.com/arachno

General: The *Journal of Arachnology* publishes scientific articles reporting novel and significant observations and data regarding any aspect of the biology of arachnid groups. Articles must be scientifically rigorous and report substantially new information. Submissions that are overly narrow in focus (e.g., local faunal lists, descriptions of a second sex or of a single species without additional discussion of the significance of this information), that have poorly substantiated observational data, or that present no new information will not be considered. Book reviews will not be published.

Manuscripts must be in English and should use the active voice throughout. Authors should consult a recent issue of the *Journal of Arachnology* for additional points of style. Manuscripts longer than three printed journal pages (12 or more double-spaced manuscript pages) should be prepared as Feature Articles, shorter papers as Short Communications. Invited Reviews will be published from time to time and unsolicited reviews are also welcomed. All reviews will be subject to the same review process as other submissions.

Submission: Manuscripts should be prepared in Microsoft Word and then submitted electronically via our online system, *PeerTrack* (http://www.editorialmanager.com/arachno). *PeerTrack* will guide you through the step-by-step process including uploading the manuscript and all of its parts. The paper can be uploaded as one piece, with tables, figures, and appendices embedded, or as text, then tables, figures, and appendices, each uploaded individually. Ultimately, *PeerTrack* will assemble all parts of the paper into a PDF that you, as corresponding author, will need to approve before the submission process can be completed. Supplemental Materials (see below) can also be uploaded, but they are not bundled into the PDF.

Voucher Specimens: Specimens of species used in your research should be deposited in a recognized scientific institution. All type material *must* be deposited in a recognized collection/institution and the identity of the collection must be given in the text of the manuscript.

Checklist—Common Formatting Errors is available as a PDF at http://www.americanarachnology.org/JOA.html#instructions

FEATURED ARTICLES

Title page.—The title page includes the complete name, address, and e-mail address of the corresponding author; the title in bold text and sentence case; each author's name and address; and the running head.

Running head.—This should be in all capital letters, not exceeding 60 characters and spaces, and placed at the top of the title page. It should be composed of the authors' surnames and a short title. Examples: SMITH—SALTICIDS OF PANAMA; SMITH & CRUZ—SALTICIDS... ; SMITH ET AL.—SALTICIDS...

Abstract.—Length: ≤ 250 words for Feature Articles; ≤ 150 words for Short Communications.

Keywords.—Give 3–5 appropriate keywords or phrases following the abstract. *Keywords should not duplicate words in the title.*

Text.—Double-space text, tables, legends, etc. throughout. Except for titles and headers, all text should be left-justified. Do not add line numbers—they are automatically added by *PeerTrack*. Three levels of heads are used.

- The first level (METHODS, RESULTS, etc.) is typed in capitals and centered on a separate line.
- The second level head begins a paragraph with an indent, is in bold type, and is separated from the text by a period and a dash.
- The third level may or may not begin a paragraph but is italicized and separated from the text by a colon.

Use only the metric system unless quoting text or referencing collection data. If English measurements are used when referencing collection data, then metric equivalents should also be included parenthetically. All decimal fractions are indicated by a period (e.g., 3.141). Include geographic coordinates for collecting locales if possible, using one of the following formats: 0°12′32″S, 29°52′17″E or 0.2089°S, 29.8714°E.

Citation of references in the text: Cite only papers already published or in press. Include within parentheses the surname of the author followed by the date of publication. A comma separates multiple citations by the same author(s) and a semicolon separates citations by different authors, e.g., (Smith 1970), (Jones 1988; Smith 1993), (Smith & Jones 1986, 1987; Jones et al. 1989). Include a letter of permission from any person who is cited as providing unpublished data in the form of a personal communication.

Citation of taxa in the text: Include the complete taxonomic citation (author, year) for each arachnid genus and/or species name when it first appears in the abstract and text proper. For example, *Araneus diadematus* Clerck, 1757. For Araneae, this information can be found online at www.wsc.nmbe.ch. Citations for scorpions can be found in the *Catalog of the Scorpions of the World (1758–1998)* by V. Fet, W.D. Sissom, G. Lowe & M.E. Braunwalder. Citations for the smaller arachnid orders (pseudoscorpions, solifuges, whip scorpions, whip spiders, schizomids, ricinuleids and palpigrades) can be found at museum.wa.gov.au/catalogues-beta/. Citations for some species of Opiliones can be found in the *Annotated Catalogue of the Laniatores of the New World (Arachnida,Opiliones)* by A.B. Kury.

Literature cited.—Use the following style and formatting exactly as illustrated; include the full unabbreviated journal title. Personal web pages should not be included in Literature Cited. These can be cited within the text as (John Doe, pers. website) without the URL. Institutional websites may be included in

Literature Cited. If a citation includes more than six authors, list the first six and add "et al." to represent the others.

Binford, G. 2013. The evolution of a toxic enzyme in sicariid spiders. Pp. 229–240. *In* Spider Ecophysiology. (W. Nentwig, ed.). Springer-Verlag, Heidelberg.

Cushing, P.E., P. Casto, E.D. Knowlton, S. Royer, D. Laudier, D.D. Gaffin et al. 2014. Comparative morphology and functional significance of setae called papillae on the pedipalps of male camel spiders (Arachnida, Solifugae). Annals of the Entomological Society of America 107:510–520.

Harvey, M.S. & G. Du Preez. 2014. A new troglobitic ideoroncid pseudoscorpion (Pseudoscorpiones: Ideoroncidae) from southern Africa. Journal of Arachnology 42:105–110.

World Spider Catalog. 2015. World Spider Catalog. Version 16. Natural History Museum, Bern. Online at http://wsc.nmbe.ch/

Roewer, C.F. 1954. Katalog der Araneae, Volume 2a. Institut Royal des Sciences Naturelles de Belgique, Bruxelles.

Rubio, G.D., M.O. Arbino & P.E. Cushing. 2013. Ant mimicry in the spider *Myrmecotypus iguazu* (Araneae: Corinnidae), with notes about myrmecomorphy in spiders. Journal of Arachnology 41:395–399.

Footnotes.—Footnotes are permitted on the first page, only to give current address or other author information, and at the bottom of tables (see below).

Taxonomic articles.—Consult a recent taxonomic article in the *Journal of Arachnology* for style or contact a Subject Editor for Systematics. Papers containing original descriptions of focal arachnid taxa should be listed in the Literature Cited section.

Tables.—Each table, with the legend above, should be placed on a separate manuscript page. Only horizontal lines (usually no more than three) should be included. When necessary, tables may have footnotes, for example, to specify the meanings of symbols about particular data.

Illustrations.—Original illustrations include photographs, line drawings, maps, and other graphic representations. All should be considered figures and numbered consecutively with other figures. You should ensure that all illustrations, at submission, are at high enough resolution to be useful to editors and reviewers; 300 dpi is usually sufficient.

At the discretion of the Editor-in-Chief, a figure can be rendered in color in the online version but in monochrome in the journal's printed version, or in color in both versions if warranted by the figure's context and content. Most figures will be reduced to single-column width (9 cm, 3.5 inches), but large plates can be printed up to two-columns width (18 cm, 7 inches). Address all questions concerning illustrations to the Editor-in-Chief of the *Journal of Arachnology*: **Robert B. Suter, Editor-in-Chief** [*E-mail:* suter@vassar.edu].

Legends for illustrations should be placed together on the same page(s). Each plate must have only one legend, as indicated below:

Figures 1–4. *A-us x-us*, male from Timbuktu: 1. Left leg. 2. Right chelicera. 3. Dorsal aspect of genitalia. 4. Ventral aspect of abdomen.

The following alternate Figure numbering is also acceptable:

Figure 1a–e. *A-us x-us*, male from Timbuktu: a. Left leg. b. Right chelicera. c. Dorsal aspect of genitalia. d. Ventral aspect of abdomen.

Assemble manuscript.—The manuscript should be assembled in the following sequence: title page, abstract, text, tables with legends, figure legends, figures. As noted above, at the time of submission the paper can be uploaded as one piece, with tables, figures, and appendices embedded, or as text, then tables, figures, and appendices, each uploaded individually.

Supplemental materials.—Authors may submit for online publication materials that importantly augment the contents of a manuscript. These may be audio files (e.g., .mp3, .m4a, .aif, .wav), video files (e.g., .mov, .m4v, .flv, .avi), or Word documents (e.g., .doc, .docx) for large tables of data. Consult with the Editor-in-Chief if you are considering submitting other kinds of files. Audio and video files should be carefully edited before submission to eliminate leaders, trailers, and other extraneous content. Individual files may not exceed 10MB; no more than five files may be included as supplemental materials for a manuscript.

Supplemental materials will be considered by reviewers and therefore must be included at the time of manuscript submission. Supplemental materials are published online at the discretion of the editors.

SHORT COMMUNICATIONS

Short Communications are usually limited to 3–4 journal pages, including tables and figures (11 or fewer double-spaced manuscript pages including Literature Cited; no more than 2 figures or tables). Internal headings (METHODS, RESULTS, etc.) are omitted. Short communications must include an abstract and keywords.

Page charges.—Page charges are voluntary, but authors who are not members of the American Arachnological Society are strongly encouraged to pay in full or in part for their articles ($75 per journal page).

Proofs.—The Journal's expectation is that the final revision of a manuscript, the one that is ultimately accepted for publication, will not require substantive changes. Accordingly, the corresponding author will be charged for excessive numbers of changes made in the proofs.

Reprints.—Hard copy reprints are available only from Allen Press via EzReprint, a user-friendly, automated online system for purchasing article reprints. If your paper is accepted, prior to its publication you will receive an e-mail containing both a unique URL (SmartLink) from Allen Press/Yurchak Press and information about the reprint order process. Clicking on the SmartLink will take you directly to a web portal where you may place your reprint order. The email will be sent to you from: reprints@authorbilling.com. PDFs of papers published in the *Journal of Arachnology* are available to AAS members at the society's web site. They are also available through BioOne (www.bioone.org) and JSTOR (www.jstor.org) if you or your institution is a member of BioOne or JSTOR. PDFs of articles older than one year are freely available from the AAS website.

COVER ARTWORK

Authors are encouraged to send high quality color photographs to the Editor-in-Chief to be considered for use on the cover. Images should be at least 300 dpi.

CONTENTS

Journal of Arachnology

Volume 44 Number 3

Featured Articles

Short Communications